INTERNATIONAL ENERGY AGENCY
Energy conservation in buildings and community systems programme

26th AIVC Conference

Ventilation in Relation to the Energy Performance of Buildings

Proceedings

Air Infiltration and Ventilation Centre
Operating Agent and Management
INIVE EEIG
Boulevard Poincaré 79

INTERNATIONAL ENERGY AGENCY
Energy conservation in buildings and community systems programme

26th AIVC Conference

Ventilation in Relation to the Energy Performance of Buildings

Proceedings

This report is part of the work of the IEA Energy Conservation in Buildings & Community Systems Programme – Annex V Air Infiltration and Ventilation Centre

Publication prepared by
Belgian Building Research Institute (on behalf of INIVE EEIG)

Practical organization of the conference by
Belgian Building Research Institute (on behalf of INIVE EEIG)

Document AIC-PROC-26-2005

ISBN 2-9600355-8-5

Annex V Participating countries:
Belgium, Czech Republic, France, Greece, The Netherlands, Norway and the United States of America.

Preface

International Energy Agency

The International Energy Agency (IEA) was established in 1974 within the framework of the Organisation for Economic Co-operation and Development (OECD) to implement an International Energy Programme. A basic aim of the IEA is to foster co-operation among the twenty-four IEA Participating Countries to increase energy security through energy conservation, development of alternative energy sources and energy research development and demonstration (RD&D).

Energy Conservation in Buildings and Community Systems

The IEA sponsors research and development in a number of areas related to energy. In one of these areas, energy conservation in buildings, the IEA is sponsoring various exercises to predict more accurately the energy use in buildings, including comparison of existing computer programs, building monitoring, comparison of calculation methods as well as air quality and studies of occupancy.

The Executive Committee

Overall control of the programme is maintained by an Executive Committee, which not only monitors existing projects but also identifies new areas where collaborative effort may be beneficial.

To date the following have been initiated by the Executive Committee (completed projects are identified by *):

1 Load Energy Determination of Buildings *
2 Ekistics and Advanced Community Energy Systems *
3 Energy Conservation in Residential Buildings *
4 Glasgow Commercial Building Monitoring *
5 Air Infiltration and Ventilation Centre
6 Energy Systems and Design of Communities *
7 Local Government Energy Planning *
8 Inhabitant Behaviour with Regard to Ventilation *
9 Minimum Ventilation Rates *
10 Building HVAC Systems Simulation *
11 Energy Auditing *
12 Windows and Fenestration *
13 Energy Management in Hospitals*
14 Condensation *
15 Energy Efficiency in Schools *
16 BEMS – 1: Energy Management Procedures *
17 BEMS – 2: Evaluation and Emulation Techniques *
18 Demand Controlled Ventilation Systems *
19 Low Slope Roof Systems *
20 Air Flow Patterns within Buildings *
21 Thermal Modelling *
22 Energy Efficient communities *
23 Multizone Air Flow Modelling (COMIS)*
24 Heat Air and Moisture Transfer in Envelopes *
25 Real Time HEVAC Simulation *
26 Energy Efficient Ventilation of Large Enclosures *
27 Evaluation and Demonstration of Residential Ventilation Systems *

28 Low Energy Cooling Systems *
29 Daylight in Buildings *
30 Bringing Simulation to Application *
31 Energy Related Environmental Impact of Buildings *
32 Integral Building Envelope Performance Assessment *
33 Advanced Local Energy Planning *
34 Computer-aided Evaluation of HVAC Systems Performance *
35 Design of Energy Hybrid Ventilation (HYBVENT) *
36 Retrofitting of Educational Buildings *
36 WG Annex 36 Working Group Extension 'The Energy Concept Adviser'
37 Low Exergy Systems for Heating and Cooling of Buildings *
38 Solar Sustainable Housing *
39 High Performance Insulation systems (HiPTI) *
40 Commissioning Building HVAC Systems for Improved Energy Performance *
41 Whole Building Heat, Air and Moisture Response (MOIST-EN)
42 The Simulation of Building-Integrated Fuel Cell and Other Cogeneration Systems (COGEN-SIM)
43 Testing and Validation of Building Energy Simulation Tools
44 Integrating Environmentally Responsive Elements in Buildings
45 Energy-Efficient Future Electric Lighting for Buildings
46 Holistic Assessment Tool-kit on Energy Efficient Retrofit Measures for Government Buildings (EnERGo)

Annex V: Air Infiltration and Ventilation Centre

The Air Infiltration and Ventilation Centre was established by the Executive Committee following unanimous agreement that more needed to be understood about the impact of air change on energy use and indoor air quality. The purpose of the Centre is to promote an understanding of the complex behaviour of air flow in buildings and to advance the effective application of associated energy saving measures in both the design of new buildings and the improvement of the existing building stock.

The Participants in this task are Belgium, Czech Republic, France, Greece, Netherlands, Norway, and the United States of America.

26th AIVC Conference

Brussels, Belgium, 21-23 September 2005

"Ventilation in Relation to the Energy Performance of buildings"

CONTENTS

Session 1 – Indoor environment and energy

Impact of Commercial Building Infiltration on Heating and Cooling Loads in U.S. Office Buildings 1
Steven J. Emmerich, Andrew K. Persily and Timothy P. McDowell

Uncertainty and sensitivity analysis to evaluate natural night ventilation design in an office building..... 3
Hilde Breesch, Arnold Janssens

Indoor environmental quality, energy usage and occupant perception in commercial office buildings..... 9
D. Novosel and L.D. Stetzenbach

Energy performance of earth-air heat exchanger in a Belgian office building 15
A. Janssens, M. Steeman, J. Desmedt, H. Hoes, M. De Paepe

Energy and Comfort performance of natural ventilation system in office buildings in China 21
Runming Yao, Baizhan Li, Koen Steemers

Ventilation, IAQ and Energy Efficiency in hot humid climates..... 27
S.C. Sekhar, K.W. Tham, K.W. Cheong

Session 2 – Whole building heat, air and moisture transfer – 1st part

Annex 41, whole building heat air and moisture response - Introduction 35
H. Hens

IEA Annex 41, Subtask 1: modelling principles and common exercises 41
Monika Woloszyn, Ruut Peukhuri, Lone Mortensen, Carsten Rode

NORDTEST Project on Moisture Buffer Value of Materials..... 47
Carsten Rode, Ruut Peukhuri, Kurt K. Hansen, Berit Time, Kaisa Svennberg, Jesper Arfvidsson, Tuomo Ojanen

Modelling of Moisture Conditions in a Cold Attic Space 53
A. Sasic Kalagasidis, B. Mattsson

Session 3 - Airthightness

Blowerdoor measurement of large buildings – with one or more blower systems 59
Sigrid Dorschky, Paul Simons, Stefanie Rolfsmeier

Airtightness of Commercial Buildings in the U.S. 65
Steven J. Emmerich and Andrew K. Persily

Airtightness field measurement of 123 new French dwellings with a simplified measuring device 71
Andrés Litvak, Anne Voeltzel, Xavier Boulanger, Robert Markiewicz, Bruno-Gilbert Royet

Criteria to define limits for building airtightness – airtightness of some Portuguese buildings 77
Armando Pinto

Rationale for Measuring Duct Leakage Flows in Large Commercial Buildings 83
Craig Wray, R. Diamond, Max Sherman

Session 4 – Measurements and monitoring

‘DIAGVENT’ guidebook – checking the performance of ventilation systems 89
Pierre Barles, Pierre-Jean Vialle, Marie-Claude Lemaire

Energy audit certification and rating of school buildings in Greece 95
Gaitani Niki, Santamouris Mat, Mihalakakou Giouli, Papaglastra Marianna1, Assimakopoulos Margarita-Niki, Sfakianaki Katerina, Pavlou Konstantinos, Doukas Paris, Korres Dimitrios

Refurbishing of the ventilation system in a school 105
Pierre-Jean Vialle, Anne Voetzel, Christian Pico

Review on ventilation rate measuring and modelling techniques in naturally ventilated buildings 111
Sezin Eren Özcan, Erik Vranken and Daniel Berckmans

Experiment of the mixing property and the heat exhaust effect under cross ventilation in a full-scale building model 123
S. Nishizawa, T. Sawachi, K. Narita, H. Seto, Y. Ishikawa and T. Gotou

Session 5 - Hybrid ventilation

Experimental characterization of hybrid ventilation systems in residential buildings..... 129
Manuel Pinto, Vasco Peixoto de Freitas, João Carlos Viegas

Study on energy conservation effect of hybrid ventilation system utilizing wind pressure for multi-family buildings..... 135
M. Tajima, T. Sawachi, Y. Hori, Y. Takahashi

On the impact of urban environment on the performance of natural and hybrid ventilation systems 141
K. Niachou, M. Santamouris

Performance evaluation of the hybrid ventilation system controlled by a pressure difference sensor..... 151
H. Yoshino, S. Yun and A. Nomura

Assessment of improvements brought by humidity sensitive and hybrid ventilation / HR-VENT project 157
J.L. Savin, S. Berthin, M. Jardinier

Session 6a – Poster session 1

Improving envelope airtightness: results of a pilot study on 31 houses..... 169
Karine Guillot, Daniel Limoges, François Rémi Carrié

Analysis method based on power balance as applied to wind driven flow..... 175
Kyosuke Hiyama and Shinsuke Kato

Ventilation related to User Habits – Considerations on Environmental Envelope Rehabilitation 181
Carolina Ganem, Helena Coch and Alfredo Esteves

Ventilation system qualité for dwellings : a pragmatic approach 187
P. Wouters and P. Van den Bossche

A simple tool for energy and comfort assessment in natural ventilation building..... 189
Runming Yao, Koen Steemers, Nan Li

Development of design guidelines for tertiary sector buildings equipped with natural ventilation systems 191
Geoffrey van Moeseke, Isabelle Bruyère, André De Herde

Performance prediction of dwelling ventilation with self-regulating air inlets 197
L. Willems and A. Janssens

Prediction of buoyancy-induced pressure difference across exterior walls of high-rise residential building 203
Jae-Hun Jo, Sung-Han Koo, Jong-In Lee, Hoi-Soo Seo, Myoung-Souk Yeo, Kwang-Woo Kim

CFD analysis of the effect of self-regulating devices on the distribution of naturally supplied air 211
J. De Neve, S. Denys, J.G. Pieters, I. Pollet, J. Denul

Session 6b – Poster session 2

Natural ventilation – some design considerations 217
Seemi Ahmed, Siraj Ahmed

Indoor humidity control with DX A/C systems in subtropical residences 229
Zheng Li, Wu Chen, Shiming Deng

Heat and Non-Heat Recovery Ventilation Performance in Energy-Efficient HUD-code Manufactured Housing 235
Michael Lubliner, Andrew Gordon, Adam Hadley, Danny Parker

Guidelines to improve efficiency of a double-skin façade in an office building 245
Elisabeth Gratia, André De Herde

Airflow simulations in double façades with a perforated inner sheet 251
Regina Bokel, Truus de Bruin-Hordijk

Atria for ventilation efficiency improvement in urban office buildings 257
Chris J. Koinakis

Application of Phoenics to Athletic halls with HVAC ventilation 265
O.I. Stathopoulou, V.D. Assimakopoulos

Indoor air climate control 271
A. Van Brecht, S. Quanten, T. Zerihundesta, D. Berckmans

Session 7 – Whole building heat, air and moisture transfer – 2nd part

Experimental evaluation of moisture buffering effect in a room .....*(paper not yet available)*
Teruaki Mitamura, Hiroshi Yoshino, Ken-ichi Hasegawa, Shin-ichi Mastumoto, Mayumi Adachi

Effect of moisture inertia models on the predicted indoor humidity in a room 287
A. Janssens, M. De Paepe

Numerical simulations of energy performance of a ventilation system controlled by relative humidity 295
M. Woloszyn, J. Shen, A. Mordelet, J. Brau

Indoor climate design for a monumental building with periodic high indoor moisture loads 301
A.W.M. van Schijndel

Session 8 - Modelling

Development and validation of a model to calculate wind speeds in urban canyons 315
C. Georgakis, M. Santamouris

Probabilistic model PROMO for evaluation of air change rate distribution..... 329
Krystyna Pietrzyk, Carl-Eric Hagentoft

Modelling and control of livestock ventilation systems and indoor environments..... 335
Zhuang Wu, Per Heiselberg, Jakob Stoustrup

Comparative analysis of the energy impact of air infiltration for different ventilation systems 341
A. Voeltzel and F.R. Carrié

Analysis of ventilation systems in high performance homes in cold climates..... 347
Christine E. Walker and Douglas Kosar

Use of the stairwell as a component of natural ventilation systems in residential buildings. Comparison of technologies for the external envelope. 353
F. Iannone, F. Fiorito

Impact of Commercial Building Infiltration on Heating and Cooling Loads in U.S. Office Buildings

[1]Steven J. Emmerich, [1]Andrew K. Persily, and [2]Timothy P. McDowell

[1]*Building and Fire Research Laboratory, National Institute of Standards and Technology*
Gaithersburg, MD USA
[2]*TESS, Inc.*
Madison, WI USA

ABSTRACT

With the exception of a few analyses of the impacts of ASHRAE Standard 62-89 and energy use in specific buildings, the energy use in commercial building due to infiltration and ventilation flows has received little attention. However, as improvements have been made in insulation, windows, etc., the relative importance of these airflows has increased. Previous work at NIST described a research plan to quantify, and assess opportunities to reduce, the energy and indoor air quality impacts of building airtightness and ventilation system control in office buildings (Emmerich et al. 1995). It included an initial estimate that infiltration is responsible for 18% of the total heating energy use and 2% of the total cooling energy use in US office buildings but also concluded that an improved estimate would require the development of a new simulation tool coupling a multizone airflow model with a building thermal analysis program.

McDowell et al. (2003) describes the incorporation of the AIRNET airflow model (the airflow simulation portion of the CONTAMW multizone IAQ modeling program) into the TRNSYS energy simulation program to be the needed tool. The resulting integrated simulation tool was then used to estimate the energy usage of 25 buildings representing the U.S. office building stock over a range of infiltration and ventilation conditions. This paper presents detailed simulation results including infiltration rates and their associated heating and cooling loads with an emphasis on the results from the buildings representing recent construction.

UNCERTAINTY AND SENSITIVITY ANALYSIS TO EVALUATE NATURAL NIGHT VENTILATION DESIGN IN AN OFFICE BUILDING

Hilde Breesch, Arnold Janssens

Department of Architecture and Urban Planning, Ghent University, J. Plateaustraat 22, B-9000 Gent, Belgium

ABSTRACT

Natural night ventilation is an energy efficient way to improve thermal summer comfort. Coupled thermal and ventilation simulation tools predict the performances. Nevertheless, the reliability of the simulation results with regard to the assumptions in the input, is still unclear. Uncertainty analysis is chosen to determine the uncertainty on the predicted performances of natural night ventilation. In addition, sensitivity analysis defines the most important input parameters causing this uncertainty. This methodology is used to evaluate one of the possible design schemes of natural night ventilation in a new office building of the Ghent University (Belgium).

KEYWORDS

Natural night ventilation, TRNSYS - COMIS, uncertainty and sensitivity analysis.

INTRODUCTION

Natural night ventilation is an interesting passive cooling method. Driven by wind and thermally (stack) generated pressures, natural night ventilation cools down the exposed building structure at night, in which the heat of the previous day is accumulated. Temperature peaks are consequently reduced and postponed. Designers utilize building simulation to predict the performances of natural night ventilation. Nevertheless, the reliability of these simulation results with regard to the assumptions, made by the user in the input, is still unclear. This uncertainty puts up a barrier to implement energy efficient cooling techniques. Therefore, this research aims to define the uncertainty of the predicted performances of natural night ventilation as well as the input parameters causing this uncertainty. This methodology is used to evaluate one of the possible design schemes of natural night ventilation in a new office building of the Ghent University (Belgium).

METHODOLOGY

The thermal comfort achieved by natural night ventilation is characterised by the weighted excess hours during occupation time (GTO). Determination of GTO is based on the comfort theory of Fanger (Fanger, 1972), which takes both indoor environmental parameters (air and radiant temperature, air velocity and relative humidity) and personal properties (metabolism, activity level and clothing) into account. The hourly weight factor (WF) takes the degree of discomfort in consideration and is directly proportional to the increase of the predicted percentage of dissatisfied people (PPD): one hour with 20 % dissatisfied people is equal to two hours with 10 % dissatisfied. A PMV of 0.5 corresponds to a WF of 1 (see Eqn. 1).

$$\text{if } PMV < 0.5 \text{ then } WF = 0 \text{ else } WF = 10 - 9.5 \exp\left[-\left(0.03353\ PMV^{4} + 0.2179\ PMV^{2}\right)\right] \quad (1)$$

A number of weighted working hours in which more than 10 % of the occupants are dissatisfied (predicted mean vote or PMV > 0.5) less than 150 - 200 h, means a good thermal summer comfort (van der Linden et al., 2002).

A coupled thermal and ventilation model, which iterates the mass and energy balance per zone till convergence, is necessary to simulate natural night ventilation (Breesch and Janssens, 2002) as the internal temperatures depend on the ventilation flow rates. Because natural night ventilation is temperature driven, the flow rate is on its turn function of the indoor air temperatures. The existing coupling between TRNSYS 16 (SEL et al., 2004), a transient multizone thermal simulation model, and COMIS 3.1 (Dorer et al., 2001), a multizone infiltration and ventilation simulation model, is chosen to predict the performances of natural night ventilation. Both simulation programs subdivide the building in various zones, mostly corresponding to the rooms, in which the air is assumed to be perfectly mixed.

To analyse the uncertainty on the predicted thermal comfort, given the uncertainty on the input factors, Monte Carlo analysis (MCA) (Saltelli et al., 2000) is chosen. MCA performs multiple evaluations with randomly selected model input parameters. The following steps are successively carried out: selection of a range and distribution for each input parameter, sample generation from these distributions, evaluation of the model for each element of this sample and uncertainty analysis. Latin Hypercube sampling (LHS) is chosen to build a N*k sample with N elements of k input parameters because LHS ensures better coverage of the range of each input parameter than random sampling. The range of each variable is divided into N non-overlapping intervals of equal probability 1/N. One value from each interval is randomly selected. These N values of the first input factor are step-by-step and at random combined with N randomly chosen values of each other input factor. The minimum number of model evaluations, required for Latin Hypercube sampling for a representative sample, is one and a half times the number of input factors (POLIS, JRC-ISIS, 2003).

Furthermore, sensitivity analysis studies how the variation in the thermal comfort is attributed to the variation in the input parameters. Global sensitivity, based on MCA, incorporates the influence of the whole range of variation and distribution of each input parameter and evaluates the effect of one parameter while all other parameters are varied as well. The standardized rank regression coefficient (SRRC) ranks and quantifies the effect of the input factors on the thermal comfort and are deduced from linear regression analysis on rank-transformed input data. Eqn. 2 defines the standardized linear regression model from a N*k sample with N elements of k input factors (with j = 1,2,…,k; i = 1,2, …,N; x = input; y = output; b_j = regression coefficient):

$$\frac{y-\bar{y}}{\hat{s}} = \sum_{j=1}^{k} \frac{b_j \hat{s}_j}{\hat{s}} \frac{\left(x_j - \bar{x}_j\right)}{\hat{s}_j}$$

$$\text{with } \bar{y} = \sum_{i=1}^{N} \frac{y_i}{N},\ \bar{x}_j = \sum_{i=1}^{N} \frac{x_{ij}}{N} \quad \hat{s} = \left[\sum_{i=1}^{N} \frac{\left(y_j - \bar{y}\right)^2}{N-1}\right]^{1/2}, \hat{s}_j = \left[\sum_{i=1}^{N} \frac{\left(x_{ij} - \bar{x}_j\right)^2}{N-1}\right]^{1/2} \quad (2)$$

The coefficients $\frac{b_j \hat{s}_j}{\hat{s}}$ are called SRRCs. Assuming the input factors x_j independent, SRRC estimates the importance of an input x_j while all other input factors remain their expected value. Both the distribution of the input x_j and its impact on the output affect the SRRC.

CASE STUDY

One of the possible design schemes of natural night ventilation by thermal stack in a new office building of the Ghent University (Belgium) is studied. The examined building, situated on the west side of a courtyard, consists of three office floors on top of a foyer and two underground service floors and is part of large complex of offices, laboratories and an auditorium in the city centre of Ghent. The office floors have a an area of 24.7 x 11 m², the height between floor and false ceiling and two floors respectively is 2.9m and 3.9m, the total height is 18m. The curtain wall façade of the offices is composed of sandwich (63%) and glass (37%) panels, the stairwell is completely finished with glass. Figure 1 shows the operation scheme of the natural ventilation (by day and night) on a floor plan and a cross section. Outside air enters the offices on each floor through top hung windows, cools down the exposed floor by night, flows through the false ceiling to the corridor and continues its way to the central stairwell on the south side of the courtyard where the air leaves the building at the top through outlet windows on both sides.

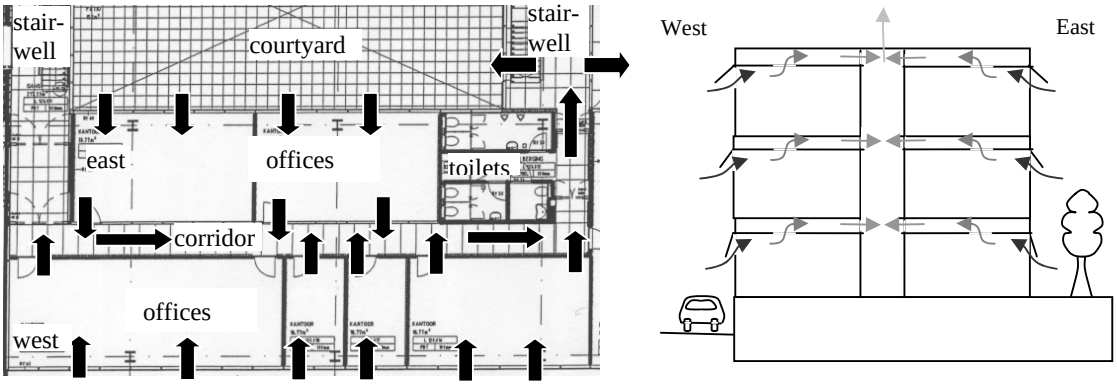

Figure 1: Operation scheme of natural ventilation on a floor plan (left) and on a cross section (right)

The simulation model simplifies the building geometry and includes on each floor one office on the west and the east side, connected by a circulation zone, i.e. the corridors and the stairwell. All the input parameters are assumed to be normally distributed. The distributions are estimated from data in the literature and standards. The given ranges correspond to $[\mu - 2\sigma; \mu + 2\sigma]$, with μ and σ respectively the mean and standard deviation.

Hourly design weather data in Uccle (Belgium) are calculated by Meteonorm (Meteotest, 2003), based on monthly average measured data from 1961-1990. Simulations are carried out from May 21 to September 15. The internal heat gains vary from 25 to 35 W/m² in the offices, 3 W/m² in the corridor. Wall compositions and material properties (BIN, 2001) are shown in table 1. Uncertainties on these values are caused by temperature and humidity variations and are calculated according to (ISO, 1999), taking into account a temperature difference of 10°C and a humidity ratio depending on kind of the material (CEN, 2000). Solar absorption coefficients are taken from (Clarke et al., 1990). The transmittance coefficient U of glass is not varied: 1.1 W/m²K, the solar transmission coefficient varies from 0.58 to 0.62. External sunblinds are provided on all windows and are automatically controlled to be lowered from an irradiation of [135;165] W/m² and have a g-value (glass included) from 0.1 to 0.2. The convective heat transfer coefficient on external surfaces depends on the local wind velocity on site (ASHRAE, 2001). In addition, the internal convective heat transfer coefficient by natural convection is function of the temperature difference between the surface and the air as shown in table 1. A time step of 15 min is chosen. Internal separations between the concerned office

and the rest of the building are assumed to be adiabatic. The offices are assumed to be occupied from Monday to Friday from 9h to 18h.

The wind velocity on site is calculated from the meteorological wind velocity taking the roughness height z_0 on site and at the meteo station into account (table 1). Figure 2 shows the wind pressure coefficients Cp influenced by the enclosed buildings, calculated with the Cp generator of Knoll et al. (1995). The air tightness of the façade is characterised by an air mass flow coefficient C from 6 to $14*10^{-5}$ kg/(s.Pa^n.m²) (Tamura and Chia, 1976) and modelled by cracks on office floor and ceiling height. The night ventilation openings in the façade are automatically controlled in each office separately (table 1). This table also defines the effective leakage area (ELA) of the openings at night in 1 office module of 2.6m wide on each floor, with a discharge coefficient C_D from 0.4 to 0.8 (Flourentzou et al., 1998). The ELA of the exhaust openings in the stairwell is 4.6m². The natural ventilation openings by day are controlled to let pass an air flow of 1 or 3 vol/h when the indoor temperature exceeds 22°C.

TABLE 1
Building data

wall	**composition**
External wall	Sandwich + 9 cm insulation
Roof	False ceiling + reinforced concrete + 12 cm insulation
Internal wall	Gypsum board + 5cm insulation
Intermediate floor	False ceiling + reinforced concrete

Internal convective heat transfer coefficient

$$\alpha_{ci} = C(\Delta\theta)^n$$

	vertical	**horizontal**	
		Buoyant	**Stably stratified**
C	[1.31; 2.30]	[1.52; 2.27]	[0.29; 0.6]
n	[0.33; 0.24]	[0.33; 0.24]	[0.13; 0.25]

Material properties		**λ (W/mK)**	**ρ (kg/m³)**	**a (-)**	**c (J/kgK)**
Aluminium	μ	203	2700	0.53	880
	σ	0	27	0.06	0
Reinforced concrete	μ	1.70	2400	0.72	1000
	σ	0.11	24	0.04	38
Light concrete	μ	0.24	850	0.72	1000
	σ	0.02	9	0.04	84
bitumen	μ	0.23	1100	0.88	1700
	σ	0	0	0.01	0
insulation	μ	0.040	50	-	840
	σ	0.001	0	-	10
Gypsum board	μ	0.25	900	0.40	1050
	σ	0.02	9	0.05	86
Air cavity: R (mK/W)	μ	0.16	-	-	-
	σ	0.01	-	-	-

Operation natural night ventilation
Previous day
$\theta_{i,max}$ > [22.5; 23.5]°C
At that moment
22h < time < 6h
θ_i > [18.5; 19.5]°C
$\theta_i - \theta_e$ > [1.5; 2.5]°C
θ_e > [9.5; 10.5]°C

Characteristics of night ventilation openings in 1 office module		
floor	**ELA supply (m²)**	**ELA circulation (m²)**
first	0.08	0.16
second	0.10	0.17
third	0.24	0.18
location	**Terrain description**	**z_0 (-)**
Meteo station	Cultivated open fields	[0.03;0.05]
On site	Mean city centre	[1;4]

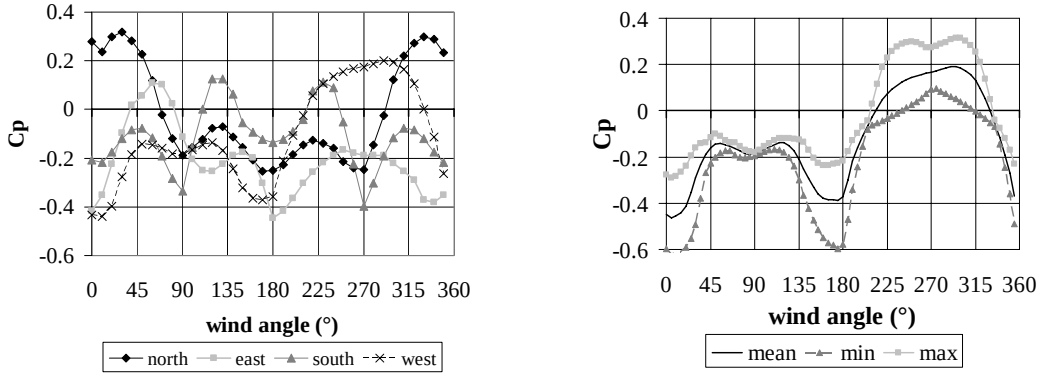

Figure 2: mean wind pressure coefficients Cp (left) and variation on Cp on the west side (right)

DISCUSSION

The thermal summer comfort in the new office building of the Ghent University (Belgium) is studied by uncertainty and sensitivity analysis. 100 independent Latin Hypercube samples (> minimum = 92 = 1.5 x 61 factors) are developed using Simlab software (POLIS, JRC-ISIS, 2003). Figure 3 (left) shows the results of the uncertainty analysis. On none of the floors a good comfort level is noticed. The probability of a reasonable comfort is higher in an office on the west than on the east side on the same floor because west winds are more frequent in Belgium and the east side of the building is more shielded against the wind. As a consequence, cross ventilation happens by night and day, causing more cooling in the offices on the west side. Furthermore, poor thermal comfort has a higher probability as the floor level rises due to smaller thermal stack height. On the 3rd level, the air is even most of the time flowing out instead of into the supply openings because the neutral pressure plane is underneath these supply openings because the height difference between the supply on the 3rd level and the exhaust in the stairwell is too small. This is shown in figure 3 (right) which compares the internal temperatures and air flows between the 2nd and 3rd level on the east side. The air flow rates flowing into the 3rd level from outside are much smaller than into the 2nd level.

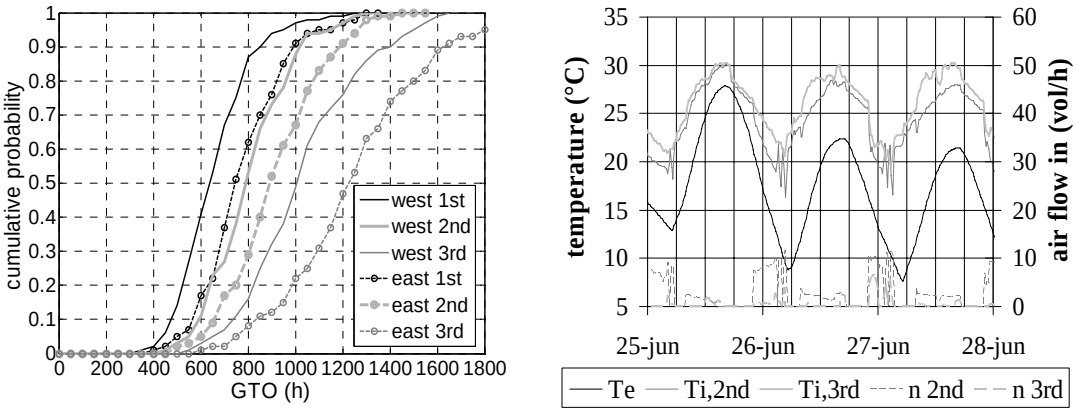

Figure 3: distribution of thermal comfort GTO (left) and comparison of temperatures and flows on the 2nd and 3rd floor on the east side in the building with mean properties (right)

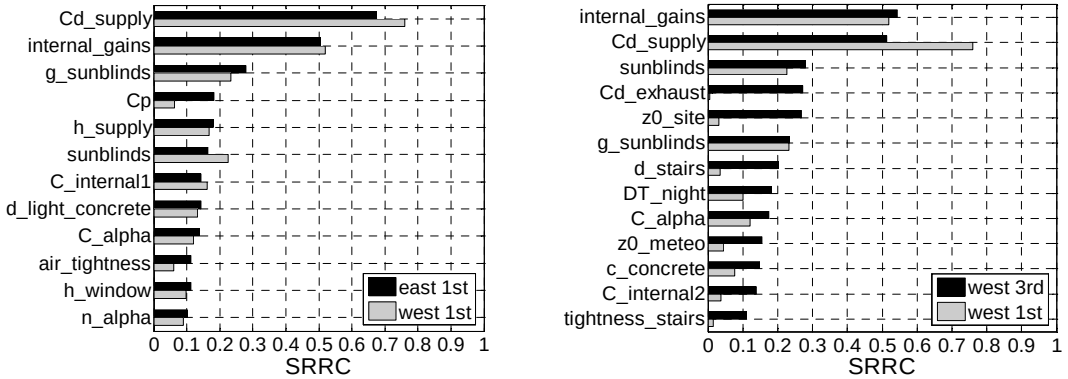

Figure 4: Most influential input parameters on thermal comfort in an office on the west and east side (left) and on the 1st and the 3rd floor on the west side compared (right)

Sensitivity analysis, characterized by SRRC, defines the impact of all input parameters on the thermal comfort, defined by GTO (figure 4). In all offices, the discharge coefficient Cd of the supply openings, the internal heat gains and the characteristics of the sunblinds have the greatest impact on the thermal comfort. At a later stage, input parameters defining the heat

transfer and storage (C_alpha, n_alpha, d_light_concrete, c_concrete), the flow resistance of the circulation (C_internal) and controlling natural night ventilation (DT_night, Ti,min-night) are important. Most influential input factors are the same on the first 2 floors. Although, differences exist between the offices on the west and the east side as shown in figure 4 (left). The wind pressure coefficient Cp and the air tightness of the façade have much more impact on the thermal comfort in the east office. This means the effect of the wind on the ventilation is higher on the east side (see above). Differences are also noticed between an office on the 1st and the 3rd level (see figure 4 (right) for 2 west offices). Generally, the absolute impact of the input parameters on the thermal comfort is higher on the 3rd than on the 1st level. In addition, the impact of the characteristics of the stairs (Cd_exhaust, d_stairs, tightness_stairs) and other offices (C_internal2, air_tightness_west) on the comfort on the 3rd level is striking as well as the impact of parameters influencing the wind velocity (z0_site, z0_meteo). The air flowing out the supply openings on the 3rd floor due to thermal stack explains these conclusions.

CONCLUSION

Uncertainty and sensitivity analysis are used to evaluate one of the possible design schemes of natural night ventilation in a new office building of the Ghent University (Belgium). On none of the floors, a good comfort level is noticed. The probability of poor comfort is larger on the east side and on a higher floor. The discharge coefficient of the supply openings, the internal heat gains and the characteristics of the sunblinds have the greatest impact on the thermal comfort. In the offices on the east side, the wind has also a high influence on the thermal comfort. On the 3rd level, the impact of the design of the stairwell and other offices and of input parameters influencing the wind velocity, is striking.

ACKNOWLEDGEMENT

The authors would like to acknowledge the temporary partnership Beel-De Geyter-SWK and the company Cenergie for the availability of the plans and design data.

REFERENCES

ASHRAE (2001). *Fundamentals Handbook (SI)*, American Society of Heating, Refrigerating and Air Conditioning Engineers, Atlanta, USA.

BIN (2001). *NBN B 62-002/A1, Calculation of thermal transmittance coefficients of walls and buildings*, Brussels, Belgium.

Breesch, H., Janssens, A. (2002). Simulating natural ventilation: coupling thermal and ventilation model. *Proceedings 3th EPIC and 23th AIVC conference: Energy Efficient & Healthy Buildings in Sustainable Cities*, Lyon, France, 741-746.

CEN (2000). *Building materials and products – Energy related properties – Tabulated design values*, EN 12524.

Clarke, J.A., Yaneske, P.P., Pinney, A.A. (1990). *The Harmonisation of Thermal Properties of Building Materials*, BRE, United Kingdom.

Dorer, V. (1999). Air, contaminant and heat transport models: integration and application. *Energy and Buildings*, **30**, 97-104.

Fanger, P.O. (1972). *Thermal comfort: Analysis and applications in environmental engineering*, McGraw-Hill, London, New York.

Flourentzou, F., Van der Maas, J., Roulet, C.-A. (1998). Natural ventilation for passive cooling: measurement of discharge coefficients. *Energy and Buildings*, **27**, 283-292.

ISO (1999). *Building materials and products – Procedures for determining declared and design thermal values*, ISO 10456, final draft.

Knoll, B., Phaff, J.C., de Gids, W.F. (1995). Pressure simulation program. *Proceedings 16th AIVC conference: Implementing the results of ventilation research*, Palm Springs, USA, 233-241.

Meteotest (2003). *Meteonorm: global meteorological database for engineers, planners and education version 5.0*, Bern, Switzerland.

POLIS, JRC-ISIS (2003). *Simlab 2.2: Reference Manual*, http://www.jrc.cec.eu.int/uasa/prj-sa-soft.asp, Ispra, Italy.

Saltelli, A., Chan. K., Scott E.M. (ed.) (2000). *Sensitivity Analysis*, John Wiley and Sons, Chichester, UK.

SEL, TRANSSOLAR, CSTB, TESS (2004). *Trnsys 16: a Transient System Simulation Program*, University of Wisconsin, Madison, USA.

Tamura, G.T., Chia, Y.S. (1976). Studies on exterior wall air tightness and air infiltration of tall buildings. *ASHRAE Transactions*, **82:1**, 122-134.

Van der Linden, K., Boerstra, A.C., Raue A.K., Kurvers, S.R. (2002). Thermal indoor climate building performance characterized by human comfort response. *Energy and Buildings* **34**, 737-744.

INDOOR ENVIRONMENTAL QUALITY, ENERGY USAGE AND OCCUPANT PERCEPTION IN COMMERCIAL OFFICE BUILDINGS

D. Novosel[1], CIAQP and L. D. Stetzenbach[2], Ph.D.

[1]National Center for Energy Management and Building Technologies, Alexandria, Virginia 22314 USA
[2]Harry Reid Center for Environmental Studies, University of Nevada, Las Vegas, Las Vegas, Nevada 89154 USA

ABSTRACT

A multi-disciplinary study to comprehensively measure and analyze operational performance and indoor environmental conditions in a sample of typical, commercial office buildings in the United States is described. The study will provide data that are currently not available. The indoor building factors that will be investigated during this study have never been formally studied in a comprehensive and systematic manner. No normative database currently exists for typical buildings making it impossible to correlate occupant indoor environmental response data to corresponding building design information and related measured microbiological and engineering data. These data are necessary to properly assess building performance.

KEYWORDS

Building performance, indoor environmental quality, normative database, perception questionnaire

BACKGROUND

There are significant gaps in knowledge relating to synergies between building energy performance, indoor environmental quality (IEQ) and building security. The National Center for Energy Management and Building Technologies ("National Center") was established in 2003 to fill these gaps (NEMI 2002). The first major task of the National Center was to develop methods and protocols to quickly and cost-effectively capture physical and operational data of existing buildings as they relate to energy performance and indoor environmental quality.

Past studies have generally focused on either issues related to energy consumption of buildings, building envelope measures and building systems improvements or on indoor air quality (IAQ) and the occupants' perception of their indoor environment. Most IAQ studies have dealt with IAQ deficiencies and their detrimental impact on the occupants. Thus, there exists a large knowledge gap with regard to what defines a typical building with acceptable indoor air quality and with acceptable energy performance.

This paper reports on a project to develop a database of typical commercial and institutional buildings. The database will contain measured environmental data that underwent rigorous statistical analyses based on numerous hypotheses, which are designed to confirm or dispute

standard industry assumptions with regard to comfort and occupant perceptions of IEQ. Building characteristics and operational and energy usage data will be incorporated as well.

INTERGRATED BUILDING PERFORMANCE DATABASE

Table 1 summarizes the four major datasets that will be incorporated in the integrated building performance (IBP) database. Questionnaires will capture the occupants' perceptions of IEQ, building characteristics and asset valuation parameters commonly used by the investment community. The building characteristics questionnaire is derived from previous ASHRAE work (2004a). Utility bills will generally serve to extract energy consumption data. Aggregation of energy usage by major equipment components or major users of energy, such as office equipment, will not be performed unless that data are made available by the facilities operator. The IBP database will contain the measured IEQ parameters, the questionnaire data and the results of the analyses of biological measurements. Multiple statistical analyses will be conducted to determine relationships that exist between selected elements of the database.

TABLE 1
Data sources and collection methods

DATA SET	DATA CAPTURED	DATA SOURCE	COLLECTION METHOD
OCCUPANTS	• IEQ perception	▸ Occupants	▸ IEQ Perception Questionnaire
BUILDING	• Characteristics • Asset Valuation • Energy Usage	▸ Facilities Manager ▸ Building Owners ▸ Utility Bills, Metered Data	▸ Questionnaire ▸ Questionnaire ▸ Downloaded in the Data Base
HVAC SYSTEM	• Operational Data	▸ Building Automation System	▸ Downloaded in the Data Base
IEQ	• Temperature, humidity, draft • Mold • VOCs • Sound • Light • CO_2	▸ (6) Typical locations within the building	*All data recorded* ▸ (6) Vivo Sampling Carts ▸ Airborne and Surface Sampling ▸ Sensor ▸ (6) Sound Level Meters ▸ (4) Meters; Luminance, Illuminance, Chromaticity and Spectral Power ▸ Sensor

The IEQ perception questionnaire was derived from previous work done by ASHRAE (1988), CBE (2004), Nakano (2003) and Spagnolo (2003) and significantly expanded in each area, particularly as it concerns acoustics and light. The questions were designed to obtain sufficient data to verify or refute their underlying hypotheses. The hypotheses were derived from current standards (ASHRAE 2004b, ASHRAE 2004c) or recent work by other researchers (ASHRAE 1998, Beranek 1993, Bies 1997, Cena 2003, Fanger 1989, Leventhall 2003, Martin 2002, Pellerin 2004, Rea 2000, Schiller 1988, Schiller 1990, Westman 1981, Witterseh 2002, Yamazaki 1998, Yizai 2000). Each hypothesis is probed by one or more of the questions. The questionnaire is computer-based and is completed by occupants during the days of monitoring in the building where measurements are collected.

The questionnaire was reviewed and approved by the University of Nevada, Las Vegas Institutional Review Board, a United States federal government requirement.

MEASUREMENT PROTOCOLS

IEQ, light and sound measurements are conducted using standard industry procedures (ASHRAE 2004b, ISO 1989; ISO 1994) or established research protocols (Cena 2003, Chun 2004, Kaynakli 2005; Kosonen 2004, Ye 2003, Zhao 2004).

The IEQ comfort parameters (air temperature, operative temperature, air velocity, relative humidity) are recorded at six typical locations within the building. Each building is monitored for three days. The measurement locations remain unchanged from day to day. Vivo instrumentation carts (Dantec Dynamics, Skovlunde, Denmark) capture the IEQ comfort parameters as specified by ANSI/ASHRAE Standard 55-2004. All data are digitized at a periodic interval of three minutes for an eight-hour span. Depending on the type of sensor either two-level averaging or three-level averaging is performed.

The concentration of carbon dioxide (CO_2) is recorded using Hobo (Telaire, Goleta, California, USA) and Bacharach (New Kensington, Pennsylvania, USA) sensors at each of the six locations as well as outdoors. Volatile organic compounds (VOCs) are measured at the six indoor locations using the RAE Systems' IAQ monitor model IAQRAE 042-1211-012 with calibration kit (RAE Systems World Headquarters, Sunnyvale, California, USA).

Sound measurements are made with portable precision sound level meters (models 912, 947 and 948 manufactured by Svantek Ltd., Warszawa, Poland) at two locations in each monitoring area where the IEQ comfort parameters are being recorded. The measurement for each position spans enough time to capture continuous sound levels of the general background sound with no building occupants present and continuous sound levels over a typical workday.

Four different lighting parameters are captured at the same locations as the IEQ parameters. Illuminance is measured at the work surface and the computer monitors using the Illuminance Meter T10 (Konica Minolta, Tokyo, Japan). Luminance of wall, partitions and the floor is recorded by the Luminance Meter LS-100 (all by Konica Minolta, Tokyo, Japan). The color temperature is measured with the Chroma Meter CS-100A (Konica Minolta, Tokyo, Japan), and spectral power distributions are measured using the Lightspex from GretagMacbeth.

Microbiology samples are collected for culturable airborne fungi and total fungal spores, and surface-associated culturable fungi at the same locations where IEQ measurements are made. Each sampling procedure has specific protocols for collection and analysis (Buttner 2002, Macher 1999) summarized in Table 2.

TABLE 2
Microbiology samples and collection and analysis methods

SAMPLE	COLLECTION METHOD	SAMPLE SIZE	ANALYSIS METHOD
Culturable fungi	Andersen single-stage impactor sampler (Graseby Andersen, Atlanta, Georgia, USA) on malt extract agar (Difco Laboratories, Sparks, MD) amended with chloramphenicol (MEAC); decontaminated with an ethanol wipe between each sample location	28.3 liter/min. for 2 minutes (0.057 m^3 of air per sample)	macroscopic and microscopic morphology
Airborne fungal spores	Burkard personal impactor sampler (Burkard Manufacturing Co., Ltd., Rickmansworth Hertfordshire, England)	10 liters/min for 2 to 5 minutes (0.02-0.05 m^3 of air)	stained and viewed with light microscopy for the presence of recognizable fungal spores
Surface sampling for culturable fungi	vacuum sampling with an individual field filter cassette attached to a vacuum pump	dust amounts collected vary by surface loading/soiling	macroscopic and microscopic morphology

INITIAL RESULTS

Initial data obtained from three large commercial buildings located in Chicago, USA are validating the utility of the protocols selected.

Table 3 summarizes the preliminary results of the comfort data. The measured comfort data are within the acceptable range of operative temperature and relative humidity according to ANSI/ASHRAE Standard 55-2004. There also seems to be good agreement between the measured data and the occupants' perceptions of the indoor air quality. The comfort indices of Predicted Percentage Dissatisfied (PPD) and Predicted Mean Vote (PMV) also indicate acceptable comfort conditions.

All three buildings were well ventilated with indoor carbon dioxide concentrations ranging from 490 to 575 ppm. The differential to outdoor concentration was between 119 and 215 ppm, well below the requirement of ANSI/ASHRAE Standard 62.1-2004 of 700 ppm or less.

TABLE 3
Summary of preliminary analyses of comfort data for three large office buildings in Chicago

Building No.	Parameters	Temperature	Relative Humidity	Velocity	Mean Radiant Temperature	PPD	PMV	Vertical Temperature Difference	Indoor to Outdoor CO_2 Concentration Differential
	Unit	°C	%	m/s	°C			°C	ppm
	Comfort Range	20-24	<60	<0.25	20-24	<10	-0.5 -0.5	<3	<700
1	Mean	22.5	17.0	0.09	22.6	7.0	-0.29	0.30	119
	95% Confidence Interval for Mean	22.4-22.6	16.7-17.4	0.08-0.1	22.5-22.6	6.7-7.2	-0.31/-0.27	0.35-0.36	106-132
	Median	22.5	17.0	0.08	22.6	6.9	-0.30	0.20	104
	Standard Deviation	0.46	1.8	0.04	0.36	1.2	0.10	0.25	61.5
	Set Point	22.2±0.5	None	N/A	N/A	N/A	N/A	N/A	None
	Perception Survey Results	Slightly Cool	Slightly Dry	Slightly Drafty	Slightly Cool	14.4	-0.65	No draft felt	Fresh some of the time
2	Mean	22.3	37.2	0.08	22.6	5.7	-0.14	0.19	215
	95% Confidence Interval for Mean	22.3-22.4	35.1-39.2	0.08-0.09	22.5-22.7	5.5-5.8	-0.16/-0.11	0.17-0.21	197-233
	Median	22.4	39.0	0.08	22.8	5.1	-0.10	0.20	208
	Standard Deviation	0.32	9.7	0.03	0.47	0.8	0.12	0.10	85.7
	Set Point	22.2±0.5	None	N/A	N/A	N/A	N/A	N/A	None
	Perception Survey Results	Comfort	Slightly Dry	Comfort	Comfort	6.0	0.21	No draft felt	Fresh most of the time
3	Mean	23.3	37.2	0.06	23.3	5.5	0.06	0.23	212
	95% Confidence Interval for Mean	23.1-23.3	35.6-38.7	0.05-0.07	23.2-23.5	5.3-5.6	0.03-0.09	0.19-0.26	201-224
	Median	23.4	33.3	0.06	23.6	5.3	0.10	0.20	211
	Standard Deviation	0.53	7.4	0.03	0.59	0.6	0.14	0.19	53.5
	Set Point	23.0±0.5	None	N/A	N/A	N/A	N/A	N/A	None
	Perception Survey Results	Comfort	Comfort	Slightly Stagnant	Comfort	9.9	0.48	No draft felt	Fresh most of the time

The sound data demonstrate that the interior noise levels were very similar in all three buildings with ambient levels below 45 dBA, which would characterize these three buildings as being quiet.

The measured illuminance of work surfaces ranged from 675 to 710 Lux, thus being higher than the recommended design range of 300 to 500 Lux. These measurements correlate well to

the occupants' perception of the brightness of their work surface with the vast majority of occupants indicating it as being bright. Similar results were obtained for the vertical illuminance of computer monitors, which ranged from 261 to 330 Lux, whereas the recommended value is 50 Lux for offices. All other lighting data (illuminance uniformity on the work surface; luminance of walls, partitions and the floor; correlated color temperature; and color rendering index) were within the recommended ranges for office environments.

Results of analyses of indoor airborne mold data indicate presence of fungal species in genus and concentrations reflective of the outdoors. Surface samples indicate similar composition.

Statistical evaluation of the data will be conducted when a larger data set is obtained. This evaluation will include comparison of data obtained during the three days of collection to determine if multiple sampling days are required or if a single collection day captures "average" values.

Comprehensive analyses of all data as well as associations between data and the hypotheses will be published at the end of this year in a report, which at that time may be downloaded from the National Center's website at www.ncembt.org.

FUTURE PLANS

The study described here is the first phase of a multi-year effort to obtain performance data from typical commercial and institutional buildings. The current phase will monitor ten office buildings in five locations in the United States. Plans are being made to study education buildings and healthcare facilities in the coming years. The IBP database has been designed to allow inclusion of data from other projects as well, and to be accessible online via web browsers. Once the current phase of this project is complete, the National Center will make the database available to other researchers to perform their own analyses.

ACKNOWLEDGEMENT

The authors gratefully acknowledge the support from the United States Department of Energy under Cooperative Agreement DE-FC26-03GO13072.

REFERENCES

ASHRAE (1998). *ASHRAE RP 921 - Field study of occupant comfort and office thermal environments in a hot arid climate*, Kris Cena (ed). American Society of Air-Conditioning, Heating and Refrigerating Engineers Inc., Atlanta, Georgia, USA.

ASHRAE (2004a). *Procedures for Commercial Building Energy Audits*, American Society of Air-Conditioning, Heating and Refrigerating Engineers Inc., Atlanta, Georgia, USA.

ASHRAE (2004b). *ANSI/ASHRAE Standard 55-2004, Thermal Environmental Conditions for Human Occupancy*, American Society of Air-Conditioning, Heating and Refrigerating Engineers, Inc., Atlanta, Georgia, USA.

ASHRAE (2004c) *ANSI/ASHRAE Standard 62.1-2004, Ventilation for Acceptable Indoor Air Quality*, American Society of Air-Conditioning, Heating and Refrigerating Engineers Inc. , Atlanta, Georgia, USA.

Beranek, L.L. (1993). *Acoustics*. Acoustical Society of America, New York, USA.

Bies, D.A. and C.H. Hansen (1997). *Engineering Noise Control: Theory and Practice*, E & FN Spon, London, U.K.

Buttner, M.P., K. Willeke, and S. Grinshpun (2002). Sampling and analysis of airborne microorganisms, pp. 814-826. In C.J. Hurst, G. Knudsen, M. McInerney, M.V. Walter, and L.D. Stetzenbach, (eds.), *Manual of Environmental Microbiology, 2nd edition*, ASM Press, Washington, D.C., USA.

Cena, K., N. Davey and T. Erlandson. 2003. Thermal comfort and clothing insulation of resting tent occupants at high altitude. *Applied Ergonomics* **34 (6)**, 543-550.

Chun, C., A. Kwok and A. Tamura (2004). Thermal comfort in transitional spaces—basic concepts: literature review and trial measurement. *Building and Environment* **39 (10)**, 1187-1192.

Fanger P.O. and A.K. Melikov (1989). Turbulence and draft. *ASHRAE Journal* **31(4),** 18-25.

ISO (1994). *ISO 7730:1994 Moderate Thermal Environments—Determination of the PMV and PPD Indices and Specification of the Conditions for Thermal Comfort.* International Organization for Standardization, Geneva, Switzerland

ISO (1998). *ISO 7726:1998 Ergonomics of the Thermal Environment—Instruments for Measuring Physical Quantities*. International Organization for Standardization, Geneva, Switzerland.

Kaynakli, O. and M. Kilic (2005). Investigation of indoor thermal comfort under transient conditions. *Building and Environment* **40 (2)**, 165-174.

Kosonen, R. and F. Tan (2004).. Assessment of productivity loss in air-conditioned buildings using PMV index. *Energy and Buildings* **36 (10)**, 987-993.

Leventhall, G., P. Pelmear and S. Benton (2003). *A Review of Published Research on Low Frequency Noise and its Effects*, Department for Environment, Food and Rural Affairs, London, U.K.

Martin, R.A., C. Federspiel, and D. Auslander (2002). Responding to thermal sensation complaints in buildings. *ASHRAE Transactions* **108**, 407-412.

Macher, J. (1999). *Bioaerosols: Assessment and Control.* American Conference of Governmental Industrial Hygienists, Cincinnati, USA, 12-1 – 12-8.

NEMI (2002). *National Center for Energy Management and Building Technologies – Final Strategic Planning Report*, National Energy Management Institute, Alexandria, Virginia, USA.

Pellerin, N. and V. Candas (2004). Effects of steady state- noise and temperature conditions on environmental perception and acceptability. *Indoor Air* **14**, 129-136.

Rea, M.S. (2000). *IESNA Lighting Handbook: Reference and Application, 9th Edition*, Illuminating Engineering Society of North America, New York, USA.

Schiller, G. (1990). A comparison of measured and predicted comfort in office buildings. *ASHRAE Transactions* **96(1)**, 609-622.

Schiller, G.E., E.A. Arnes, F.S. Bauman, C. Benton, M. Fountain and T. Doherty (1988). A field study of thermal environment and comfort in office buildings. *ASHRAE Transactions* **94 (2)**, 280-308.

Westman, J.C., and J.R. Walters (1981). Noise and stress: a comprehensive approach. *Environmental Health Perspectives* **41**, 291-309.

Witterseh, T., G. Clausen and D.P. Wyon (2002). Heat and noise distraction effects on performance in open offices. *Proceedings of Indoor Air 2002* **4**, 1084-1089.

Yamazaki, K., S. Nomoto, Y. Yokota and T. Murai (1998). The effects of temperature, light, and sound on perceived work environment. *ASHRAE Transactions* **104**, 711-720.

Ye, G., C. Yang, Y. Chen and Y. Li (2003). A new approach for measuring predicted mean vote (PMV) and standard effective temperature (SET*). *Building and Environment* **38 (1)**, 33-44.

Yizai, X. and Z. Rongyi. 2000. Effect of turbulent intensity on human thermal sensation in isothermal environment. *Qinghua Daxue Xuebao/Journal of Tsinghua University* **40 (10)**, 100-103.

Zhao, R., S. Sun and R. Ding. 2004. Conditioning strategies of indoor thermal environment in warm climates. *Energy and Buildings* **36 (12)**, 1281-1286.

ENERGY PERFORMANCE OF EARTH-AIR HEAT EXCHANGER IN A BELGIAN OFFICE BUILDING

A. Janssens[1], M. Steeman[1], J. Desmedt[2], H. Hoes[2], M. De Paepe[3]

[1]*Department of Architecture and Urban Planning, Ghent University (UGent), B-9000 Gent, Belgium*
[2]*Flemish Institute for Technological Research (VITO), Energy technology, B-2400 Mol, Belgium*
[3]*Department of Flow, Heat and Combustion Mechanics, Ghent University (UGent), B-9000 Gent, Belgium*

ABSTRACT
An earth-air heat exchanger (EAHX) has been implemented in a low-energy office building in Kortrijk, Belgium. An extensive monitoring campaign was conducted to define the energy consumption in the building and the contribution of the EAHX to energy savings. This paper presents the results of the measurements and compares the measured performance of the EAHX to the building energy use and to results of a simulation model for 3D transient heat transfer.

KEYWORDS

Earth-air heat exchanger, energy use, monitoring, simulation

INTRODUCTION

Earth-air heat exchangers (EAHX), also called ground tube heat exchangers, are a possible technique to reduce energy consumption for heating and cooling in buildings. Tubes are put into the ground, through which ventilation air is drawn. Thus EAHX can cool or heat the ventilation air, using the soil as a heat source or sink. Their performance depends on the air flow rate, convective heat transfer at the tube surface, depth, dimensions and number of pipes and soil properties (De Paepe and Janssens, 2003). Only a moderate climate having a large temperature difference between summer and winter is suited for EAHX. As the heat exchanger has a good peak performance but a limited seasonal capacity, it is an interesting technique in combination with other energy saving measures. For instance, the EAHX may prevent frosting of a conventional air-air heat exchanger during cold weather, thus increasing the number of operation hours of the heat exchanger combination. Furthermore, in combination with other low-energy cooling techniques (eg night cooling) and good thermal building design, the EAHX may eliminate the need for an air conditioning system (IEA-Annex 28, 1999).
In several European countries this technique is gradually introduced, both in housing as in office buildings (Pfafferot 2003). Also in some new office buildings in Belgium, EAHXs have been implemented (Breesch et al. 2005). The Belgian moderate climate is suitable for an adequate operation of earth to air heat exchangers, with a yearly mean temperature of 9.8 °C and normal extremes of –8.6°C and 29.9°C (RMI, 2004). Architects and building service designers are often interested in installing EAHX, but still lack confidence to apply these techniques in the absence of information on design methods and on the performance of existing applications in Belgium. Therefore, this paper discusses the energy performance of an EAHX applied in a low-energy office building in Kortrijk, Belgium. The EAHX was designed according to a design method published by De Paepe and Janssens (2003). In a first part of the paper this design method is briefly explained, and the expected design performance of the EAHX is presented. Further, the energy performance of the EAHX is evaluated based

on an extensive monitoring campaign conducted by VITO in 2003 (Desmedt et al. 2004). The performance is related to the building gas and electricity use. In a last part the EAHX is evaluated using a simulation model for 3D transient heat transfer. Differences between simulation and measuring results are discussed.

OFFICE BUILDING DESCRIPTION

The office building 'SD Worx' is located in Kortrijk, Belgium and consists of two office floors on top of a limited ground floor with building services (design: Stramien arch., study: Cenergie cvba). On the south side, the floors are connected with an open stairwell and circulation zone. The building is in operation since spring 2002. Figure 1 shows a vertical section. It was the ambition of the project to create an office building (total floor area: 1350 m²) with good thermal comfort and with half the energy consumption of a standard office building. This was achieved by several means: very good thermal insulation, energy efficient ventilation, solar shading, passive cooling techniques, enhanced control automation,… In winter, two condensing boilers of 46 kW each supply hot water to a hydronic radiator system. Fresh air is provided by means of a demand controlled, balanced ventilation system. The ventilation flow rate is controlled from a minimum of 2000 m^3/h up to 8000 m^3/h in response to measurements of IAQ and temperature in the offices. The supply air passes through an EAHX and is further pre-heated by a regenerative heat exchanger (RHX, nominal thermal effectiveness 90%). The EAHX includes two concrete pipes with an internal diameter of 80 cm and a length of 40 m each, buried in clay ground under groundwater level at depths of 3 and 5 m and connected to the ventilation system by PE-pipes with an internal diameter of 40 cm. In summer, the building is cooled by passive means. By night a natural night ventilation system is active: outside air enters the office floors through bottom hung windows, located near the ceiling in the offices on the north side. The air cools down the exposed ceiling and leaves the building in the circulation zone through outlet windows. By day, the ground tubes precool the supply air. The supply flow rate increases proportionally from 5400 m³/h at 23 °C indoor temperature to 8000 m³/h at 26 °C and above. In cooling mode, the exhaust air leaves the building through the outlet windows on top of the circulation zone. In addition to the passive cooling techniques a packaged water chiller (21 kW) is installed to remove excess heat from a server and computer room located on the ground floor.
Previously, Breesch et al. (2005) reported on the thermal comfort during summer in this office building and on the contribution of the EAHX to achieve good comfort, relative to the contribution of night cooling. Breesch et al. used a coupled thermal and building simulation model to demonstrate that the night cooling system was more efficient than EAHX to improve thermal comfort. However only the combination of both techniques appeared capable to achieve an acceptable comfort without additional active cooling in the offices.

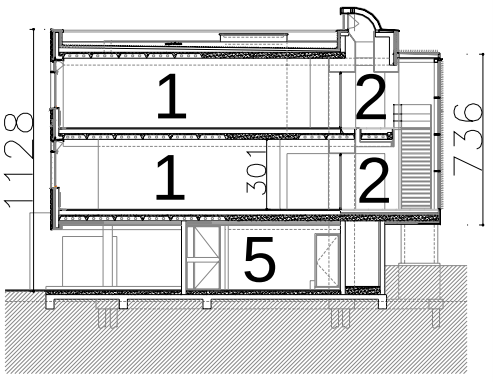

Figure 1: vertical section

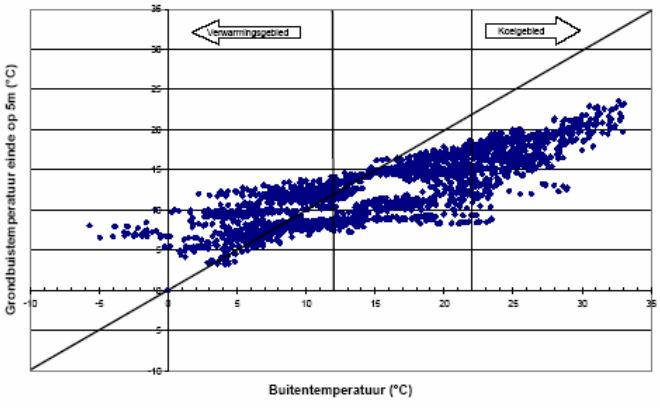

Figure 2: Measured outlet vs inlet EAHX temperature

DESIGN PERFORMANCE

The EAHX was designed according to a sizing method based on thermal and pressure drop optimization (De Paepe and Janssens 2003). In this method the thermal performance of the heat exchanger is characterized by means of the steady state effectiveness ε:

$$\varepsilon = \frac{T_a - T_e}{T_s - T_e} = 1 - \exp\left(-\frac{\pi h L D}{\dot{m}_a c}\right) \quad (1)$$

with T_a the air temperature after passing the EAHX, T_e the exterior air temperature at the inlet, T_s the constant tube wall temperature, h the convection coefficient inside the tube (W/m²K), L and D the tube length and diameter (m), m_a the air flow rate per tube (kg/s) and c the thermal capacity of air (J/kgK). The convection coefficient is also function of the air flow rate and the diameter of the ground tubes.
The desired effectiveness follows from the design requirements and climate conditions, but often an effectiveness of 80% is considered to be an optimum for an EAHX (IEA Annex 28 1999). In the original design of the EAHX for the building an effectiveness of 80% was proposed. However, due to difficulties during construction, the original design was abandoned and the configuration with two 80 cm diameter tubes was built. Since the ventilation rate in the office building is demand controlled, the effectiveness of the EAHX changes as a function of the actual ventilation rate. Table 1 lists the EAHX performance indicators for the minimum, mean and maximum ventilation rate. As the table shows the design effectiveness of the built configuration is rather low, in between 38 and 48%. On the other hand, the pressure drop across the tubes is very small, so the presence of the EAHX has a negligible effect on the electricity consumption of the fans. The table further shows that the ventilation rate may be varied over a wide range with minor change in effectiveness.

TABLE 1: Design performance as a function of ventilation rate

Ventilation rate (m^3/h)	2000	5400	8000
Effectiveness (%)	48	40	38
h (W/m²K)	2.2	4.7	6.3
Pressure across tube (Pa)	0.2	1.3	2.5

MEASURED PERFORMANCE IN RELATION TO BUILDING ENERGY USE

This section presents the measured energy consumption of the building in the year 2003 and discusses the energy performance of the earth-air heat exchanger (Desmedt et al. 2004). It is good to bear in mind that the year 2003 was exceptionally warm: the yearly mean temperature was 11.1°C where 9.8°C is a normal value in Belgium (RMI 2004). This high yearly mean was primarily caused by high temperatures in spring and summer (with a 13 day long heat wave in august). Therefore the heating degree days were only 7% lower than the normal value: $G_{eq}(16.5/16.5)$ = 2296°d in stead of 2458°d.
Table 2 lists the measured gas and electricity consumption in the building. The results show that the designers met the ambition to decrease the energy consumption by two compared to typical values for office buildings in Belgium.

Table 2: Measured gas and electricity consumption in 2003 (Desmedt et al. 2004)

	Energy consumption	Normalized consumption per heated floor area	Typical values for offices in Belgium (VITO 2002)
Gas (space heating)	7317 m^3	61 kWh/m²*	147-214 kWh/m²
Electricity		65 kWh/m²	75-133 kWh/m²
- Fans	10130 kWh		
- Chiller	5244 kWh		
- Other	72376 kWh		

* calorific value: 10.5 kWh/m^3 and corrected to normal heating degree days

The EAHX and the RHX that pre-heat the ventilation air reduce the space heating demand. The energy delivered by the heat exchangers was measured by monitoring the ventilation flow rates of the fans and the temperature differences across the heat exchangers. Figure 2 shows the measured air temperature at the exit of the deepest ground tube (5m) as a function of the external air temperature. The graph confirms that the EAHX has a good peak performance. A temperature difference of 9 to 14°C is achieved across the EAHX during weather extremes, resulting in a maximum heat gain of 10 kW and a maximum heat removal of 25 kW measured across the EAHX. However in milder weather the EAHX may have an adverse effect: it still cools the air during part of the time when the building has a space heating need (at outside temperatures below 12°C).
The energy supplied by the heat exchangers is shown in Figure 3 relative to the net total heat delivered by the hydronic system (assuming a system efficiency of 85%). The yearly sums are listed in Table 3. Here it is assumed that the energy delivered by the EAHX is always in line with the heating or cooling needs of the building. This way the energy performance of the EAHX is overestimated. Still the results show that the amount of energy saved by the EAHX is relatively small but not unimportant, considering its limited steady state effectiveness. Without the EAHX the gas and electricity consumption in 2003 would have increased by a maximum of 5 and 7%, respectively. The cooling performance of the EAHX outweighed its heating performance. This is related to the increased number of operation hours, to the increased airflow rate and to the extremely warm weather during summer 2003. The avoided equivalent electricity use for cooling is in the same order as the electricity consumed by the 21kW chiller.

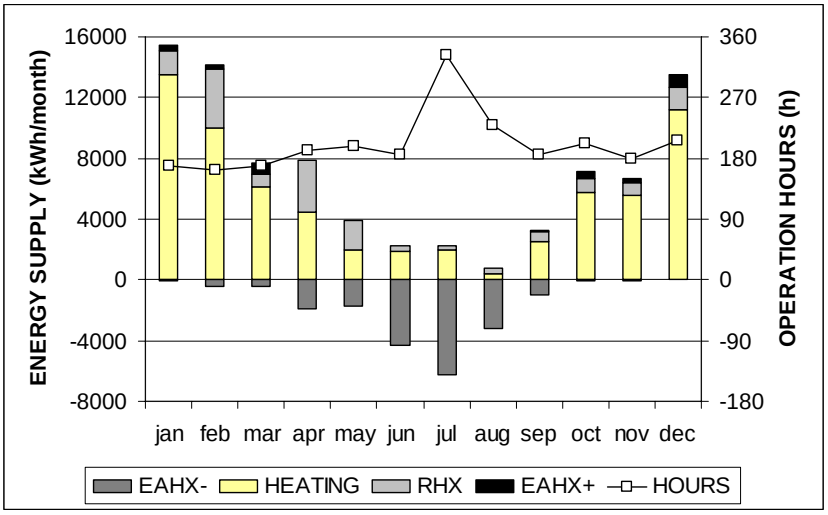

Figure 4: Measured energy supply (Desmedt et al. 2004)

Table 3: Yearly sums of sensible heat supplied by heat exchangers

	Heating			Cooling	
	EAHX	RHX	Heating system	EAHX	Eq. Electricity
Energy supply (kWh/a)	3044	16513	65300	19367	6455 (COP = 3)
Relative to measured needs	5%	25%			7%

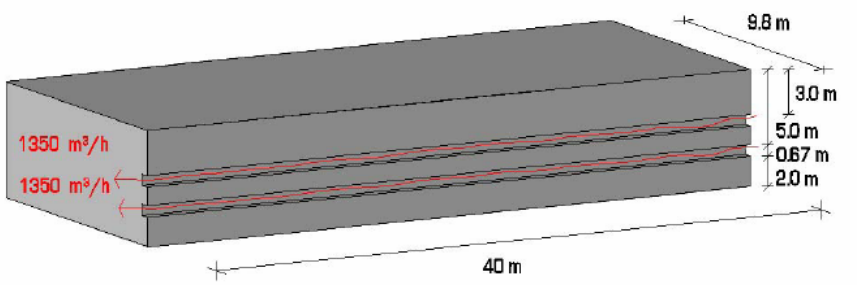

Figure 4: Model geometry and calculation domain (Steeman 2005)

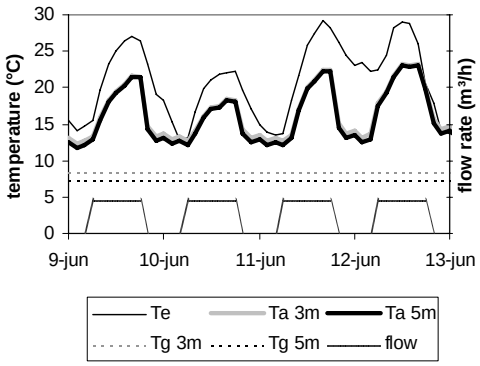

Figure 5: Simulation output

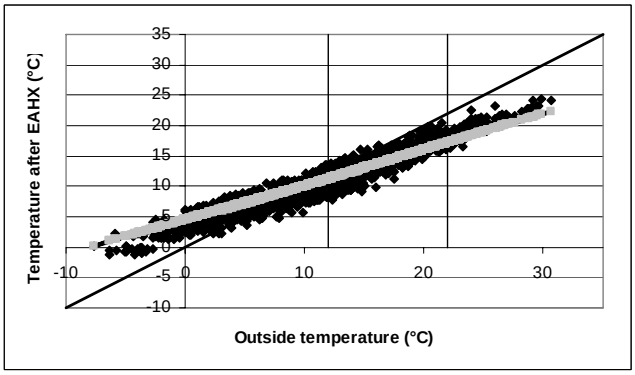

Figure 6: Predicted outlet vs inlet EAHX temperature

SIMULATED PERFORMANCE OF EAHX

This section presents results of dynamic thermal simulations of the case study EAHX (Steeman 2005). The predicted performances are compared to the measured performance and to performance indicators reported in literature. For this purpose the software VOLTRA was used (Physibel 2003). This is a numerical calculation tool for 3D transient heat transfer (control volume based). Apart from heat conduction and storage in solids, the model also takes convective heat transfer into account. The user may introduce mass flow rates and convective surface coefficients in a predefined flow path as a specific boundary condition. Figure 4 shows the calculation domain for the symmetric problem of the EAHX. Only the horizontal part of the EAHX is considered. The ground is assumed to be homogeneous clay: λ = 1.5 W/m²K, ρc = 3 MJ/m^{3}K. A climatic data file with hourly mean values for temperature and solar radiation defines the boundary conditions at the ground surface and at the inlets of the EAHX. In order to evaluate the performance under normal climatic conditions the Test Reference Year (TRY) for Ukkel, Belgium is used. It is assumed that ventilation is active during 12 hours a day (6-18h) at a rate of 3000 m^3/h from November to March and of 5400 m^3/h from April to October. The convection coefficient in the ground tubes is adjusted accordingly (Table 1).

Figure 5 shows a typical output of the calculations during a warm week in June: when ventilation ceases over night, the temperature in the EAHX falls back to a constant ground temperature. However, operation of the EAHX tends to heat the ground in summer: this is clear by comparison with the undisturbed ground temperatures in absence of EAHX, also indicated on the graph. Figure 6 shows the predicted air temperature at the exit of the deepest ground tube (5m) as a function of the external air temperature. The results of the dynamic simulations are compared to calculations with the steady state method (Equation 1), assuming a constant tube wall temperature equal to the outside yearly mean (10°C). As the graph shows there is a good correlation between both results, but the simple steady state method overestimates the peak performance relative to the transient simulations.

DISCUSSION

The results of measurements and simulations are compared by means of two performance indicators. The characteristic thermal response presented in Figures 2 and 6 is the first. The yearly sensible heat supply is the second. In order to derive representative values, the monthly heat supply following from the simulations is corrected in order to match the measured number of operation hours of the EAHX. Further it is common to express the heat supply as a specific value, relative to the wall surface area of the ground tubes. This number is often used in literature to compare energy performance of EAHX. Table 4 lists the resulting numbers. The measured and simulated energy gains are in the same order as the values reported in literature, except for the very large measured cooling energy supply. The comparison further shows that the simulations underestimate the performance of the EAHX compared to the measured performance. The differences in energy performance may partly be attributed to climatic differences: in 2003 the number of days with temperature extremes above 25°C was the double of a normal year (RMI 2004), resulting in a larger cooling supply. The warm summer may also have caused higher ground temperatures during autumn, resulting in a larger heating supply. During a normal year the heating and cooling energy gain from the EAHX would therefore have been smaller. Still, when comparing the predicted with the measured temperatures (Figures 2 and 6), it is clear that the differences between simulated and measured performance is not the result of climatic differences alone. The heat exchange in the EAHX is underestimated in the simulations, as appears from smaller temperature differences between inlet and outlet air compared to measurements. The reason for these deviations is unclear. Perhaps the thermal properties of the soil entered for the simulations are incorrect. The calculations may also be sensitive to the correct schedule and flow rate of the ventilation system. In this respect it is known that short operation hours result in better peak performance (IEA Annex 28 1999).
Still, considering that at ambient temperatures of 30°C the maximum measured air temperature at the outlet of the EAHX was 22°C, it is clear that the EAHX alone is not suited to effectively cool a building during warm weather. It merely eliminates ventilation heat gains and should be combined with other measures that reduce room cooling loads, in order to help avoid the need for active cooling.

Table 4: Energy gains for heating and cooling across the EAHX, relative to ground coupling area

	Measurement	Simulation	Literature (Pfafferot 2003)
Specific heating	15 kWh/(m²a)	11 kWh/(m²a)	16-51 kWh/(m²a)
Specific cooling	96 kWh/(m²a)	31 kWh/(m²a)	12-24 kWh/(m²a)
Operation hours	2412 h	2412 h	3701-4096
Specific surface area	0.05 m²/(m³/h)	0.05 m²/(m³/h)	0.08-0.18 m²/(m³/h)
Heating degree days	2296 °d	2458 °d	±2600

REFERENCES

Breesch H., A. Bossaer and A. Janssens. (2005) Passive cooling in a low-energy office building. Accepted for publication in Solar energy.
De Paepe, M. and A. Janssens (2003) Thermo-hydraulic design of earth-air heat exchangers. Energy and Buildings 35, 389-397.
Desmedt, J., N. Robeyn and P. Jannis. (2004) ANRE-Demonstratieproject: energiezuinig kantoorgebouw met horizontale grondbuizen ne regeneratieve warmtewisselaar bij kantoorgebouw SD Worx, Kortrijk (in Dutch: Low-energy office builiding with EAHX and RHX), VITO, 49 p.
IEA Annex 28 (1999) Low energy cooling: early design guidance. International Energy Agency, ECBCS Annex 28 Subtask 2 Report 2.
Pfafferot, J. (2003). Evaulation of earth-air heat exchangers with a standardized method to calculate energy efficiency. Energy and buildings 35, 1129-1143.
Physibel (2003) Voltra & Sectra: computer program to calculate 3D & 2D transient heat transfer in objects described in a rectangular grid using the energy balance technique, version 4.0w (manual).
RMI. (2004). Royal Meteorological Institute: yearly report 2003. Brussels.
Steeman, M. (2005) 3D-Dynamisch modelleren van passieve koeltechnieken: aarde-lucht warmtewisselaars (in Dutch: 3D-dynamic modelling of passive cooling techniques: EAHX), Master thesis, Ghent Universtity.
VITO (2002) Energiekengetallen in de tertiaire sector in Vlaanderen 2000 (Aernouts & Jespers) (in Dutch: energy indicators in the tertiary sector in Flanders), VITO, Mol, Belgium.

Energy and Comfort performance of natural ventilation system in office buildings in China

Runming Yao[a], Baizhan Li[b], and Koen Steemers[a]

[a]*The Martin Centre for Architectural and Urban Studies Department of Architecture University of Cambridge, UK*

[b] *Key laboratory of the Three Gorges Reservoir Region's Eco-Environment, Ministry of Education, The Faculty of Urban Construction and Environmental Engineering, Chongqing University, P R China*

ABSTRACT

This paper presents an analysis of energy and comfort performance of typical office buildings for summer cooling in five climate zones in China using the natural ventilation assessment tool, which is developed based on the integrated thermal and airflow model. Harbin, Beijing, Shanghai, Kunming and Guangzhou are selected as the five representative cities for Very Cold, Cold, Hot Summer and Cold Winter, Mild and Hot Summer and Warm Winter zones respectively. The cooling energy consumption with air conditioning system is compared to that with natural ventilation system. The simulation results show that for daytime air-conditioning system in conjunction with night ventilation can reduce cooling energy significantly for each zone. Part time air-conditioning operation can reduce cooling energy in Very Cold and Mild zones significantly but not in Hot summer zones such as Guangzhou and Shanghai. In natural ventilation cooling system design, climatic factor must be considered because it is a very important factor, which influences the effectiveness of natural ventilation and cooling energy consumption.

KEYWORDS

Natural ventilation, climate, energy saving, thermal comfort, China

INTRODUCTION

China's buildings sector currently accounts for 23% of China's total energy use and is projected to increase to one-third by 2010[4]. Energy consumption in buildings becomes the major source of greenhouse gas emission in China. Natural ventilation is being increasingly proposed as a mean of low energy design method in "green buildings" community; because it has the potential to significantly reduce energy cost required for mechanical ventilation of buildings. However potential cooling energy saving depends on the climate, internal heat gains and the building design. The climate of China is extremely diverse and variable with a tropical climate in the south and sub-arctic in the north. Therefore, it is very important to evaluate the potential effectiveness of natural ventilation and thermal comfort at the strategic design stage. A natural ventilation assessment tool [5] developed based on the coupled thermal and airflow model at the Martin Centre for Architectural and Urban Studies in University of Cambridge has been used to assess the thermal comfort of natural ventilation system of the typical office buildings in China's Five Climate Zones. The cooling energy consumptions of different cases have been analyzed.

CLIMATE

China is a large country with an area of about 9.6million km^2. About 98% of the land area stretched between a latitude of 20^{o}N to 50^{o}N, from subtropical zones in the south to the temperate zones (including warm-temperate and cold temperate) in the north. For building thermal design, five climate zones have been presented by "Thermal design code" [1]. There are different design codes for different zones. Table 1 lists the U-value of building envelopes.
In this paper the five cities, Harbin (HB), Beijing (BJ), Shanghai (SH), Kunming (KM) and Guangzhou (GZ), which represent the five climate zones in China, have been selected for office building energy and comfort studies. The latitudes of the cities are 44.46, 39.56, 31.0, 25.51, and 25.01 respectively from north to south.

Table 1 U-value of envelope in each zone (W/m^2.K)

	Very Cold Zone (Harbin)	Cold Zone (Beijing)	Hot summer and cold winter zone(Shanghai)	Mild zone (Kunming)	Hot summer and warm winter zone(Guangzhou)
External wall	0.52	1.16	1.5	1.5	1.5
Glazing	2.5	4	4.7	6.0	6.0

SIMULATION FOR TYPICAL OFFICE BUILDING

Method

The coupled thermal and airflow model is developed for natural ventilation and energy performance analysis. The detailed theoretical model will not be illustrated in this paper. This paper focuses on the analysis of the simulation results. Preliminary energy and discomfort rate are the two indices for energy and comfort performance analysis used in this paper. The discomfort rate is defined as the ratio of the number of hours in which internal air temperature exceeds the fixed comfort temperature over the occupied hours in hot summer days.

Basic Information

The office room can be grouped into two types: one is the high standard fully central air-conditioned cell office and another is the traditional office room equipped with split room air-conditioner. In tradition, the layout of the office building is designed as south-north orientation with a corridor in the middle. A typical office room is selected for this case study, of which the required information for thermal simulation is listed in the table 2 and as following:

- Room dimension is 3.6m in length, 5.4m in depth and 3.0m in height;
- Orientation is south-north orientation;
- Glazing ratio in the south wall is 0.35 and 0.25 in north wall;
- Occupied period is from 8:00 to 18:00;
- Thermal mass is assumed as medium mass;
- Internal shading devices is applied in southern window in summer;
- The office room is located in city.

Table2 Basic information of traditional office building

Fresh air requirement (m^3/h.person)	Gain of occupant			Gain of lighting (W/m^2)	Gain of equipment (W/m^2)
	Density (person/m^2)	Heat emit of people (W/person)	Moisture content emit from people(Kg/h)		
30	0.1	64	0.084	10	10

Natural Ventilation

The dynamic simulations for the typical office rooms in the five cities have been performed for summer season. The "all day and night" ventilation strategy has been applied. According to the Chinese Thermal Design code, the internal design air temperature is selected as 26^{o}C and not exceeding 28 ^{o}C. The simulation results are shown in Fig.1. From the figure we can see that generally, in June and September, natural ventilation can improve office internal thermal comfort condition in the most cities, but the internal air temperature in Guangzhou exceeds 28^{o}C. In the hottest months July and August, natural ventilation can improve office internal thermal comfort in Harbin and Kunming, where the monthly average internal air temperature is below 26 ^{o}C; but it cannot fully improve that in Beijing, Shanghai, and Guangzhou. In particular, the thermal conditions in the afternoon in these cities cannot achieve comfort level. Table 3 lists the discomfort rate of the offices with all day and night ventilation systems in the five cities. Tc is the comfort temperature. In order to reduce discomfort risk, obviously mechanical cooling system is desired.

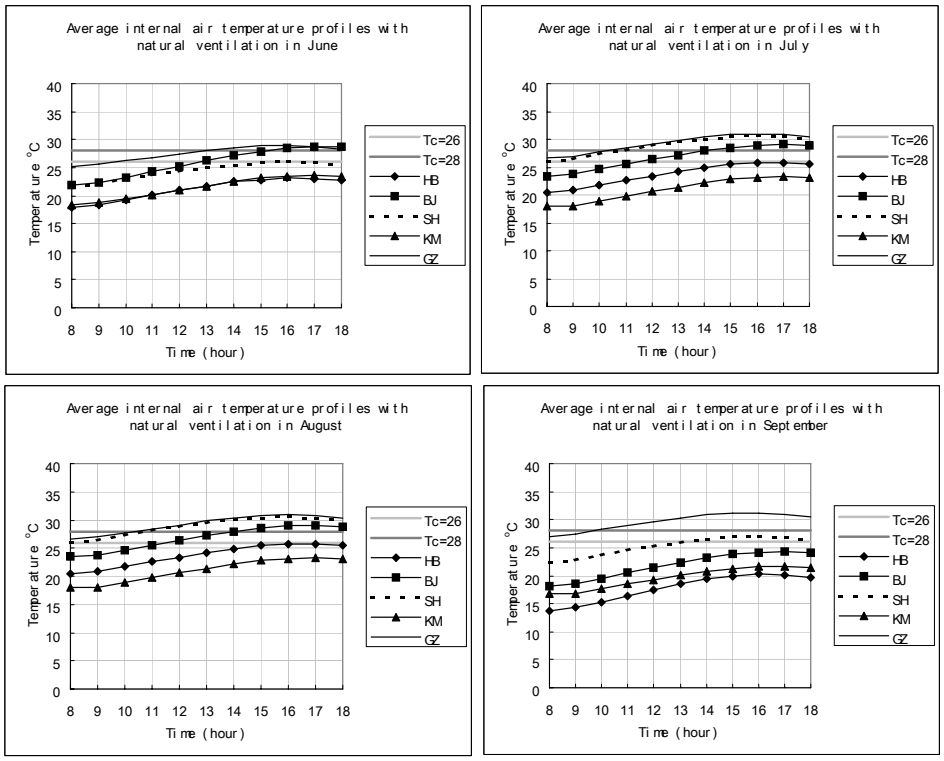

Fig.1 Monthly average temperature profiles in the five cities.

Table 3 Discomfort rate of the office with night natural ventilation in summer season

Discomfort rate %	Harbin	Beijing	Shanghai	Kunming	Guangzhou
Tc=28	5	21	34	2	48
Tc=26	11	35	49	6	58

Cooling strategies

The mechanical measures are necessary in order to improve office thermal comfort in summer in most zones in China because natural ventilation cannot work properly by its own. The hourly auxiliary cooling load has been simulated for different cases in order to calculate the cooling

energy consumption. The setting up of the internal comfort temperature is a key factor, which influences the cooling energy consumption and thermal comfort. The effects of indoor air movement on human thermal comfort in hot climate have been extensively studied. Air movement may provide desirable cooling in warm and humid conditions. Air velocities increase the body's convective and direct evaporative heat loss rate. Li states that people, who feel warm, find air movement pleasant in China [3]. Ceiling or table fans for cooling are the most common measures used by Chinese people in summer. People choose higher operating speeds when the indoor air temperature is higher. Usually, in the occupied parts of rooms, the air velocity is below 0.1 m/s, and then the air temperature is a sufficient index of the warmth of the environment. However, when a ceiling or table fan is used as a cooling measure for body comfort, the comfort temperature should be corrected to take account of the effect of air movement. The correction for air movement indicates that the effect of increasing the air movement to 1 m/s is equivalent to lowering the globe temperature (if the air temperature and the mean radiant temperature are equal) by 3^{o}C. Air velocities higher than this are unlikely to be acceptable in offices, because of the risk of disturbing papers. When ceiling fans are provided for summer 'cooling', it may not be necessary to measure the air movement; it would usually be sufficient to assume that their provision gave a benefit potentially equivalent to a 3 degree drop in temperature [2].

In order to assess the energy performance of natural ventilation and mechanical cooling systems, three cases for traditional office room equipped with split air-conditioner have been selected for energy consumption analysis. We suppose the discomfort rate of each case is under 2%.

(1) Air-conditioner operates during the working period (0800 to 1800)
This is proposed as a base case for comparisons. In this case the occupants can freely select the desired internal air temperature. According to the Chinese design standard, the desired internal air temperature can be set as 26^{o}C. Considering the adaptive comfort and the survey in China, 28^{o}C is the acceptable temperature. The energy consumptions of these two setting temperatures have been simulated for each city in summer season.
(2) Daytime air-conditioning in conjunction with night time natural ventilation
In order to assess the impact of night ventilation on energy performance, the simulation for this case has been performed.
(3) Part time air-conditioning in the afternoon and fan operation in the morning
The table fan and the ceiling fan are the most common cooling measures in offices in China. The equivalent comfort temperature is 3^{o}C lower than internal air temperature due to the air movement with fan.

Computer simulations for the above cases for each city have been performed.

RESULTS ANALYSIS

(1) Night ventilation can save cooling energy

Fig.2 shows the percentage of cooling energy saving of the case "daytime air-conditioning with night ventilation" comparing to the case "daytime air-conditioning without night ventilation. Tc=28 means the comfort temperature is set as 28^{o}C and Tc=26 is set as 26^{o}C. From the figure we can see that the saving percentage is slightly higher when comfort temperature is set higher. In the Very Cold and Mild zones, there is a significant energy saving due to the implementation of night ventilation. For example, in Harbin, the average energy saving can achieve about 80% and in Kuming about 90%. This is because in these two zones,

the differences of day and night air temperature are high. There is about 60% of energy saving in Beijing and 50% in Shanghai. Even in the Hot Summer and Warm Winter zone –Guangzhou, there is about 40% of energy saving by implying nigh ventilation. To explain this situation, the temperature and load profiles of July 21st in Beijing of the cases "Daytime air-conditioning without night ventilation" and "Daytime air-conditioning with night ventilation" are illustrated in Fig.3, in which Ta is outdoor air temperature; T1 is the internal air temperature without night ventilation; T2 is the internal surface temperature without night ventilation; T1nv is the internal air temperature with night ventilation; T2nv is the internal surface temperature with night ventilation; Load cooling is the cooling load without night ventilation and Loadnv is the cooling load with night ventilation. From the figure we can see that the internal surface and air temperature of this case with night ventilation is lower than those without night ventilation. The cooler outdoor air offset the heat stored in the building structure and this reduces cooling load for the next day morning. The air-conditioning operating hour can delay two hours.

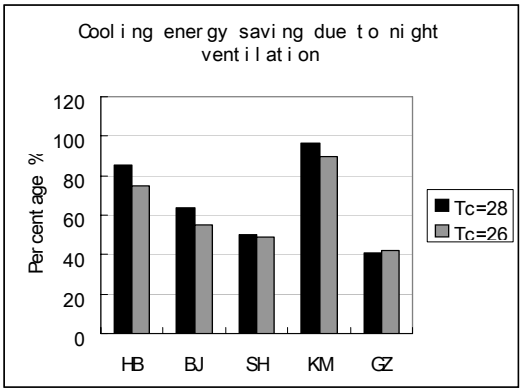

Fig.2 Percentage of energy saving

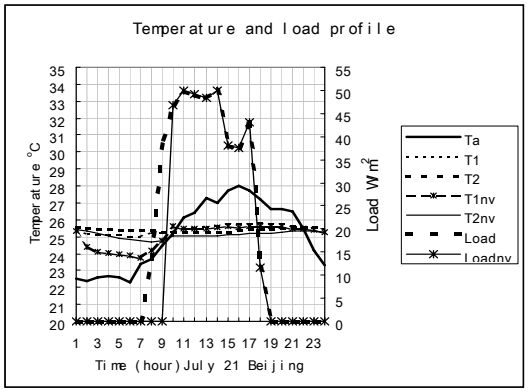

Fig.3 Temperature and load profiles

(2)Part time air-conditioning operation in the afternoon

From the natural ventilation simulation analysis we can see that office internal thermal condition in the morning can be improved by natural ventilation in the most cities except hottest month. This will give the opportunity for the integration of natural ventilation and mechanical cooling measures. It is noted that fan is the commonly used measures for thermal comfort improvement, which can equivalently offset air temperature by 3 ^{o}C. Fig. 4 shows the energy saving of part time air-conditioning operation. From the figure we can see that the case of "fan cooling in the morning and air-conditioning in the afternoon" can save about 85% energy comparing "all day air-conditioning without night ventilation" in Kunming, about 60% in Harbin, about 25% in Beijing and 15% in Shanghai. However there is less than 10% saving for comfort setting temperature of 28^{o}C and almost no saving for that of 26^{o}C in Guangzhou. This is because the daytime outdoor air temperature in the morning in Guangzhou is higher than that in the other four cities. When outdoor air temperature is high there will be no benefit for energy saving using natural ventilation. In contrast, all day air-conditioning operating can immediately remove the internal gains, while the afternoon part time air-conditioning operating system cannot remove the internal gains due to the high outdoor air temperature and the heat will be stored in the building structure and furniture and this will cause the higher cooling load in the afternoon. To explain this situation, the temperature and load profiles of July 17th in Guangzhou of the cases "Full time daytime air-conditioning" and "Part time air-conditioning" are illustrated in Fig.5, in which Ta is the outdoor air temperature; T1 is the internal air temperature with full time air-conditioning; T1p is the internal air temperature

with part time air-conditioning; T1p-eq is the equivalent air temperature internal air temperature considering air movement due to fan operation with par time air-conditioning; Load is the cooling load of full time air-conditioning and Load-p is the cooling load of part time air-conditioning. From the figure we can see that there is no significant saving for the part time air-conditioning operation comparing with full time air-conditioning, because there is a high peak cooling load when air-conditioning starts to operate in the afternoon. From the above analysis we can see that when outdoor air temperature is high, natural ventilation cannot save cooling energy.

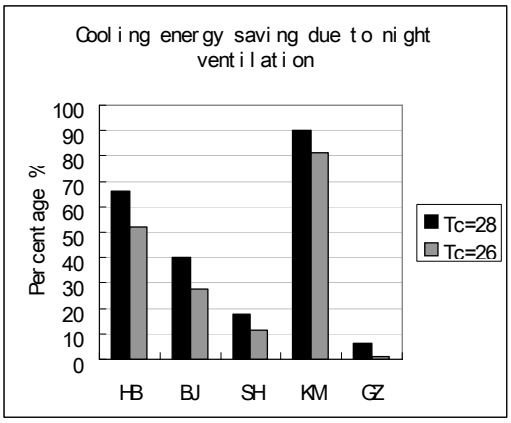

Fig.4 Percentage of energy saving

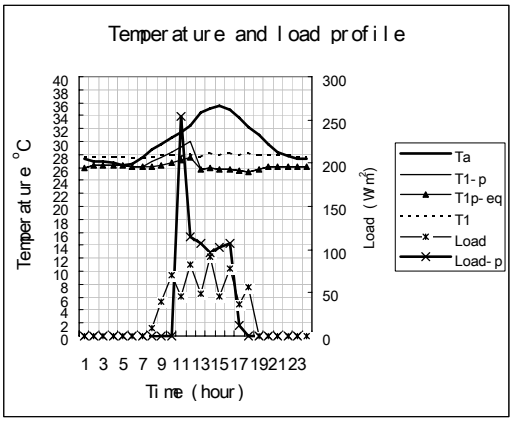

Fig. 5 Temperature and load profile in Guangzhou

CONCLUSION

The computer simulations for the typical office building in Chinese five cities, which represent the five climate zones in China, have been performed with different cases. Natural ventilation is a sufficient measure for improving summer thermal comfort however local climate plays an important role in energy saving. Night ventilation can reduce cooling energy. Air-conditioning in conjunction with natural ventilation system can achieve significant energy saving in Very Cold Zone and Mild zone and less saving in Hot summer zones.

ACKNOWLEDGEMENT

The authors wish to acknowledge the funding from CMI (Cambridge-MIT Institute) for the project Sustainable Building Design. The authors thank the financial support form UK FCO GOF Program. The authors thank Samantha Lawton for the administrative support provided.

REFERENCE

1. China Standard GB 50176-93(1993): Thermal design for civil building, 1993-10-01
2. Humphreys M.A., Nicol J. F. (1995), An adaptive guideline for UK office temperatures, UK adaptive temperature guideline. Standard for thermal comfort, E & FN SPON, 190-195.
3. Li B., Peng X., Yao R.(1997): The report on improving indoor thermal comfort in south China., Chongqing University.
4. Yao R., Li B. and Steemers K.(2005): Energy policy and standard for built environment in China, International Journal of Renewable Energy, 2005 1-16.
5. Yao R. and Steemers K.(2005): Project Report, Sustainable building design, CMI project, The Martin Centre for Architectural and Urban Studies

VENTILATION, IAQ AND ENERGY EFFICIENCY IN HOT HUMID CLIMATES

S.C. Sekhar, K.W.Tham and K.W.Cheong
Department of Building, National University of Singapore,
4 Architecture Drive, Singapore 117566

ABSTRACT

At the conceptual design stage, one needs to pay considerable attention to both the energy as well as indoor air quality (IAQ) requirements. Often, designers tend to overlook ventilation and IAQ issues and conceptualise the HVAC design more from energy considerations. An energy efficient design of air-conditioning system in hot and humid climates is quite challenging in view of the high humidity levels prevailing all-year round. This paper outlines some of the key factors that could lead to inadequate or inefficient ventilation and, thereby, poor IAQ. An overview of some integrated IAQ-energy audit case studies conducted in Singapore in the mid nineties is presented. Finally, a couple of emerging technologies related to air-conditioning and air distribution that are particularly ideal for hot and humid climate are presented.

KEYWORDS

Indoor air quality, energy efficiency, ventilation, hot and humid climate, air-conditioned buildings

INTRODUCTION

In hot and humid climates, one of the biggest challenges to overcome from an air-conditioning system design perspective is dehumidification or moisture removal. In this regard, the "H" can be conveniently removed from HVAC as Heating is seldom considered and designers are confronted only with the Ventilation and Air-Conditioning aspects. The process of cooling and dehumidification in practical air-conditioning system designs is one in which the dynamically varying sensible and latent cooling requirements are to be met in the correct proportion in which they occur in the occupied zones, and consequently at the cooling and dehumidifying coil. In other words, the dynamically varying Room Sensible Heat Ratio (RSHR) needs to be appropriately handled by the cooling coil performance. Invariably, this is the challenge as an improperly selected coil may lead to either inadequate dehumidifying performance, resulting in elevated humidity levels in the occupied zones or overcooling, resulting in an energy penalty. It is, thus, evident that the call for higher ventilation rates is always going to be perceived with trepidation in view of the energy issues. However, the lack of good ventilation would almost certainly lead to poor indoor air quality (IAQ) and eventually lead to rectification measures that could be more expensive than if it were to have been addressed in the

original design. This paper deals with some of the ventilation, IAQ and energy related code of practice requirements in Singapore, following which an overview of ventilation and IAQ measurements conducted in air-conditioned buildings in Singapore in the mid nineties will be presented. Finally, a couple of emerging energy efficient technologies for effective and practical zone-level ventilation control that shows promise for the hot humid climates is discussed.

INTEGRATED IAQ AND ENERGY AUDIT STUDIES

A comprehensive study of five air-conditioned buildings in Singapore was undertaken in the mid nineties, which included measurements of exposures and technical characteristics as well as occupants' perception and symptoms (Sekhar et al., 2003). A summary of the research framework and the findings of this study are now discussed.

The measured concentration levels of the physical, chemical and biological pollutants were compared with relevant local and international standards/guidelines to establish the IAQ status of the building. In particular, continuous chemical monitoring data of carbon dioxide, carbon monoxide, formaldehyde and TVOC allows the profiling of the prevailing concentration levels over a weekly period, resulting in an "IAQ signature". In order to express the quality of indoor air in different premises, an indoor pollutant standard index (IPSI) was proposed, which recognises that the characteristics of indoor air pollutants are significantly different from each other and their effect on human health and comfort are also different from one another.

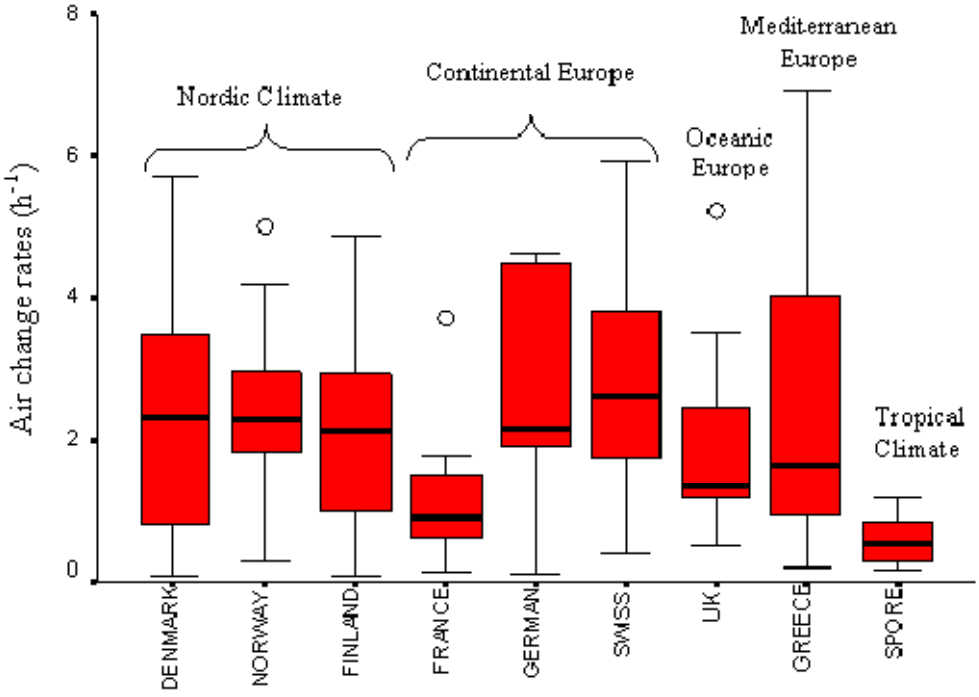

Figure 1 : Air change rates (ACH) measured in the European and Singapore buildings studied

Tracer gas techniques were employed to determine the ventilation characteristics such as the air change per hour (ACH), Air Exchange Effectiveness (AEE) parameters and the global air exchange efficiency. The ventilation index (lps/sq.m), normalized on the basis of air-conditioned floor area, is based on the actual amount of fresh air provided, calculated from measured air change rates (ACH). A comparison of the outdoor ACH between Singapore studies and those in other countries is shown in Figure 1, which indicates a high recirculation rate in air-conditioned buildings in hot humid climates (Zuraimi et al., 2005).

The IAQ-energy audit methodology, adopted in this study was based on a system-zone concept, which implies that all the indoor sampling points for a measurement set-up belong to a zone(s) that are served by the same air-conditioning and ventilation system. In the event of a zone(s) that constitute a control volume of space being served by more than one Air Handling Unit (AHU), then all the relevant AHUs serving the set of zones are included in the study as part of the same set-up. Such a "system-zone" concept was employed to ensure that the prevailing IAQ levels in the occupied zones could be attributed to the characteristics of the air-conditioning and the air distribution system. This was also envisaged to facilitate a study of the energy consumption at the micro level associated with a certain level of IAQ.

Building Symptom Index (BSI) was another parameter computed, which is an indicator of the well-being and health condition of the occupants as deduced from a questionnaire survey. It is the average number of sickness symptoms declared per person, out of a selected list. In deriving the BSI, only the symptoms that disappear after leaving the building are considered, in conformance to the notion of sick building syndrome terminology. BSI values were also computed separately for male and female occupants to explore the differences in perceptions between genders, as this has been observed to be a significant consideration in earlier studies.

A total of 5 buildings were studied and although large differences in the mean values of all the measured and computed parameters between individual buildings were observed, it is to be noted that they generally met the requirements of the local guidelines in Singapore. In the case of thermal comfort parameters, despite the mean values of operative temperatures for each building being reasonable, certain measured locations indicated air temperatures in the low range of the recommended values. A slight increase in these temperatures would imply an energy saving potential. The monthly energy consumption per air-conditioned floor area varied by a factor of 4.6 for the least energy consuming building to the most energy consuming building, which showed a reasonable theoretical economy potential as well as a significant diversity of conditions. The air temperatures measured in the occupied spaces of the audited buildings were generally in the lower range of the recommended values, and raising the air temperature set-points could provide an energy saving potential. Among the five buildings studied in this project, four of the buildings did not exhibit any clear relationship of poor IAQ and low energy consumption or vice versa.

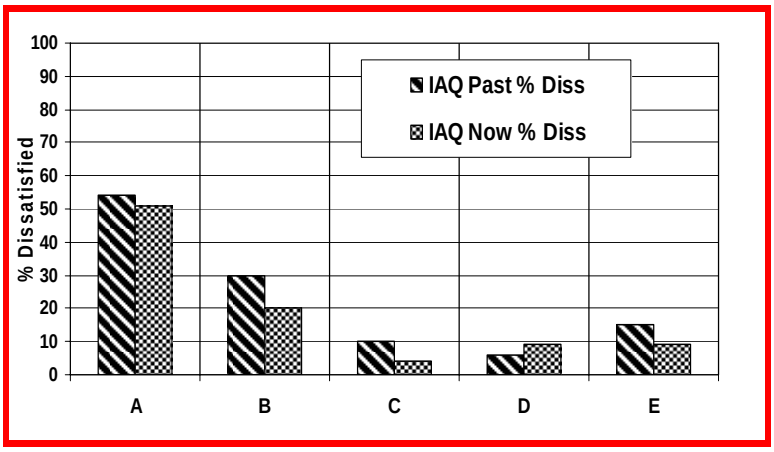

Figure 2 : IAQ acceptability rated by occupants expressed in percentage dissatisfied

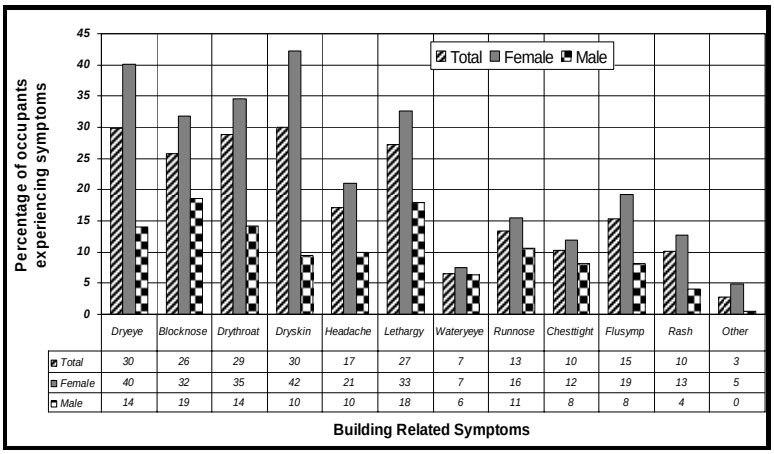

Figure 3 : A comparison of MALE and FEMALE Building Related Symptoms (Mean of all 5 buildings) – Here and Now (%)

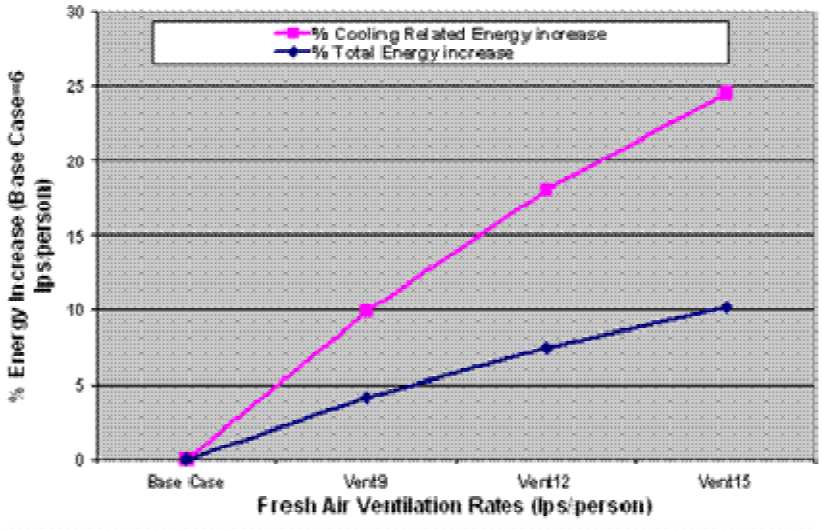

Figure 4 : Ventilation rates – Energy implications in hot and humid climate

Occupants' satisfaction with their indoor air quality is presented in Figure 2. The level of overall acceptability for thermal comfort was better than indoor air quality in general. Female occupants register significantly higher building related symptoms in comparison to their male counterparts in both the "past month" and the "here and now" periods, as shown in Figure 3. These observations were consistent with those seen in European studies (Bluyssen et al., 1996). The study suggested that the occupants' perception of symptoms experienced as well as environmental acceptability is quite distinct from IAQ acceptability determined from empirical measurements of indoor pollutants, which reinforces the complex nature of IAQ issues.

ENERGY EFFICIENCY AND ENHANCED IAQ

It is apparent that there would be a significant energy penalty with increased ventilation rates in conventionally designed air-conditioning and air distribution systems. A comparison of energy implications with varying ventilation rates is shown in Figure 4. The cooling energy increase between a ventilation rate of 6 lps/person to 15 lps/person could be as high as 25%. The challenge, then, is to explore the possibility of providing the ventilation to the occupied zones in such a way that adequate ventilation is provided at all times during human occupancy. A couple of technologies that are found promising are now discussed, with a particular emphasis for hot humid climate.

Single Coil Twin Fan (SCTF) System

The SCTF concept involves two variable air volume (VAV) systems employing one compartmented cooling and dehumidifying coil. A prototype unit was developed and installed to serve conditioned air to two rooms of an IAQ chamber in the Department of Building at the National University of Singapore (Sekhar et al., 2004). A schematic diagram of the SCTF air-conditioning and air distribution system is shown in Figure 5. The fresh air is conditioned in the "fresh air" compartment of the air handling unit (AHU) and distributed to the various VAV boxes that form part of the air distribution network. Each of these F/A VAV boxes is controlled by its own localized carbon dioxide (CO_2) sensors, which will ensure an adequate ventilation (F/A) provision at all times. As the main purpose of the F/A VAV box is to ensure adequate fresh air quantity based on occupant density, it helps in achieving energy conservation in the event of reduced occupant loads.

The return air from the various zones of the same distribution network is conditioned in the "recirculated air" compartment of the same AHU and distributed to a separate set of the various VAV boxes. Each of these R/A VAV boxes is controlled by its own localized zone thermostats, which addresses diversity in cooling loads, and consequently helps in achieving significant energy savings at part load operating conditions resulting from non-occupancy related factors. Based on our preliminary findings, energy savings up to 12% in conjunction with significantly improved IAQ have been observed in comparison with conventional air-conditioning systems (Sekhar et al., 2004). The conditioned Fresh Air and the conditioned Return Air travel in parallel ducts and do not mix until just before the supply air diffusers in the mixing chamber of the modified VAV box.

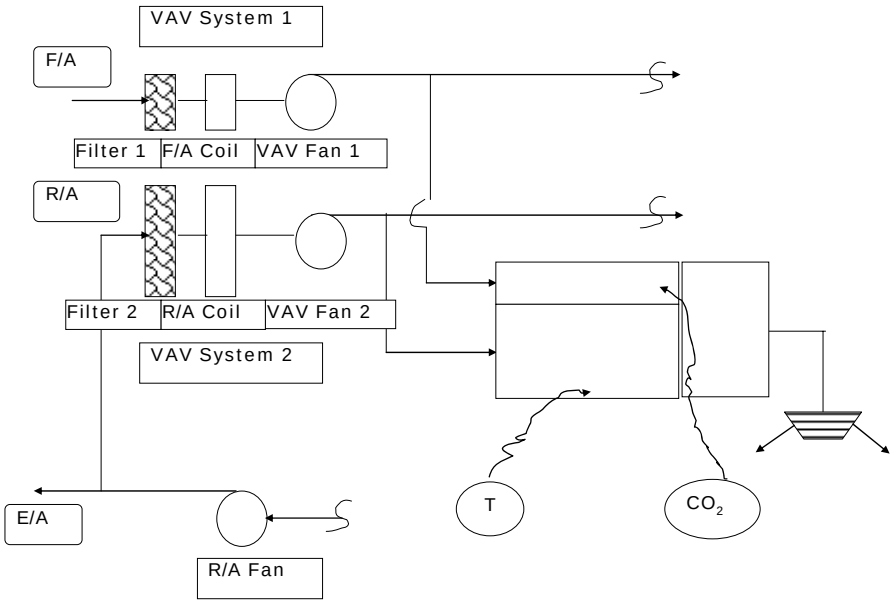

Figure 5 : The Single Coil Twin Fan (SCTF) system

Personalised Ventilation (PV) System

Whilst the concept of personalised ventilation (PV) is still primarily at the research stage in the area of air-conditioning, it shows tremendous promise for the future designs of buildings and is fundamentally based on improving ventilation to every individual in the built environment (Kaczmarczyk et al. 2004; Kaczmarczyk et al., 2002; Melikov et al., 2002). The PV concept has tremendous potential in enhancing the acceptability of Ventilation, Indoor Air Quality and Thermal Comfort in air-conditioned buildings by supplying clean fresh air directly to the occupant breathing zone without mixing with recirculated air, which is usually contaminated with indoor pollutants. The inability of conventional air-conditioning systems to do so often leads to occupant dissatisfaction.

Preliminary findings from a pilot study conducted at the National University of Singapore suggest that the use of PV system in conjunction with a secondary air-conditioning system significantly enhances thermal comfort and IAQ acceptability as well as the perception of freshness in the air (Sekhar et al., 2005). It was observed that the ventilation effectiveness of the PV system is significantly higher than conventional mixing ventilation system. Based on the responses of thermal comfort and IAQ acceptability, it is evident that the subjects do find the PV system to be significantly better than total mixing system. The pilot study has also indicated that the PV system has a potential to save energy in tropical designs.

The combination of the SCTF system and the PV system has attractive benefits to several building types, particularly those where considerable occupant and functional diversity are expected. For example in a health care facility, the fresh air supplied by the SCTF

system can be easily configured as a PV air terminal device to provide in such a way that it flows through the doctor's immediate breathing zone before going towards the patient. This is envisaged to offer better infection control between the doctor and a sick patient.

CONCLUSIONS

This paper has highlighted the ventilation, IAQ and energy issues in air-conditioned buildings in a hot and humid climate. The Sick Building Syndrome symptoms experienced in the Singapore studies were quite similar to those observed in European studies. A couple of emerging air-conditioning and air distribution technologies are presented that could offer significant benefits both in terms of enhanced IAQ as well as energy efficiency.

REFERENCES

Bluyssen, P.M., de Oliviera Fernandes, E., Groes, L., Clausen, G., Fanger, P.O., Valbjorn, O., Bernhard, C.A. and Roulet, C.A. (1996) "European indoor air quality audit project in 56 office buildings", *Indoor Air*, Vol.6, pp.221-238

Kaczmarczyk, J., Melikov, A.K. and Fanger, P. O., 2004. Human response to personalised ventilation and mixing ventilation, Indoor Air, Vol.14, Supplement 8, pp. 17-29

Kaczmarczyk, J., Zeng, Q, Melikov, A and Fanger, P. O., 2002. The effect of a personalized ventilation system on perceived air quality and SBS symptoms. Proceedings of Indoor Air 2002, Monterey, USA.

Melikov, A., Cermak, R. and Mayer M., 2002. Personalised ventilation : Evaluation of different air terminal devices. Energy and Buildings, Vol. 34, No. 8, pp. 829-836.

Sekhar, S.C., Gong Nan, K.W.Tham, K.W.Cheong, A.K.Melikov, D.P.Wyon and P.O.Fanger, 2005. Findings of Personalized Ventilation Studies in a Hot and Humid Climate. International Journal of Heating, Ventilating, Air-conditioning and Refrigerating Research (HVAC&R Research), ASHRAE, USA. *To appear.*

Sekhar, S.C., Uma Maheswaran, C.R., Tham, K.W, and Cheong K.W, 2004. Development of energy efficient single coil twin fan air-conditioning system with zonal ventilation control, ASHRAE Transactions, Volume 110, Part 2, pp 204-217.

Sekhar, S C, K W Tham and K W Cheong, 2003. Indoor air quality and energy performance of air-conditioned office buildings in Singapore. Indoor Air - International Journal of Indoor Air Quality and Climate. Vol 13, Issue 4, pp 315-331.

Zuraimi, MS, C-A Roulet, K W Tham, S C Sekhar, K W Cheong, N H Wong and H K Lee, 2005. A Comparative Study of VOCs in Singapore and European Office Buildings. Building and Environment.

Annex 41
Whole building heat, air and moisture response

H. Hens
Department of Civil Engineering, Laboratory of Building Physics, K.U.Leuven
B-3001 Leuven, Belgium

ABSTRACT

Combined heat, air and moisture (HAM) simulation at the envelope level and building simulation have been two separate activities for many decades now. In HAM-models, inside temperature and inside relative humidity are handled as known boundary condition, while all building simulation tools predict inside temperatures and net energy demand without any consideration for relative humidity.

Things started to change when airflow modeling became doable. That step not only allowed a better quantification of ventilation related energy consumption but it also permitted a refinement of the humidity balances in the building. However, at least two linkages between the building and the indoor environment remained poorly explored: (1) the fact that many adventitious air flows enter and leave the building across the envelope causing a complex pattern of indoor air washing, wind washing, air looping, infiltration and exfiltration in it and (2), the fact that moisture buffering in indoor finishes and furniture delays and dampens the inside relative humidity. Both phenomena have an impact on the energy consumed for heating, cooling and air conditioning, on durability and on perceived indoor air quality. Analyzing those linkages which are at the basis of whole building heat, air and moisture transport and studying the impact on energy consumption, durability and perceived indoor air quality are at the core of the annex 41 activity.

KEYWORDS

Combined heat, air and moisture transport, moisture buffering, air leakage, energy, durability, perceived indoor air quality

INTRODUCTION

Although it is well known that the heat, air and moisture flows (called HAM) generated by building use and entering from outside, that the HAM flows that traverse the enclosure and the HAM flows that are injected by the HVAC system are in permanent and mutual balance, simulation tools and the designers that use them do not currently consider that reality. Building designs are scrutinized on the heat needed, while HVAC-systems are dimensioned as to deliver that heat with as main goal to keep the indoor temperature at comfort level. Yet, indoor relative humidity is typically kept free floating, except when full air conditioning is applied, as it is perceived to be less important. Few designers detail the envelope taking into account the full hygrothermal load from inside and from outside, while hardly anyone considers the whole heat, air and moisture balance that develops between the building's interior, its envelope and the outside environment. This is a pity as air pressure differences inside the building and between the building and the outside for example may generate airflows that change the heat, air and moisture response of the envelope and the building drastically, while buffering effects could dampen relative humidity fluctuations significantly. Resulting air ingress, possible rain penetration and the moisture deposits both cause in the envelope could not only negatively affect energy consumption but also trigger the envelope's durability. Simultaneously, inside relative humidity, if not well managed, may affect perceived indoor air quality and become a driving force for mold infection and dust mite multiplication.

Clearly, the whole building heat, air moisture response has impact on human comfort, indoor air quality, energy consumption and envelope durability. Enough reasons to start an Annex on the subject, termed as Annex 41, Moist-En (Hens, 2003)

STATE OF THE ART

Building modeling started in the fifties. From the beginning, the goals were quantifying the net energy demand, analyzing the ways that demand could be reduced by building related measures and getting information on the temperature without heating and cooling as this allowed to evaluate overheating. Later-on, HVAC-models were added and energy consumption became the quantity quantified. Hardly any model, however, was able to model the air and humidity balances in the building. Instead rough estimates on infiltration and ventilation air flows were used and humidity remained untouched (ASHRAE, 2001)

During the same period, the research effort on heat, air and moisture transport focused on the envelope. In the sixties, a few simple evaluation tools became popular. They scaled reality down to two steady state transport modes: heat flow by conduction and water vapor flow by diffusion (Glaser, 1958, Glaser 1958, ASHRAE, 2001). Today highly sophisticated one- and two-dimensional full heat and moisture models are available that allow modelling vapor and liquid flow, that are transient in nature, that consider moisture sources such as wind-driven rain, rising damp, initial moisture, sorption and desorption, interstitial condensation and surface condensation and that allow to quantify some of the consequences of unfitted moisture tolerance, such as hygrothermal stress and strain, mold infection, corrosion and frost damage (Pedersen, 1990)(Carmeliet, 1992)(Künzel, 1994)(Grünewald, 1997)(Sedlbauer et al., 2003). Examples of such models are: Match, Wufi, Latenite and HygIRC. In Europe, the one-dimensional full models are even in the process of becoming standardized procedures. All envelope models, however, take the indoor climate (temperature, relative humidity, air pressures) as known boundary condition. This of course is fiction, except in case of full air conditioning, when the indoor is completely uncoupled from the outdoor. Also a correct implementation of wind driven rain and its impact on the building envelope remained a weakness. In fact, although wind and wind driven rain has been a research topic for many decades, one had to wait until CFD became a commonly used tool before a turn could be made from experiment and simple calculation to full simulation and prediction of the rain load on the envelope (Lacy et al., 1962)(Blocken et al., 2004)

As already said, the analysis of the airflow patterns within a building was an important step on the road to whole building HAM analysis. Basic work on inter-zonal flow has been done by the Comis group and Annex 23 (Allard et al., 1990). The last decade, large numbers of researchers use CFD to analyze intra-zonal flow (Baker et al., 1994). The linkage between the flows in the building and those in the envelope, however, is hardly established, although the study of air flows in and through envelope parts has underlined their importance for a correct evaluation of the hygrothermal response (Kronvall, 1982)(Trechsel ed., 1994).

Finally, the last years, we saw a renewed interest in indoor moisture buffering by finishing layers and furniture (see figure 1) (Svennberg et al., 2004). A few software packages have been developed, which allow evaluating the effect. Measurements on buffering capacity of finishing materials and furniture are performed in several laboratories. Nordtest initiated a research program on the subject, included a round robin on buffering (Rode, 2003).

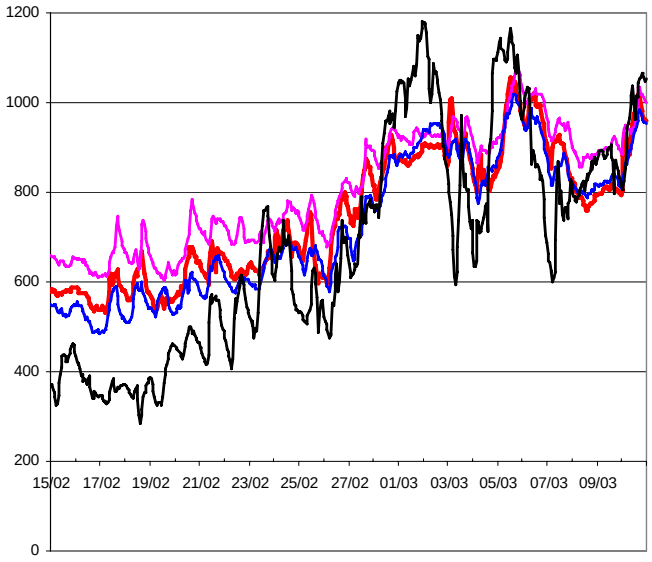

Figure 1 Inside vapor pressure in a naturally ventilated office. Black shows the outside vapor pressure, purple, red and blue the inside vapor pressure. Hygric inertia dampens the swings and causes the inside excess to turn negative when the weather changes from cold to moderate

ANNEX OBJECTIVES

The annex is meant to establish a holistic view on the overall HAM transfer in buildings and their envelopes. The specific objectives are:

1. Exploring the physics involved in whole building HAM response. That includes basic research, a further development of models, measuring the moisture storage function of finishing materials and furniture, mock up testing and field testing. Test results will be used to verify and validate models by inter-comparison and confrontation with measured data. Objective 1 should establish a basic understanding of the overall HAM-flows that come from inside and outdoors under different weather conditions (cold, warm and dry, warm and humid and maritime) and their effect on the building's overall hygrothermal response.

2. Analyzing the effects of whole building HAM on comfort, indoor air quality, on energy consumption and enclosure durability. Good comfort and good indoor air quality are part of overall users satisfaction. As everyone spends up to 80% of her/his time in buildings, the whole society is benefiting when comfort conditions are optimal. Avoided energy consumption helps sustainability. From that point of view, humidity changes, termed as latent energy, are very significant in warm moist regions, where latent heat often makes over 50% of the annual cooling load. Optimal moisture storage solutions may reduce that percentage. The result is a net saving in energy resources and less CO_2 produced, not only now but even more in the future when the desire for well-controlled indoor environments will further increase. Better durability finally also means more sustainability. A long service life in fact economizes on material use, embodied energy and embodied pollution. Damage statistics learn that bad moisture management is the most important cause of shortened service life. Objective 1 should translate itself in original research, damage case evaluation and literature reviews. Simultaneously, measures must be studied as to moderate possible negative impacts of combined HAM transfer with air- and rain-tightness, correct moisture management, optimal thermal insulation, well balanced humidity storage and lower energy demands as some of the focal points.

ANNEX ORGANISATION

The work is structured in four subtasks:

Subtask 1: modeling principles and common exercises

Subtask 1 concentrates on whole building HAM modeling with special emphasis on HAM-transfer between the surroundings and the outside surface of the building envelope, HAM transfer in the envelope, HAM transfer between the inside surface of the envelope and indoors, HAM transfer from outdoors to indoors and vice versa through leakages, purpose designed ventilation grids and HVAC-coupled in- and outlets, HAM transfer between the building envelope and the interior partitions, HAM transfer between the indoor air and furniture and HAM transfer between the different zones in a building. Models that result from the subtask will take into account parameters such as location and orientation of the building, the heating, ventilation and air conditioning systems, adventitious and user defined air flows, moisture response by hygroscopic and capillary-active materials in the building enclosure and furniture, the type of room (bathroom, living room, etc.) and user's behavior (number of people, activities (moisture and energy production, etc.), frequency and duration of window ventilation). Numerical codes that integrate the above mentioned elements will be verified and validated and their applicability demonstrated, using common exercises as the main vehicle. The actual schedule of common exercises looks as follows:

Exercise 0	Dry BESTEST for validating the thermal part of the models (done)
Exercise 1	Wet BESTEST. Generating vapor in the BESTEST building, predicting of the inside relative humidity in isothermal and transient conditions (done)
Exercise 2	Simulating experimental results at room level under isothermal conditions
Exercise 3	Simulating experimental results at room level under non-isothermal conditions
Exercise 4	Simulating a coupled room configuration under isothermal conditions
Exercise X	Real world case, evaluating the impact of adventitious ventilation flows that traverse the envelope on durability and energy consumption

Exercise 2, 3 and 4 are meant as validation steps. In all three cases experiments have been done and the objective of the exercise is to simulate the experiments, to compare the calculated with the test data and to judge the agreement between both

Subtask 2: experimental investigation

Subtask 2 primarily considers the impact of moisture buffering in finishing materials and furniture on the relative humidity in the indoor environment. For that purpose material property data, surface film coefficient values and design parameters required for modeling will be generated. More specific goals of the subtask are to collect material property data needed for modeling and characterizing buffer effects, to study the parameters affecting moisture transfer between the air and a material surface both in steady state and transient conditions, to provide the data for validation of the models through well monitored benchmark mock-up cases and to generate concepts and practical applications of moisture buffering systems. For that purpose, the Annex 24 material database will be extended by adding more data on vapor permeability, specific moisture capacity and air permeance. Also a round robin on measuring vapor permeability, specific moisture capacity and buffering ability of unpainted and painted gypsum board is going on and well monitored mock-up tests are performed.

Subtask 3: boundary conditions

Subtask 3 concentrates on outdoor and indoor climatic conditions, on the heat and moisture loads, on air pressures generated by wind, stack and fans as parameters to be used in whole building HAM model(s). The subtask has as specific objectives to characterize wind and wind driven rain patterns around buildings, to analyze absorption and runoff properties of exterior cladding, to quantify the moisture load due to condensation on exterior building surfaces by clear sky radiant cooling, to collect data on interior heat and moisture release, on interior temperature and interior relative humidity in different types of buildings and to come to a usable classification of indoor climates

Subtask 4: long term performance and technology transfer

Subtask 4 starts from a clear fit for purpose concept. Buildings should provide required indoor environment and comfort at low energy costs during an economically feasible service life, what the exterior climate and usage pattern may be. Special attention will go to the effects of moisture on the indoor environment, on durability and energy consumption with problems in buildings caused by a high indoor humidity as specific topic. Predicting long term performances, of course, demands a frame of reference. That may for example involve extending the limit state approach to durability assessment. Within subtask 4, this will be done for some types of decay, mould being one of them. In such limit state approach, two levels intervene: risk assessment at the design stage and prevention methods for use during the building's service life.

Also an effective communication with practitioners, building services engineers, project managers, administrators and educators is of importance. Subtask results should be accessible to everybody outside the scientific community. Because of different priorities and training, end-users have different perspectives. That means, it is necessary to put the results into a form which is easy to understand and to use by the following groups: (1) private industry, (2) practitioners, (3) educational establishments. Of course, this cannot be realized globally within subtask 4. The report of subtask 4 will anyhow focus on it.

ANNEX PRODUCTS

The products of the annex will be designed for use by the building research community, by engineering offices that focus on building physics, energy, HVAC and sustainable construction, by material and building system developers, by corporations with an interest in high performance systems, by building designers and by educational institutions. These products will include

In general	An internet site. The site contains all meeting proceedings, all annex papers and common exercise results and the drafts of the final reports (http://www.kuleuven.ac.be/bwf/projects/annex41/).
Subtask 1	Final report on whole building HAM modeling with an appendix discussing the results of the common exercises
Subtask 2	Final report documenting all experimental investigations (round robin on gypsum board, test room measurements) and a database with moisture storage properties of finishing materials and furnishings.

Subtask 3 Final report on indoor and outdoor boundary conditions for whole building HAM simulation with special emphasis on wind driven rain, undercooling, air pressure differences that may exist between the inside and outside and moisture, measured inside climate data and heat and moisture sources within buildings

Subtask 4 Final report on long term performances in relation to comfort, durability and energy, demonstrating the benefits of a well controlled whole building HAM response

All final reports will be published in hard copy form and on CD-ROM.

CONCLUSION

Annex 41 has a huge program to cover. The initiative yet motivated 18 countries and more than 50 experts to participate, underlining the interest in the topic and the expectation people has that the activity will not only generate a better understanding of the whole building heat, air and moisture response but also establish ways how to benefit from that knowledge in the design and construction of buildings and HVAC-systems in terms of better comfort, better indoor air quality, better durability and less energy consumed. The work started 18 months ago and will proceed for another 30 months.

REFERENCES

Alard F., Dorer V.B., Feustel H.E. (1990), Fundamentals of the multi-zone air flow model-COMIS, Technical Note 29, AIVC

ASHRAE (2001), Handbook of Fundamentals, chapters 23 and 31, Atlanta, Georgia

Baker A. J., Williams P.T., Kelso R.M. (1994), Development of a robust finite element CFD procedure for predicting indoor room aor motion, Building and Environment, Vol.29, No 3, pp 261-273

Blocken B., Roels S., Carmeliet J. (2003), A numerical study of wind nuisance for a high-rise building group, Research in Building Physics, Balkema, 981-990

Carmeliet J. (1992), Durability of fiber-reinforced renderings for exterior insulation systems, Doctoraal Proefschrift

Glaser H. (1958), Temperatur und Dampfdruckverlauf in einer homogene Wand bei Feuchteausscheidung, Kältetechnik 6, pp 174-181

Glaser H. (1958), Vereinfachte Berechnung der Dampfdiffusion durch geschichtete Wand bei Ausscheiden von Wasser und Eis, Kältetechnik 11, 12, pp 358, pp 386-390

Grünewald J. (1997), Konvektiver und diffusiver Stoff- und Energietransport in kapillarporösen Baustoffen, Dissertation an der TU Dresden, Fakultät Bauingenieurswesen

Hens H. (2003), Proposal for a New Annex, 17 p (accepted by the EXCO as Annex 41 in the fall meeting of 2003)

Kronvall J. (1982), Air flows in building components, Report TVBH-1002, Division of Building Technology, Lund University of Technology

Künzel H.M. (1994), Verfahren zur ein- und zweidimensionalen Berechnung des gekoppelten Wärme und Feuchtetransport in Bauteilen mit Einfachen Kenwerten, Abhandlung zur Erlangung der Würde eines Doktor-Ingenieurs, Stuttgart

Lacy R., Shellard H. (1962), An index for driving rain, The Meteorological Magazine 91, no 1080, pp 177-184

Pedersen C. R. (1990), Combined heat and moisture transfer in building constructions, Report no 214, TUD

Rode C. editor (2003) Nordtest, Workshop on Moisture Buffer Capacity, DTU, 33 p.

Sedlbauer K., Krus M. (2003), A new model for mold prediction and its application in practice, Research in Building Physics, Balkema, 921-928

Trechsel H, editor (1994) Moisture Control in Buildings, ASTM Manual Series: MNL 18, 485 p.

Svennberg K., Hedegaard L, Rode C. (2004), moisture Buffer performance of a fully furnished room, Proceeding of the Performance of Exterior Envelopes of Whole Buildings IX International Conference (CD-ROM)

IEA ANNEX 41, SUBTASK 1 – MODELLING PRINCIPLES AND COMMON EXERCISES

Monika Woloszyn[1], **Ruut Peuhkuri**[2], **Lone Mortensen**[2], **Carsten Rode**[2]

[1] *Centre de Thermique de Lyon, CNRS UMR 5008, UCBL, INSA Lyon, France*
[2] *Department of Civil Engineering, Technical University of Denmark, DK-2800 Kgs. Lyngby, Denmark*

ABSTRACT

The paper gives an outline of existing modelling capabilities as well as an overview of current developments in integral modelling of hygrothermal conditions for whole buildings as presented within IEA Annex 41. Such models deal with the heat, air and moisture conditions of most relevant elements of buildings: The indoor air, the building envelope, inside constructions and furnishing. These building elements interact with each other and they are influenced by the use of the building, the building services, and the outside climate. The transport processes for heat, air and moisture also interact with each other, and everything has an impact on the energy consumption of the building and the quality of indoor air.

A suite of Common Exercises for computational modelling are developed and executed within this modelling subtask. The common exercises test the current capabilities of existing models and, very importantly, they stimulate the development of new models or the expansion of capabilities of existing models. The first two Common Exercises have been executed already. Some further plans for the subsequent Common Exercises will be outlined in the paper.

KEYWORDS

Heat, Air, Moisture, Whole buildings, Modelling

INTRODUCTION

Annex 41 of the International Energy Agency's (IEA) Energy Conservation in Buildings and Community Systems programme (ECBCS) is a cooperative project on "Whole Building Heat, Air and Moisture Response". The project seeks to deepen the knowledge about the integrated heat, air and moisture transport processes when the whole building is considered. That means it is necessary to consider all the elements: the separate building materials, the composite constructions, furniture and the indoor climate with its users, systems for heating, cooling and air-conditioning, as well as the outdoor climate. All these elements have an effect on each other. Also, the nature of the transport processes for heat, air and moisture (HAM) make them depend on each other. While research projects in the past have been focusing only on some of these elements at a time, Annex 41 seeks to develop further understanding of how the elements function together. This will be done by concerted actions which seek to further and develop the common experiences in modelling and experimenting on the involved topics. Elementary processes which have also been studied in the past, such as moisture transport in materials, or wind-driven rain on facades are also studied in the Annex, but only with the objective to study how such processes influence the whole building performance.

The four-year project started in November 2003 and has succeeded to gather significant international contributions from researchers of four continents in the world. Altogether

researchers from some 39 institutions representing 19 different countries participate in the project. The project has the two homepages: http://www.ecbcs.org/annexes/annex41.htm (hosted by the IEA ECBCS programme), and http://www.kuleuven.be/bwf/projects/annex41/ (by the project's Operating Agent, the Catholic University of Leuven, Belgium).

This paper focuses on activities in the IEA Annex' Subtask 1: *Modelling Principles and Common Exercises*. Other subtasks are: Subtask 2 - *Experimental Investigations*; Subtask 3 - *Boundary Conditions*; and Subtask 4 - *Long Term Performance and Technology Transfer*.

MODELLING OF HYGROTHERMAL CONDITIONS IN WHOLE-BUILDINGS

Traditionally, computational models that cover the whole building have been focusing mainly on the thermal aspects, since this has been complicated enough to cope with for all the different building elements, the HVAC systems, and the users. Today however, although some developments are still ongoing, this kind models have been quite well established for at least one decade. On the other hand, models which deal with several processes, such as the flow of heat, air and moisture have mainly been focussing on one building element at a time. Such models have also been reasonably well established for about one decade.

However, it is well known, that the different hygrothermal processes interact with each other: E.g. moisture conditions cannot be predicted without knowledge about the thermal state, mass flows such as by air or moisture also have and impact on the thermal conditions, and air flows may severely impact the moisture behaviour. Likewise, the hygrothermal conditions in individual building components interact importantly with the indoor climate they surround. One could not predict the conditions in the envelope of building without knowing or assuming something about the indoor conditions, and those indoor conditions are, among other things influenced by the building elements.

Today we have begun to see the development of models that cope with these issues in an integrated way. Subtask 1 of IEA Annex 41 seeks to stimulate this development. Obviously, there are three possible ways to approach the whole building HAM simulation:

- To improve existing building simulation tools so they can better account for processes linked with the envelope,
- Extension of building component simulation tools,
- A combination of both building simulation and building component simulation tools.

Generally, the models used are either hygrothermal models for components of the building envelope which are expanded with models for indoor air volumes and by making provision for simultaneous calculation of several building components – e.g. Holm et al. (2003). Alternatively, building energy simulation models, which already have capabilities for making thermal analysis of whole buildings, are expanded with models for transient moisture transport in the building components - e.g. Rode & Grau (2003).

The mission of IEA Annex 41's Subtask 1 is to stimulate this development by inspiring the research work and gathering the experiences. To qualify as an IEA Annex 41 contribution, research work, including modelling, must comprise at least two of the processes: Heat, Air and Moisture, and it must comprise building elements on various levels from the individual building material to the whole building.

The Annex also invites more fundamental research contributions from the participants as long

as they relate to the overall subject of the Annex. Such research is presented in so-called “free papers”, and there has until today been free papers on subjects such as: CFD-models for air-moisture transport in rooms; analytical solutions; toolboxes such as MATLAB; sensitivity studies on energy effects; zonal approaches; algorithm development; material–air interaction; and case studies. Further free papers are invited particularly within the nominated topics: Sensitivity studies; convective vs. heat and moisture flows (e.g. by CFD); surface coefficients; integration aspects; simplified models; multidimensional effects; integration of systems; energy impacts.

COMMON EXERCISES

The purpose of the common exercises being part of Subtask 1 of the Annex is to test the possibilities of the existing models or models under development to predict the integrated hygrothermal behaviour of buildings and to stimulate new development in this area. Besides this, common exercises provide elements of validation of HAM building simulation tools. The following elements necessary for code validation will be included in common exercises:

- analytical verification
- empirical validation vs experimental data
- finally comparative testing, which is the heart of all the common exercises.

As of to date the following Common Exercises (CE) have been executed as part of Subtask 1 of Annex 41:

- Common Exercise 0 (CE0). Validation of thermal aspects of the employed models. This was done by repeating the building energy simulation test BESTEST of IEA SHC Task 12 & ECBCS Annex 21 (Judkoff and Neymark, 1995).
- Common Exercise 1 (CE1). Expanding on CE0 and the BESTEST case by adding considerations about moisture interactions between building constructions and indoor climate.

Both these exercises study the IEA BESTEST building. The IEA BESTEST building is also referenced in ASHRAE Standard 140 (ASHRAE, 2004). The building shown in Figure 1 has a simple structure with two windows facing south. It is superficial, so no measurement data exist. The cases serve to provide comparison between different modelling results.

Along with the numerical results, reports on the program and modelling choices were filled in by the participants. These reports contribute to the documentation of the state-of-the-art of models that can be used for whole building heat, air and moisture transfer simulations.

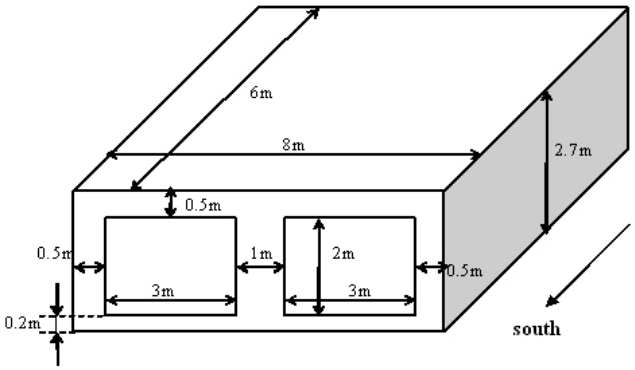

Figure 1 BESTEST base case building.

CE 0 Thermal Building Simulation

For the purpose of Annex 41, four cases where chosen from the original BESTEST procedure, adapted for whole building approach, including a lightweight building and a heavyweight building. There were also cases with free floating thermal conditions as well as cases with active heating and cooling systems. More information on the cases is given by Judkoff and Neymark (1995).

13 sets of results were collected coming from 11 institutions from 9 countries using the following different programs: *BSim*; *Clim2000*; *EnergyPlus*; *ESP-r*; *HAMLab*; *HAMTool*; *IDA ICE*; *ITT DELPHIN*; *TRNSYS*; *Wufi+*. The programs participating in CE0 are both public domain and commercial software, and their common feature is continuous development of physical models. Different solution methods are used in these models, such as explicit and implicit finite difference algorithms, or response factor type methods. Both fixed and auto-adaptative time steps are equally represented. Also, the reconstruction of outdoor climate from meteorological data varies. Some programs use linear interpolation while the others assume that the climate remains constant over the sampling interval. All models used include moisture in the balance of the air zone, but at the time of executing CE0 only a few programs represented moisture transfer through the envelope.

CE 1 Hygrothermal Building Simulation

Common Exercise 1 expanded on Common Exercise 0 by adding the indoor and building envelope moisture conditions for the BESTEST building used in CE0. The first results of the Common Exercise 1 showed, however, that the original case had too many uncertainties even within the thermal calculation, e.g. the presentation of the material data, window models etc. Therefore, a step back was taken with Common Exercise 1A (an analytical case) and Common Exercise 1B (a more “realistic” case). The constructions were made monolithic, the material data were given as constant values (CE1A) or functions (CE1B) and the solar gain through windows was modelled simplified.

Altogether 16 institutions participated in at least some parts of Common Exercise 1. The tools used were: *1DHAV+*; *BSim*; *Clim2000*; *EnergyPlus*; *Esp-r*; *HAMLab*; *HAMTool*; *HAM-VIE*; *IDA ICE*; *ITT DELPHIN; NPI*; *PowerDomus*; *SPARK*; *TRNSYS*; *Wufi+*; and *Xam*; Some of the institutions have used the same code for all the exercises – with or without modifications from case to case – while others have used 2 different codes or have not taken part in a single exercise.

Conclusions to Draw from the Common Exercises

The Common Exercises 0 and 1 stimulated some developments of different software as well as some original use of existing programs. They also showed that there is a need for some consensus data concerning heat and moisture properties of the materials. In the following, some experiences from the exercises are discussed. Attention is paid both to the new achievements and to the problems that occurred.

CE 0 (Heat)
Common Exercise 0 stimulated some improvement of existing programs, namely concerning the “H” (Heat) part of HAM-models, and specially radiation heat transfer calculations. Both

short wave radiation (computation of incident solar radiation and heat gains through the windows) and long wave intra-zone exchanges were enhanced in some programs. As heat, air and moisture closely interact with each other in a building, a correct description of energy behaviour is needed before assessing whole building moisture performance.

The deviation of results within a reasonable range gives also some more confidence in energy models and provides a valuable reference case for some future sensitivity study on the impact of moisture on energy loads.

CE 1 (Heat and Moisture)
The results from the original case (CE1) showed however that now there was not even agreement in the way the models calculated the thermal conditions. However, one should be reminded that this was a first attempt ever of trying to compare the results of this kind of models with moisture.

It was concluded after presentation of these results that the exercise should be redesigned to become significantly simpler in order to avoid deviations due to factors that are not central for the hygrothermal modelling itself.

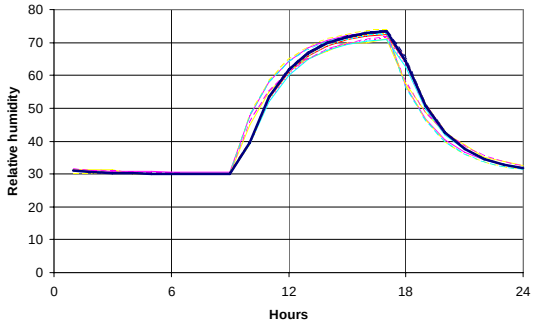

Figure 2: CE1A. Indoor relative humidity. Isothermal exposure. Construction surfaces are tight. The numerical results are compared with the analytical consensus solution.

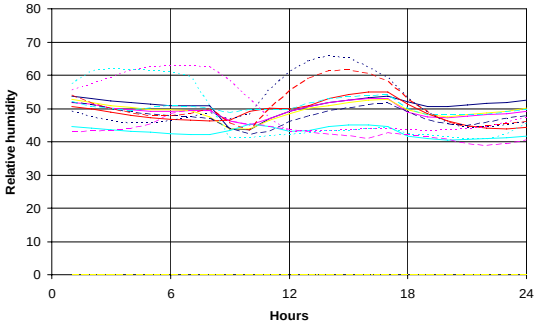

Figure 3: CE1B. Indoor relative humidity. Non-isothermal conditions and open surfaces. A day in July with solar and long wave radiation through the windows and on external opaque surfaces.

The first part of the revised exercise (CE1A), was a very simplified isothermal case with tight or open indoor surfaces, which showed very good agreement between both the analytical solutions and the numerical calculations (see Figure 2). These results gave an increased belief that it was possible to predict the indoor RH with a whole building hygrothermal calculation. However, in this case some important building elements like windows were neglected.

The second and more realistic part of the revised exercise (CE1B) illustrated again the complexity of the whole building hygrothermal modelling: New deviations could not be neglected. The differences in the thermal calculation could not fully explain the deviations as they occurred also for the case with constant indoor temperature. Figure 3 illustrates the variation in the resulting indoor RH for the case where the solar and long wave radiation were included.

FURTHER WORK

The experience from the Common Exercises so far tells that there is a need to execute more

cases, especially with comparison with measurement data. Also adding furniture to the set-ups and considering the air flows has to be considered as well.

The actual challenge in whole building Heat Air and Moisture modelling is to develop good paradigms for modelling the correspondence between the numerous different and physically coupled phenomena rather than to develop new models where the elementary processes are dealt with separately. Another important issue is the relative importance of different phenomena and their interactions. Sensitivity analysis and the future common exercises should help to answer the fundamental question when and which interactions can be neglected and in which cases they must be represented. The plan for further exercises is as follows:

- CE 2: Based on experimental data from climate chamber tests at Tohoku University, Japan. The tests have known wall claddings and air flow conditions.
- CE 3: Based on double climatic chamber tests carried out by the Fraunhofer Institut für Bauphysik, Germany, using two identical chambers with different cladding materials.
- CE 2007. A two-storey climatic chamber test carried out at Concordia University, Canada, will serve as basis for this exercise.
- CE "X". Based on data from a real life row house located in Belgium. with some known indoor climate/moisture problems which also involve effects of adventitious airflow.

GENERAL CONCLUSIONS

The Common Exercises executed as a part of the Annex 41 Subtask 1: Modelling have illustrated the complexity of the whole building hygrothermal modelling: It was possible to find a consensus among the solutions with different calculation models only for an extremely simple isothermal case - a building with monolithic walls and without windows.

On the other hand, these results also underline the importance of this type of exercises: The existing codes are "tested" for their suitability for the whole building hygrothermal simulation and the new ones are created, including upgrading and developing the existing codes to be able to handle also the moisture calculations.

REFERENCES

ASHRAE. 2004. *Standard Method of Test for the Evaluation of Building Energy Analysis Computer Programs*. ANSI/ASHRAE Standard 140-2004. Atlanta, GA: American Society of Heating, Refrigerating and Air-Conditioning Engineers, Inc.

Holm, A., Künzel, H.M. and Sedlbauer, K. 2003. The Hygrothermal Behaviour of Rooms: Combining Thermal Building Simulation and Hygrothermal Envelope Calculation. *Eighth International IBPSA Conference*. Eindhoven, the Netherlands

Judkoff, R., and Neymark, J. 1995. *Building Energy Simulation Test (BESTEST) and Diagnostic Method*. NREL/TP-472-6231. Golden, CO: National Renewable Energy Lab..

Rode, C. and Grau, K. 2003. Whole Building Hygrothermal Simulation Model. *ASHRAE Transactions*, V. 109, Pt. 1. Atlanta, GA: American Society of Heating, Refrigerating and Air-Conditioning Engineers, Inc.

NORDTEST PROJECT ON MOISTURE BUFFER VALUE OF MATERIALS

Carsten Rode[1], Ruut Peuhkuri[1], Kurt K. Hansen[1], Berit Time[2], Kaisa Svennberg[3], Jesper Arfvidsson[3], Tuomo Ojanen[4]

[1] Department of Civil Engineering, Technical University of Denmark, DK-2800 Kgs. Lyngby, Denmark
[2] Materials and Structures, Norwegian Building Research Institute, N-7491 Trondheim, Norway
[3] Department of Building Physics, Lund Institute of Technology, S- 221 00 Lund, Sweden
[4] VTT Materials and Products, Technical Research Centre of Finland, FIN-02044 VTT, Espoo, Finland

ABSTRACT

Building materials and furnishing used in contact with indoor air have some effect to moderate the variations of indoor humidity in occupied buildings. Very low humidity can be alleviated in winter, as well as can high indoor humidity in summer and during high occupancy loads. Thus, materials can possibly be used as a passive means of establishing indoor climatic conditions, which are comfortable for human occupancy.

But so far there has been a lack of a standardized figure to characterize the moisture buffering ability of materials. It has been the objective of a Nordic project, which is currently being completed, to develop a definition, and to declare it in the form of a NORDTEST method. Apart from the definition of the term Moisture Buffer Value, the project also declares a test protocol which expresses how materials should be tested. Finally as a part of the project, some Round Robin Tests have been carried out on various typical building materials.

The paper gives an account on the definition of the Moisture Buffer Value, it outlines the content of the test protocol, and it gives some examples of results from the Round Robin Tests.

KEYWORDS

Moisture, materials, transport properties, indoor air, buffer capacity, Round Robin Test.

INTRODUCTION

Indoor humidity is an important parameter to determine the occupants' perception of indoor air quality (Fang et al. 2000), and is also an important parameter as a cause of processes which are harmful to the health of occupants (Bornehag et al., 2003). Materials that absorb moisture and release it in other periods can be used positively to reduce peaks of humidity levels in indoor climates. Some investigations indicate that the use of hygroscopic materials can improve the indoor climate and comfort of occupants because of the way the materials moderate the indoor humidity variations (Simonson et al., 2001).

For these reasons, and because of the role played by indoor moisture conditions on the durability of the envelope of buildings, there is significant interest in characterizing both the moisture transmitting and buffering properties of absorbent, porous building materials.

At present there is no consensus on how to describe the moisture buffer property of building materials. Therefore, there is a need for a robust definition of a term for the moisture buffer

effect of materials, which is technically sound, yet comprehensible and indisputable for the industry and users that will apply it: i.e. a number that is able to indicate the rate and amount of moisture flowing between a material and its surrounding climate in a dynamic situation.

Also, a test method to determine the moisture buffer performance according to the definition needs to be defined. A Round Robin Test should be executed in order to ensure that testing laboratories are able to handle the test method, and to establish the first reference measurements on a limited number of representative materials. The purpose of the NORDTEST project described in this paper is to fulfil these needs, and that was also the conclusion at a workshop that was arranged prior to starting the NORDTEST project (Rode, 2003). We propose to call this desired property the *Moisture Buffer Value*.

Partners in the NORDTEST project are the Technical University of Denmark (DTU) (as project leader); Technical Research Centre of Finland (VTT); Byggforsk, Norway (NBI); and Lund Institute of Technology, Sweden (LTH). In addition the project is followed by an international reference group with participants from six other research institutions.

DEFINITION OF MOISTURE BUFFER VALUE

The Moisture Buffer Value (MBV) indicates the amount of moisture uptake or release by a material when it is exposed to repeated daily variations in relative humidity between two given levels. When the moisture uptake or release from beginning to end of the exposure to a new relative humidity is reported per open surface area and per % RH variation, the result is the MBV. The unit for MBV is kg/(m^2·% RH). The concept of moisture buffer value can easily be appreciated and understood from an experimental standpoint, and likewise, it is relatively straightforward to measure. Theoretically, the MBV can be associated with the effusivity for moisture exchange, a definition parallel to thermal effusivity (Hagentoft, 2001).

The value is a direct measure of the amount of moisture transported to and from a material when the exposure is given. The value is mainly, but not only a property of the material. Also the mass transfer coefficient at the boundary layer plays a role, and thus, the moisture buffer value becomes a true material property only in the limit of the convective mass transfer coefficient tending to infinity. For many materials the internal resistance to moisture transport is considerably larger than the convective surface resistance.

TEST PROTOCOL

The NORDTEST project defines a test protocol for experimental determination of the moisture buffer value. The principle is based on climatic chamber tests, where a specimen is subjected to environmental changes that come as a square wave in diurnal cycles.

The test protocol proposes to use climatic exposures which vary in 8 h + 16 h cycles: 8 hours of high humidity followed intermittently by 16 hours of low humidity. The reason for the asymmetry in this time scheme is twofold: (1) It replicates the daily cycle seen in many rooms, e.g. offices or bedrooms, where the load comes in approximately 8 hours, and (2) for practical reasons during testing if the climatic chamber conditions are changed manually, it is a scheme which is easier to keep than a 12 h + 12 h shift.

TABLE 1. Materials tested in the Round Robin, and indication of institutions performing the tests.

Material/Product	DTU	VTT	LTH	NBI
Spruce Plywood (pre-test)	x	XX	x	x
Spruce boards from *Woodfocus*, FIN	x	XX		x
Concrete from *Betonelementforeningen*, DK	XX		x	x
Gypsum from *Gyproc*, S		x	XX	x
Laminated Wood from *Annebergs Limtræ*, DK	XX	x		x
Light weight aggregate concrete from *maxit*, DK	XX		x	x
Cellular concrete from *H+H Celcon*, DK	XX	x	x	
Brick from *Kalk- og Teglværksforeningen*, DK	XX	x	x	
Birch wood panels from *Tresenteret*, N		x	x	XX

XX - country responsible for supplying the material

The low humidity is proposed to be 33% RH, while the high should be 75% RH. However, the NORDTEST project also proposes the following alternatives: 33/54%, 54/75%, and 75/93%. These humidity levels are chosen because they can be maintained by saturated salt solutions, but some other conditioning system may also be used. The choice of RH-level may have some impact on the results as the sorption and permeability properties depend on humidity. Therefore, testing should be done in a range which reflects a relevant level for the application of the material. During the tests, it is important that the equipment is able to make rapid RH-changes. Testing should always be carried out at 23°C as a reference.

Specimens will normally be sealed on all but one or two surfaces so the minimum exposed surface area should be 0.01 m^2. The thickness of the specimen should be at least the moisture penetration depth for daily humidity variations, or 10 mm, whichever is larger. At least three specimens should be used for testing.

Using an accurate scale, the specimens should be weighed continuously or intermittently during the test. At least five weight measurements should be carried out during the 8 hour high humidity part of the last cycle. A minimum of three cycles have to be carried out, and the weight amplitude must not vary by more than 5% from day to day. This is defined as the three stable cycles (see Figure 2 for an example of a measurement sequence). The stable cycles are also characterized by the fact that the daily amounts of moisture uptake and release are approaching each other as shown in Figure 3. The mass change should be plotted and normalized as mass change ($m_{8\ hours}$-m_0) per m^2 and per ΔRH to give the MBV (see Figure 3).

ROUND ROBIN TEST AND INITIAL RESULTS

A Round Robin Test is carried out within the NORDTEST project to try the testing paradigm and to obtain some initial results for typical building materials. In addition, and to guide the formulation of the test protocol, a preliminary test was carried out on some spruce plywood boards that were distributed to all project partners. The materials tested and the institutions doing the tests are listed in Table 1. Each material is tested by three partners.

The institutions do not have quite the same experimental equipment available and some of the operational routines were also dissimilar, although in accordance with the common test protocol. E.g., some institutes made manual weighing of the specimen, while it for others took place by automated logging of a scale. Thus, it has been part of the Round Robin Test to see if it were possible to obtain similar and agreeable results by all institutes.

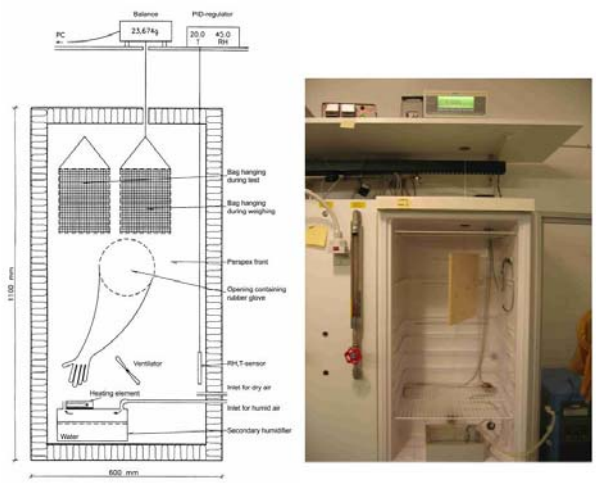

Figure 1: Drawing and picture of one of the climatic chambers used at DTU.

Figure 1 shows a drawing and photograph of one of the climatic chambers used at DTU. The humidity control of the chamber works by supplying it with either humid or dry air in an intermittent mode, such that the desired humidity in the chamber is achieved.

Figure 2 shows the measured weight change response of one of the specimens when it was subjected to cycles that varied the ambient humidity between 33% and 75 % RH for 16 and 8 hrs respectively. The choice of stable cycles and the moisture uptake is marked in the figure.

Figure 3 shows for three different specimens of the same type of material how the moisture uptake and moisture release varied from cycle to cycle until the three stable cycles were attained. Thus the results of measurements of one type of material give the following background for statistical analysis: Three specimens with results from three cycles of both moisture uptake and release - altogether 3x3x2 = 18 bids for the MBV result. The results should be represented at least with their mean value and standard deviation together with information about the number of tested specimens and stable cycles (if different from 3x3).

Figure 4 shows the MBV for the materials tested by the participating institutions until the day of completing this paper. The materials are labelled M1, M2, ..., M8, and the bar diagrams indicate for each material and testing laboratory the average of the MBV-value and its standard deviation. More results need to be obtained before statements can be issued about how agreeable the results are, and it is also too early to give statements about how well the different materials perform as moisture buffers. However, it seems that the order of magnitude for the tested materials is around 1 g/(m^2·%RH), and there may be approximately a factor 3 of a difference between the materials with the highest and lowest MBV among those tested.

PRACTICAL APPLICATION OF THE MOISTURE BUFFER VALUE

The Moisture Buffer Value is primarily meant as a number that can be used to appraise a material's ability to absorb and release moisture from an adjacent space. For practical application it can also be useful as a number for estimation of the moisture balance of rooms, as indicated by the following example.

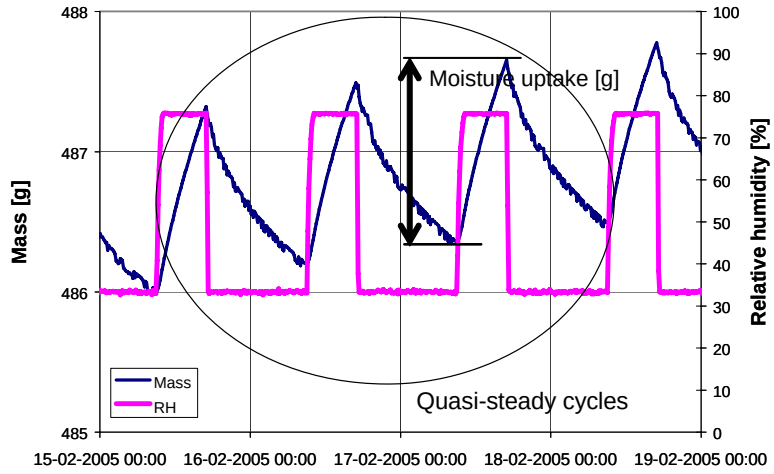

Figure 2: Moisture uptake and release cycles for M6. Exposure between 33 and 75% RH.

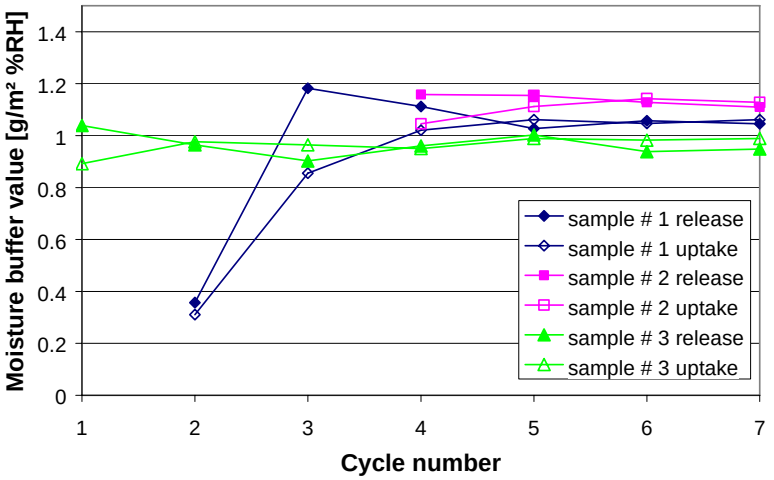

Figure 3: MBV of material M1 as a function of cycle number and uptake versus release. The last 3 cycles are the stable cycles (=quasi-steady)

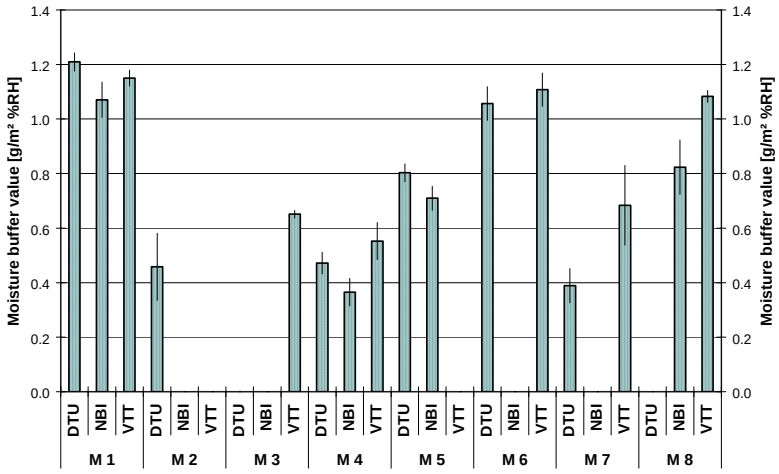

Figure 4: Moisture Buffer Values found by different institutions for the different materials. Each bar indicates the average of three specimens over three stable cycles. The thin vertical line-bars indicate standard deviations.

Example

An unventilated room has dimensions 4 x 5 x 2.5 m = 50 m^3, and temperature 23°C. In the room is released G = 100 g of moisture per hour. The room is clad with A = 45 m^2 of material with MBV = 1.2 g/(m^2·ΔRH). By how much will the indoor humidity increase in 8 hours?

First, the wall cladding is neglected. The saturation water vapour concentration at 23°C is 20.6 g/m^3. Thus, the air itself has a moisture buffer value of 0.206 g/(m^3·%RH), so in 8 hours ΔRH will be $\frac{8h \cdot 100\ g/h}{50\ m^3 \cdot 0.206\ g/(m^3 \cdot \%RH)} = 78\%\ RH$ (or condensation may occur before then).

Next, if the room cladding is considered, but the buffer capacity of the air is neglected, the RH increase can be calculated by assuming that all the released moisture will be absorbed by the wall cladding material. The increase in indoor relative humidity will be:

$$\Delta RH = \frac{G \cdot \Delta t}{\mathrm{MBV} \cdot A} = \frac{100\,\mathrm{g/h} \cdot 8\,\mathrm{h}}{1.2\,\mathrm{g/(m^2 \cdot \%RH)} \cdot 45\,\mathrm{m^2}} = 15\,\%\,\mathrm{RH}$$

Finally, if as in reality, the room experiences an air change with other environments, its humidity would be governed also by the air change rate and vapour content of the ventilation air, and this could well be more important than the buffer capacity of the air and materials.

CONCLUSION

The described work declares a uniform definition of a term such as *Moisture Buffer Value* as well as an experimental protocol for its determination. *Moisture Buffer Value* can be used to appraise the ability of materials used in buildings to moderate indoor humidity variations. The term should replace an inconsistent variety of other numbers used till now to appraise this quality of building materials. A Round Robin Test is carried out in which the moisture buffer value has been determined for some examples of common building materials. The results of the described project will be published in the form of a NORDTEST method.

REFERENCES

Bornehag, C.G., Sundell, J., and Hägerhed, L., DBH Study Group (2003) Dampness in dwellings and sick building symptoms among adults: a cross-sectional study on 8918 Swedish homes. Proceedings of Healthy Buildings 2003, Singapore, Vol. 1, pp. 582 (2003)

Fang, L., Clausen, G., Fanger, P.O. (2000) Temperature and humidity: important factors for perception of air quality and for ventilation requirements. ASHRAE Transactions, 106, Pt. 2

Hagentoft, C.-E. (2001) Introduction to Building Physics. Studentlitteratur.

Rode, C. (2003) Workshop on Moisture Buffer Capacity – Summary Report. Report R-067. Department of Civil Engineering, Technical University of Denmark.

Simonson, C.J.; Salonvaara, M. and Ojanen, T. (2001) Improving Indoor Climate and Comfort with Wooden Structures. VTT Publ. 431. Technical Research Centre of Finland.

MODELLING OF MOISTURE CONDITIONS IN A COLD ATTIC SPACE

A. Sasic Kalagasidis and B. Mattsson

Department of Building Technology, Chalmers University of Technology, Gothenburg, S-41296, SE

ABSTRACT

This study investigates numerically the occurrence and duration of higher relative humidities in a cold attic space, which are a consequence of excessive moisture supply from ventilating the attic and from air infiltration from inside the dwelling. Hygrothermal states of the attic air zone and the adjacent construction elements are calculated by a whole building heat, air and moisture simulation tool. Airflows to the attic are determined by taking into account the total distribution of pressure around and inside a building. The role of attic ventilation is analyzed by comparing naturally ventilated and unventilated attics in an open landscape or a city zone. For air infiltration from inside the dwelling only scenarios with the airflow directed mostly to the attic are analyzed. The simulations show that, if indoor air infiltrates through the attic floor, it is necessary to ventilate the attic. In that case, a building situated in a sheltered position is more susceptible to moisture problems in the cold attic than the same building in an unsheltered position. However, in the absence of air infiltration from inside the dwelling, the attic should not be ventilated. Simulations are performed for real climatic conditions.

KEYWORDS

Cold attics, moisture problems, mold in attics, air infiltration, attic ventilation, attic floor.

INTRODUCTION

The 1973 energy crises led to increased thermal insulation levels in buildings in Sweden. A common procedure was to add insulation to the attic floor in houses, which nowadays has the thickness of 384 mm on average (STEM, 2001). As a result, the climate of the attic turns colder during wintertime and becomes close to the one outdoors. Over the years, cold attics have shown to be susceptible to transfer of moist air from the environment, by ventilation, or, by infiltration from a living space. In that case, appearance of mold on internal wooden sides of the roof may be encountered. Although it is 30 years ago since moisture problems in attics became widespread, few investigations have been made which focus on attic ventilation only (Samuelson 1995, Arfvidsson and Harderup 2005). They show the more an attic is ventilated, the higher the relative humidity reached. The cited studies also include numerical investigations of ventilation airflow rate, moisture buffering capacity of the insulating material, the role of a heat source, etc. (Larsson 1996, Sasic 2004, Arfvidsson and Harderup 2005).

Attics are kept ventilated by tradition, a practice established in the past on uninsulated attics, aiming to reduce the melting of snow and the appearance of icicles on the roof. By introducing cold attics, the main purpose of ventilation is not appropriate any more. However, it may acquire another purpose, such as to remove humid air that can be transported from inside the dwelling by air infiltration through the attic floor. Three decisive causes for air infiltration – wind speed, wind pressure on the building envelope and location of leakage paths –can only be roughly estimated without performing extensive measurements. Although

the majority of airflow experiments on attics focus on air infiltration or air change rates (Gustén, 1989, Forest and Walker, 1995), little can be gained with respect to the impact of wind on air infiltration through attic floors.

The present work reports results from numerical investigations of the impact of wind and air infiltration from a living space on the moisture conditions in a cold attic. The role of attic ventilation is analyzed by comparing ventilated and unventilated attics, with and without air infiltration from inside the dwelling. Air infiltration rates are modeled by taking into account the pressure distribution around and inside the building as a whole. The aim of the paper is to find out whether ventilation (governed by wind) may help in removing convectively transported moisture through the attic floor. The simulations are performed using a CFD-tool (Fluent) for attic ventilation rates and HAM-Tools (Sasic, 2004a) for air infiltration rates through the attic floor and the hygrothermal states in the attic.

THE MODELLED BUILDING AND ASSUMPTIONS REGARDING BOUNDARY CONDITIONS

The model building is a one storey single-family house with a cold attic under a 30^o pitched roof, Figure 1. The floor area is 8 by 12 m and the wall height is 2.5 m. The volume of the attic is 110 m^3. The roof is covered with concrete tiles on the outer side, followed by an underlay and lined with 19 mm thick wooden spruce boards on the internal side. Gable sides are constructed of wooden boards and painted on the outer side. The attic floor is insulated with a 500 mm thick loose-fill insulation with an air barrier below and gypsum board as internal lining. The roof sides face south and north respectively.

The airtightness of the house is specified to be 0.8 $l/(m^2 \cdot s)$ of the surface area that separates the indoor climate from the outdoor one, or from any unheated space. The indicated value meets the requirement of the Swedish building code (BBR, 2002) and is related to a pressure difference of 50 Pa across the building envelope, in which case the air change rate for the building is equivalent to 3.5 ACH.

To have naturally correlated weather parameters (air temperature and relative humidity, solar and long-wave radiation and wind), measured climate data are used in the simulations. The data are recorded in the southwest coastal area of Sweden, characterized by mild winters and summers, but with heavy and lengthy rainy periods throughout the year. The data cover one year. The climate in the house is designed in the following way: air temperature is constant and equals 22^oC, while the air relative humidity varies between 40 % in wintertime and 70 % in summer, according to recommendations in CEN TC 89. This gives approximately 4 g/m^3 higher moisture content in the indoor air than in the outdoor.

CALCULATIONS OF AIRFLOW

Ventilation airflow of the attic

In the simulations the attic is denoted as ventilated when there are ventilation openings below the eaves, as it is shown in Figure 1a. Otherwise, the attic is unventilated. However, in such cases also, it is assumed that air infiltrates the attic through this path, since attention is usually not paid to make this detail completely airtight.

For ventilated attics the airflow through the ventilation openings dominates the total air balance of the attic. This implies that, although the pressure difference across the roof can be substantial, air will mainly enter and exit the attic through these openings. The roof decking of the modeled building is assumed to be perfectly airtight (as being covered with a roofing felt underlay, a procedure rather common for Swedish single-family houses).

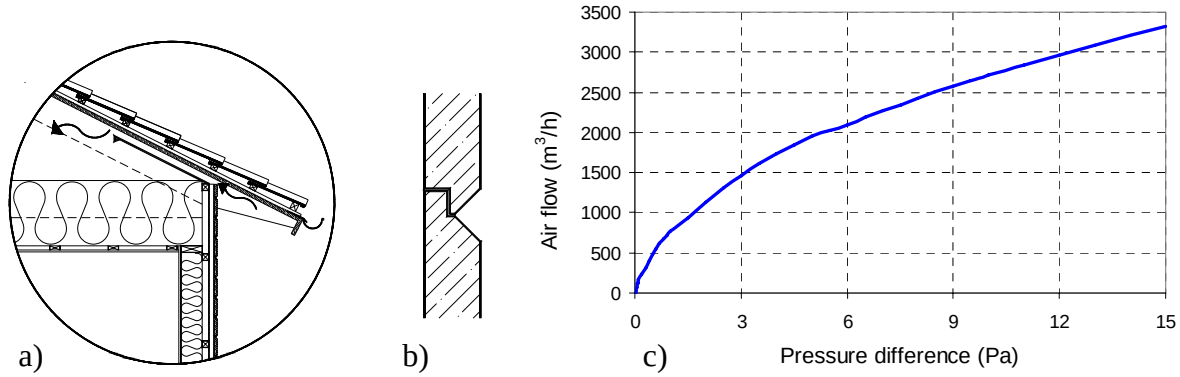

Figure 1: a) The common design of the ventilation opening below the eaves. b) The possible air leakage path through the joint between wooden boards at the gables. c) The airflow through the ventilation openings as a function of the pressure difference between the outdoor pressure and the pressure in the attic.

The airflow through the ventilation openings is modeled as a function of the pressure difference across the openings, according to Figure 1c. The air leakage rate for this detail (when there are no intentional openings) is assumed to be 1/20 of the airflow rate in the case when intentional ventilation openings are present. The air leakage paths through the gables consist of gaps between the wooden boards in the façade, as it is shown in Figure 1b, with the airflow assumed to be laminar (Mattsson, 2005).

The total ventilation airflow rate of the attic represents the resulting airflow through the openings (or leakages) on the roof eaves and through the leakages on the gables. The flow is calculated for real climate data and for two different exposures to the wind, Figure 2, taking into account the wind direction The prevailing wind is from the south-west with average speed of 4.2 m/s. Wind pressure coefficients are obtained from Orme et al. (1998).

Airflow through the attic floor

The stack effect governs the transport of air from a living space to the attic during wintertime. However, the type of house ventilation system may alter the air direction; in case of mechanical exhaust ventilation, the system makes such under pressure in the house, which, in turn, counteracts the stack effect and, as a result, the air from the attic is sucked into the house. Finally, the effect of wind on a building can support or decrease the airflow through the attic floor, depending on the position of air leakages or intentional openings on a house, as well as on the house exposure to the wind.

A number of different scenarios and interactions between these effects is analyzed in the work of Mattsson (2005). The present investigation is focusing on some of the cases from the work cited, i.e. those with the largest risk of indoor air infiltration. Thus, the model house is assumed to be equipped with the mechanical exhaust-supply ventilation system that extracts 120 m^3/h and supplies 90 % of this ventilation rate when the climate does not influence the ventilation system, i.e. when the outdoor and indoor temperatures are equal and there is no wind. Air leakages on the house are distributed in such a way that the stack effect has its

maximal impact - when half of the leakages are concentrated at the floor level and half at the ceiling.

The airflow through all leakages is modeled using a power-law equation with a flow exponent of 0.67, (see for example ASHRAE, 2001). As in the case of attic ventilation, the air flow through the attic floor is calculated for the real climate data and for two different exposures to wind. Some results are shown in Figure 3.

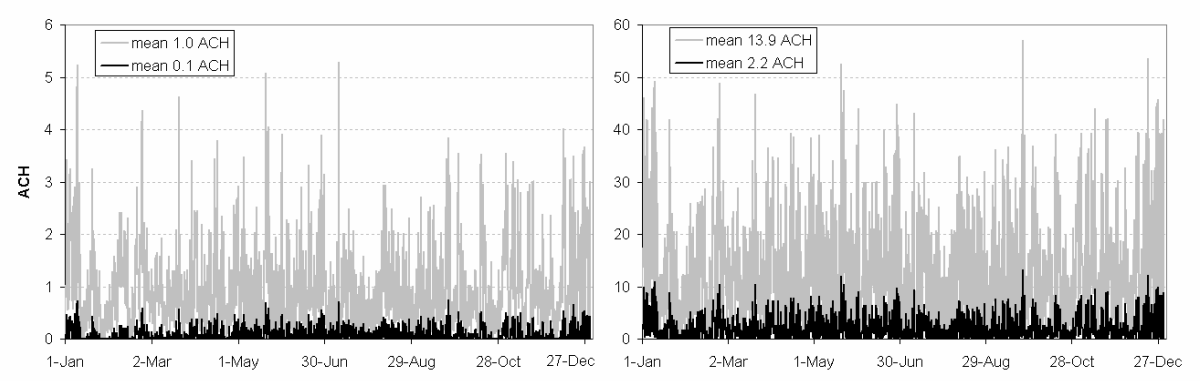

Figure 2: The diagram to the left shows the ventilation air change rates of the unventilated attic for the house in open position to the wind (the gray line) and in closed (city) position to the wind (the black line). The diagram on the right shows the same for the ventilated attic. The volume of the attic is 110 m^3.

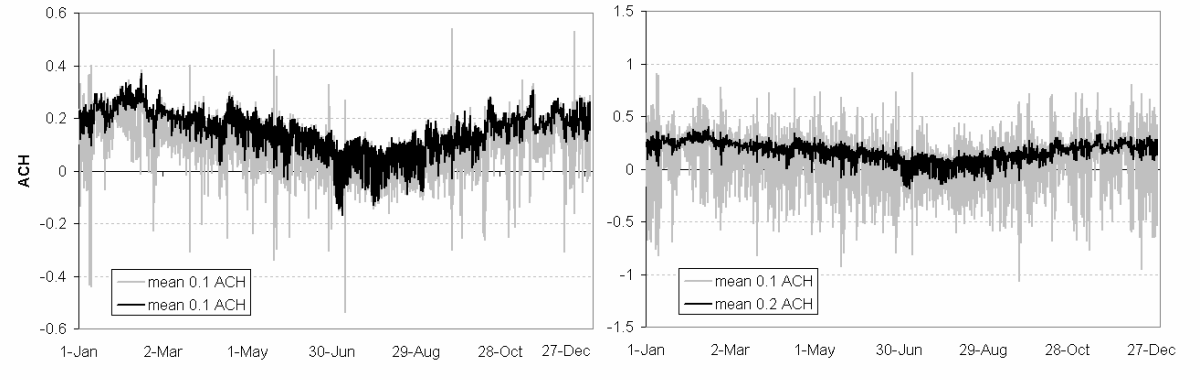

Figure 3: Airflow through the attic floor for the unventilated (to the left) and ventilated attic (to the right). Gray lines denote results for the house in open position to the wind, blacks for the house in closed position to the wind. Positive values represent flows directed upwards to the attic.

HYGROTHERMAL CALCULATIONS

The hygrothermal states in the attic are calculated by taking into account the outdoor climate load, the airflows by ventilation and infiltration, as well as the heat and moisture transfer through construction elements (roof sides, gable walls and attic floor). The attic is treated as a single air zone, while heat and moisture transfer through construction elements is calculated as an one-dimensional phenomenon.

The attic indoor climate varies with respect to the attic ventilation, air infiltration from the living space and the attic exposure. The overview of all cases concerned is given in Table 1, together with the reference case – the absolutely airtight attic (e.g. no ventilation or infiltration).

Repeating the climate and air infiltration load, year by year, each case is run until a periodical behavior is reached. For the majority of them, it is in the second simulated year. Final results for the reference case are used as initial conditions (i.e. initial temperature and relative humidity in construction elements and indoor air) for all other cases where the air load appears. Material properties, transfer coefficients and other parameters of interest are carefully modeled in order to represent reality in a credible way, (Sasic, 2004b).

TABLE 1
Overview of the cases concerned

Roof ventilation	**R**eference case	**V**entilated				**U**nventilated			
Wind exposure		**O**pen		**C**ity		**O**pen		**C**ity	
Air-tightness of the floor	Unventilated and absolutely air-tight attic	**T**ight	**L**eaky	**T**ight	**L**eaky	**T**ight	**L**eaky	**T**ight	**L**eaky
Notation	**R**	**VOT**	**VOL**	**VCT**	**VCL**	**UOT**	**UOL**	**UCT**	**UCL**

Results for air relative humidity in the attic are given as duration curves, Figure 4a, for all nine cases. This method, also presented in Samuelson (1995), illustrates the differences between the cases in a straightforward way. The time (per year) when a certain relative humidity is exceeded is given on the x-axis. In case of the reference attic the relative humidity never exceeds 80 %; for the ventilated attics in open position it is over 85 % half of the year. The highest values are found in the UCL attic, where the relative humidity is greater than 85 % the most of the time. Besides, results for the ventilated attics are quite grouped indicating the similar climate. On the other hand, the results for the unventilated attics are very spread and the presence of air infiltration from the outside and from the inside the dwelling are easily distinguished.

Mold growth risk on wooden surfaces can be assessed from the duration of favorable conditions for growth which are ranked in respect to the temperature and relative humidity in the attic (Hukka and Viitanen, 1999). To illustrate this, the duration of some characteristic ranges of relative humidity and temperature at the internal side of the southern roof slope are shown in Figure 4b. The data are given for two different ventilation airflow rates and they complement the results in Figure 4a.

CONCLUSIONS

There are considerable differences in relative humidity variations for the cases analyzed. In the absence of air infiltration from the dwelling, the climate in the attic becomes drier as the ventilation rate decreases. Having in mind that mold growth risk increases with increasing relative humidity, it seems that attics, in general, should not be ventilated. However, when air infiltration from inside the dwelling is present, attic ventilation helps in removing excessive moisture. In this case, the effect of ventilation is more pronounced as airflow rates become higher, but the final upgrade is nevertheless limited, since ventilation itself brings moisture to the attic. The simulations also reveal that a building situated in a sheltered position is more susceptible to moisture problems in the cold attic compared to the same building in an unsheltered position. Future work will focus on more detailed investigations on air leakage paths through the attic floor, as well as on the moisture analyses in other climate conditions.

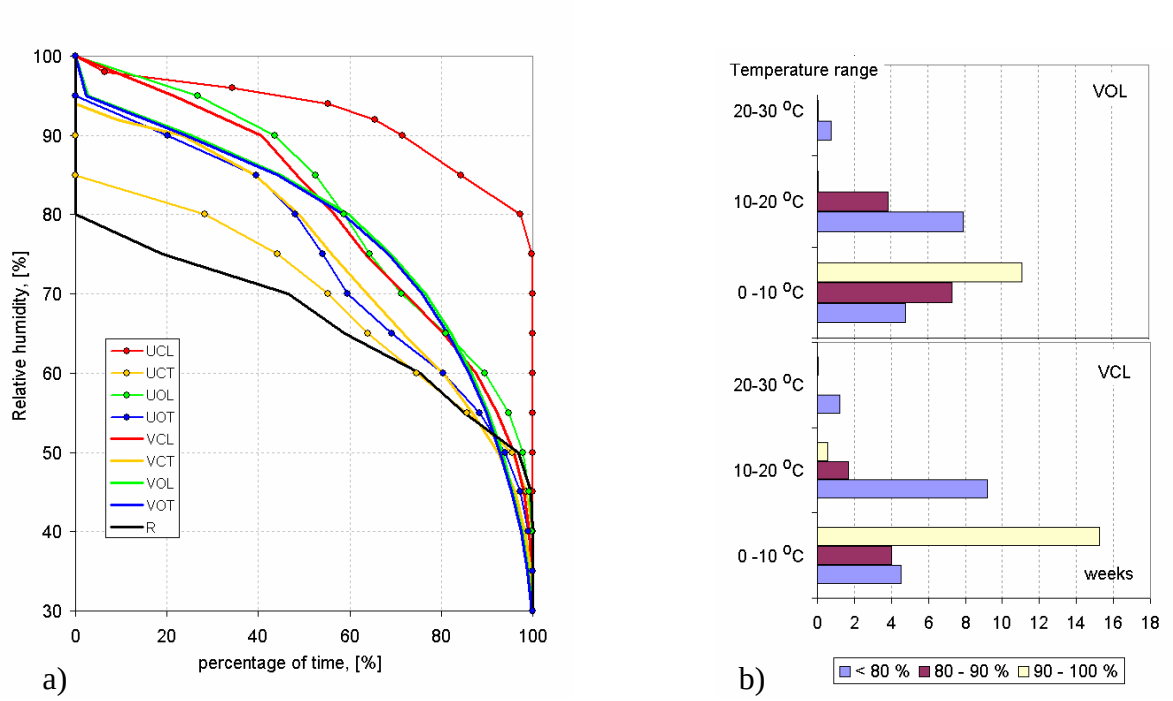

Figure 4 a) Results for the air relative humidity for all cases, sorted in descending order. b) Duration of some characteristic ranges of relative humidity and temperature at internal wooden side of a southern roof slope, for ventilated attics in two different positions and with leakages from a dwelling.

References

Arfvidsson, J. and Harderup, L-E. (2005). Moisture Safety in Attics Ventilated by Outdoor Air. The 9th Symposium in Building Physics, Island.

ASHRAE. (1997). *The Book of Fundamentals*. American Society of Heating, Refrigerating and Air-Conditioning Engineers. Atlanta. USA.

BBR. (2002). *Building code BFS 1993:57 with changes up till 2002:19*. In Swedish. Karlskrona, Sweden.

CEN/TC 89 WI 29.3. Hygrothermal performance of building components and building elements – Assessment of moisture transfer by numerical simulation. Draft.

Forest, T. W. and Walker I. S. (1995). Field Measurements of Ventilation Rates in Attics. *Building and Environment* **30:3**, 333-347.

Gustén, J. (1989). *Wind pressure on low-rise buildings*. Doctoral thesis. Chalmers University of Technology, Gothenburg, Sweden.

Hukka, A. and Viitanen, H. A. (1999). A mathematical model of mould growth on wooden material. *Wood Science and Technology* 33:6 475-485.

Larsson, L-E. (1996). Cold attics. Calculation model for moisture transfer analysis and practical implementations. In Swedish. Publication P-96:1. Department of Building Physics, Chalmers University of Technology, Sweden.

Mattsson, B. (2005). A sensitivity analysis of assumptions regarding the position of leakages when modelling air infiltration through an attic floor. The 9th Symposium in Building Physics, Island.

Orme, M., Liddament, M.W. and Wilson, A. (1998). *Numerical Data for Air Infiltration & Natural Ventilation Calculations, AIVC TN 44.* Air infiltration and Ventilation Centre, Coventry, England.

Samuelson, I. (1995). Hygrothermal performance of attics. In Swedish. SP Report 1995:68, Sweden.

Sasic Kalagasidis, A. (2004a). HAM-Tools. *An Integrated Simulation Tool for Heat, Air and Moisture Transfer Analyses in Building Physics.* Doctoral Thesis. Chalmers University of Technology, Gothenburg, Sweden. ISBN 91-7291-439-4.

Sasic Kalagasidis, A. (2004b). The whole model validation for HAM-Tools. Case study: hygro-thermal conditions in the cold attic under different ventilation regimes. 9th Int. Conference on Performance of the Exterior Envelopes of Whole Buildings. Clearwater Beach, Florida.

STEM (Swedish Energy Agency). (2001). Today's small houses in Sweden. In Swedish. Publications. Eskilstuna.

www. fluent. com

BLOWER DOOR MEASUREMENT OF LARGE BUILDINGS - WITH ONE OR MORE BLOWER SYSTEMS

Sigrid Dorschky, Paul Simons, Stefanie Rolfsmeier

BlowerDoor GmbH, Energie- und Umweltzentrum, D-31832 Springe, Germany

ABSTRACT

This article describes five blower door measurements – each made with a different objective – carried out on large buildings. Proof of air tightness is required to guarantee the operational capability of ventilation systems or to enable fire protection by nitrogen gas inerting. Air tightness measurements of large buildings can be carried out without difficulty using a number of blower systems. With appropriate planning it is easy to achieve very good values, because of the low A/V ratio in these particular buildings – e.g. the level of air tightness required for passive houses ($n_{50} > 0.6\ h^{-1}$) or even better.

KEYWORDS

Blower door, fire protection, energy, air tightness, ventilation systems, quality assurance

INTRODUCTION

The blower door system has been used to measure the air tightness of single-family houses in Germany since 1989. The applications and reasons for measuring air tightness are varied: quality assurance, production of expert reports and provision of energy advice, avoidance of convection-related building damage as well as protection against allergens in the home. Similar experience with apartment buildings (multiple dwellings) has been gained since 1991. Since the introduction of the Energy Saving Directive [EnEV 2002], the air tightness of large administration and industrial buildings is increasingly being checked too – and not just on energy-related grounds: quality assurance, sealing of clean rooms and fire protection are becoming more and more important.

DESCRIPTION OF THE BUILDINGS

The large buildings described here are distributed throughout the whole of Germany. A number of blower door systems had to be used for the measurement of each building.

Figure 1: External view of Building A, installation of 5 (out of 7) blower door systems: either 2 or 3 units were installed per external door opening using an aluminium frame and special panels (2 or 3-hole panels)

TABLE 1
Building data and photographs of the measured buildings

Building No.	Building data and installed number of blower doors	Photograph of the building
Building A	Care Centre in Karlsruhe, Baden-Württemberg, built 2004, proof of tightness required in accordance with [EnEV 2002] (building with ventilation system): $n_{50\ max.} \leq 1.5\ h^{-1}$ Volume (internal): 27,400 m³ 7 blower door systems installed	
Building B	Industrial building in Cloppenburg, Lower Saxony, built 2004, proof of tightness required to guarantee effective function of ventilation system: $n_{50\ max.} \leq 1.5\ h^{-1}$ Volume (internal): 17,100 m³ 3 blower door systems installed	
Building C	Office building in Hamm, North Rhine-Westphalia, built 2003, quality assurance of the air barrier at the construction phase: envisaged limit in accordance with [DIN 4108-7] (building with natural ventilation) $n_{50\ max.} \leq 3\ h^{-1}$ Volume (internal): 31,500 m³ 3 blower door systems installed	
Building D	Industrial building in Brunswick, Lower Saxony, built 2002, proof of tightness required in accordance with passive house standard ("zero emission building", with ventilation system): $n_{50\ max.} \leq 0.6\ h^{-1}$ Volume (internal): 46,500 m³ 4 blower door systems installed	
Building E	Industrial warehouse in Marl, North Rhine-Westphalia, built 2004, proof of tightness for fire prevention system (gas inerting by injection of nitrogen) required: $n_{50\ max.} \leq 0.02\ h^{-1}$ Volume (internal): 191,000 m³, 1 blower door installed	

METHODOLOGY

We were commissioned to carry out a blower door measurement each time in accordance with [EN 13829] and to determine the n_{50} (air change rate per hour at a 50 Pa pressure difference). The number of blower door systems required was determined as follows:

Allowed air flow rate at 50 Pa = Volume V x $n_{50\ max.}$

No. of blower systems = allowed air flow at 50 Pa / max. blower door capacity [TEC]

If the building is leakier than planned, i.e. the $n_{50\ max.}$ figure is exceeded, the 50 Pa pressure difference cannot be created with the calculated number of fans.

Example – Building A (uncorrected volume advised by the client):

35,000 m³ x 1.5 h^{-1} = 52,500 m³/h

52,500 m³/h / 7200 m³/h at 50 Pa = 7.3 blower systems

Several blower units were installed per door opening. Airtight nylon panels with 2 or 3 fan holes are provided for this, with the panels installed in external door openings using adjustable aluminium frames. If internal doors create a pressure drop within the building, the blower systems have to be distributed around the building shell. The measurement then has to be carried out by a number of people who can communicate with each other by mobile phone. In other cases, the blower door systems can be installed at a single point and operated by just one person.

Figure 2: External view, installation of 3 blower door units in one external door

Figure 3: Internal view; aluminium frame with 2 middle cross bars; 3 blower door units (open, without reducing rings); APT 8 - Automated Performance Testing system in case; notebook with TECLOG and BlowerDoor plus

More people are needed to check the complete building envelope at approx. -50 Pa depressurization for large leakages and failings of temporarily sealed openings (preliminary check in accordance with [EN 13829], 5.3.1). By completion of the building preparation, some fans could gradually be switched off and covered on 2 of the buildings, e.g. on Building D, after fully closing and securing the sliding gates (2 of the 4 installed blower systems), on Building C after closing a number of windows that had opened under depressurization because they were not completely locked (2 of the 3 installed blower systems).

The readings (natural pressure difference, pressure difference sequence) were recorded with the TECLOG logging program and then analysed with the BlowerDoor-plus Excel worksheet and the test report prepared. [EN 13829].

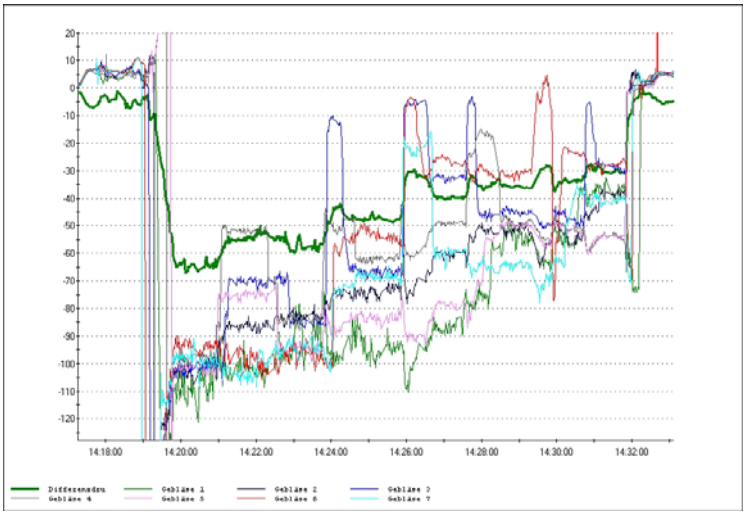

Figure 4: Building A, recording of the pressure difference sequence with TECLOG: natural pressure difference, applied pressure differences -65 to -30 Pa (green fat line), fan pressures of 7 fans

Blower door												
Number			1	2	3	4	5	6	7	8		
Model:	3 or 4		4	4	4	3	4	4	4			
Fan Configuration:	0, A, B, C, D, E		0	0	0	0	0	0	0			
Fan Configuration coefficient:		C [m³/hPa]	682.73	682.73	682.73	818.24	682.73	682.73	682.73			
Fan Configuration exponent:		n	0.4993	0.4993	0.4993	0.4947	0.4993	0.4993	0.4993			
Readings Building		**Readings BlowerDoor**									**Summary**	
											V_{Fan}	Δp_{Fan}
zero flow Δp_0	-4.7	--	--	--	--	--	--	--	--	--	--	--
Δp_1 [Pa]	-64.4	$\Delta p_{Fan,i}$ [Pa]	108.6	102.4	102.0	98.1	101.5	94.0	98.0		--	--
	--	$V_{Fan,i}$ [m³/h]	7091.5	6886.4	6872.9	7909.7	6856.1	6598.3	6737.0		48952	5202.9
Δp_2 [Pa]	-53.7	$\Delta p_{Fan,i}$ [Pa]	102.1	86.4	70.5	52.3	74.9	99.2	101.9		--	--
	--	$V_{Fan,i}$ [m³/h]	6876.3	6326.3	5715.4	5794.6	5890.8	6778.1	6869.6		44251	4250.4
Δp_3 [Pa]	-57.1	$\Delta p_{Fan,i}$ [Pa]	89.1	82.9	85.3	84.5	94.3	97.1	94.4		--	--
	--	$V_{Fan,i}$ [m³/h]	6424.3	6197.0	6286.0	7346.8	6608.8	6706.1	6612.3		46181	4629.8
Δp_4 [Pa]	-47.5	$\Delta p_{Fan,i}$ [Pa]	93.9	74.0	66.6	61.6	83.4	52.8	68.4		--	--
	--	$V_{Fan,i}$ [m³/h]	6594.8	5855.4	5555.3	6283.3	6215.7	4947.2	5629.8		41081	3662.5
Δp_5 [Pa]	-35.7	$\Delta p_{Fan,i}$ [Pa]	54.4	51.3	45.0	47.4	49.9	31.3	64.3		--	--
	--	$V_{Fan,i}$ [m³/h]	5021.5	4876.5	4567.7	5519.4	4809.6	3810.4	5458.7		34064	2516.8
Δp_6 [Pa]		$\Delta p_{Fan,i}$ [Pa]									--	--
	--	$V_{Fan,i}$ [m³/h]									0	0.0
Δp_7 [Pa]		$\Delta p_{Fan,i}$ [Pa]									--	--
	--	$V_{Fan,i}$ [m³/h]									0	0.0
Δp_8 [Pa]		$\Delta p_{Fan,i}$ [Pa]									--	--
	--	$V_{Fan,i}$ [m³/h]									0	0.0
zero flow Δp_0	-4.5	--	--	--	--	--	--	--	--	--	--	--

Figure 5: Building A, entry of the depressurization readings in BlowerDoor-plus: difference pressures and fan pressures / air flow rate of the 7 BlowerDoor systems

RESULTS

Table 2
Number of blower door units used / air tightness results

Building	Number of blower door units installed/required	Measured air flow rate (m^3 / h)	Measured n_{50} (h^{-1})	Target value of n_{50} not to be exceeded (h^{-1})
Building A	7 / 7	45,111	1.6	1.5
Building B	3 / 3	22,260	1.3	1.5
Building C	3 / 1	6,742	0.21	1.5
Building D	4 / 2	10,089	0.22	0.6
Building E	1 / 1 (low flow ring A)	2,613	0.014	0.02

For an international comparison of the results, e.g. with the publications from GB [AIR 2004], [AIVC Prague 2004], the results of the air permeability q_{50} (per envelope area A_E) in addition would have been meaningful, but A_E values were not determined during these investigations.

DISCUSSION

Building A: proof of tightness in accordance with EnEV not achieved

The care centre was built using traditional methods of construction without special regard for air tightness. Because a ventilation system was installed and included in the heat requirement analysis, proof of air tightness is obligatory. The air tightness limit was just exceeded and remedial works were necessary. The measurement itself was very expensive as 7 blower door units had to be installed to deliver the required leakage flow. By installing 2x2 and 1x3 fans in parallel, the measurement could be carried out with 3 people.

Building B: securing effective operation of ventilation systems

The industrial building under test, located near Cloppenburg in Lower Saxony, has an internal volume of 17,100 m^3 and is used for producing special cables. The building is equipped with an ultramodern ventilation system. The precondition for satisfactory operation of this ventilation system is a sufficiently airtight building envelope (in this case an air change rate of less than 1.5 h^{-1} at a building pressure difference of 50 Pa), to allow controlled air distribution . Using three blower door systems (maximum total capacity of around 24,000 m^3/h) a air flow rate of 22,000 m^3/h was measured under test conditions, corresponding to an air change rate of 1.3 h^{-1}. As a result, adequate air tightness of the building envelope – as the precondition for correct performance of the ventilation system - could be successfully proved.

Building C: quality assurance

The administration building in Hamm with an internal volume of 31,000 m^3 could be measured with just one blower door unit (initial calculations indicated that four units would be required) and achieved excellent results – because there was a very good air tightness design concept. The air tightness constructional details were examined by the author at the design stage and suggestions for improvement were made.

Building D: high energy efficiency

An early blower door measurement (preliminary measurement of the air barrier) was carried out during the construction phase on the zero-emission industrial building (internal volume approx. 46.500 m^3). This was necessary because, besides the thermal insulation, the air

tightness of the building is an essential factor in ensuring high energy efficiency. The planned controlled ventilation with heat recovery can only achieve its aim if the air exchange for provision of the required clean, fresh air actually takes place via the heat exchanger and not through joints and cracks. Following remedial works, two of the four blower door units could be switched off during the course of the measurement – the final measurement was carried out with just two blower door systems.

Building E: fire protection

The industrial warehouse in Marl with an internal volume of around 190,000 m³ is protected by a fire prevention system (gas inerting). By injecting nitrogen, this system reduces the oxygen content in the warehouse to such an extent that a fire is no longer possible. As a result, no sprinkler system is required. Instead, extremely demanding requirements are imposed with regard to air tightness: under the terms of the contract, the facade – made from mineral fibre sandwich panels – must not exceed an air change rate of 0.02 h^{-1} at 50 Pa (n_{50}). Once again here - because of the tightness of the building envelope– this meant that a single blower door system was adequate for the required proof: 2,613 m³/h were delivered with low flow ring A, an air flow rate specified as standard for multiple-dwellings in the [EnEV 2002].

CONCLUSION

The measurement results show that - with a good air tightness design concept - the cost of the measurement is low and the capacity of one blower door system (7800 m³/h) is often sufficient. Where there is no real design concept and the buildings are very large and leaky, air tightness measurements are carried out with up to eight systems. For the measurements, up to three blower door units can be installed in the sturdy aluminium frame per door opening, or they can be distributed individually over the openings in the facade (ground floor), according to the characteristic properties of the building.

REFERENCES

[EN 13892]: European Committee for Standardization: EN 13829: Thermal performance of buildings – Determination of air permeability of buildings – Fan pressurization method (ISO 9972:1996, modified). Brussels, Nov. 2000.

[DIN 4108-7]: Normenausschuss Bauwesen (NABau) im DIN Deutsches Institut für Normung e.V.: DIN 4108-7: Wärmeschutz und Energie-Einsparung in Gebäuden. Teil 7: Luftdichtheit von Gebäuden, Anforderungen, Planungs- und Ausführungsempfehlungen sowie -beispiele. Berlin 2001.

[TEC] The Energy Conservatory / BlowerDoor GmbH: Manual/Handbuch Minneapolis BlowerDoor. Minneapolis/Springe-Eldagsen 1988-2005.

[EnEV 2002]: Bundesregierung: Verordnung über energiesparenden Wärmeschutz und energiesparende Anlagentechnik bei Gebäuden (Energieeinsparverordnung – EnEV). Vom 16. November 2001. Berlin.

[AIR 2004]: S. Sharples and S. Class, Airtightness: the largest building ever tested. In: IEA AIVC (publisher): Air Information Review Vol. 25, No. 3, June 2004. Brussels.

[AIVC Prague 2004]: S. Sharples and C. Goodacre, Air leakiness of non-standard housing: impact of upgrading measures. In: 25th AIVC Conference Ventilation and Retrofitting – Proceedings. Brussels, 2004.

Airtightness of Commercial Buildings in the U.S.

Steven J. Emmerich and Andrew K. Persily

Building and Fire Research Laboratory, National Institute of Standards and Technology
Gaithersburg, MD, USA

ABSTRACT

In 1998, Persily published a review of commercial and institutional building airtightness data that found significant levels of air leakage and debunked the "myth" of the airtight commercial building. This paper updates the earlier analysis for the United States by including data from over 100 additional buildings. The average airtightness of 28.4 $m^3/h \cdot m^2$ at 75 Pa is essentially the same as reported by Persily in 1998. This average airtightness is in the same range as that reported for typical U.S. houses and is also similar to averages reported for commercial buildings built in the United Kingdom prior to recent airtightness regulations. Additionally, the trend of taller buildings being tighter and the lack of correlation between year of construction and building air leakage observed are consistent with the earlier report. This new analysis also found a trend (with considerable scatter) towards tighter buildings in colder climates. Although this study more than doubles the number of buildings in the air leakage database, any conclusions from this analysis are still limited by the number of buildings and lack of random sampling.

KEYWORDS

Airtightness, commercial buildings, infiltration, ventilation

INTRODUCTION

Persily (1998) published a review of commercial and institutional building airtightness data that found significant levels of air leakage and debunked the "myth" of the airtight commercial building. That analysis also failed to support correlations between airtightness and building age or construction. This paper updates the earlier analysis by adding over 100 U.S. buildings – more than doubling the number of U.S. buildings in the database.

Many discussions in the popular press and the technical literature still refer to commercial and institutional buildings, and newer buildings in particular, as being airtight. "Tight buildings" often are blamed for a host of indoor air quality problems including high rates of health complaints and more serious illnesses among building occupants. Furthermore, discussions and analyses of energy consumption in commercial and institutional buildings frequently are based on the assumption that envelope air leakage is not a significant portion of the energy used for space conditioning. These statements are almost never supported by any test data or airflow analysis for the buildings in question.

Building envelope airtightness is also one critical input to building airflow models, such as CONTAM (Dols and Walton 2002), which predict air leakage rates through the building envelope induced by outdoor weather and ventilation system operation. These predicted

airflow rates can be used to estimate the energy consumption associated with air leakage and to investigate the potential for energy savings through improvements in envelope airtightness and in ventilation system control (Emmerich et al. 2005). Importantly, these airflow rates can also be used to predict indoor contaminant levels and occupant exposure to indoor pollutants, and to evaluate the impacts of various indoor air quality control strategies. Therefore, it is important to have reliable values of envelope airtightness for commercial and institutional buildings.

In mechanically ventilated buildings, a tight envelope is desirable, as envelope leakage has several potentially negative consequences. These include uncontrolled and unconditioned outdoor air intake, thermal comfort problems, material degradation and moisture problems that can lead to microbial growth and serious indoor air quality problems.

This paper reports on the analysis of measured envelope airtightness data from over 200 U.S. commercial and institutional buildings assembled from both published literature and previously unpublished data. The buildings include office buildings, schools, retail buildings, industrial buildings and other building types. It is the largest such collection and analysis that has been presented to date. This paper summarizes the data, analyzes the data for trends, and compares the results to the earlier study.

MEASURING ENVELOPE AIRTIGHTNESS

The airtightness of building envelopes is measured using a fan pressurization test in which a fan is used to create a series of pressure differences across the building envelope between the building interior and the outdoors. The airflow rates through the fan that are required to maintain these induced pressured differences are then measured. Elevated pressure differences of up to 75 Pa are used to override weather-induced pressures such that the test results are independent of weather conditions and provide a measure of the physical airtightness of the exterior envelope of the building.

ASTM Standard E779 (ASTM 1999) is a test method that describes the fan pressurization test procedure in detail, including the specifications of the test equipment and the analysis of the test data. In conducting a fan pressurization test in a large building, the building's own air-handling equipment sometimes can be employed to induce the test pressures. A Canadian General Standards Board test method, CGSB 149.15, describes the use of the air-handling equipment in a building to conduct such a test (CGSB 1996). In other cases, a large fan is brought to the building to perform the test such as described by the Chartered Institution for Building Services Engineers' test method, CIBSE TM-23 (CIBSE 2000).

Often, the test results are reported in terms of the airflow rate at some reference pressure difference divided by the building volume, floor area or envelope surface area. Such normalization accounts for building size in interpreting the test results. In other cases, the pressure and flow data for measurements performed at multiple pressure differences are fitted to a curve of the form:

$$Q = C \cdot \Delta p^n \qquad (1)$$

where Q is the airflow rate, Δp is the indoor-outdoor pressure difference, C is referred to as the flow coefficient, and n is the flow exponent. Once the values of C and n have been

determined from the test data, the equation can be used to predict the airflow rate through the building envelope at any given pressure difference.

The airtightness data presented here are collected from a number of different studies that use different units and reference pressure differences. The results are presented here as airflow rates at an indoor-outdoor pressure difference of 75 Pa normalized by the above-grade surface area of the building envelope. When necessary, this conversion was based on an assumed value of the flow exponent of 0.65. The values of envelope airtightness are given in units of $m^3/h \cdot m^2$, which can be converted to cfm/ft^2 by multiplying by 0.055.

DATA AND DISCUSSION

Table 1 contains a summary of the air leakage data for the 201 U.S. commercial and institutional buildings that are considered here. Sources of data included 9 buildings tested by NIST (Persily and Grot 1986, Persily et al. 1991, Musser and Persily 2002), 90 buildings tested by the Florida Solar Energy Center (Cummings et al. 1996 and 2000), 2 buildings tested by Pennsylvania State University (Bahnfleth et al. 1999) 23 buildings tested by Camroden Associates (Brennan et al. 1992 and previously unpublished data), and 79 buildings tested by the U.S. Army Corps of Engineers (previously unpublished data including some partial school buildings). The buildings were tested for a variety of purposes and were not randomly selected to constitute a representative sample of U.S. commercial buildings. None of the buildings are known to have been constructed to meet a specified air leakage criterion, which has been identified as a key to achieving tight building envelopes in practice.

TABLE 1
Summary of Building Characteristics and Airtightness Data

		Air Leakage at 75 Pa ($m^3/h \cdot m^2$)			
Dataset	#	Mean	Standard Deviation	Min	Max
NIST	9	15.1	11.5	3.9	43.3
FSEC	88	41.7	34.3	4.0	168
Brennan	23	14.0	13.3	2.7	60.6
ACoE	79	19.7	10.3	3.4	63.4
PSU	2	9.8	0.4	9.5	10.1
All buildings	**201**	**28.4**	**35.8**	**2.7**	**168**

As seen in Table 1, the average air leakage at 75 Pa for the 201 buildings is 28.4 $m^3/h \cdot m^2$, which is essentially the same as the average of 28.7 $m^3/h \cdot m^2$ for U.S. buildings included in the earlier analysis by Persily. This average airtightness is tighter than the average of all U.S. houses but leakier than conventional new houses based on a large database of residential building airtightness (Sherman and Matson 2002). The average of the U.S. commercial buildings is also similar to averages reported by Potter (2001) of 21 $m^3/h \cdot m^2$ for offices, 32 $m^3/h \cdot m^2$ for factories and warehouses, and 26.5 $m^3/h \cdot m^2$ for superstores built in the United Kingdom prior to new building regulations which took effect in 2002.

The airtightness data were also analyzed to assess the impact of a number of factors on envelope airtightness including number of stories, year of construction, and climate. It is

important to note that the lack of random sampling and sample size limits the strength of any conclusions concerning the impacts of these factors. Also, not all of these parameters were available for all buildings in the database. Figure 1 is a plot of the air leakage at 75 Pa vs. the reported number of stories of the building and shows a tendency toward more consistent tightness for taller buildings. The shorter buildings display a wide range of building leakage. This result is consistent with the earlier analysis by Persily (1998).

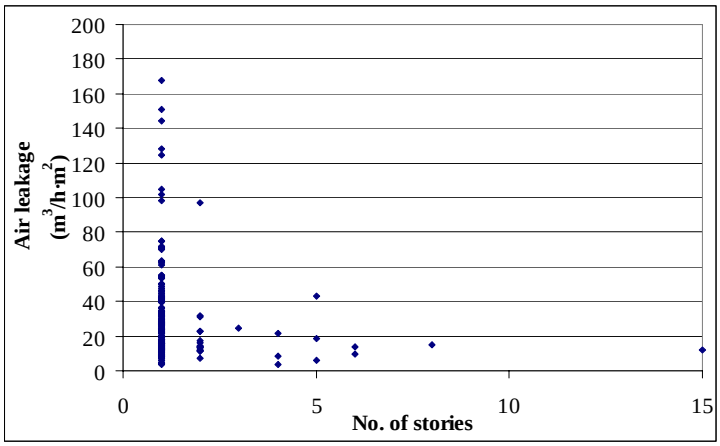

Figure 1: Normalized building air leakage vs. height of building (in stories)

Figure 2 is a plot of the air leakage at 75 Pa vs. the year of construction of the building for buildings built more recently than 1955. While common expectation is that newer commercial buildings must be tighter than older ones, the data simply give no indication that this is true. This result is also consistent with the earlier analysis by Persily (1998) despite the addition of numerous newer buildings in this dataset.

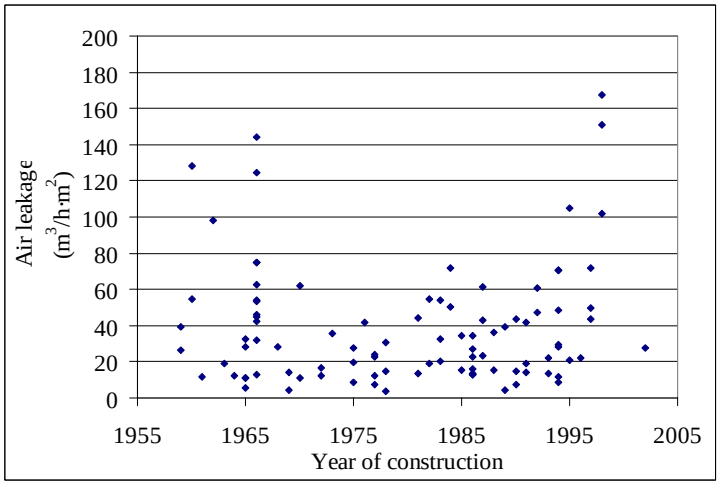

Figure 2: Normalized building air leakage vs. year of construction

Figure 3 is a plot of the air leakage at 75 Pa vs. the climate where the building is located as measured by annual heating degree-days base 18 °C for buildings of 3 stories or fewer (189 of the buildings). Approximate heating degree-day values were used for some of the building as either the locations were not precisely known or they were in locations without published heating degree-day data. Although the data show considerable scatter, they do indicate a general trend toward somewhat tighter constructions in the colder climates. The average air leakage was 33 $m^3/h \cdot m^2$ for buildings in locations with less than 2000 heating

degree-days compared to 18 $m^3/h \cdot m^2$ for building in locations with more than 2000 heating degree-days. Although there are data from numerous locations, there are little data from the northern U.S. and even less from the western U.S. If possible, future efforts should focus on collecting data in those regions.

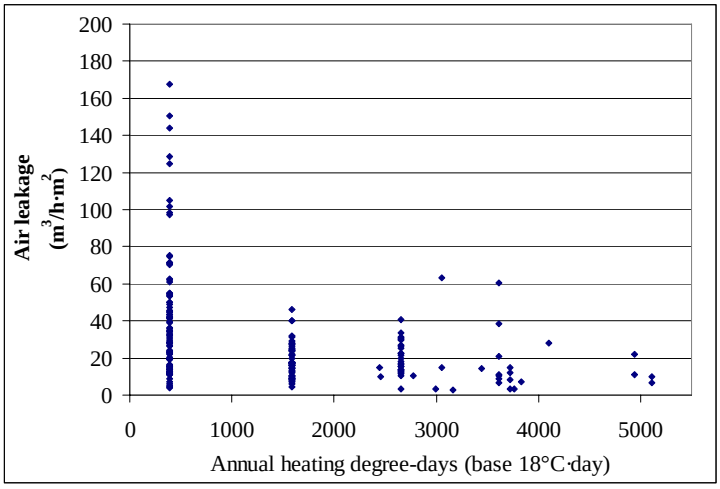

Figure 3: Normalized building air leakage vs. climate (in heating degree-days base 18 °C).

SUMMARY

This paper presents a summary of available measured U.S. commercial and institutional building airtightness data. The overall average airtightness of 28.4 $m^3/h \cdot m^2$ at 75 Pa is essentially the same as reported by Persily in 1998. This average airtightness is in the same range as that reported for typical U.S. houses and is also similar to averages reported for commercial buildings built in the United Kingdom prior to recent airtightness regulations. Additionally, the trend of taller buildings being tighter and the lack of correlation between year of construction and building air leakage observed are consistent with the earlier report. This study also found a trend (with considerable scatter) towards tighter buildings in colder climates. Although this study more than doubles the number of buildings in the air leakage database, any conclusions from this analysis are still limited by the number of buildings and lack of random sampling.

ACKNOWLEDGMENTS

This work was sponsored by the US. Department of Energy, Office of Building Technologies under Agreement No. DE-AI01-01EE27615. The authors acknowledge the contributions of data from Terry Brennan of Camroden Associates, James Cummings of Florida Solar Energy Center and Donald Dittus of the U.S. Army Corps of Engineers.

REFERENCES

ASTM. (1999). E779-99, Standard Test Method for Determining Air Leakage Rate by Fan Pressurization. West Conshohocken, PA: American Society for Testing and Materials.

Bahnfleth, W.P., Yuill, G.K. and Lee, B.W. (1999). "Protocol for Field Testing of Tall Buildings to Determine Envelope Air Leakage Rate," ASHRAE Transactions, Vol. 105 (2).

Brennan, T., Turner, W., Fisher, G., Thompson, B., and B. Ligman. (1992). “Fan pressurization of school buildings.” Proceedings of Thermal Performance of the Exterior Envelopes of Buildings V, American Society of Heating, Refrigerating and Air-Conditioning Engineers, Inc., pp. 643–45.

CGSB. (1996). *CAN/CGSB-149.15-96, Determination of The Overall Envelope Airtightness of Buildings by the Fan Pressurization Method Using the Building’s Air-Handling Systems*. Canadian General Standards Board.

CIBSE. (2000). *TM-23, Testing Buildings for Air Leakage*. The Chartered Institution of Building Services Engineers.

Cummings, J.B., Withers, C.R., Moyer, N., Fairey, P. and B. McKendry. (1996). Uncontrolled Airflow in Non-residential Buildings. Florida Solar Energy Center, FSEC-CR-878-96.

Cummings, J.B., Shirey, D.B., Withers, C., Raustad, R. and Moyer, N. (2000). *Evaluating the Impacts of Uncontrolled Air Flow and HVAC Performance Problems on Florida's Commercial and Institutional Buildings*, Final Report, FSEC-CR-1210-00.

Dols, W.S., and Walton, G.N. (2002). *CONTAMW 2.0 User Manual. Multizone Airflow and Contaminant Transport Analysis Software*. NISTIR 6056.

Emmerich, S.J., McDowell, T., and Anis, W. (2005). *Investigation of the Impact of Commercial Building Envelope Airtightness on HVAC Energy Use*. NISTIR 7238.

Musser, A. and Persily, A. (2002). Multizone Modeling Approaches to Contaminant-Based Design. Proceedings of ASHRAE Transactions Vol. 108.2.

Persily, A.K. (1998). Airtightness of Commercial and Institutional Buildings: Blowing Holes in the Myth of Tight Buildings. Proceedings of Thermal Performance of the Exterior Envelopes of Buildings VII, pp. 829-837.

Persily, A.K. and Grot, R.A. (1986). “Pressurization testing of federal buildings.” Measured Air Leakage of Buildings, ASTM STP 904, H.R. Treschsel and P.L. Lagus, Eds., American Society for Testing and Materials, pp. 184-200.

Persily, A.K., Dols, W.S., Nabinger, S.J. and Kirchner, S. (1991). Preliminary Results of the Environmental Evaluation of the Federal Records Center in Overland Missouri. NISTIR 4634.

Potter, N. (2001). Air Tightness Testing – A Guide for Clients and Contractors. BSRIA Technical Note 19/2001.

Sherman, M.H. and Matson, N.E. (2002). Airtightness of New U.S. Homes: A Preliminary Report. LBNL-48671, Lawrence Berkeley National Laboratory.

AIRTIGHTNESS FIELD MEASUREMENT STUDY OF 123 NEW FRENCH DWELLINGS WITH A SIMPLIFIED MEASURING DEVICE

Andrés LITVAK [1]* – Anne VOELTZEL [2] – Xavier BOULANGER [3]
Robert MARKIEWICZ [4] – Bruno-Gilbert ROYET [5]

[1] *CETE Sud Ouest – Département Aménagement et Infrastructures Rue P. Ramond – Caupian BP C 33165 SAINT MEDARD EN JALLES Cedex FRANCE*

[2] *CETE de Lyon – Département Villes et Territoires 46, rue St Théobald BP 128 38081 L'ISLE d'ABEAU Cedex FRANCE*

[3] *ALDES AERAULIQUE Prologue 2, rue Ampère BP 9707 31312 LABEGE Cedex FRANCE*

[4] *CETE Nord Picardie – Département Villes et Territoires 2, rue de Bruxelles – BP 275 59019 LILLE FRANCE*

[5] *CETE de l'Est – Laboratoire Régional de Strasbourg - BP 9 67035 STRASBOURG Cedex FRANCE*

* *corresponding author :* tel : int/ 33 5 56 70 66 40 fax : int/ 33 5 56 70 66 68 e-mail : andres.litvak@equipement.gouv.fr

ABSTRACT

Studies on buildings' airtightness have shown that several issues can arise from uncontrolled airflow leakages in buildings (e.g., higher energy cost, thermal comfort and health of occupants, building components and equipment preservation). The new French thermal regulation, RT2000, applicable since June 2001, has set explicitly airtightness performance levels for new buildings. Yet, buildings' airtightness performance knowledge is only possible by means of on site controls and measurements. A recent study has shown that the development of a simplified buildings' airtightness measuring devices (IMPEC), can reduce the duration and the number of people involved in the measurement controls, and therefore can significantly decrease the associated costs of controls.

In this work, we aim at developing an IMPEC in a commercial version and at performing a nation wide field measurement study in order to increase the knowledge of the construction field actors both on the airtightness performance of new French dwellings and on the availability of lower cost controls. We present the characteristics of an automated model of IMPEC, developed under the brand PERMEASCOPE®. The IMPEC's measurement protocol is based on dwellings' depressurisation by means of a portable fan connected to the air distribution systems, through the kitchen or bathrooms ventilation exhausts. The results of a field measurement study of the airtightness of 123 new French dwellings are presented and compared to the results of former studies. Finally, we discuss the control performances of IMPEC devices in terms of potentials to reduce negative impacts on energy consumption and occupant's health and comfort.

KEYWORDS

Field measurements ; Infiltration ; Airtightness ; Building Envelope ; Dwellings; Thermal Regulation

BACKGROUND

The negative impact of air infiltration through buildings envelope – namely, by negative consequences on occupant's health and comfort, on building systems and fabrics' pathologies and on energy consumption - has been thoroughly detailed in the literature. The French thermal regulation RT2000, applicable since June 2001, has set airtightness performance levels for new buildings. If regulatory thermal calculations account explicitly for airtightness performance levels, progress need yet to be done to develop means of controlling the effective performance of buildings. Indeed, development of reliable, simplified and low-cost

airtightness measurement tools has been identified as a necessary condition to widespread on site controls and therefore buildings' airtightness performances. A former work by CETE de LYON, ALDES and EDF has led to develop a pre-commercial version of a simplified dwelling airtightness measuring device (IMPEC), Litvak et al. (2002).

OBJECTIVES

In the continuity of former efforts on development of commercial versions of IMPEC with a view to widespread onsite measurement controls, this article presents a work of four Technical Study Center (CETE), as part of the technical and scientific network of the French ministry of Equipment, in partnership with ALDES. This work aims at answering to a double concern : to develop an IMPEC in a commercial version and to perform a nation wide field measurement study in order to increase the knowledge of the construction field actors both on the airtightness performance of new French dwellings and on the availability of lower cost controls.

METHODOLOGY

Airtightness indicators and air leakage assessment

The modelling of airflow patterns through cracks of the building envelope follows from the early works on hydrodynamics of pipes, that allowed to assess the airflow rates $Q_{[m^3/h]}$ through elementary holes, as a function of differential pressure between indoor and outdoor, $\Delta P_{[Pa]}$, see Eqn 1 :

$$\mathbf{Q = K \cdot \Delta P^n} \qquad \mathbf{(1)}$$

where $n_{[-]}$ and $K_{[m^3/h/Pa^{-n}]}$ are the flow exponential and the airtightness constant.

For their specific requirements, some European countries, including France with RT2000, have decided to consider the leakage index $I_{\Delta P}$ [m³/h/m²], defined as the infiltration airflow rate at ΔP_0 weighted by envelope surface areas the most susceptible to promote the infiltration of air leakages. In accordance to RT2000, we considered the specific *unheated surfaces*, defined as the *« surfaces that separate the indoor heated volume from the outdoor air and indoor unheated air, excluding the floor »*. For RT2000, leakage airflow rates are assessed by extrapolating to 4 Pa the Equation 1, determined by measurements in the pressure intervals [10-70 Pa] as recommended by the EN NF 13829 norm.

State-of-the-art of onsite measurement techniques

To date, the most reliable manner to determine the airtightness of a building consists in measuring its infiltration airflow rate. A standardized method, using a fan depressurization technique (known as the "blower-door method") is commonly used and follows the procedure described in the norm NF EN 13829. It consists in replacing a large opening of a dwelling (usually the doorway) by a "blower-door" frame, with an incorporated extracting fan capable of depressurizing the dwelling. All commercially available airtightness measuring devices are based on this "blower-door" technique. Yet, to our knowledge, very few commercially available devices are distributed in France to measure the airtightness of buildings' envelope.

The "blower-door technique" is particularly adapted to measure the air leakages in relatively small buildings. For larger constructions and/or extremely leaky buildings, the building depressurization usually becomes impossible, due to the power limitation of the fan. For this

buildings, CETE de Lyon has developed an equipment, unique in France, that measures infiltration airflow rates up to 65 000 m^3/h, Bringer (1997). One should know that this 5 meter long equipment is towed by a truck to operation site.

Although earlier studies have occasionally succeeded in depressurising large multi-family buildings with commercially available Blowerdoor devices, Litvak (2001), a main concern remains the capacity of assessing the airtightness of these types of buildings from individual measurements (e.g., apartment measurements), for technical and economical reasons. Yet to our knowledge, no work has determined an experimental relationship between individual and global measurements of multi family dwelling buildings. Since RT2000 mandatory performance levels refer exclusively to the whole building characteristics, such knowledge would offer valuable information in order to develop lower costs controls.

Measurement protocol

If the "Blowerdoor" technique appears to be a very accurate method to determine the infiltration airflow rate of a building's envelope, its main drawback remains the possible occultation of air infiltrations through the large opening where the extracting fan is mounted. The IMPEC's protocol, developed in this work and extensively described elsewhere, Litvak (2002), relies on the "Blowerdoor technique", but it connects to the mechanical ventilation network as exhaust, if available, or as an alternative, to a small trap in a wooden frame.

Figure 1. IMPEC onsite measurement protocols: connected to the mechanical ventilation network (left) or to a wooden "fake trap" (right)

The operative IMPEC's measurement protocol follows the recommendation of EN 13829. A field measurement campaign was led nationwide with 5 Perméascope®, a commercially available model of the IMPEC, distributed by ALDES, in order to assess the infiltration airflow rates of 123 new French dwellings. Complementary measurements were performed with a Minneapolis Blowerdoor® instrument, on 4 large multi family buildings of the sample, in order to compare global and individual dwelling measurements in these buildings.

Characteristics of the 123 nationwide dwelling sample

The main characteristics of the 123 dwellings, spread over 58 buildings and composed of 71 % of multi-family dwellings and 29% of single family dwellings, are presented in Table 1.

Single Exhaust Ventilation	Humidity Controlled Ventilation	Exhaust and Supply ventilation
42%	58%	0%
52	71	0

1	2	3	4	5	6
2%	24%	40%	25%	9%	0%
2	30	49	31	11	0

Number of main rooms of each dwelling

Electricity	Gas	other
41%	57%	2%
51	70	2

Type of Heating Energy

Masonry	Concrete	Timber frame	Metal frame
28%	67%	3%	2%
35	82	4	2

Building Structure

Table 1 : Characteristics of buildings and dwellings

FIELD MEASUREMENT RESULTS AND DISCUSSION$

Leakage pathway observations

The air leakage pathways of 123 dwellings were carefully investigated under the IMPEC's test depressurization conditions by qualitative observations. The onsite observations, from a total of 189, have been reported for each dwelling and were classified according to the occurrence of different air leakage pathway types. The most recurrent and major locations observed for air infiltration are the electrical conduits and window and door frames, see Figure 2.

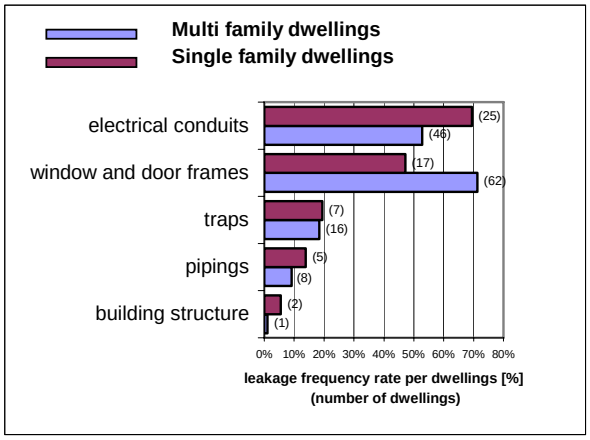

Figure 2 : Leakage pathway rate frequency

If these results corroborate the earlier findings on a field measurement study (performed with Minneapolis Blowerdoor® instruments) on airtightness of 71 French dwellings, Guillot (2000), a significant increase in air leakage pathways through doorway frames, as compared to this former study, shows evidence that this type of leakage can be occulted if measurements are performed with a conventional Blowerdoor technique, i.e. through a large opening such as a doorway.

Pressure test results

Median values of the measured I_4 indicators show good performances as related to the mandatory performance levels of RT2000 for airtightness for single family dwellings : 46% of the dwellings are more airtight than the *reference* value of 0.8 $m^3/h/m^2$, and 72% show better results than the *default* values of 1.3 $m^3/h/m^2$. As a reminder, one should note that all the dwellings (i.e., houses and apartments) were considered as single-family dwellings. These good results concern mainly concrete and masonry constructive types, which are more airtight than metal or timber frame, that have appeared to show lower performances in earlier work, Guillot (2000).

I_4 : single family dwellings = 0.77 $m^3/h/m^2$ (SD = 0.42)
I_4 : multi family dwellings = 1.06 $m^3/h/m^2$ (SD = 0.67)

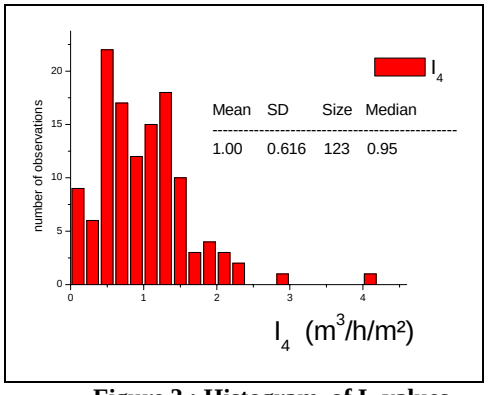

Figure 3 : Histogram of I_4 values

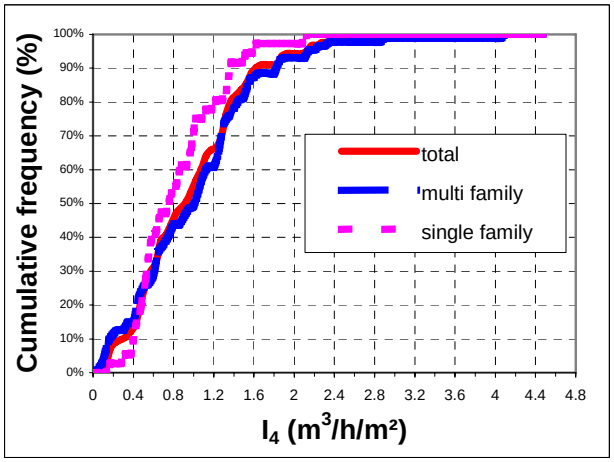

Figure 4 : Cumulative Frequencies of I_4 values

Potential improvements by corrective actions

The relationship between n and I_4, was studied both on the 123 measured values on individual dwellings and on the 4 multi family dwelling buildings. The observed hyperbolic-type decrease, see Figure 5, shows that a gain on the flow exponent from n = 0.60 (that represents turbulent regime caused by larger holes in the building envelope) to n = 0.66 (which is generally the median value observed in onsite measurements) can lead to a net gain of 60 % on I_4 :

$$I_4(0.60) / I_4(0.66) = 1.6 .$$

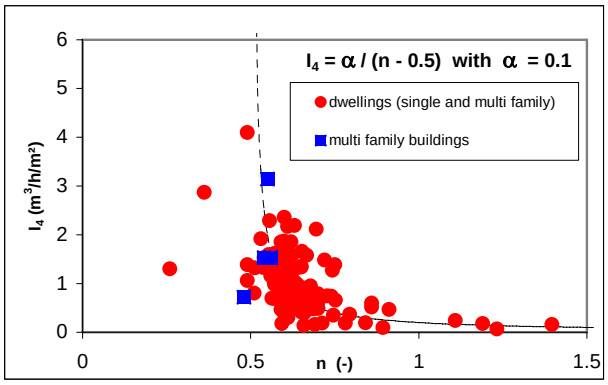

Figure 5. Influence of the flow exponent value on the infiltration rate. *The dotted line represents the hyperbolic fit $I_4 = 0.1 / (n-0.5)$*

In the ligh of this result, complementary onsite depressurizing tests have been performed on 14 dwellings, after sealing with adhesive tape the major air leakage pathways observed, namely through larger holes. The types of corrections concerned mainly door frames and doorsteps, window frames, electrical rack boards and traps. Results of these 14 complementary test show that simple sealing after onsite visual inspection, can lead up to 70% of improvement on the air infiltration rate I_4, with an observed median value of 36%. These results show that significant improvements on the airtightness performance of buildings can be done by very simple means, e.g. by sealing with pointing or adapted joints, major defects observed through the building envelope. Such observations can easily be achieved by quality control inspections associated with onsite measurement controls.

Relationship between individual airtightness measurements and building measurements

Individual measurements done with the IMPEC instrument (Perméascope®) among different dwellings of 4 buildings of the nationwide sample have been compared to the global building infiltration airflow rate measured with a Blowerdoor commercial instrument (Minneapolis Blowerdoor®). If no empirical relationship was assessed between these four cases, one can note that the (I_4 IMPEC, I_4 BD) measured couples show good correspondence with the RT2000 mandatory levels for single family dwelling and multi family dwelling buildings (respectively, 0.8 $m^3/h/m^2$ and 1.2 $m^3/h/m^2$), see Figure 6. This trend, that would need to be confirmed by further research, would then offer to regulatory performances an interesting correspondence with low cost means of control.

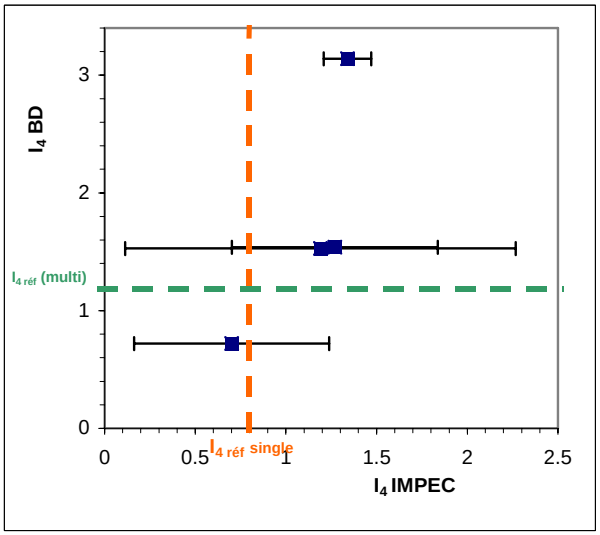

Figure 6. Comparison between individual apartment measurements – median values – done with IMPEC (I_4 IMPEC) and whole building measurement done with Blowerdoor instrument (I_4 BD). *The error-bars correspond to the standard deviation of the median values of the IMPEC's measurement on the different dwellings of the building. Measurements on individual dwellings with IMPEC were done on 3, 5 (twice) and 10 dwellings.*

Impact of airtightness on associated energy cost

Most of RT2000 thermal calculations of the 58 inspected buildings take into account a *default* value, 0.5 $m^3/h/m^2$ less airtight than the *reference* value of 0.8 $m^3/h/m^2$ for single family dwellings and 1.2 $m^3/h/m^2$ for multi family dwelling buildings. By accounting for this reference value, designers do not need to justify any airtightness performance. This late reason, coupled with frequent lack of knowledge on airtightness issues, makes the *reference* value to be the predominant choice for engineers in their RT2000 thermal calculations. Numerical simulations from 40 buildings of the field measurement sample (36 single family dwellings and 4 multi family dwellings) have been done through a sensitive analysis of airtightness on the RT2000 energy consumption coefficient C. Calculations have been done by modelling dwelling well known case studies and varying the airtightness airflow rate, when assessing the C coefficient with the engine of calculation developed by the CSTB, *THC 2000* (version 2.1.1). Detailed methodology has been described elsewhere, (Litvak, 2005). Results show that almost 75 % of the single family dwellings and 3 buildings out of 4 would improve the C coefficient by up to 6% for single family and 2% for multi family dwellings, if the actual (i.e. measured) airtightness value would have been chosen, instead of the default value leading to $C_{déf}$.

CONCLUSION AND FUTURE WORK

A commercial version of IMPEC, under the name Perméascope®, has been developed and tested successfully on a 123 dwelling nationwide field measurement campaign. The results corroborate earlier findings on the major infiltration locations and on the performance of concrete and masonry constructive types, that appear to be particularly airtight as referred to the present French thermal regulation RT2000. If, air infiltration impacts on energy consumption and hygienic air renewal are shown to be significant, simple corrective actions provided after measurement tests show that potentials for improving performance can reach up to 70%. Moreover, development of onsite low-cost measurement instruments, as part of quality assurance tools, appear to be a major solution to reduce the likelihood of infiltration pathways, caused by lack of care during the construction phase. It can also help designer to optimise the airtightness performance level in their regulation thermal calculations.

ACKNOWLEDGEMENTS

This work was supported by the Direction Générale de l'Urbanisme de l'Habitat et de la Construction (DGUHC) and by the Agence de l'Environnement et de la Maîtrise de l'Energie (ADEME), under contract n° 03 04 C 0120. The authors wish to thank Philippe LOHIER, Sébastien GUIRAUD, Michel BARBE, Bernard LAMARQUE (CETE Sud Ouest), Matthieu FOURNIER, Aline GAGNIARRE, Rémi CARRIE, Daniel LIMOGES, Sylvain BERTHAULT (CETE Lyon), Didier FLUCK, Fabrice CONIN (CETE Est) and Olivier LEMAITRE, Marc BRUANT, Laurent DELEERSNYDER (CETE Nord-Picardie) for their valuable contribution to the nationwide field measurement tests.

References

Bringer, J. (1997). Mesure de la perméabilité à l'air de bâtiments de grands volumes, CETE LYON, CERTU, 1997.
Guillot, K. (2000). Campagne de mesures de la perméabilité à l'air de 70 logements, CETE LYON, ADEME, 2000.
Litvak, A. (2001) Résultats de mesures de perméabilité à l'air sur un logement collectif – opération « Le Manguély » , CETE de LYON, novembre 2001
Litvak, A. (2002) Elaboration d'un instrument de mesure portable de l'étanchéité à l'air des constructions , CETE de LYON/ALDES/EDF, ADEME-PUCA, juin 2002
Litvak, A. (2005) Campagne de mesure de l'étanchéité à l'air de 123 logements , CETE Sud Ouest – report n°DAI.GVCH./05.10, ADEME-DGUHC
NF EN13829 (2001) . Performance thermique des bâtiments - Détermination de la perméabilité à l'air des bâtiments – méthode de pressurisation par ventilateur. AFNOR, 2001.

CRITERIA TO DEFINE LIMITS FOR BUILDING AIRTIGHTNESS

Airtightness of some Portuguese dwellings

Armando Pinto

Building Components Division, National Laboratory of Civil Engineering LNEC

Lisboa 1700-066, Portugal

ABSTRACT

The increasing concern on energy conservation in buildings and the increasing insulation level of buildings, lead to the introduction of limits for building airtightness, to minimize building heat losses. In some countries the recommended limits are very strict and could be difficult achieved with standard construction practices. Usually the limits are established according construction (best) practices and in some countries it takes in account the building type, ventilation system and weather. Usually those limits don't take in account the air flow rate for background ventilation.
In Portugal the concern about building airtightness is limited to air permeability of windows. In the study curried out it was assessed the importance of whole building airtightness, versus window air permeability and the importance of whole building airtightness to define limits that take in account, energy losses, indoor air quality and ventilation requirements and the action that promote the pressure difference across building envelope (wind actions, thermal buoyancy and ventilation systems).

KEYWORDS
Airtightness, Air permeability, Ventilation, Energy conservation, Natural ventilation, Mechanical ventilation

BUILDING AIRTIGHTNESS VS WINDOWS AIR PERMEABILITY

In Portugal since 1987 there are limits to windows air permeability Mimoso (1987). The air permeability of windows could have a relatively large range. For aluminium windows tested at LNEC (Pinto, 2002), the sliding windows on average belong to class 2 of air permeability (EN 12207: 1999), and the side hung casement on average belong to class 3.

If we suppose that the glazed area is 20% of the floor area, the air permeability of windows corresponds to n50 of 0.6 for sliding windows and 0.3 for side-hung, on average.

The airtightness of Portuguese buildings was first studied at FEUP by Afonso et al (1988), where it was measured the airtightness of 7 buildings (6 dwellings and 1 detached single family house), using the blower door test method (ISO 9972: 1996). In other study, it was measured the air tightness of 12 detached single houses, Silva (1991).

In the previous studies it wasn't assessed the importance of the air permeability of different components of building shell. To try to address the importance of windows in whole building airtightness, in this study, in four buildings, the airtightness was measured sealing windows and sealing the roller shutters boxes, the two major discontinuities in building shell. The results of those 4 tests show that the window air permeability is responsible for only 5 to 11% of building air leakage and that crack around roller shutters could be responsible for 15% to 50% air leakage, figure 1. In one building, with one anemometer, some of the remaining leaks

were identified in joints between floors and walls and electric pipes. This results are similar to other obtained in other countries, Wouters (1986), Moyé 1985), or obtained by extrapolation Orme (1999), ASHRAE (1997).

These results show that to minimise air leakage in building, it will be necessary to recommend limits to whole building airtightness and not only to some components, such as windows.

The air tightness of 23 Portuguese buildings is represented in figure 2. For apartments the n50 on average belong to the range 2 to 4, and in the detached dwellings n50 belong to the range 4 to 10, which mans an airtightness classified as average according to EN ISO 13790, but over some limits imposed in some European countries, justifying the studied of reasonable limits for airtightness of Portuguese buildings.

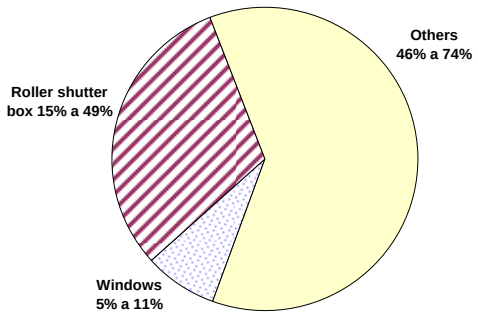

Figure 1 – Average leakage distribution in four buildings

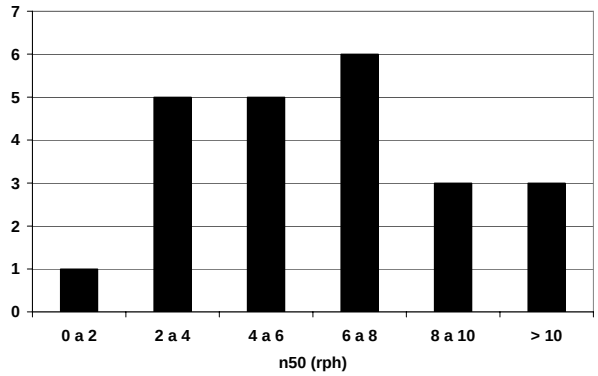

Fig.2 – n50 of 23 Portuguese buildings

CRITERIA TO DIFINE AIRTIGHTNESS OF BUILDINGS

In Portugal and other countries, the intake of fresh air for ventilation of residences usually is done directly from outdoor, using small opening, trickle ventilator. One first approach to define limits for building airtightness could be that the building air leakage should be less than the background ventilation rate (Q_b in m^3/h) at 10 Pa for building with natural and hybrid ventilation systems and 20 Pa for building with centralised mechanical ventilations systems, eqn 1 (**Criteria I**). The 10 Pa and 20 Pa, pressure difference are based on standards to design ventilation system (NP 1037-1:2000, NF XP P 50-410: 1995). This criteria when applied, gives very stringent airtightness limits for buildings, table 1.

$$n50 \le Q_b \times (50/20)^{0.67} \quad \text{for buildings with mechanical ventilation}$$
$$n50 \le Q_b \times (50/10)^{0.67} \quad \text{for buildings with natural or hybrid ventilation} \qquad (1)$$

The criteria I, doesn't take into account the action that promote air infiltrations so, another criterion could be: the limitation of air infiltration (total air flow rate) to the double of background flow rate under strong wind action, for example, for wind speed with a probability of being exceeded only on 5% of time, in one year (**Criteria II**) This criteria focus on the major concern of airtightness which is air infiltration in buildings, conservation of energy and thermal comfort. This second criteria lead to different limits according to building wind exposure and ventilation system.

To get wind effect on buildings, it was analysed the data of the test reference years of Lisbon and Paris (table 2), where we can see the larger difference in air temperature.

Since building have different exposure to wind, it was considerer 3 types of terrain, and 5 height, which gives the wind Reduction Factor ($U = RF \times U_{meteorological}$) presented in table 3 (BS 5925:1991). With this wind Reduction Factor and the wind speed exceeded only in 5% of the time (assure reasonable air infiltrations in 95% of the time) we can calculate the dynamic pressures of wind and define 8 classes of exposure to wind, table 3.

To define and appreciate the impact of building airtightness it was considered the four buildings indicated in table 1, and it was studied in more detail two buildings (table 4): one apartment building with two opposite façades exposed to wind (the most stringent) and one detached dwelling with four façades exposed to wind (the less stringent).

AIRTIGHTNESS FOR BUILDINGS WITH MECHANICAL VENTILATIONS SYSTEMS

To define the limits for "over ventilation" in buildings it was used a simple air flow network with one internal node and one node for each façade exposed to wind. In the simulations of mechanical ventilations system it was considered the 8 wind classes, continuous extraction of Q_b, the intake of fresh air trough trickle ventilator with the performance shown in figure 3 and the air infiltrations trough each façade given by the power low, eqn 2 (nfac, is the number of façades exposed to wind). For wind pressure coefficient it was adopted the data for the low-rise building (table F1, Orme, 1999) and the wind angle 0º.

With the results of the simulation (table 5), it was concluded that the limits for airtightness of buildings could be calculated by eqn 3, which is equivalent to limit the air flow trough crack around building envelope to Q_b. The limits obtained by eqn 3, are 6% lower than the limits obtained by the air flow network for P_{dyn}=80Pa and 25% lower for P_{dyn}=10Pa. The constants 47 and 63, are calculated by: $47 = 50^{0.67} \times 2/[(C_p0º - C_p180º)/2]$, $63 = 50^{0.67} \times 4/[C_p0º - (C_p0º + C_p90º + C_p180º + C_p270º +)/4]$).

$$Q = n50/nfac/50^{0.67} \times \Delta P^{0.67} \qquad (2)$$

$$n50 \le 47 \times Q_b/Vol \times (P_{dyn})^{0.67} \quad \text{for buildings with 2 exposed facades}$$

$$n50 \le 63 \times Q_b/Vol \times (P_{dyn})^{0.67} \quad \text{for buildings with 4 exposed facades} \qquad (3)$$

The application of these limits to case studies (table 4), gives the results presented in table 5, where we see the decrease of the requirements of building airtightness as wind exposure decrease. To test the validity of these limits, the two case studies were evaluated in more detail with ESP-r, for wind classes 1, 2, 5 and 8. For the wind class 5, it was studied four scenarios: 1, zero airtightness, only air intake devices; 2, air intake devices and criteria I of building airtightness; 3, air intake devices and n50 respecting criteria II; 4, air intake devices and n50 comply with criteria flow rate fourth of the background ventilation in no more than 5% of the time. In scenarios 5, 6, 7 air intake devices and n50 comply with criteria II.

From ESP results (table 6) we can conclude:

- It is reasonable to recommend limits that depend of wind exposure and depend on the number of façades exposed to wind;
- The limit of the air infiltration to the double of background ventilation in less than 5% of the time seems reasonable, because if we admit 4 times the background ventilation (case 4) we have a large increase on heating demand (internal air temperature of 20ºC);
- If we compare criteria I (case 2) with the other cases satisfying criteria II we observe a slight increase on heating demand. But this slight increase could be overcome if the number of air intake devices is reduced proportionally to the airtightness;

AIRTIGHTNESS FOR BUILDINGS WITH NATURAL VENTILATIONS SYSTEMS

The limit for airtightness in building with natural ventilations systems is relatively more cumbersome to achieve, because in a first stage we must assure the background ventilation rate in more than 50% of the time between November and April (the heating season) and we should also limit the over ventilation because of thermal comfort, and energy consumption.

To limit air leakage it was considered the trickle ventilator (figure 3). To calculate the number of trickle ventilator to assure the background ventilation rate it was used the model ESP-r. The air flow trough chimneys was evaluated using the model ($m=C.\rho.\Delta P^{0.5}$) with a stack height of 5 m, where the values of C comply with NP 1037-1 (C=46 for chimney in kitchen and 21 for chimney in bathroom). In the detached dwelling it was considered a larger chimney in kitchen with C of 110 and C of 21 for the 3 bathrooms. The cowl was simulated with the model of Gonzales (1984), (∅300mm, C_p=-0.55, ζ=1.22, B=0.8, n=0.18).

In ESP-r were analysed four scenarios: case 1, determination of the number of air intake devices to get background ventilation in 50% of the time between November and April, with zero building airtightness; case 2, determination of the n50 required to assure the background ventilation in 50% of the time with zero air intake devices; case 3, simulations with 75% of the air intake devices and 25% of n50 of case 2; case 4, simulations with 25% of the air intake devices and 75% of n50 of case 2. The results are presented in table 7, and we can conclude:

- In buildings with natural ventilations systems we need much more air intakes than in mechanical ventilation systems to assure the background ventilation rate in a reasonable period of time, stated here as 50% of the time between November and April, period when we have the lowest outdoor temperatures, and the greater stack effect. This number is much higher than the one obtained with the 10 Pa criteria. The analysis of whole year show that these air are enough to assure the background ventilation in 50% of the time of the year in Lisbon and only 30 to 50% in Paris.
- This larger air permeability required for background ventilation agrees with the results obtained by the simple model proposed by Perino et all (2002), which require a slightly higher air permeability.
- Because we need much more air intakes in natural ventilations system, it seems reasonable to admit a larger air leakage to building envelope, than in buildings with mechanical ventilations systems. But, from the results of wind class 8 it is recommended to limit n50 to 25%, which gives a value near criteria II, eqn 3.
- Another interesting result is that, buildings with natural ventilation have a heating demand larger than buildings with mechanical ventilations system, because of the greater variability of air flow rates; in Lisbon, the air flow rate is higher than $2\times Q_b$ in 20% of the time. This value could compensate partly the energy consumption of fans.
- Because of the higher air temperature in Lisbon, than in Paris, the air permeability required for background ventilation in Lisbon is higher than in Paris.

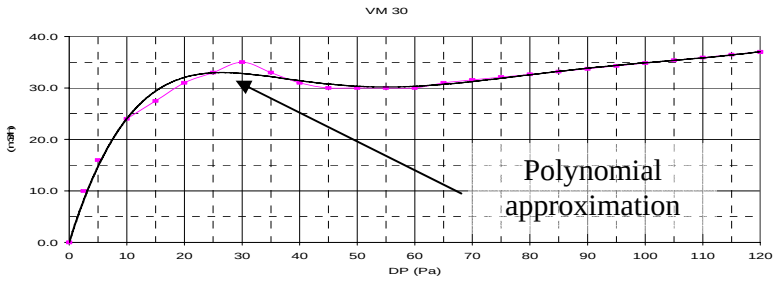

Figure 3 – Performance of auto-regulate air intake device with module 30 m^3/h at 20 Pa

CONCLUSIONS

In this paper it was presented some data about Portuguese building airtightness. The values measured in 23 building, show good agreement with the proposed requirements for sheltered buildings, but these values could be excessive for more exposed buildings.

The leakage distribution of Portuguese buildings agrees with measurements made in other countries and show that we should limit the whole building airtightness and not only some of their components.

From the study done it is proposed that the building airtightness for mechanical and natural ventilated buildings should be limited to double the background ventilation in less than 5% of the time, which could be obtained by eqn 3, taking into account wind exposure (table 3) and background ventilation.

To get better building behaviour the airtightness of the building should be measured, to verify the compliance with criteria and to decrease the number of air intake devices proportionally to the air flow rate across cracks in building shell.

With these limits it could be expected a decrease in the heating demand and a negligible reduction in cooling loads.

The method for the calculations of air intake for buildings with natural ventilation systems should be revised because the values obtained with 10 Pa criteria are insufficient.

I would like to express my gratitude to Prof. E. Maldonado (FEUP) for lending the blower door.

References

Afonso, C.; Maldonado, E. (1988) - Determinação de níveis de infiltrações típicos em edifícios portugueses. 3ª Jornadas de física e tecnologia de edifícios. Lisboa, 1988.

ASHRAE (1997) - 1997 ASHRAE handbook, Fundamentals. ASHRAE, Atalanta.

Concannon, P. (2002) - Residential ventilation. AIVC, Conventry.

Gonzalez, M. A. (1984) - On the aerodynamics of natural ventilators. Building and Environment.

Mimoso (1987) - Recommendations for the use of graded windows according to their exposure. LNEC, Lisboa, Portugal.

Moyé, C. (1985) - La perméabilité à l'air des bâtiments d'habitation. CSTB, Paris.

Orme, M. (1999) - Applicable models for air infiltration and ventilation calculations. AIVC, Conventry.

Perino, M. (2002) et al - A simple tool to assess the feasibility of hybrid ventilations systems. IEA Annex 35.

Pinto, A. (2002) – Windows heat balance in heating season. Efficient thermal heat transfer coefficient. XI-Congresso Ibérico e VI-Congresso Ibero-Americano de energia solar. Vilamoura.

Silva, A.M.C.R. - Caracterização das infiltrações médias anuais em edifícios portugueses através do método de pressurização. FEUP, Porto, 1991. Tese de Mestrado.

Wouters, P. (1986) - La ventilations et l'infiltration dans les bâtiments: la situation en Belgique. CSTC, Bruxelles.

Table 1 – Application of criteria I to some buildings types

Typology	Apart 1 bed	Apart 2 bed	Apart 3 bed	Apart 4 bed	DSFH
Floor area (m^2)	53	65	82	105	135
Q_b (m^3/h)	86	130	180	235	285
n50 Nat. Venti.	1.9	2.3	2.6	2.6	2.5
n50 Mec. Ven.	1.2	1.5	1.6	1.7	1.6

Table 2 – Weather data

	v (m/s) > 50% time	v (m/s) > 5% time	T_{air} (ºC) < 50% time	DD_{20}	Heat. Seas. (month)	I_{sul} kWh/m^2.month
Lisbon	3.6	8.9	11.5	1750	6	90
Paris	3.6	8.9	5.5	2890	8	28

Table 3 – Wind effect class

Terrain / H (m)	Reduction factor RF			P_{dyn} (Pa) exc. 5% time			Wind effect Class		
	Open flat	City	Urban	Open flat	City	Urban	Open flat	City	Urban
5	0.89	0.89	0.52	40	10	10	4	1	1
10	1.01	1.01	0.62	50	20	10	5	2	1
18	1.11	1.11	0.72	60	20	10	6	2	1
28	1.20	1.20	0.81	70	30	20	7	3	2
60	1.36	1.36	0.97	80	50	30	8	5	3

Table 4 – Data of the two detailed case studies

	Floor (m^2)	Volume (m^3)	Q_b (m3/h)	Uwall (W/m^2K)	Uwin (W/m^2K)	Uroof (W/m^2K)	A_{win}/A_{floor}
Apartment	53	135	86	0.78	3.5	-	20%
Detached	135	340	286	0.78	3.5	0.50	20%

Table 5 – Limits of building airtightness for two case studies according wind exposure class

Typology	V (m^3)	Q_b (m^3/h)	Nº air intake	n50							
				1	2	3	4	5	6	7	8
Dwelling	135	86	3	6.4	4.0	3.1	2.5	2.2	1.9	1.7	1.6
DSFH	340	285	10	11.3	7.1	5.4	4.5	3.8	3.4	3.1	2.8

Table 6 – Heat demand (kWh) and over ventilation with mechanical ventilation

Case	Wind Class	Apartment (3 air intake)					Detached Apartment (3 air intake)				
		n50	Lisbon		Paris		n50	Lisbon		Paris	
			Heat	Q>2Q	Heat	Q>2Q		Heat	Q>2Q	Heat	Q>2Q
1	5	0	90	0.0%	1 865	0.0%	0	3 554	0.0%	13 174	0.0%
2	5	1.2	103	0.1%	1 914	0.0%	1.0	3 607	0.0%	13 373	0.0%
3	5	2.2	115	0.4%	1 999	0.3%	3.8	3 920	1.7%	14 450	2.7%
4	5	5.1	220	17.0%	2 575	10.0%	9.2	4 986	20.7%	17 819	20.6%
5	1	6.4	105	0.2%	1 911	0.1%	11.3	3 644	0.1%	13 489	0.3%
6	2	4.0	126	2.0%	2 042	1.2%	7.1	3 916	2.1%	14 419	3.0%
7	8	1.6	135	2.2%	2 122	1.3%	2.8	4 054	3.3%	14 922	4.0%

Table 7 – Heat demand (kWh) and over ventilation with natural ventilation

Wind Class	Apartment 2 exposed façades								Detached dwelling 4 exposed façades							
	Lisbon				Paris				Lisbon				Paris			
	N	n50	Heat	%	N	n50	Heat	%	N	n50	Heat	%	N	n50	Heat	%
1	130	0	559	26%	58	0.0	2,351	12%	260	0	4,566	14%	92	0	13,711	2%
1	98	8.4	486	25%	44	4.7	2,314	11%	195	7.6	4,462	13%	69	3.4	13,688	1%
1	33	25	358	23%	15	14	2,288	8%	65	22.9	4,269	9%	23	10.3	13,629	1%
1	0	34	295	20%	0	19	2,239	7%	0	30.6	4,172	7%	0	13.7	13,602	1%
5	18	0	241	25%	12	0.0	2,141	15%	60	0	4,325	18%	36	0	13,755	3%
5	14	2.2	265	25%	9	1.5	2,179	15%	45	2.8	4,394	18%	27	1.7	13,913	6%
5	4.5	6.7	314	24%	3	4.5	2,295	15%	15	8.3	4,498	17%	9	5.2	14,187	9%
5	0	9.0	331	23%	0	6.0	2,318	14%	0	11.1	4,537	17%	0	7.0	14,311	9%
8	12	0	181	24%	8	0.0	1,871	0%	40	0	3,988	10%	27	0	13,345	0%
8	9	1.5	219	24%	6	1.0	1,993	4%	30	1.9	4,148	14%	20	1.2	13,616	3%
8	3	4.5	307	25%	2	3.1	2,229	14%	10	5.7	4,410	30%	7	3.6	13,980	9%
8	0	6.0	344	25%	0	4.1	2,319	17%	0	7.6	4,521	19%	0	4.8	14,170	12%

% - percentage of time between November and April when Q>2 Q_b; N- nº of air intake devices

RATIONALE FOR MEASURING DUCT LEAKAGE FLOWS IN LARGE COMMERCIAL BUILDINGS

Craig P. Wray, Richard C. Diamond, and Max H. Sherman[1]

[1]*Energy Performance of Buildings Group, Lawrence Berkeley National Laboratory*
Berkeley, California 94720, USA

ABSTRACT

Industry-wide methods of assessing duct leakage are based on duct pressurization tests, and focus on "high pressure" ducts. Even though "low pressure" ducts can be a large fraction of the system and tend to be leaky, few guidelines or construction specifications require testing these ducts. We report here on the measured leakage flows from ten large commercial duct systems at operating conditions: three had low leakage (less than 5% of duct inlet flow), and seven had substantial leakage (9 to 26%). By comparing these flows with leakage flows estimated using the industry method, we show that the latter method by itself is not a reliable indicator of whole-system leakage flow, and that leakage flows need to be measured.

KEYWORDS

Ducts, leakage, commercial, commissioning, measurements, diagnostics.

INTRODUCTION

Typically in North American large commercial buildings (floor area more than 1,000 m^2), central HVAC systems continuously supply heated or cooled air to conditioned spaces through a complex network of ducts. Large fan pressure rises are needed to move the supply air through the typically long duct runs, and the associated fan power is a substantial fraction (35-50%) of HVAC energy use. Fan energy can be reduced by using tight ducts that deliver conditioned air to where it is needed.

Although little is known about the duct system characteristics of existing buildings, three characteristics are notable. One is that the thousands of field-assembled joints between duct sections and duct-mounted accessories (e.g., VAV boxes) create numerous opportunities for leakage. The size and distribution of the leaks depends on the duct construction materials, and on the installation workmanship. Leakage testing of representative duct sections is necessary to verify that the installed system meets design specifications.

For a hole in a duct to be a problem, there must also be a pressure difference across it to drive the leakage airflow. Therefore, a second important characteristic is the pressure distribution in the duct system. Some duct sections operate at high static pressures (e.g., 100 to 2,500 Pa), but other sections, such as those downstream of VAV boxes, operate at much lower pressures (e.g., 10 to 100 Pa). In some systems, as much as 50 to 75% of the ducts may operate at the lower pressures (Fisk et al. 1999). Because of the spatial distribution of leaks and sometimes temporal variations in pressure, it is practically impossible to know the pressure difference across each leak. Although this lack of information means that leakage flows cannot be

estimated with any quantifiable certainty, a common industry practice for estimating leakage flows is to assume that an average duct static pressure applies to every leak.

A third important characteristic is the location of the ducts relative to conditioned space. Leakage from a supply duct directly into a conditioned space is of little importance, except perhaps in terms of uniformity of air delivery, noise, and draft potential. In North American large commercial buildings, duct systems tend to be located inside ceiling return plenums, which are not conditioned space. In this case, supply air leakage can short-circuit the air distribution system, and the supply fan airflow must increase to compensate for the thermal energy lost through leakage.

Because the relationship between supply fan power and airflow is somewhere between a quadratic and cubic function, the increase in airflow to compensate for duct leakage means that fan power consumption increases significantly, with a large fraction used just to move the leaking air. Recent field measurements (Diamond et al. 2003) indicate that supply air leakage can increase fan power requirements considerably: a leaky system (10% leakage upstream of VAV boxes, and 10% downstream at operating conditions) uses 25 to 35% more fan power than a tight system (2.5% leakage upstream and 2.5% downstream at operating conditions).

The objective of this paper is to discuss the merits of duct leakage metrics and test methods that are used today by the building industry, and to present measured data that demonstrate the need for measuring duct leakage flows.

COMMON LEAKAGE METRICS

The building industry uses numerous metrics to describe duct leakage. A common metric is leakage rate (ASHRAE 2005), which is the leakage flow that would occur per unit of duct surface area if all the leaks were exposed to the same reference pressure. Leakage class is a related metric and is simply the leakage rate divided by the reference pressure to the 0.65 power. Standards and design specifications describe a wide range of reference pressures, and the reference is not necessarily the same as the average operating pressure in the system. ASHRAE suggests that the average leakage rate for unsealed (leaky) metal ducts at a reference pressure of 250 Pa is 2.5 $L/(s \cdot m^2)$; recommended leakage rates for tight ducts are 5 to 10 times smaller. Unfortunately, none of these estimates account for leaks at connections to grilles and diffusers, access doors, or duct-mounted equipment such as VAV boxes.

Another common metric in design specifications is leakage flow fraction, which is the leakage flow divided by a reference airflow. For an entire duct system or for “high pressure” ducts upstream of VAV boxes, the appropriate reference is the supply fan airflow. For “low pressure” ducts downstream of VAV boxes, the appropriate reference is the flow entering the box. For average unsealed leaky ducts, SMACNA (1985) suggests that leakage fractions of 6 to 77% can occur, depending on the system airflow and duct static pressure. To use this metric, one must know or estimate both the leakage flow and the reference flow. The following section describes the tests that industry currently uses to estimate these parameters.

DUCT LEAKAGE TEST METHODS

Instead of measuring total leakage flows at operating conditions, test and balance companies typically estimate the leakage rate using an industry-wide method (SMACNA 1985):

pressurize a sealed duct section using an auxiliary fan and, using a flow meter integrated with the injection apparatus, measure the airflow required to maintain a reference pressure difference (assumed to be the same across every leak).

Unfortunately, because it is difficult to temporarily seal and test the often numerous "low pressure" ducts downstream of VAV boxes with this method, few guidelines or construction specifications require testing these ducts. Thus, testing focuses on the "high pressure" ducts (anecdotal evidence suggests that such tests sometimes are carried out even before branch ducts are attached). Not testing "low pressure" ducts downstream of VAV boxes is a problem, because these "branch" ducts can be a large fraction of the system and, as shown later in Figure 1, these ducts tend to be much leakier than upstream "main" ducts. Testing only the "high pressure" ducts does not guarantee a tight system if the "low pressure" ducts are leaky. Both parts of the duct system need to be tested.

Even if the pressurization test was used to assess the leakage of the "low pressure" ducts, the variability of operating pressures in these ducts makes it difficult to define an appropriate reference pressure. To overcome this difficulty, whole-system leakage airflows at operating conditions can be determined by measuring the airflow out of each supply grille, and by measuring the supply fan airflow; the difference between the sum of the grille airflows and the supply fan airflow is the leakage. If desired, the leakage of individual duct sections can also be tested by measuring the inlet flow to the section. It is necessary to keep the supply fan airflow and all VAV box damper positions (when applicable) constant during the test.

In practice, conventional flow measurement methods generally are not accurate enough to assess duct leakage flows. For example, pitot-static tube traverses to measure duct and fan airflows have an accuracy of only about 5 to 10%. Our recent laboratory tests of commercially-available flow capture hoods indicate that many hoods have substantial bias and precision errors (10 to 20%), although some hoods are quite accurate (2 to 5%).

Less-conventional methods can accurately measure leakage flows. These tests involve constant-injection tracer gas techniques (with expensive gases and analyzers and with careful attention to mixing) to measure supply fan airflows (accuracy of 3 to 4%), and powered flow-hoods to measure supply grille airflows (accuracy of 1 to 2%). Powered hoods are insensitive to the flow non-uniformities that lead to errors with conventional hoods. However, powered hoods are slow and cumbersome to use, especially in occupied buildings (e.g., it took five people 12 hours to measure airflows from about 100 supply grilles in one building). To make leakage flow measurements more practical, inexpensive, rapid, and accurate tracer-gas based systems with enhanced mixing need to be made commercially available.

DUCT PRESSURIZATION TEST RESULTS

Figure 1 shows the few duct pressurization test data that researchers have collected over the past several years in nine U.S. large commercial buildings (Xu et al. 1999, 2000; Fisk et al. 1999; Diamond et al. 2003). These data include VAV, CAV (constant-air-volume), and dual-duct systems, and both "high-pressure" ("main") and "low-pressure" ("branch") duct sections. For VAV systems, the data include fan-powered boxes ("VAV Fan") and cooling-only boxes. Most of the systems supply air through rectangular diffusers, but some use slot diffusers.

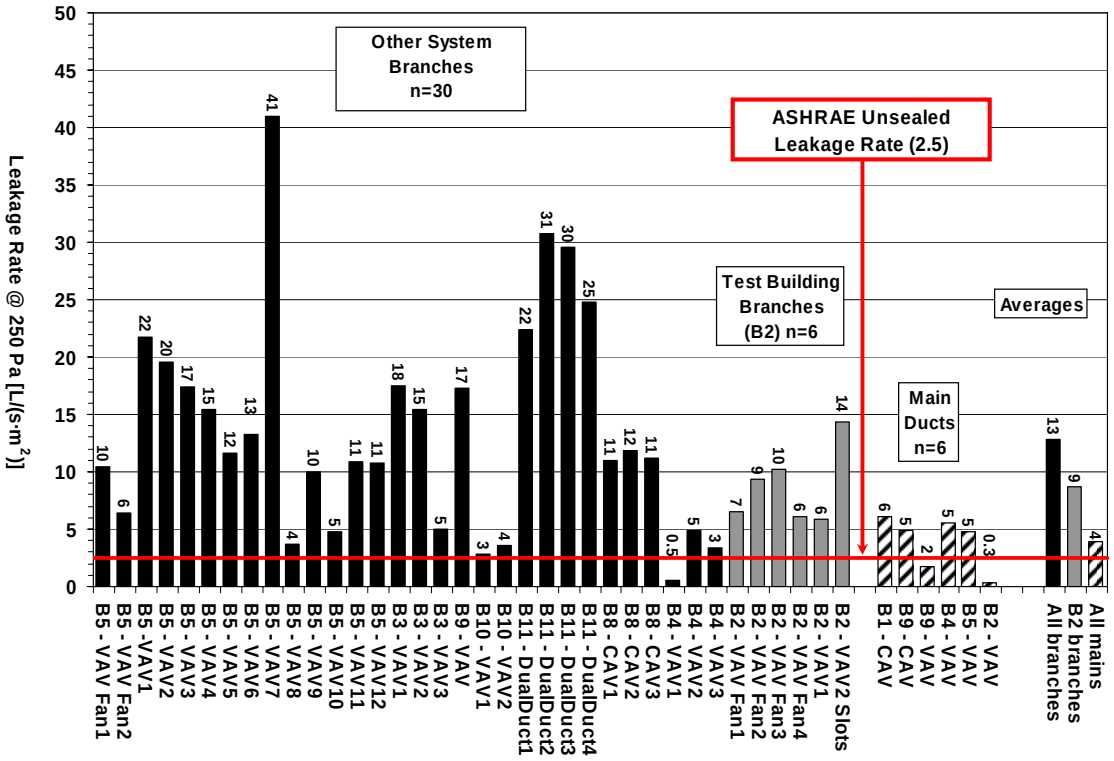

Figure 1: Duct Leakage Rates

Figure 1 suggests that there is a wide range of duct leakage in U.S. large commercial buildings. On average, branch ducts are about three times leakier than main ducts (perhaps in part because the branch ducts are not usually tested). Even many of the main ducts, which might have been tested during post-construction test and balance activities, are leakier than the average unsealed leakage rate suggested by ASHRAE.

Building 2 (B2) contains the system used by Diamond et al. (2003) to assess the fan power impacts of duct leakage. The intent of the study was to seal leaky ducts and to measure the resulting change in fan power. The pressurization test data in Figure 1 indicate that the branch ducts are leaky; however, as described in the next section, it turned out that the duct system was actually very tight in terms of leakage flows, and substantial duct leakage had to be added instead to carry out the study.

DUCT LEAKAGE AIRFLOW TEST RESULTS

Figure 2 shows measured leakage flow fractions for 10 systems in nine U.S. large commercial buildings. The data are for whole-systems, as well as duct branches. The reference flows that we measured at operating conditions are listed for each test. Where corresponding duct pressurization test data are available, we used these data to estimate the leakage fraction that the tested part of the duct system would experience at its average operating pressure. In other words, for the conditions at which the leakage flow measurements were made, we calculated the leakage fraction that would be implied by the standard industry pressurization test (if it were applied to the duct sections included in the measured leakage flow test). For whole-systems, we estimated leakage flows section by section using the average operating pressure associated with each section, and then divided the sum by the total inlet flow for the system.

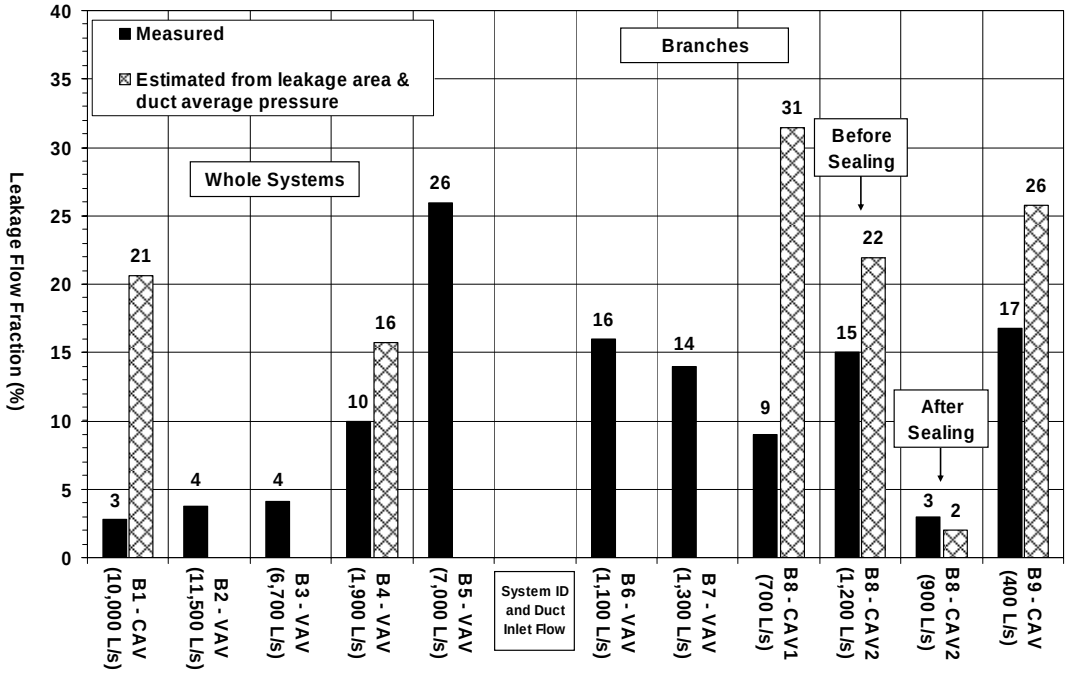

Figure 2: Duct Leakage Flow Fractions

The discrepancies between measured and estimated leakage flow fractions mean that the estimates are not a reliable indicator of actual leakage, and leakage flows need to be measured. In particular, the estimated fraction for Building 1 is seven times greater than the measured fraction. This estimate is not useful to show compliance with design specifications, and could lead to adversarial relations between designers, installers, and test and balance contractors. One can imagine the installer being told to do a better job, because the estimate indicates the ducts are leaky, when in fact the workmanship is good and the ducts are tight.

The principal reasons for discrepancies are that the pressurization tests unintentionally included gaps between diffusers and the ceiling grid, and the operating pressures at these gaps and at other leaks are lower than the average operating pressure. During the test, diffusers were sealed with a covering fastened to the adjacent ceiling grid, which means that the diffuser-grid gaps were inside the sealed system during the test. Consequently, the gaps appear to be duct leaks, even though they are not leaks during normal operation.

Figure 2 indicates that there may be a substantial number of leaky duct systems in the building stock: three systems had low leakage (less than 5% of duct inlet flow), and seven had substantial leakage (9 to 26%). There is also good news: some installers already can produce tight duct systems. Rather than requiring new construction and sealing techniques, it appears that installers of leaky systems only need training to use industry best practices. Measuring duct leakage flows would help demonstrate progress toward this goal.

As a retrofit to reduce leakage, the duct systems in Building 8 were sealed using aerosol-based sealants. Our tests on Branch 2 indicate that the sealing substantially reduced leakage. Note that the reduced inlet airflow after sealing is likely because the building operators adjusted the fan speed between tests, and is not caused by the sealing itself. The estimated leakage flow fraction agrees well with the measured fraction for the “sealed” case. Small estimated fractions are good indicators of a tight system; the converse is not true for large fractions that indicate a system is leaky.

SUMMARY

Duct leakage can considerably increase fan energy use in large commercial buildings. Industry-wide methods of assessing leakage are based on pressurization tests of "high pressure" ducts, and make broad assumptions regarding the interactions between leaks and duct static pressure. Even though "low pressure" ducts can be a large fraction of the system and tend to be leaky, few guidelines or construction specifications require testing these ducts. Both parts of a duct system need to be tested.

We have used complex techniques to measure leakage flow fractions for ten large commercial duct systems at operating conditions: three had low leakage (less than 5% of duct inlet flow), and seven had substantial leakage (9 to 26%). Comparisons of these fractions with fractions estimated using the industry method show that small estimated fractions are a good indicator that a system is tight; the converse is not true for large fractions that indicate a system is leaky. Leakage flows need to be measured to properly commission a duct system.

ACKNOWLEDGEMENTS

This work was supported by the Assistant Secretary for Energy Efficiency and Renewable Energy, Building Technology Program of the U.S. Department of Energy, under Contract no. DE-AC02-05CH11231.

REFERENCES

ASHRAE. (2005). *Handbook of Fundamentals: Chapter 35, Duct Design*. American Society of Heating, Refrigerating and Air-Conditioning Engineers, Inc.; Atlanta, GA. pp. 35.14-35.16.

Diamond, R.C., C.P. Wray, D.J. Dickerhoff, N.E. Matson, and D.M. Wang. (2003). *Thermal Distribution Systems in Commercial Buildings*, Lawrence Berkeley National Laboratory Report to the California Energy Commission. LBNL-51860.

Fisk, W.J., W. Delp, R. Diamond, D. Dickerhoff, R. Levinson, M. Modera, M. Nematollahi, and D. Wang. (1999). "Duct Systems in Large Commercial Buildings: Physical Characterization, Air Leakage, and Heat Conduction Gains". *Energy and Buildings*, Vol. 32.

SMACNA. (1985). *HVAC Air Duct Leakage Test Manual*. Sheet Metal and Air Conditioning Contractors' National Association, Inc.; Chantilly, VA.

Xu, T., O. Bechu, R. Carrie, D. Dickerhoff, W. Fisk, E. Franconi, O. Kristiansen, R. Levinson, J. McWilliams, D. Wang, M. Modera, T. Webster, E. Ring, Q. Zhang, C. Huizenga, F. Bauman, and E. Arens. (1999). *Commercial Thermal Distribution Systems Final Report for CIEE/CEC*. Lawrence Berkeley National Laboratory, Berkeley, CA. LBNL-44320.

Xu, T., M. Modera, R. Carrie, D. Wang, D. Dickerhoff, and J. McWilliams. (2000). *Commercial Thermal Distribution Systems: Performance Characterization and Aerosol-Sealing Technology Development*. Draft Final Report for the U.S. Department of Energy, Lawrence Berkeley National Laboratory, Berkeley, CA. LBNL-46283.

“DIAGVENT” GUIDEBOOK - CHECKING THE PERFORMANCE OF VENTILATION SYSTEMS

Pierre BARLES[1], Pierre-Jean VIALLE[2], Marie-Claude LEMAIRE[3]

[1] Pierre Barles Consultant, BP4 - 83460 Les Arcs, France
[2] CETIAT, BP2042 - 69603 Villeurbanne, France
[3] ADEME, 500 rte des Lucioles - 06560 Sophia-Antipolis, France

ABSTRACT

Ventilation in buildings is necessary first for hygienic reasons and also to preserve the building structure. This is more essential, today, because the buildings are more and more airtight, mainly due to energy regulations. It is also evident that air renewal energy losses and fan consumption become more and more important in relation with the total energy consumption of buildings.

Nevertheless, many defaults are encountered on installed ventilation systems. It seems necessary to check the installations, at the starting up and regularly in time, and not only when the problems occur.

In France, today, there is no obligation for regular inspections of ventilation systems, whereas it is a legal requirement in other countries like Sweden.

DIAGVENT method has been established on the basis of many inspections on different residential and commercial buildings, and on the Swedish experience which where applied in France.

This method is described in a small practical guidebook (around 30 pages). It includes three levels of inspections or diagnosis:

- DIAGVENT 1: no measurements, only visual checking, for commissioning new installations. The main objective is to verify that the installed system is in accordance with the expected one. The system is started on ;
- DIGVENT 2: is the main part in the method ; it is a more detailed inspection, both for new and existing installations ; it includes not only visual checks but also performances measurements (total and local air flow rates, pressures, electrical power) ; it also includes analysis of the results and indications for feasible improvements or more detailed investigations, if necessary ;
- DIAGVENT 3: corresponds to specific measurements, when a strong problem has been revealed after DIAGVENT 1 or 2, or after a complaint from the users. It may lead to a very detailed inspection and may include sophisticated measurement techniques (for acoustics, air leakages, air pollution transfers, etc.). Specific measurements are not detailed in the guidebook, but it is shown, depending on the nature of the problem, which point should be checked and what kind of measurement or analysis should be made.

DIAGVENT guidebook should be a practical tool for the professionals: engineering consultants, inspectors, installers, maintenance companies …
It gives, for example, practical information on standard measurement devices for DIAGVENT 2: which type of device and where it can be bought. It gives some useful reference values (air flow rates, duct air leakages, fan electrical consumption…) to help the professional during the analysis of the results.

This guidebook can be free downloaded on the CETIAT website. French professional training bodies are already interested in including this ventilation diagnosis method in their training programs.

KEYWORDS

Ventilation, Checking, Performances, Guidebook, Inspections, Commissioning.

INTRODUCTION

It is not new to say that the performances of ventilation systems, in practice, do not always properly achieve initial objectives, which are to bring hygienic air to the occupants in buildings. Of course, a lot of installations are also in a good situation and give satisfaction to the owner and to the occupants. But some observations are not acceptable; other situations are very poor quality and often there is no appropriateness between the results and the intrinsic performances of the ventilation components.

As this situation goes on, it seems necessary to check the installations, at the starting up and regularly in time, and not only when the problems occur. In France, today, there is no legal requirement for systematic inspection on ventilation installations; only very few of the new ones are visited.

The aim of DIAGVENT guidebook is to help the professionals: engineering consultants, inspectors, installers, maintenance companies … to make inspections on ventilation installations. Complementary with the method, DIAGVENT gives practical information on standard measurement devices and also some useful reference values (air flow rates, duct air leakages, fan electrical consumption…) to help the professional during the analysis of the results.

SOME RESULTS ON PERFORMANCES OF VENTILATION SYSTEMS IN FRANCE

During the last years, many investigations were driven by the authors on the performance of ventilation systems in different buildings. Many of them were made for ADEME, others for ALDES [1], and others for private bodies. One initial objective of ADEME was to test a method, like the Swedish method Boverket [2]; for that, a Swedish inspector took part in some investigations on commercial buildings [3].

Observations and measurements, on more than thirty buildings (residential, offices, schools, hotel, etc.) and fifty ventilation systems (majority of simple exhaust systems, some balanced systems) show the main following results:

- Total air flow rate at the fan case :
    - Half the number of fan units do not give the total scheduled air flow in the range of ± 20 % ;
    - When the total flow rate is not obtained, 75 % of the fans give less than 80 % of the air flow rate, and 25 % give more than 120 % ;
- Global air leakage of the ductwork :
    - In residential applications (multifamily buildings), new or existing, the global air leakage of ventilation system is between 15 % and 45 % !
    - In commercial applications, existing, the global air leakage of ventilation system is between 10% and 35 %
    - This is in accordance with previous studies [5] ;
- Air flow rate in the rooms :
    - Due to the previous results, air flow rates in rooms are not always in accordance with the hygienic values or with the scheduled values ;
    - The situation is more difficult in some buildings like the schools where we found air flow rates in the range of 30 % to 100 %.
- Electrical consumption of fan motors :

- On about thirty installations (simple exhaust or balanced systems), it was found that 2/3 were below 0,25 W/m3/h, which is the reference in the French thermal regulation (it is quite a good result) ; and 1/5 were above the double of this reference value.

Also, other observations can be made on:

- available documentation : it is very difficult to get a complete documentation, even any documentation in many cases,
- air inlets and outlets : the main problem seems to be the connection defaults between exhaust air terminal devices and ducts ;
- controls : the users are not aware about the possibilities in the management of the systems ; many installations are running all the time instead of being switched off when the building (commercial) are not occupied ;
- dirtiness of components and ducts : air inlets and exhaust air terminal devices are very often dirty, sometimes completely blocked ; there is no general concern about cleaning ducts, which are often very dirty ; new European standards on accessibility could help in the future.

Picture 1: Air inlet, very dirty

Picture 2: Open duct (!)

Picture 3: Leakages, ductwork

DIAGVENT METHOD AND GUIDELINE

The DIAGVENT method is described in a thirty eight pages small book (A5 format)which is divided in three main parts :

- Typology of the more common installations ;
- Methods: description of the three diagnostic levels DIAGVENT 1 2 and 3 ;
- Annexes and useful information.

First Part: Typology

DIAGVENT presents a typology of the more common ventilation installations, in France:

- in residential applications :
  - simple exhaust system, self regulated
  - simple exhaust system, humidity controlled
- in commercial applications :
  - same that residential
  - air conditioning systems

It gives some simple drawings, to show the above principles.

Then, a description of the main components which will be found in the different installations is given, just to show what the inspector could find on site.

Second Part: Methods

●*DIAGVENT 1: Completeness checking and starting on.*

It seems useful to describe very simple investigations to verify that the installed system is in accordance with the expected one. No measurements are made, only visual checking. It is mainly applicable for commissioning new installations. At the end of the inspection, the system is started on.
DIAGVENT 1 follows the main steps for inspection:

- Electrical box: supply characteristics, emergency command …
- Ductwork: nature, accessibility, connexions quality, supports…
- Fan case: type, accessibility, doors, belt, supports…
- Fan is started on: rotation direction, vibrations…
- Rooms: inlets, outlets, presence of drafts, noise (the fan is running)…

At the end of DIAGVENT 1, a summary sheet is performed, listing the 5 main points of the inspection and indicating the defaults which were encountered.
A model of this sheet is given in the guidebook.
The inspector should also directly explain the results to the owner, with the support of photos.

●*DIAGVENT 2: Checking the performance of the ventilation system.*
This is the main part in the DIAGVENT method. It is a more detailed inspection, both for new and existing installations. It includes not only visual checks but also performances measurements (total and local air flow rates, pressures, and electrical power). It also includes analysis of the results and indications for feasible improvements or more detailed investigations, if necessary.
The preparation of the inspection is important: explanations to the owner; trying to get the documentation, in advance, to understand the system, to identify or select the main parts which will be inspected; questions about the feeling of the occupants; checking the maintenance reports…
Then, on site, DIAGVENT 2 will follow both the experience of the inspector (for example to adapt the inspection to the real system configuration) and the main following steps:

- Documentation : drawings, schedule of conditions, maintenance… if possible, documentation is examined in advance (see above, preparation);
- Fan(s) : visual checking (DIAGVENT 1) and measurements (air flow rate, pressures/under pressures, electrical power);
- Ductwork: visual checking mainly, partial air flow rates, pressures/under pressures, air leakage visualisation with smoke…;
- Air diffusion in rooms: visual checking (great attention to the connections between ducts and air terminal devices), local air flows, pressures/under pressures (for example between rooms)…;
- Command and controls: information, electrical supply, connections, time switch…

After inspection, analysis of the results is made: for example comparison between the scheduled air flow rates and the existing ones, calculation of a specific power ratio (W/m3/h), global air leakage evaluation…
A summary sheet is performed; a model is given, which include the main parts:

DIAGVENT 2 – Diagnostic sheet - Performance of the ventilation system				
Important default to correct ☐			Nothing or minor default ☐	
General data: address, building, occupation, owner, ventilation system, inspector name and qualification…				
Point	Default	Note *	Other observation	OK**
…				

…				

*: note=1 if the default is important or critical (for example half the scheduled air flow rate); note=2 if the default is minor (for example dust in the exhaust fan box) (as in the Swedish inspection method [2] & [3])
**: it seems to be interesting to mention, not only the defaults (see above) but also the different points which are observed and which lead to no specific remark (just to show that this point has been observed and that it is OK)

Practical information and description of the useful measurement devices is given and, at the end of the manual, Internet addresses are listed (not an exhaustive list) to help the user to find this kind of devices.

In the DIAGVENT guidebook, an indication is given on the duration of DIAGVENT 2 inspection for different sizes and types of buildings; a table is established. It is only an informative data, just to give an idea to the inspectors and to the owners.

Of course, after DIAGVENT 2, it is necessary to meet the owner and to explain the results (photos are useful) ; general observations are listed and some improvement ways are shown to the owner. Sometimes, depending on the heaviness of some defaults, it could be necessary to go to the DIAGVENT 3 diagnostic level.

●*DIGVENT 3: Specific measurements on ventilation system.*
When a strong problem has been revealed after DIAGVENT 1 or 2, or after a complaint from the users it may be necessary to go to a very detailed inspection which may include sophisticated measurement techniques (for acoustics, air leakages, air pollution transfers, etc.). Specific measurements are not detailed in the guidebook, but it is shown, depending on the nature of the problem, which point should be checked and what kind of measurement or analysis should be made, with the reference to measurement techniques and standards.

The problems addressed are:

- Air flow rate deficiency (global or local)
- Acoustic disturbance
- Exaggerated electrical consumption
- Transfer of odours
- Presence of moisture
- Drafts

For example, in case of presence of moisture once the absence of any water infiltration has been verified, the inspections listed are:

- Measurements in the rooms concerned for temperature and humidity levels over representative periods in order to evaluate the humidity generation.
- Analysis of the design conditions of the ventilation system and of the effective conditions of use of the buildings to check if there is a real adequation or not.

Third Part: Annexes and useful information
DIAGVENT guidebook also includes:
- Bibliography (standards, guidebooks, measurement methods…)
- Websites (measurement devices manufacturers, technical centres for DIAGVENT 3)
- Annex 1: DIAGVENT 1 and 2 inspection sheet models
- Annex 2: Reference values (air flow rates, fan consumption, ductwork leakage)
- Annex 3: Detailed inspection method for typical residential ventilation system
- Annex 4: Method for measuring the air flow in duct

- Annex 5: Method for measuring the electrical fan power
- Annex 6: Examples of photos

		
Picture 4: In duct air flow measuring with hot wire anemometer	Picture 5: Measuring the electrical power at the fan unit	Picture 6: Local air flow measuring at an exhaust ATD in a bar

PERSPECTIVES

DIAGVENT guidebook tries to be the translation of a practical experience, from many investigations on residential or commercial buildings ventilation installations. Swedish experience in checking the performances of ventilation systems was an example for starting this work.

One aim is to help inspectors with a practical tool, and useful information.

DIAGVENT does not describe an exhaustive method, but a flexible one which will be adapted to the situation and the experience of the practitioners.

DIAGVENT is in French, but it could easily be translated in English.

It can be free downloaded on the CETIAT Website: www.cetiat.fr.

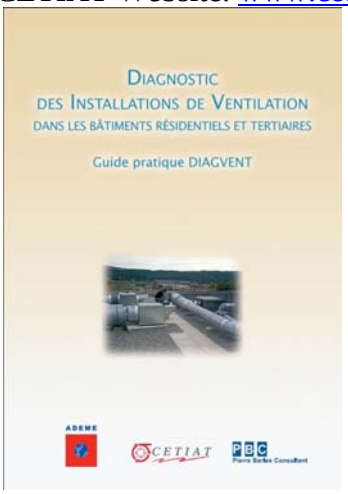

Picture 1: DIAGVENT Guidebook cover

References

[1] « Testing a method for the evaluation of the airtightness of the ventilation systems in existing buildings », P. Barles, X. Boulanger, S. Buseyne, 25e Conférence AIVC, 2004
[2] Checking the performance of ventilation systems »The Swedish National Board of Housing, Building and Planning. General Guidelines 1992 : 3E
[3] « Testing a method for checking the performances of ventilation systems in commercial buildings, in France », P. Barles, M-C. Lemaire, R. Larsson, 22e Conférence AIVC, 2001
[4] EN12599, Ventilation for Buildings – Test Procedures and Measuring Methods for Handling over Installed Ventilation and Air Conditioning Systems
[5] European Project SAVE-DUCT Improving Ductwork – A time for Tighter Air Distribution Systems, Final Report CE DG XVII, 1999

ENERGY AUDIT CERTIFICATION AND RATING OF SCHOOL BUILDINGS IN GREECE

Gaitani Niki[1], Santamouris Mat[1], Mihalakakou Giouli[2], Papaglastra Marianna[1], Assimakopoulos Margarita-Niki[1], Sfakianaki Katerina[1], Pavlou Konstantinos[1], Doukas Paris[1], Korres Dimitrios[1]

[1]*Department of Applied Physics, Faculty of Physics, University of Athens*

Building Physics 5, University Campus, 157 84 Athens, Greece

Tel: +302107276849, Fax: +302107276847, e-mail: ngaitani@phys.uoa.gr

[2]*University of Ioannina, Department of Environment & Natural Resources Management, Greece*

ABSTRACT

The present paper presents the results of the energy and environmental evaluation of ten school buildings in the Greater Athens Area. The research included measurements of the indoor air quality, evaluation of the situation of the building envelope, recording of energy and ventilation systems and generally all the systems that influence the energy output of the school buildings. Experimental investigations were performed in ten different schools and the concentration levels of CO2, CO and VOC's were measured. The analysis of the educational buildings included measurements of several environmental parameters such as temperature, relative humidity and air velocity inside each classroom, while ventilation was examined by estimating the air changes using the tracer gas technique. The thermal comfort conditions have been calculated using two different thermal comfort bioclimatic indices developed to be used for indoor spaces. The investigation of the above parameters was assessed in relation to the energy consumption of the school buildings. Finally the energy performance of school buildings was rated using a kmeans clustering technique.

KEYWORDS

Energy performance, indoor air quality, thermal comfort, school buildings

INTRODUCTION

Energy efficiency, indoor air quality and thermal comfort conditions are the three main factors influencing the school buildings environment [1,5].
The concentration levels of various pollutants such as CO_2, CO, HCHO were measured in ten school buildings located in the Greater Athens Area and the results were presented and analyzed in [6]. The experimental investigation included measurements of several environmental parameters such as temperature, relative humidity and air velocity inside each classroom while ventilation was examined by estimating the air changes using the

tracer gas technique. In order to evaluate the energy performance of the school buildings, the energy consumed for heating, cooling, lighting, mechanical and electrical systems, has been measured and analysed. The thermal behaviour has also been simulated using a dynamic simulation program and various energy conservation scenarios have been proposed in order to improve the buildings' energy efficiency. Finally, the thermal comfort conditions have been calculated using a thermal comfort bioclimatic index developed to be used for indoor and outdoor spaces.

2. SCHOOL BUILDINGS' DESCRIPTION

Measurements were carried out in ten school buildings. Seven of them are located at the centre of Athens while the remaining three school buildings in the Greater Athens Area. Various classrooms in each school building were provided for measuring the indoor air quality. All measurements were performed during the month of October and November 2004. All ten schools were equipped with central heating systems for the winter period.
Table 1 shows a brief description of the ten experimented school buildings.

3. RESULTS AND DISCUSSION

Analysis of physical parameters

In Tables 2 and 3 can be seen the minimum, maximum, and mean measured indoor air temperature and relatively humidity values respectively for the ten school buildings as well as the mean ambient air temperature and the relative humidity. As shown, the mean indoor temperature and relative humidity values do not present significant differences from those of the ambient air. However, the maximum indoor relative humidity values are in some cases remarkably higher than those of the ambient environment, while frequently exceed the 65%, which is a limit value for achieving thermal comfort conditions. The observed high indoor relative humidity values could be related to condensations in the building shell.
In Table 4 it can be seen the mean, maximum and minimum measured indoor air velocity values for the ten school buildings. The mean indoor air velocity values could be regarded as acceptable. However, the maximum values in several cases are considered to be significantly high and they do not contribute to the achievement of thermal comfort conditions.

Analysis of chemical parameters

Measurements of the most important pollutants concentration levels were carried out. Thus, the concentration levels of CO_2, CO and VOCs have been measured in the classrooms of the ten investigated schools. Analytically:

For CO_2: Table 5 shows the minimum, mean and maximum CO_2 concentration values for the ten school buildings. There is also the percentage of each school classrooms where the concentrations are higher than the health and comfort limit. This limit according to ASHRAE is 1001 ppm for an eight hours continuous exposure. However, CO_2

concentration values higher than 600 ppm are usually regarded as nearly the limit. As shown, the CO_2 concentration values are very close or higher than the limit ones. The inadequate ventilation mainly causes this. All measured values of CO_2 are not considered to impose healthy risks, however, the observed CO_2 concentration values can be responsible for a serious reduction of productivity and mental activity, which are very important especially in schools.

For CO: In Table 6 it can be seen the minimum, mean and maximum CO concentration values for the ten school buildings. As shown, the maximum measured value in all classrooms was equal to 4.47 ppm, a value much lower than the limit of 35 ppm of ASHRAE, the limit of 26 ppm defined by WHO, (World Health Organisation), or the limit of 50 ppm recommended by the Technical Chamber of Greece. Thus, it was not observed any risk for the health of students and staff.

For VOCs: Table 7 shows the minimum, mean and maximum VOCs concentration values for the ten school buildings as well as the percentage of each school classrooms where the concentrations are higher than the health and comfort limit. As shown, the maximum concentration values fluctuated between 0.21 and 5.34 ppm. VOCs concentration levels between 0.80 and 6.64 ppm could be responsible for some health problems such as headaches. Concentrations above the limit of 6.64 ppm could cause more serious than headaches neurological problems.

Ventilation measurements

All measurements of the natural ventilation were performed using the tracer decay method. From the measurements the air changes per hour (ACH), have been calculated for all investigated areas. Table 8 presents the results of the experimental investigation concerning the air changes per hour for various experimented classrooms of the ten school buildings for infiltration and for natural ventilation. Values in bold are considered being insufficient ventilation rates.

Thermal comfort conditions investigation

Human thermal comfort is defined as a condition of mind that expresses satisfaction with the thermal environment [2], the person would prefer neither warmer nor cooler surroundings, [4].
In the present research the thermal comfort conditions have been investigated using the wet-bulb globe temperature index, which is a heat stress indicator that considers the effects of temperature, humidity and radiant energy.
Wet Bulb Globe Temperature (WBGT) is commonly used as guidance for environmental heat stress to prevent heat stroke during physical exercise or while at work.
The wet bulb globe temperature is calculated using the following equations [3]:

- For outdoor environment with direct sun exposure:

$$WBGT=0.7*T_w+0.2*T_g+0.1*T_{air}$$

- For indoor environment or outdoor without direct sun exposure:

  $WBGT=0.7*T_w+0.3*T_g$

Where: T_w is the wet bulb temperature, T_g is the temperature measured using a black globe thermometer and T_{air} is the ambient air temperature (conventional thermometer). All temperatures should be expressed in °C.
Table 9 shows the WBGT-index criterion of heat stress warning specified in order to prevent heat stroke. WBGT index has been calculated for the ten examined school buildings. In Table 10 it can be seen the minimum, mean and maximum values of the calculated index for the ten school buildings. As shown, all values are lower than the considered limits, thus, the occupants of the investigated buildings do not experience any heat stress.

Energy performance investigation

Energy consumption calculations

Furthermore, the energy behaviour of the ten school buildings was calculated using the transient simulation program TRNSYS [7]. These calculations aim primarily at the buildings energy evaluation and assessment and secondly at improving the thermal comfort conditions and minimizing the energy consumption especially during the heating period of the year, as school buildings are not occupied during the months of July and August. Energy calculations were performed for the whole set of the ten school buildings using hourly values of climatic data for the city of Athens and for one year. The main inputs to the model were the following:

a. The construction elements of the ten school buildings: which mainly are the materials of the external and internal walls, of the roof and floor as well as the openings.
b. The geometric elements of the examined buildings including dimensions and orientations
c. The climatic data including air temperature, relative humidity, solar radiation, and wind velocity
d. The internal gains including lighting, occupancy and electric equipment.
e. Infiltration and ventilation of the each building.

The main output is the energy consumption, (heating and cooling load), of the building in kWh/m^2. Primarily, the thermal performance of the ten buildings in their existing situation was simulated. Figure 1 shows the calculated energy consumption values, (heating and cooling load), of the ten schools in their existing situation. These values represent the heating load and the cooling load that corresponds to the months of May, June, and September, (July and August schools are closed). As it can be seen the heating load varied in the range of 22.3 to 50.7 kWh/m^2 while the cooling load fluctuated between 6.9 and 18.9 kWh/m^2. In order to improve thermal comfort conditions and to reduce the energy consumption levels several improving scenarios have been proposed.

CONCLUDING REMARKS

The indoor air quality, the energy behaviour and the thermal comfort conditions in ten school buildings, located in the greater Athens area, were investigated in the present paper. The main concluding remarks from the above research are the following:
Regarding the indoor air quality, the CO_2 concentration values are usually higher than the comfort limit values. The CO concentrations are lower than the limit and do not present any danger for the occupants health. VOCs concentrations are, in a high percentage, higher than the limits. Moreover, ventilation levels are insufficient.
As regards the thermal behavior, the ten investigated school buildings were simulated using a dynamic simulation program, in order to calculate the buildings' energy consumption. After calculating the energy consumption various improvements were proposed and the energy saving was estimated. Improving scenarios such as external walls and roof insulation, ceiling fan, and night ventilation present a significant contribution to the energy consumption reduction.
The WBGT-index was used for calculating the thermal comfort conditions inside the classrooms. From the calculations it was found that the thermal comfort values were lower than the considered limits.

References

[1] Argiriou A., Asimakopoulos D.N., Balaras C., Dascalaki E., Lagoudi A., Loizidou M., Santamouris M., and Tselepidaki I., "On the energy consumption and indoor air quality in office and hospital buildings in Athens, Hellas", *Energy Conserv. Manag*., Vol. 35, pp**.** 385-394, 1994.
[2] ASHRAE (American Society of Heating and Refrigerating Engineers), Handbook of Fundamentals: Physiological Principles, Comfort, Health, New York, 1997.
[3] Aynsley R. and Spruill M., "Thermal comfort models for outdoor thermal comfort in warm humid climates and probabilities of low wind speed", Journal of Wind Engineering and Industrial Aerodynamics, Vol. 36, Part 1, pp. 481-488, 1990.
[4] Fanger, P.O., "Thermal comfort", Mc Graw-Hill, 1972.
Givoni B., "Man, Climate and Architecture", 2nd Ed., Applied Science Publishers, London, 1976.
[5] Papadopoulos A.M., and Avgelis A., "Indoor environmental quality in naturally ventilated office buildings and its impact on their energy performance", Int. J. of Ventilation, Vol.2, No.3, pp.203-212, 2003.
[6] Synnefa A., Polichronaki E., Papagiannopoulou E., Santamouris M., Mihalakakou G., Doukas P., Siskos P.A., Bakeas E., Dremetsika A., Geranios A., Delakou A., "An experimental investigation of the indoor air quality in fifteen school buildings in Athens, Greece", Int. J. of Ventilation, Vol.2, No.3, pp.185-202, 2003.
[7] TRNSYS 15.1, A transient system simulation program developed from Solar Energy Laboratory, University of Wisconcin-Madison and Transsolar of Stuttgart, 2002

TABLE 1
Description of the ten school buildings

School Number	Year of Construction	Number of students	Number of Classrooms	Working hours
1	1980	100	20	8:00-20:00
2	1981	215	11	8:00-16:00

3	1980	200	7	8:00-20:00
4	1980	260	12	8:00-22:00
5	1989	297	12	8:00-14:00
6	1980	210	13	8:00-17:30
7	1979	218	11	8:00-19:00
8	1980	140	6	8:00-16:00
9	1985	280	7	8:00-16:00
10	1982 & 1996	340	19	8:00-14:00 & 18:30-23:30

TABLE 2
Minimum, mean and maximum measured indoor air temperature values for the ten school buildings

School Number	Minimum indoor air temperature, (°C)	Mean indoor air temperature, (°C)	Maximum indoor air temperature, (°C)	Mean ambient air temperature, (°C)
1	23.0	25.8	27.2	27.5
2	19.5	20.2	21.0	19.0
3	20.1	21.9	23.0	17.5
4	22.0	24.4	26.1	23.5
5	22.6	25.3	27.1	26.7
6	19.3	22.7	24.3	21.1
7	17.3	19.4	21.1	19.0
8	23.0	24.5	26.5	23.0
9	22.0	24.7	25.7	25.7
10	23.3	26.0	27.8	26.9

TABLE 3
Minimum, mean and maximum measured indoor relative humidity values for the ten school buildings

School Number	Minimum indoor relative humidity, (%)	Mean indoor relative humidity, (%)	Maximum indoor relative humidity, (%)	Mean ambient relative humidity, (%)
1	60	66	76	57
2	40	43	48	24
3	51	53	56	49
4	56	65	70	59
5	47	57	66	42
6	61	66	75	63
7	56	61	69	54
8	54	60	70	59
9	60	68	86	52
10	50	53	57	48

TABLE 4
Minimum, mean and maximum measured indoor air velocity values for the ten school buildings

School Number	Minimum indoor air velocity, (m/sec)	Mean indoor air velocity, (m/sec)	Maximum indoor air velocity, (m/sec)

1	0.07	0.18	0.60
2	0.05	0.15	0.31
3	0.07	0.10	0.17
4	0.05	0.07	0.10
5	0.05	0.09	0.20
6	0.01	0.09	0.30
7	0.03	0.10	0.25
8	0.07	0.12	0.20
9	0.00	0.12	0.31
10	0.05	0.13	0.23

TABLE 5
Minimum, mean and maximum measured CO_2 concentration values for the ten school buildings

School Number	Minimum CO_2 concentration, (ppm)	Mean CO_2 concentration, (ppm)	Maximum CO_2 concentration, (ppm)	Percentage of classrooms in which concentrations are higher than the limit, (%)
1	408	600	1246	38
2	867	1258	1628	100
3	446	833	1373	57
4	367	602	1040	33
5	363	576	786	70
6	105	661	1133	50
7	772	1070	1873	100
8	413	675	1298	50
9	424	813	1664	100
10	396	598	846	45

TABLE 6
Minimum, mean and maximum measured CO concentration values for the ten school buildings

School Number	Minimum CO concentration, (ppm)	Mean CO concentration, (ppm)	Maximum CO concentration, (ppm)	Percentage of classrooms in which concentrations are higher than the limit, (%)
1	1.27	1.70	2.25	0
2	0.74	1.42	2.67	0
3	0.28	0.88	1.70	0
4	0.25	0.36	0.44	0
5	0.19	0.32	0.61	0
6	0.52	0.92	1.45	0
7	3.80	4.08	4.47	0
8	0.28	0.67	1.05	0
9	0.30	1.09	3.10	0
10	0.14	0.57	1.15	0

TABLE 7
Minimum, mean and maximum measured VOCs concentration values for the ten school buildings

School Number	Minimum VOCs concentration, (ppm)	Mean VOCs concentration, (ppm)	Maximum VOCs concentration, (ppm)	Percentage of classrooms in which concentrations are higher than the limit, (%)
1	0.58	1.28	2.29	100
2	0.0	0.60	1.32	100
3	0.02	0.74	2.55	71
4	0.24	0.93	2.15	100
5	0.02	0.08	0.21	90
6	0.01	0.76	1.53	92
7	1.42	2.45	5.34	100
8	0.14	0.40	0.78	100
9	0.23	1.34	3.62	100
10	0.05	0.60	1.68	100

TABLE 8
Infiltration and natural ventilation levels, in ACH, in various classrooms of the ten investigated school buildings

School number	Infiltration (ACH)	Infiltration & natural ventilation (ACH)
1 Classroom 1	0.1	3.5
1 Classroom 2	0.2	2.8
2 Classroom 1	0.4	9.0
3 Classroom 1	1.2	4.6
3 Classroom 2	1.9	6.9
4 Classroom 1	0.1	7.4
5 Classroom 1	0.2	1.7
5 Classroom 2	0.3	3.8
6 Classroom 1	0.9	7.3
6 Classroom 2	0.3	2.4
7 Classroom 1	0.5	12.1
7 Classroom 2	0.9	10.2
8 Classroom 1	1.3	5.9
8 Classroom 2	6.2	11.7
9 Classroom 1	0.4	1.3
9 Classroom 2	0.4	1.4
10 Classroom 1	0.3	2.0
10 Classroom 2	0.2	4.8

TABLE 9
The WBGT-index criterion of heat stress warning specified in order to prevent heat stroke

WBGT [°C]	Types of warning and required rest
Below 21	Safe (needs occasional supply of water)
21 - 25	Note (needs immediate supply of water)
25 - 28	Caution (needs to take rest)
28 - 31	Warning (Stop active physical exercise)
Above 31	Dangerous (Cancel physical exercise)

TABLE 10
Minimum, mean and maximum WBGT-index values for the ten school buildings

School Number	Minimum WBGT, (°C)	Mean WBGT, (°C)	Maximum WBGT, (°C)
1	22	22	23
2	14	15	16
3	16	18	19
4	19	21	23
5	19	21	23
6	18	20	21
7	14	16	18
8	19	21	22
9	21	22	22
10	19	21	22

FIGURE 1
Energy consumption values for heating and cooling for the ten investigated school buildings in their existing situation.

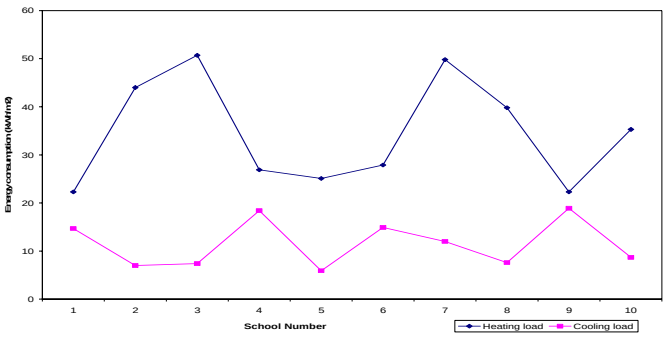

"REFURBISHING OF THE VENTILATION SYSTEM IN A SCHOOL"

Pierre-Jean Vialle[1], Anne Voeltzel[2], Christian Pico[3]

[1] *CETIAT, BP2042 - 69603 Villeurbanne, France*

[2] *CETE de Lyon, 38 081 l'Isle d'Abeau, France*

[3] *Ville de Lyon, 69 205 Lyon, France*

ABSTRACT

This project aims to demonstrate via a refurbishing operation, how a mechanical ventilation system can both provide a good indoor air quality and limit the energy consumption due to air renewal. The field of this operation concerns the improvement of indoor air quality for sensitive people as young children in classrooms, associated to a rational use of energy by the ventilation systems. Several series of measurements have been carried out before and after the refurbishing of the ventilation system to investigate the performances of the systems installed, evaluate the feeling of the occupants, and compare with the previous situation. The results obtained show a real improvement of the indoor air quality and also a possibility for energy savings up to 70% due to the use of demand control ventilation.

KEYWORDS

School, Indoor Air Quality, Refurbishing, Mechanical Ventilation, Energy Savings, Demand Control Systems.

INTRODUCTION

Currently in France most of the schools are naturally ventilated by opening windows. Depending on the external conditions, in case of noisy surrounding or during winter time, people might be reluctant to the aperture of the windows. In these conditions the indoor air quality in classrooms can reach rather poor levels, with high CO_2 concentration and humidity levels. This indoor environment is of course not favourable for sensitive people like young children, and has negative effect on their capacities to be concentrated.

The purpose of this project was to analyse how an adequate mechanical ventilation system can provide a good indoor air quality in classrooms, and in parallel allow substantial energy savings, comparing with airing by opening windows. This study has been supported by the regional branch in Rhône-Alpes of Ademe (french Agency for Environment's Defence and Energy Savings) in the frame of its experiments and demonstration program. The project team including the building owner Ville de Lyon, the consultant Tellitech, and two laboratories CETIAT and CETE de Lyon has been built since the beginning of the project and maintained till the reception of the new installations and validation of their performances.

This paper describes first the objectives of the project, and the approach retained. Then a row description of the building and of the new ventilation systems is given. After, the main results of the different measurements performed before and after refurbishing are presented. Finally,

analysing the data collected an estimation, of the energy savings is given by referring to the previous situation and to a mechanical exhaust ventilation system.

OBJECTIVE AND APPROACH

The objective of this project was to demonstrate how a mechanical ventilation system can both optimise the indoor air quality in the school, and limit the energy consumption due to air renewal.
To achieve this objective different choices have been made :

- assess the needs of the occupants;
- adapt air flow rate to the occupation rate of the rooms as far as possible;
- pay attention to the air tightness of the ductworks (class B);
- install a performing balanced ventilation system with heat recovery.

The collaboration established between the different partners all along the project has allowed a sharing of competencies and knowledge favourable to the optimisation of the definition of the systems and to the controls and validations during and after refurbishing. Inspections have been performed by CETE de Lyon and CETIAT.

DESCRIPTION OF THE SCHOOL

The school complex consists of five buildings. Two buildings are from the year 1960, the others have been added in 1982. In these buildings there are mainly a primary school, a nursery school, a general purpose room and a canteen. In total 25 classrooms are present.
Since the beginning in 1982, new buildings have been equipped with a mechanical balanced ventilation system. But due to several lacks in the installation and maintenance, these systems have not worked properly on a long period, and have rapidly been shut off. So in fact, even if a mechanical system was present, the school was naturally ventilated by opening the windows for already many years.
Most of the ducts were flexible ducts ruined by outdoor conditions. The air handling units could run but they were old patterns without insulation adapted to outdoor conditions. These elements have led to the decision to remove completely the old systems and install new ones.

The refurbishing operation exposed here has only concerned rooms located in the buildings built in 1982.

DESCRIPTION OF THE NEW SYSTEMS INSTALLED

As it was a first step, the refurbishing of the ventilation systems has concerned only 6 classrooms of the nursery school, 2 classrooms of the primary school and the general purpose room. In this paper we only consider the operation concerning the classrooms.
The systems installed in the classrooms are mechanical balanced systems (see figures 1 and 2). One unit supplies the air in two rooms. According to the French regulation for hygiene (15 m3/h for pupil and 25 m3/h for adults) and to the maximum number of people expected in each room (30 children, 2 adults) one system has an air flow rate capacity of 1100 m3/h. An heat recovery unit with an efficiency of 65%, an F7 type filtration unit and an electrical heater are also included. The ventilation unit is installed outdoor on the terrace-roof of the

classrooms. The ductworks are made with double skin rigid ducts, including a 50 mm thick layer of mineral wool for thermal insulation and acoustical absorption. Junctions are sealed with mastic and adhesive tape. Three air diffusers supply the fresh air in each room. The exhaust is located in the corridors. Acoustic grilles are installed in doors bottom for air transfer.
For all these systems, the air flow rate is regulated according to the $C0_2$ level detected in the classroom. A damper is present in each branch supplying the air in the rooms. The aperture of the damper is function of the CO_2 level detected.

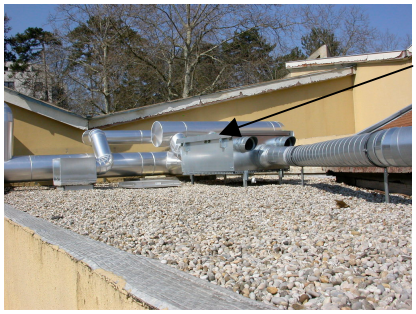

Figure 1 : Air handling unit on terrace roof

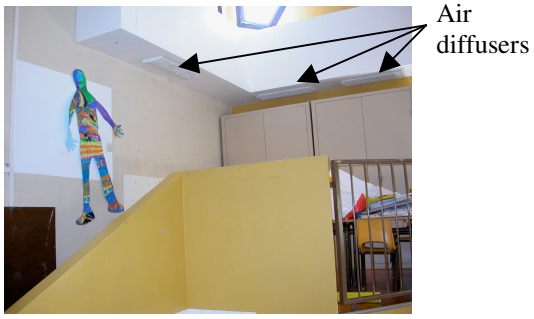

Figure 2 : Air diffusers in classrooms

INSPECTIONS PERFORMED

Preliminary inspections

In order to help for the design of the future ventilation systems, a first inspection has been made at the very beginning of the project, in order to :
- get useful information about the activities and occupation rate in the different rooms of the school supposed to be refurbished;
- estimate the quality of the building, regarding especially the air tightness of the walls.

Questionnaire

To get information about the use of the classrooms several interviews have occurred between the teachers of the primary and nursery schools and the members of the project team. A questionnaire has also been circulated. Main points addressed by the questionnaire were concerning the activity and the occupation rate in the classrooms and also the way people perceived the indoor air quality.
The results of this survey have shown that from 8h30 to 11h30 and from 13h30 to 16h30 the number of people present in classrooms varies. Due to the fact that all the rooms are not occupied, the teachers are used to separate the pupils in several groups for different indoor activities. Activities outside the school also happen during the week.

Airtightness of the building

Using a specific fan connected to a false door in the entry of the classroom, it is possible to create a depression in the room. An airflow-meter measures the air flow rate leakage. Tests performed have shown that the building was rather leaky, with 2.6 to 3.8 Vol/h under 4 Pa. These values are very high compared to the reference value of 0.9 Vol/h recommended in guidelines for this kind of buildings. Highest value 3.8 Vol/h was due to the casing of the shutters that was almost not fixed. The other leaks were mainly located around the frame of the windows and to the junction between walls and ceiling.

Inspections after refurbishing of ventilation systems

Once the new ventilation systems have been installed, different inspections have been performed. Tests to assess the air tightness of the new ductworks have been carried out first. Then a measurement campaign during the heating period in the classrooms has been organised to evaluate the indoor air quality level and the capability of the systems to adapt the air flow rate to the occupation rate. These last measurements have been performed with and without the new mechanical ventilation system running in order to compare the new situation with the previous one.

Airtightness tests

The tests have been performed two times on the first ductworks installed, according to the standard EN 12237. Results obtained the first time were rather poor. The leakage was more than ten times superior to the limits of the air tightness class B required. The reasons identified were mainly leaky junctions between the ducts and the inlet of the air diffusers. A second test has been performed once the defaults have been eliminated. The results obtained satisfied the air tightness class C. The requirements were so quite respected.

Measurements of indoor air quality in classrooms

The parameters controlled during this campaign were temperature, relative humidity, CO_2 concentration (indoor and outdoor), ventilation air flow rates and occupation rate. Air flow rates were not directly measured but deduced from the damper position. Preliminary measurements had actually allowed to determine the relationship between these two parameters. Tests have been performed over two weeks in two primary classrooms and two nursery classrooms.

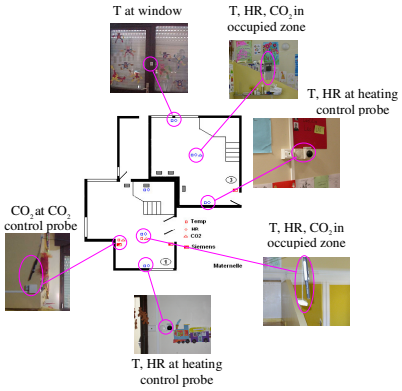

Figure 3 : Map of the nursery classrooms and sensors positioning

The sensors have been installed in the rooms in order to get CO_2 level, temperature and HR in the middle of the occupied zone, and also in the proximity of the CO_2 and temperature sensors used to drive respectively the ventilation system and the heating system. Temperature sensors have also been put near the windows or doors used to naturally ventilate the rooms in winter when mechanical ventilation was not running. The figure 3 gives an illustration of the sensors positioning in the nursery classrooms.

The results obtained during this campaign show that the CO_2 level is generally higher during periods where the ventilation mechanical is not running. The maximum concentration are 1400 ppm in nursery classrooms without mechanical ventilation and 1000 ppm with mechanical ventilation. In primary classrooms the values are similar. Figure 2 show the variation of the temperature, $C0_2$ concentration and relative humidity for a nursery school classroom and figure 3 for a primary school classroom. The blue underlined periods in the graphs correspond to the periods where mechanical ventilation is running.

Concerning the ability of the system to adapt the air flow rate to the occupation rate, the results are rather good. As it is shown in figure 4, since the people enter the classrooms the CO_2 level is increasing and the air flow rate follows within a certain delay but without ever that the CO_2 level overtakes a threshold value of 1000-1100 ppm. We can notice that during unoccupied periods the air flow rate is maintained at a rather high level, from 170 to 390 m^3/h depending on the classrooms. This is in fact because of the safety of the preheating system of fresh air that is shut off if pressure in the casing of air handling unit is too high. So it prevents from closing the damper more than a certain point and maintains rather high the air flow rate level.

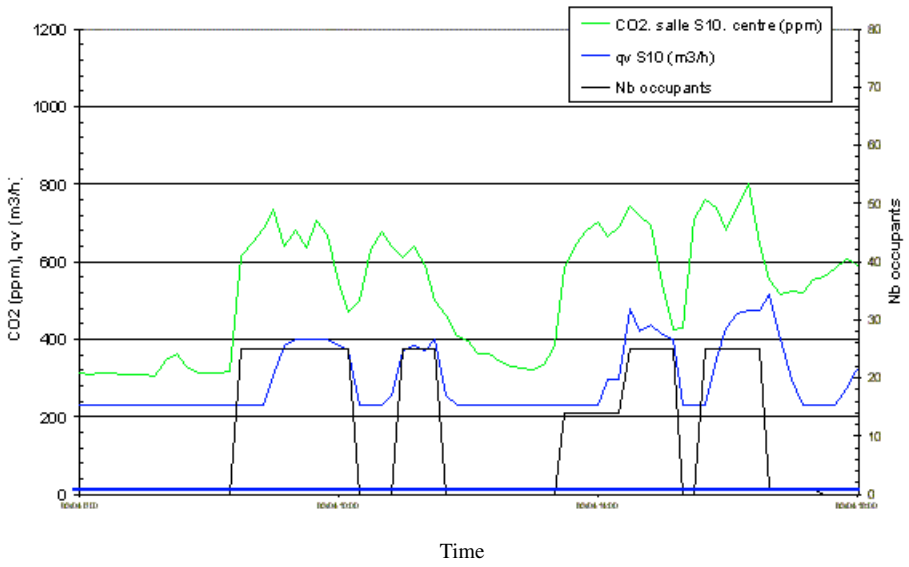

Figure 4 : CO_2, occupancy and ventilation air flow rate in a primary school classroom

PREDICTION OF ENERGY SAVINGS

Analysing the air flow rate measurements it appears that the average air flow rate in the different classrooms compared with a constant air flow rate system is reduced by 17 to 60 %. Adapting the minimum air flow rate during unoccupied periods (fixing at 50 m^3/h only) the reduction could reach 53 % to 77 %.
Calculation of the global energy consumption can be made considering the electrical consumption of the fans and energy necessary to heat the fresh air. The average outdoor conditions retained correspond to the French climatic zone H1 (3174 degree.day heating for indoor temperature 21°C).
Estimation of the energy savings have been made comparing with constant air flow exhaust system (respecting regulation level) and with a natural ventilation system by opening windows. For this last one the reference air flow rate, defined in French thermal regulation, is 1,8 times the regulation level. The average heat recovery efficiency retained is 60%. Results are given in table 1.

TABLE 1

Level of energy savings

Cases	Part of gains due to demand control	Part of gains due to heat recovery	Global gain
Comparing with constant air flow rate mechanical exhaust system	39 % (70 %)*	61 % (30 %)*	14 289 kWh/an (16 792 kWh/an)* 62 % (73 %)*
Comparing with ventilation by opening windows	72 % (85 %)*	28 % (15 %)*	30 962 kWh/an (33 465 kWh/an)* 78 % (85 %)*

*: Values in brackets are corresponding to the gains calculated with an optimised air flow rate of 50 m3/h when rooms are unoccupied.

The potential of energy savings is important. The main gains are due to the modulation of the air flow rate more than to the heat recovery to the condition to have a real reduced ventilation air flow rate during periods where classrooms are unoccupied.

CONCLUSION

Considering the objectives of this study, demonstration has been achieved that the mechanical ventilation can provide a good indoor air quality, with limiting energy consumption comparing to airing by opening windows. The use of demand control systems to adapt the air flow rate to the occupation rate seems quite adapted for schools. The reduction of the airflow rate can reach at least 50% compared to a constant air flow system. Corresponding energy savings are also important from 40 % to 70%, and more again if the comparison is made with ventilation by opening windows.

REVIEW ON VENTILATION RATE MEASURING AND MODELLING TECHNIQUES IN NATURALLY VENTILATED BUILDINGS

Sezin Eren Özcan[1], Erik Vranken[1], and Daniel Berckmans[1]

[1]*Laboratory forAgricultural Buildings Research, Catholic University of Leuven, Kasteelpark Arenberg, 30, B-3001, Heverlee , Belgium*
Tel. +32(0)16 32 17 26 E-mail:daniel.berckmans@agr.kuleuven.ac.be

ABSTRACT

Direct and indirect measuring techniques are available for determination of ventilation rate in naturally ventilated buildings. Direct measuring methods include measuring fan, propeller gauge, hot wire anemometer, particle image velocimetry, laser Doppler anemometer, and transit time sonic anemometer. Basic disadvantage of direct measuring techniques is that they are generally used for point or local measurements of air velocity. In order to have the total ventilation rate through the whole building, a "system" is required to measure simultaneously the airflow both in magnitude and direction at a number of locations.

Indirect measuring techniques are; heat balance, CO_2 balance, pressure difference, CFD analysis, tracer gas measurements, multizone modelling, and zonal models. These methods consider the whole system, and therefore, provide a possible tool for determining air flux through the building envelopes. Methods based on computer simulations (CFD, multizone models, etc.) should be validated against experimental data. However, in most of the cases, those validations are lacking, or do not indicate the accuracy of the method. Tracer gas measurements are mostly used as reference method in validations. However, accuracy of this technique should also be studied. Most indirect measuring techniques suffer from the problem of imperfect mixing of air within the ventilated structure. Therefore, the accuracy of tracer gas measurements should be improved by using information of imperfect mixing within the building.

KEYWORDS

Ventilation rate, natural ventilation, measuring techniques, accuracy

INTRODUCTION

Due to limited energy sources, countries are looking for alternative solutions to decrease energy needs. In that context, natural ventilation can be seen as a very attractive sustainable technique in building design (Simonson, 2005). However, understanding of ventilation dynamics is needed to provide an efficient control.

Ventilation rate has to be determined not only in terms of energy, but also for controlling indoor air quality and emissions. For these reasons, agricultural buildings (livestock houses, greenhouses, etc.), naturally ventilated industrial buildings, and residences require a reliable ventilation rate measuring technique.

Objective of this study was to review available techniques for ventilation rate measurement while putting emphasise on their accuracies. Additionally, operational principals and advantages/disadvantages of available methods were discussed. At the end, a summary table can be found with related reference list.

DIRECT MEASURING TECHNIQUES

Direct measuring techniques are mostly practical and accurate tools for air speed measurements. Although some techniques can be used to measure air flux through the buildings in and outlet sections such as free running impeller, most of them can only measure air speed at certain point in the air stream. Those measurements can be converted into ventilation rate by multiplying with the cross section area where the flow is passing through. However, since the flow through an opening is not uniform especially in naturally ventilated buildings, measuring a point at the opening does not give the total ventilation. Therefore, the accuracy on air speed does not indicate the accuracy on ventilation rate.

One common solution to point measuring problem is to use multiple sensors at the opening. However, this application is costly and affects the behavior of flow due to physical impedance.

Free Running Impeller

These types of sensors can also be called as measuring fan, free impelling turbine or propeller fans. The sensor is placed in a circular duct or ventilation opening and directly measures the air stream through it (Berckmans, 1986; Vranken, 1999; Berckmans et al., 2001). They are the most common means of measuring ventilation rate in mechanically ventilated stables. Operational ventilation rate of these sensors is high, that is, from 60 m^3/h to 14,000 m^3/h. The inaccuracy of fans depends on design. Nowadays, they can measure down to 5% inaccuracy.

These fans cannot be used in all kinds of naturally ventilated buildings, since they need defined inlet/outlet and circular cross-section.

Propeller Gauge

With this method, air speed is measured using a small propeller. Depending on the quality, accurate measurements of air velocity are possible (2 %) within a range of 0.2 – 30 m/s (Kinsey *et al*., 2004; NovaLynx Corporation, 2005; Davis Instruments, 2005).

This method also measure local air speed, which may not be representative for overall ventilation rate. Additionally, if the instrument is not properly calibrated, the inaccuracy can reach up to 25 %.

Hot Wire Anemometer

Basic principle of the hot wire anemometers is based on heat loss of a thin heated wire or amount of heat needed to keep the wire at constant temperature along the air stream. They can measure steady-state to transient temperature differences and air speed of 0.05 to 20 m/s (Perry, 1982; Scholtens and van ‘t Ooster, 1994).

Although these devices can measure very accurately (0.5 %), if calibration and calculations are not done accurately the inaccuracy can go up to 25%. One apparent disadvantage of these devices is that they are very susceptible to dust and thus corrosion. Moreover, as mentioned before, since they measure gas velocity at a certain point, a representative measuring point should be determined. Due to lack of physical robustness, these instruments are very fragile. Finally, the cost of installation is considerably high.

Laser Doppler Anemometer

Laser Doppler Anemometry, or LDA, is a technique for measuring the flow velocity of fluids or gases. Acoustic pulses sent and received by transducers at a fixed frequency collide with particles in water, allowing for a determination of velocity. It is a non-intrusive technique with a high frequency response and large dynamic range capabilities. The method’s other particular advantages are: high spatial and temporal resolution, no need for calibration and the ability to measure in reversing flows (DeGraaff and Eaton, 2001). LDA is one of the most popular methods to validate CFD results (Posner *et al.*, 2003, Temperley *et al.*, 2004).

This method is also accurate at determining air velocities (< 2 %). But main shortcomings are; they can only log local speeds, expensive, and sufficient transparency is required between laser source and target. Besides, accuracy is highly dependent on alignment of emitted and reflected beams.

Particle Image Velocimetry

Particle image velocimetry is a technique which allows the fluid velocity to be measured simultaneously throughout a region illuminated by a two-dimensional light sheet. The PIV monitor the motion of particles, with velocities of particles being taken as representative of local element (Hu *et al.*, 2002).

PIV is accurate in velocity measurements (< 3 %). However, it can also be used for local measurements. Like LDA, this method is also used in CFD validations.

Transit Time Sonic Anemometer

A pair (or pairs) of transducers, each having its own transmitter and receiver, are placed on the pipe wall, one (set) on the upstream and the other (set) on the downstream. The time for acoustic waves to travel from the upstream transducer to the downstream transducer t_d is shorter than the time it requires for the same waves to travel from the downstream to the upstream t_u. From this time difference and reflection angle, average air flux through the path can be found.

Since there is no obstruction in the flow path, the equipment causes no pressure drop. It has low maintenance cost due to no moving parts. Multi-path models have higher accuracy for wider ranges of Reynolds number. Portable models are also available for field analysis and diagnosis.

This type of anemometers is already used in practice to measure ventilation rates through long openings. However, airflow variation in space and time is usually found under natural ventilation results certain inaccuracy. In order to have a general picture of air movement through the whole building, a "system" was required to measure simultaneously the airflow both in magnitude and direction at a number of locations. Additionally, the instrument has a higher initial set up cost and the uncertainties caused by the geometry of the system, that is, the difference between the internal diameter and roughness of the meter body and the measuring section, influence the final accuracy (Calogirou et al., 2001; Iooss et al., 2002).

Average accuracy of the instrument changes between 0.1 to 4 % in a velocity range of 0 to 60 m/s. In a current project, sonic anemometer technique has been improved using multiple measuring points (Van Buggenhout *et al*., 2005). This method was suggested as a practical technique to be used in naturally ventilated buildings taking contactless measurements.

INDIRECT MEASURING TECHNIQUES

Indirect measuring techniques are based on measuring certain parameters that related to ventilation rate, such as pressure, temperature, and concentration and modelling the relation between them. Indirect measuring techniques are the ones that used mostly to determine the ventilation rate in naturally ventilated buildings. These methods are subject to constant improvement.

Complexity of the models does not necessarily indicate a better accuracy (for example, CO_2 balance versus CFD). In addition, more complex systems can hardly be used for online control purposes. On the other hand, they may provide a useful tool for design purposes.

Pressure Difference

Techniques based on this method calculate pressure difference between indoor and outdoor and correlates it to air exchange (Bruce, 1978; Brockett and Albright, 1987; Boulard and Baille, 1995; Demmers, 1997; Richardson et al., 1997). Main advantage of pressure difference systems is being cheap and direct measuring technique. If it is coupled with tracer gas experiments, physical description of ventilation mechanism can be acquired, and ventilation rate per opening depending upon physical environment can be predicted.

Basic disadvantage of pressure difference methods in naturally ventilated buildings is inaccuracy due to low wind speed and low pressure difference. Additionally, accuracy depends on type, size, and number of the ventilation opening(s), the position of the openings and building size. These devices are also sensitive to corrosion. High fluctuation in and around the buildings (6.5 – 250 Pa) affects also the robustness of the method. An

inaccuracy of 2 % is possible with pressure difference method, but due to above mentioned reasons, inaccuracy would be more.

CO_2 Balance

CO_2 balance is performed by continuous or intermittent measurement of CO_2. This method already used in naturally ventilated buildings in number of studies (Penman and Rashid, 1982; Van Ouwerkerk, 1993; Van't Klooster and Heitlager, 1994; Pedersen et al., 1998). Main handicaps of this method are originated from CO_2 produced from other sources (respiration, manure, etc.) and solubility of CO_2 in water. High numbers of living organisms are needed to obtain high concentration differences. Since at low concentration levels, small error in concentration measurement can result larger error in ventilation rate. This method also depends on organism type, activity level, etc. It is possible to measure ventilation rates between 18 – 1400 m^3/h with an inaccuracy of 15 to 40 %.

Heat Balance

Ventilation rate can be calculated from heat loss through building by means of simple temperature measurements (Kotani *et al*., 2003). However, this indirect method needs complex calculations afterwards (Yam *et al*., 2003, Fatnassi *et al*., 2004). It is difficult to determine exact heat gains and loses. At high k-values, measurement of radiation, wind speed and direction are also needed. Furthermore, this method is not suitable for fast and simple determination of ventilation rate (Van't Ooster, 1994). It can be used in mechanically ventilated buildings where sources are better known, although for those buildings easier methods are already available. This method can be used with ventilation rates of maximum 696 m^3/h with an inaccuracy of -31 to +101 %.

Tracer Gas

Tracer gas method is one of the most popular methods used in ventilation rate determinations in naturally ventilated buildings. The method is based on conservation of mass of a inert tracer gas injected to a building section. Three types of measurement techniques are available: i. rate of decay (Snell et al., 2003), ii. rate of accumulation (Zhang *et al*., 1995), iii. constant rate (Demmers *et al*., 2000).

In current calculations with tracer gas method, perfect mixing assumed in the volume. Therefore, injection and sampling points should be chosen carefully to represent the average air flow in the room. Measurements up to 235,000 m^3/h are possible with an inaccuracy range of 10 to 50% (Sandberg and Blomqvist, 1985).

CFD Analysis

CFD softwares use Navier-Stokes equations to simulate the whole system. The volume is divided into huge number of cells and interactions between the cells are calculated (Ayad, 1999). The main advantage of CFD models is that they can be applied to any type of the building. However, these models have many disadvantages. First of all, good assumptions are needed for system parameters (Demmers et al., 2000). Due to complexity of the

software, expertness is needed and calculations are time consuming. Final results reflect a condition at certain time step; therefore, dynamic analyses are not possible. Although these models cannot be used at online control of ventilation rate, they can be effective tools for early building design purposes. Any range of ventilation rate can be simulated. Inaccuracy of CFD models are estimated around 30% (Campen and Bot, 2003).

Multizone Modelling

In classical multizone modelling, air speed or temperature is simulated using doors and windows as connectors. These models also use mass transfer between the zones as CFD models. However, since number of zones is much far less than former one, calculations can be done quickly (Feustel, 1999). This method can also be used at any range of ventilation rate.

Zonal Models

Zonal models are based on the same principal that multizone modelling utilises. The main difference in zonal modelling is that they aim to model large halls or empty zones by assuming fictitious zones in these spaces (Inard et al., 1996). Again, mass balances were constructed among imaginary zones, and those equations are solved successively to define the whole system. Zonal models uses less time and computer memory in their calculations compared to CFD.

CONCLUSIONS AND DISCUSSIONS

Available techniques used for ventilation rate measurement and simulation for naturally ventilated buildings were summarised. While both direct and indirect measuring techniques have particular advantages, they have also certain drawbacks that cannot be disregarded. Main disadvantage of direct measuring techniques is providing local measurements that cannot be representative for whole system. On the other hand, simulation techniques are laborious and not accurate enough.

Nowadays, none of the methods provides accurate and robust mechanism for natural ventilation measurements. Constant evaluation and improvement of current methods observed in the last decades. Alternatively, combination of measuring and modelling techniques can provide a reliable online control system in these buildings.

Table 1. Literature Survey on Measuring Techniques for Ventilation Rate and Air Velocities

METHOD	ADVANTAGE	DISADVANTAGE	INACC.	REFERENCE
Direct Measuring Techniques				
Free Running Impeller	- used in most of the mechanically ventilated stables	- need defined inlet/outlet - circular cross-section	5-25%	Berckmans et al., 1991; Vranken, 1999; Berckmans et al. 2001
Propeller Gauge	- Depending on the quality, accurate measurements are possible	- local measurements - accuracy depend on pressure difference, temperature, static pressure, and density measurements	2 – 25 %	NovaLynx Corporation, 2005; Davis Instruments, 2005; Kinsey et al., 2004
Hot wire anemometer	- can measure steady-state to transient temperature differences	- susceptibility to dust - need for a representative measuring point due to local measurement - lack of physical robustness	0.5 - 25 % *	Perry and Morrison, 1971; Scholtens and van 't Ooster, 1994; Watmuff, 1995; Dantec Dynamics, 2005
Laser Doppler Anemometer	- accurate - non-intrusive - no need for calibration - ability to measure reversing flows	- local measurements - accuracy is highly dependent on alignment of emitted and reflected beams - expensive - sufficient transparency is required between laser source and target	< 2 % *	Yeh and Cummins, 1964; George, 1988; De Graaff and Eaton, 2001 Dantec Dynamics, 2005
Particle Image Velocimetry	- accurate - non-intrusive	- local measurements	< 3 % *	Shandas et al., 1995; Hu et al., 2000, 2002; Meyer et al., 2002; Dantec Dynamics, 2005
Transit Time Sonic Anemometer	- accurate - no obstruction in the flow path - low maintenance cost - can be used in corrosive environments - portable models are available	- local measurements - high initial set up cost - susceptible to construction errors	0.1 - 4 % *	Quaranta et al., 1985; Wang et al., 1999; Windsonic, Gill Instruments; Airflow UA6, Davis Instrumets

* inaccuracies in terms of air velocities

METHOD	ADVANTAGE	DISADVANTAGE	INACC.	REFERENCE
Indirect Measuring Techniques				
Pressure Difference	- cheap and direct measuring technique for mechanical ventilation - if coupled with tracer gas experiments, physical description of ventilation mechanism, ventilation rate per opening depending upon physical environment can be predicted - local ventilation rates can be determined	- depends on type size, and number of the ventilation opening(s), the position of the openings and building size. - at low wind speed inaccuracy is bigger - sensitive to corrosion -mostly underestimation - high fluctuation in and around the buildings	20 - 35 %	Bruce, 1978; Brockett and Albright, 1987; Boulard and Baille, 1995; Demmers, et al., 1997; Richardson et al., 1997; Boulard et al., 1998
CO_2 balance	- used in naturally ventilated buildings	- CO_2 from other sources (respiration, manure, etc.) - solubility of CO_2 in water - small error in concentration can result larger error in ventilation rate	15 - 40 %	Penman and Rashid, 1982; Van't Klooster and Heitlager, 1994; Pedersen et al., 1998
Heat Balance	- only temperature measurements are enough - can be used in naturally ventilated buildings	- complex calculations and difficulty in determination of heat gains/loses - not suitable for fast and simple determination of ventilation rate - for high k-values, measurement of radiation, wind speed and direction is needed	31 - 101 %	Van't Ooster, 1994; Wang and Deltour, 1996; Kotani et al., 2003; Yam et al., 2003 ; Fatnassi et al., 2004
Tracer Gas	- can be used for total ventilation rate calculations - suitable for natural ventilation	- perfect mixing assumed	10 - 50%	Abu-Jarad et al., 1982 Sandberg and Blomqvist, 1985; Jung et al., 1994; Zhang et al., 1995;
CFD Analysis	- can be applied to any type of the building	- good assumptions are needed for system parameters -requires huge processing time	10 - 40%	Ayad, 1999; Demmers et al., 2000; Campen and Bot, 2003; Jiang et al., 2003
Multizone Modelling	- mostly used in building design calculations	- boundary conditions should be well defined	15 - 50%	Sherman, 1989; Feustel and Dieris, 1992; Dascalaki et al., 1995, 1999; Roulet et al., 1999; Posner et al., 2003
Zonal Models	-less zone is needed than CFD - less execution time	- need a good reference method for comparison -more experimental validation needed	20-50 %	Inard et al., 1996; Wurtz et al., 1999; Brehme and Krause, 2001; Ren and Stewart, 2003

References

Abu-Jarad, F., Sithamparanadarajah, R., Thompson, J.M. and Fremlin, J.H. (1982). Comparison of various techniques for measuring natural ventillation in rooms. *Physics in Medicine and Biology*, Volume: 27 :11, 1393-1400.

Ayad, S.S. (1999). Computational study of natural ventilation, *Journal of Wind Engineering and Industrial Aerodynamics*, 82 :1-3, 49-68.

Berckmans, D., Vandenbroeck, P. and Goedseels, V. (1991). Sensor for continuous ventilating rate measurement in Livestock Buildings. *Journal of Indoor Air*, **3** : 323-336.

Berckmans, D., Vranken, E. and Janssens, K. (2001). Method and apparatus for determining a flow pattern of a fluid in a space. *International Patent* WO 01/01082, International application published under the patent cooperation treaty (PCT)

Boulard, T. and Baille, A. (1995). Modelling of air exchange rate in a greenhouse equipped with continuous roof vents. *Journal of Agric. Engineering Research*, **61**: 37-48.

Boulard, T., Kittas, C., Papadakis, G. and Mermier, M. (1998) Pressure Field and Airflow at the Opening of a Naturally Ventilated Greenhouse, *Journal of Agricultural Engineering Research*, **71 :1**, 93-102.

Brehme, G. and K.-H. Krause. (2001). Compartmental airflow simulation in stables with natural ventilation. *Agricultural Engineering International: the CIGR Journal of Scientific Research and Development.* Manuscript BC 01 003. Vol. **IV**.

Brockett, B. L. and Albright, L. D. (1987). Natural ventilation in single airspace buildings. *Journal of Agric. Engineering Research*, **37 :2,** 141 – 154.

Bruce, J. M. (1978). Natural convection through openings and its application to cattle building ventilation. *Journal of Agric. Engineering Research*. **23:** 151-167.

Calogirou, A., Boekhoven, J. and Henkes, R.A.W.M. (2001). Effect of wall roughness changes on ultrasonic gas flowmeters. *Flow Measurement and Instrumentation*, **12 :3**, 219 – 229.

Campen, J.B. and Bot, G.P.A. (2003). Determination of greenhouse-specific aspects of ventilation using three-dimensional computational fluid dynamics. *Biosystems Engineering*, **84 :1,** 69 – 77.

Dantec Dynamics. (2005). http://www.dantecdynamics.com/

Dascalaki, E., Santamouris, M., Argiriou, A., Helmis, C., Asimakopoulos, D., Papadopoulos, C. and Soilemes, A. (1995). Predicting single side natural ventilation rates in buildings, *Solar Energy*, **55 :5,** 327-341.

Dascalaki, E., Santamouris, M., Bruant, M., Balaras, C.A., Bossaer, A., Ducarme, D. and Wouters P. (1999). Modeling large openings with COMIS. *Energy and Buildings*, **30 :1**, 105-115.

Davis Instruments. (2005). http://www.davis.com/showl5.asp?L5ID=1&L4ID=6

DeGraaff, D. B. and Eaton, J. K. (2001). A high-resolution laser Doppler anemometer: design, qualification, and uncertainty, *Experiments in Fluids*, **30 :5**, 522 – 530.

Demmers, T.G.M., Burgess, L.R., Short, J.L., Phillips, R., Clark, J.A. and Wathes C.M. (1997). The use of pressure difference measurements in determining ammonia emissions from naturally ventilated UK Beef building. *Proocedings of the Fifth International Symposium ILES-V*. p.56-64.

Demmers, T. G. M., Burgess, L. R., Phillips, V. R., Clark, J. A. and Wathes, C. M. (2000). Assessment of techniques for measuring the ventilation rate, using an experimental building section, Journal *of Agricultural Engineering Research*, **76 :1**, 71-81.

Fatnassi, H., Boulard, T. and Lagier, J. (2004). Simple Indirect Estimation of Ventilation and Crop Transpiration Rates in a Greenhouse, *Biosystems Engineering*, 88 :4, 467-478.

Feustel, H.E. and Dieris, J. (1992). A survey of airflow models for multizone structures, *Energy and Buildings*, 18 :2, 79-100.

Feustel, H.E. (1999). COMIS--an international multizone air-flow and contaminant transport model, *Energy and Buildings*, 30 :1, 3-18.

George, W.K. (1988). Quantitative measurement with the burst-mode laser Doppler anemometer, *Experimental Thermal and Fluid Science* **1 :**29–40.

Hu, H., Saga, T., Kobayashi, T. and Taniguchi, N. (2002). Simultaneous measurements of all three components of velocity and vorticity vectors in a lobed jet flow by means of dual-plane stereoscopic particle image velocimetry. *Physics of Fluids*, **14 :7,** 2128-2138.

Hu, H., Kobayashi, T., Saga, T., Segawa, S. and Taniguchi, N. (2000). Particle image velocimetry and planar laser-induced fluorescence measurements on lobed jet mixing flows. *Experiments in Fluids*, **29 :7,** 141-157.

Inard, C., Bouia, H. and Dalicieux, P. (1996). Prediction of air temperature distribution in buildings with a zonal model, *Energy and Buildings*, 24 :2, 125-132.

Iooss, B., Lhuillier, C. and Jeanneau, H. (2002). Numerical simulation of transit-time ultrasonic flowmeters: uncertainties due to flow

profile and fluid turbulence. *Ultrasonics*, 40 :9, 1009 – 1015.

Jiang, Y., Alexander, D., Jenkins, H., Arthur, R. and Chen, Q. (2003). Natural ventilation in buildings: measurement in a wind tunnel and numerical simulation with large-eddy simulation, *Journal of Wind Engineering and Industrial Aerodynamics*, **91 :3**, 331-353.

Jung, A. and Zeller, M. (1994). An analysis of different tracer gas techniques to determine the air exchange efficiency in a mechanically ventilated room. *Fourth Int. Conf. on Air Distribution in Rooms - ROOMVENT '94.* pp.315-332.

Kinsey, J.S., Swift, J. and Bursey, J. (2004). Characterization of fugitive mercury emissions from the cell building at a US chlor-alkali plant, *Atmospheric Environment*, **38 :4,** 623-631.

Kotani, H., Satoh, R. and Yamanaka, T. (2003). Natural ventilation of light well in high-rise apartment building, *Energy and Buildings*, **35 :4**, 427-434.

Meyer, K. E., Özcan, O. and Westergaard, C. H. (2002). Flow Mapping of a Jet in Crossflow with Stereoscopic PIV. *Journal of Visualization.* 5 :3, 225-231.

NovaLynx Corporation. (2005). http://www.novalynx.com/200-2201.html

Pedersen, S., Takai, H., Johnsen, J.O., Metz, J.H.M., Koerkamp, P.W.G.G., Uenk, G.H., Phillips, V.R., Holden, M.R., Sneath, R.W., Short, J.L., White, R.P., Hartung, J., Seedorf, J., Schroder, M., Linkert, K.H. and Wathes, C.M. (1998). A comparison of three balance methods for calculating ventilation rates in livestock buildings. *J. Agric. Engineering Research*, **70 :1,** 25 – 37

Penman, J. M. and Rashid, A. A. M. (1982). Experimental determination of air-flow in a naturally ventilated room using metabolic carbon dioxide, *Building and Environment*, 17 :4, 253-256.

Perry, A. E., and Morrison, G. L. (1971). A Study of the Constant Temperature Hot-Wire Anemometer, J. *Fluid Mech.* **47** : 577-599.

Posner, J. D., Buchanan C. R. and Dunn-Rankin, D. (2003) Measurement and prediction of indoor air flow in a model room, *Energy and Buildings*, **35 :5**, 515-526.

Ren Z. and Stewart J. (2003). Simulating air flow and temperature distribution inside buildings using a modified version of COMIS with sub-zonal divisions. *Energy and Buildings*, **35 :**257-271.

Richardson, G.M., Hoxey, R.P., Robertson, A.P. and Short, J.L. (1997). The Silsoe Structures Building: Comparisons of pressures measured at full scale and in two wind tunnels. *Journal of Wind Engineering and Industrial Aerodynamics*, **72 :1-3,** 187 - 197

Roulet, C.A., Furbringer, J.M. and Cretton, P. (1999). The influence of the user on the results of multizone air flow simulations with COMIS. *Energy and Buildings*, **30 :1**, 73 - 86

Quaranta, A.A., Aprilesi, G.C., Dedicco, G. and Taroni, A. (1985). A microprocessor based, 3 Axes, ultrasonic anemometer, *Journal of Physics*, e-Scientific Instruments, **18 :5,** 384 -387.

Sandberg, M. and Blomqvist, C. (1985) A quantitative estimate of the accuracy of tracer gas methods for the determination of the ventilation flow rate in buildings, *Building and Environment*, **20 :3**, 139-150.

Scholtens, R. and Van 't Ooster, A. (1994). Performance and accuracy of methods for measuring natural ventilation rates and ammonia emissions. *Proceedings of the International Conference on Agricultural Engineering, AGENG '94.* p.240.

Shandas, R., Gharib, M., Sahn, D., Valdes-Cruz, L. (1995). Digital Particle Image Velocimetry: A New Technique for Verification of Color Doppler Flow Mapping Data, *Journal of the American College of Cardiology*, 25 :2, 380A.

Sherman, M.H. (1989). On the estimation of multizone ventilation rates from tracer gas measurements. *Building and Environment.* **24 :4,** 355 – 362.

Simonson, C. (2005). Energy consumption and ventilation performance of a naturally ventilated ecological house in a cold climate, *Energy and Buildings*, **37 :1**, 23-35.

Snell, H. G. J., Seipelt, F. and Van den Weghe, H. F. A. (2003). Ventilation Rates and Gaseous Emissions from Naturally Ventilated Dairy Houses, *Biosystems Engineering*, 86 :1, 67-73.

Temperley, N.C., Behnia, M. and Collings, A.F. (2004). Application of computational fluid dynamics and laser Doppler velocimetry to liquid ultrasonic flow meter design, *Flow Measurement and Instrumentation*, **15 :3**, 155-165.

Van Buggenhout, S., Lemaire, J., Vranken, E., Van Malcot, W., and Berckmans, D., (2005). Ontwikkeling van een eenvoudige meettechniek voor debietmeting in natuurlijk geventileerde gebouwen. HOBU-project, HOBU 020078, pp. 80.

Van Ouwerkerk, E. N. J. (1993). *Meetmethoden NH3-emissie uit stallen. Onderzoek inzake de mest- en ammoniakproblematiek in de veehouderij*. DLO Rapport, Wageningen, the Netherlands

Van 't Klooster, C. E. (1994). *Implementation of natural ventilation in pig houses*. Ph.D. Thesis Landbouwuniversiteit Wageningen (NL). 153 pp.

Van 't Klooster, C. E. and Heitlager. B.P. (1994). Determination of minimum ventilation rate in pig houses with natural ventilation based on carbon-dioxide balance. *J. Agric. Engineering Research*, **57 :4,** 279 – 287.

Van 't Ooster A. (1994). Using natural ventilation theory and dynamic heat balance modelling for real time prediction of ventilation rates in naturally ventilated livestock houses. *International Conference on Agricultural Engineering, AGENG '94*. p.206-207.

Vranken, E. (1999). *Analysis and optimisation of ventilation control in Livestock Buildings.* PhD-thesis No 392 at the Faculty of Agricultural and Applied Biological Sciences: K.U.Leuven.

Wang, S., and Deltour, J. M. (1996). An experimental ventilation function for large green-houses based on a dynamic energy balance model. *International Agricultural Engineering Journal.* **5 :1-4**, 103-112.

Wang, S., Yernaux, M. and Deltour, J. (1999). A networked two-dimensional sonic anemometer system for the measurement of air velocity in greenhouses. *J. Agric. Engineering Research*, 73 :2, 189 – 197.

Watmuff, J.H. (1995). An investigation of the constant-temperature hot-wire anemometer, *Experimental Thermal and Fluid Science*, **11 :2**, 117-134.

Windsonic. (2004). http://www.gill.co.uk/products/anemometer/anemometer.htm

Wurtz, E., Nataf, J.M. and Winkelmann, F. (1999). Two- and three-dimensional natural and mixed convection simulation using modular zonal models in buildings, *International Journal of Heat and Mass Transfer*, **42 :5,** 923 - 940

Yam, J., Li, Y. and Zheng, Z. (2003). Nonlinear coupling between thermal mass and natural ventilation in buildings, *International Journal of Heat and Mass Transfer*, 46 :7, 1251-1264.

Yeh Y. and Cummins H.Z. (1964). Localized fluid flow measurements with a He-Ne laser spectrometer. *Applied Physics Letters*, **4:**176

Zhang, J.S., Shaw, C.Y. and Magee, R.J. (1995). On the accuracy and repeatability of the pulse and step-down tracer gas methods for measuring mean ages of air. ASHRAE Transactions, **101 :1**, 239-248.

EXPERIMENT OF THE MIXING PROPERTY AND THE HEAT EXHAUST EFFECT UNDER CROSS VENTILATION IN A FULL-SCALE BUILDING MODEL

S. Nishizawa[1], T. Sawachi[2], K. Narita[3], H. Seto[1], Y. Ishikawa[1] and T. Gotou[3]

[1] *Building Research Institute, 1 Tachihara, Tsukuba 305-0802, Japan*
[2] *National Institute for Land and Infrastructure Management, 1 Tachihara, Tsukuba 305-0802, Japan*
[3] *Nippon Institute of Technology, 4-1 Gakuendai, Miyashiro, Saitama 345-8501, Japan*

ABSTRACT

Cross ventilation is one of the most important techniques for achieving energy conservation and for maintaining a comfortable indoor environment in summer. But it is difficult to evaluate the effect of cross ventilation quantitatively and to design based on a quantitative evaluation, because the indoor environment is uneven and changes with the outside conditions under cross ventilation.
The full-scale model experiment has been done under cross ventilation, and the properties of airflow in and around the full-scale model have been examined. In this paper, the mixing property and heat exhaust effect of cross ventilation are discussed.
Concentration decay in the full-scale model is measured by using tracer gas technique, and the spatial unevenness of mixing property is examined. And it is shown that the different mixing properties are formed with the airflow pattern. In the experiment of the heat exhaust effect, the temperature of air and surface and exhaust heat is measured. The relation between the temperature reduction and the flow path is examined. Two experiments show that ventilation rate is the most effective factor to decide the exhaust heat and the room mean age of air. But air flow pattern also has a influence.

KEYWORDS

Cross ventilation, Full-scale model experiment, Mixing property, Heat exhaust effect

INTRODUCTION

Cross ventilation driven by wind is one of the most important techniques for achieving energy conservation and for maintaining a comfortable indoor environment in summer for the temperate regions. But it is difficult to evaluate the effect of cross ventilation quantitatively and to design based on a quantitative evaluation, because the indoor environment has unevenness and changes dynamically with outside conditions under cross ventilation. It is difficult to predict the air flow rate under cross ventilation due to variational wind. And it is still difficult to estimate indoor comfort condition given by cross ventilation.
In the previous study, the full-scale model experiment has been done under cross ventilation, and the properties of air flow (velocity field, pressure distribution on surface, discharge coefficient of openings, …) have been examined. In this paper, it is discussed the influence of the air flow pattern on the mixing property and heat exhaust effect under cross ventilation.

EXPERIMENTAL METHOD

The plan and section of the wind tunnel for cross ventilation is shown in Figure 1. The wind tunnel was constructed to examine the property of air flow in and around a full-scale building model. Its form is different to a conventional boundary layer wind tunnel, but it is possible

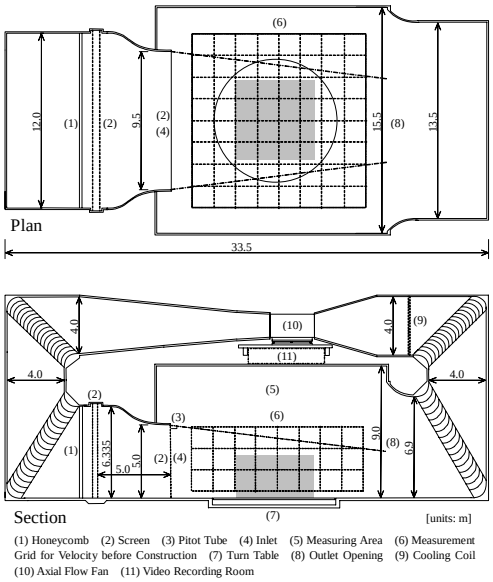

Figure 1: Plan and section BRI's cross ventilation laboratory wind tunnel

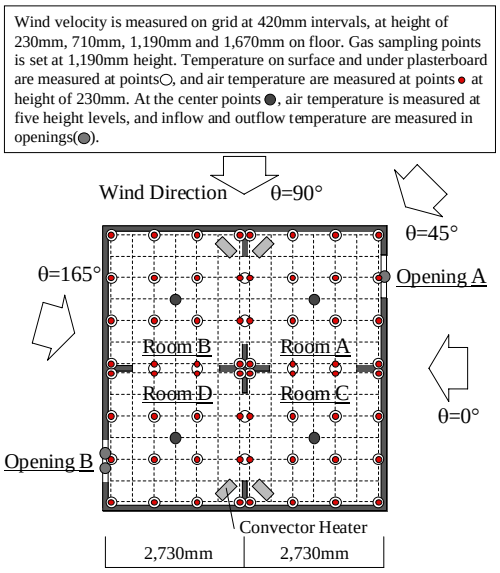

Figure 2: Building model and measuring points

that the full-scale building model gets same wind pressure condition repeatedly. In the wind tunnel, the air flow pattern and the wind pressure has already been measured in detail.

The building model is shown in Figure 2. It has dimensions W=D=5,560mm and H=3,000mm and has four rooms. It has two large openings (W=860mm, H=1,740mm), which are set at diagonal position of the model for cross ventilation. Wind direction is set at every 15 degree (0° – 165°) by rotating the model. Air flow velocity is measured on indoor grid using 3-dimentional ultrasonic anemometer (Kaijo, WA-390). The average velocity at the inlet is set at 3m/s.

The automatic doors are set at both openings in the experiments of the mixing property and heat exhaust effect. The mixing property in the uneven space under cross ventilation is evaluated applying repeatedly the tracer gas technique with changing the door-opening interval. The concentration decay is measured at 0.05 sec intervals at 17 or 18 sampling points, which are set at 1,190mm height every wind direction. And the average concentration decay is also measured at intervals of door-opening setting.

In the experiment of the heat exhaust effect, foam plastic insulation boards 50mm thick are set on floor, wall and ceiling in the model, and plasterboards 12.5mm thick are set on floor as thermal storage. Before opening the doors, indoor air is heated evenly about 10 degrees centigrade higher than wind tunnel temperature by using heaters and mixing fans. And the change of temperature of air and floor surface is measured every 15 seconds at points in Fig.2 after opening the doors.

RESULTS

Mixing Property

The results of typical three cases (Wind directions are 15°, 45° and 105°) are shown in Figure 3–11. Figure 3 shows the visualized flow pattern in 15°. Figure 4 shows the air flow field in and around the model at 1,190mm height and the local air change index (ε_p) at sampling points. And Figure 5 shows the decay of normalized concentration at some points. In the case of wind directions 15°, the main current appears clearly, and the concentration decrease

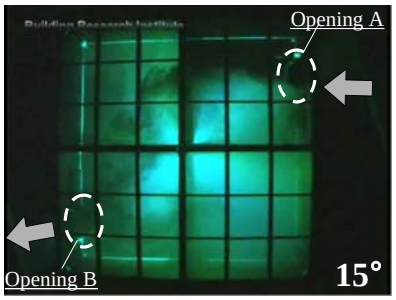

Figure 3: Air flow visualization (15°)

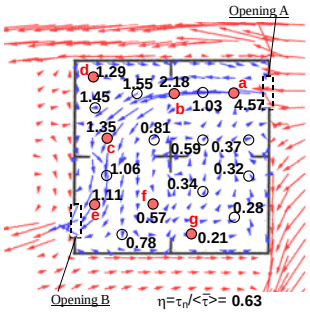

Fig. 4: Sampling points and local air change index (15°)

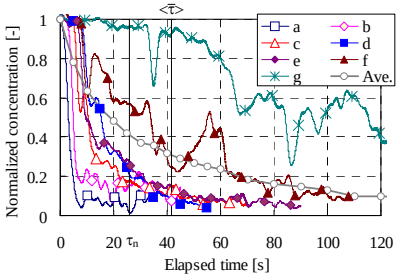

Fig. 5: Concentration decay (15°)

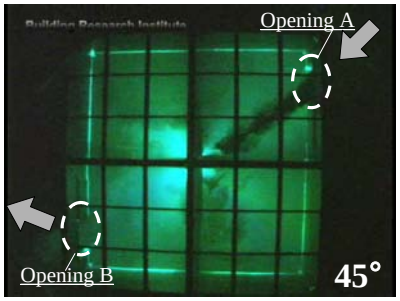

Figure 6: Air flow visualization (45°)

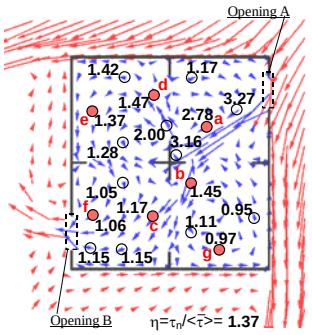

Fig. 7: Sampling points and local air change index (45°)

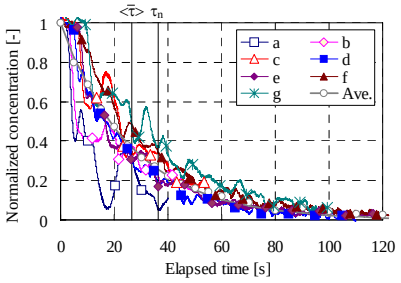

Fig. 8: Concentration decay (45°)

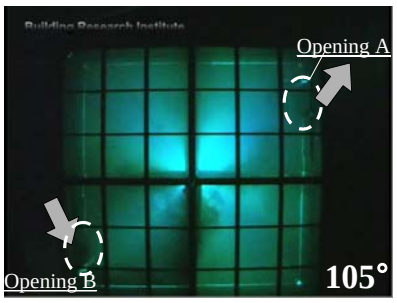

Figure 9: Air flow visualization (105°)

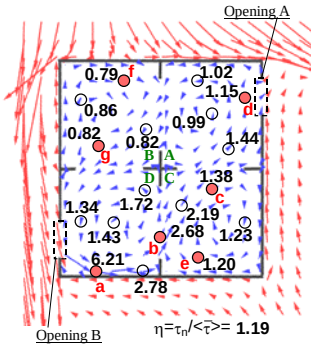

Fig. 10: Sampling points and local air change index (105°)

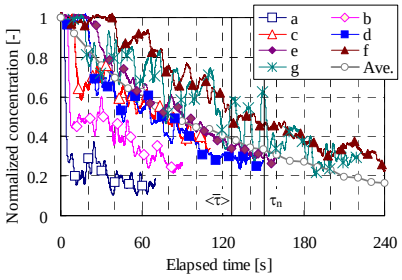

Fig. 11: Concentration decay (105°)

quickly at the points in main current (point **a**, **b** in Figure 4 and 5). In the edge of the main current (point **f**), the concentration decay is slow, and has large periodic fluctuation. The periodic fluctuation is caused by vortices, which are made by mixing of main current and retention air (Figure 3). At point **g**, which is far from main current, the concentration attenuates very slowly (Figure 5). The average concentration decay is also shown in Figure 5.

In the case of wind direction 15°, the room mean age of air ($<\bar{\tau}>$) is 41.5s, and the coefficient of air change performance (η) is 0.63. This is the similar characteristic of poor mixing ventilation and shows the tendency that the air in the main current is smoothly discharged, and the air is kept in the retention area for a long time.

In the case of wind direction 45°, the current collides with the pillar and walls at center in the model, and diverges in two directions (Figure 6, 7). The coefficient of air change performance (η) is 1.37, and the air flow field shows the characteristic of the piston flow (Figure 7). There is not so much of difference in the speed of concentration decay, except points **a**, **b** (Figure 8). And the distribution of the local air change index (ε_p) is more even than wind direction 15°. Therefore, indoor air is discharged effectively ($<\bar{\tau}>_{(15°)}$=41.5s, $<\bar{\tau}>_{(45°)}$=28.5s) though the air flow rate in 45° is smaller than 15° ($Q_{(15°)}$=9,700m^3/h, $Q_{(45°)}$ =7,000m^3/h).

In the case of wind direction 105° (Figure 9 – 11), the air flow rate is smaller ($Q_{(105°)}$=1,700m^3/h), and the room mean age of air is longer (<$\bar{\tau}$>=126.4s) than 15° and 45°. The coefficient of air change performance (η) is 1.19, and the total mixing property in the model is close to the perfect mixing, but the distribution of the local air change index (ε_p) shows the unevenness along the flow (ε_p has the tendency of Room **D** > **C** > **A** > **B** (Figure 10)). The concentration at point **g** has large periodic fluctuation because of air exchange between Room **C** and **B** (Figure 10, 11).

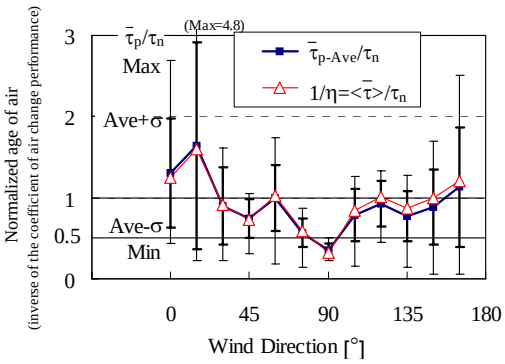

Figure 12: Distribution of local mean age of air

Figure 12 shows the age of air normalized by the nominal time constant (τ_n). When the value of normalized room mean age of air (<$\bar{\tau}$>/τ_n) becomes larger (η becomes smaller), the difference of $\bar{\tau}_p$ between the sampling points becomes larger, and the unevenness of mixing property between main current and retention area makes clear in the space. And when <$\bar{\tau}$>/τ_n approaches 0.5 (η approaches 2) and the air flow field comes to show the tendency of the piston flow, the difference of $\bar{\tau}_p$ becomes small, and mixing property is formed uniformly.

Heat Exhaust Effect

Air temperature distribution (height of 230mm above floor level) and temperature distribution on floor surface in the case of wind direction 15° are shown in Figure 13, 14. Temperature is expressed normalized by initial inside-outside temperature differences. In the case of wind direction 15°, Air temperature quickly falls in the main current, and decreasing rate of air temperature is smaller in the retention area and at the back of pillar and side walls. The temperature of floor surface falls slower than the air temperature. The normalized temperature on floor is 0.6 - 0.8 at 5 minute after opening doors, and still keeps 0.2 – 0.3 under the main current and about 0.5 in the retention area 20 minutes later.

Figure 15 shows the exhaust heat from inside the model and the heat flow from floor in wind direction 15°. The exhaust heat flow H [W/K], which is normalized by initial inside-outside temperature differences, is obtained by follows.

$$H = \rho C_p Q(T_{out} - T_{in})$$

Where ρ is air density [kg/m^3], C_p is heat capacity of the air at constant pressure [J/kg K], Q is air flow rate [m^3/s], and T_{in} and T_{out} is the normalized temperature in the inflow and outflow [-]. Air flow rate Q was measured by integrating the velocity at 48 points in opening area. And the normalized heat flow from floor H_f [W/K] is calculated by follows.

$$H_f = \Sigma h A(T_f - T_a)$$

Where h is the convective heat transfer coefficient [W/m^2K], A is surface area [m^2], T_f is the normalized temperature on the floor surface [-] and T_a is the normalized temperature of air at height 230mm [-]. The convective heat transfer coefficient h was calculated from the moisture transfer coefficient, which is measured by evaporation from the filter paper at 196 points on floor in the wind direction 15°. Figure 16 shows the distribution of the convective heat transfer coefficient in the case of wind direction 15°. The convective heat transfer coefficient is high under main current, and it has higher value at collision point at sidewall (**a** in Figure

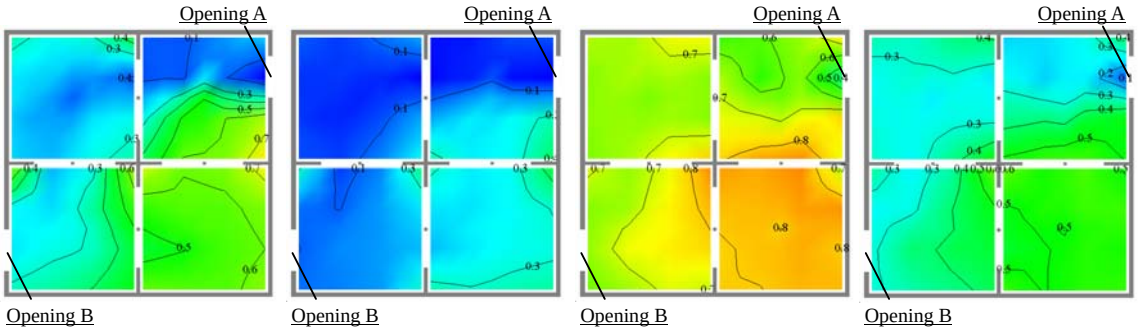

a) 1 minute b) 5 minutes

Figure 13: Air temperature distribution (15°)

a) 5 minutes b) 20 minutes

Figure 14: Temperature distribution on floor (15°)

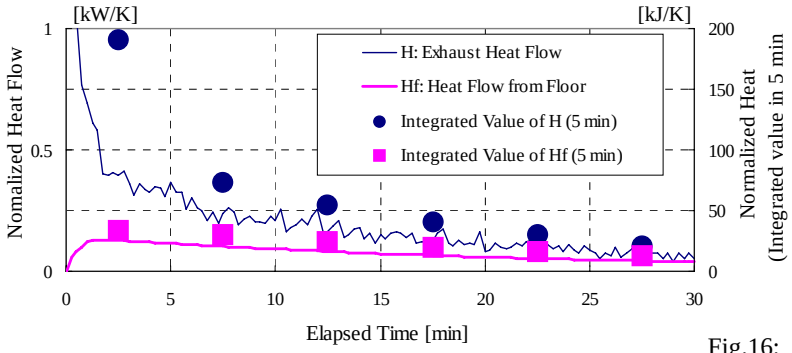

Figure 15: Heat transfer in 15°

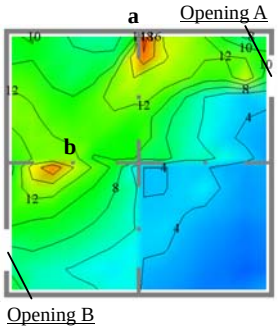

Fig.16: Distribution of the convective heat transfer coefficient (15°)

16) especially. Another higher point is influenced by pillar **b**.

In Figure 15, the heat flow from floor (H_f) is smaller than the exhaust heat flow (H). Total H_f is only 40% of total H, because of the heat capacity other than plaster boards, aluminum sash and glass of partitions, and heat bridge of the frame. In the experiment, insulation boards are set on floor, walls, and ceiling, but don't covered partitions that are made of aluminum frame and glass. And the partitions are connected with steel frame and heat bridge is formed through insulation division. Therefore partitions keep large amount of heat before opening doors, and supply heat to ventilated air. Figure 17 shows the total exhaust heat normalized by initial temperature differences and the summation of heat capacity in insulation division of the model. Total H_f in 15° is almost equal to the heat capacity of plaster boards on the floor, so the experiment and the convective heat transfer coefficient is appropriate. Total H is uneven in the condition of wind direction, compared with the heat capacity in the insulation division, because of influences of the heat capacity of the ceiling and underfloor space that is connected by heat bridge.

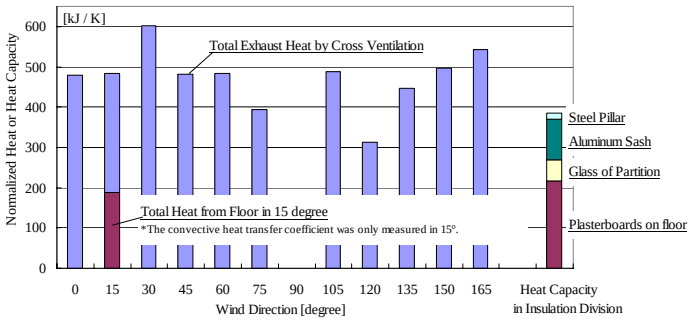

Figure 17: Total exhaust heat and heat capacity of the model

Figure 18 shows the relation between the air flow rate Q and the summation of exhaust heat H for 5 and 10 minutes from opening the doors (wind directions are shown in [ ]). It is shown that the ventilation rate is the most effective factor to decide the exhaust heat. And there is little difference in the wind direction at low ventilation rate, but there is difference in the wind direction at high ventilation rate; internal heat is smoothly exhausted in 30° and 45°, and not

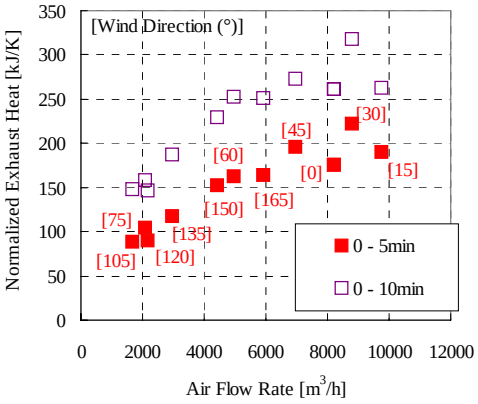

Figure 18: Air flow rate and exhaust heat

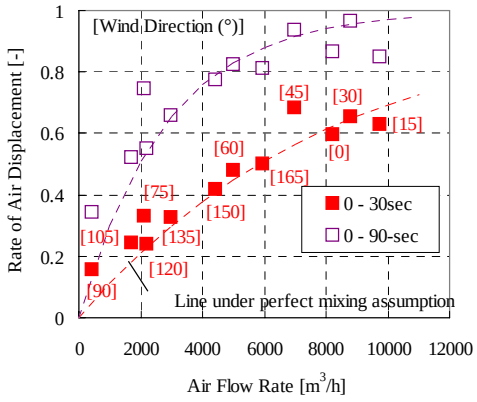

Figure 19: Air flow rate and air displacement

easily exhausted in 0° and 15°. The difference also appears in the rate of air displacement in the experiment of mixing property (Figure 19), and it is considered that the air flow pattern have an influence on the indoor convective heat transfer as well as the mixing property.

CONCLUSIONS

The mixing property and heat exhaust effect are examined experimentally in the uneven space under cross ventilation. Conclusion is as follows.

1) Relation between air flow pattern and mixing property is examined by the concentration decay. In the case that the main current appears clearly, the coefficient of air change performance (η) becomes smaller, and the uneven distribution of the local air change index (ε_p) appears clearly, and the speed of decay is different in measurement point. In the case that the airflow field has the characteristic of the piston flow, the coefficient of air change performance (η) approaches 2, and the distribution of the local air change index (ε_p) becomes uniform.
2) Temperature distribution of air and floor surface is measured and air temperature in main current decrease quickly. And the temperature on floor falls slower than air temperature, but the temperature under main current has faster decrease than the temperature in retention area reflecting the distribution of convective heat transfer coefficient.
3) The exhaust heat speed and the rate of air displacement are mainly affected by ventilation rate, but are reflected the difference of air flow pattern at large ventilation rate.

References

Carrilho da Graça, G., P.F. Linden. (2002). Simplified modeling of cross ventilation airflow, *ASHRAE Transactions* **109: 1**, 65-79

Nishizawa, S., Enai, M., Hayama, H. and Mori, T. (2003). The Index to evaluate the space with unevenness in consideration of time scale. *Ventilation 2003 Proceedings*, 97-102.

Nishizawa, S., Sawachi, T., Narita, K., Seto, H. and Ishikawa, Y. (2004). Examination of the space with cross ventilation by tracer gas technique and zoning concept of the space with unevenness. *Roomvent 2004 Proceedings CD*.

Sawachi, T., Narita, K., Kiyota, N., Seto, H. Nishizawa, S. and Ishikawa, Y. (2004). Wind pressure and air flow in a full-scale building model under cross ventilation. *The International Journal of Ventilation* **2: 4**, 343-358

Yuguo Li and Jimmy Chi Wai Yam (2004). Designing thermal mass in naturally ventilated buildings. *The International Journal of Ventilation* **2: 4**, 313-324

EXPERIMENTAL CHARACTERIZATION OF HYBRID VENTILATION SYSTEMS IN RESIDENTIAL BUILDINGS

Manuel Pinto[1], Vasco Peixoto de Freitas[2], João Carlos Viegas[3]

[1]Department of Civil Engineering, Viseu Polytechnic Institute,
Repeses Campus, 3504-510 VISEU, PORTUGAL
[2]Department of Civil Engineering , Faculty of Engineering - University of Porto
Rua Dr. Roberto Frias, 4200-465 PORTO, PORTUGAL
[3]National Laboratory of Civil Engineering,
Av. do Brasil, 101, P-1700-066 LISBOA, PORTUGAL

ABSTRACT

In the recent past, residential buildings in temperate climates were ventilated by the daily opening of windows and by exaggerated window and door permeability. Energy conservation concerns have led to better quality windows and lower air permeability that consequently increased the risk of condensation whilst decreasing indoor air quality.
Because of the variation in natural factors, such as wind speed and the stack effect, natural ventilation systems are unlikely to permanently provide ideal ventilation rates. As such, we will characterize the performance of hybrid ventilation systems (air intake through automatically regulated louvers in bedrooms and living rooms, natural exhaust in bathrooms and fan exhaust systems in kitchens) that are a possible solution to this drawback.
In March of 2002 and January of 2003, we measured air change rates in a 2-bedroom apartment using the PFT technique. This method has the advantage of measuring air renewal rates in inhabited apartments during a reasonable period and thereby reveals air renewal rates in the dwelling and also in each compartment.
This article will demonstrate the results obtained at a standard apartment and will present the experimental study characterising the hybrid ventilation system in a 100-apartment residential complex in the Porto area. The study evaluates the façade's permeability and the respective air exchange rates per compartment using the PFT and the constant concentration techniques.

KEY WORDS: ventilation, dwellings, air change rate (ACH), PFT, constant concentration technique.

INTRODUCTION

Following the 1970s energy crisis, the need to cut down on energy consumption led to lower air change rates (ACH) in residential buildings with an impact on air quality and relative indoor humidity levels. Moreover, the use of window frames with improved sealing properties decreased permeability to outside air and resulted in the risk of condensation and the consequent deterioration of building materials, Piedade and Rodrigues (2001), Freitas (2002).

The National Laboratory of Civil Engineering, Viegas (1995), and the Portuguese standard, IPQ (2002) for the natural ventilation of residential buildings recommend an average of one ACH in main rooms (bedrooms and living/dining rooms) and four ACHs in service rooms (kitchens and bathrooms).

Most recently built residential buildings might not comply with these rates. It is necessary to implement "general and permanent ventilation" systems with continuous air admission through the main rooms and air exhaust in the service rooms, Viegas (2002), Viegas (2004), Ferreira (2004).

SURVEY

In the spring of 2000, a survey of approximately 6,700 construction companies (Association of the Northern Industrialists of Civil Construction and Public Works, AICCOPN) was conducted in order to characterize the ventilation systems of residential buildings under construction in the northern region.

One hundred and forty valid replies were obtained covering 2,693 dwellings. The vast majority of the dwellings (2651) are located in the northern region. The survey includes approximately 6% of the dwellings built in the northern region in 2000, INE (2001).

The buildings under study presented the following characteristics, Pinto (2002):

- flats (93%) made up the vast majority of the surveys;
- the most widely represented typologies were two- and three-bedroom dwellings (31 and 46%, respectively);
- a large part of the dwellings were four (22.5%), five (18.8%) and six (22.9%) storey buildings.

The systems under study generally had the following main characteristics, Pinto (2002):

- no measures were taken to provide the dwellings with specific devices for the intake of air in the main rooms (bedrooms and living/dining rooms), only about 8% have fixed air inlets;
- mainly in the bathrooms (59%), or kitchens (77%), air exhaust is carried out through mechanical extraction, continuous or discontinuous;
- static ventilators are rarely used.

Under these circumstances, one can say that "general and permanent ventilation" is not a current practice in Portugal. We consider the implementation of these ventilation systems of great importance.

MEASUREMENT IN A STANDARD FLAT

Two trials were conducted over an extended period (2 weeks each) in order to estimate the ventilation rates (May 2002 and January 2003; Location: near Porto) using the PFT technique (more precisely, the homogeneous emission technique - Stymne and Boman (1994)), in a two-bedroom flat, Pinto (2003).

In the homogeneous emission techniques, the tracer gas emission rates from the sources are arranged to yield equal emission rates per volume unit in the measurement object. The local tracer concentration will be proportional to the "local mean age of air (τ_p[h])" (see Eq. 1).

$$\tau_p = \frac{M_p}{kt(s/V)} \tag{1}$$

Where (s/V) is the constant tracer gas emission rate per volume [g/($h^{-1} \cdot m^{-3}$)], M_p [g] is the mass of tracer gas collected in an adsorption sampling during a time period t [h] and k is the sampling rate for a passive sampling [m^3/h]. Therefore, this particular technique can be used to map the air distribution in a building. The inverted value of the local mean age of air can be interpreted as a "local air change rate" (ACH_{local}).

The flat's ventilation system admitted air via self-adjustable inlets (one inlet per room and two inlets in the living room) with a flow rate of 30 m^3/h under a 20 Pa pressure differential; natural exhaust in bathroom (ϕ125); individual discontinuous mechanical extraction in the kitchen; self-ventilated laundry (admission/exhaust via fixed inlets). The following is a layout of the flat showing the location of the respective instruments (Figure 1).

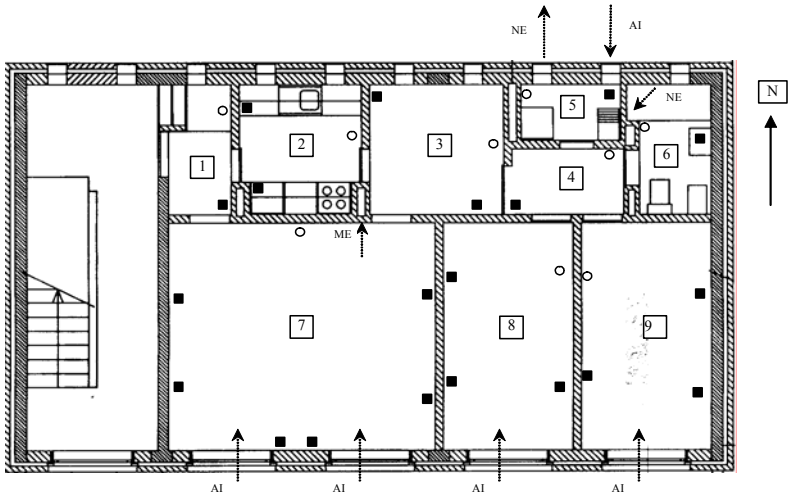

Figure 1: Layout of the flat showing the position of equipment used

Results and discussion

Knowing that the inlets guarantee an admission rate of 120 m^3/h, and considering that the flat has a volume of 160 m^3, the expected ACH rate should be 0.75 h^{-1} (on average for the whole flat). The low rates obtained (Table 1) can be explained by the relative lack of cross-ventilation, the windows are practically all on one side, facing south, while prevailing winds vary from the northwest and east. The lack of stack effect due to the small indoor/outdoor temperature difference and to the discontinuous mechanical extraction in the kitchen may also explain the low rate obtained. The habits of the residents, who kept their windows open for long periods during the May trial, may also explain the higher ACH rate during this period.

Local variation in each room's renewal rate, ACH_{local}, can be found in Table 1, where the rooms with the greatest ACH rate are the laundry and kitchen. It was found that the bathroom had a slightly higher ACH rate, probably caused by a slightly higher stack effect rate.

TABLE 1
ACH in each room and in the flat

Room	No.	ACH_{local} (h^{-1})	
		May	January
Hall	1	0.42	0.42
Kitchen	2	0.49	0.41
Hall A (bedroom C)	3	0.40	0.35
Hall B	4	0.37	0.33
Laundry	5	0.85	0.68
Bathroom	6	0.37	0.38
Living room	7	0.40	0.35
Bedroom A	8	0.46	0.28
Bedroom B	9	0.33	0.26
Prevailing wind direction		NW-26.8%	E-34.9%
Average wind speed (km/h)		19.8	14.4
Average indoor temperature (ºC)		16.0	12.2
Average outdoor temperature (ºC)		14.6	9.4
ACH_{total} (h^{-1})		0.41	0.33

MEASUREMENTS IN A GROUP OF MODIFIED STANDARD FLATS

Continuing previous tests, the study will analyse seven flats, six of which have a hybrid ventilation system (continuous exhaust system in the kitchen and natural exhaust in the bathroom). The seventh flat has a natural ventilation system in order to compare the performance of the two systems. The flats were selected to represent different orientations and different heights above ground (see Figure 2).

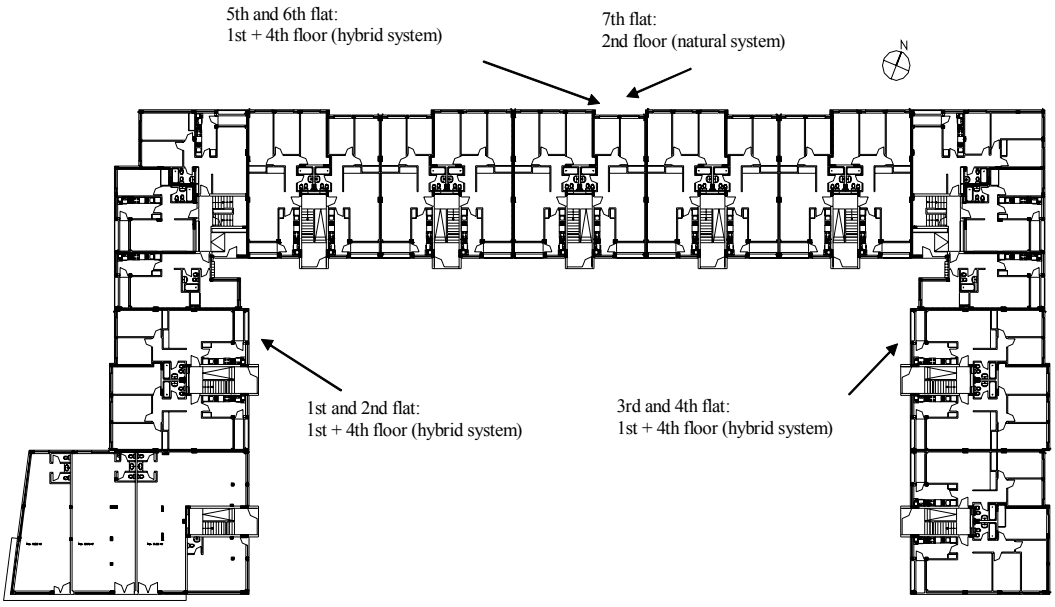

Figure 2: Residential building containing the seven flats to be tested

Table 2 describes the ventilation system implemented in each flat and the expected air renewal rates.

TABLE 2
Ventilation system in the flats

Flat no.	Orientation	Floor	Ventilation System	Diameter of the bathroom duct	Exhaust in the kitchen (Φ150)&	ACH_{total} (forecast)	Diameter of the heater duct#
1	SW	1st	Hybrid	Φ110* + static ventilator	Mechanical: 60 - 160 m^3/h	0.7 – 1.3	Φ175 - collective
2		4th	"	Φ110* + static ventilator	Mechanical: 60 - 160 m^3/h	"	Φ125 - individual
3	NE	1st	"	Φ125* + static ventilator	Mechanical: 60 - 160 m^3/h	0.75 – 1.3	Φ175 - collective
4		4th	"	Φ125* + static ventilator	Mechanical: 60 - 160 m^3/h	"	Φ125 - individual
5	NW	1st	"	Φ110* + static ventilator	Mechanical: 60 - 160 m^3/h	0.7 – 1.3	Φ175 - collective
6		4th	"	Φ110* + static ventilator	Mechanical: 60 - 160 m^3/h	"	Φ125 - individual
7	NW	2nd	Natural	Φ110	Natural	0.9	Φ175 - collective

* - Bathroom duct with insulation;
& - The schedule is: 12h-14h and 18h30-21h30 with 160 m^3/h and in the remaining hours with 60 m^3/h;
# - The need for fresh air for the heater is of about 4.3*heating power ≈ 100 m^3/h.

Figure 3 shows a standard apartment and the location of the various ventilation system devices.

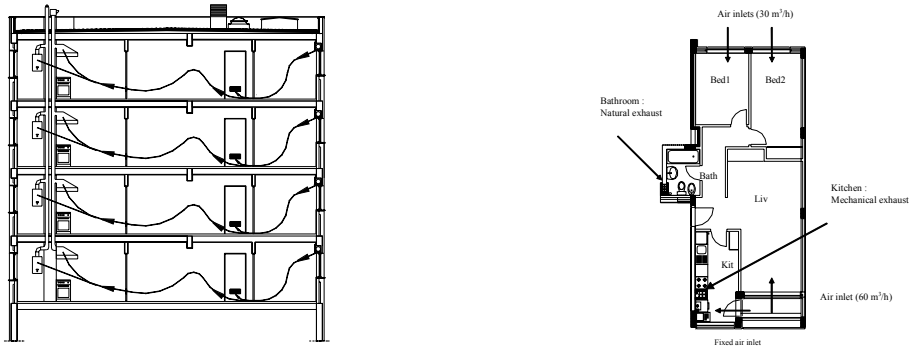

Figure 3: Standard flat to be tested

PLANNED TESTS

The following tests will be performed:

- to determine the pressure coefficients in the building's surrounding area;
- to determine window permeability – in laboratory;
- to determine the load loss and depression coefficient of the static ventilators;
- to determine the possibility of inverting the flow in the bathroom's duct and of stopping the boiler's exhaust;
- to determine the permeability of the surrounding components (e.g. windows, window-blind cases and air intake grates) – "*in situ*";
- to determine the overall permeability of the apartments;
- PFT test (one week) simultaneously in the seven apartments when uninhabited (summer of 2005) and inhabited (winter of 2007);
- PFT test in the seven apartments, uninhabited, simultaneously and applying the constant concentration technique (one week at each apartment; winter of 2006);

– to determine the comfort conditions: PMV - Predicted mean vote; PPD - Predicted percentage of dissatisfied).

Figure 4 shows some of the devices implemented at the apartments.

a) b)

Figure 4: Air intake devices, a) fixed inlets for air intake in the kitchen, b) self-adjustable inlets for the air intake in rooms and living room

In addition to the previously announced tests, the study also aims to examine the effects of alterations to the ventilation system, in particular the following: the efficiency of the thermal insulation in the bathroom ducts; the efficiency of using wider diameter ducts in bathrooms; the effect of ventilation with localised exhaust when the exhaust is stopped and the effect of an air transfer device on kitchen and bathroom doors.

CONCLUSION

Previous test results show that the ventilation rates of dwellings may be too low. Not using heating devices in dwellings results in a poor stack effect that consequently reduces ventilation rates. Wind did not increase ventilation rates to the level required in the previously studied building. Hybrid systems may be the solution for providing adequate ventilation rates. This experimental programme will provide the means to examine the performance of a system alternative to the natural ventilation. This system will equip apartment buildings with hourly renewal rates compatible with current regulations. Since hybrid ventilation systems are now being used in Portugal, there is an interest in determining the utilisation conditions under which they will provide adequate ventilation. This study is expected to reveal the performance of hybrid ventilation and any opportunities to improve its use.

ACKNOWLEDGEMENTES

The authors would like to acknowledge the support of FCT (POCTI/ECM 45555/2002).

REFERENCES

Ferreira, M., Corvacho, H. and Alexandre, J. L. (2004). Natural ventilation of residential buildings in Portuguese winter climatic conditions. *25th AIVC Conference,* Prague, Czech Republic.

Freitas, V. P. (2002). Building condensation. How to solve the problem in Portugal. *XXX IAHS Congress*, Coimbra, Portugal.

INE - National Institute of Statistics (2001). *Monthly Statistics Bulletin* [in Portuguese], November. Portugal.

IPQ - Instituto Português da Qualidade [Portuguese Institute of Quality] (2002). NP 1037-1. Ventilation and evacuation of combustion products from places with gas appliances. Part 1: Dwellings. Natural ventilation [in Portuguese], Lisbon, Portugal.

Piedade, A. C. and Rodrigues, A. M. (2001). Ventilation deficiencies in the origin of the signs of dampness in buildings: a case study [in Portuguese]. *Congresso Nacional da Construção*, Lisbon. Portugal.

Pinto, M. and Freitas, V. P. (2002). Characterization of natural ventilation systems in residential buildings in Portugal. The importance of standardization. *XXX IAHS Congress*, Coimbra, Portugal.

Pinto, M. *et al* (2003). Air change rates in multi-family residential buildings in northern Portugal, *7th Healthy Buildings Conference*, National University of Singapore, Singapore.

Stymne, H. and Boman, C. A. (1994). Measurement of ventilation and air distribution using the homogeneous emission technique. A validation. *4th Healthy Buildings Conference*, Budapest, Hungary.

Viegas, J. C. (1995). Natural ventilation of residential buildings [in Portuguese]. *National Laboratory of Civil Engineering*, Lisbon. Portugal.

Viegas, J. C. *et al* (2002). Assessment of the performance of natural ventilation in an apartment building. *8th Roomvent Conference*, Copenhagen, Denmark.

Viegas, J. C., Matias, L. and Pinto, A. (2004). Natural ventilation of an apartment: a case study. *9th Roomvent Conference*, Coimbra, Portugal.

STUDY ON ENERGY CONSERVATION EFFECT OF HYBRID VENTILATION SYSTEM UTILIZING WIND PRESSURE FOR MULTI-FAMILY BUILDINGS

M. Tajima[1], T. Sawachi[1], Y. Hori[2] and Y. Takahashi[2]

[1]*National Institute for Land and Infrastructure Management*
1 Tachihara, Tsukuba, 3050802 JAPAN
[2]*Building Research Institute*
1 Tachihara, Tsukuba, 3050802 JAPAN

ABSTRACT

According to the R&D Project on Low Energy Housing with Validated Efficiency, the CO_2 emissions due to operation of ventilation systems are estimated to be 7 to 12% of total CO_2 emissions of a unit of multi-family buildings in mild climate regions of Japan. Using network model calculations, CO_2 emissions of a hybrid ventilation system using Natural Ventilation Openings and other ventilation systems were estimated. The input power needed by the ventilation system can be reduced by 79 % when it employs the hybrid ventilation system compared with when it employs the balanced ventilation system. The hybrid ventilation system features not only sufficient ventilation performance, which is estimated by using the Overall Supply Rate Fulfilment index, but also reduced power input.

KEYWORDS

Hybrid ventilation, Multi-family buildings, Energy conservation, CO_2 emissions

INTRODUCTION

It is required under the Kyoto Protocols to reduce greenhouse gas emissions by 6% from the 1990 level for Japan between 2008 and 2012. However, in 2002, CO_2 emissions from housing use increased by as much as 28.8% from the 1990 level. In addition, since July 2003, the amended Japanese Building Standard Law has required whole house mechanical ventilation systems for new dwellings to improve indoor air quality. Hence, reducing energy consumption of housing use including whole house ventilation systems has been an important issue in Japan. Therefore, this paper is intended to estimate CO_2 emissions of whole house ventilation systems, especially hybrid ventilation systems utilizing wind pressure, installed in a unit of multi-family buildings with sufficient ventilation performance.

The R&D Project of Low Energy Housing with Validated Efficiency

MLIT (Ministry of Land, Infrastructure and Transport), NILIM (National Institute for Land and Infrastructure Management) and BRI (Building Research Institute) have carried out the R&D Project of Low Energy Housing with Validated Efficiency (LEHVE) to reduce CO_2 emissions from dwellings. In the LEHVE project, two units in a test multi-family building, which were called the Reference unit and Energy Conservation unit respectively, were utilized for estimating CO_2 emissions. The Reference unit employs typical equipments, consumer electronics and thermal insulation material, which is based on the Japanese Energy

Conservation Standard of 1999. At the same time, the Energy conservation unit has better heat insulation properties, the latest energy efficient equipments and consumer electronics. Both of the units employ identical whole house ventilation systems, which are balanced ventilation with heat recovery, to set the same ventilation aspects and same ventilation loads. Experimental results of CO_2 emissions of the two units are shown in Figure 1. The CO_2 emissions of the ventilation system are estimated to be 7 % to 12 % of total CO_2 emissions in mild climate regions of Japan. It is expected that energy conservation methods on whole house ventilation systems have a definite effect for reducing CO_2 emissions of multi-family buildings.

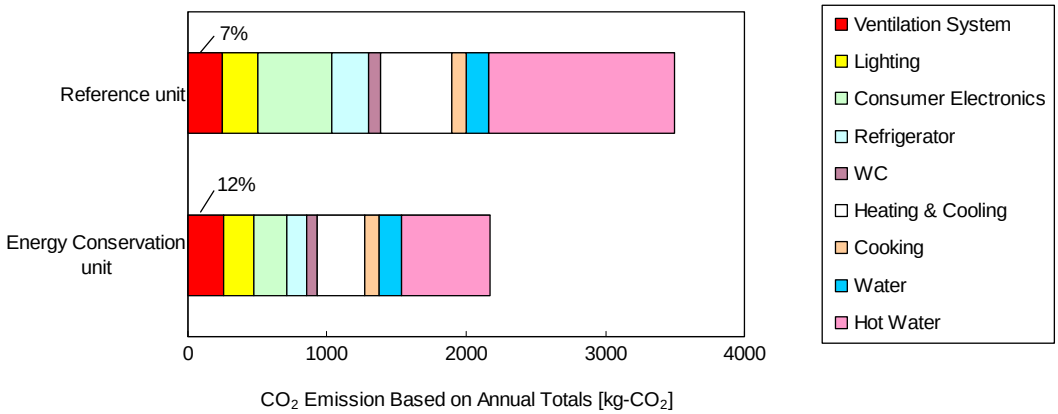

Figure 1: CO_2 emissions based on annual totals in Tsukuba city (mild climate region in Japan)

METHODS

Natural Ventilation Opening

A Natural Ventilation Opening utilizing wind pressure, which employs a constant air flow damper, is shown in Figure 2. The opening limits inflow with the damper when the pressure difference is larger than 8 Pa. This opening was used as a component of a hybrid ventilation system for simulations. The ΔP-Q characteristic of the opening was measured on a test chamber. Furthermore, by tracer gas measurement, ventilation performance and total ventilation rates were estimated by installing the natural ventilation openings on a full scale unit model, which was built outdoors. Therefore, the performance of this opening was certified in actual conditions.

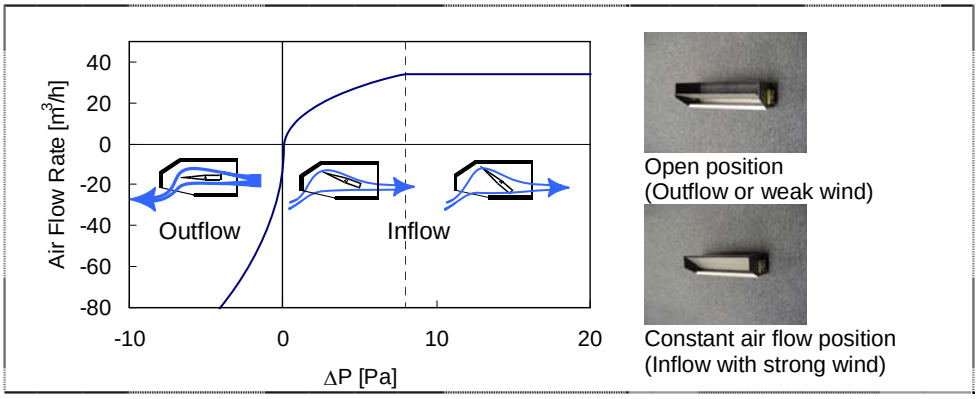

Figure 2: ΔP-Q characteristics of "Natural Ventilation Opening"

Network Model Simulation

Figure 3 shows a model of a typical unit of multi-family buildings, which were simulated by a network model VENTSIM. This unit employs a hybrid ventilation system with a typical exhaust fan system and the Natural Ventilation Openings. The Standard Expanded AMeDAS (Automated Meteorological Data Acquisition System) weather data of Tokyo and Cp distribution data of multi-family buildings (shown in Table 1), which were collected by wind tunnel measurements, were given for simulations. Fresh air supply rate and ventilation performances based on the Supply Rate Fulfilment index were calculated as outputs. Simulation cases are shown in Table 2.

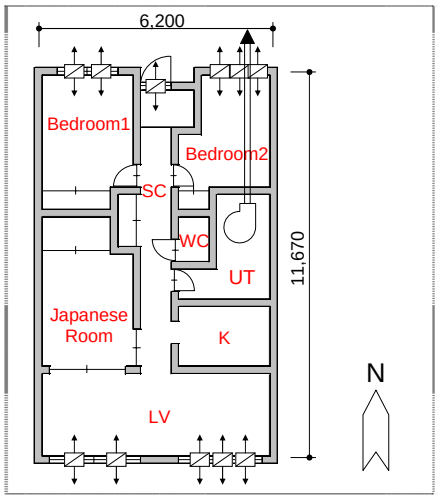

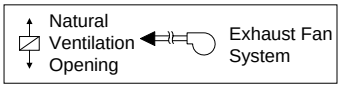

Required fresh air supply rate P_i of each zone

Zone	P_i
LV + Japanese Room + K	50 m^3/h
Bedroom 1	20 m^3/h
Bedroom 2	20 m^3/h

Applying to Japanese Energy Conservation Standards of 1999

Figure 3: Model of unit for simulation

Table1: Scale models of multi-family buildings for wind tunnel testing

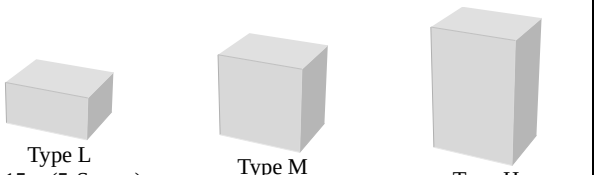

Type L	Type M	Type H
H: 15m (5-Storey)	H: 30m (10-Storey)	H: 45m (15-Storey)

W: 30m D: 15m

Terrain: Urban or City (Coefficient = 0.27)

Table 2: Simulation

CASE 01	Exhaust ventilation
CASE 02	Natural ventilation (utilizing only wind pressure)
CASE 03	Hybrid ventilation

Ventilation Performance Terminology

The SRF index was used to evaluate ventilation performance. This terminology is based on the theory of conservation law of fresh air rate. The index is given by Eqn.1 and defined as the ratio of the effective supply rate S_i (Eqn.3) to the substantial required fresh air supply rate P_i'. The SRF value ranges from 0 to 1 and SRF=1 means the referenced room has sufficient effective fresh supply air rate compared to P_i'. S_i and P_i' are calculated by using α_i (surplus fresh air supply rate of the zone i, which is obtained by solving Eqn.2 or Eqn.2'). α_i can be calculated when all airflow rates among zones in a building are known. The maximum value of α_i, 1.0 represents purely fresh air like outside air, and a negative value means there is no

fresh air. The Overall Supply Rate Fulfilment (OSRF) is defined as the geometric mean of SRF values of rooms as shown in Eqn.4.

$$SRF_i = \frac{S_i}{P_i - \sum_{j=1}^{n} \min(0, \alpha_j Q_{ij})} = \frac{S_i}{P_i'} \quad (1)$$

Steady condition

$$0 = A_i + \sum_{j=1}^{n} \alpha_j \cdot Q_{ij} - \alpha_i \left(\sum_{j=1}^{n} Q_{ji} + B \right)_i - P_i \quad (2)$$

Transient condition

$$\frac{d\alpha_i}{dt} V_i = A_i + \sum_{j=1}^{n} \alpha_j \cdot Q_{ij} \alpha_i \left(\sum_{j=1}^{n} Q_{ji} + B \right) - P_i \quad (2)'$$

$$S_i = A_i + \sum_{j=1}^{n} \max(0, \alpha_j \cdot Q_{ij}) - \sum_{j=1}^{n} \max(0, \alpha_i \cdot Q_{ji}) - \max(0, \alpha_i \cdot B_i) \quad (3)$$

$$OSRF \equiv \left(SRF_1 \times SRF_2 \times \cdots \times SRF_M \right)^{1/M} \quad (4)$$

where

A_i	direct fresh air supply rate, the rate of air that is supplied directly from outside to room i [m^3/h]
B_i	rate of air exhausted directly to the outside from room i [m^3/h]
M	number of rooms for which the required fresh air supply rate is specified
P_i	required fresh air supply rate for room i [m^3/h]
P_i'	substantial required fresh air supply rate of room i [m^3/h]
Q_{ij}	transferred airflow rate, rate of air flowing from room j to room i [m^3/h]
S_i	effective fresh air supply rate of room i [m^3/h]
V_i	air volume of room i [m^3]
n	number of rooms
α_i	surplus fresh air supply rate contained in the air exhausted from room i

RESULTS AND DISCUSSION

Ventilation performance

Relationships between OSRF and pressure differences between the north external wall and the south external wall are shown in Figure 4. Hybrid ventilation operation (CASE 03) uses an exhaust fan when wind pressure is less than 2 Pa and larger than -2 Pa, and gives better OSRF values than other ventilation operations. Annual OSRF of each case is shown in Figure 5. These OSRF values indicate this hybrid ventilation system provides sufficient ventilation performance.

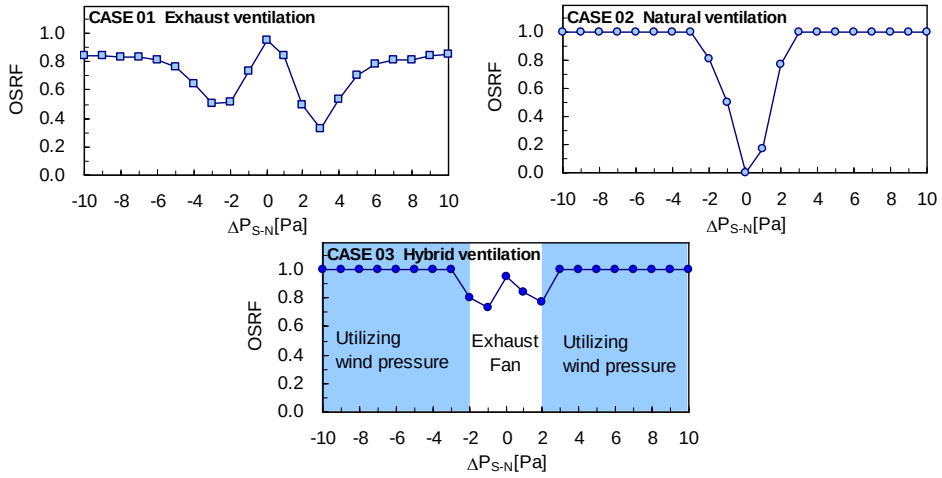

Figure 4: Relations between OSRF and wind pressure, which is based on the north external wall pressures

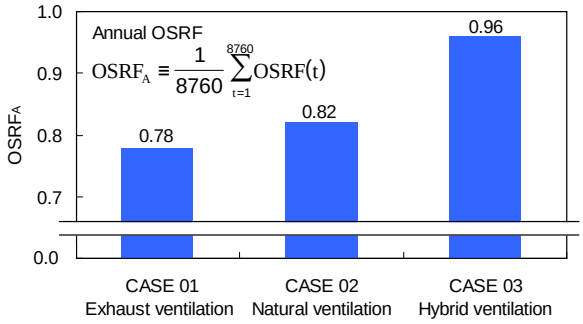

Figure 5: Calculated annual OSRF (Central Unit of 8th floor in TYPE-H)

Estimation of CO_2 emissions of Hybrid ventilation system

Annual percentages of multi-family buildings in Tokyo utilizing only wind pressure, which are based on results of CASE 03 in Figure 4, are shown in Figure 6. In Figure 6, the average percentages of available times are larger than 50%. Specifically, wind pressure can be utilized 70% of the time on many of the units in Type H. These results indicate the hybrid ventilation system features not only sufficiently ventilates but also reduces power input.

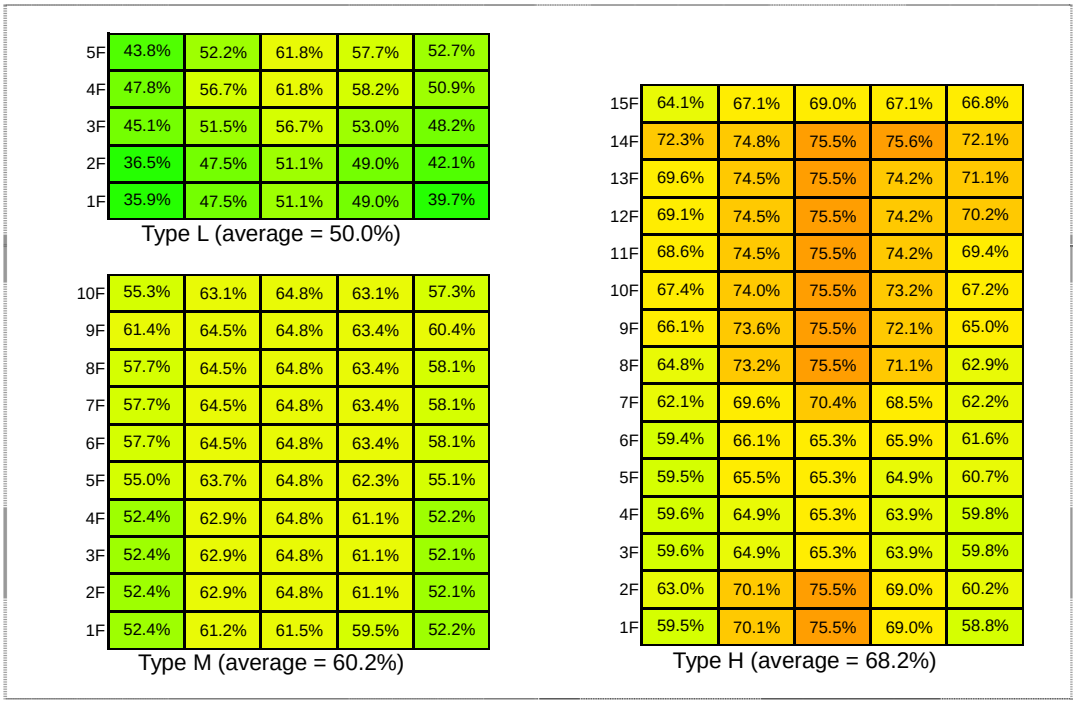

Figure 6: Annual available percentages of utilizing only wind pressure in multi-family buildings at Tokyo (SECTION)

Estimated CO_2 emissions and power consumption of ventilation systems are shown in Figure 7. These results are based on survey results of performance data of ventilation systems available in Japan. These data indicate that input power due to operation of a ventilation system can be reduced by 79 % when the hybrid ventilation system is employed compared with when the balanced ventilation system is employed, according to survey result in 2000. This means that the total CO_2 emissions on the Reference unit of LEHVE project will be reduced by 6%. Furthermore, on the Energy conservation unit, it will be reduced by 10%. In

addition, input power reduction will be more efficient when the most up-to-date ventilation systems are employed, which were surveyed in 2004.

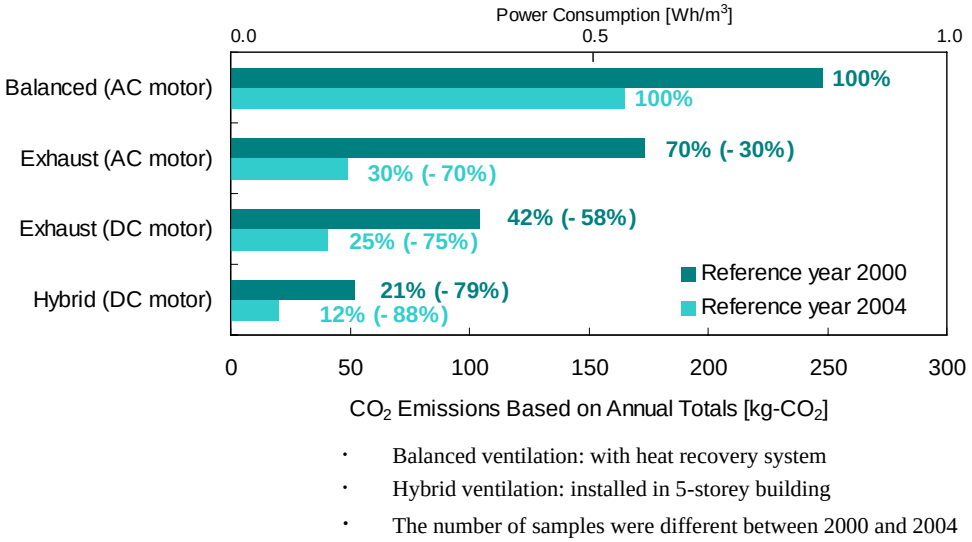

- Balanced ventilation: with heat recovery system
- Hybrid ventilation: installed in 5-storey building
- The number of samples were different between 2000 and 2004

Figure 7: Estimated CO_2 emissions of ventilation system

CONCLUSIONS

In the present study, CO_2 emissions of a hybrid ventilation system using Natural Ventilation Openings and other ventilation systems were estimated by network model simulations. From the result of R&D project of Low Energy Housing with Validated Efficiency, the CO_2 emissions due to operation of ventilation systems are estimated to be 7% to 12% of the total CO_2 emissions of a unit of multi-family buildings in mild climate regions of Japan. The input power of ventilation systems can be reduced by 79% when the hybrid ventilation system is employed compared with when the balanced ventilation system is employed. The hybrid ventilation system using the Natural Ventilation Openings features not only sufficient ventilation performance but also reduces power input. The hybrid ventilation system under conditions in an actual installation will be validated by measurements in future work.

REFERENCES

NILIM, BRI. (2005) Guidelines for designing the Low Energy Housing with Validated Efficiency. Institute for Building Environment and Energy Conservation

Takao Sawachi, Yoshinori Taniguchi, Shigeki Ohnishi, Haruki Ohsawa and Hironao Seto. (1998) A new experimental approach for the evaluation of domestic ventilation systems, *ASHRAE Transactions: Research*, pp.570-611.

ON THE IMPACT OF URBAN ENVIRONMENT ON THE PERFORMANCE OF NATURAL AND HYBRID VENTILATION SYSTEMS

K. Niachou and M. Santamouris

Group Building Environmental Studies, Physics Department, Section of Applied Physics, National Kapodistrian University of Athens, 15784 Athens, Greece

ABSTRACT

The impact of the urban environment on natural and hybrid ventilation was investigated through experimental and computational procedures in the framework of RESHYVENT European Project. An experimental campaign was organized in two urban street canyons in Athens, during summer 2002, consisting of field and indoor experiments. The experiments aimed at the investigation of the impact of the various urban features on the efficiency of different ventilation systems. Natural, mechanical and hybrid ventilation experiments were carried out in three building apartments under different ambient conditions. A comparison analysis, in terms of air exchange rates and air-exchange efficiency, was performed between the studied ventilation systems. Besides, computational calculations of air flow characteristics were carried out for advanced RESHYVENT hybrid ventilation systems considering a great number of simulation scenarios. The most important constraints of the urban environment on the performance of hybrid ventilation systems are highlighted.

KEYWORDS

Urban environment, hybrid ventilation, field experiments, ventilation experiments, computational procedures.

INTRODUCTION

The potential of natural ventilation systems can be seriously reduced in the urban environment because of its ambient characteristics and mainly due to low wind speeds, high ambient temperatures and increased external pollutant and noise levels. Hybrid ventilation is known to exploit the benefits of both natural and mechanical ventilation modes, to optimize the performance of ventilation, both from the thermal comfort and the indoor air quality point of view (Heiselberg, 2002). It is particularly important in urban canyons where the potential of natural ventilation is reduced due to attenuation of wind speeds (Santamouris, 2001). Thus, it is important to investigate the performance of hybrid ventilation systems under specific urban conditions in order to improve our knowledge and to attain optimum performance of these systems.

An urban measurement campaign was organized in two street canyons very near to the centre of Athens during summer period. Air and surface temperatures, wind speeds, wind directions and outdoor air characteristics (TVOC's, CO_2, CO and NO_x) were measured inside and outside the street canyons together with ventilation and air quality measurements inside the buildings. Infrared thermographies were taken on an hourly basis together with surface temperatures on street level and on the opposite building walls. Ventilation experiments were performed consisting of natural, mechanical and hybrid ventilation. The experiments were implemented on a 24-hour basis, for a number of five consecutive days for each canyon. The

results obtained from experimental procedures were analysed in order to evaluate the impact of the urban parameters on the performance of hybrid ventilation. Also the air exchange rates and air-exchange efficiency were estimated in the three building apartments. A comparative study of the performance of different ventilation systems in urban canyons was performed. In order to complete the work on the parameters that influence hybrid ventilation in urban environment, computational calculations of air flow characteristics were implemented using the multizone airflow and thermal model COMIS/TRNSYS. A detailed sensitivity analysis was made, considering a great number of simulation scenarios.

The aim of this study is to summarize the work performed within RESHYVENT project in order to investigate the impact of the urban environment, as well as, to identify the most important limitations on the performance of natural and hybrid ventilation systems.

EXPERIMENTAL RESEARCH OF NATURAL AND HYBRID VENTILATION IN URBAN CANYONS

The total experimental campaign was based on field and indoor experiments aiming at the investigation of the impact of the various urban features on the applied ventilation system efficiency.

Site Description and Field Measurements

The field measurements were performed every 30secs for a number of 5 consecutive days, during June to September 2002 and they are illustrated in Figure 1.

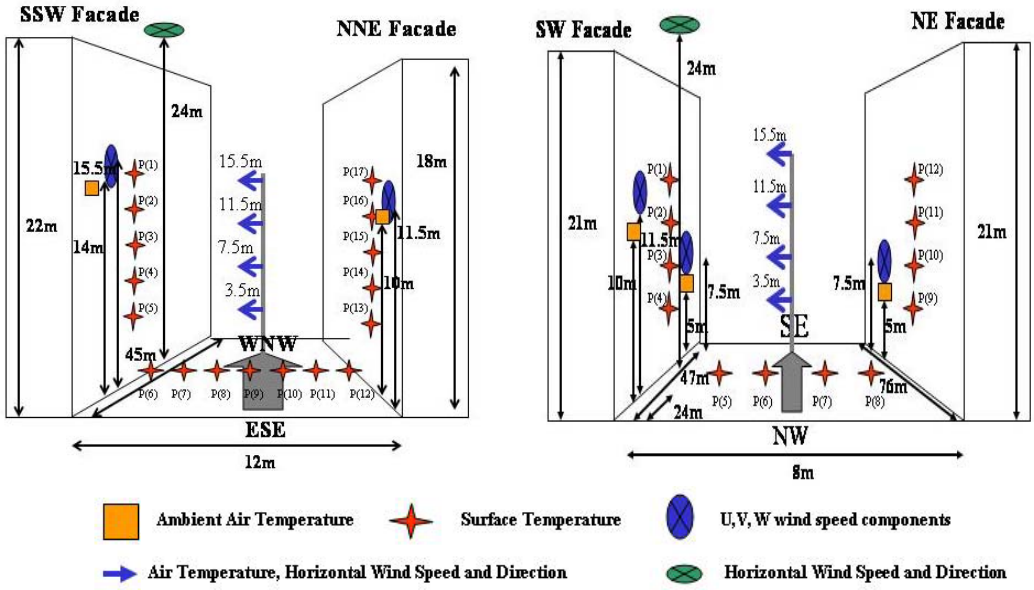

Figure 1: A schematic representation of the field measurements performed inside and outside the two urban street canyons (left is Ragavi and right is Ag. Fanouriou canyon)

The two studied canyons are different, in terms of geometrical characteristics and orientation (Table 1). Namely, Ragavi street is an almost regular and asymmetric street canyon, whereas Ag. Fanouriou is a deep and symmetric canyon. Both canyons are typical with regard to the surrounding urban scale, however they presented a different microclimate, as it was investigated from the analysis of measured parameters (Niachou et al, 2005c).

TABLE 1
Characteristics of studied street canyon and building apartments

Canyon	Orientation from North	H/W	L/H	Measured Period	Apartment	Area (m^2)	Volume (m^3)
Ragavi	100	1.7	2.3	19/07-23/07/02	A_1	65	112
Ag. Fanouriou	137	2.6	3.6	28/08/-2/09/02	A_2	78	130
				11/09-15/09/02	A_3	50	120

Ventilation Experiments

A total number of 114 ventilation experiments were conducted consisting of 3 infiltration, 30 natural, 34 mechanical and 47 hybrid ventilation experiments. Each experiment consisted of two parts. At first the tracer gas was injected inside the rooms and afterwards the tracer decay concentration was measured. Internal fans were used to homogenize to the extend that it was possible the internal concentrations. In A_2 and A_3 experiments two tracer gases (N_2O, SF_6) were injected during the first stage in two different zones.

Natural ventilation experiments were performed with single-sided and cross ventilation configurations. In case of single-sided ventilation, openings were considered either, from the canyon or, the rear canyon facade. Cross ventilation experiments were studied with two or more openings placed at the front and back canyon side. Mechanical ventilation was tested experimentally with one or two fans operating in inlet or extract modes. All possible configurations were studied with the fans placed on both building external walls.

Hybrid ventilation experiments were focused on fan-assisted natural ventilation, where supply and extract fans were used to enhance pressure differences by mechanical fan assistance. The fans were installed to openings adjacent to the canyon and rear façades operating in inlet or extract modes together with natural ventilation through one or two openings.

EVALUATION OF THE EXPERIMENTAL RESULTS IN URBAN CANYONS

Field Measurements

In order to understand the impact of the urban environment on the potential of natural and hybrid ventilation, a detailed analysis of air and surface temperature distribution, as well as, of the observed airflow characteristics inside the two studied street canyons was performed. The observed differentiations of wind and temperature distribution have been discussed in order to get a better insight of the urban canyon microenvironment. The latter has been shown to have a direct impact on the ventilation performance in urban buildings (Niachou et al, 2005a, 2005b).

Ventilation Measurements

The investigation focused on air-exchange rates and air-exchange efficiency in the three urban building apartments. A comparative study of the performance of different ventilation systems in urban canyons has been performed (Niachou et al, 2005a, 2005b), as shown in Figure 2. Besides a comparison was made between single and multi-zone methodologies. The multi-zone approach, in spite of its better theoretical basis, has been found more sensitive to the accuracy of the measured concentrations, especially when a single tracer is used. Moreover, a methodology to determine the ventilation efficiency in two tracer gas experiments is proposed (Niachou et al, 2005b).

Natural cross ventilation has been shown to lead to higher ACH values than single-sided natural ventilation under different ambient conditions. Hybrid ventilation has been shown to be associated with rather lower ACH than natural cross-ventilation, but slightly higher ACH under single-sided ventilation or calm conditions. This, of course, does not mean that hybrid ventilation may not be of use during winter times, or during those few days during the summer that natural ventilation is not an effective means of cooling, either due to low winds or due to high ambient temperatures.

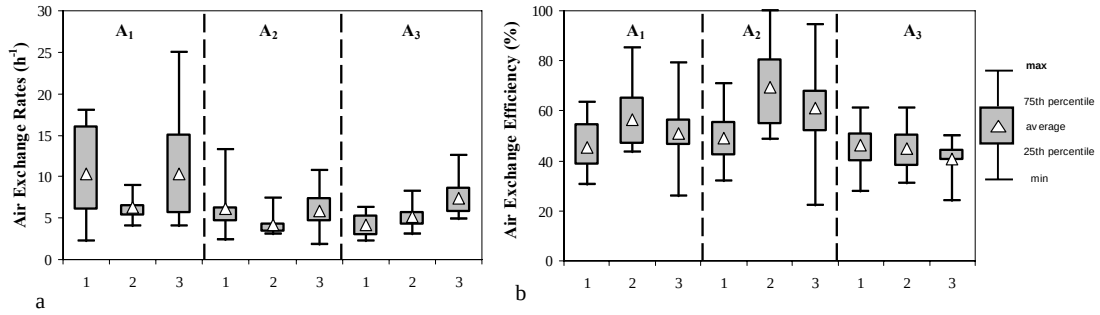

Figure 2: Boxplots of estimated air-exchange rates and air-exchange efficiency values (%) based on multi-zone method (h^{-1}) for natural (1), mechanical (2) and hybrid (3) ventilation experiments under different ambient conditions

Nevertheless, there is more to evaluating hybrid ventilation than comparing the mean values of the air exchange rates, which have a relatively high spread for natural ventilation. Despite the small number experiments performed under calm conditions (wind speed lower than 0.2m/s), it was confirmed that hybrid ventilation has an advantage over natural under windless conditions (Figure 3). It should also be stated that apart from the comparison of estimated air exchange rates, there is a qualitative difference between natural and hybrid ventilation, in terms of air-exchange efficiency. Higher air-exchange efficiency values have been estimated in hybrid ventilation experiments in comparison with single-sided ventilation. In most cases, there is also an improvement relative to natural cross ventilation.

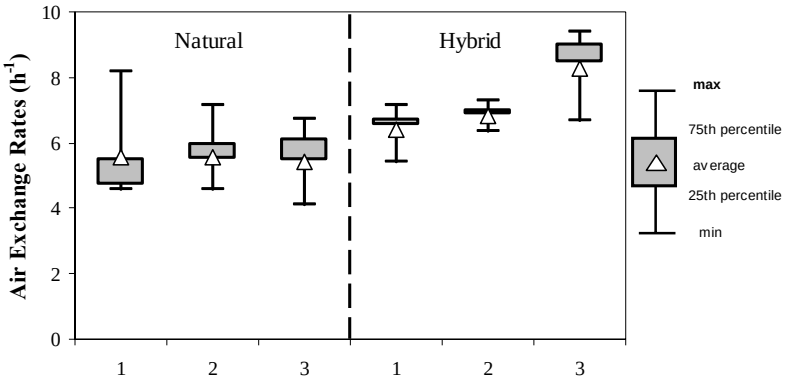

Figure 3: Boxplots of estimated air exchange rates (h^{-1}) for natural (single-sided) and hybrid ventilation experiments at A_3 apartment, under calm conditions based on the single-zone (1,2) and multi-zone (3) methodologies

COMPUTATIONAL CALCULATIONS OF AIRFLOW CHARACTERISTICS IN URBAN CANYONS

In order to complete the work on the parameters that influence hybrid ventilation in urban environment, computational calculations of airflow characteristics were performed, using the multizone airflow and thermal model COMIS/TRNSYS. The reference building is a single-family house, namely an apartment, located inside an urban street canyon. Advanced hybrid ventilation systems have been studied, based on RESHYVENT concept and on RESHYVENT consortiums. Five different canyon configurations have been studied, having an aspect ratio (H/W) equal to 1, 1.5, 2, 2.5 and 3. The rear canyon facades were studied either with local or with no local obstructions. The undisturbed wind speed data has been translated into canyon data based on the developed research methodology within URBVENT European Project. The Cp-values for the two external building facades and for the five canyon geometries were estimated by "CP-generator" by TNO.

A detailed sensitivity analysis has been performed considering all the following parameters:

- Canyon Geometry
- Canyon Layout
- Outdoor Urban Air Characteristics
- Indoor Pollutant Emissions
- Building Leakage
- Demand Control

A set of simulations under steady state and dynamic conditions have been performed. The dynamic simulations were performed on an hourly basis within a year period for different climates. A full data basis with all simulation scenarios and results are given in final report of WP10 of RESHYVENT project (Niachou and Santamouris, 2005). These airflow characteristics helped to get a better insight of the impact of the urban environment on the ventilation effectiveness.

Description of Hybrid Ventilation systems

The two hybrid ventilation systems were studied consisting of demand control, a low-pressure system supported by wind and buoyancy and balancing supply and exhaust.

Pilot RESHYVENT Ventilation System

The first studied hybrid ventilation system (Figure 4) is a pilot ventilation system, based on RESHYVENT concept. It consists of two inlet/extract fans attached on the external building walls (canyon and rear canyon facades), a balancing supply and exhaust system (with a corresponding performance of 795m^3/h at 0 Pa pressure difference) and a low pressure system supported by wind and buoyancy.

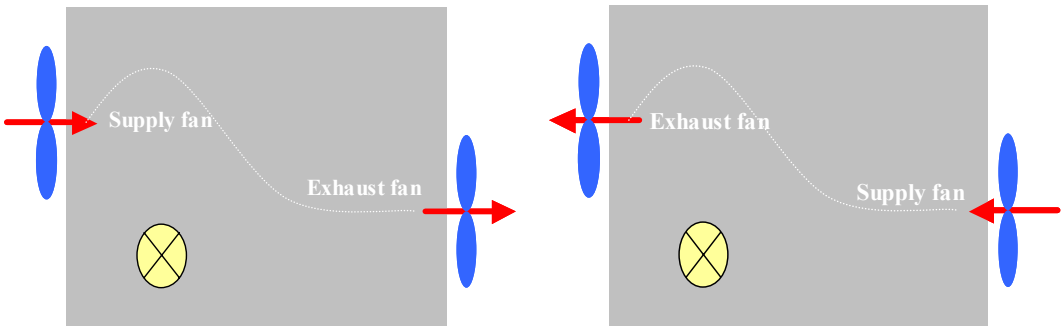

Figure 4: A representation of the pilot hybrid ventilation system with the two inlet/extract fans installed at the two external building walls. An inverse operation of the fans is considered on the right photo

RESHYVENT Hybrid Ventilation System for Moderate Climates

The second studied ventilation system is one of the four RESHYVENT ventilation systems which was developed for moderate climates and employs natural air supply and natural or mechanical air exhaust duct system. Heating and cooling were also specified for the apartment (zone). The heating set point was 16°C and the cooling set point was 26°C.

The system consists of self-regulating air inlets, DC fan, motorized damper, flow meter, central control unit, CO_2 sensors and ductwork. The roof outlet is considered 1m above the building roof in all canyon geometries. The demand control of the ventilation system is based on monitoring of CO_2 in rooms. There is a CO_2 sensor and a self-regulating air inlet in each room. The self-regulating inlets are usually positioned above windows. These inlets are able to maintain a constant flow rate for the pressure difference across the facade higher than 1 Pa. The exhaust fan is used when the air exhaust through the duct is lower than the demanded flow. The efficiency of the hybrid ventilation system in the different canyon geometries was also investigated with pressure-dependent grilles in order to better realize the canyon effect. When the CO_2 concentration is below a threshold value (etc. 1200 ppm) then ventilation system ventilates only at the minimum level ($10 dm^3 s^{-1}$). When the concentration of CO_2 in a room increases to 1200 ppm, then the inlet in this room opens. The inlet opens to a certain target flow rate, which depends on the nominal flow rate of the inlet and the gradient of increase of the CO_2 concentration. The airflow rate in the exhaust increases to a value which is the sum of the basic ventilation flow rate and the target flow rates of the opened inlets. The ventilation system first tries to achieve the exhaust flow rate by adjusting the motorized damper in the vertical exhaust duct (stack). If natural driving forces are not sufficient then the fan is switched on and its speed adjusted to match the demanded flow rate. The RESHYVENT ventilation system was examined either with natural or hybrid exhaust modes. In the natural ventilation exhaust mode, the exhaust airflow rate from the duct was affected by the natural driving forces. The total demanded flow rates (dm^3/s) was based on occupancy and activity schedule within the 24-hour period (Table 3). In case of the hybrid ventilation system, the exhaust fan had to meet the total demanded airflow rate.

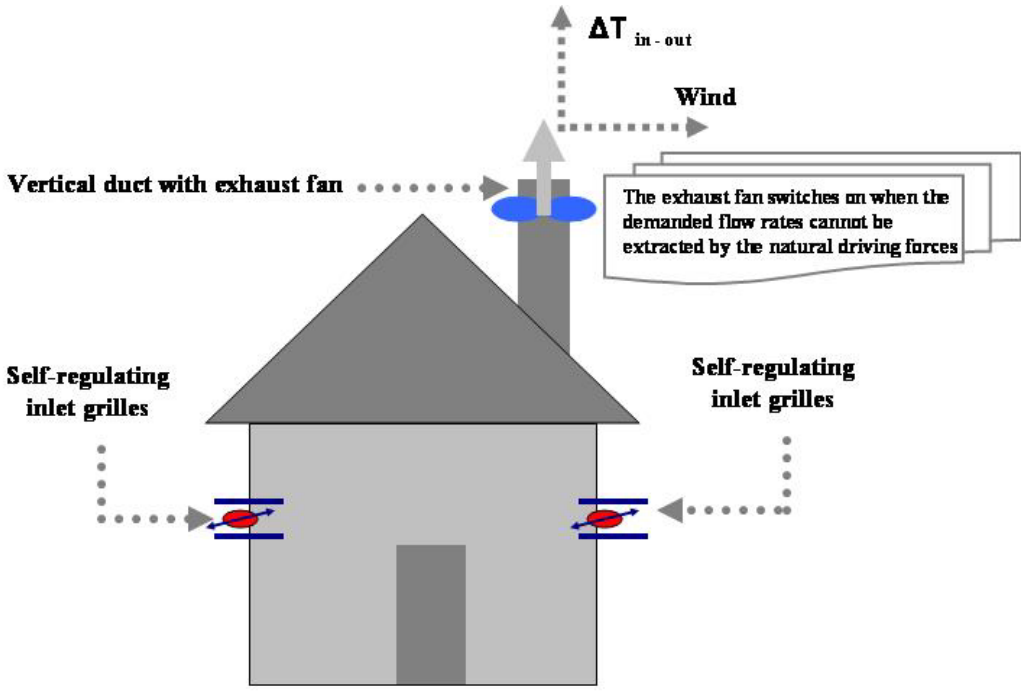

Figure 5: Representation of the RESHYVENT hybrid ventilation system for moderate climates

The inlet grilles were considered fully open between 0Pa and 0.5 Pa. Above 0.5 Pa the self-regulating inlet grilles started to control and there was no longer a standard relation between pressure and airflow. The airflow admission (dm^3/s) in relation with the pressure difference for self-regulating and pressure-dependent air inlets given in Tables 4-5.

TABLE 3
Demanded exhaust flow (dm^3/s)

Time	Demanded flow (dm^3/s)
0-6h	28
6-8h	42
8-17h	21
17-19h	42
19-22h	28
22-23h	42
23-24h	28

TABLE 4
Characteristics of self-regulating inlets

ΔP (Pa)	Flow rate (dm^3/s)
0	0
0.1	8.2
0.2	11.6
0.3	14.2
0.4	16.4
0.5	18.4
0.6	19.0
0.7	21.7
0.8	22.5
0.9	24.0
1	26
50	26

TABLE 5
Characteristics of pressure-dependent inlets

ΔP (Pa)	Flow rate (dm^3/s)
0	0
0.1	8.2
0.2	11.6
0.3	14.2
0.4	16.4
0.5	18.4
0.6	19.0
0.7	21.7
0.8	22.5
0.9	24.0
1	26
2	36.7
5	58.0
10	82.1
50	183.6

COMPUTATIONAL RESULTS

A detailed analysis of the efficiency of the pilot and RESHYVENT ventilation systems has been performed in different urban situations. The main concluding results regarding the performance of these systems are discussed in the following paragraphs.

Concerning the efficiency of the pilot RESHYVENT hybrid ventilation system, based on the RESHYVENT concept, the most important results are:

- The combined effect of wind and temperature difference resulted in greater airflow rates inside the reference building. However, a better performance was observed when wind direction was towards the building walls without local obstructions around it, rather than, when the wind blows towards the shielded building walls. The absolute minimum total ventilation rates were observed, either for windless conditions, or for parallel to the canyon axis flow.

- The impact of the outdoor air characteristics showed that when the ambient TVOC's concentration was increased, then greater ventilation supply and exhaust rates were required in order to sustain the indoor TVOC's concentration below the desirable levels. The better IAQ levels were related with strong natural driving forces (wind and temperature difference) and better outdoor air characteristics.

- A comparison analysis was performed considering that the inlet/extract fans would operate in a reverse mode. Namely, the supply fan is considered at the canyon (shielded) façade and the inlet fan at the rear canyon (unshielded) wall (Figure 5). The two hybrid ventilation systems were found to have a different performance under variable outdoor conditions. However, for each studied system the better performance, in terms of air change rates, was observed for winds towards the mechanical supply fan. Nevertheless, better indoor air quality is obviously expected when the mechanical supply fan is attached on the unshielded building walls, due to increased pollutant concentrations originating mainly from traffic sources, especially when air circulation is reduced inside the canyon.

The efficiency of RESHYVENT ventilation system for moderate climates will be discussed mainly with pressure-dependent inlet grilles in order to realize better the canyon effect. Both natural and hybrid ventilation exhaust systems were studied.

- From the study of hybrid ventilation system in the five canyon geometries, it was estimated that RESHYVENT ventilation system would operate more hours in natural exhaust ventilation mode, when there were available natural driving forces. The performance of the ventilation system with the natural duct exhaust system in different canyon geometries showed that wind effect is dominant driving force in canyons with lower aspect ratios (regular or avenue canyons). Stack effect is maximum in deeper canyons (H/W greater than 2), when the average height of buildings is increased. Under the combined wind and stack effect, then the air exhaustion through the duct depends on the dominating natural driving force.

- From the estimated pressure differences across canyon facades with the natural exhaust ventilation system, it was found that the majority of pressure differences range between 0Pa-1Pa for all canyon geometries. The smaller the aspect ratio of canyon is, the maximum % of values between 0Pa-1Pa becomes. Thus, the range between 0Pa-1Pa

becomes of high interest for pressure-dependent or self-regulated air inlets when installed at canyons facades and the ventilation exhaust system operates in natural mode.

- The study of two different canyon configurations, with and without surrounding obstacles at the rear building walls, showed that wind effect is reduced a lot near shielded facades. Higher exhaust flow rates were estimated with the natural exhaust system in canyons without local obstructions. Besides, the hours of operation of the exhaust fan and thus the fan energy are increased in canyons with local obstructions around the buildings, as a result of the reduced wind effect.

- The effect of different outdoor air characteristics on the efficiency of the hybrid ventilation system has been shown through TVOC's, seeing that its concentration in the urban environment can be very variable. A better IAQ was observed (with regard to TVOC's), when the control of the inlet grilles was based on TVOC's rather than when was based on CO_2. The control strategy of the inlet devices is very crucial, since it is possible with appropriate control to improve the effectiveness of the hybrid ventilation system, so as to meet indoor IAQ, without increasing the demanded flow rates of the system. Thus, the energy cost for heating or cooling will be reduced when IAQ is achieved with the minimum required flows.

- A parametric study has been performed considering two indoor TVOC's emissions. Namely, an average TVOC's emission equal to 1.1mg$h^{-1}m^{-2}$ (emission factor for 30 vinyl floorings reported by Gustafsson et al, 1993) and a high emission of 2.2mg$h^{-1}m^{-2}$. It was resulted that when high indoor pollutant emissions are expected in urban buildings, then it is very important to consider effective control strategies in order ensure the required IAQ levels with the minimum demanded flow rates. First of all, it important to reduce source emissions inside the building and then to increase ventilation rates, thus to avoid increased energy costs.

- The impact of the building leakage on the efficiency of the IC2 ventilation system was studied considering different leakage classes (0.6, 2.5 and 5h^{-1}@50Pa). It has been found that when the building leakage is increased, then the introduced airflow through the inlet grilles is reduced, as a result of the increased infiltration rates.

- Finally, from the sensitivity analysis with different control strategies for the opening of inlet grilles, it was resulted that it is very important to apply effective control strategies for the operation of inlet grilles. When appropriate control is applied, it is possible to achieve the best thermal comfort and indoor air quality with the minimum demanded flow rates and thus with the minimum energy cost. Passive cooling or combined control strategies with passive cooling and CO_2 or TVOC's were found very effective.

CONCLUSIONS

Natural and hybrid ventilation in urban areas is highly affected by a number of urban parameters. Effective design of hybrid ventilation in urban buildings requires a good understanding of the urban climate characteristics. The most important parameters (canyon geometry and layout, wind and temperature distribution inside canyons, pollutant concentrations, external noise, solar/daylight access, humidity and wind pressure on building facades) have been identified and analyzed in the framework of RESHYVENT Project. The most important limitations and constraints of the impact of the urban environment on the

performance of natural and hybrid ventilation have been identified through a number of experimental and computational procedures.

ACKNOWLEDGEMENTS

The present research has been performed in the framework of the research project RESHYVENT and it is financed by the Fifth Framework Programme of the European Commission, Directorate General for Science, Research and Technology under the contract ENK6-CT2001-00533. The contribution of the Commission is gratefully acknowledged.

REFERENCES

1. Gustafsson, H. and Jonsson, B. (1993), Trade standards for testing chemical emissions from building materials, Part I: Measurements of flooring materials, Proc. Indoor Air '93, Vol.2, 437-443, Helsinki, Finland.
2. Heiselberg, P. (2002). *Principles of Hybrid Ventilation*, IEA, Annex 35, Hybrid Ventilation Centre, Aalborg University.
3. Knoll B., Phaff, J.C., and. De Gids, W.F (1996) Pressure Coefficient Simulation Program, Air Infiltration Review, Vol. 17, No 3.
4. Niachou K. and Santamouris M. (2005). WP10, 'Urban Impact in EU', Final Report, National and Kapodistian University of Athens, RESHYVENT, ENK6-CT2001-00533, February 2005.
5. Niachou, K., Hassid, S., Santamouris, M. and Livada, I. (2005a). Comparative Monitoring of Natural, Hybrid and Mechanical Ventilation Systems in Urban Canyons, *Energy and Buildings* **37:5**, 503-513.
6. Niachou, K., Santamouris, M. and Hassid, S. (2005b). Performance of Natural, Hybrid and Mechanical Ventilation Systems in Urban Canyons, *Proc. PALENC Conference*, Vol.1, 433-439, Santorini, Greece.
7. Niachou, K., Livada, I. and Santamouris, M. (2005c). A Study of Temperature and Wind Distribution Inside two Urban Street Canyons in Athens, *Proc. PALENC Conference*, Vol.1, 125-131, Santorini, Greece.
8. RESHYVENT (2002). Cluster Project on Demand Controlled Hybrid Ventilation in Residential Buildings with specific emphasis of the Integration of Renewables, European Joule Project, Contract No ENK6-CT2001-00533, 2002.
9. Santamouris, M. (2001). *Energy and Climate in the Urban Environment*, James and James, LTD, London
10. URBVENT (2000). European Research Project on Natural Ventilation in Urban Areas, Optimal Openings Design, WP2 Final report, Joule Programme, Project Contract No ENK 6-CT-2000-00316**.**

PERFORMANCE EVALATION OF THE HYBRID VENTILATION SYSTEM CONTROLLED BY A PRESSURE DIFFERENCE SENSOR

H. Yoshino[1] , S. Yun[1] and A. Nomura[2]

[1]*Department of Architecture and Building Science, Graduate School of Engineering, Tohoku University, Sendai 980-8579, JAPAN*
[2]*Ventilation Equipment and Systems Division, TOSHIBA CARRIER CORPORATION, 336 Tadewara, Fuzi 416-8521, JAPAN*

ABSTRACT

A hybrid ventilation system controlled by a pressure difference sensor was installed on a detached test house. Performance of this ventilation system was evaluated through the field measurement taken into account the different conditions of the air supply and the exhaust systems. The results of the measurement revealed that the exhaust airflow rate was relatively stable while the indoor-outdoor temperature difference varied and the wind velocity changed. The exhaust airflow rate met the target airflow rate of 64% during the whole measuring period. From the comparison about the air supply systems, the crawl space air supply system showed better result than the passive air supply system not only for the balance of air supply in the first floor and the second floor but also for the stability against various outdoor condition.

KEYWORDS

Hybrid ventilation system, Control strategy, Pressure difference sensor,
Crawl space air supply system, Balance of infiltration airflow rate

INTRODUCTION

Hybrid ventilation systems utilize not only the mechanical force but also the natural forces such as buoyancy and wind effects. The mechanical system can stabilize the irregular natural forces such as buoyancy and wind effect instead of consuming energy. It has to be taken into account seriously, therefore, how these different systems should be combined and controlled[1].

From the previous research[2] about the performance of hybrid ventilation system installed on a two-storey building, the followings were reported that the hybrid ventilation system controlled by the temperature difference between indoor and outdoor cannot deal with the influence of outdoor wind on the ventilation airflow rate while the supplemental fan is off. Moreover, the infiltration airflow rate was very insufficient in the second floor by the influence of buoyancy effect under the condition of heating.

To make an alternative for such problems, a hybrid ventilation system using the pressure difference sensor for controlling the airflow rate with supplemental fan and damper was introduced in this study. The crawl space air supply system was adopted for maintaining the balance of infiltration airflow rate in the first floor and the second floor and compared with the passive air supply system.

ABSTRACT OF THE HYBRID VENTIATION SYSTEM AND THE TEST HOUSE

Hybrid ventilation system

Figure 1 shows the conceptual drawing of the control strategy of the hybrid ventilation system. The airflow rate passing the vertical exhaust duct is monitored by a pressure difference sensor stored in the system unit. A supplemental fan and a damper are controlled automatically according to the monitored results to meet the target airflow rate. The fan has 35 stages of rotation speed and the damper has 7 stages of angle.

Test house

Figure 2 shows the floor plans and sectional view of the test house used for the measurement. Total floor area of the house is 78.9m^2 and the volume is 163.9m^3. The equivalent leakage area of the building envelope per unit floor area is 2.8cm^2/m^2 obtained by the measurement of the fan pressurization method. A stairwell in the hall connects the first floor with the second

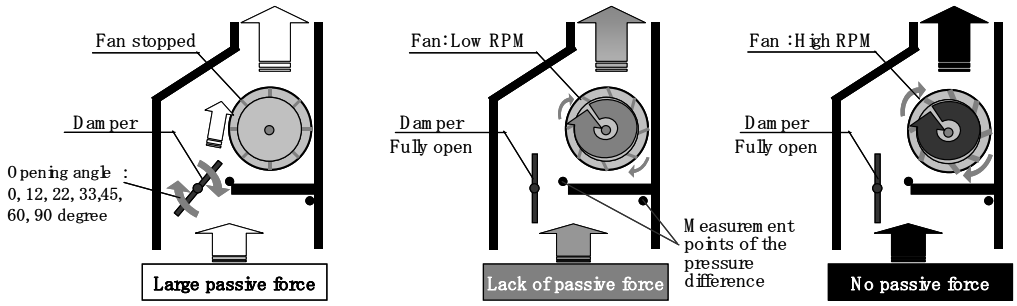

Figure 1. The control strategy of the hybrid ventilation system

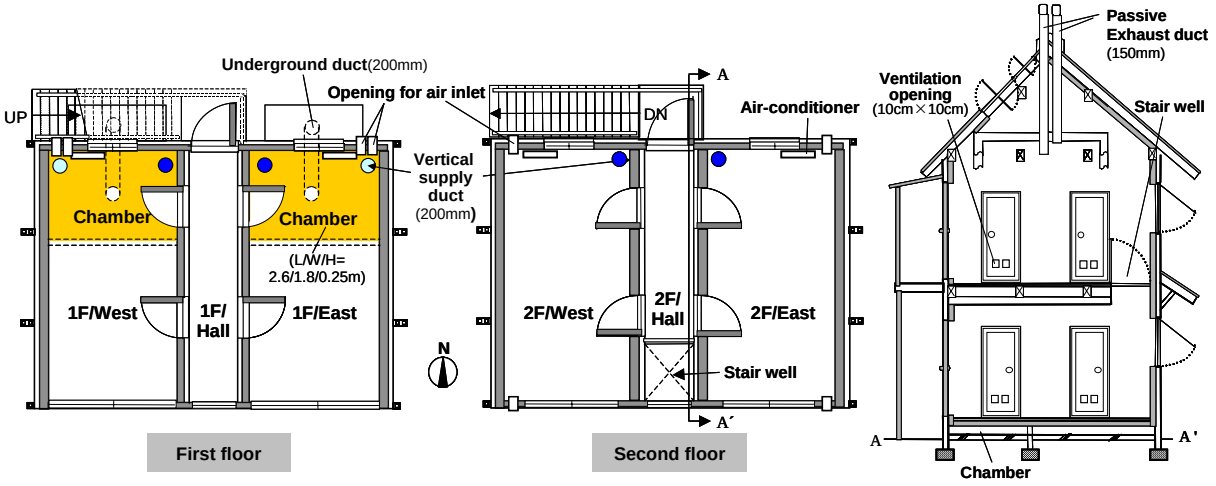

Figure 2. Floor plans and sectional view

floor and two openings are set on every internal doors for ventilation. Openings for air inlet are installed on the external wall of each room except halls which could be used as the passive air supply system. As well as, underground ducts, chambers installed in the crawl space and vertical supply ducts can be used as the crawl space air supply system. The hybrid ventilation system is installed at the top of the second floor hall and it is connected via ducts to each rooms and outdoor space.

METHODS AND CONDITIONS OF MEASUREMENT

The infiltration airflow rates of each room were measured by the constant concentration method with SF_6 gas as a tracer. The airflow rate of the exhaust duct was measured by the constant injection method using CO_2 gas. The operating conditions of the supplemental fan and the damper of hybrid ventilation system were monitored. Indoor-outdoor temperature difference, indoor-outdoor pressure difference and outdoor wind speed and direction were measured. Table 1 shows the measurement cases for comparing the influences of the air supply system and the difference of places where the exhaust executed. Figure 3 shows the conceptual drawings of Case A and Case B. The exhaust airflow rate of ventilation system was set to 95～125m^3/h for satisfying 0.6～0.75ACH.

RESULTS & DISCUSSIOIN

Variation of each measurement item

Figure 4 shows a part of the measurement result from Case A-1 and Case B-2, including the infiltration airflow rate and exhaust airflow rate, outdoor wind velocity and direction, indoor-outdoor temperature difference and pressure difference, operating conditions of the fan and the damper, respectively.

The total infiltration airflow rate and the airflow rate of the exhaust duct were generally stable while the indoor-outdoor temperature difference varied and the wind velocity changed. But the operating conditions of the fan and the damper of Case A-1 and Case B-2 are varied under the same direction of wind from the northwest at 0:00-6:00 in the day of January 24th and 19th, respectively. This caused by the different influences of wind on each cases where the air supply systems of different feature are introduced.

Table1. Case of measurement

	Place of exhaust	Air supply system	Period (Jan)	Time (hr)
CaseA-1	2nd Floor	Passive	20～25th	117
CaseA-2	All rooms		25～29th	88
CaseB-1	2nd Floor	Crawl space	5～12th	160
CaseB-2	All rooms		17～20th	66

※Set temperature : 30℃ (Crawl space : free floating temp.)

※Opening area of vertical supply duct in the 1st floor adjusted to 1/4

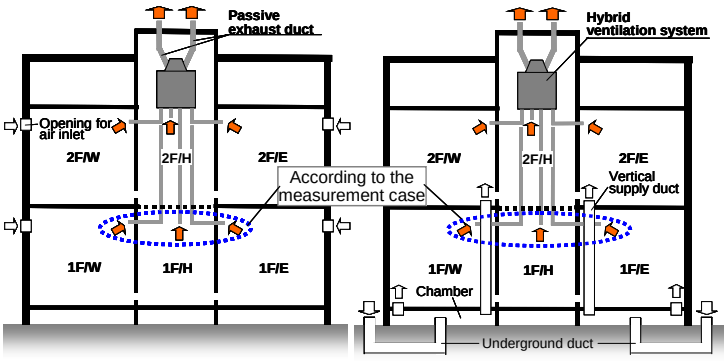

(1) Case A (2) Case B

Figure 3. Conceptual drawing of Case A, Case B

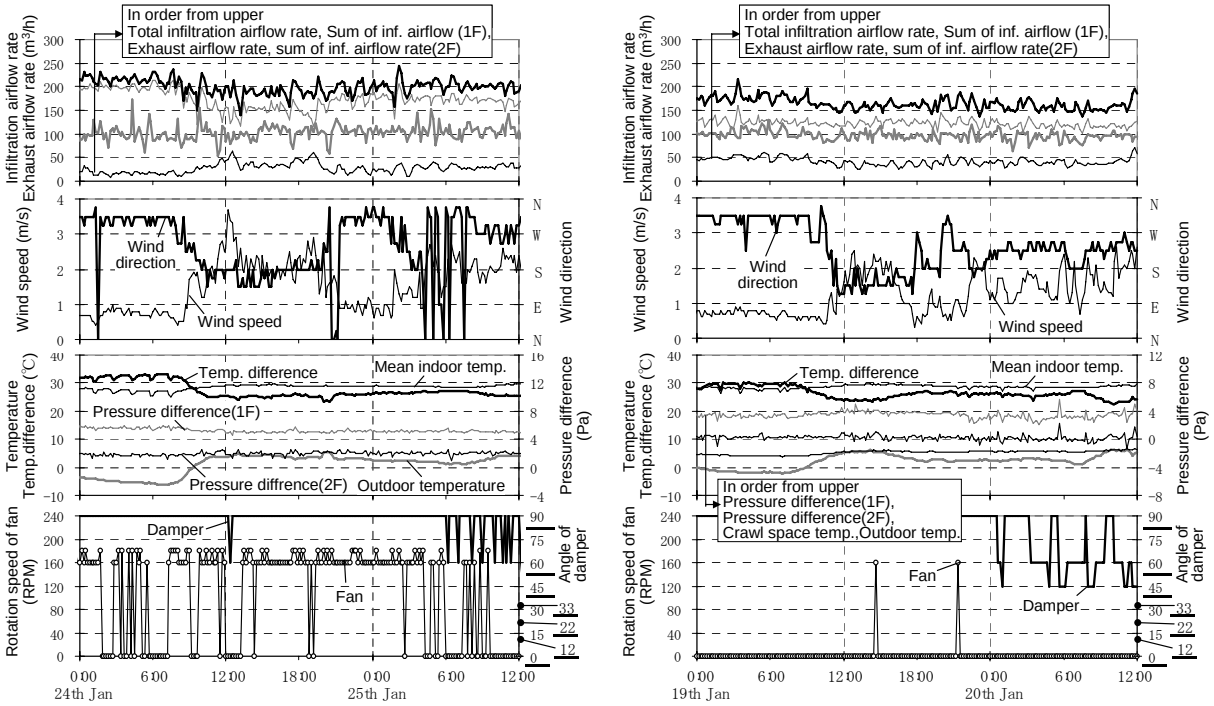

Figure 4. Measurement results of Case A-1(left), Case B-2(right)

Table 2. Operating modes and mean value of each measurement item (Case A)

Operating mode	Rotation speed of fan (RPM)	Opening angle of damper (degree)	Total time (hr)	Total infiltration airflow rate (m³/h)	Exhaust airflow rate (m³/h)	Temp. difference (℃)	Pressure difference(1F) (Pa)	Pressure difference(2F) (Pa)	Wind speed (m/s)
1	0	45	1	206	97	28.0	5.6	2.0	2.5
2		60	6	205	103	27.9	5.4	1.8	2.3
3		90	134	200	96	28.6	5.7	1.9	1.1
4	160		45	203	106	28.1	5.6	2.0	1.1
5	180		20	204	106	28.4	5.6	2.0	1.0

Table 3. Operating modes and mean value of each measurement item (Case B)

Operating mode	Rotation speed of fan (RPM)	Opening angle of damper (degree)	Total time (hr)	Total infiltration airflow rate (m³/h)	Exhaust airflow rate (m³/h)	Temp. difference (℃)	Pressure difference(1F) (Pa)	Pressure difference(2F) (Pa)	Wind speed (m/s)
1	0	45	7	158	89	26.8	3.6	0.2	1.3
2		60	15	160	93	26.9	3.6	0.3	1.3
3		90	196	167	97	28.8	3.4	0.3	0.8
4	160		7	162	105	25.1	3.8	0.7	1.0
(5)	180		0.3	163	113	25.0	4.1	0.8	0.6

Comparison about the operating conditions

The operating conditions of the supplemental fan and the damper appeared in Case A and Case B (206 hours, 225.3 hours in total respectively) could be divided into five modes. Table 2 and Table 3 shows the mean value of the infiltration airflow rate and exhaust airflow rate, indoor-outdoor temperature difference and pressure difference with outdoor wind speed for each operating mode. The mean exhaust airflow rate almost met the target airflow rate (95～125m^3/h). But the total infiltration airflow rates of Case B show lower value than Case A because of the large resistance of the air supply system by using the underground ducts and crawl spaces. No relationships are found between the operating modes and indoor-outdoor temperature difference, and pressure difference.

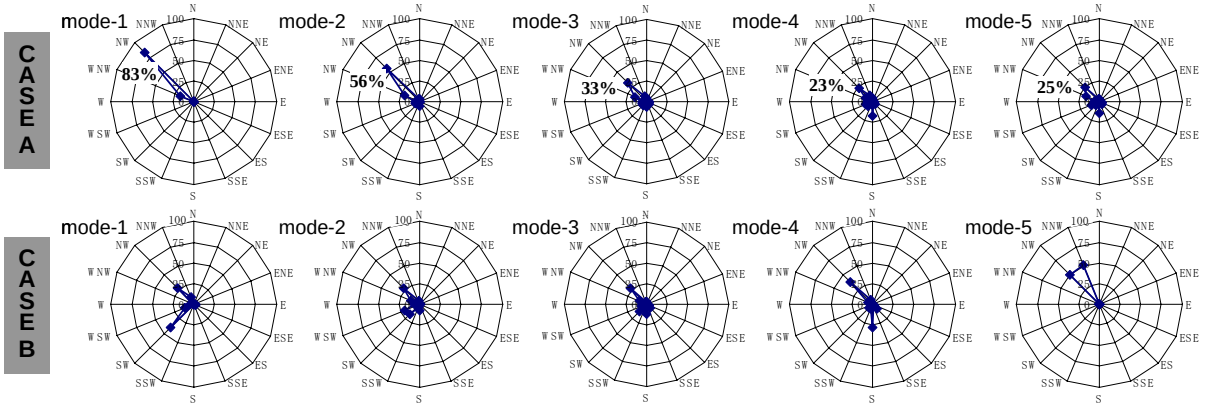

Figure 5. Wind rose for each operating mode

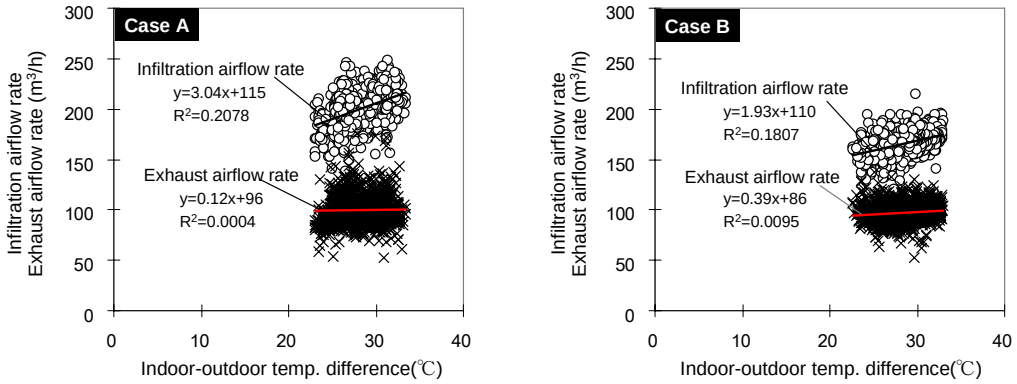

Figure 6. Relationship between temp. difference and ventilation airflow rate in Case A(left), Case B(right)

Influence of the wind on the ventilation airflow rate

Figure 5 shows the wind rose for each operating mode of Case A and Case B. In Case A, the proportion of wind from the northwest becomes the higher from mode-5 to mode-1 with increase of the mean value of wind speed(reference Table 2). In Case B, on the other hands, there are no correlation between the operating modes and outdoor wind. This reveals that the crawl space air supply system provides more stability for system control than the passive air supply system against the influence of outdoor wind.

Influence of the indoor-outdoor temperature difference on the ventilation airflow rate

Figure 6 shows the relationship between the indoor-outdoor temperature difference and the total infiltration airflow rate, and the exhaust airflow rate about Case A and Case B. The airflow rate of passive exhaust duct was maintained by the control of hybrid ventilation system even the indoor-outdoor temperature difference changed. But the total infiltration airflow rate increases according to the rise of temperature difference, especially in Case A.

Proportion of the target airflow rate

Figure 7 shows the histogram of each operating mode. Figure 8 shows that the proportions of target airflow rate are occupying about 60% and 70% for whole periods in Case A and Case B, respectively.

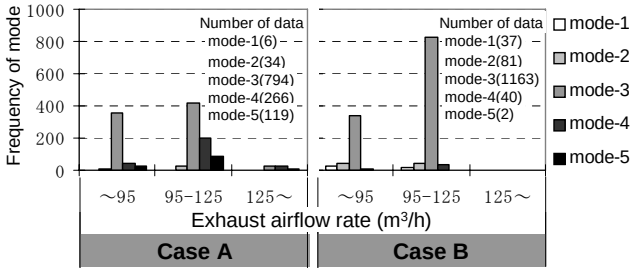

Figure 7. Histogram of each operating mode

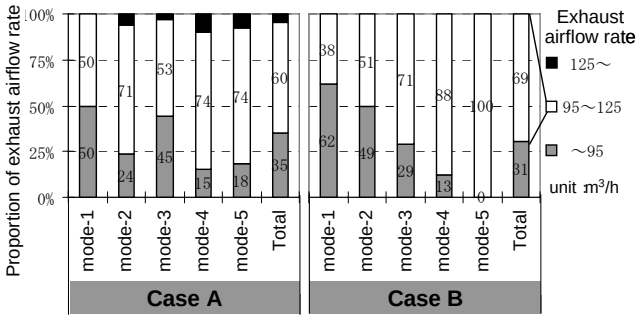

Figure 8. Proportion of exhaust airflow rate

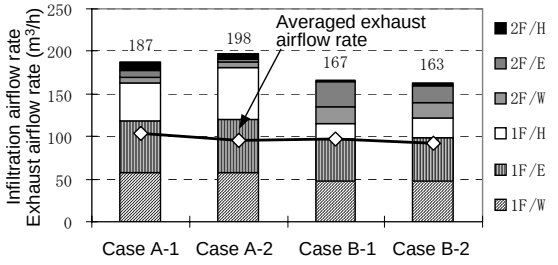

Figure 9. Distribution of infiltration airflow rate

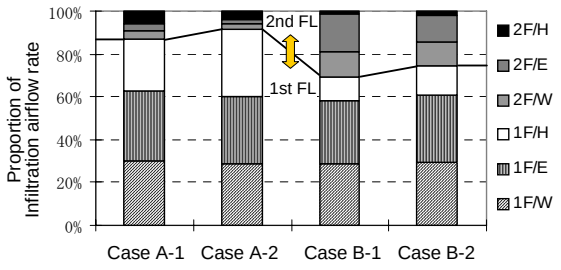

Figure 10. Proportion of infiltration airflow rate

Balance of the infiltration airflow rate for the first floor and the second floor

Figure 9, Figure 10 shows the distribution of averaged infiltration airflow rate and its proportion respectively. Mean value of the exhaust airflow rate has been added as well and it met the target airflow rate in any cases. The infiltration airflow rate on the second floor increased to 30% in Case B while it reached only 10% in Case A. From the comparison about the place of exhaust, Case A-1 and Case B-1 in which the second floor has been exhausted showed better balance of the infiltration airflow rate than Case A-2 and Case B-2.

CONCLUSION

The exhaust airflow rate was generally stable and met the target airflow rate in average under the condition of varying indoor-outdoor temperature difference and outdoor wind. The crawl space air supply system showed higher proportion of target airflow rate than the passive air supply system. Combination of the crawl space air supply system with the exhaust from the second floor is recommended for getting the balance of infiltration airflow rate in the first floor and the second floor.

Acknowledgement

The hybrid ventilation system introduced in this study has been developed by SEKISUI HOUSE Ltd. and TOSHIBA CARRIER Ltd..

References

[1] P.J.M. Op't Veld.(2004).Development of demand controlled hybrid ventilation systems RESHYVENT. *Air Information Review(AIVC).* **Vol 25, No 2**

[2] Yoshino H. and Lee JH. Et al.(2003).Study on the performance evaluation of hybrid ventilation system for detached house - Part 1. *Journal of Environmental Engineering(Transactions of AIJ).* **No 566**, 57-64

ASSESSMENT OF IMPROVEMENTS BROUGHT BY HUMIDITY SENSITIVE AND HYBRID VENTILATION / HR-VENT PROJECT

Savin, J.L., Berthin, S. and Jardinier, M.

Aereco S.A., 9 allée du Clos des Charmes, Collégien
F - 77615 MARNE LA VALLEE Cedex 3

ABSTRACT

Introduced for the first time at 25th AIVC Conference in Prague in September 2004, the HR-Vent project still delivers new rich teachings since its start in January 2004. Until December 2005, more than 700 million data have been recorded on 180 extract units in 5 occupied collective buildings located in NANGIS (France).

Directly linked to the local meteorological data, these measurements aim at evaluating the ability of the new installed hybrid ventilation system to erase the back draught effects as well as to improve the natural draught and the connected gas appliance operation ; They also allow to show the effectiveness of the connected humidity sensitive extract grilles in the wet rooms by recording every minute the data of relative humidity, temperature, pressure and opening surface. All these data are measured by specifically developed sensors integrating a high accuracy low pressure manometer.

Specific and statistical analysis on pressures and airflow, comparisons between rooms, between storeys and buildings, influences of wind speed and outdoor temperatures are very interesting teachings for all of us who need a really significant monitoring to improve their knowledge on natural and hybrid ventilation behavior.

The first results can particularly show the IAQ and energy effectiveness in a microscopic view as in a macroscopic analysis.

KEYWORDS

Measurements, monitoring, HR-VENT, passive stack ventilation, mechanical assistance, hybrid ventilation, humidity sensitive, needs, punctual, mean.

INTRODUCTION

The behavior of ventilation, especially the passive stack and the hybrid ventilation, is still a source of speculations for all of us who try to assess its performances. It is to come out its deep secrets that a large-scale project named HR-VENT has been monitored. This project, located in France in the City of NANGIS, is being applied from January 2004 until December 2005 in 5 occupied collective buildings. Not less than 700 million data are being recorded on 180 extract units to collect information on humidity, temperature, pressure, grille opening surface and gas appliance working. After a first presentation at 25th AIVC Conference in Prague in September 2004[1], some new major results and teachings regarding the improvements brought by the humidity sensitive extract grilles and the mechanical assistance are presented in this article.

PROJECT REMINDER – MEASURED PARAMETERS

HR-VENT project consists in recording every minute the following parameters:

WC and bathroom equipped with a humidity sensitive extract unit.	**Kitchen with domestic boiler**	**Outdoor conditions**
Measured parameters		
Temperature (°C) Relative humidity (%) Aperture of the grille (cm^2) Pressure difference (Pa)	Temperature (°C) Relative humidity (%) Temperature of the combustion gas (°C) Pressure difference (Pa)	Temperature (°C) Relative humidity (%) Wind velocity (m/s) Wind direction (°)
Calculated parameter		
Airflow (m^3/h)	Airflow (m^3/h)	

The 5 buildings are equipped with the following components:

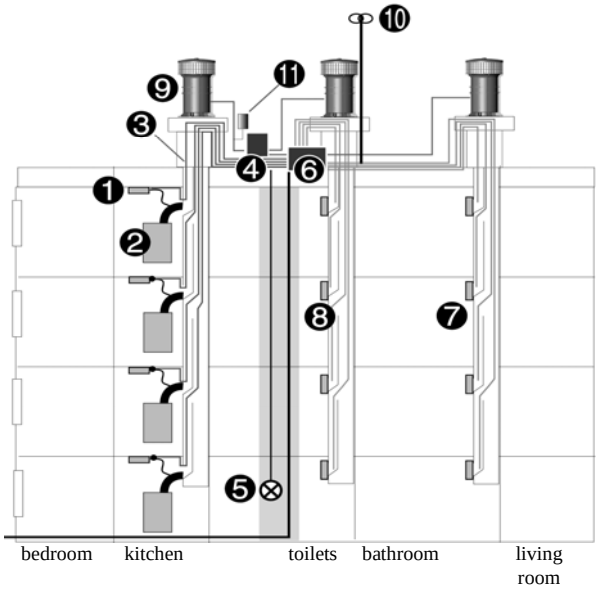

Figure 1 :

Cut of a schematic view of a building stack (example with 4 levels)

[1] Siret, F., Savin, J.L., Jardinier, M. and Berthin, S. (2004). " Monitoring on hybrid ventilation project - first results." *25th AIVC conference.*

	Component	*Function*
1	**Instrumented grille - Kitchen**	Acquisition of : Pressure / Burnt gas Temperature / Room temperature / Room Relative humidity. Frequency : each minute.
2	Connected gas appliance	Hot water production for domestic use.
3	**Data bus cable**	Carry data acquired by components 1,3 and 8.
4	Complete control panel	Transformation of 230 VAC to 15VDC Electrical protection Fan power supply management Simultaneous working of fans management.
5	Working indicator	Indication of good working of the fans equipping this stack of dwellings.
6	**Instrumentation box**	Registers data acquired by components 1,3 and 8.
7	**Instrumented grille - bathroom**	Acquisition of : Pressure / Grille opening section / Room temperature / Room Relative humidity. Frequency : each minute
8	**Instrumented grille - Toilets**	Acquisition of : Pressure / Grille opening section / Room temperature / Room Relative humidity. Frequency : each minute.
9	VBP very low pressure fan	Very low pressure fan for passive stack ventilation assistance.
10	**Meteorological station**	Acquisition of : Wind speed / Wind direction / External local temperature / External local relative humidity. Frequency : each minute.
11	Temperature sensor	Controls the VBP fans speed according to temperature (normal speed / low speed).

Note : Components in charge of registering data are mentioned in bold.

CONTRIBUTION OF THE MECHANICAL ASSISTANCE

The installation of a very low pressure mechanical assistance fan (VBP) has allowed to report various results on the pressures measured at the 100 cm² fix extract grille in the kitchen[2].

Note : the case of the fix extract grille in the kitchen (instead of a humidity sensitive extract grille) allows to "isolate" the impact of the mechanical assistance.

On the charts Figure 2 are presented the airflow on the different floors of a duct column equipped with VBP assistance fan, which has been cut off during one hour (from 13.45 to 14.45 [3]).

We can report that the airflow at the kitchen fix extract grille remains almost constant at 70 m3/h in this period inside each kitchen when the assistance is working. Not only the assistance provides a quasi-constant airflow although the external temperature thus the thermal draught varies, but it also equalizes the airflow between the different floors. When the fan is cut off, the airflow – thus the pressure- varies more greater during this short time inside the room ; it also varies according to the different floors, due to the thermal draught effect, from 20 m3/h up to 50 m3/h.

The assistance fan has not only increased the airflow (x 1.75 on average) to reach a better level but it has also allowed to stabilize the pressure (thus the airflow as it is a fix grille) inside the room and between the floors.

[2] The kitchen is desserved by a fix extract grille which connects the gas appliance.
[3] Data recorded on the 05/17/05, on one stack of 5 kitchen.

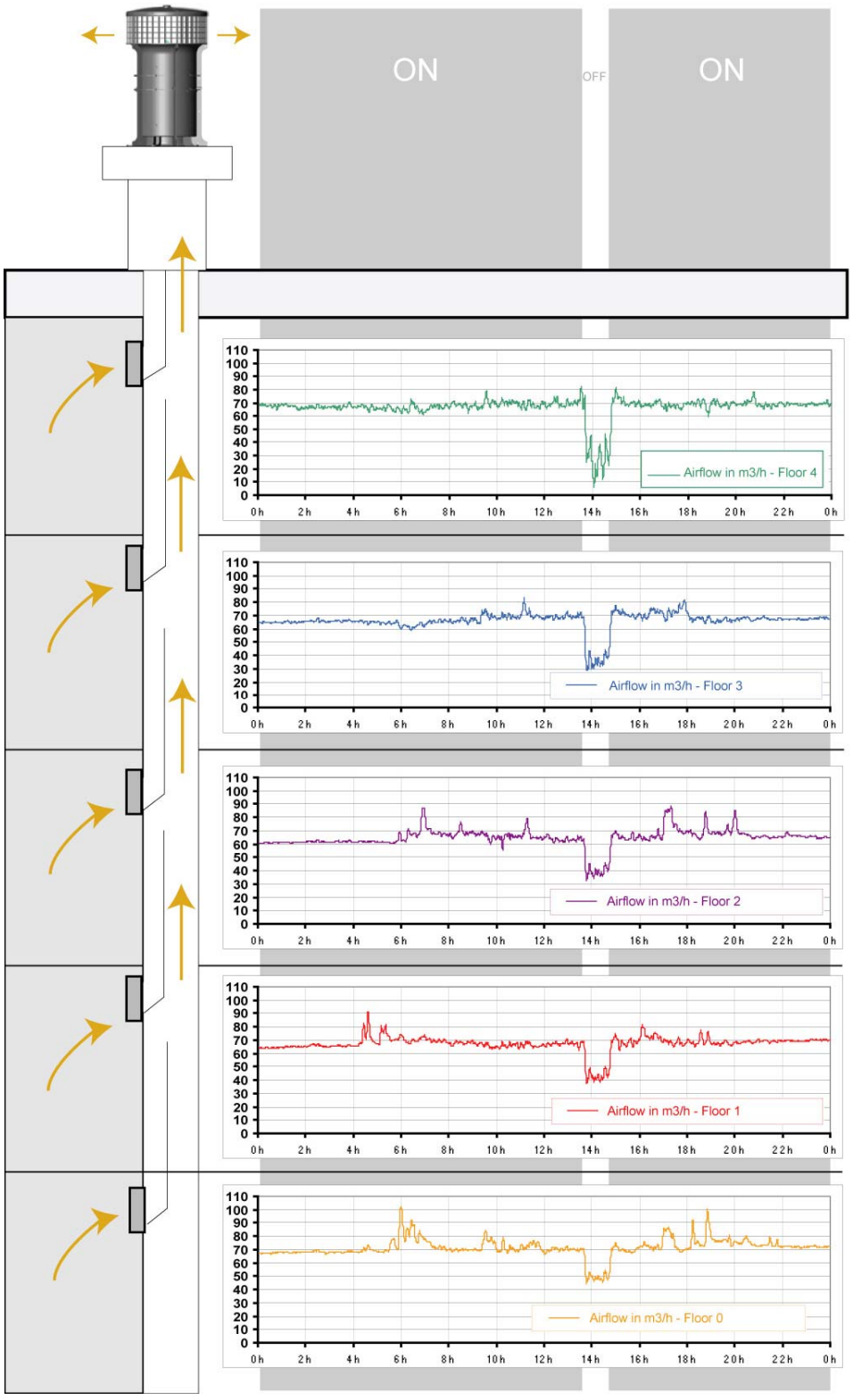

Figure 2 : Comparison on fix extract grille airflow in the kitchen on 5 dwellings connected to the same duct ; with (ON) / without (OFF) fan assistance (example on one day).

CONTRIBUTION OF THE HUMIDITY SENSITIVE EXTRACT GRILLES

This part intends at showing the contribution of the humidity sensitive extract grilles in improving the performances of the natural or hybrid ventilation.

Instantaneous behavior of the humidity sensitive extract grille

On the following chart (Figure 3) is presented the day variation of aperture vs. relative humidity for a humidity sensitive extract grille located in a bathroom. We can notice that the variations of aperture follow well the evolution of relative humidity, with a fast reactivity ; it succeeds in following the large variation of relative humidity.

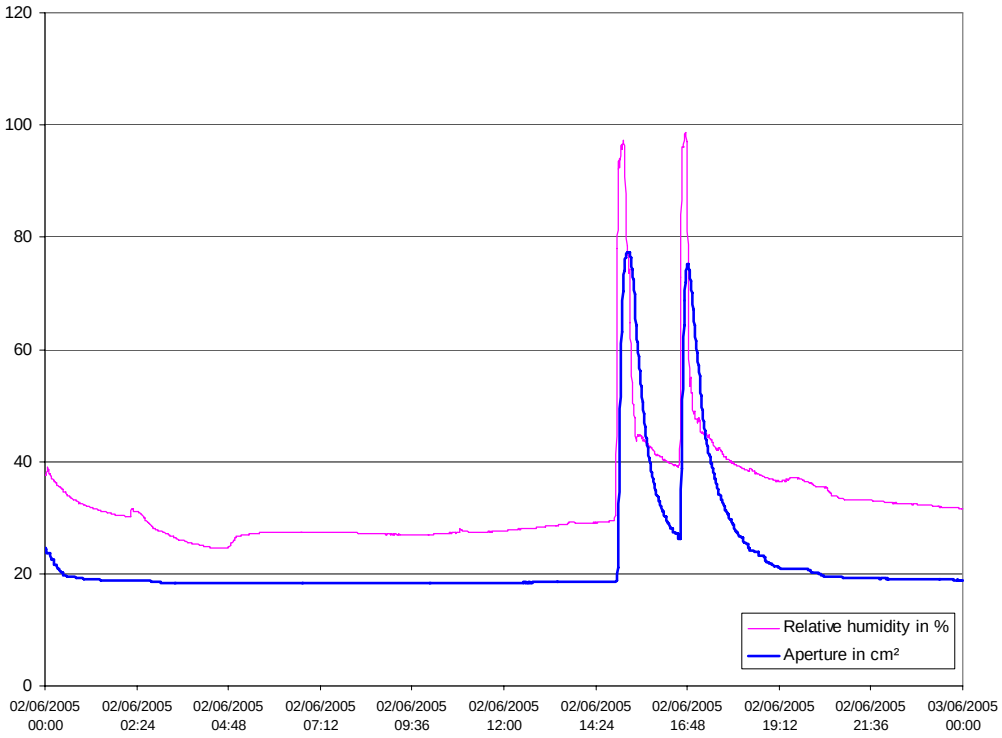

Figure 3 : Aperture vs. relative humidity of a humidity sensitive extract grille in the bathroom

Statistical behavior of the humidity sensitive extract grilles

On the chart Figure 4 can we see both the punctual variability of the grille aperture vs relative humidity and the relative stability of the mean aperture according to the thermal season. Due to the evolution of the mean internal relative humidity all the year long, the grille is mainly close to the closed position in the cold season ; in the hot season the grille aperture becomes wider. The charts on Figure 3 as on the left column of Figure 4 show that **the humidity sensitive extract grille detects permanently the punctual humidity variations to adapt its aperture.**

Only the mean level of aperture varies according to the thermal season during the year. This lower airflow level during the cold season allows to erase over-ventilation thus allows to save energy on thermal losses due to ventilation, while optimizing IAQ as it remains adapted to the punctual needs of air renewal.

Instantaneous / punctual behavior	Statistical behavior
Microscopic view (one day) of Aperture vs Relative humidity variations for one humidity sensitive extract grille in one bathroom, for different thermal seasons.	Macroscopic view (all minute points of the month) of Aperture vs Relative humidity variations for one humidity sensitive extract grille in one bathroom, for different thermal seasons. (only 95% of points)
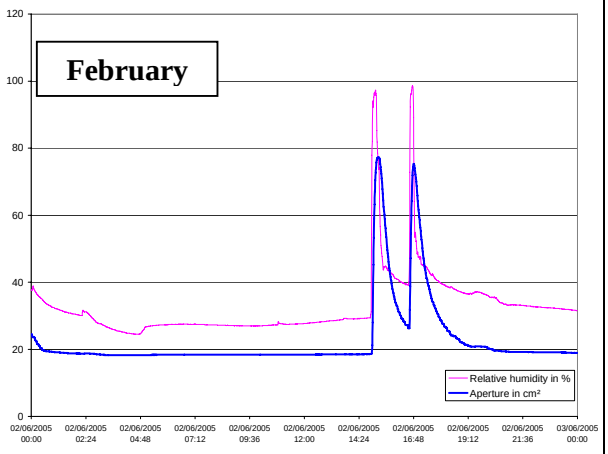	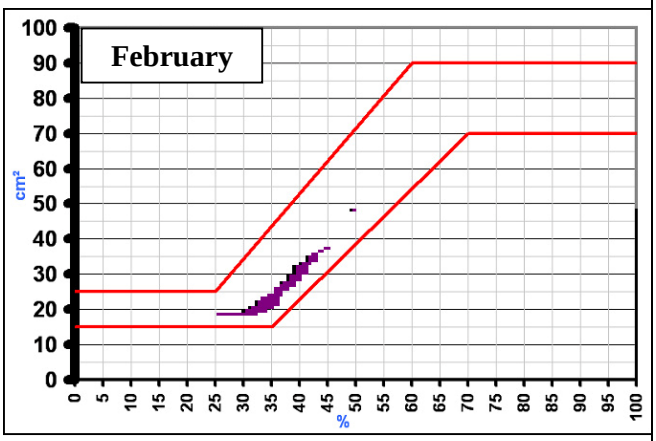
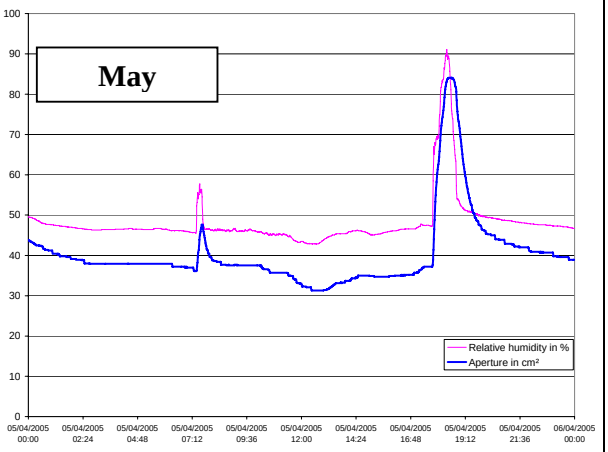	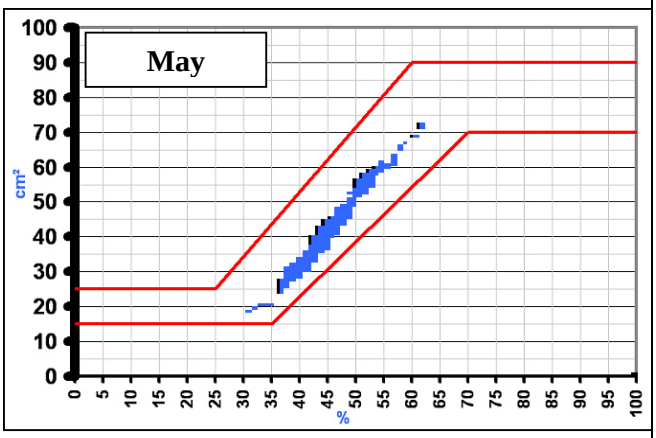
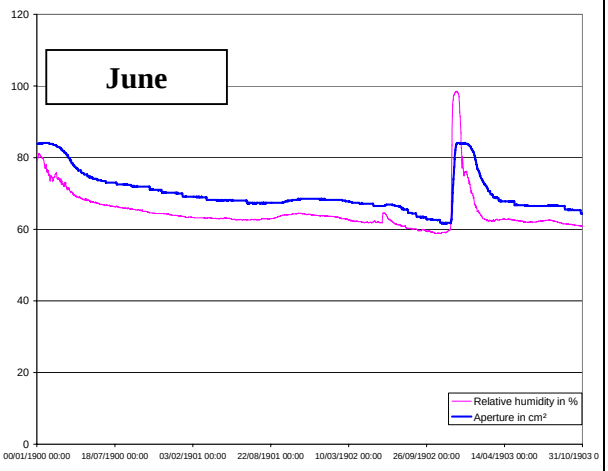	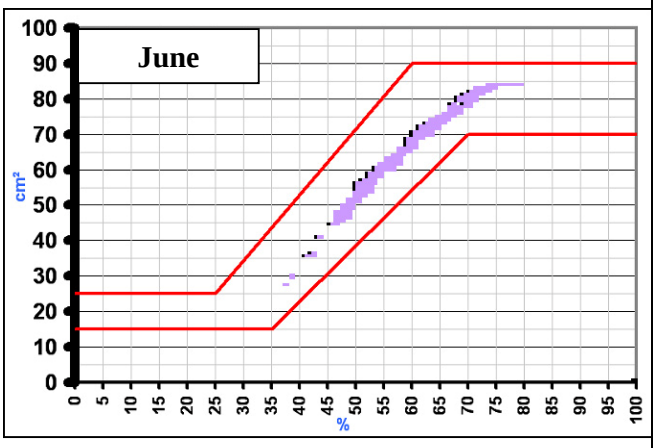

Figure 4 : Microscopic day-view and macroscopic monthly view of the variation of Aperture Vs Relative humidity of one humidity sensitive extract grille in one bathroom.

COMPARISON BETWEEN FIX, HUMIDITY SENSITIVE AND ASSISTED VENTILATION

The following analysis concerns the study of the mean monthly airflow, which is naturally different from the instantaneous airflow which is variable in the case of the humidity sensitive ventilation (see previous chapters).

- *Fix extract grille in PSV (Figure 5)*

If we consider the variation of airflow according to the pressure for a fix grille of 50 cm² for example, we know that the airflow depends directly and mainly on the stack effect, thus on the thermal season (Figure 5).

Due to the thermal draught, the pressure thus the airflow is higher in winter, and decrease to go to null or reverse airflow in summer.

The variation of the mean airflow is thus important, although the mean needs are similar. As airflow are more important in winter, it directly increases the thermal losses. The fix extract grille is not able to adapt its airflow to the punctual variations of needs of air renewal.

- *Fix extract grille with assistance fan (Figure 6)*

On Figure 6 can we notice the improvement brought by a mechanical assistance on a fix extract grille. The airflow are increased as the pressure, and the variation of airflow between February and July is reduced from Δ=30 m3/h to Δ =20 m3/h.

It is also remarkable to report that the mechanical assistance has allowed to erase reverse airflow, all year long.

- *Humidity sensitive extract grille in PSV (**Error! Reference source not found.**)*

As seen before, we know that the mean value of aperture of the humidity sensitive extract unit is reduced in winter, increased in summer. So the change of aperture compensates the variation of natural forces ; the humidity sensitive extract unit can be consequently considered as an airflow stabilizer (**Error! Reference source not found.**).

But the main fact to remember is that the mean airflow variations are limited, and the winter mean airflow is decreased up to 50% compared to a fix grille, which make the humidity sensitive extract grille an important contributor for energy saving.

- *Humidity sensitive extract grille with assistance fan (Figure 8)*

By putting a mechanical assistance on the vertical duct connected to the humidity sensitive extract grilles (Figure 8), the ventilation tends to be optimal : higher in hot season when the aim is to fight against reverse airflow, lower in cold season when the enemy is the thermal loss.

The mixed-effect of mechanical assistance and humidity sensitive extract grilles allows to reach an higher IAQ in winter as in summer, and improve its anti-reverse airflow power in summer.

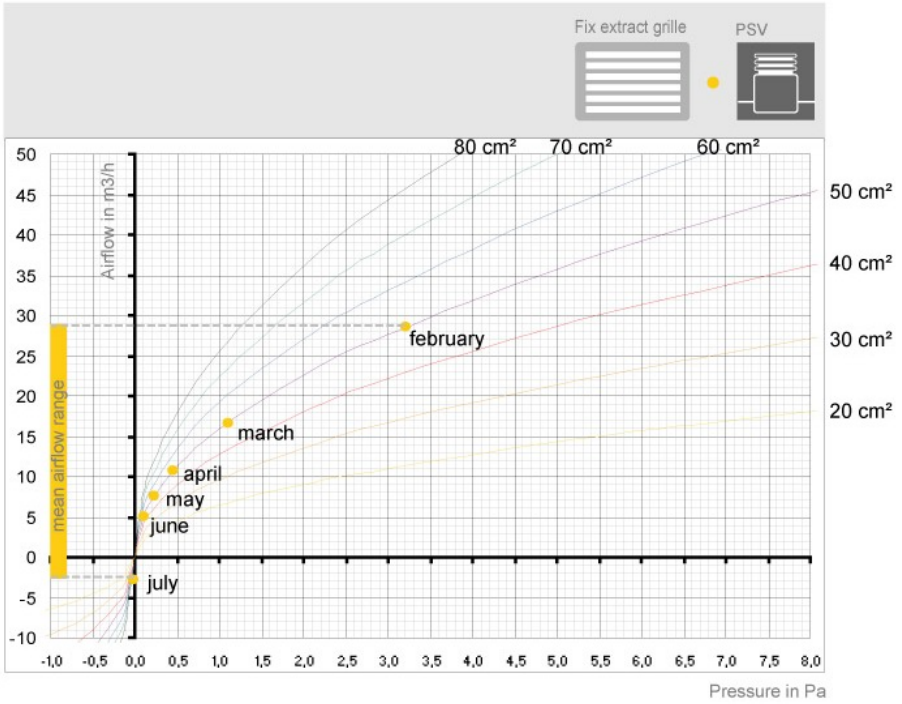

Figure 5 :

Fix extract grille + PSV – **Mean*** monthly value of airflow / pressure

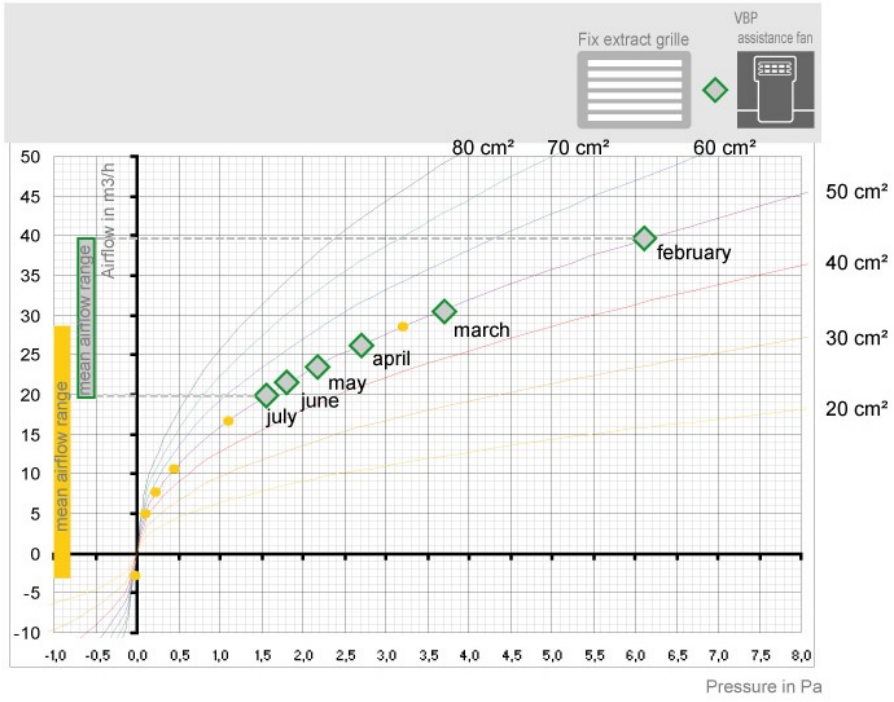

Figure 6 :

Fix extract grille +assistance fan – **Mean*** monthly value of airflow / pressure

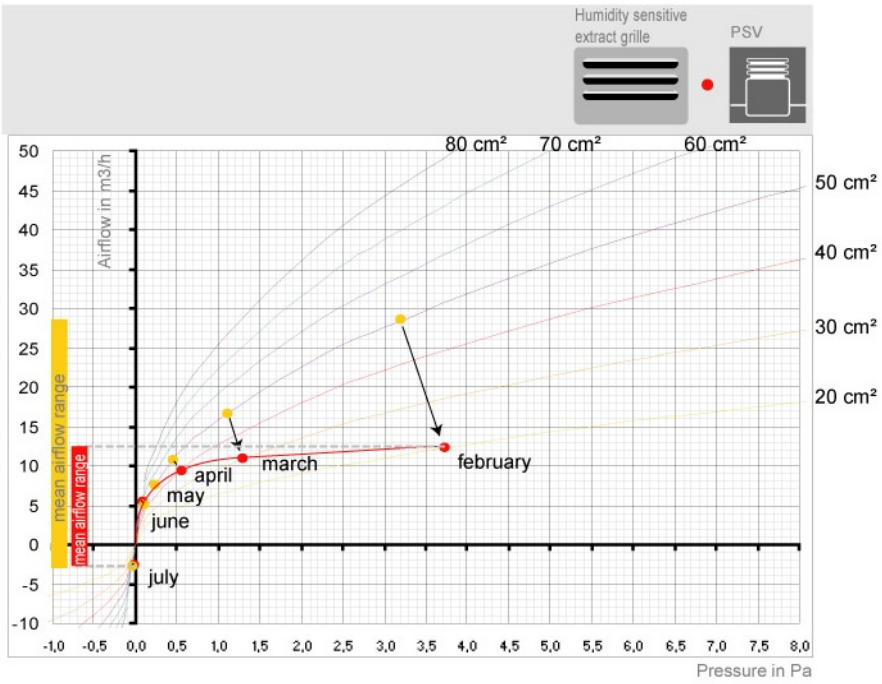

Figure 7 :

Humidity sensitive extract grille + PSV – **Mean*** monthly value of airflow / pressure

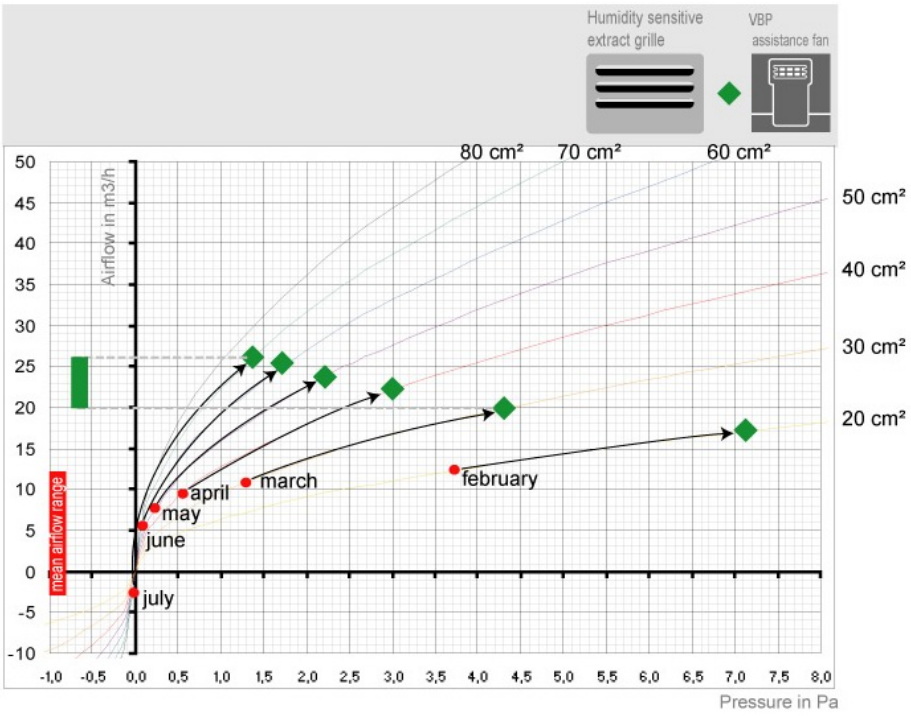

Figure 8 :

Humidity sensitive extract grille + assistance fan – **Mean*** monthly value of airflow / pressure

* : the mean value of the airflow corresponds to the average of all the airflow / pressure points on one month on one bathroom extract grille **; the instantaneous behavior of the humidity sensitive extract grille remains <u>variable</u>, adapted to the needs** (see Figure 3 and Figure 4).

This example, for determined conditions of meteorology, type of building, floor level, type of dwelling, is representative of the majority of the cases. All the details of the study will be available in the final monitoring report in the 1st 2006 semester.

AIRFLOW RANGE REPORT FOR SEVERAL TYPES OF BUILDINGS

The mixed-effect of humidity sensitive ventilation and fan assistance is illustrated in an other way in the Figure 9, which represents the average airflow range from winter to summer in 4 types of buildings (2, 3, 4 and 5 floors) depending on the floor level and on the technical room.

This synthesis intends at showing the influence of parameters such as height of buildings, number of floor, working of assistance fan and type of extract unit.

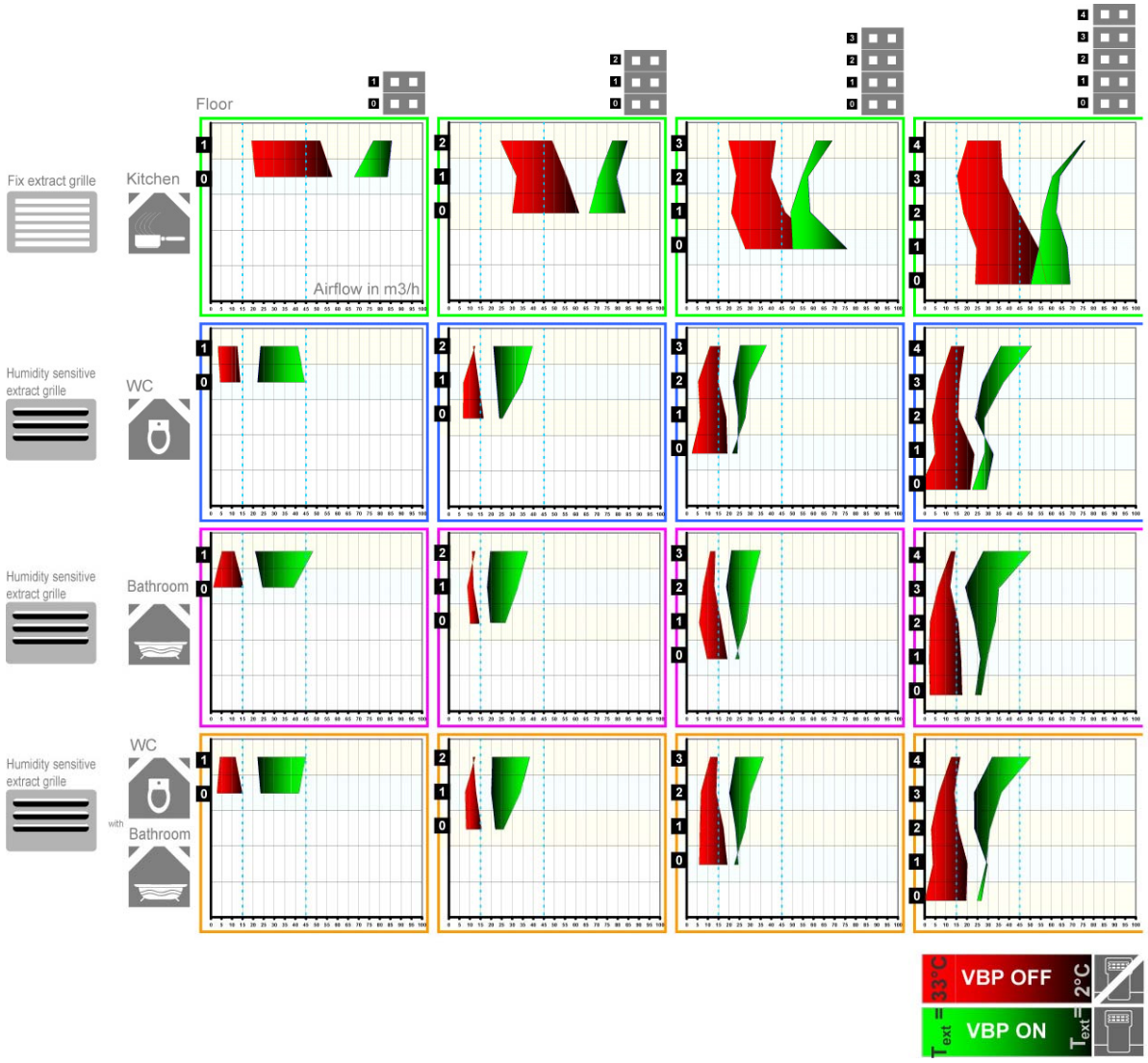

Figure 9 : Comparison on airflow range for different types of technical rooms, different types of buildings (2 to 5 floors), with / without fan assistance.

Legend:
The width of the spectrums corresponds to the range of external temperature. In red (left) is the airflow with mechanical assistance OFF. In green (right) is the airflow with mechanical assistance working. Compilation of all year long data, all extract units (166).

In the kitchen where the grille is fix, we can notice that the range of airflow is wider than in the bathroom and WC where extract grilles are humidity sensitive. It is also remarkable to report that the mean airflow (not the punctual airflow) is considerably lower with the humidity sensitive ventilation.

This variability of airflow for one technical room is reduced with the mechanical assistance, in the fix grille as in the humidity sensitive grille. The mechanical assistance tends to favor the higher floors while the PSV favors the lower floors (in winter), and increases widely the mean airflow of the range.

The higher is the building, the more we have airflow variation between the floors. But these differences are reduced by both humidity sensitive extract units and mechanical assistance.

CONCLUSION

HR-VENT project has allowed to confirm and to discover more behaviors of passive stack and hybrid ventilation. It confirms the efficiency of the humidity sensitive ventilation as an IAQ provider and energy saver by showing its ability to adapt instantaneously the airflow to the punctual needs of air renewal, while the mean airflow is lowered in winter. It also shows that the mechanical assistance ensures an anti-reverse airflow power required in summer, which, mixed to the humidity sensitive extract grilles, provides a complete optimized solution for energy savings as IAQ.

More teachings and information will be available in the final report of HR-VENT, to be issued in the 1st 2006 semester.

REFERENCES

Siret, F., Savin, J.L., Jardinier, M. and Berthin, S. (2004). " Monitoring on hybrid ventilation project - first results." *25th AIVC conference.*
Savin, J.L., Jardinier, M. and Siret, F. (2004). "In-situ performances measurement of an innovative hybrid ventilation system in collective social housing retrofitting". *25th AIVC conference.*
Siret, F. and Jardinier, M. (2004). "High accuracy manometer for very low pressure." *25th AIVC conference.*

IMPROVING ENVELOPE AIRTIGHTNESS : RESULTS OF A PILOT STUDY ON 31 HOUSES

Karine Guillot, Daniel Limoges, François Rémi Carrié

Centre d'Etudes Techniques de l'Equipement de Lyon
46 rue Saint Théobald
F – 38081 L'Isle d'Abeau Cedex, France

ABSTRACT

This paper presents the results of a field study conducted on 31 houses owned by a French social housing management body. The central objective of our investigation was to propose and evaluate rehabilitation scenarios to improve the envelope airtightness. For this, pre- and post- envelope leakage measurements were performed together with infrared thermography analyses. In parallel, the occupants were interviewed to better understand their interaction with the thermal functions and what their feeling was about the thermal comfort and indoor quality in their homes. These detailed investigations performed on 8 houses showed that the airtightness could be significantly improved (median at 0.3 $m^3/h/m^2$ at 4 Pa), and that the refurbishment lead to better thermal comfort.

KEYWORDS

air leakage, envelope, survey, infrared thermography, thermal performance, low-income housing

INTRODUCTION

This work is part of a broader research program supported by ADEME and EDF that aims at evaluating the significance of envelope leakage and at improving the airtightness of new and existing buildings [1][3][4].

In this particular study, OPAC de l'Ain (social housing management body) decided to evaluate the significance of envelope leakage of a group of 31 semi-detached electrically heated houses, to better understand its interactions with occupants' comfort and energy use, and to propose, conduct, and evaluate retrofitting actions.

This paper concentrates on the evaluation of the overall process. More information regarding the pre-characterization and definition of scenarios can be found in an earlier paper [2].

PROJECT PHASES

The project phases are briefly described herebelow :

Phase I **(**Winter 2001-2002) entailed pre-characterization and definition of refurbishment scenarios. It included :

- Airtightness tests on 8 residences and identification of major leak sites with IR thermography
- Heating energy use monitoring during 2 winter months in 9 residences
- Temperature and humidity monitoring at different locations during 2 winter in 9 residences
- Airflow rate measurements at Air Terminal Devices (ATDs)

Phase II (2003) consisted in implementing the retrofitting measures on site. CETE was involved in the assistance to building owner to raise awareness among the companies involved, and a few spot controls.

Phase III (winter 2003-2004) consisted in analysing and evaluating the overall process based on post-characterization of envelope leakage, indoor environment monitoring, and questionnaires among occupants.

SUMMARY OF REFURSBISHMENT MEASURES AND COST

Retrofit actions have been derived for each type of defect, based on guidelines detailed in reference [1] and interactions with professionals. Most actions consist in sealing cracks with mastic joints or insulation foam. The total cost per house was of 2 100 Euros including 1 300 Euros for the replacement of windows. In other words, the extra cost due to the manual sealing of cracks is 800 Euros.

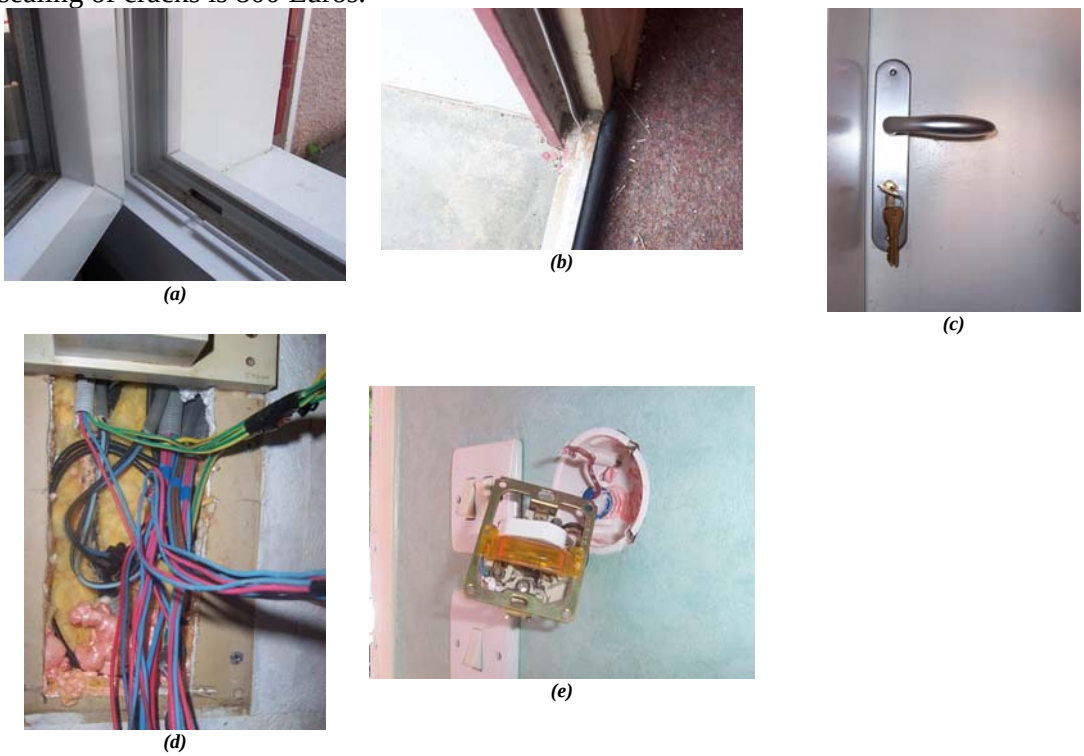

Figure 1. Examples of refurbishment measures. (a) replacement of windows. (b) Replacement of undercut joint and joint around the opening. (c) Replacement of the garage lock. (d) Injection of insulation foam to close the passageways to the air gap in the wall. (e) Insulation foam behind the plug boxes in cold walls.

MAJOR RESULTS OF PHASE III

Envelope airtightness improvement

The pre- and post- envelope leakage measurement results are synthesized in Figure 2. The value of I_4 ranged between 0.63 and 1.64 $m^3/h/m^2$, with a median at 1.15 $m^3/h/m^2$. Except for one, the envelopes are considerably leakier than the reference used in the French building code (0.8 $m^3/h/m^2$). After refurbishment, the I_4 ranged between 0.67 and 1.29 $m^3/h/m^2$, with a median at 0.79 $m^3/h/m^2$. The median of the airtightness improvement is 0.3 $m^3/h/m^2$.

The IR thermography analyses have shown that significant improvement at window frame-opening interfaces, garage doors, access panels to attic. However, significant leakage remained at window frame-wall interfaces, and electrical boards and conduits.

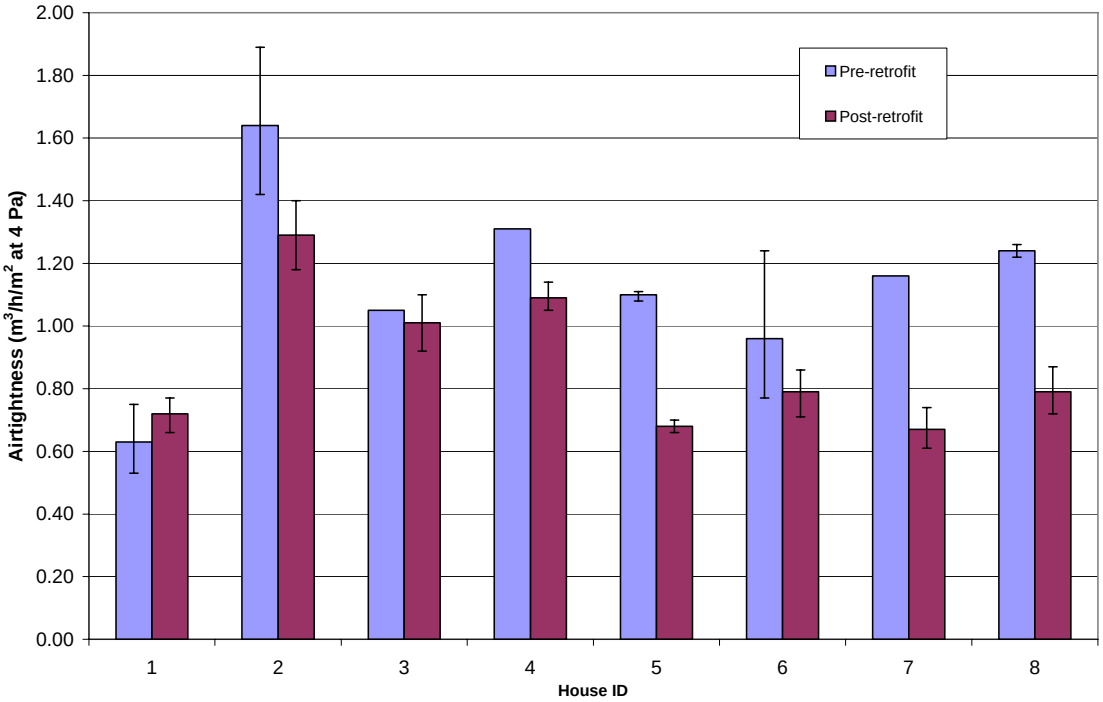

Figure 2. Pre- and post- airtightness measurements in m^3/h per m^2 of cold walls (except lower floor) at 4 Pa.

Evaluation of potential energy use reduction

The uncontrolled airflow rate due to envelope leakage has been evaluated using a simplified model developed by CSTB similar to the calculation procedures adopted in the former energy performance regulation (Th-G, 1991). Figure 3 and Figure 4 show that the additional unwanted airflow rate ranges from –4% up to +18% and leads to heating energy losses ranging from –215 up to 1320 kWh. The gain on the ventilation energy losses is estimated to be of 10% on average for a heating season.

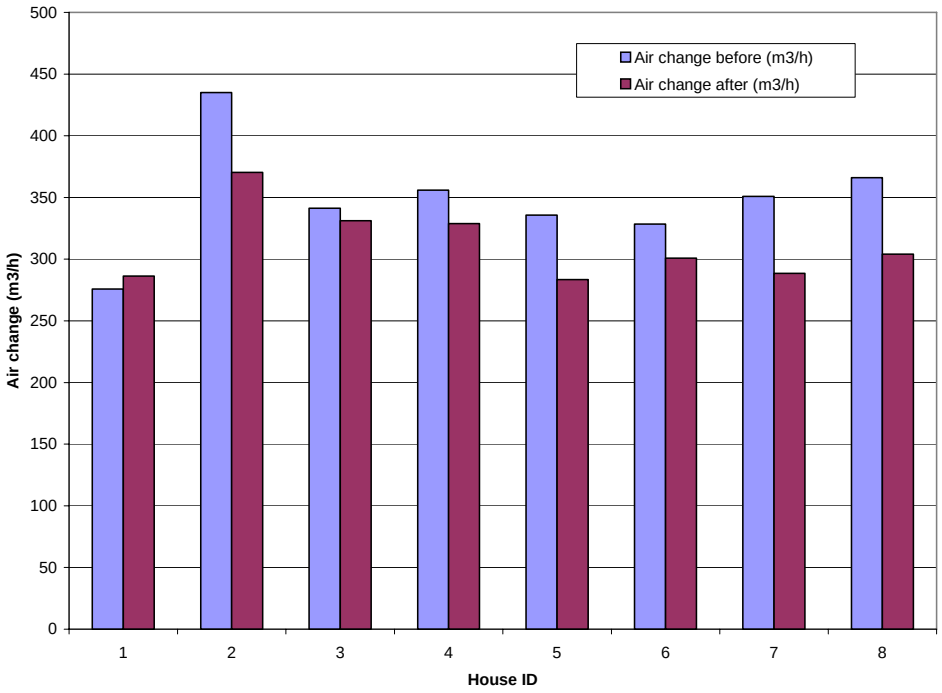

Figure 3. Estimates of air change rate before and after refurbishment.

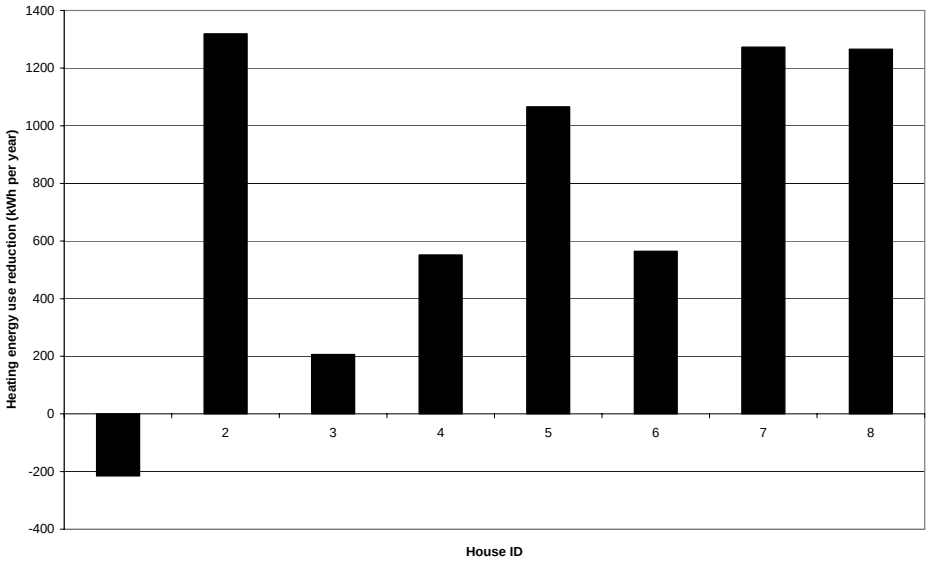

Figure 4. Estimates of heating energy use reduction on a heating season (2500 degree days).

Occupants' behaviour and acceptance, perceived thermal comfort

The energy savings results should be used with care as the calculation does not take into account the effect of occupants' behaviour. The analysis of our questionnaires shows that the occupants have not changed their thermostat setting before and after retrofitting and that they continue window airing during long time periods even during cold days, despite the information given during the experimentation.

The replacement of the windows has been seen as a very positive measure by the occupants. This major work has shaded the considerable efforts made by the contractors on manual sealing. Interviews among the occupants show that the measures that are perceived most effective are : first, the replacement of windows; second, the electrical boards and garage doors. On the other hand, 5 of them are disappointed with the work performed on the main door. In fact, in many cases, it was so distorted that the new sealing joints could not be effective.

All occupants interviewed were satisfied with the progress made with regard to thermal comfort. They all described this progress in terms of reduction of cold draughts and/or feeling of cold.

Tips and traps

Here is a list of major tips and traps that have been identified in this study.

Tips :

- carefully locate cracks
- check the ventilation system performance and define retrofit actions to be undertaken if necessary
- discuss the definition of the work together with the contractors and manufacturers
- carefully define the requirements to the contractors regarding the products to apply and their installation

Traps :

- degradation of materials too significant, making any measure ineffective
- reluctance to undertake work with costly side effects (ex. skirting boards)
- economic context making unattractive manual sealing for the contractors
- lack of awareness, need for skilled labour

Ways of progress and reproducibility

Several ways of progress have been identified :

- to raise the principal barriers, in particular, by integrating the concern of airtightness in all the actions of maintenance – maintenance of real estate, by writing clear requirements ;
- to develop pedagogy and the communication near the professionals and occupants on the objectives of ventilation, the principle of mechanical ventilation, the possibilities of saving energy while satisfying comfort, in order to avoid behaviours detrimental to energy and comfort ;
- to stimulate the quality of the work in order to put forward good practice and skilled labour, which remains an key aspect in the construction process ;
- finally, at research level, to improve knowledge on the contribution of the various components and connections of the envelope to air leakage. This more precise

knowledge could make it possible to concentrate efforts towards the trades most concerned.

The reproducibility of this action on a large scale highly depends on progress made regarding those questions, as well as the awareness of building owners and managers, contractors, and occupants.

CONCLUSION

The objective of this experimentation was to test the feasibility of reducing envelope leakage in existing buildings. Globally, the evaluation of this project shows that simple measures can be implemented with success. It also shows that sealing cracks can result in significant energy savings and better comfort. These issues are all the more important as the buildings is highly insulated with energy efficient equipment. This is why the improvement of envelope air tightness is an important question that should be addressed in the context of the energy performance of buildings directive; rehabilitation projects (mentioned in particular in article 6 of the EPBD) should take into account the benefits of reducing envelope leakage.

ACKNOWLEDGEMENTS

This study was performed on houses that are managed by OPAC de l'Ain. It was supported in part by ADEME, EDF, and the French Ministry of Equipment (DRE Rhône-Alpes). This work is part of a broader research program supported by ADEME and EDF that aims at evaluating the significance of envelope leakage and at improving the airtightness of new and existing buildings.

REFERENCES

[1] EDF – CETE de Lyon. (2001). *Perméabilité à l'air des bâtiments d'habitation – Guide améliorer la performance des logements existants.* July 2001.

[2] Guillot, K., et al. 2003. Field characterization of the envelope leakage of houses for determining rehabilitation priorities. In 24th AIVC Conference, Washington, D.C., October 2003. pp. 265-270.

[3] Guillot, K., Litvak, A., Kilberger, M., Boze, D. (2000). *Ventilation performances in French dwellings: results from field observations and measurements*. UK, Air Infiltration and Ventilation Centre, proceedings of "Innovations in Ventilation Technology", 21st AIVC Annual Conference, held The Hague, Netherlands, 26-29 September 2000, paper 50.

[4] Litvak, A., Guillot, K., Kilberger, M., Boze, D. (2000). *Airtightness of French dwellings: results from field measurement studies*. UK, Air Infiltration and Ventilation Centre, proceedings of "Innovations in Ventilation Technology", 21st AIVC Annual Conference, held The Hague, Netherlands, 26-29 September 2000, paper 60.

[5] Th-G. (1991). Règles de calcul du coefficient GV. Référence AFNOR DTU P 50-704. avril 1991.

ANALYSIS METHOD BASED ON POWER BALANCE AS APPLIED TO WIND DRIVEN FLOW

Kyosuke Hiyama[1] and Shinsuke Kato[2]

[1]*Nikken Sekkei Ltd., Tokyo 102-8117, Japan*
[2] *Institute of Industrial Science, The University of Tokyo, Tokyo 153-8505, Japan*

ABSTRACT

Currently, various studies have demonstrated some doubt about the accuracy of the orifice equation when applied to the calculation of cross-ventilation. As a result, a computational fluid dynamic (CFD) simulation is considered the best method of analyzing cross-ventilation properties under present conditions. However, repetition of CFD analysis to determine the optimum ventilation performance is particularly complex. Accordingly, a flow network model that corresponds to cross-ventilation was developed and suggested as a more efficient means of determining the optimal opening conditions. At least one instance of CFD analysis using a model with openings is necessary to investigate the airflow property around a building. The suggested flow network model was established by utilizing the results of the CFD analysis, and relaxing the total pressure loss coefficients.

KEYWORDS

Power Balance, Ventilation Rate, Network Model Analysis, Pressure Loss Coefficient

INTRODUCTION

The fluid mechanics of cross-ventilation with open windows are different from those of air infiltration through cracks. Various studies have provided useful information for the understanding of different aspects of cross-ventilation phenomena (Karava P 2004). As referred by Sandberg (2004), airflow approaching the building has a choice, to flow through the opening or past the building. When the opening is sufficiently large, the wake behind the building disappears with the result that the airflow properties investigated by a sealed model do not correspond to those for cross-ventilation. Various studies have proposed the modeling of cross-ventilation (Murakami et al. 1991, Sandberg 2002, Ohba et al. 2004, Kurabuchi et al. 2004). The application of a power balance model (energy conservation law) was proposed by Kato (2004). This modeling noted that the dynamic pressure, neglected in the assumption of small openings (i.e. the static pressure difference between the front and the back of an opening is considered to be equal to the total pressure difference), must always be taken into account. Non-standard values for outlet pressure loss coefficients have been reported through wind tunnel experiments. However much more work needs to be done to provide design data for the calculation of ventilation.

CFD analysis is considered the optimal method to predict cross-ventilation properties under present circumstances. However, repetition of CFD analysis to determine the opening conditions for optimal ventilation performance is excessively troublesome. A flow chart for planning the optimal ventilation property by CFD analysis alone is shown in Figure 1. It

might be useful in reducing the number of repetitions of CFD analysis and calculation costs by developing a more efficient method of predicting an outline of the ventilation properties. At least one instance of CFD analysis using a model with openings is necessary to investigate the airflow property around a building. Then, the developed flow network model which corresponds to the cross-ventilation characteristics analyzed by the CFD analysis is suggested as a more streamlined method of determining the optimal opening conditions; especially the opening sizes. A flow chart for planning the optimal ventilation property by CFD analysis and the developed flow network analysis is shown in Figure 2. In order to develop the flow network model correspond to cross-ventilation, the parameter for the airflow network model –total pressure loss coefficient – was reconsidered.

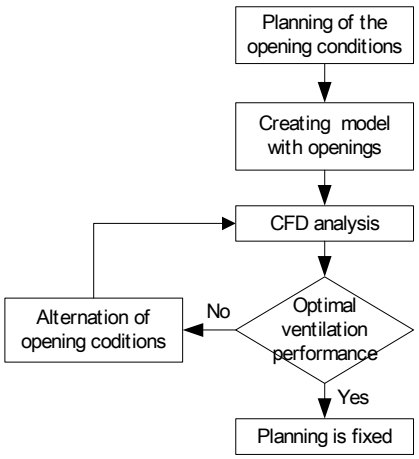

Figure 1. Flow chart for planning by only CFD

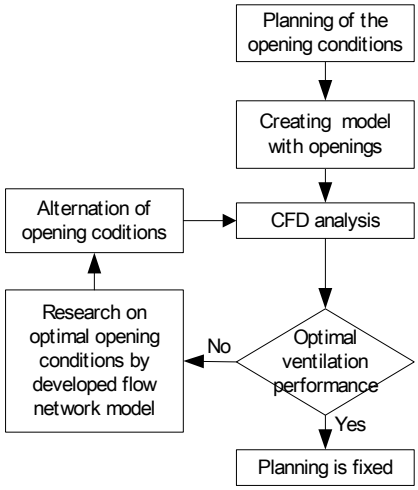

Figure 2. Flow chart for planning by CFD and developed flow network model analysis

TOTAL PRESSURE LOSS COEFFICIENT CORRESPONDING TO CROSS-VENTILATION

If the openings for cross-ventilation are not small enough, the airflow through those openings still preserves part of their dynamic pressure when they stay inside the room. That is, they reach the leeward windows before completely dissipating their kinetic energy into heat. This means that the total pressure losses at openings vary greatly according to the degree of energy preservation after the opening. The total pressure loss is much smaller if the dynamic pressure is preserved and dissipation decreases. The degree of energy preservation is influenced by the flow fields inside and outside formed by the configuration of the building and each window. A simplified energy preservation equation (Equation 1) is as follows (Kato 2004):

$$\sum_m Q_m \frac{1}{2}\left(\frac{Q_m}{A_m}\right)^2 + \sum_m Q_m \left(P/\rho\right)_m + LP = 0 \tag{1}$$

By establishing a room as a control volume, Equation 2 is obtained:

$$\sum_i PW_i = \sum_j PW_j + LP \tag{2}$$

When it is assumed that the airflows discharged from the openings dissipate most of their kinetic energy as heat at the leeward openings, the total lost power of the airflow through a room is expressed as follows:

$$LP = \sum_i Q_i \cdot P_{ti} - \sum_j Q_j \cdot P_{sj} \tag{3}$$

Then, the total lost power of each room in a CFD analysis is obtained using Equation 3.

On the other hand, total lost power evaluated in a flow network model analysis is expressed as follows:

$$LP = \sum_i \zeta_i \frac{1}{2} \rho \left(\frac{Q_i}{A_i} \right)^2 \cdot Q_i + \sum_j \zeta_j \frac{1}{2} \rho \left(\frac{Q_j}{A_j} \right)^2 \cdot Q_j \tag{4}$$

The calculation results from Equations 4 and 5 should be the same to make the airflow network model analysis correspond to cross-ventilation. Then the individual total pressure loss coefficients are obtained using the suggested function $f(\theta_{ij})$ as follows:

$$\zeta_i = f_i(\theta_{ij}) \cdot \xi = \min\{r(1 - \sin^{0.7}(1.8\theta_{ij})) + 1.1\sin^{0.7}(1.8\theta_{ij})\} \cdot \xi \quad (j = 1,....,n) \tag{5}$$

$$\zeta_j = f_j(\theta_{ij}) \cdot \xi = \min\{r(1 - \sin^{0.7}(1.8\theta_{ij})) + 1.1\sin^{0.7}(1.8\theta_{ij})\} \cdot \xi \quad (i = 1,....,n) \tag{6}$$

where θ_{ij} is defined as the angle between a perpendicular line from the windward opening surface through the center and a line from the center of the windward opening to the center of the leeward opening, as shown in Figure 3. $f(\theta_{ij})$ is a function defined to approximate the experimental result from investigating the correlation between θ_{ij} and the total pressure loss coefficient by Ishihara (1969), as shown in Figure 4. $f(\theta_{ij})$ is based on the idea that the value range from r to 1.1 depends on a variable θ_{ij}. The unknown value r for each room is obtained to solve simultaneous equations: Equations 3 ~ 6 using one instance of CFD analysis. However, if θ_{ij} is more than $\pi/9$, it is assumed that the conventional pressure loss coefficients could be adapted and $f(\theta_{ij})$ is considered to equal 1.

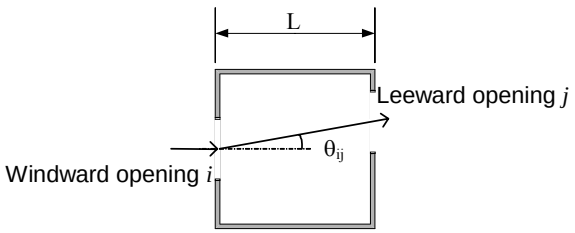

Figure 3. Definition of θ_{ij}

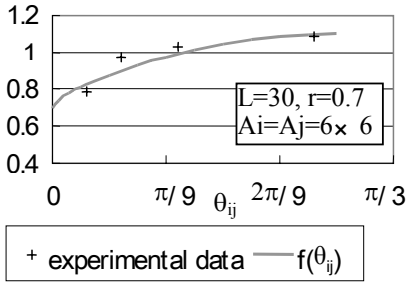

Figure 4. experimental data (Ishihara 1969) and $f(\theta_{ij})$

CASE STUDY USING DEVELOPED FLOW NETWORK MODEL

A case study of the developed flow network model was performed to validate the suggested total pressure loss coefficients. The Model House at Hanoi built in Hanoi, Vietnam, was used as a model building for the case study. The cross sections of the building are shown in Figure 4. This building is an apartment house comprising six dwellings; Houses A~F. In this study, Room C3 which are arranged in the center of the apartment were selected for analyses. The plans of the room, and the locations of the openings (3a~3c) are shown in Figure 5.

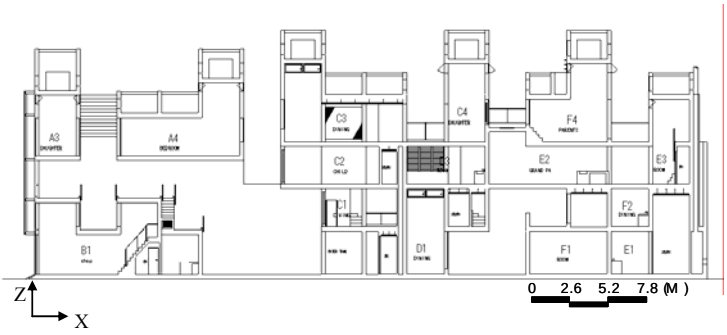

Figure 4. Cross section of the building model

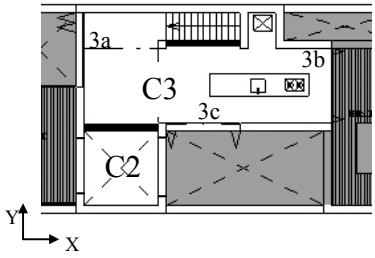

Figure 5. Plan of Room C3

Four flow network model analyses using the suggested total pressure coefficient were performed. The calculation conditions were the same in all cases apart from the opening areas, as shown in Table 1. The values for the pressure coefficients were obtained by one instance of CFD analysis under the opening conditions in Basic Case. (See Appendix A) As the wind pressure for calculating the pressure coefficient, total pressure is assumed on windward openings and the static pressure on the leeward wall around the openings is asuumed on leeward openings, as shown in Figure 6. Then the total pressure loss coefficients were set as suggested in the former sections using the CFD results.

In order to validate the results, CFD analyses were made under the same conditions in each case and the results were compared. The airflow rates analyzed by the developed flow network model and CFD are shown in Table 1. The values estimated by the developed flow network model analyses agree well with those from the CFD analyses. It is considered that the developed flow network analysis could calculate the airflow rate sufficiently well to predict the results using CFD analysis.

Table 1. Comparison of predicting results by developed flow network model and CFD

Room C3	Opening area [m^2]		Airflow rate [m^3/s]		Differential [%]
	3a	3b	Q_{new}	Q_{cfd}	$(Q_{new}-Q_{cfd})/Q_{cfd}\times10^2$
Basic Case	2.0	3.9	-	1.02	-
Case1	1.2	3.9	0.62	0.59	6.5
Case2	2.7		1.38	1.41	-2.1
Case3	2.0	3.1	1.01	1.02	-0.9
Case4		4.7	1.02	1.03	-1.1

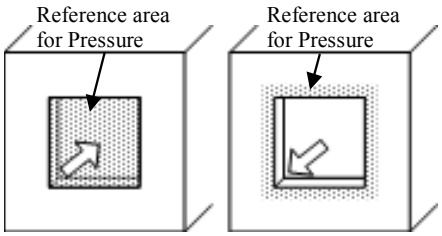

a) windward b) leeward

Figure 6. Reference area for pressure coefficient

CONCLUSION

There is some doubt about the accuracy of the conventional flow network model based on the orifice equation for calculating cross-ventilation properties. CFD analysis is considered the best method of analyzing cross-ventilation properties under present conditions. However, repetition of CFD analysis to determine the optimum ventilation performance is particularly complex. Accordingly, a flow network model that corresponds to cross-ventilation was developed and suggested as a more efficient means of determining the optimal opening conditions. Through the validation of the suggested flow network model, it was concluded that the model could calculate the airflow rate sufficiently well to predict the results by CFD analysis. This might result in reducing the time spent determining the optimal opening conditions; especially the opening sizes.

APPENDIX A

The dimensions of the analyzed area for CFD analysis were: length 241.6 m, width 206.25 m, and height 113.5 m, as shown in Figure 7. The building models were located in the center of the area. The wind directions were from the front of the building models as shown by the arrow in Figure 7. The wind flow was assumed to be incompressible and steady. In the process, the High Reynolds Number Quadratic k-ε model (Shih, T.H. et al. 1993) was employed to solve the governing equation for transport of mass, momentum, energy and other flow parameters, wherein thermal transfer was not taken into consideration in these analyses. The pressure and velocity coupling was achieved by using the Semi-Implicit Method for Pressure Linked Equation (SIMPLE) algorithm. The principle of discretization was obtained by applying the Quadratic Upstream Interpolation for Convection Kinematics (QUICK) scheme to advection terms (scalar and momentum equation), and the second-order central differencing scheme to other terms. The boundary conditions are summarized in Table 2. The mesh has approximately 300,000 grid points.

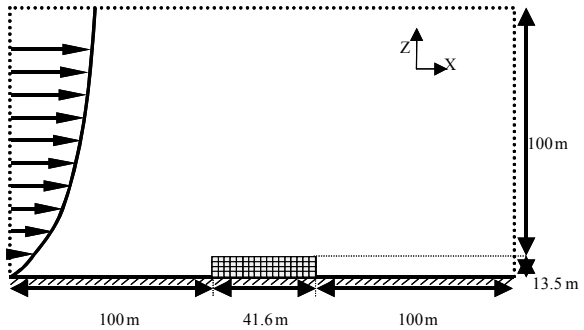

Figure 7. Dimensions of analyzed area

Table 2. Boundary conditions

Inlet	$U(Z)/U_D = (Z/D)^{1/4}, V = 0,\ W = 0, \varepsilon(Z) = C_\mu k(Z)^{3/2}/l(Z),$ $l(Z) = 4(C_\mu k(Z))^{1/2} D^{1/4} Z^{3/4}/U_D, D = 13.5, U_D = 1.0$
Outlet	Mass balanced
Side and upper planes	Symmetrical planes
Ground plane	Generalized log law
Building surface	Generalized log law

Note: k is from experimental data (Murakami et al 1988)

NOMENCLATURE

A	: area of opening [m^2]	C_μ	: constant = 0.09
D	: height of building model [m]	k	: turbulent kinetic energy [m^2/s^2]
L	: length between windward opening and leeward opening [m]	LP	: lost power [W]
l	: turbulence length scale [m]	P	: pressure [Pa]
PW	: rate of energy transport (PW = Pd·Q + Ps·Q) [W]		
U, V, W	: velocity components in the X, Y, Z directions [m/s]	Q	: airflow rate [m^3/s]
ε	: turbulent energy dissipation rate [m^2/s^3]	ρ	: fluid density [kg/m^3]
θ	: angle between windward opening and leeward opening [rad]	ξ	: conventional pressure loss coefficient [-]
ζ	: total pressure loss coefficient [-]		

SUBSCRIPTS

0	: reference value	s	: static pressure
t	: total pressure	*m*	: m^{th} control volume surface
i	: i^{th} windward opening	*j*	: j^{th} leeward opening
new	: result from developed flow network model analysis	cfd	: result from CFD analysis

REFERENCES

Ishihara M (1969), *Kenchiku kanki sekkei*, Asakura, Tokyo, Japan.

Jensen JT, Sandberg M, Heiselberg P, Nielsen PV (2003), "Wind driven cross-flow analyzed as a catchment problem and as a pressure driven flow, *The International Journal of Ventilation*, 1, pp 89-101.

Karava P, Stathopoulos T and Athienitis AK (2004), "Wind driven flow through openings – a review of discharge coefficients", *International Journal of Ventilation*, 3, (3), pp 255-266

Kato S (2004), "Flow network model based on power balance as applied to cross-ventilation", *International Journal of Ventilation*, 2, (4), pp 395-408.

Kurabuthi T, Ohba M, Endo T, Akamine Y and Nakayama F (2004), "Local dynamic similarity model of cross ventilation part1 – theoretical framework", *International Journal of Ventilation*, 2, (4), pp 371-382.

Murakami S, Mochida A and Hayashi Y (1988), "Modification of Production Terms in *k*-ε Model to Remove Overestimation of *k* Value around Windward Corner", *Proceedings of 10th National Symposium on Wind Engineering*, pp199-204, Tokyo, Japan.

Murakami S, Kato S, Akabayashi S, and Mizutani K and Kim YD (1991), "Wind tunnel test on velocity pressure fields of cross ventilation with open windows", *ASHRAE Transactions*, 97, (1), pp 525-538.

Ohba M, Kurabuthi T, Endo T, Akamine Y, Kamata M and Kurahashi A (2004), "Local dynamic similarity model of cross ventilation part2 – application of local dynamic similarity model", *International Journal of Ventilation*, 2, (4), pp 383-393.

Shih T.H.; Zhu J. and Lumley J.L. (1993), "A realizable Reynolds stress algebraic equation model", NASA TM-105993.

Sandberg M (2002), "Airflow through large openings – a catchment problem", *Proceedings of Roomvent 2002*, pp541-548, Copenhagen, Denmark.

Sandberg M (2004), "An alternative view on theory of cross-ventilation", *International Journal of Ventilation*, 2, (4), pp 400-418.

VENTILATION RELATED TO USER HABITS.
Considerations on Environmental Envelope Rehabilitation.

Carolina Ganem[1,2], Helena Coch[1] and Alfredo Esteves[2]

[1]Arquitectura i Energia. ETSAB-UPC, Diagonal 649, 08028. Barcelona (SPAIN)
[2]Laboratorio de Ambiente Humano y Vivienda. LAHV-CRICYT-CONICET,
Av. Ruiz Leal s/n - Parque Gral. San Martín CC. 131, 5500. Mendoza (ARGENTINA)

ABSTRACT

Application of ventilation techniques, as well as the use of any passive environmental solution in a rehabilitation, requires knowledge of the particularities of the **climate** and the specific characteristics of the **building stock**. In a theoretical approach, these two variables would be enough to predict indoor behaviour. Nevertheless, in practice, one third variable needs to be considered, as **user habits** can completely change the equation. This study is referred to a continental dry template climate, particularly to the city of Mendoza (32.88º south latitude, 68.85º west longitude and 827 m.a.s.l. Annual cooling DD (base 23°C): 138 °C day/year, Annual heating DD (base 18°C): 1384 °C day/year). The selection of the studied buildings was based in presenting the most common housing typologies and their envelope characteristics. There were selected three different low density housing typologies. The actual thermal performance of each building was monitored a 20–day period each season. Different hypothetical scenarios were compared in order to understand the influence of ventilation as a passive technique in rehabilitation and the relationship of this strategy with user habits. Conclusions address the possibilities of ventilation as a passive technique in rehabilitation. Criteria of intervention is provided according to user habits.

KEYWORDS
ventilation, building stock, user habits, envelope, rehabilitation

INTRODUCTION

As the rate of replacement of old buildings with new buildings is very slow, the existing building stock in cities will eventually be rehabilitated in order to reach certain desired "up grading" levels of comfort and modernity to create the necessary conditions to put the dwelling back into the market with an economic redevelopment. This modernization, however, usually leads to increased energy needs, which are usually covered by conventional, non renewable, energy resources, with the consequent contribution to the pollution of the city environment and thus, to global warming. (Ganem et al, 2003)

A series of studies carried out world wide over the last decades have shown that the improvement of the environmental behaviour of existing buildings is a key factor for the rationalisation of non-renewable energy consumption in cities. The objective of this paper is to understand the possibilities of ventilation as a passive technique in rehabilitation.

Application of **ventilation techniques**, as well as the use of any passive environmental solution in a rehabilitation, requires knowledge of the particularities of the **climate** and the specific characteristics of the **building stock**. In a theoretical approach, these two variables would be enough to predict indoor behaviour. Nevertheless, in practice, one third variable needs to be considered, as **user habits** can completely change the equation.

CLIMATE

The site's particular climatic characteristics would present advantages and constraints in an intervention. Analysing both, the passive ventilation strategy will begin to take a general shape. This study is referred to a continental dry template climate, particularly to the city of Mendoza (32.88º south latitude, 68.85º west longitude and 827 m.a.s.l. Annual cooling DD (base 23°C): 138 °C day/year, Annual heating DD (base 18°C): 1384 °C day/year).

Figure 1 shows Bio-climatic Chart and Wind characteristics for Mendoza. Temperatures vary from –6ºC in Winter to 37ºC in Summer, with daily swings of about 10 to 20ºC. Our concern for this work is to focus on temperatures that exceed the comfort boundary, where **ventilation** strategies can make a difference to prevent overheating. Ventilation is proposed as a potential strategy to be used in first steps of environmental rehabilitation. Summer maximum temperatures exceed the comfort range. In Autumn and Spring temperatures also may pass this limit. Overheating may happen nine month out of twelve, with the certainty that the three summer months will actually be hot.

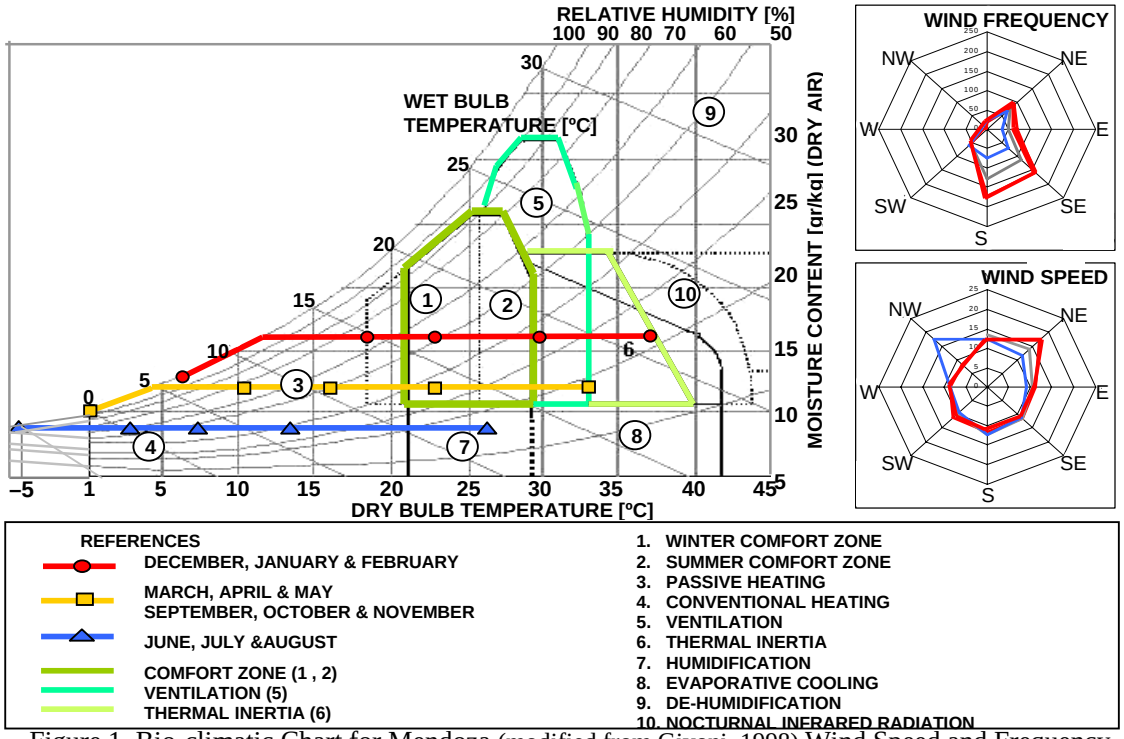

Figure 1. Bio-climatic Chart for Mendoza (modified from Givoni, 1998) Wind Speed and Frequency

According to the Bio-climatic chart, **Ventilation** and **Thermal Inertia** are suggested as adequate passive strategies to regain internal comfort. It is important to know wind's characteristics to analyse how to best profit from this natural resource. As observed in Figure 1, in summer, winds come usually from the **South, South-East** with an speed of 12 km/hour.

There are two ways in which **Ventilation** can improve comfort: One is by a direct effect providing a higher indoor air speed by opening the windows to let the wind in, thus enhancing the cooling sensation of the inhabitants. This strategy is termed **Comfort Ventilation.** The other way is to ventilate the building only at night and thus cool the interior mass of the building. During the following day the cooled mass reduces the rate of indoor temperature rise. This strategy is termed **Nocturnal Ventilative Cooling** (Givoni, 1998) Both strategies will be analysed and criteria of use will be given for environmental rehabilitation.

BUILDING STOCK

The city of Mendoza presents an homogeneous distribution of the density of constructions, with a noticeable preference of inhabitants to live in individual houses. Today, buildings up to 10 meters high conform the 90% of the existent urban tissue. Due to the age distribution of the building stock and economical needs in the city of Mendoza, the demand in the coming years will increasingly reside in the maintenance, rehabilitation and adaptation of the building stock.

The selection of the studied buildings was based in presenting the most common housing **typologies** and their **envelope** characteristics related to ventilation possibilities. There were selected three different low density housing typologies.

(1) 1880 – 1930: Mediterranean Half Patio House

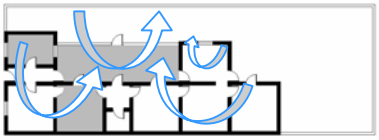

Form/Comp Coeff.[1]	Open / 0.70
Walls Conductance	1.42 W/m^2.K
Roofs Conductance	0.44 W/m^2.K
Average Weight	> 1500 kg/m^3
Openable Surface	15% simple glass
Ventilation Possib.	Within spaces
Envelope Flexibility	High

(2) 1930 – 1945: Modern Movement Rational House

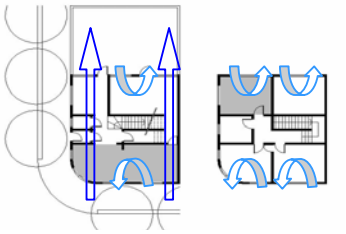

Form/Comp Coeff.[1]	Compact /0.95
Walls Conductance	2.10 W/m^2.K
Roofs Conductance	0.93 W/m^2.K
Average Weight	> 1500 kg/m^3
Openable Surface	20% simple glass
Ventilation Possib.	Crossed/Within [2]
Envelope Flexibility	Low

(3) 1940 – 2000: New-Colonial House

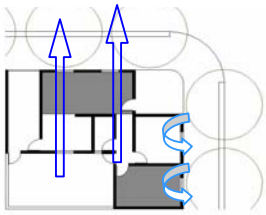

Form/Comp Coeff.[1]	Semi-compact/ 0.85
Walls Conductance	2.10 W/m^2.K
Roofs Conductance	0.52 W/m^2.K
Average Weight	> 1500 kg/m^3
Openable Surface	10% simple glass
Ventilation Possib.	Crossed/Within [2]
Envelope Flexibility	Medium

The actual thermal performance of each building was monitored a 20–day period each season. Data was recorded on a 15 minute basis. Figures 2 to 4 show a selection of 5 days.

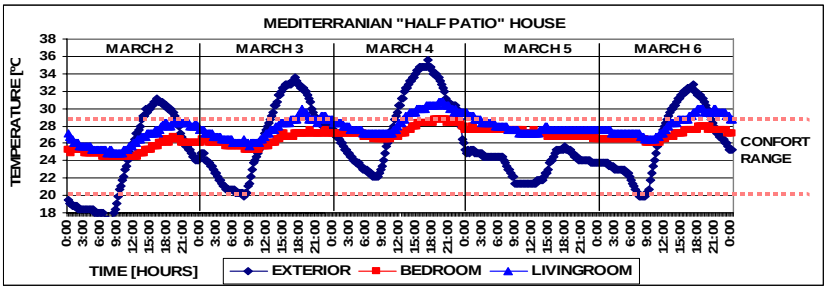

Figure 2. Temperature Measurements. Mediterranean “Half Patio” House.

[1] Compactness Coefficient: from 0 to 1, been 1 the most efficient relationship between envelope and volume. (Serra and Coch, 1991)

[2] Easily crossed in public areas and mostly within each space in private areas of the house.

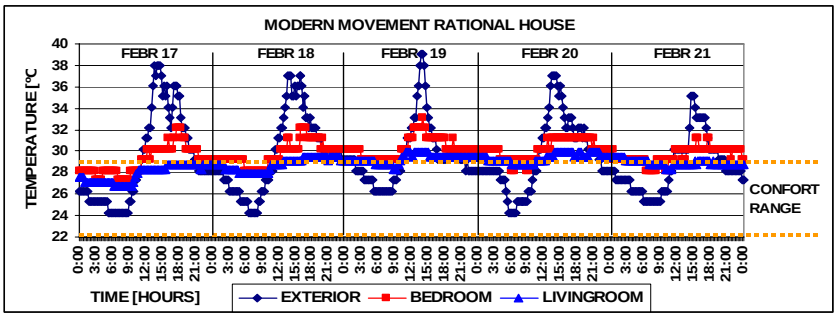

Figure 3. Temperature Measurements. Modern Movement Rational House.

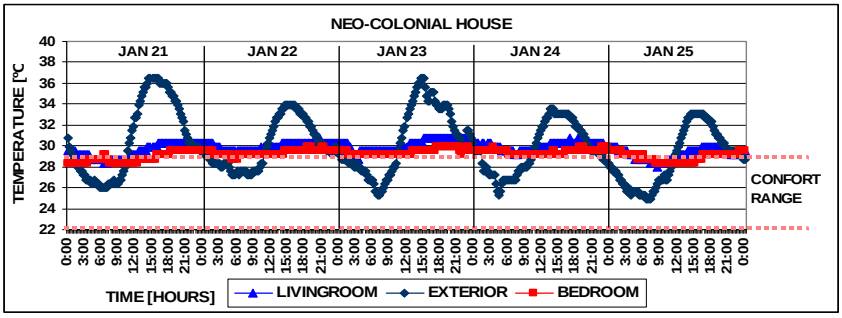

Figure 4. Temperature Measurements. Neo-Colonial House.

USER HABITS

It must be noticed that measurements were performed in inhabited houses. Occupants managed envelope openings as desired and not always leading to reach comfort. From now on, measurement analysis will be regarded from the climate and building point of view adding the user component leading to a holistic comprehension of the phenomena.

Buildings' thermal inertia stand out in a **first** analysis of measurements. The important flattering of the interior temperature curves is accomplished by the high mass that present all typologies. This is a general characteristic of Argentinean construction. However, all inertia flatted curves are not the same, been less variable the Neo-Colonial Chalet typology which presents the smaller percentage (10%) of openable surface. The Modern Movement Rational House with 20% of openable surface reports the highest temperatures in hottest hours of the afternoon. This situation is related to the lack of sun shading in openings and daytime ventilation, resulting in the approach of indoor temperatures to the outdoor situation.

The **Second** observation will be regarding discomfort interior temperatures registered in all typologies on hottest days. Nowadays economic issues prevent the abuse of air conditioning in Argentina. Even though most houses have this type of mechanical equipment, they are not in all rooms and they are on a few hours a day. As discomfort exists in a permanent basis in summer, as soon as people can economically spear the cost, mechanical condition will probably be the solution they would apply to regain comfort increasing pollution and non-renewable energy consumption. The need of a an **environmental** rehabilitation is clear.

Third observation points attention into the fact that there are important differences in day-night exterior temperatures and houses remain 10 to 15ºC above external temperature at night time. There is therefore an opportunity to apply Nocturnal Convective Cooling and show users how a different management of the envelope approaches comfort without added costs and

avoiding pollution. The crucial issue is therefore the prediction of how energy efficient the ventilation strategy will actually be in a rehabilitation. At this point it is important to quantify the potential influence in the lowering of interior temperature of envelope regulation of openings and filters (ventilation). Figure 5 shows temperatures of a Modern Movement Rational House identical to the first one presented in Figure 3, and also measured in the same period of time. It has a completely different temperature behavior because it is instinctively managed by is occupants with the Nocturnal Ventilative Cooling strategy.

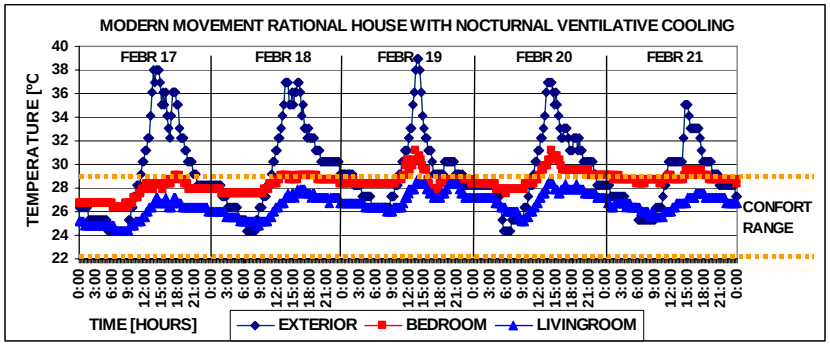

Figure 5. Modern Movement Rational House with Nocturnal Ventilative Cooling.

Even though the bedroom presents some temperatures above comfort, the general situation has improved greatly. Night temperatures in the Living-room reach the minimum exterior measurements. By natural strategies this is the lowest you may go! The private area of the house (bedrooms) is more difficult to cross ventilate due to privacy partitions. The ventilation strategy may be complemented to guaranty comfort even in hottest days of summer.

Potential of successful rehabilitation with ventilation techniques as a first rehabilitation improvement in the hot season has worked very good for the Modern Rational House (Figure 5). In order to quantify the Nocturnal Ventilative Cooling potential of the Mediterranean Half-Patio House and the Neo-Colonial Chalet, simulations were performed with the transitional simulation program SIMEDIF (Flores et al, 2000). Results are shown in Figures 6 and 7.

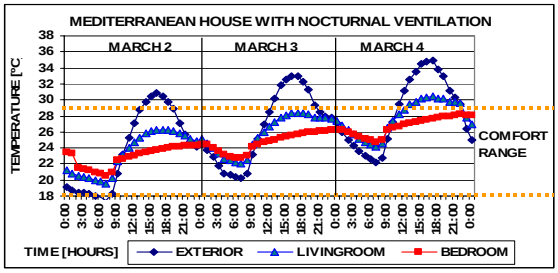

Figure 6. Simulated Mediterranean Half-Patio House with Nocturnal Ventilative Cooling.

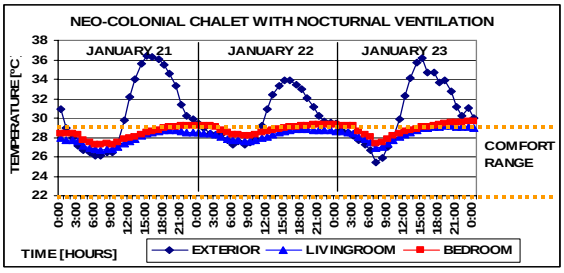

Figure 7. Simulated Neo-Colonial Chalet House with Nocturnal Ventilative Cooling.

Simulations of the Neo-Colonial Chalet (Fig. 7) present the same advantages and constraints that the Rational House (Fig.5), but with less openable area. This difference results in less variable cycles and a more constant temperature. The Mediterranean House presents a different scenario. Without the possibility of cross ventilation, the hottest rooms are the ones with more envelope area exposed to the exterior, in this case the Living-room. An envelope rehabilitation strategy to prevent overheating, probably related to sun shading, is needed as a complement. Nevertheless, internal temperatures lower considerably with the Nocturnal Ventilative Cooling strategy been a very recommendable and cost-effective way to start environmentally ameliorating comfort.

CONSIDERATIONS ON ENVIRONMENTAL ENVELOPE REHABILITATION WITH VENTILATION

- Nocturnal Ventilative Cooling: envelope management

This is the main strategy recommended for climates such as Mendoza's with diurnal temperature swing of more than 15ºC and a high mass building stock. This strategy works best combined with an appropriate insulation and sun shading of the envelope to prevent daytime heat gain that end in overheating. The final performance depends greatly on users'daily habits.

- Comfort (daytime) Ventilation: air movement management

When indoor conditions exceed comfort limits during daytime but temperatures are still lower than the outdoor ones. Air movement with ceiling or wall fans with the maintenance of the house completely closed will upper the limit of the comfort range 2-3ºC from the established one. In Mendoza, usually this may be enough to regain indoor comfort without compromising the rising of temperatures to the point that they could equal the ones registered or to be registered outside by opening the windows.

Daytime ventilation, by opening the house during the day, results in the behaviour of indoor spaces following the outdoor. It is only recommended in Mendoza when, due to an special meteorological situation, the outdoor temperature did not descended during night-time. The building is overheated from the day before and internal and external temperatures are the same. The movement of air gives occupants a psychological perception of coolness. It is important to be aware that temperature will not go bellow outside levels.

CONCLUSIONS

This paper has identified ventilation opportunities as a passive technique in first steps of summer rehabilitation. Choosing appropriately the ventilation type required for each climatic situation, it is possible to improve the interior temperature performance without added costs.

Nocturnal Ventilative Cooling is a very recommendable strategy in the city of Mendoza and similar climates with important day-night temperature swings. By analysing the existent building stock in the particular case of Mendoza, it was demonstrated that this strategy works in all existent typologies, even though each one presents a different potential of cooling by ventilation. Nevertheless, final temperature performance will depend on users' correct envelope management and not on typology .

There were also identified cases where the nocturnal ventilation strategy must be complemented in hottest days in order to maintain comfort during the day. This may be achieved by suitable sun protections and by diurnal air movement by fans.

REFERENCES

FLORES, S. et al. (2000). *SIMEDIF para Windows*. INENCO - UNSA. www.inenco.net.
GANEM, C. and ESTEVES, A. (2003) *A better quality of life through the refurbishment of buildings' façades with glazed balconies.* Proceedings of 20th PLEA Conference, Santiago de Chile.
GIVONI, B. (1998) *Climate considerations in buildings and urban design*. Van Nostrand Reinhold.
SERRA, R and COCH, H. (1991) Arquitectura y Energía Natural. Edicions UPC.

AKNOWLEDGEMENTS

The authors would like to aknowledge Families Racconto, Borruel, Polici and Maglione, that allowed us to perform thermal measurements in their homes within their premises.

VENTILATION SYSTEM QUALITY FOR DWELLINGS: A PRAGMATIC APPROACH

P. Wouters, P. Van den Bossche
Division of Building Physics an Indoor Climate, Belgian Building research Institute (BBRI), B-1342 Limelette, Belgium

ABSTRACT

As a result of the EPB directive, the Flemish government has established a new regulation due as from January 1ste, 2006. This regulation also imposes the presence of minimal ventilation equipment in new buildings. Various Belgian as well as international investigations report a lack of quality of installed ventilation systems, in individual dwellings as well as in utility buildings. Possible problems range from missing inlets, leaking air ducts to inadequate flow rates and acoustical complaints. In order to improve performance and comfort perception, a quality tool is developed, assisting the installers to commission ventilation systems. An inspection list enables to check the conformity of the installation with the requirements imposed by law or design team. These check points can be visual or require measurement of air flow or acoustical performance. The aim is to establish a basic and pragmatic tool to improve customer satisfaction.

A simple tool for energy and comfort assessment in natural ventilation building

Runming Yao[a]*, Koen Steemers[a], Nan Li[b]

[a] *The Martin Centre for Architectural and Urban Studies Department of Architecture University of Cambridge, UK*
[b] *Key laboratory of the Three Gorges Reservoir Region's Eco-Environment, Ministry of Education, The Faculty of Urban Construction and Environmental Engineering Chongqing University, P R China*

Abstract

A simplified coupled thermal and airflow model has been developed. The British Standard natural ventilation calculation method for a single zone has been integrated within a four-node thermal resistance network model. The user friend interface has been developed using Delphi language. The software is suitable for natural ventilation design for summer cooling at the strategic building design stage. The case studies for UK building have been presented in the paper.

Keywords: strategic design, ventilation effectiveness, coupled thermal and air flow, thermal comfort, summer cooling, interface, software

Introduction

This paper develops a simple single zone model for ventilation analytical solutions by integrating an empirical airflow model into a simplified thermal resistance network model. It is usually sufficient for the first-cut calculation and can also perform quick comparisons between different building configurations. This method is useful because it offers a fast, first estimation of airflow rates related to different ventilation configuration of building design. The existing tools that are available require a reasonable degree of user training and good ability to interrupt the results. Thus most architects and designers will not feel very comfortable using them and may even feel distrustful of them. Therefore it is important to develop a simple method for ventilation effectiveness for the early design stage.

Methodology

Thermal and airflow interactions are characteristic of natural ventilation airflow systems. An integrated thermal and air flow model has been developed as a server of this tool.

Interface

The Delphi language is used to develop user friendly interface. The intuitive software leads the building designers to perform natural ventilation design and energy and comfort assessment.

Case Studies

Case studies for UK office buildings have been performed using this tool to demonstrate the usability.

Conclusion

In this paper the authors introduces a tool for energy and comfort assessment of natural ventilation building.

DEVELOPMENT OF DESIGN GUIDELINES FOR TERTIARY SECTOR BUILDINGS EQUIPPED WITH NATURAL VENTILATION SYSTEMS

Geoffrey van Moeseke[1], Isabelle Bruyère, André De Herde

[1]Université Catholique de Louvain – Architecture et Climat – Place du Levant, 1 à 1348 Louvain-la-Neuve, Belgique. Phone : +32 10 47 21 38, fax : +32 10 47 12 50, ref. author email: vanmoeseke@arch.ucl.ac.be

ABSTRACT

This study considers the link between tertiary buildings design and equipments known as natural and hybrid ventilation or cooling. It focuses on the case of cross ventilated buildings and the envelope choices able to ensure comfort along with energy savings. This link is studied by simulating with TRNSYS various cross ventilation systems: by night, day or both. These are applied to typical situations as individual office, open-plan office, or meeting rooms. Studied rooms are chosen south oriented and subjected to medium internal gains. Thermal behaviour of these rooms is analysed and compared when architectural characteristics vary: insulation level, shading strategy, glassed surface and thermal inertia. These results will be used to develop feasibility criteria for low energy cooling and design guidelines for these rooms for both typical year and heat wave. The case of a complementary mechanical cooling is also studied.

KEYWORDS

Natural ventilation, comfort, energy savings, design

INTRODUCTION

Thinking about natural cooling by ventilation can not be done without talking about architecture. Usually building and HVAC design are made by different teams with few interactions. But to determine architecture from energy efficiency point of view may lead to high performance buildings, as illustrated by Breesh et al (2005) and other authors. A promising technique is natural ventilation. But for this one to ensure thermal comfort some architectural choices have to be made. This paper tries to give design guidelines for architects and HVAC designers in order create efficient buildings with natural cooling systems. Four parameters are investigated here: inertia, insulation, glazing surface and shadow devices. Other parameters are important to consider, like internal gains, control modes, orientations, dimming strategies for example. These will be part of further studies.

ENERGY SAVINGS BY NATURAL COOLING

Dynamic simulations were performed on typical tertiary rooms (depicted in table 1) with TRNSYS16 for a typical Belgian year and the measured heat wave of July 1976, depicted in figure 1.

TABLE 1 : Main characteristics of investigated rooms

	Office module	Landscape office (2 opposite facades)	Meeting room
Surface	19.44 m²	142.6 m²	58.3 m²
Facade surface	9.72 m²	64.8 m²	32.4 m²
Infiltration	0.2 air change by hour		
Glazing surface	6.84 m², including 18% for the frame.	45.36 m², including 18% for the frame.	22.68 m², including 18% for the frame.
Orientation	South	North-south	South
Shadow devices	Low-emissive selective glazing. Solar factor=0.42, U=1.23W/M²K		
Mean inertia	200 kg/m²		
Insulation	Façade: U=0.437 W/m²K, other walls are considered adiabatic		
Internal gains	28 W/m²	40 W/m²	46.9 W/m²
Occupation hours	From 8h00 to 18h00, including 3 hours of ½ occupation		

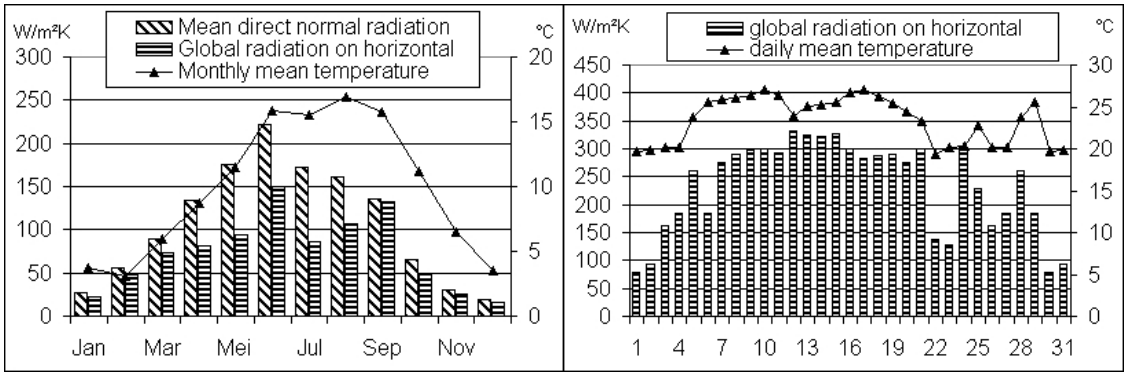

Figure 1 Weather data used for the simulations: a typical Belgian year made of assembled representative month (monthly mean values, left) and the measured heat wave of July 1976 (daily mean values, right)

Investigated outputs are energy demand and thermal comfort. No technological productivity is considered for energy demand. Although Brager et al. (2002) showed adaptative comfort criterions are suited for naturally ventilated rooms, the first steps of this study use a well established among practitioners criterion considering 100 hours above 25.5°C as comfort acceptance limit, as defined by ISSO (1994). Adaptative criterions will be used in parallel in the next steps of this study.

For each office, four systems are modelled: traditional mechanical cooling, and 3 natural ventilation modes (Figure 2). These are defined with constant air flow rate. Such efficient control may be obtained by fan assisted ventilation. For the mechanical case, cooling set point is set to 24°C in winter and spring and 25°C in summer and fall. Heating set point is of 20.5°C with night interruption. Night cooling consists of 8 air changes by hour between 21pm and 5am. Night cooling begins if internal temperature exceeds 22.5°C with an automatic stop if inside temperature falls under 18.5°C. For day cooling, lower inside temperature limit is 21°C. Air change by hour is modulated following outside temperature, from 0.5 ach bellow

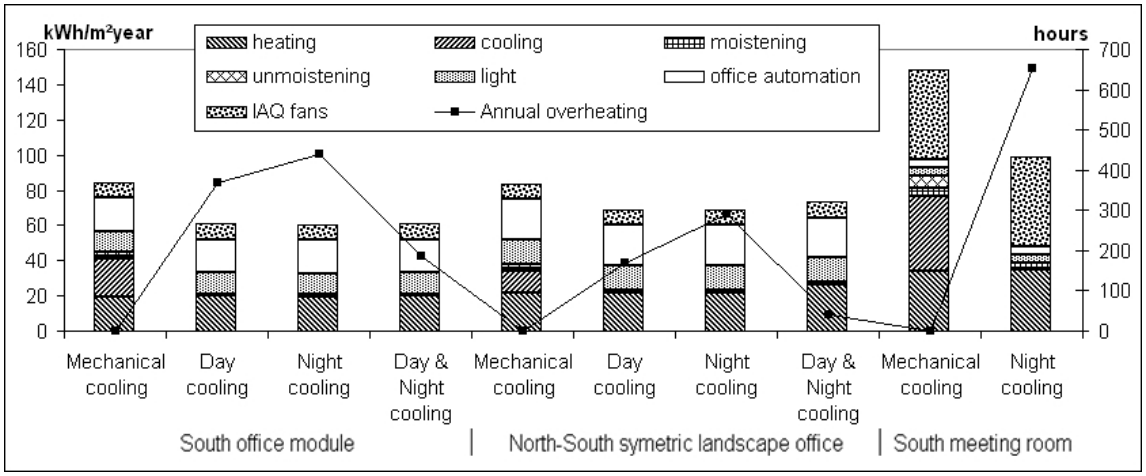

Figure 2 : Energy demand and overheating hours for rooms depicted in table 1. Neither light dimming nor internal gain reduction modelled.

11°C to 3 ach above 15°C. For the meeting room, only night cooling is modelled in addition to mechanical cooling. Indeed, natural day ventilation makes no sense as hygienic ventilation brings already a high air change rate.

Results may seem quite low compared to monitored situations, for example in the HYBVENT state-of-the-art report, Delsante (2002). It can be justified by many favourable management hypotheses. Choice has been made to modelled highly efficient cases. Natural cooling techniques allow important energy savings: 28% in an office module, 13% in a landscape office and 35% in a meeting room, but for the chosen example these seem unable to ensure comfort during a typical year, especially in the meeting room. These poor performances may dissuade designer interested in natural ventilation.

IMPACT OF ARCHITECTURAL CHOICES ON COMFORT

By modifying building design choices like insulation, inertia, glazing surface and shading, it is possible to reach a satisfactory comfort level, both with larger energy savings. But some building design choices may also make things worst. Choices presented in figure 3 varies from the best (40% glazing surface with g=0.82 blinds, high insulation, high inertia: 375kg/m² for office module and 430kg/m² for the meeting room) to the worst (100% glazing without shading, low inertia and low insulation: Uwall=1.46W/m²K and 0.5ach infiltration rate) from the energy point of view. Results for the office module shows good insulation allows lower energy demand. Comfort level of maximum100 hours can not be reached without shading, whatever the glazing surface. Blinds always give sufficient comfort. Chosen management is closing when irradiation exceeds 250W/m² simultaneously with internal temperature above 23°C. Selective glazing may or not be efficient following other choices. Also low inertia is not favourable for comfort.

Comfort criterion is always met in the landscape office because solar gains are relatively smaller (higher floor area for the same façade) and thanks to the north façade losses. Design parameters nevertheless bring to different energy demands. In a meeting room, high internal

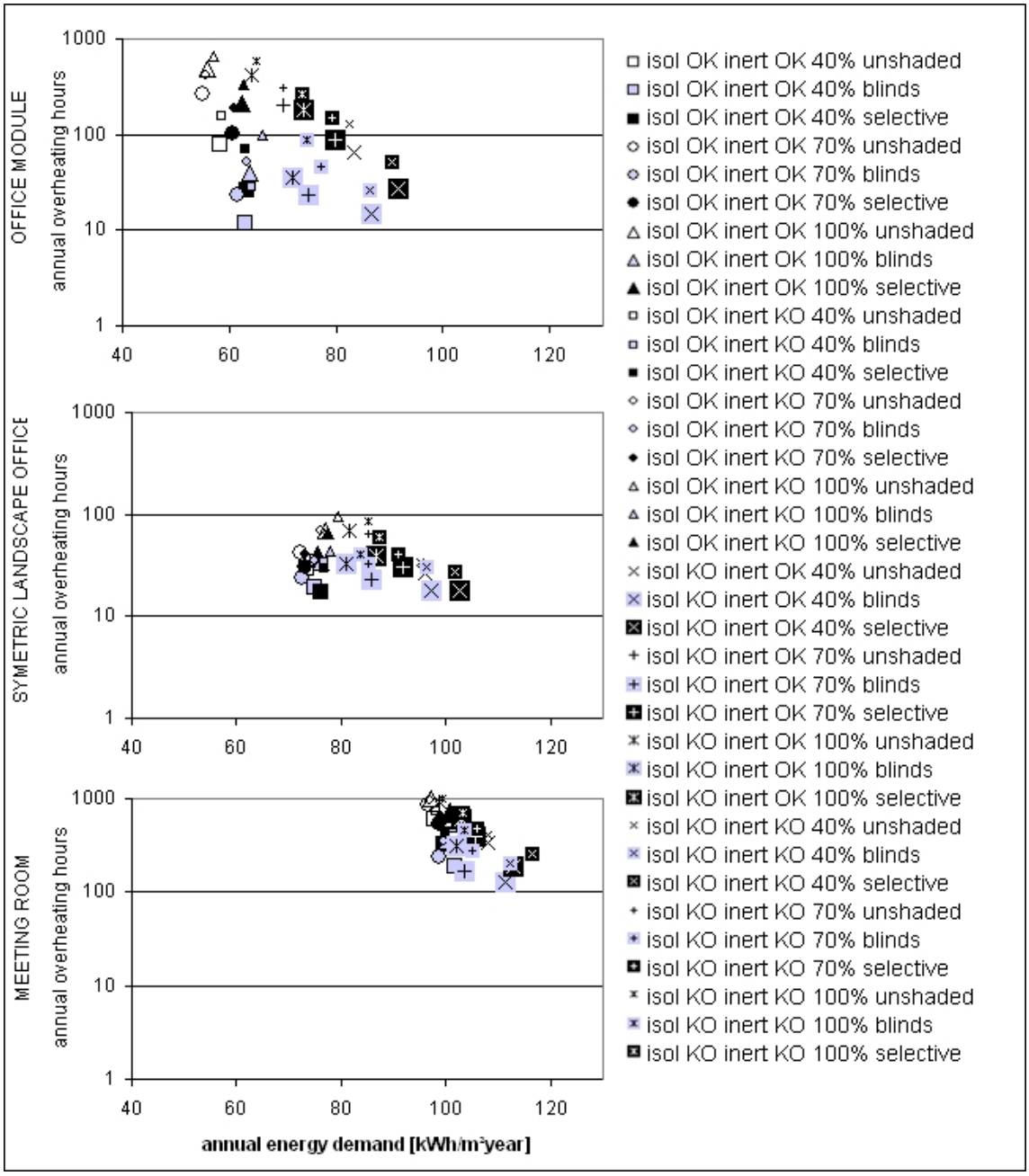

Figure 3 Impact of architectural choices on overheating hours and energy demand for an office module, a landscape office and a meeting room, day and night natural ventilation

gains always make overheating too large.

Considering a heat wave, comfort is more difficult to reach. Figure 4 shows internal temperatures for two cases considered comfortable for a typical year. The optimal solution maintains comfort conditions without mechanical cooling, internal temperature being around 5°C lower than outside. But replacing a 40% glazing surface with blinds by a 70% selective glazing leads to too high internal temperatures during day, even with an efficient night cooling. Internal temperature may even rise above outside temperature because of inadequate shadow device. It shows natural cooling may ensure thermal comfort, even for a heat wave, but all architectural choices must be considered with this objective in mind.

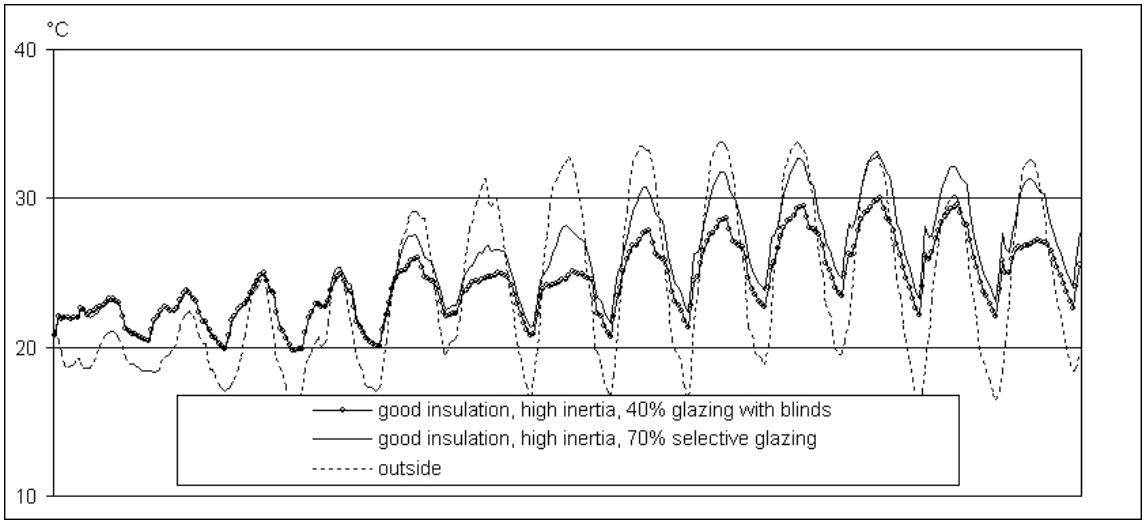

Figure 4 Internal temperature for a high and a medium energy efficiency design during a heat wave. Simulated case: south oriented office module with 0.2 ach infiltration rate, 28W/m² internal gains

HYBRID COOLING

When architectural choices are so that natural cooling is insufficient to create satisfactory indoor conditions, a mechanical device may be installed to give a complementary cooling. Figure 5 illustrates energy saving reached with natural cooling when mechanical cooling maintains a 25°C set point.

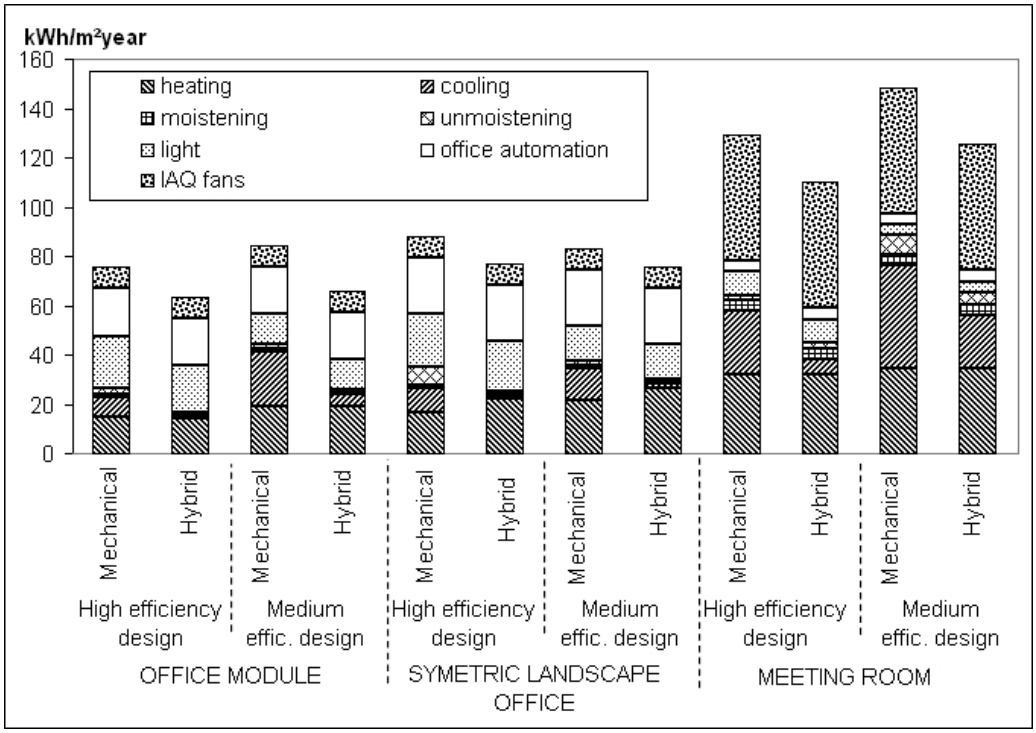

Figure 5 Energy demand for an office module, a landscape office and a meeting room. Impact of natural ventilation used in combination with mechanical cooling. High efficiency: 40% blinded glazing, high inertia and high insulation. Medium efficiency: 70% selective glazing, high insulation and medium inertia

Combination of mechanical and natural cooling allows substantial energy savings in the modelled situations: 16 to 22% for an office module, 10 to 13% for a landscape office and 15% in a meeting room. Complementary mechanical cooling is not very energy costing. The only arguments against it are investment cost and the risk of too large use of the mechanical cooling once it is installed.

Savings are only a few smaller than without mechanical cooling in the case of office modules or landscape offices. For the meeting room, reduction in savings is larger but natural ventilation used alone was never capable to ensure thermal comfort.

CONCLUSIONS

This paper shows free cooling strategies have to be considered both with architectural choices. Best performances are reached when efficient natural cooling is managed in massive, well insulated and efficiently shaded buildings. All parameters must be met to reach comfort in a heat wave. If not possible, as for retrofitting cases, a complementary mechanical cooling can be added. Free cooling is then still very useful, allowing large energy savings.

AKNOWLEDGEMENT

This research was made possible by contribution from the Institut Bruxellois pour la Gestion de l'Environnement. The authors gratefully acknowledge their support of this project.

BIBLIOGRAPHY

Brager, G.S., De Dear, R.J. (2002). Thermal adaptation in the built environment: a literature review. *Energy and Buildings* **27**, 83-96

Breesch, H., Bossaer, A., Janssens, A. (2005). Passive cooling in a low-energy office building. To be published in *Solar Energy*

Delsante, A, Vik, T.A. (2002). *Hybrid ventilation: State of the art review*, IEA Annex 35

ISSO (1994). *Energie-efficiënte kantoorgebouwen: binnenklimaat en energiegebruik*. SBR publicatie 300, Rotterdam

PERFORMANCE PREDICTION OF DWELLING VENTILATION WITH SELF-REGULATING AIR INLETS

L. Willems, A. Janssens

Department of Architecture and Urban Planning,
Faculty of Engineering, Ghent University
J. Plateaustraat 22, B-9000, Belgium
Tel. 09/264.37.49, Fax 09/264.41.85, e-mail: Lieven.Willems@ugent.be

ABSTRACT

This paper presents simulation results of the performance of ventilation systems with self-regulating inlets in different types of typical Flemish dwellings. Normal free air inlet vents have one major disadvantage: the complete dependence on the variable outside weather conditions (wind and temperature). The use of *self-regulating inlets* should minimize this impact, optimize the indoor comfort (no draught) and reduce the waste of energy by ventilation.
The multizone infiltration and ventilation simulation model COMIS has been used to investigate the impact of the use of self-regulating inlets. Different types of self-regulating inlets, corresponding to the different classes of inlets as mentioned in the new Flemish *Energy Performance Regulation* have been implemented in the ventilation model of different types of dwelling.
The paper presents the model premises and discusses the results of the simulations. To assess ventilation performance, the infiltration and ventilation flow rates, the *indoor air quality* and the reduction of *ventilation heat loss* by the use of self-regulating inlet vents are predicted and compared for the various types of inlets.

KEYWORDS

Self-regulating inlet, ventilation heat loss, Energy Performance Regulation, indoor air quality

INTRODUCTION

This research is part of the research project 'EL²EP residential buildings' that aims at developing a methodology for a global optimization of residential buildings with an extremely low energy consumption and pollution level. The methodology looks for as well an economic, energetical and ecological optimum. These optima must also guarantee a good performance in relation to comfort, health, functionality and durability.
The optimization of the ventilation system takes up an important place in this research. Ventilation and infiltration heat loss is one of the major energy waists in a building. Otherwise is good ventilation primordial to guarantee a good indoor air quality. Free air inlets or 'trickle vents' are one of the possible ways to supply fresh outside air in dwellings. Normal inlet vents have one major disadvantage: the complete dependence on the variable outside weather conditions (wind and temperature). The purpose of self-regulating inlets is to minimize this impact and ideally deliver an almost constant fresh air supply indoors. The use of these self-regulating inlets should thus optimize indoor comfort (no draught) and should minimize the waste of energy by ventilation. This research evaluates the impact of the use of these self-regulating inlets regarding the energy savings and the indoor air quality. This is done with simulations on two typically Flemish building types.

CASE STUDY HOUSES

This research focuses on two of the moist common Flemish dwelling types: the multiple-storied detached house and the row house (35 % and 31 % of total Flemish housing stock). For reasons of equivalence each dwelling type has the same quantities volumes (= 450 m³), surfaces of room and have common properties (inclined roof, open kitchen).

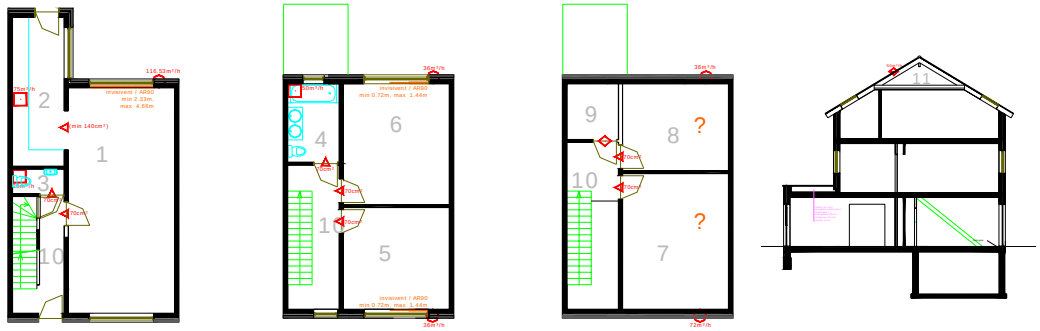

FIGURE 1: Dwelling types

TABLE 1
test values for the air-tightness of dwellings

n_{50} (1/h)	Leakage air change rate for a pressure difference of 50 Pa
5.3 / 9.5	Average air-tightness of new Flemish row house / freestanding house (BBRI 1998).
3	Minimal air-tightness for house with balanced mechanical ventilation (NBN D 50-001)
1	Minimal air-tightness balanced mechanical ventilation with heat recovery (NBN D 50-001)
0.6	Minimal air-tightness for passive house standard

The air-tightness of a building has a great impact on the ventilation performance of a building. Therefore the investigation is done at four different levels for each dwelling type.
Climatic data is taken from the Test Reference Year Ukkel, witch gives hourly information about outdoor temperature, wind velocity and wind direction. The row house is implanted in a city landscape (wind velocity profile exponent $\alpha = 0{,}35$). The detached house is situated in the flat open country ($\alpha = 0.20$).To deal with a realistic use of the house, both houses are occupied by a four-headed family (two adults and two adolescents) and an indoor temperature schedule determine an optimal day and night temperature for each room.

VENTILATION MODEL AND SYSTEM

The ventilation of the dwellings is investigated with COMIS. This multizone infiltration and ventilation simulation model predicts the airflows in and trough the building, taking in account several intern and extern conditions.

The implemented ventilation system is designed with the Belgian Ventilation Standard (NBN D 50-001). This Standard stipulates that every normal room should receive enough (fresh) air as figured in TABLE 3. To create a almost permanent airflow the supply of the fresh air should take place in the dry rooms (living room, bedrooms, study) and the exhaust of the vitiated air in the humid rooms (kitchen, bathroom, toilet, washroom). Transfer between dry and humid rooms occurs through ventilation registers or gaps under the doors of the intervening rooms (hall) between the dry and the humid rooms.

TABLE 2
required airflow rates according to the Belgian Ventilation Standard and Flemish EPR

Required airflow rates according to the Belgian ventilation standard NBN D 50-001 (1991) and flemish EPR*		NBN D 50-001				ROW HOUSE		DETACHED HOUSE	
		type of ventilation requirement	basic require-ment airflow	min	max	floor aera of room	nominal air-flow rate	floor aera of room	nominal air-flow rate
Type of room	ROOM		m^3/hm^2	m^3/h	m^3/h	m^2	m^3/h	m^2	m^3/h
dry rooms	living room	inlets	3.6	75.	150.	32.37	116.53	35.67	128.41
	bedroom 1		3.6	25.	72*	14.59	52.51	16.97	61.07
	bedroom 2		3.6	25.	72*	17.36	62.48	18.23	65.62
	bedroom 3		3.6	25.	72*	19.46	70.06	18.27	65.78
	study		3.6	25.	72*	12.48	44.93	8.04	28.93
humid rooms	open kitchen in livingroom	exhausts	3.6	75.	150.	10.42	75.	10.24	75.
	toilet		3.6	25.	25.	1.71	25.	1.68	25.
	bathroom		3.6	50.	75.	5.48	50.	8.04	50.
	washroom		3.6	50.	75.	3.9	50.	7.68	50.
intervening rooms	hall					29.91		28.53	
	all transfer openings			25.			25.		25.

SELF-REGULATING INLETS

Free air inlets or 'trickle vents' are one of the possible ways to supply fresh outside air in the dry rooms of the dwellings. Most common they are integrated in the upper part of the windows. Wind pressure and temperature differences between in- and outside create a pressure difference over the inlet witch causes an airflow through the inlet.

$$Q = C_q \Delta P^n \quad \text{(eqn. 1)}$$

The power law (eqn. 1) expresses the dependency of the airflow Q (m^3/s) from the pressure difference ΔP (Pa). The flow exponent n express the type of flow: values from 0.5 (turbulent) till 1 (laminar). The mass flow coefficient C_q ($m^3/s.Pa$) is related with the size of the opening and the density of the air flowing through the opening.
This means that sometimes the naturally created pressure difference is so low that the supply of fresh air in a room is insufficient. At other times the supply of fresh air is much higher than necessary for an acceptable indoor air quality. Self-regulating inlets minimize this impact and ideally deliver an almost constant fresh air supply indoors, independent of the pressure difference across the inlet. A self-regulating inlet will reduce the section through witch the incoming airflow at increasing pressure differences. Theoretically the mass flow coefficient C_q will thus decrease at high pressures. Most of the existing self-regulating inlets create this effect by a flap witch is, due to the pressure of the airflow pushed or rotated in front of the opening and so reducing this opening.

FLEMISH ENERGY PERFORMANCE REGULATION (EPR)

From January 2006 the new Flemish Energy Performance Regulation (EPR) will come operative. The imposed minimal thermal isolation requirements and the maximal E-value (representing the primary energy consumption) tries to minimize the energy consumption of the building and their installations. The included ventilation requirements guaranty a good indoor air quality. The ventilation requirements of the EPR oblige to apply the Belgian ventilation standard NBN D 50-001 (1991).
Using self-regulating inlets reduces the E-value of the building. To calculate the E-value of a building and its installations, the average infiltration and exfiltration airflow $\dot{V}_{in/exfil,heat}$ and the average dedicated ventilation airflow $\dot{V}_{dedic}$ (through inlets and exhaust openings) have to be determined. If we only take in account variable air-tightness and self-regulating inlets, EPR propose the following (simplified) formulas:

$$\dot{V}_{in/exfil,heat} = 0{,}04 * n_{50} * V_{EPW} \qquad \text{(Eqn. 2)}$$

$$\dot{V}_{dedic} = \left[0{,}2 + 0{,}5 * EXP(-V_{EPW}/500)\right] * V_{EPW} * \left[1 + 0{,}5\left(\frac{r_{nat.\sup} + 0{,}2 + 0{,}025}{0{,}425}\right)\right] \qquad \text{(Eqn. 3)}$$

TABLE 3
Classification of self-regulating performances of inlet in function of the pressure difference

pressure difference P (Pa)	Airflow relatively to the nominal air flow q_N at 2 Pa								
	Class P0	**Class P1**		**Class P2**		**Class P3**		**Class P4**	
0 Pa ≤ P ≤ 2 Pa		≥ 0.8√(P/2)	≤ 1.2 q_N	≥ 0.8√(P/2)	≤ 1.2 q_N	≥ 0.8√(P/2)	≤ 1.2 q_N	≥ 0.8√(P/2)	≤ 1.2 q_N
2 Pa	q_N	q_N		q_N		q_N		q_N	
2 Pa ≤ P ≤ 5 Pa		≥ 0.8 qN	≤ 1.8 q_N	≥ 0.8 qN	≤ 1.8 q_N	≥ 0.8 qN	≤ 1.5 q_N	≥ 0.8 qN	≤ 1.2 q_N
5 Pa ≤ P ≤ 10 Pa		≥ 0.7 qN	≤ 2.3 q_N	≥ 0.7 qN	≤ 2 q_N	≥ 0.7 qN	≤ 1.5 q_N	≥ 0.8 qN	≤ 1.2 q_N
10 Pa ≤ P ≤ 25 Pa		≥ 0.5 qN	≤ 3 q_N	≥ 0.5 qN	≤ 2 q_N	≥ 0.5 qN	≤ 1.5 q_N	≥ 0.8 qN	≤ 1.2 q_N
25 Pa ≤ P ≤ 50 Pa		≥ 0.3 qN	≤ 3 q_N	≥ 0.3 qN	≤ 2 q_N	≥ 0.3 qN	≤ 1.5 q_N	≥ 0.3 qN	≤ 1.5 q_N
50 Pa ≤ P ≤ 100 Pa		/	≤ 3 q_N	/	≤ 2 q_N	/	≤ 2 q_N	/	≤ 2 q_N
100 Pa ≤ P ≤ 200 Pa		/	≤ 4 q_N	/	≤ 3 q_N	/	≤ 3 q_N	/	≤ 3 q_N
correction factor $r_{nat.sup}$	**0.2**	**0.18**		**0.14**		**0.08**		**0.02**	

TABLE 4
average infiltration and ventilation airflow of row house $\dot{V}_{in/exfil,heat} + \dot{V}_{dedic}$,

air-tightness n50 (1/h)	**Class P0**	**Class P1**		**Class P2**		**Class P3**		**Class P4**	
	V_{P0}	V_{P1}	V_{P1}/V_{P0}	V_{P2}	V_{P2}/V_{P0}	V_{P3}	V_{P3}/V_{P0}	V_{P4}	V_{P4}/V_{P0}
5.3	300.3	296.7	*99%*	289.5	*96%*	278.7	*93%*	267.9	*89%*
3	269.5	265.9	*99%*	258.7	*96%*	247.9	*92%*	237.1	*88%*
1	242.6	239.0	*99%*	231.8	*96%*	221.1	*91%*	210.3	*87%*
0.6	237.3	233.7	*98%*	226.5	*95%*	215.7	*91%*	204.9	*86%*

The V_{EPW} is the volume of all the rooms witch are thermally isolated from the exterior. To determine the correction factor of the energy saving qualities of the self-regulating inlets $r_{nat.sup}$, the inlets are divided in 5 different classes: P0 (not self-regulating) up to P4 (good self-regulating), see TABLE 3.
TABLE 4 presents the calculated $\dot{V}_{in/exfil,heat} + \dot{V}_{dedic}$. According to the EPR the use of good selfregulating inlets (P4) should be able to decrease the infiltration and ventilation airflow with 11 to 14 % depending of the air-tightness of the building.

SIMULATION RESULTS

In the different test house models we have implemented theoretical self-regulating inlets of each class. These inlet models react as follow: from 0 up to the upper pressure difference limit

for each inlet class, the airflow rate through the inlet follows the power law. The upper pressure difference limit is taken at the range of 2 up to 5 Pa. At higher pressure differences the airflow rate remains constant. For example an inlet of class P2 with a nominal airflow rate (at 2 Pa) of 100 m³/h will follow the power law up to 180 m³/h (= 1.8 * q_N). This will be at a pressure difference of 6.48 Pa. At higher pressure differences the airflow rate remains constant at 180 m³/h.
The *total airflow rate* (infiltration and ventilation) is calculated with COMIS for the different classes of inlets and for the different air-tightness values. The absolute results and the results relative to non self-regulating inlets is given in table 5.

TABLE 5
average infiltration and ventilation airflow rate of row house and detached house

air-tightness n50 (1/h)	Class P0	Class P1		Class P2		Class P3		Class P4		
	V_{P0} (m³/h)	V_{P1} (m³/h)	V_{P1}/V_{P0}	V_{P2} (m³/h)	V_{P2}/V_{P0}	V_{P3} (m³/h)	V_{P3}/V_{P0}	V_{P4} (m³/h)	V_{P4}/V_{P0}	
5.3	345	345	99.9%	345	99.9%	345	99.7%	343	99.3%	ROW HOUSE
3	282	281	99.9%	281	99.9%	281	99.7%	279	99.1%	
1	224	224	99.9%	224	99.9%	223	99.5%	221	98.6%	
0.6	212	212	99.9%	212	99.9%	211	99.5%	208	98.4%	
5.3	370	367	99.2%	367	99.2%	365	98.5%	359	97.2%	DETACHED HOUSE
3	303	299	98.9%	299	98.9%	296	98.0%	291	96.1%	
1	239	235	98.4%	235	98.4%	232	97.0%	226	94.6%	
0.6	225	221	98.2%	221	98.2%	218	96.8%	212	94.2%	

The main total airflow rate decreases almost 1 % for the row house and 3 to 6 % for the detached house by using the best self-regulating inlets. Comparing with the results of EPR, the gains are in these two cases a bit overestimated in the EPR.
To have an idea of the *energy loss* by ventilation we approximate the ventilation heat loss (or the enthalpy) for a whole heating season with the following formula:

$$E = \sum_{i=1}^{hoursofheatingseason} 3600 \rho c_p Q_i \left(T_{\mathrm{int}(i)} - T_{ext(i)}\right) \qquad \text{(J)} \quad \text{(eqn. 4)}$$

The total air infiltration and ventilation rate at hour i Q (m³/s) will have to be heated from outside temperature $T_{ext(i)}$ (K) to the indoor temperature $T_{int(i)}$ (K). When we neglect the moisture, the sensible heat (enthalpy) can be calculated when we know the air density ρ (kg/m³) and the specific heat of dry air c_p (J/kg.K). By placing self-regulating inlets, the energy demand is reduced with about 1% in the row house and 2.3 to 4.8 % in the detached house. The absolute impact of placing self-regulating inlets is greater in air-tight dwellings but nevertheless the energy impact of increasing the air-tightness of a house is much greater than the impact of placing self-regulating inlets.

TABLE 6
energy impact of ventilation and air infiltration

air-tightness n50 (1/h)	ROW HOUSE				DETACHED HOUSE			
	Class P0	Class P4	ΔE	ΔE	Class P0	Class P4	ΔE	ΔE
	E_{P0} (kWh)	E_{P4} (kWh)	E_{P0}-E_{P4} (kWh)	E_{P4}/E_{P0}	E_{P0} (kWh)	E_{P4} (kWh)	E_{P0}-E_{P4} (kWh)	E_{P4}/E_{P0}
5.3	6240	6197	42	0.7%	6684	6528	156	2.3%
3	5144	5100	44	0.9%	5537	5358	179	3.2%
1	4135	4078	57	1.4%	4434	4238	196	4.4%
0.6	3921	3859	62	1.6%	4194	3994	200	4.8%

The impact of self-regulating inlets on the *indoor air quality* is evaluated with the European Standard EN 13779. Although the scope of this Standard is not the naturally ventilated residential buildings, the mentioned classification of the indoor air quality (IDA classification) is useful to compare the different situations. To evaluate the indoor air quality, the percentage of time with at least a moderate indoor air quality (IDA 3 or better) is calculated. To have at least IDA 3 the CO2-concentration in the room must be lower than 1000 ppm above the outdoor concentration level.

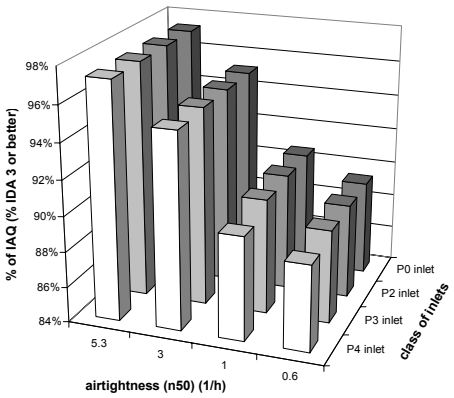

Figure 2: time % of IDA 3 or better for the row house

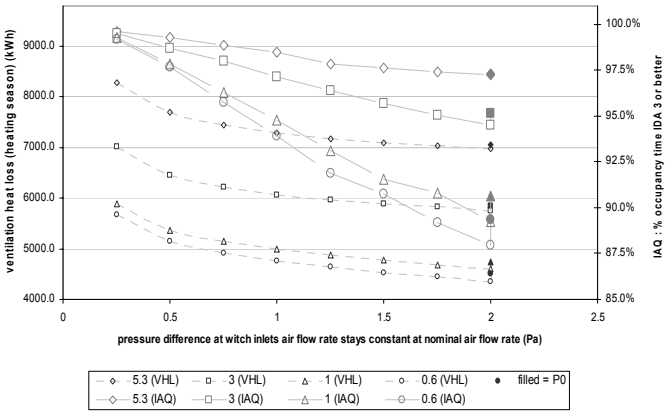

Figure 3: ventilation heat loss (VHL) and Indoor Air Quality (IAQ) with varying self-regulating startpoints (0.25 Pa -> 2 Pa)

Figure 2 shows that the use of self-regulating inlets on the indoor air quality is almost nihil (< 0.8 %). The influence of self-regulating inlets on the indoor air quality takes place at moments that the indoor air quality is already good (the low CO_2-concentrations become a bit higher).
When the *pressure difference starting point for self-regulating* is situated between 0 en 2 Pa we observe some quiet remarkable phenomena (figure 3). The lower the pressure difference starting point the higher the airflow rates, the better the IAQ, but also the higher the ventilation heat loss. The use of '1,75Pa'-inlet gives the *same* ventilation heat loss than non self-regulating inlets (P0). The '0,25Pa-inlet' will have 18 % (n_{50} = 5,3 h^{-1}) to 28 % (n_{50} = 0,6 h^{-1}) *more* ventilation heat loss than with non self-regulating inlets.
In reality the self-regulating starting point is more a range of pressure differences in witch the inlet evaluate to an almost constant airflow. To evaluate the effect of the self-regulating inlet on the ventilation heat loss the complete airflow rate path must be known, certainly in the range from 0 to 2 Pa. At this moment this information is rarely available for the available inlets. A second important problem is the different design regulations of ventilation. Installing a good Dutch inlet (with a design nominal airflow rate at *1 Pa*) in a building designed with the Belgium Ventilation Standard gives more or less a similar effect as the ideal '1Pa'-inlet from our previous simulation. This means 6 % more ventilation heat loss than with normal non self-regulating inlets.

CONCLUSION

Self-regulating inlets can have a positive impact on the ventilation heat loss, but the influence predicted in the EPR occurs to be overestimated in the tests. A expert choice of self-regulating inlets and a good ventilation system design is primordial for a good performance.

REFERENCES

Belgian Building Research Institute (BBRI) and Wenk Sint-Lukas Gent. (1998). *SENVIVV: Studie van de Energieaspecten van Nieuwbouwwoningen in Vlaanderen: Isolatie, Ventilatie, Verwarming. Eindverslag.* Project 930.256/WTCB, Brussels.

BIN. (1991). *Ventilatievoorzieningen in woongebouwen*, Belgian Institute for Standardisation, NBN D 50-001, Brussels.

CEN. (2004), *Ventilation for non-residential buildings –Performance requirements for ventilation and room-conditioning systems*, EN 13779, European Committee for Standardization (CEN), Brussels

De Gids W.F. (1997), Controlled air flow inlets. *Air Infiltration and Ventilation Centre, Proceedings of "Ventilation and Cooling", 18th Annual Conference*, Athens, Greece, 23-26 September 1997, **Volume 1**, pp 245-256.

Liddament, M.W. (1996), *A Guide to Energy Efficiënt Ventilation,* Air Infiltration and Ventilation Centre, Coventry, Great Britain.

Maeyens, J. & Janssens, A. (2003). Air exchange rates, energy losses and indoor air quality duet o the application of the Belgian ventilation standard. *Proceedings of the 2nd International conference on research in building physics,* Belgian, Leuven, 14-18 September.

Maeyens, J. & Janssens, A. (2003a). Impact of residential natural ventilation and air-tightness techniques on the energy loss and indoor air quality. *proceedings of the 24th AIVC conference & BETEC conference - Ventilation, Humidity control and energy*, pp 289-294.

PREDICTION OF BUOYANCY-INDUCED PRESSURE DIFFERENCE ACROSS EXTERIOR WALLS OF HIGH-RISE RESIDENTIAL BUILDINGS

Jae-Hun Jo[1], Sung-Han Koo[1], Jong-In Lee[2], Hoi-Soo Seo[3]
Myoung-Souk Yeo[1], Kwang-Woo Kim[1]

[1] *Department of Architecture, College of Engineering, Seoul National University, San 56-1, Shillim-dong, Kwanak-gu, Seoul 151-744, South Korea*

[2]*POSCO E&C Technical Research Institute, 79-5, Youngchon-ri, Dongtan-myun, Hwasung-shi, Gyunggi-do 445-810, South Korea*

[3]*POSCO E&C Architecture Division, 227-7, Jayang-dong, Kwangjin-gu, Seoul 143-190, South Korea*

ABSTRACT

It is very important to estimate the stack pressure difference across exterior walls for understanding the energy impacts of infiltration and ventilation in high-rise buildings, because stack pressure is likely to significantly affect energy load and is sustained over a long period. This paper presents a simple prediction strategy for estimating the pressure distribution in high-rise residential buildings, using key parameters that affect the magnitude and distribution of stack pressure. The strategy is composed of two procedures: first, the stack pressure is predicted from parameters such as the height of the elevator shaft, the location of the neutral pressure level for each shaft, and the interior temperature of each shaft. Then, the pressure distribution of each floor is calculated using the equivalent leakage areas of the exterior and interior walls, by which finally the pressure difference across the exterior walls can be estimated. To verify the feasibility of this strategy, the predicted pressure differences across exterior walls were compared to measured data of a high-rise residential building with multiple elevator zoning. The results show that this strategy can predict pressure distribution quickly with satisfactory results for both the architectural designer and HVAC engineer.

KEYWORDS

Stack effect, Pressure distribution, Residential building, High-rise

INTRODUCTION

Numerous high-class residential buildings of over 30 stories are being planned in Korea, and problems due to stack pressure differences are becoming an issue. It is crucial that the pressure differences across exterior walls be considered in these buildings, as they affect the heating load from infiltration and adequate ventilation planning. Stack pressure differences have been used often as a major variable in previous infiltration calculation models (Liddament 1986, Lyberg 1997), though they are limited in the case of low-rise buildings. The use of network models such as COMIS (Feustel 1990) and CONTAMW (Dols et al. 2002) is effective, but it requires accurate data for many airtightness variables and may only be employed by a few number of experts. Based on the observation results from field measurements and simulations (Jo 2005), this paper presents a simple prediction strategy for

pressure distribution that may be used to quickly predict buoyancy-induced pressure differences in the early design stages for heating load calculations and ventilation planning.

SIMPLIFIED PREDICTION APPROACH

To predict the buoyancy-induced pressure distribution for a building, the magnitude of the total pressure difference over the entire building must first be determined, and then the proportion of pressure differences across the exterior wall and interior separations must be calculated. Since high-rise buildings have various vertical airflow routes and complicated interior floor plans, this study adopts the following simplifications.

Simplifications in Wind and Equipment Effects

Generally, wind pressure affects the airflow routes in the case of high-rise buildings. However, the effect of wind pressures is instantaneous, unlike stack pressure which is sustained over a long period. Sometimes, the effect of wind pressure is combined with the effect of stack pressures in a procedure called superposition (e. g., Walker 1993). This study focuses on stack pressure during the winter season when indoor-outdoor temperature differences are great, and excludes the effect of wind pressure. In high-rise buildings in Korea, the each residential unit has a separate heat recovery ventilator on the grounds that the exterior walls are airtight, and a minimal amount of ventilation is supplied to the indoor corridor zones to provide a balanced pressure. Therefore, this study excludes the effect of ventilation equipment.

Simplifications in the Shape of the Building

Simplification in vertical shafts

The vertical airflow routes in a high-rise building consist of elevator shafts, stairwells, and various mechanical shafts. As shown in the field measurements and airflow simulations of previous studies (Jo 2005), the main vertical airflow routes with the most significant effect on the pressure distribution of each floor are the passenger elevator shafts, which are connected to each serving floor. The emergency elevator shaft or stairwells which are inevitably included in high-rise buildings are also highly vulnerable to stack pressure difference problems, as building code requirements usually force them to be connected to all floors and create vertical airflow routes. However, additional partitions and vestibules are installed to increase their airtightness as measures against excessive pressure differences. Also, these shafts are rarely used in daily routines, so that they do not render a great impact on the airflow of the entire building. Therefore, this study focuses only on the heights of passenger elevator shafts in predicting the pressure distribution of a building.

Simplification in typical floor plans

Buoyancy-induced pressure differences are proportioned over building elements according to the structure of the building and the leakage area of each building element. An effective means of reflecting this proportion is the Thermal Draft Coefficient (TDC), which is defined by ASHRAE (2001) as the sum of top and bottom pressure differences across the exterior walls divided by the total theoretical pressure differences, and which has been discussed in detail by Tamura (1967, 1994). Hayakawa (1989) indicated that the proportions of pressure differences will be similar if the typical floor plans are similar, and interpreted the TDC as the proportion of pressure difference supported by the exterior walls. Looking at the typical floor

plans of high-rise residential buildings in Korea, each floor can be simplified to be separated by a first partition formed by the exterior walls, a second partition formed by the entrance and wall between the residential unit and the corridor, and a third partition formed by the elevator door and the wall of the elevator shaft. In this study, the equivalent leakage area of the exterior walls and the equivalent leakage area of interior separations were used to determine the pressure difference across the exterior walls of each floor.

PREDICTION OF BUOYANCY-INDUCED PRESSURE DIFFERENCE

The prediction strategy is composed of the following two procedures, and the key parameters are as follows in each step:

1. Predicting the vertical stack pressure distribution: the height of each elevator shaft (h_{low}, h_{high}), the location of the neutral pressure level for each shaft ($h_{NPL,low}$, $h_{NPL,high}$), the outdoor and interior temperatures of each shaft (t_o, t_s)
2. Predicting the horizontal stack pressure distribution: the equivalent leakage areas in exterior walls (A_w) and interior partitions including the vertical shafts (A_e)

To readily show the strategy of predicting buoyancy-induced pressure distribution, a model building was selected, with which the strategy may be demonstrated. The key parameters for the model building are given in Table 1. Here, the location of NPLs and ratio of equivalent leakage areas are based on measurement data of 15 high-rise residential buildings of over 30 stories (Jo 2005), and the other values are based on the design conditions of the model building.

TABLE 1 Parameters for the model building

Parameter	Symbol	Value
Outdoor temperature	t_o	-12℃
Indoor temperature	t_s	22℃
Location of NPL (two zone type)	$h_{NPL,high}$	64 % (best estimate)
	$h_{NPL,low}$	32 % (best estimate)
Height of elevator shaft (two zone type)	S_{high}	210 m
	S_{low}	105 m
Ratio of equivalent leakage areas	A_e/A_w	0.67~0.82 (best estimate: 0.73)

Predicting the Vertical Stack Pressure Distribution

To predict buoyancy-induced pressure distribution over a building, the magnitude of maximum pressure difference must be calculated for each floor by first assuming the position of the neutral pressure level. The main parameters affecting the buoyancy-induced pressure difference are the building height, the indoor-outdoor temperature difference, and also the height of the neutral pressure level, which may differ depending on the proportion of openings on the upper and lower parts of a building. The building height is closely related to the height of the vertical shafts within the building, and as previous study (Jo 2005) has shown that the main airflow within a building depends on the heights of the passenger elevator shafts, the heights of the vertical zoning of such shafts must be considered. The vertical distance from the neutral pressure level of each passenger elevator shaft, along with the indoor-outdoor temperature difference, are used to complete the basic calculation equation, and consequently, the vertical stack pressure distribution may be predicted by determining the magnitude of

buoyancy-induced pressure difference for each floor. The "prediction of vertical stack pressure distribution" follows the process shown below, and the results are shown in Fig. 1.

(1) Draw a line with a slope representing the absolute pressure ($P_{outside}$) for the outdoor temperature (see Fig. 1 a).

- Outdoor temperature, t_o : -12℃

(2) Mark the position of the estimated neutral pressure level for each elevator shaft on the absolute pressure line (see Fig. 1 b).

- Position of the NPL for the upper level elevator shaft, $h_{NPL,high}$: 64 % of building height
- Position of the NPL for the lower level elevator shaft, $h_{NPL,low}$: 32 % of building height

(3) Mark the height of each passenger elevator shaft on the vertical axis, and draw parallel horizontal lines (see Fig. 1 c).

- Height of the upper level elevator shaft (equal to building height), S_{high} : 210 m
- Height of the lower level elevator shaft, S_{low} : 105 m

(4) For each elevator shaft, draw a line that passes the neutral pressure level of the corresponding shaft, with a slope representing the absolute pressure ($P_{low\text{-}rise\ elevator}$, $P_{high\text{-}rise\ elevator}$) for the temperature inside the shaft (see Fig. 1 d).

- Temperature inside the elevator shafts (equal to the indoor temperature), t_s : 22℃

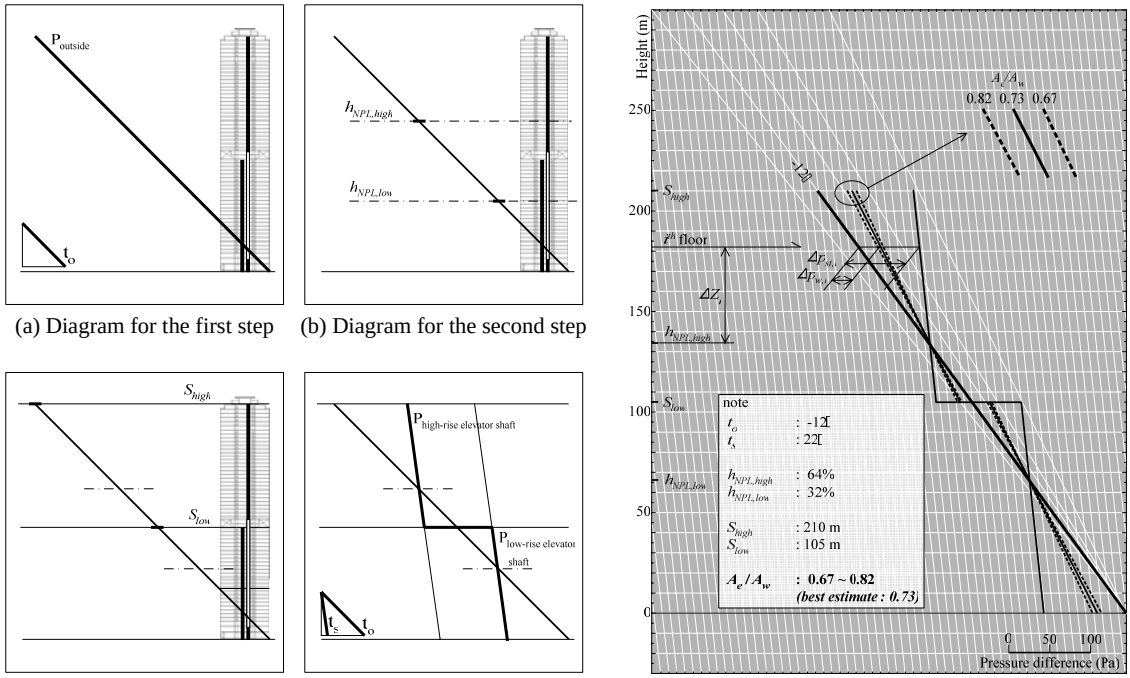

(a) Diagram for the first step (b) Diagram for the second step

(c) Diagram for the third step (d) Diagram for the forth step (e) Predicted results

Figure 1: Diagrams for the prediction procedure of stack pressure distribution and the predicted results

Predicting the Horizontal Stack Pressure Distribution

As in the previous section, a model building is used and the procedure of predicting the horizontal stack pressure distribution is demonstrated in this section. First, the pressure distribution across the exterior wall and indoors is predicted by utilizing the TDC, which represents the proportion of pressure difference for the exterior wall. Then, the pressure difference across the exterior wall may be calculated by multiplying the pressure difference for each floor, obtained in predicting the vertical stack pressure distribution. In the same

manner, the pressure distributions across specific interior separations may be calculated also, by using the equivalent leakage areas for the specific interior separations. The "prediction of horizontal stack pressure distribution" follows the process shown below, and the results are shown in Fig. 1 e.

(1) Calculate the TDC using the equivalent leakage area of the interior separations (A_e) and the equivalent leakage area of the exterior wall (A_w).
   - A_e/A_w : 0.67 ~ 0.82 (best estimate: 0.73), and γ_i : 0.31 ~ 0.40 (best estimate: 0.35)

(2) Multiply the TDC to the stack pressure difference for each floor ($\Delta P_{st,i}$) to obtain the pressure difference across the exterior wall ($\Delta P_{w,i}$). ΔZ_i is a vertical distance from the neutral pressure level of each passenger elevator shaft to ith floor (see Fig. 1 e).
   - $\Delta P_{st,i} = 3460 \times [1/(t_o+273) - 1/(t_s+273)] \times \Delta Z_i$
   - $\Delta P_{w,i} = \Delta P_{st,i} \times \gamma_i$

VERIFICATION OF THE PREDICTION STRATEGY

To show the applicability of the prediction strategy for buoyancy-induced pressure difference, the strategy is applied to a case study for which field measurements were obtained in a previous study, so that the prediction results may be compared with the measurement results. Figure 2 shows that the buoyancy-induced pressure differences, which represent the pressure difference between the outdoors and inside the vertical elevator shaft, are the same for most of the floors except for the upper levels and the 54th floor (the transfer floor). Also, as the results well reflect the change in absolute pressure at each vertical separation area, the airflow at each floor may easily be determined. The reason for the discrepancy in the results of the upper levels is regarded to lie in the difficulty, and hence inaccuracy, in measuring the airflow of the upper levels during the field measurement, and the reason for the discrepancy in the results for the 54th floor is because the upper and lower elevator shafts meet on the same floor and create airflow routes that are difficult to account for using the prediction strategy of this study. However, the elevator shaft of the typical high-rise residential building, which yields the height of the main vertical zone, is usually a single zone type or a two zone type without a transfer floor, so that by using the prediction strategy of stack pressure distribution presented in this study, the buoyancy-induced pressure difference may effectively be obtained for all typical floors of the building.

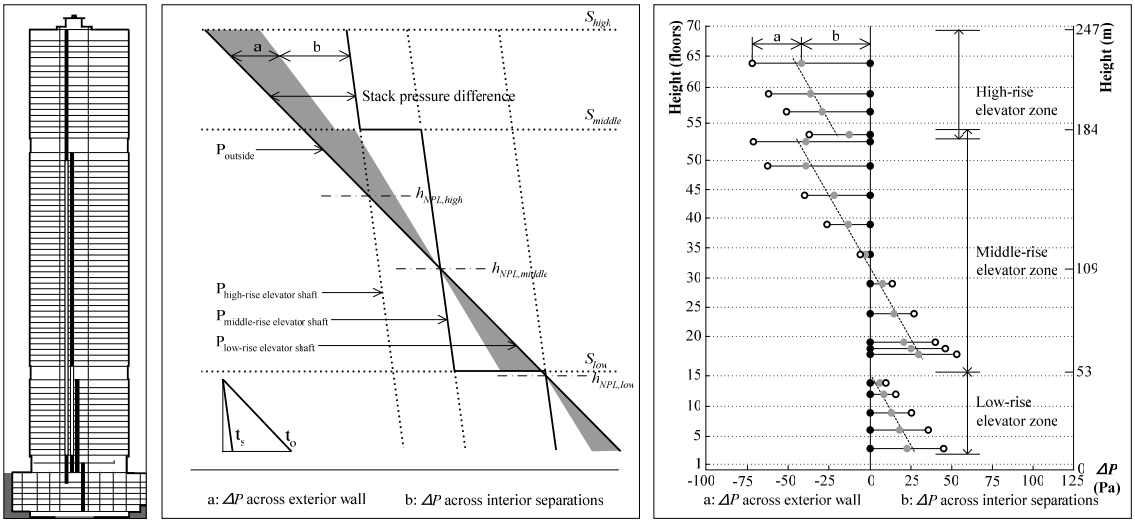

(a) Section (b) Predicted data (c) Measured data

Figure 2: Pressure distribution comparisons of predicted results and measured results

CONCLUSIONS

This paper presents a simple prediction strategy for estimating the pressure distribution in high-rise residential buildings to be utilized in the early planning stages. The strategy is composed of two main procedures: first, "prediction of the vertical stack pressure distribution," in which the pressure difference over the entire building is determined, and second, "prediction of the horizontal stack pressure distribution," in which the pressure difference across the exterior wall for each floor is calculated from the stack pressure difference obtained from the first procedure. In calculating the magnitude of pressure difference over the entire building and on each floor, such parameters as the height of the elevator shaft, the location of the neutral pressure level for each shaft, and the indoor-outdoor temperature difference were considered. Next, in calculating the pressure distribution on each floor, the leakage area of the exterior wall was utilized, as well as the equivalent leakage area of the interior walls, which includes the airtightness of the shafts. Using these procedures, the buoyancy-induced pressure difference across the exterior walls can be estimated.

Limitations

In this paper, the procedure of predicting the buoyancy-induced pressure difference across exterior walls in high-rise residential buildings assumes that the typical floor plan is uniform and that the temperature of all indoor zones are kept constant. Therefore, it may not be applied to buildings with non-uniform floor plans or many zones with different indoor temperatures. Also, further research is necessary that supplies reliable data on the equivalent leakage areas of exterior walls and interior separations and the locations of neutral pressure levels for various elevator shafts in various kinds of buildings, for a more accurate prediction of pressure distribution.

References

ASHRAE. (2001). *ASHRAE Handbook-Fundamentals*. American Society of Heating, Refrigerating and Air-Conditioning Engineers, Atlanta, USA.

Dols, W.S. and Walton, G.N. (2002). *CONTAMW 2.0 user manual*. NISTIR 6921, National Institute of Standards and Technology, USA.

Feustel, H. (1990). *Fundamentals of the multizone air flow model-COMIS mote AIVC 29.* Air Infiltration and Ventilation Centre, UK.

Hayakawa, S. and Togari, S. (1988). Study on the stack effect of tall office building (part 1). *Journal of Architectural Institute of Japan* **387**, 42-52.

Jo, J.-H. (2005). *Prediction of pressure distribution due to stack effect in high-rise buildings and evaluation of its impact*. Ph. D. thesis, Seoul National University.

Jo, J.-H., Yeo, M.-S., Yang, I.-H. and Kim, K.-W. (2004). Solving the problems due to stack effect in tall buildings. *the CIB World Building Congress 2004*, Toronto, Canada.

Liddament, M.W. (1986). *Air infiltration calculation techniques-An application guide.* Air Infiltration and Ventilation Centre, UK.

Lyberg, M.D. (1997). Basic air infiltration. *Building and Environment* **32:2**, 95-100.

Tamura, G.T. (1994). *Smoke movement and control in high-rise buildings*, National Fire Protection Association, USA.

Tamura, G.T. and Wilson, A.G. (1967). Pressure differences caused by chimney effect in three high buildings. *ASHRAE Transactions* **73:2**, 1.1- 1.10.

Walker, I.S. and Wilson, D.J. (1993). Evaluating models for superposition of wind and stack effect in air infiltrarion. *Building and Environment* **28:2**, 201-210.

CFD ANALYSIS OF THE EFFECT OF SELF-REGULATING DEVICES ON THE DISTRIBUTION OF NATURALLY SUPPLIED AIR

J. De Neve[1], S. Denys[1], J.G. Pieters[1], I. Pollet[2] and J. Denul[2]

[1] *Department of Biosystems Engineering, Ghent University, Ghent, B 9000-Belgium*
[2] *Renson Ventilation NV, Waregem, B 8790-Belgium*

ABSTRACT

Thermal comfort in living rooms or bedrooms is among others determined by the spatial distribution of the supplied ventilation air. In this work, the performance of a self-regulating (pressure-sensitive) air transfer device, in terms of air flow rate and human comfort, was investigated by means of CFD. Self-regulating ventilators limit the air supply rate according to the pressure difference across the ventilator as to reduce draught risks. The CFD analysis was carried out as much as possible according to the experimental method for evaluating such devices, described in the European Standard EN 13141-1. Pressure differences across the air transfer device of 2 and 10 Pa were studied, at a temperature difference between inside and outside climate of 20 °C. Results revealed that self-regulating air transfer devices are able to achieve a uniform flow rate for the pressure differences under investigation. Besides, they decrease the risk on draught compared with non-regulating devices.

KEYWORDS

Natural ventilation, energy performance of buildings, modelling, computational fluid dynamics, thermal comfort, draught

INTRODUCTION

Many buildings throughout the world are naturally ventilated. In the past, natural ventilation relied on an arbitrary combination of uncontrolled air infiltration and opening or closing windows and doors. Nowadays, ventilation requirements can be very demanding, as modern systems must provide greatly improved reliability and control. Natural ventilation is driven by wind and thermally generated pressure differences (so-called stack pressures). For a given configuration of openings, the rate of natural ventilation varies according to the prevailing driving forces of wind and indoor/outdoor temperature differences. Therefore, in the design of natural ventilation devices, provision is often made for the occupant to be able to adjust ventilation device openings to meet the demand. Besides user adjustable systems, some air inlet systems respond automatically to climate parameters such as temperature, humidity or pressure. So-called ‘pressure-sensitive vents’ have been specifically designed for operation at the normal driving pressures of natural ventilation (i.e., < 10 Pa). The aim of designers is to enable an almost uniform flow rate to be achieved throughout a wide pressure range, thus permitting good control of natural ventilation.

For assessing and designing natural ventilation devices, physical models can be very useful. Single-compartment and multi-compartment mass balance models have been designed to estimate the impact of sources, sinks and control options on indoor pollutant concentrations

(e.g., AIVC, 1990; Koontz and Nagda, 1991; Sparks *et al.*, 1996). However, for assessing the performance of natural ventilation devices in terms of flow rate and pressure sensitivity, mass balance models do not provide the desired information. In such cases, models based on computational fluid dynamics (CFD) provide more detailed information. CFD models predict air velocity, temperatures, pressures and pollutant concentrations at individual points in a room instead of the average values predicted by mass balance models. As a result, CFD models are especially useful for studying the distribution of air and air movement in rooms and buildings (Jones and Whittle, 1992; Nielsen, 1996), and for evaluating thermal comfort (Dorer *et al.*, 2005). In this work, ventilation devices placed in the window or outer wall as natural air supply (so-called background ventilators), were studied using CFD. In particular, the performance of a self-regulating (pressure-sensitive) air transfer device, in terms of air flow rate and human comfort feeling, was investigated. The CFD-analysis was carried out as much as possible according to the experimental method for evaluating such devices, described in the European standard EN 13141-1.

MATERIALS AND METHODS

Climate room

A CAD design of a climate room was generated as shown in Figure 1. The room had three interior walls and one exterior wall. The exterior wall (thickness 40 cm) had a centrally located window opening of 1.18 m × 1.45 m (H×W). The window opening was positioned at 0.82 m above the floor. Hence, the top of the opening was at 2 m. The window consisted of an exterior and interior frame, an air transfer device with opening length of 1 m and a window glass.

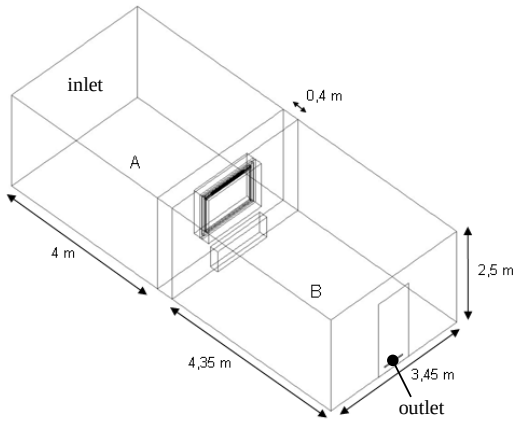

Figure 1: Geometry of the calculation domain with (A) the outdoor environment and (B) the room

The wall opposing the window wall contained a door of 2 m × 0.83 m with an opening of 3 cm × 50 cm (H×W) placed at 15 cm above the floor. This opening served as the outlet of the climate room. A rectangular block (0.55 m × 0.20 m × 1.35 m), placed under the window at a height of 15 cm, served as the heating device.

The investigated air transfer device (Figure 2) was placed on top of the window frame. It had a manually adjustable outlet lid and a self-regulating, pressure-sensitive interior flap (Figure 2). The self-regulating flap was simulated in two positions, corresponding to pressure

differences of 2 and 10 Pa over the air transfer device. The corresponding positions of the flap were experimentally determined.

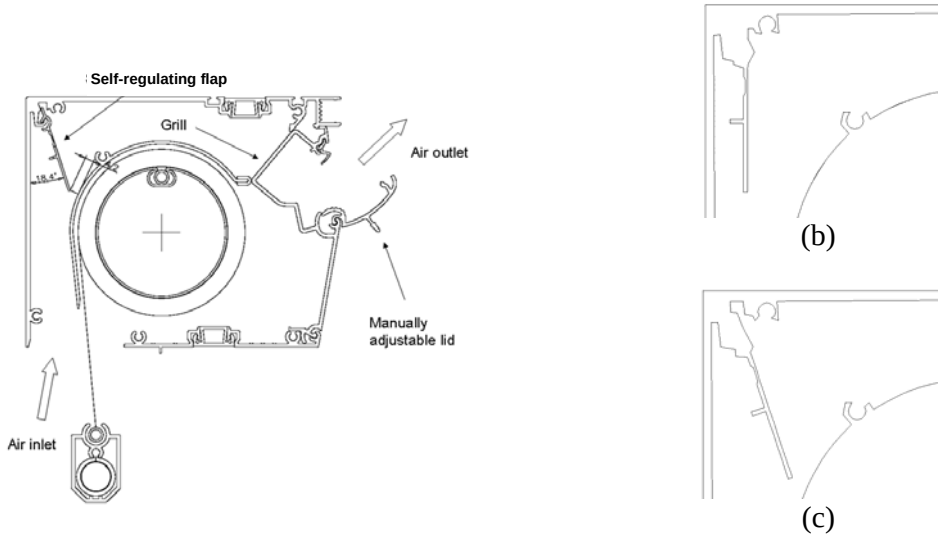

Figure 2: (a) Geometry of the air transfer device with its manually adjustable outlet lid and pressure-sensitive interior flap and a detail of the geometry of the interior flap in its position of (b) 2 Pa and (c) 10 Pa.

CFD-model and procedures

The CFD analysis was performed using the commercial CFD software Fluent (Fluent Inc., Lebanon, U.S.). This software uses the finite volume method. The segregated solver was used to obtain steady-state solutions. The numerical discretisation was conducted by a first order upwind scheme. Turbulence was simulated by a k-ω model, modified for low Reynolds number effects and hence applicable to wall-bounded flows and free shear flows. Natural convection was simulated by including gravity and temperature dependent air densities according to the ideal gas law.

Simulations were done for two positions of the pressure-sensitive interior flap, corresponding to pressure differences of 2 (POS2) and 10 Pa (POS10) over the air transfer device (Figure 2). For these simulations, a relative pressure of 2 or 10 Pa was applied at the inlet of the calculation domain. Besides simulations for corresponding pressure differences and flap positions (simulations POS2-2Pa and POS10-10Pa), a simulation was performed for a non-regulating case whereby a pressure difference of 10 Pa was considered for a flap position corresponding to the design at 2 Pa (POS2-10Pa). The latter simulation was done for evaluating the ability of the air transfer device to achieve a uniform flow rate throughout a wide pressure range.

Except for the inlet face, all other faces of the calculation domain (door, interior walls, floor and the ceiling) were treated as adiabatic walls. The exterior wall, the window frame and the window glass were solids with a thermal conductivity of respectively 0.2 W/(m·K), 0.12 W/(m·K) and 0.065 W/(m·K). The pressure at the outlet was adapted in such a way that the pressure difference over the air transfer device was 2 or 10 Pa. Pressure adaptations were needed to overcome the flow resistance at the outlet (door opening).

The experimental method for evaluating air transfer devices, described in EN 13141-1, imposes a constant temperature in the test room. A central heating-like thermal regulation procedure was therefore incorporated in the model to control the temperature inside the ventilated room. The control procedure adapted the surface temperature of the heating device, during the CFD calculation, so the desired temperature was achieved in the middle of the room. The outdoor temperature was 0 °C and the desired temperature in the middle of the room was set at (20 ± 0.5) °C.

RESULTS AND DISCUSSION

Air transfer device performance

Results for the three cases are included in Table 1. The self-regulating performance of the air transfer device can be clearly seen: at a pressure difference of 10 Pa, almost the same flow rate was achieved as at a pressure difference of 2 Pa (40.36 m³/h and 43.56 m³/h, respectively). As a result, similar air patterns were observed in both pressure-regulated cases (see Figure 3a). In the case where the pressure-sensitive interior flap was not positioned according to the prevailing pressure difference (POS2-10Pa), the higher pressure difference resulted in a much higher flow rate of 108.84 m³/h. Apparently, the position of the interior flap caused an extra flow resistance at higher pressure differences, decreasing the flow rate.

TABLE 1
Simulation results of the three cases

Simulation	POS2-2Pa	POS10-10Pa	POS2-10Pa
Position self-regulating device (Pa)	2	10	2
Pressure difference (Pa)	2.02	10.08	10.04
Flow rate (m³/h)	43.56	40.36	108.84
Heating device temperature (K)	345	345	377
Heating device capacity (W)	362	329	616
Average draught risk (%)	4.56	5.89	8.87

Human comfort

High flow rates have a negative influence on the human comfort. Figure 3a shows the velocity contours with isolines of 0.2 m/s, in the vertical plane of symmetry, perpendicular to the window. The higher flow rate in the case POS2-10Pa resulted in an air jet that penetrated horizontally into the room. For the self-regulating cases POS2-2Pa and POS10-10Pa, the velocities at the air transfer device were lower, allowing for a downward movement of the cold and heavy infiltrating air as a result of gravity. Besides velocities, also the temperature distribution in the room contributes to the feeling of comfort (Figure 3b). The air jet, observed in the non-regulating case POS2-10Pa, brought a significant amount of cold air deep into the room, while in the other cases, infiltrating cold air was heated up by the heating device and subsequently distributed within the room, which resulted in better mixing. As a result, a significantly higher heating device capacity was needed to reach the desired room temperature in the case POS2-10Pa (see Table 1). The model approximation of the heating device as a rectangular block with low contact area, and the fact that no radiation was taken into account, gave rise to unrealistically high heating device temperatures, specially in the latter case. In the cases where flow rates were regulated, the required heating device temperature and the

corresponding capacity were lower due to a better contact between cold infiltrating air and the heating device, and better mixing.

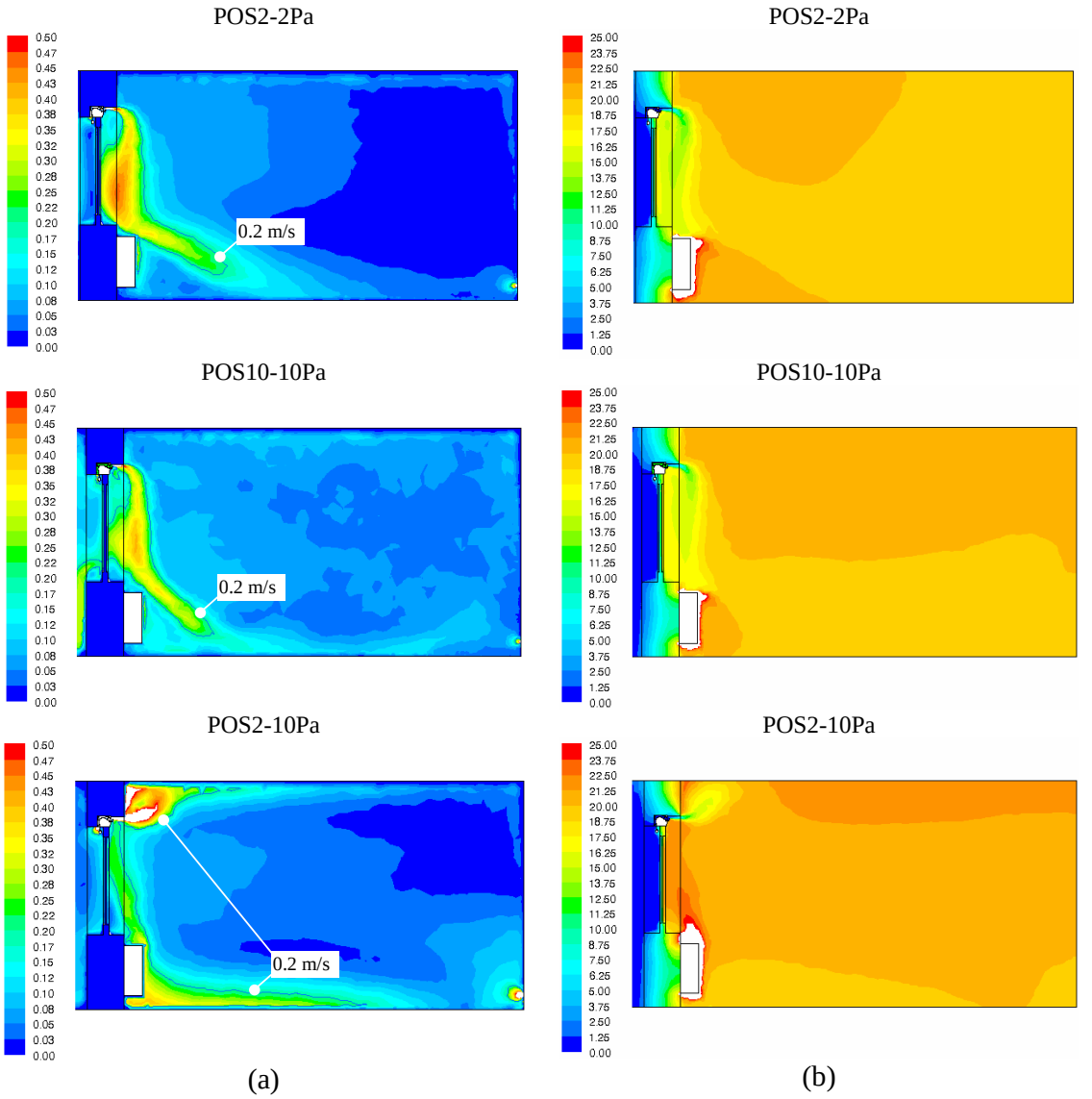

Figure 3: (a) Velocity magnitude (m/s) with isolines of 0.2 m/s and (b) temperature distribution (°C) for POS2-2Pa, POS10-10Pa and the POS2-10Pa

Effects of air velocity and temperature fields on the human comfort feeling can be brought together in the 'draught rate'. Draught is defined as an undesirable local cooling of the body caused by air movement, and is the most common complaint in relation to indoor climate. ISO 7730 defines draught rate *DR* (%) by means of the following equation, used to estimate the percentage of people likely to be dissatisfied because of air movements:

$$DR = (34 - t_a) \times (v_a - 0.05)^{0.6223} \times (0.3693 \times v_a \times TU + 3.143)$$

where t_a is the air temperature (°C), v_a the local mean air velocity (m/s) and *TU* the turbulence intensity (%). Figure 4 shows profiles of the draught rate on the plane of symmetry for the self-regulating case POS10-10Pa and the non-regulating case POS2-10Pa. Since only one plane is shown, it is difficult to draw conclusions. For comparison, volume-average values of

DR within the room are included in Table 1. The volume-averaged *DR* was higher for POS10-10Pa than for POS2-2Pa, since higher velocities were required in order to achieve the same flow rate at a higher pressure difference (smaller opening). The volume-averaged *DR* for the non-regulating case POS2-10Pa was only slightly higher (8.87 vs. 5.89 for the regulating case), but it should be kept in mind that the high heating device capacity (almost doubled as compared to the self-regulating case), causes a reduction of *DR* by increasing the room temperature.

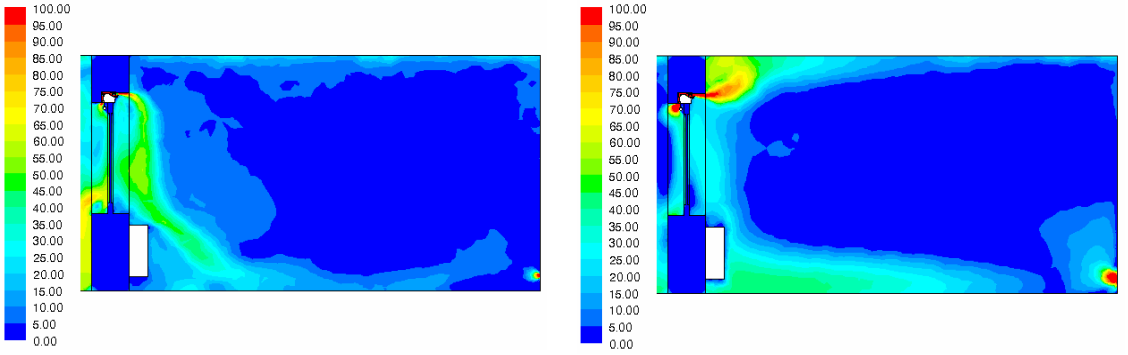

Figure 4: Draught risk [%] for (a) the self-regulating case POS10-10Pa and (b) the non-regulating case POS2-10Pa

CONCLUSION

CFD was used as a valuable tool for demonstrating the ability of a self-regulating pressure-sensitive air transfer device to achieve a uniform flow rate throughout the normal range of pressure differences for natural ventilation. Besides, CFD proved very useful for studying air distribution and movement in a climate room, and for evaluating effects of the air transfer device on human comfort by assessing draught risk. CFD results demonstrated that self-regulating air transfer devices can decrease the risk on draught compared with non-regulating devices. Besides, mutual effects of air transfer devices and heating devices can be studied.

REFERENCES

AIVC (1990). Fundamentals of the multizone air flow model-COMIS. *AIVC Technical Note 29*.

Dorer, V., Pfeiffer, A. and Weber, A. (2005). Parameters for the design of demand controlled hybrid ventilation systems for residential buildings. *AIVC Technical Note 59.*

Jones, P.J. and Whittle, G.E. (1992). CFD for building air flow prediction – current status and capabilities. *Building and Environment* **27:3**, 321-338.

Koontz, M.D. and Nagda, N.L. (1991). A multichamber model for assessing consumer inhalation exposure. *Indoor Air* **4**, 593-605.

Nielsen, P.V. (1992). Description of supply openings in numerical models for room air distribution. *ASHRAE Transactions* **98:1**

Sparks, L.E.B.A., Tichenor, B.A., Cang, J. and Guo, Z. (1996). Gass-phase mass transfer model for predicting volatile organic compound (VOC) emission rates from indoor pollutant sources. *Indoor Air* **6**, 31-40.

Natural Ventilation –Some Design Considerations

*Seemi Ahmed ** Siraj Ahmed

Abstract

Natural ventilation reduces energy consumption for fans and mechanical cooling and in most cases gives occupants control over their office space. Further benefits include no fan noise and in some cases elimination of the mechanical cooling system. The information in this paper has been presented to help building designers, owners and managers understand how certain key factors affect the performance and energy efficiency of the ventilation system, and to operate ventilation systems at minimal energy cost. Improving the air tightness of older buildings will reduce air leakage and cold drafts, and help reduce energy use by improving the performance of ventilation systems. There are three strategies for achieving acceptable indoor air quality: ventilation, source control and cleaning/filtration. Depending on the building and the specific characteristics of its location, these strategies may be used singly or in combination. When identifiable contamination sources are present in a building, it is necessary to reduce contamination sources as much as possible either by using environmentally friendly furnishings, materials and products, or by exhausting contaminants at the source, if possible. General Ventilation should then be used. For buildings where the number of occupants varies significantly with time, such as office complexes and schools, it may be possible to further improve energy efficiency by turning off ventilation systems during the non-occupied periods and controlling their ventilation rates during occupied periods based on the actual number of occupants at a given time.

Natural Ventilation

Natural ventilation relies on the natural porosity of the building and/or a combination of vents, chimneys and open able windows to provide the primary source of ventilation. Small extractor fans may be used to augment needs (e.g. in 'wet' rooms such as kitchens, bathrooms etc.).

Throughout the world many buildings are naturally ventilated. While natural ventilation may mean little more than relying on a arbitrary combination of uncontrolled air infiltration and window opening, the present need for energy efficiency and good indoor air quality now demands well designed natural ventilation systems. This can be achieved by understanding the flow mechanisms and evaluating the impact on air change of the natural driving forces of wind and temperature

Natural ventilation systems rely on pressure differences to move fresh air through buildings. Pressure differences can be caused by wind or the buoyancy effect created by temperature differences or differences in humidity. In either case, the amount of ventilation will depend critically on the size and placement of openings in the building. It is useful to think of a natural ventilation system as a circuit, with equal consideration given to supply and exhaust. Openings between rooms such as transom windows, louvers, grills, or open plans are techniques to complete the airflow circuit through a building.

*Lecturer,
Deptt. of Architecture and Planning
M.A.N.I.T,
Bhopal, India,
Email:seemiahmed2002@yahoo.com

*Sr.Lecturer,
Deptt. Of Mechanical Engineering
M.A.N.I.T,
Bhopal, India,
Email:sirajahmed23@yahoo.com

Code requirements regarding smoke and fire transfer present challenges to the designer of a natural ventilation system. Historic buildings used the stairway as the exhaust stack, a technique now prevented by code requirements in many cases

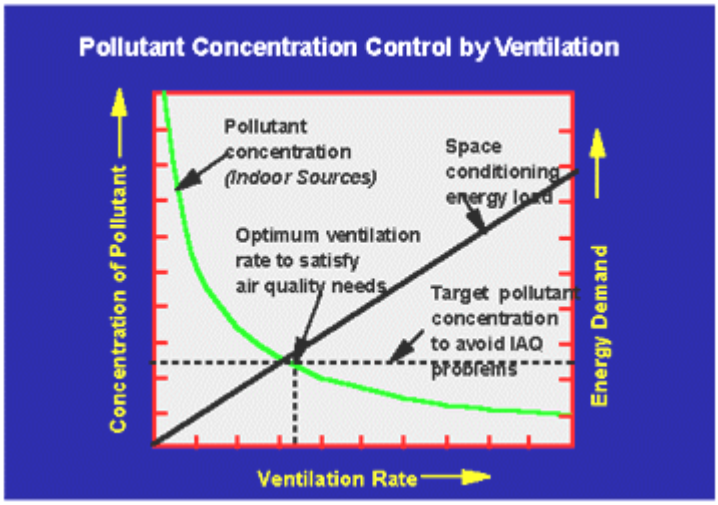

Fig. 1.1 Pollutant Concentration Control by Ventilation

The indoor pollution emissions are controlled by 'diluting' or 'displacing' indoor air with 'clean' outdoor air. For a fixed emission rate, the steady state concentration level is reduced as the ventilation rate is increased. If the air is 'conditioned' (i.e. heated or cooled to maintain optimum thermal comfort.

Technical Information

There are two basic types of natural ventilation effects: buoyancy and wind. Buoyancy ventilation is more commonly referred to as temperature-induced or stack ventilation. Wind ventilation supplies air from a positive pressure through apertures on the windward side of a building and exhausts air to a negative pressure on the leeward side.

Wind

Wind causes a positive pressure on the windward side and a negative pressure on the leeward side of buildings. To equalize pressure, fresh air will enter any windward opening and be exhausted from any leeward opening. In summer, wind is used to supply as much fresh air as possible while in winter, ventilation is normally reduced to levels sufficient to remove excess moisture and pollutants

Sometimes wind flow prevails parallel to a building wall rather than perpendicular to it. In this case it is still possible to induce wind ventilation by architectural features or by the way a casement window opens. For example, if the wind blows from east to west along a north-facing wall, the first window (which opens out) would have hinges on the left-hand side to act as a scoop and direct wind into the room. The second window would hinge on the right-hand side so the opening is down-wind from the open glass pane and the negative pressure draws air out of the room.

It is important to avoid obstructions between the windward inlets and leeward exhaust openings. Avoid partitions in a room oriented perpendicular to the airflow. On the other hand, accepted design avoids inlet and outlet windows directly across from each other (you shouldn't

be able to see through the building, in one window and out the other), in order to promote more mixing and improve the effectiveness of the ventilation.

Buoyancy

Buoyancy ventilation may be temperature-induced (stack ventilation) or humidity induced (cool tower). The two can be combined by having a cool tower deliver evaporatively cooled air low in a space, and then rely on the increased buoyancy of the humid air as it warms to exhaust air from the space through a stack. The cool air supply to the space is pressurized by weight of the column of cool air above it. Although both cool towers and stacks have been used separately, the author feels that cool towers should only be used in conjunction with stack ventilation of the space in order to ensure stability of the flow. Buoyancy results from the difference in air density. The density of air depends on temperature and humidity (cool air is heavier than warm air at the same humidity and dry air is heavier than humid air at the same temperature). Within the cool tower itself the effect of temperature and humidity are pulling in opposite directions (temperature down, humidity up). Within the room, heat and humidity given off by occupants and other internal sources both tend to make air rise. The stale, heated air escapes from openings in the ceiling or roof and permits fresh air to enter lower openings to replace it. Stack effect ventilation is an especially effective strategy in winter, when indoor/outdoor temperature difference is at a maximum. Stack effect ventilation will not work in summer (wind or humidity drivers would be preferred) because it requires that the indoors be warmer than outdoors, an undesirable situation in summer. A chimney heated by solar energy can be used to drive the stack effect without increasing room temperature, and solar chimneys are very widely used to ventilate composting toilets in parks.

An expression for the airflow induced by the stack effect is:

$$Q_{stack} = C_d * A[gh(T_i - T_o)/T_i]^{1/2} \quad \text{....(1.1)}$$

where
Q_{stack} = volume of ventilation rate (m^3/s)
C_d = 0.65, a discharge coefficient.
A = free area of inlet opening (m^2), which equals area of outlet opening.
g =9.8 (m/s^2). the acceleration due to gravity
h = vertical distance between inlet and outlet midpoints (m)
T_i = average temperature of indoor air (K), note that 27°C = 300 K.
T_o = average temperature of outdoor air (K)

The cool tower ventilation is only effective where outdoor humidity is very low. The following expression for the airflow induced by the column of cold air pressurizing an air supply is based on a form developed by Thompson (1995), with the coefficient from data measured at Zion National Park Visitor Center. This tower is 7.4 m tall; 2.4 m square cross section, and has a 3.1 m^2 opening.

$$Q_{cooltower} = 0.49 * A * [2gh(T_{db} - Twb)/T_{db}]^{1/2} \quad \text{....(1.2)}$$

where
$Q_{cool\ tower}$ = volume of ventilation rate (m^3/s)
0.49 is an empirical coefficient calculated with data from Zion Visitor Center, UT, which includes humidity density correction, friction effects, and evaporative pad effectiveness.
A = free area of inlet opening (m^2), which equals area of outlet opening.
g =9.8 (m/s^2). The acceleration due to gravity
h = vertical distance between inlet and outlet midpoints (m)
T_{db} = dry bulb temperature of outdoor air (K), note that 27°C = 300 K.
T_{wb} = wet bulb temperature of outdoor air (K)

The total airflow due to natural ventilation results from the combined pressure effects of wind, buoyancy caused by temperature and humidity, plus any other effects from sources such as fans. The presence of mechanical devices that use room air for combustion, leaky duct systems, or other external influences can significantly affect the performance of natural ventilation systems.

DESCRIPTION

Natural ventilation, unlike fan-forced ventilation, uses the natural forces of wind and buoyancy to deliver fresh air into buildings. Fresh air is required in buildings to alleviate odors, to provide oxygen for respiration, and to increase thermal comfort. At interior air velocities of 160 feet per minute (fpm), the perceived interior temperature can be reduced by as much as 5°F. However, unlike true air-conditioning, natural ventilation is ineffective at reducing the humidity of incoming air. This places an upper limit on the application of natural ventilation in warm humid climates.
In order for air to move through or around a space, there needs to be some driving force. One often sees the obligatory blue and red arrows indicating the movement of air through an architect's latest design. Unfortunately, these arrows seldom make it into the final building, leaving the air confused and unsure of where to go next. It is then left up to natural forces to direct the air through the building.

The building form and construction determines the relative strength of these natural forces. This basically comes down to the size and location of air inlets and outlets as well as any ability to capture or funnel prevailing breezes. The building form can be designed to enhance ventilation, using atria, narrow building depths, open plan environments, massive concrete structures, sun-assisted chimneys, wind-wings and twin facades. In hybrid systems, motorised windows can be used as active regulators to achieve control over air change rates and heat load reduction.

Inducing Air Movement

Air will move only when it is pushed, pulled, heated up or cooled down. In a passive design, the pushing and pulling has to be done by the prevailing wind, whilst the heating and cooling can be done by solar radiation, evaporation and/or thermal mass.

Wind-Driven Ventilation

Air can only be pushed and pulled by producing localised areas of high or low pressure. Thus building form is fundamental to any wind-driven natural ventilation system. Anything that diverts or changes the path of the air will act to impede its flow. This impedance is significantly higher if the air is forced to move upwards or downwards to navigate a barrier without any corresponding increase or decrease in temperature.

Wind causes a positive pressure on the windward side and a negative pressure on the leeward side of buildings. To equalise this pressure, outside air will enter any windward openings and be drawn out of leeward openings. In summer, wind is usually used to supply as much fresh air as possible while in winter ventilation is normally reduced to levels sufficient only to remove excess moisture and pollutants.

Stack-Effect Ventilation

Buoyancy results from differences in air density. The density of air depends on temperature and humidity. Cool air is heavier than warm air at the same humidity and dry air is heavier than humid air at the same temperature. Thus, heat and humidity given off by occupants and other internal sources tend to make air rise. The stale, heated air escapes from openings in the ceiling or roof, drawing fresher air in through lower openings to replace it.

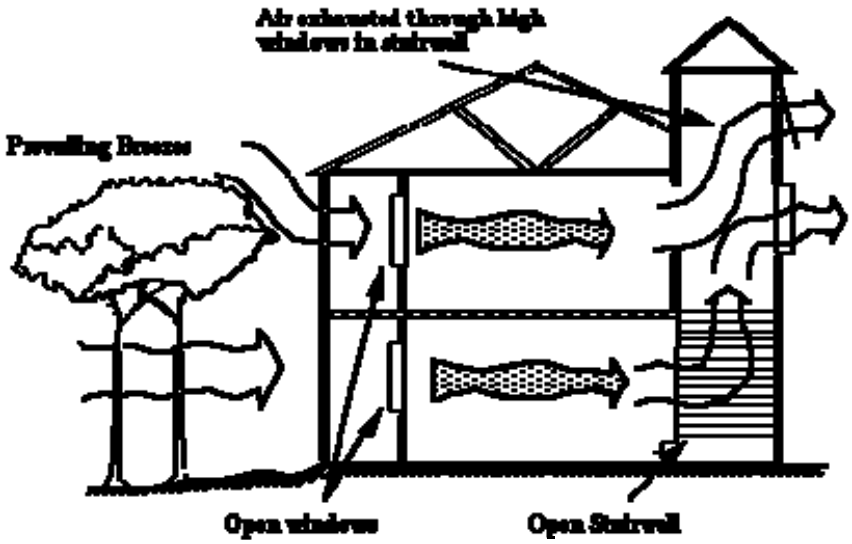

Fig. 1.2 Stack Effect Built into Home

Thermo-Syphon Effect

Operating in much the same way as the stack effect, a thermo-syphon makes use of direct sunlight to warm the air in a building. This requires a large amount of equator-facing glass. Dark surfaces beneath the glass absorb the direct sunlight, increase in temperature and re-radiate long-wave infrared radiation heat back into the enclosed space. As glass is opaque to long-wave infrared radiation, the heat energy is trapped within the space and eventually absorbed by the air. This is basically the greenhouse effect at work.

If allowed to vent out the top, the heated air will rise - drawing new cooler in at the bottom. This causes quite a strong convection current within the building. By not venting the warm air out the top, but letting it move through internal vents, this convection current can be used for heating in winter, even on a relatively cloudy day.

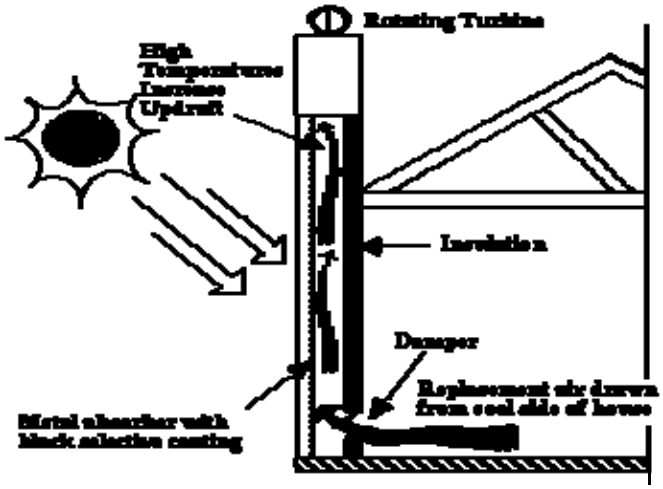

Fig. 1.3 Thermal Chimney

Principles Of Natural Ventilation

Natural ventilation methods date back to the first time animals were confined in shelters, when farmers left the barn door open to reduce moisture or heat buildup. Today's naturally-ventilated livestock shelters, although more sophisticated, operate on exactly the same principles. Natural ventilation occurs primarily because of the difference in wind pressure across a building, and to a lesser extent because of a difference in inside and outside temperature. A natural system works best in a building with no ceiling but having small openings at the eaves and ridge (peak) of the roof, and having large sidewall openings (Figure 1.4).

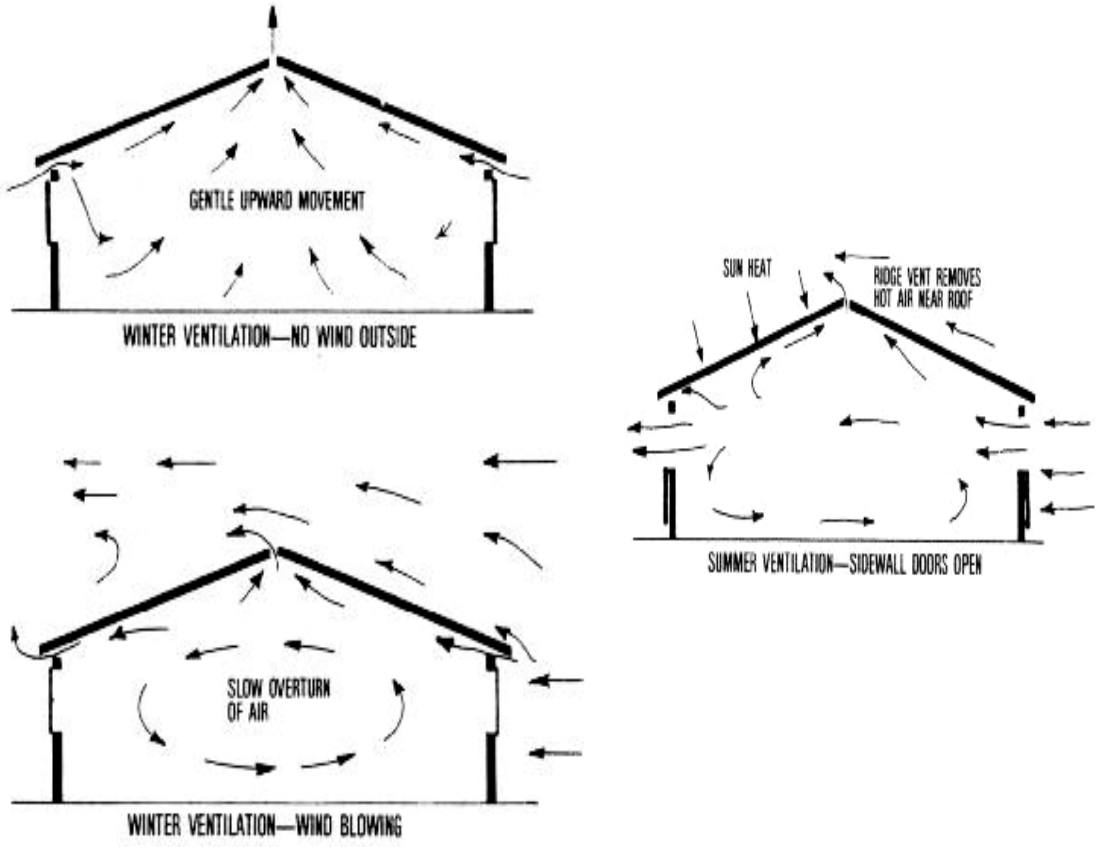

Fig. 1.4 Natural ventilation in a gable-roof building occurs primarily because of the wind blowing over the ridge and, to a lesser degree, because of the temperature difference inside and out.

Winter ventilation occurs as wind blows across the open ridge of the gable-roof building. Suction is created which draws warm, moist air out of the building and fresh air in through the eave openings. If wind velocity is great enough, the downwind (leeward) eave openings can also act as air outlets. On calm winter days, the hot, moist air still rises and eventually finds its way out the ridge opening. This chimney or `stack' effect accounts for only about 10 percent of the total ventilation, because there is not a great difference between inside and outside temperatures in most naturally-ventilated buildings, except on very cold days.

Summer ventilation is provided by opening up large portions (typically one-third to one-half) of each sidewall to allow a cross-flow of air; the ridge opening has little effect in summer.

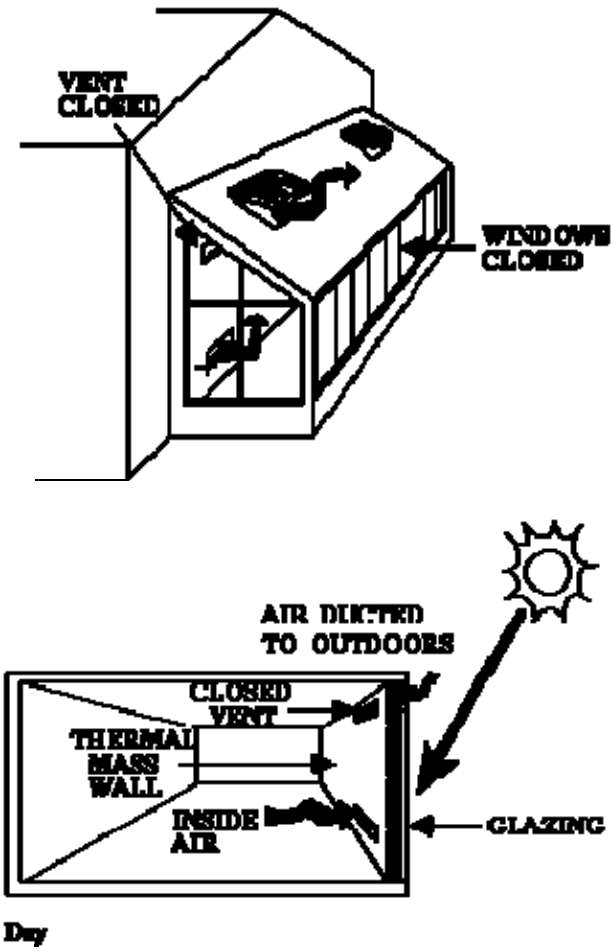

Fig.1.5 Summer Venting Thermal MassWall

Design Recommendations

The specific approach and design of natural ventilation systems will vary based on building type and local climate. However, the amount of ventilation depends critically on the careful design of internal spaces, and the size and placement of openings in the building.

- Maximize wind-induced ventilation by siting the ridge of a building perpendicular to the summer winds.
  - Approximate wind directions are summarized in seasonal "wind rose" diagrams available from the National Oceanographic and Atmospheric Administration (NOAA). However, these roses are usually based on data taken at airports; actual values at a remote building site can differ dramatically.
  - Buildings should be sited where summer wind obstructions are minimal. A windbreak of evergreen trees may also be useful to mitigate cold winter winds that tend to come predominantly from the north.
- Naturally ventilated buildings should be narrow.
  - It is difficult to distribute fresh air to all portions of a very wide building using natural ventilation. The maximum width that one could expect to ventilate

naturally is estimated at 45 ft. Consequently, buildings that rely on natural ventilation often have an articulated floor plan.

- Each room should have two separate supply and exhaust openings. Locate exhaust high above inlet to maximize stack effect. Orient windows across the room and offset from each other to maximize mixing within the room while minimizing the obstructions to airflow within the room.
- Window openings should be operable by the occupants.
- Provide ridge vents.
    - A ridge vent is an opening at the highest point in the roof that offers a good outlet for both buoyancy and wind-induced ventilation. The ridge opening should be free of obstructions to allow air to freely flow out of the building.

Operable windows that permit natural ventilation can be used in offices and other commercial structures.

Fig. 1.6

- Allow for adequate internal airflow.
    - In addition to the primary consideration of airflow in and out of the building, airflow between the rooms of the building is important. When possible, interior doors should be designed to be open to encourage whole-building ventilation. If privacy is required, ventilation can be provided through high louvers or transoms.
- Consider the use of clerestories or vented skylights.
    - A clerestory or a vented skylight will provide an opening for stale air to escape in a buoyancy ventilation strategy. The light well of the skylight could also act as a solar chimney to augment the flow. Openings lower in the structure, such as basement windows, must be provided to complete the ventilation system.
- Provide attic ventilation.
    - In buildings with attics, ventilating the attic space greatly reduces heat transfer to conditioned rooms below. Ventilated attics are about 30°F cooler than unventilated attics.
- Consider the use of fan-assisted cooling strategies.
    - Ceiling and whole-building fans can provide up to 9°F effective temperature drop at one tenth the electrical energy consumption of mechanical air-conditioning systems.
- Determine if the building will benefit from an open- or closed-building ventilation approach.
    - A closed-building approach works well in hot, dry climates where there is a large variation in temperature from day to night. A massive building is ventilated at night, then, closed in the morning to keep out the hot daytime

air. Occupants are then cooled by radiant exchange with the massive walls and floor.

- An open-building approach works well in warm and humid areas, where the temperature does not change much from day to night. In this case, daytime cross-ventilation is encouraged to maintain indoor temperatures close to outdoor temperatures.

- Use mechanical cooling in hot, humid climates.
- Try to allow natural ventilation to cool the mass of the building at night in hot climates.
- The long façade of the building and the majority of the openings should be oriented with respect to the prevailing summer breezes (i.e., north-south orientation if prevailing westerly wind).
- Exhaust vents or outlets should be on the leeward side as high as possible in the building.
- Vegetation and site objects should not obstruct inlet openings.
- Rooms should have inlet and outlet openings located in opposing pressure zones, e.g. windward and leeward walls, windward wall and roof.
- Inlets should supply air low in the room. Outlets should be located across the room and at high level.
- The vertical distance between the inlet and exhaust openings should take advantage of the stack effect.
- all occupied spaces should have an inlet and outlet opening, one or both of which may be an operable window
- The total area of outlet openings should be operable and accessible by the occupants.
- Inlet openings should not be obstructed by furniture and interior partitions.
- Enclosed staircases used to take advantage of stack effect ventilation should be designed such that their function as fire exits is not compromised.
- Floor to ceiling heights should be at least 3 m.

In order for natural ventilation to be effective as a space cooling system, it is important to keep solar and internal gains to a minimum. The lower these gains are, the less air flow is required to remove the heat and the greater the likelihood that a mechanical cooling system can be avoided. Some techniques to reduce solar and internal gains are given below.

- Window areas should not be excessive and be protected by exterior shading devices.

Shading with Vegetation

- Design for high thermal capacity and exposed ceilings for night cooling.
- Minimize warming of the walls by the sun through use of light-coloured building exteriors, trees and shrubs to provide shading and evaporative cooling, grass and other groundcover to keep ground temperatures low, and ponds and fountains to enhance evaporative cooling

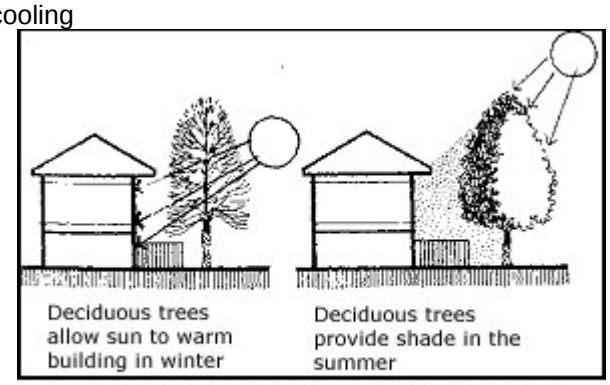

Examples of side landscape features that help to conserve energy

Fig. 1.7

- Internal loads should be low, e.g. high-efficacy lighting, lighting controls, high-efficiency mechanical equipment, pipe and duct insulation

Natural ventilation in most climates will not move interior conditions into the comfort zone 100% of the time. Make sure the building occupants understand that 3% to 5% of the time thermal comfort may not be achieved. This makes natural ventilation most appropriate for buildings where space conditioning is not expected. As a designer it is important to understand the challenge of simultaneously designing for natural ventilation and mechanical cooling. It can be difficult to design structures that are intended to rely on both natural ventilation and artificial cooling. A naturally ventilated structure often includes an articulated plan and large window and door openings, while an artificially conditioned building is sometimes best served by a compact plan with sealed windows. Moreover, interpret wind data carefully. Local topography, vegetation, and surrounding buildings have an effect on the speed of wind hitting a building. Wind data collected at airports may not tell you very much about local microclimate conditions that can be heavily influenced by natural and man-made obstructions. Hints about what type of natural ventilation strategies might be most effective can often be found in a region's historic and vernacular construction practices.

Materials and Methods of Construction

Some of the materials and methods used to design proper natural ventilation systems in buildings are solar chimneys, wind towers, and summer ventilation control methods. A solar chimney may be an effective solution where prevailing breezes are not dependable enough to rely on wind-induced ventilation and where keeping indoor temperature sufficiently above outdoor temperature to drive buoyant flow would be unacceptably warm. The chimney is isolated from the occupied space and can be heated as much as possible by the sun or other means. Air is simply exhausted out the top of the chimney creating suction at the bottom which is used to extract stale air.

Wind towers, often topped with fabric sails that direct wind into the building, are a common feature in historic Arabic architecture, and are known as "malqafs." The incoming air is often routed past a fountain to achieve evaporative cooling as well as ventilation. At night, the process is reversed and the wind tower acts as a chimney to vent room air. A modern variation called a "Cool Tower" puts evaporative cooling elements at the top of the tower to pressurize the supply air with cool, dense air.

In the summer, when the outside temperature is below the desired inside temperature, windows should be opened to maximize fresh air intake. Lots of airflow is needed to maintain the inside temperature at no more than 3-5 °F above the outside temperature. During hot, calm days, air exchange rates will be very low and the tendency will be for inside temperatures to rise above the outside temperature. The use of fan-forced ventilation or thermal mass for radiant cooling may be important in controlling these maximum temperatures.

Analysis & Design Tools

Handbook methods such as those presented in ASHRAE's *Handbook of Fundamentals* or Bansal and Minke's *Passive Building Design: A Handbook of Natural Climatic Control* are very useful in calculating airflow from natural sources for very simple building geometries.

Computational Fluid Dynamics (CFM): In order to predict the details of natural airflow, numerical computational fluid mechanics models can be used. These computer simulations are detailed and labor intensive, but are justified where accurate understanding of airflow is

important. They have been used to analyze new buildings including the atrium of a courthouse in Phoenix and the hangar of an air and space museum in the Washington, DC area.

An extensive list of journals, books, and other reference material regarding natural ventilation and other passive technologies is included in the Solstice Archive. For example,

BTS Building Standards & Guidelines Program (BSGP)
EREC Fact Sheet: Cooling Your Home Naturally

Software packages for natural ventilation analysis include:

FLUENT: A computational fluid dynamics program useful in modeling natural ventilation in buildings. It models airflow under specified conditions, so additional analysis is required to estimate annual energy savings.
AIRPAK: provides calculation of airflow modeling, contaminant transport, room air distribution, temperature and humidity distribution, and thermal comfort by computational fluid dynamics.
FLOVENT: calculates airflow, heat transfer, and contamination distribution for built environments using Computational Fluid Dynamics.

Building models incorporate very limited features for deliberate natural ventilation, but they do include the calculation of natural air infiltration as a function of temperature difference, wind speed, and effective leakage area, or schedules and user defined functions for infiltration rates.

DOE-2: A comprehensive hour-by-hour simulation; daylighting and glare calculations integrate with hourly energy simulation. IBM or compatible Pentium is advisable.
Designing Low Energy Buildings with Energy-10: An hour-by-hour simulation program designed to inform the earliest phases of the design process. Runs on IBM-compatible platforms. Best operated with Pentium or higher processor and 32 Megs of RAM.
ENERGY PLUS: A building energy simulation program designed for modeling buildings with associated heating, cooling, lighting, ventilating, and other energy flows.

REFERENCES

1) ANSI/ASHRAE Standard 62.2-2003, Ventilation and Acceptable Indoor Air Quality for Low-Rise Residential Buildings, ASHRAE, Atlanta.
2) ASHRAE, Fundamentals Handbook, ASHRAE, Atlanta, 2001.
3) L. Fang, G. Clausen and P.O. Fanger, Impact of temperature and humidity on the perception of indoor air quality. Indoor Air 8 (1998), pp. 80–90.
4) M. Nyman and C.J. Simonson, Life cycle assessment (LCA) of air-handling units with and without air-to-air energy exchangers. ASHRAE Transactions 110 1 (2004), pp. 399–409.
5) T. Ojanen, Criteria for the hygrothermal performance of wind barrier structures, in: B. Saxhof (Ed.), Proceedings of the 3rd Symposium of Building Physics in the Nordic Countries, 1993, pp. 643–652.
6) prEN 832, Thermal Performance of Buildings—Calculation of Energy Use for Heating—Residential Buildings, European Committee for Standardization, final draft, February 1998.
7) M. Schell and D. Int-Hout, Demand control ventilation using CO2. ASHRAE Journal 43 2 (2001), pp. 18–29.
8) C.J. Simonson, Moisture, Thermal and Ventilation Performance of Tapanila Ecological House, Espoo, VTT Research Notes 2069, http://www.inf.vtt.fi/pdf/tiedotteet/2000/T2069.pdf, 2000, p. 141, app. p. 5.
9) C.J. Simonson, M. Salonvaara, T. Ojanen, Moisture content of indoor air and structures in buildings with vapor permeable envelopes, in: Proceedings (CD) of Performance of Exterior Envelopes of Whole Buildings VIII: Integration of Building Envelopes, ASHRAE, Clearwater Beach, Florida, 2001, p. 16

INDOOR HUMIDITY CONTROL WITH DX A/C SYSTEMS IN SUBTROPICAL RESIDENCES

Zheng Li[1], Wu Chen[2] and Shiming Deng[3]

[1,2,3]*Department of Building Services Engineering, The Hong Kong Polytechnic University*
Kowloon, Hong Kong SAR, China

ABSTRACT

Direct expansion (DX) air conditioning (A/C) systems are most commonly used in residential buildings in hot and humid subtropics. They are normally equipped with single-speed compressors and supply fans, relying on on-off cycling compressors to maintain indoor dry-bulb temperature only, leaving indoor humidity uncontrolled. The reason for this situation is the mismatching between an equipment sensible heat ratio (SHR) and an application SHR. This paper reports a study on this mismatching problem for DX A/C systems used in subtropical residences. With the aid of a building energy simulation program, EnergyPlus, the indoor humidity control problem with two SHRs' mismatching is discussed. An experimental station has been built, humidity control strategy with variable-speed compressor and supply fan is presented; and a complete simulation model representing DX systems, based on the design parameters and test data of the experimental station is developed.

KEYWORDS

DX A/C systems, humidity control, modeling, subtropical residences

1. INTRODUCTION

For residential buildings located in the subtropics, residential air conditioning is very often provided by the use of a discrete system, i.e., room air conditioners (RACs) which are generally of direct expansion (DX) type. In the hot and humid subtropics, it is more challenging and difficult to deal with space latent cooling load than space sensible load, using a RAC. This is partly due to the fact that the current trend in designing a RAC is to have a smaller moisture removal capacity, in an attempt to boost energy-efficiency ratings (EER) and coefficient of performance (COP) (Kittler 1996). This can potentially lead to a situation where a RAC will provide a desired temperature control but not a desired indoor humidity control, which will influence the occupants' thermal comfort, indoor air quality (IAQ) and energy efficiency (Murphy 2002, Westphalen 2004 and Shirey 1993). Sensible heat ratio (SHR), which is defined as a ratio of sensible cooling load to the total cooling load, is an important parameter in studying the ability of cooling and dehumidification for the cooling coil of a RAC. The SHR for an air conditioned space is normally called an application SHR and that for an air conditioner an equipment SHR. An equipment SHR is largely a function of the design of a cooling coil, an application SHR depends mainly on the characteristics of space sensible and latent cooling load (Amrane et al 2003).

A number of reported studies discussed this humidity control issue under part load conditions, and briefly mentioned that the mismatching between two SHRs can significantly influence indoor RH levels using RACs (Murphy 2002, Shirey 1993 and Amrane et al 2003). However, the quantitative analysis for the dismatching between equipment SHR and application SHR and its impacts on indoor humidity control were rarely addressed. For this purpose, With the aid of a building energy simulation program, EnergyPlus, the mismatching problem is analyzed, a multi-purpose experimental station and a complete simulation model representing DX systems, based on the design parameters and test data of the experimental staion is developed. Humidity control strategy with variable-speed compressor and supply fan is presented.

2. INDOOR HUMIDITY CONTROL PROBLEM

A hypothetic 30-story residential block, which was modeled after those widely used in Hong Kong was used as the platform for performing the EnergyPlus simulation study. The apartment facing west, one of a total of eight apartments in a floor, was used in this study. The floor plan of the selected west-facing apartment is shown in Figure 1.

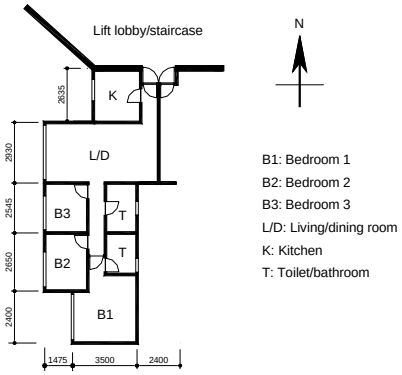

Figure 1: Floor plan of a west-facing apartment under study

The simulation conditions and assumptions, which were the required inputs to EnergyPlus, including construction details, activity levels of occupants, internal heat gain from lights, electric appliances, ventilation rate etc. were previously given (Lin 2004). Some essential details would be described here. It was assumed that this apartment was occupied by a four-person family and the living/dining room was occupied by all family members at daytime; and the master bedroom (i.e., bedroom 1) by the two adults and the other two bedrooms, each by one of the two children, respectively, at nighttime.The living/dining room and all bedrooms were equipped with window-type room air conditioners (WRACs), but no A/C was provided in the toilet/bathrooms and the kitchen. Simulations were performed under two operating modes. One was daytime operating mode (DOM), where the WRAC for the living/dining room operated daily from 7:00 to 21:00. The other was nighttime operating mode (NOM), where the WRAC in the master bedroom operated daily from 22:00 to 6:00. According to ASHRAE (ASHRAE 2004) and HK-BEAM (HK-BEAM 2001), 24°C and 50% RH were selected as the indoor setpoints. The outdoor cooling design conditions with summer design day for Hong Kong were used (Lam 1995).

Figure 2 shows the profiles of hourly space sensible and latent cooling loads for the living/dining room at DOM in the summer design day. It can be seen that the space latent cooling load stayed

almost constant except for the first hour due to pull-down load at the beginning of DOM, the sensible load varied significantly and peaked at 17:00. Over all the operating hours, the hourly application SHRs ranged between 0.55 and 0.72, with an average being 0.63 which was smaller than 0.7-0.8, the equipment SHR for a standard DX WRAC (Kittler 1996, Amrane et al 2003). This implied that for subtropical residences, their application SHRs would be lower than the equipment SHRs if standard WRACs were used. Figure 3 shows the simulated indoor air RH levels at the three different equipment SHRs (0.65, 0.75 and 0.85) in the living/dining room in the summer design day. It is understood that air conditioners with different equipment SHRs would have the different ability to handle space sensible and latent loads. The smaller an equipment SHR of a RAC is, the larger its ability to deal with space's latent cooling load.

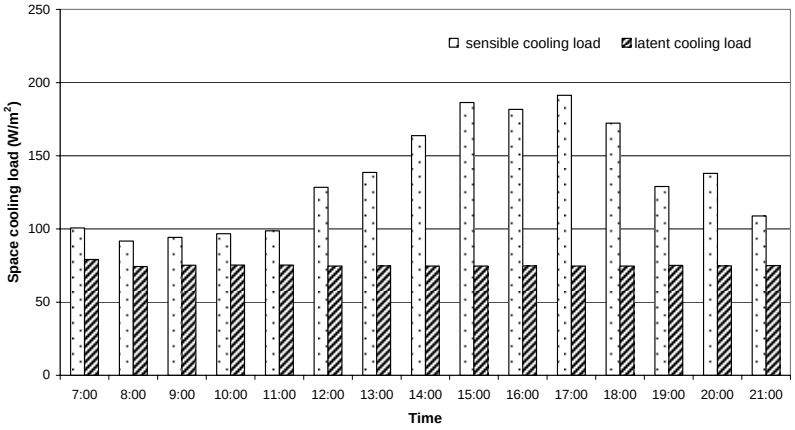

Figure 2: Profiles of hourly space sensible and latent cooling loads for the living/dining room at DOM in the summer design day

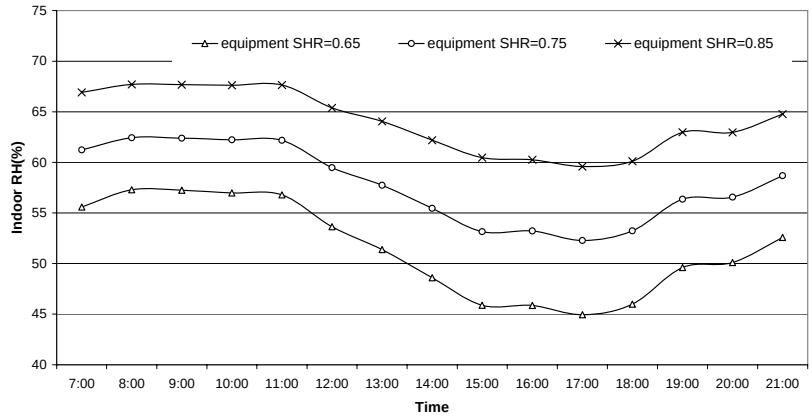

Figure 3: Indoor RH levels at different RAC's equipment SHRs in the living/dining room at DOM in the summer design day

Figure 4 shows the profile of both hourly space sensible and latent cooling loads for the master bedroom at NOM in the summer design day. It can be seen that while the sensible cooling load varied significantly with its peak occurring at the beginning, space latent load stayed relatively constant except for the first hour due to pull-down load at the beginning of NOM. Moreover, the hourly application SHRs for the bedroom ranged between 0.6 and 0.85, with an averaged value being 0.69. Figure 5 shows the indoor air RH levels at three different equipment SHRs (0.65, 0.75 and 0.85) in the master bedroom at NOM in the summer design day. It can be seen that there

were also noticeable differences in the resulted indoor RH levels when RACs with different SHRs were used. Given that the averaged application SHR was 0.69, the use of a RAC with its equipment SHR being 0.85 would cause the indoor RH level to deviate more from the setting of 50% RH than the use of the RAC with their equipment SHRs being closer to 0.69.

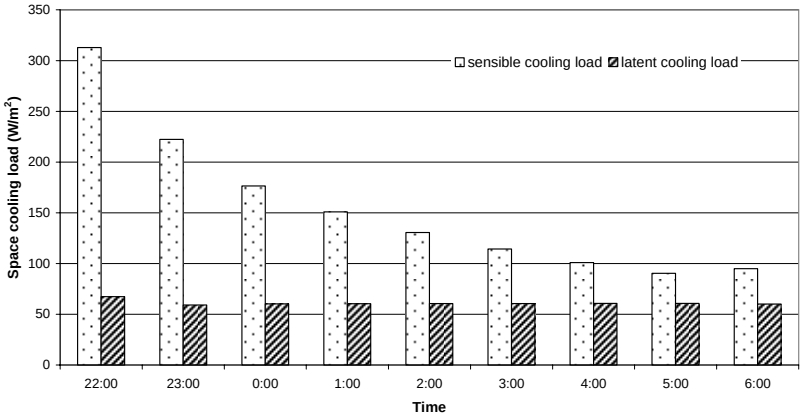

Figure 4: Profile of the hourly space sensible and latent cooling loads for the master bedroom at DOM in the summer design day

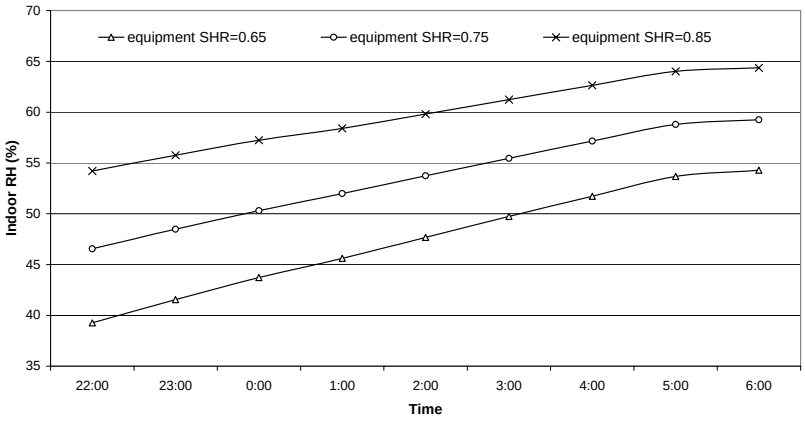

Figure 5: Indoor RH levels at different RACs' equipment SHRs in the master bedroom at NOM in the summer design day

3. DESCRIPTION OF EXPERIMENTAL STATION

A multi-purpose DX VAV A/C experimental station has been set up in the HVAC Laboratory of Building Services Engineering (BSE) Department of the Hong Kong Polytechnic University. The schematics of the air handling system and DX refrigerant plant of the experimental station are shown in Figure 6 and Figure 7, respectively. In the DX refrigerant plant, there is a condensing unit comprising of a rotor compressor driven by variable speed drive (VFD), an air cooled condenser with its axial fan driven by VFD. An electronic expansion valve (EEV) is used in the station. The refrigerant used is R22. The nominal cooling capacity is 10 kW and its modulation range is 30 to120% of the normal capacity. The air handling system includes an air handing unit (AHU) and an air conditioned room. Inside the AHU, the evaporator of the DX refrigerant plant is placed to be used as a DX air cooling coil. The supply fan in the AHU is of centrifugal type and VFD-driven. There are two sensible heat and moisture load generation units (LGU) inside

room. Sensible heat and moisture load can be varied manually or automatically with the pre-set pattern by operator's programming.

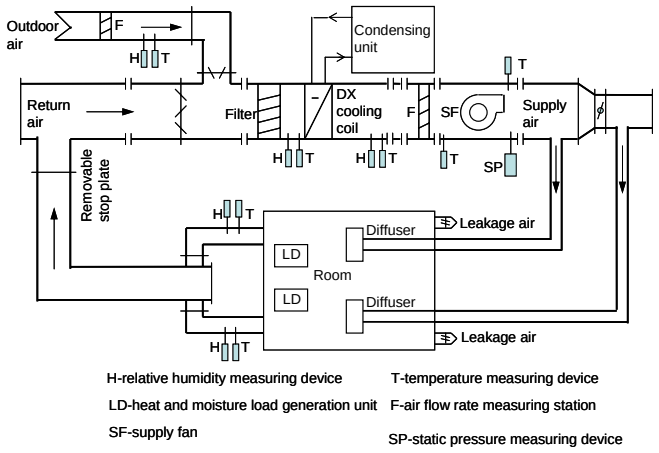

Figure 6: The schematic of the air handling system of the experimental station

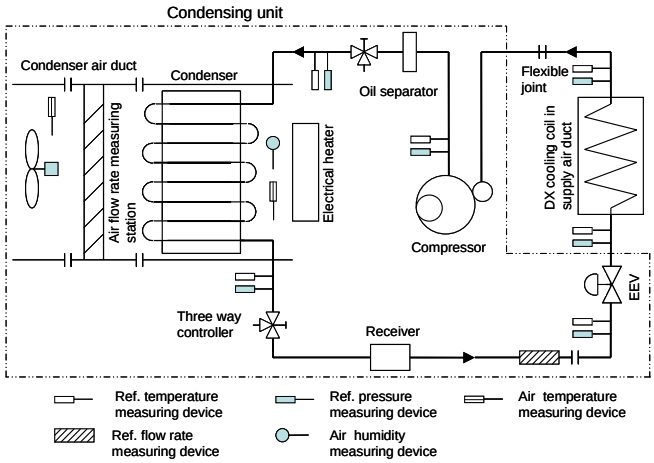

Figure 7: The schematic of the DX refrigerant plant of the experimental station

4. **DYNAMIC MODELING FOR DX SYSTEMS**

A complete dynamic simulation model representing a DX system, based on thermodynamic principle and test data of the experimental station, is developed. The complete system's simulation model is component-based, and takes the dynamic characteristics of a DX refrigeration plant into consideration. The complete conceptual model which depicts the zoning of the DX system is shown in Figure 8; each zone is treated as a stirred tank. The well-known A.C. Cleland Equations and air state equations recommended by ASHRAE are used to describe various thermodynamic and thermophysical properties of refrigerant and air, respectively. During the modeling of compressor, a polytropic compression process is assumed and a quasi-steady model is established by the traditional theoretical thermodynamic approach. EEV is represented by an orifice equation, and a varying valve opening that was modulated by refrigerant superheat at evaporator exit. The evaporator refrigerant side is basically divided into two regions: a two-

phase region and a superheated region. The two-phase region is further divided into liquid and vapor zones. The counter-flow heat exchange between the refrigerant and the air is assumed for the air-cooled plate-fin-tube condenser. Discharged vapor from compressor is delivered into the vapor zone, the boundary layer and the liquid zone.

With this model and experimental station presented in Section 3, the investigation of humidity control with varied-speed compressor and supply fan could be carried out.

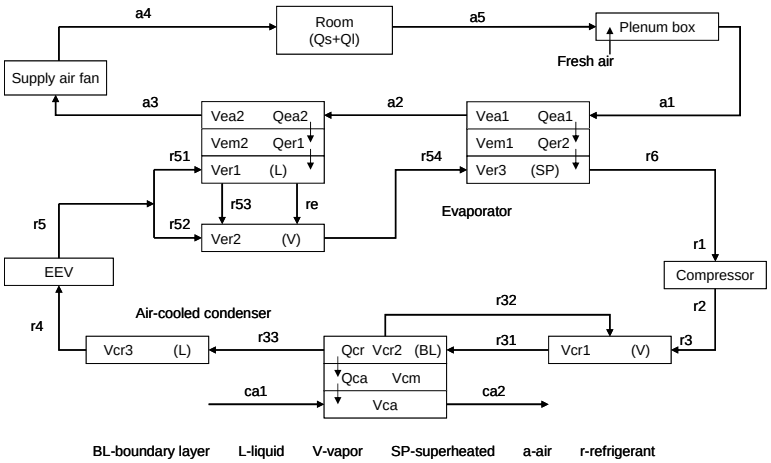

Figure 8: The conceptual model of the DX system

5. CONCLUSION

With the simulation results, for residential buildings located in hot and humid subtropics, the average application SHR was 0.63 and 0.69 for DOM and NOM, respectively, which were smaller than 0.7-0.8, the equipment SHR for a standard DX WRAC. This mismatching leaded to a situation that RH levels would be higher than the setpoint of 50%. The control strategy based on varied-speed compressor and fan would improve the humidity performance. The related experimental and simulation study will be reported in the future work.

References

Amrane, K., Hourahan, G.C. and Potts, G. (2003) Latent performance of unitary equipment. *ASHRAE Journal* **45:1**, 28-31.

ASHRAE. (2004). *ANSI/ASHRAE Standard 55-1992, Thermal Environment Conditions for Human Occupancy.*

HK-BEAM. (2003). *An Environment Assessment for New Building Developments.*

Kittler, R. (1996). Mechanical Dehumidification Control Strategies and Psychromatrics. *ASHRAE Transactions* **102:2**, 613-617.

Lam, C.J. and Hui, C.M. (1995). Outdoor design conditions for HVAC system design and energy estimation for buildings in Hong Kong. *Energy and Buildings* **22**, 25-43.

Lin, Z.P. and Deng, S.M. (2004). A study on the characteristics of nighttime bedroom cooling load in tropics and sub-tropics. *Building and Environment* **39:8**, 1101-1114.

Murphy, J. (2002). Dehumidification performance of HVAC systems. *ASHRAE Journal* **46:3**, 38-46.

Shirey, DB III. (1993). Demonstration of efficient humidity control techniques at an art museum. *ASHRAE Transactions* **99:1**, 694-703.

Westphalen, D. (2004). New approach to energy savings for rooftop AC. *ASHRAE Journal* **44:3**, 23-31.

HEAT AND NON-HEAT RECOVERY VENTILATION PERFORMANCE IN ENERGY-EFFICIENT HUD-CODE MANUFACTURED HOUSING

Michael Lubliner;[1] Andrew Gordon;[1] Adam Hadley;[2] Danny Parker[3]

[1] Washington State University Energy Program, Olympia, WA 98502, USA
[2] Bonneville Power Administration, Portland, OR 97208, USA
[3] Florida Solar Energy Center, Cocoa, FL 32826, USA

ABSTRACT

The Zero Energy Manufactured Home Project demonstrates and promotes innovative energy saving technologies to the manufactured housing industry and home buying public, while evaluating those technologies' energy performance. The project, funded by the Bonneville Power Administration, and the U.S. Department of Energy's (DOE) Building America Industrialized Housing Program (BAIHP), examines two 147 square meter ($m^{2)}$ (1600 ft^2) two-section manufactured homes, built by the same manufacturer, using an identical floor plan. Heating ventilation and air-conditioning (HVAC) measurements, envelope and duct leakage tests were conducted and remote monitoring equipment installed to track the performance of each home over a three year period.

Both homes were built in the summer of 2002 and sited in the cold, dry climate of Lewiston, ID. The Zero Energy Manufactured Home (ZEMH) has been built with highly efficient and cutting edge technologies including a photovoltaic system, sun-tempering, solar water heating, spray-in foam insulation, heat recovery ventilation, and Energy Star appliances, HVAC and lighting The comparison (ESTAR) home is built to Energy Star Program requirements as part of the Northwest Energy Efficient Manufactured Home program, which includes a quiet 20 watt whole house exhaust fan ventilation system. Energy Star is the most energy efficient home that meets the U.S. Department of Housing and Urban Development code available in the United States market today (NEEM).

This paper presents the field testing and monitoring results of both homes' heat recovery (HRV) and non-heat recovery (NHRV) ventilation system energy performance, based on in-situ monitoring data. Energy Gauge USA computer simulation software is used to compare the ventilation, envelope and duct leakage induced infiltration in the ZEMH and ESTAR homes. Anecdotal and occupant related observations are presented, along with some conclusions.

KEYWORDS

Heat recovery ventilation, indoor air quality, energy efficiency

INTRODUCTION

More than 200,000 factory homes are built in the United States each year to the federal manufactured housing standards (HUD 1994). Issues related to energy efficiency, heating, ventilation and air-conditioning standards and performance in these homes has been presented in previous AIVC papers (Lubliner 2000, 2003), (Persily 2003).

HUD code manufactured homes tend to be built tighter than site built homes, which is why codes require whole house mechanical ventilation systems. (HUD 1994), (TenWolde 1996), (Stevens 1997). HUD requires ventilation systems capable of ventilating the ZEMH and ESTAR homes be at least 26 liters per second (l/s) (56 ft^3/min). For these homes the sizing approach in the American Society of Heating, Refrigerating and Air-Conditioning Engineers (ASHRAE) Standard 62 (ASHRAE 2003) would require a comparable 29 l/s (61 ft^3/min).

The ZEMH was built with energy efficiency and renewable energy as a high priority, in an effort to evaluate proposed future energy efficiency targets. The BAIHP targets seek to demonstrate future whole house energy savings of 60-70 percent over current practice, while improving indoor air quality and durability. (Lubliner 1994) Energy modeling of the ZEMH suggests that it achieves the 60 percent target. The ESTAR home achieved the current BAIHP 30 percent target. Analysis that compares modeled and actual total and end-load technology energy use in ZEMH and ESTAR home is currently under way.

HVAC System Descriptions:

Heat Pump: Both the ZEMH and ESTAR homes are all-electric homes with HVAC systems located in the utility room. They both have 7 kilowatt (kW) (2 ton) ducted unitary air-to-air heat pumps with electric resistance backup. All heat pump components, including the outdoor coil, are located inside a small closet in the house. The heat pump draws air from the crawlspace, directs it across the outdoor coil, and exhausts it through the ceiling and roof cap. Investigations are currently under way to determine the heating and cooling performance of the heat pump compared with typical split system heat pumps and electric furnaces.

Ductwork: The heat pump duct system has a single return air grill located in the utility room. Supply ducts distribute conditioned air to floor registers in the other rooms via *riser* and *trunk* ductwork located above the floor insulation as shown in Figure 1. A *crossover duct* in the vented crawlspace connects the trunk ducts of the two home sections. The use of duct mastic and air-tight Icynene ™ foam floor insulation in the ZEMH ensures that the supply riser and trunk ducts are airtight and well within the indoor pressure and insulation boundary with minimal heat transfer between the house and the crawlspace. The ESTAR home has a leakier duct system as a result of the use of foil duct tape and because the ducts are located in a loose-fill insulation. Since 2003 all Energy Star homes in the Pacific Northwest are required to use mastic instead of tape to seal ductwork. The forced air distribution system introduces inefficiencies caused by conduction heat transfer between the ducts and the crawlspace, duct leakage to the crawlspace, and duct leakage induced infiltration. Duct leakage induced infiltration results when supply air duct leakage causes negative pressures within the home relative

to the outdoors. Supply duct leakage has been shown to be a significant contributor to uncontrolled air infiltration that increases with the HVAC operational time. (Palmiter 1992) (Persily 2000, 2003). During the winter heating season, longer HVAC operation time combined with greater stack infiltration result in high air change rates. In homes with leaky ducts and envelopes this can result in significant over ventilation and reduces the need for the continuous mechanical ventilation system to operate. The ZEMH's tighter ducts and building envelope reduce winter periods of *over ventilation* making the HRV an important component to the philosophy "build tight; ventilate right."
Table 1 provides a comparison of supply duct and envelope leakage in ZEMH and ESTAR homes using Duct Blasters™ and Blower Doors™ typically employed to test energy efficient homes. Both the ductwork and envelope are considerably tighter in the ZEMH. The difference in both total duct leakage and duct leakage to outside in the ZEMH show the ducts are tighter and that more air leaked through the ducts goes back into the house instead of the crawlspace.

HRV Operation: HRVs are typically used in cold climates to efficiently supply a steady flow of fresh outdoor air. As stale warm air is expelled, the heat recovery core warms the incoming fresh, colder air before it is distributed throughout the home. The result is a constant supply of fresh air, no unpleasant drafts, and greater home comfort. In addition to heat recovery and improved air quality, the HRV provides necessary ventilation while controlling excess humidity. The HRV in the ZEMH is a Venmar 3000™, which is designed to save energy while ventilating and providing High Efficiency Particulate Air Filters (HEPA) filtration of outside and re-circulated air. The Venmar 3000 has a replaceable HEPA filter and separate pre-filter.
The ZEMH HRV measured flow rates were 33-42 l/s (70-90 ft^3/min) of *fresh* outside air and exhausts a comparable amount of *stale* indoor air. The operation of the *balanced* HVR does not cause house depressurization and associated air leakage. Stale exhaust air is drawn through the heat exchanger core. The occupant controls include a normal mode for continuous operation 33 l/s (70 ft^3/min) and a higher *boost* mode that can be used by occupants when higher levels of indoor air pollutants are present 42 l/s (90 ft^3/min). The occupant controls also include a re-circulation mode where HEPA filtration occurs with no air exhausted or introduced and hence no ventilation. The Venmar HEPA 3000 promotes filtration and associated improved indoor air quality (IAQ), unlike many HRV systems specifically designed solely for heat recovery. The ZEMH HRV provides 66 l/s (140 ft^3/min), of re-circulated HEPA filtered air and mixes it with a measured 33 l/s (70 ft^3/min) of pre-heated outdoor air for a total of 104 l/s (220 ft^3/min) supplied to the home on normal speed. The 104 l/s (220 ft^3/min) delivered from the HRV is ducted 9 meters (30 ft) using 20 centimeter (8 in) diameter flexible plastic duct located under the attic foam insulation to a ceiling grill in the bedroom hallway at the other end of the home from the HRV return.

Defrost Mode: To ensure that the HRV does not freeze the HEPA 3000 employs a defrost mode with variable timing depending on the outside temperature. When the outside air temperature is between -5º C and -15ºC (23ºF and 5ºF), a mechanical damper shuts the outside air entering the HRV for six minutes every 30 minutes as the defrost mode. This allows the re-circulation air to warm the core. When the outside temperature

is between -15ºC and -27ºC (5ºF and -17ºF), the HRV runs in defrost mode for nine minutes every 30 minutes, and 20 minutes every 30 minutes when the outside temperature is below -27º C (-17ºF). (Forest) During 2003-2004, the HEPA 3000 was in defrost mode for about 9 hours.

HRV Distribution Effectiveness: The HRV duct design in the ZEMH is independent of the heat pump ducts and not directly ducted to bedrooms. Connecting the HRV to the heat pump ducts would require the 350 watt heat pump blower fan to operate continuously, causing electricity use of up to 3300 kilowatt-hours (kWh) per year. The ZEMH independent duct design reduces energy use. However, it also reduces spatial mechanical ventilation effectiveness in bedrooms when the heat pump is not operating. Research has shown that spatial ventilation effectiveness is improved as the central forced air heating/cooling system operates more frequently to mix the fresh air from the HRV with the indoor air. (Persily 2000)

Figure 2 shows the percentage runtime as a function of outdoor temperature for both the ZEMH and ESTAR home. As expected the runtime increases as the outdoor temperature gets lower during the heating season and increases as the outdoor temperature get higher during the air-conditioning season. The lower runtime in the ZEMH during heating is because the home is more energy efficient and both homes use identical heat pumps. The higher runtime in the ZEMH during the cooling season is a result of the occupant using the heat pump in air-conditioning mode more often in part due to dust, simplicity, and daytime occupancy. The ESTAR occupant relies more on opening windows at night to provide diurnal cooling, instead of using the heat pump. Both occupants will typically open windows when the outside temperature falls within this temperature range. When the heat pump system runs at night, occupants benefit from greater air distribution to the bedrooms. A Venmar duct accessory product currently under development will integrate both duct systems and allow for HRV fresh air to be supplied to all ducted rooms without requiring the operation of the higher wattage heating/cooling fan. This product will improve spatial ventilation effectiveness, will have no negative impact on heating and cooling systems if it uses the same ductwork, and will reduce fan energy use by not relying on the operation of the air handler blower. Another innovative ventilation control used to improve ventilation effectiveness in many energy efficient site built homes is the Fan Recycler™, which ensures that ventilation and indoor air are mixed by the existing forced air system a minimum set time period every hour, by monitoring the HVAC fan runtime. (Rudd)

HRV Maintenance and Operation: The HEPA filter is recommended to be replaced every year. The pre-filter of the HEPA cartridge, HRV core filters and inside of the HRV should be cleaned every six months. The difference in flow rates between the clean and dirty pre-filter was found to be less than 10%, with the HVR core 6-months old. The occupants were asked to run the HRV continuously and use the boost mode when they desired additional ventilation. The HRV in the ZEMH was operated primarily in normal mode. The boost mode was rarely used. The re-circulation mode eliminates outside air. This mode is intended for use during periods when outdoor pollutants are present. Instead of using the re-circulation mode, the occupants shut the HRV off because of

problems with dust, insects and barbeque smoke, which they associated with the HRV. These issues resulted in the HRV being turned off for extended periods of time during the summer of 2003. Discussions with occupants and resolution of problems resulted in HRV continuous operation in 2004-05.

HRV Efficiency: The tested HRV *net efficiency* is 56% provided by Venmar for the HEPA 3000. The net efficiency varies with outside air temperature and flow rate. While there is no industry approved method or test to evaluate the energy recovery efficiency of multifunction products such as the Venmar HEPA 3000, laboratory testing was conducted using CSA C439-00 C439-00 (Standard Laboratory Methods of Test for Rating the Performance of Heat/Energy-Recovery Ventilators) with some adaptations to take into account the impact of blending indoor air inside the unit. The net efficiency has been evaluated from the gross temperature recovery efficiency (defined as apparent effectiveness in CSA C439) to which several penalties were subtracted: unbalance factor, exhaust air transfer, casing air leakage, casing heat gain/losses, defrost energy (when applicable) and fan energy. (Forest)

The measured power consumption of the HRV blower motor in the ZEMH was 164 watts and 228 watts on normal mode and boost mode, respectively. The manufacturer reports that 85 percent of the heat generated from the motor is transferred to the incoming air downstream of the heat exchanger core with the remaining 15 percent transferred to the exhaust air downstream of the core. The high wattage of the Venmar 3000 blower is a result of the HEPA filtration option. Other small wattage Venmar HRV models such as the Duo 1.2™ do not employ HEPA filters and uses only 68 watts to provide 32 l/s (68 ft^3/min) at an 87 percent apparent sensible effectiveness at 0º C, (32º F).

NHRV: The ESTAR home utilized a Panasonic #FV-08Q2 Whisper Ceiling™ whole house exhaust fan. The fan is located in the utility room to provide non-heat recovery ventilation. The fan is designed and controlled to operate continuously. A circuit breaker must be turned off to disable operation. The exhaust flow rate was measured at 37 l/s (78 ft^3/min) using a flow grid that measures average velocity. Unlike the HRV, the NHRV fan causes a slight depressurization of the home relative to the outdoors. This depressurization causes outside air to enter the home via air leakage pathways in the thermal envelope and ductwork. The location of these leakage pathways dictates the spatial ventilation effectiveness associated with the NHRV system when the heat pump is not operating. Depressurization from the supply duct leakage and NHRV increases ventilation rates. The NHRV exhaust fan flow rate is added in quadrature to the stack effect because of changes in the vertical neutral pressure location. This results in higher flow rate capacity fan required to provide equal mechanical ventilation as the balanced HRV system. For the balanced HRV, the flow rate and stack effect are simply additive.

Energy Gauge USA Simulation: Energy Gauge USA version 2.4 was used to estimate the space heating, cooling and ventilation fan energy for the ZEMH and ESTAR homes as shown in Table 2a. Table 2b compares energy use for a variety of real and theoretical cases. All ventilation cases assume 33 l/s (70 ft^3/min). The difference between runs No.1 to No.2 in ZEMH and No.5 to No.6 in ESTAR show the energy savings associated with

not using the HEPA option when using an HRV. The difference between runs No.2 to No.3 in the ZEMH and No.6 to No.7 in ESTAR show the energy savings associated with the HRV over the NHRV. The difference between the Non-ventilation Case 8 over the other ventilation cases highlights the cost of ventilation to achieve improved IAQ. The ventilation system case comparisons in Table 2b indicate greater savings for the ESTAR home than the ZEMH. This is believed to be a result of ZEMH having both lower house and heat pump balance points.

Costs: The HEPA 3000 costs $1,100 U.S., Duo 2 costs $700 U.S. and the NHRV costs $150 U.S. These are costs of the equipment and do not reflect installation, and markups. The HEPA 3000 has a $100 U.S. annual maintenance cost to replace the HEPA filter. The other units have no annual maintenance costs; cleaning maintenance is assumed to be provided by the occupants at no cost. The useful life of these systems is unknown. It should also be noted that the HEPA filtration non-energy benefits to indoor air quality need to be considered when looking at first and operating costs. These benefits may include the avoidance of health care expenses—such as the cost of a respiratory inhaler and doctor visits—which can far outweigh the cost of energy recovery.

Conclusions:

- HRV systems can improve energy efficiency in new U.S. manufactured housing especially in homes with tighter duct and envelope systems.
- Low fan energy is a factor in HRV and NHRV systems energy performance.
- HRV systems with HEPA filtration require additional fan energy, but provide non-energy related IAQ filtration benefits.
- HRV and NHRV continuous operating systems provide effective ventilation IAQ filtration benefits with varying associated energy costs.
- Controls that reduce over-ventilation are needed especially in homes with leakier ductwork and envelopes (i.e. many non-ESTAR homes).
- Innovative controls and duct components that integrate heating/cooling ductwork with the HRV may improve spatial and temporal ventilation effectiveness.
- Cost analysis alone may not provide “apples-to-apples” comparisons in terms of IAQ benefits.

ACKNOWLEDGMENTS

This work is sponsored in large part by the U.S. Department of Energy Office of Building Technology’s Building America Industrialized Housing program under Cooperative Agreement DE-FC36-99GO10478. Special thanks to Daniel Forest, Venmar Ventilation Inc. Additional support has been provided by: The Bonneville Power Administration, the Florida Solar Energy Center, the Washington State University Extension Energy Program, the Nez Perce Tribe, Kit Manufacturing, Clearwater Homes and the Northwest Energy Efficient Manufactured Home Program

REFERENCES

American Society of Heating, Refrigerating and Air-Conditioning Engineers (1988) ASHRAE Standard 119-1988, Air Leakage Performance for Detached Single-Family Residential Buildings.
American Society of Heating, Refrigerating and Air-Conditioning Engineers (2003) ANSI/ASHRAE Standard 62.2, Ventilation for acceptable indoor air quality.

Canadian Standards Association (2000) CSA C439-00. Standard Laboratory Method Test for Rating the Performance of Heat/Energy Recovery Ventilators.
ECOTOPE 2003 Summary of SGC Manufactured Home Field Data 1997-98: Sitings in Idaho and Washington. Ectope, Inc., Seattle, WA.
Forest, D. Conversations with Danial Forest, Venmar AVS, 2005.
U.S. Department of Housing and Urban Development (1994) Manufactured Home Construction and Safety Standards, Part 3280. Washington, D.C.
Lubliner, M.; Stevens, D.T.; and Davis, B. (1997) Mechanical ventilation in HUD-code manufactured housing in the Pacific Northwest. *ASHRAE Transactions*, 103 (1), pp. 693-705.
Lubliner, M. et al (2003) Building Envelope, Duct Leakage and HVAC System Performance in HUD-code Manufactured Homes. *24th AIVC Conference Proceedings*. Brussels, Belgium.
Lubliner, M. et al (1997) Mechanical ventilation in HUD-code manufactured housing in the Pacific Northwest. *ASHRAE Transactions*, 103 (1), pp. 693-705.
Lubliner, M.; Gordon, A. (2000) Ventilation in U.S. Manufactured Homes: Requirements, Issues and Recommendations. *21st AIVC Conference Proceedings*.
Lubliner, M, et al (2004) Manufactured Home Performance Case Study: A Preliminary Comparison of ZeroEnergy and Energy Star. Performance of Exterior Envelopes of the Whole Building IX International Conference, American Society of Heating, Refrigerating and Air-Conditioning Engineers.
NEEM (2004) Northwest Energy Efficient Manufactured Home Program In-Plant Inspection Manual, Oregon Office of Energy.
Palmiter, et al (1992) Measured Infiltration and Ventilation in Manufactured Homes. Ecotope, Inc.
Persily, A.K. (2000) A Modeling Study of Ventilation in Manufactured Homes. National Institute of Standards and Technology, Gaithersburg.
Persily, A.K., et al (2003) Ventilation Characterization of a New Manufactured Home. *24th AIVC Conference Proceedings*. Air Infiltration and Ventilation Centre, Brussels, Belgium.
Rudd, Armin F.; Lstiburek , Joseph W. (2000) Measurement of Ventilation and Interzonal Distribution in Single-Family Homes. *ASHRAE Transactions 2000*, MN-00-10-3, V. 106, Pt.2., American Society of Heating Refrigeration and Air-Conditioning Engineers, Atlanta, GA.
Stevens, D.T; Lubliner, M; Davis, B. (1997) Mechanical ventilation in HUD-code manufactured housing in the Pacific Northwest. *ASHRAE Transactions*, 103 (1), pp. 693-705.
TenWolde, A.; Burch, D.M. (1996) Ventilation, Moisture Control, and Indoor Air Quality in Manufactured Houses. Forest Products Laboratory, National Institute of Standards and Technology.

Table 1: Duct & Envelope leakage and Ventilation System Flow Rates

Test	ZEMH	ESTAR
Envelope Leakage[1]	2.0 ACH @ 50Pa	3.6 ACH @ 50Pa
Total Duct Leakage[2]	145 CFM @ 25Pa (68 L/s @ 25PA) 15% of HVAC flow	211 CFM @ 25Pa (100 L/s @ 25PA) 20% of HVAC flow
Duct Leakage to Outside[2]	37 CFM @ 25Pa (17 L/s @ 25PA) 4% of HVAC flow	150 CFM @ 25Pa (71 L/s @ 25PA) 15% of HVAC flow
Whole House Ventilation	70 CFM (33L/s)[3]	78 CFM (37L/s)

[1] Tested per ASTM Standard E779-87
[2] Measured per ASHRAE Standard 152-2002
[3] Measured on low-speed with clean pre filter and 3 month old HEPA filter

Table 2a: Energy Gauge Simulation Energy Use Results							
Case	**Home**	**Type**	**Efficiency**	**Watts**	**Heat kWh/yr**	**Cool kWh/yr**	**Heat+Cool**
1	ZEMH	HEPA	56%	164	7124	286	7410
2	ZEMH	DUO	87%	70	5759	236	5995
3	ZEMH	NHRV	0%	20	7730	256	7986
4	ZEMH	NONE	0%	0	5045	204	5249
5	ESTAR	HEPA	56%	164	8523	455	8978
6	ESTAR	DUO	87%	70	7034	394	7428
7	ESTAR	NHRV	0%	20	9310	424	9734
8	ESTAR	NONE	0%	0	6268	358	6626

Table 2b: Case Comparisons	
HEPA filtration Cost:	**kWh/yr**
HEPA vs. Duo in ZEMH	1415
HEPA vs. Duo in ESTAR	1550
HRV Savings vs. NHRV:	**kWh/yr**
Duo vs. NHRV in ZEMH	1991
Duo vs. NHRV in ESTAR	2306
Cost of Vent vs. None:	**kWh/yr**
HEPA vs. None in ZEMH	2161
HEPA vs. None in ESTAR	2352
Duo vs. None in ZEMH	746
Duo vs. None in ESTAR	802
NHRV vs None in ZEMH	2737
NHRV vs None in ESTAR	3108

Figure 1: Cross Section of trunk, riser and crossover ducts

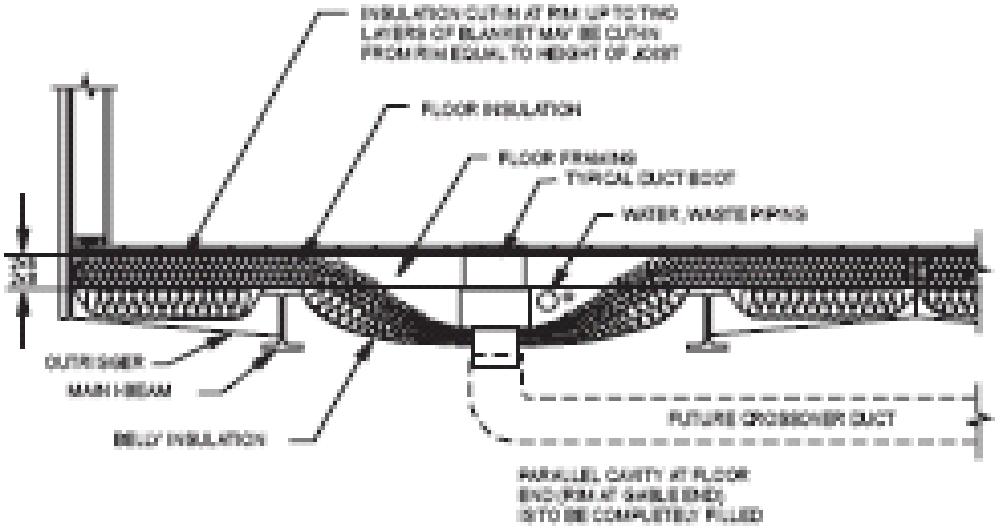

Figure 2: Run time of the ZEMH and ESTAR homes vs. Outside Temperature

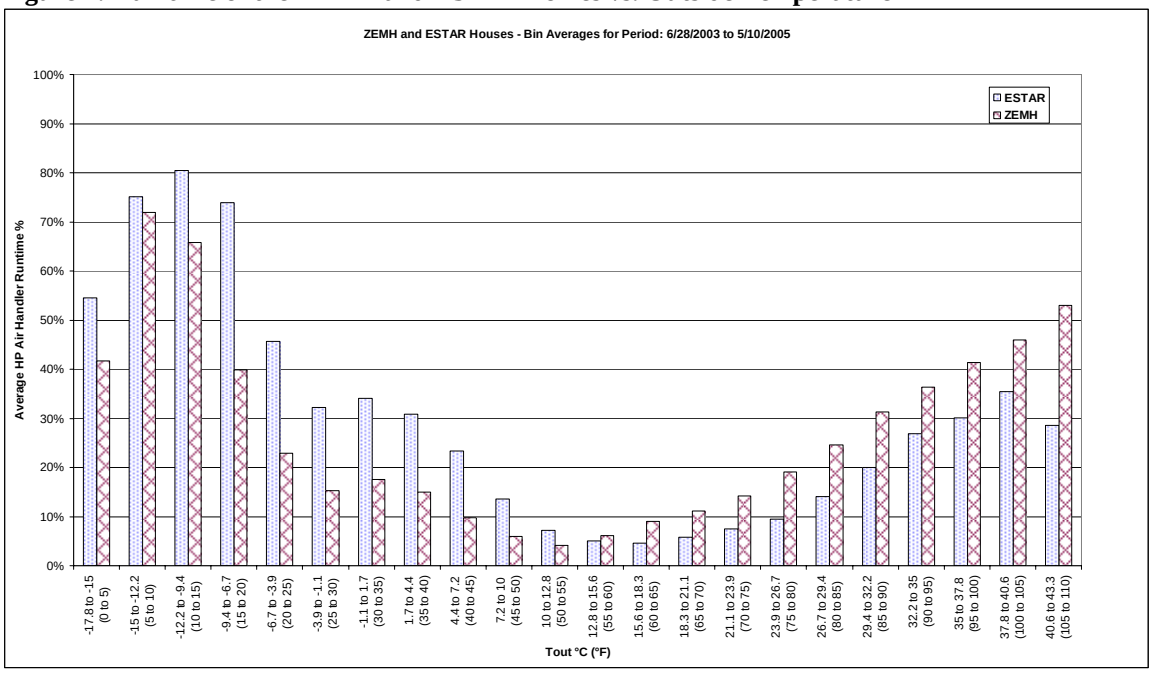

GUIDELINES TO IMPROVE EFFICIENCY OF A DOUBLE-SKIN FAÇADE IN AN OFFICE BUILDING

Elisabeth Gratia, André De Herde

Université Catholique de Louvain
Architecture et Climat
Place du Levant 1, B-1348 Louvain-La-Neuve
gratia@arch.ucl.ac.be, deherde@arch.ucl.ac.be

ABSTRACT

In these last years, a great deal of interest has been devoted to double-skin façades due to the advantages claimed by this technology (in terms of energy saving in the cold season, high-tech image, protection from external noise and wind loads).
Simulations where performed on building with and without multistory double-skin facades. The operation of this one must be obligatorily related to the climatic conditions as well external as interior.
To preserve comfort and reduce cooling loads, it is important to apply natural cooling strategies among which the natural ventilation.
Some argue that double façades are designed to improve natural ventilation in buildings by stack effect, and to allow this one where this is in general not possible due to high outdoor noise levels and/or high wind speed levels.
But a faulty operation of the double-skin façade openings can generate catastrophic scenarios such as the injection of the hot air of the double-skin façade in the offices as well as a contamination of the offices of the upper stages by the polluted air from the offices of the lower stages.
This study examines how improve efficiency of a double-skin façade in an office building during the different seasons in Belgium.

KEYWORDS

Double-skin façade; Thermal modelling; Office building; Natural ventilation.

INTRODUCTION

The double-skin façade is an architectural phenomenon driven by the aesthetic desire for an all-glass façade.
The transparency is often seen as the main architectural reason for a double skin façade, because it creates close contact to the surroundings. This in fact is also derived from a client's point of view saying that physical transparency of a company gives a signal of a transparent organization with a large degree of openness (Hendriksen et al., 2000)
This "emerging technology" of heavily glazed façades is also often associated with buildings whose design goals include energy efficiency, sustainability, and a "green" image.
The success of these façades also lies in that they admit a high degree of daylight and have an outdoor uniformity and attractive aesthetics.
The costs of double-skin façades are higher than normal façades, but claims of energy and productivity savings are used to justify some of them (Poirazis, 2004).
The recent advent of computers and other office equipments increased the internal heat gains in most offices. Highly glazed façade, often with poor shading, have become very common.

This, together with the extra heat gains from the electric lighting made necessary by deep floor plans, and the wider use of false ceilings, increased the overheating risk (Gratia et al., 2003)
In the 1990's, concern about global warming has resulted in a resurgence of interest in naturally ventilated offices (Allard, 1998), (Liddament, 1996), (Dickson, 1998).
On the other hand, there is an increasing demand for higher quality office buildings. Occupants and developers of office buildings ask for a healthy and stimulating working environment (Rennie et al., 1998). Mostly, that is provided by an air conditioning system. But in many cases, with some efforts to reduce internal gains (equipment well chosen and solar protections), natural ventilation may be sufficient to ensure good comfort levels in occupied buildings.
In that case, air conditioning system will not be necessary. This will result in considerable energy and cost savings and also indirectly in a reduced burden on the environment, since the use of energy is always associated with the production of waste materials (Wong et al., 2003).

Double-skin façades are already a common feature of architectural competitions in Europe; but there are still relatively few buildings in which they have actually been realized, and there is still too little experience of their behaviour in operation. There are many unknowns: optical and thermal modelling of these systems is not routine, and coupling heat transfer and air flow from an isolated façade system to the whole building is complex. A variety of thermal coupling strategies between the façade and the whole building must be adequately simulated.
More, it is extremely difficult to find any objective data on the performance of actual buildings implementing double-skin façades. Only, subjective claims abound in the architectural literature.
So, it is important to verify if use of natural strategies is yet possible when the building is equipped with a double-skin.

METHOD

TAS program

The simulations where realized with TAS. It is a software package for the thermal analysis of buildings. It is a complete solution for the thermal simulation of a building, and a powerful design tool in the optimization of a building environmental, energy and comfort performance (Jones, 2000).

Studied building

The simulations where realized on the building proposed in the frame of the subtask A of the Task 27 (Performance of solar façade components) of the International Energy Agency, Solar Heating and Cooling Program. Some modifications were made to adapt this one to the practices of Belgium.

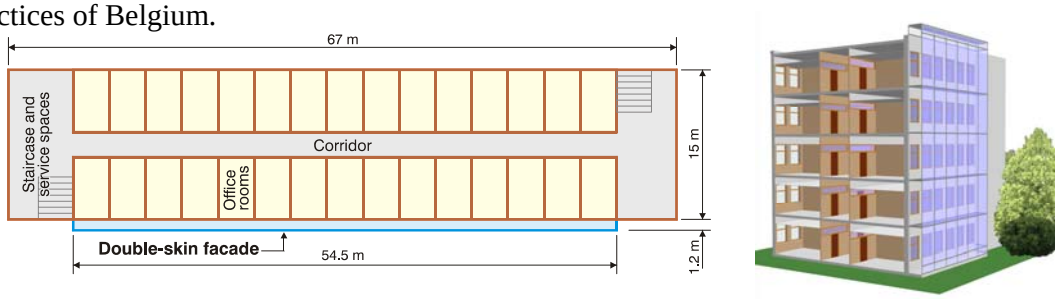

Fig. 1. View of the office building studied.

The building is a middle-size office building with office modules aligned on two façades, separated by a central corridor, with staircase/service spaces at both ends of the building.
The office building comprises 150 office modules, distributed over 5 floors and 2 orientations: 15 office modules per floor at each of the two orientations. The schemes are shown in Fig. 1.
Geometrical data of the office building are described here. Vertical cross section of office module with main measures is shown in Fig. 2.
The internal wall between office module and corridor has an openable window above the door to facilitate the air flow between northern and southern spaces (the false floor is not comprised in the drawing).
Each office has four windows (two top and two below) to allow natural day or night ventilation.

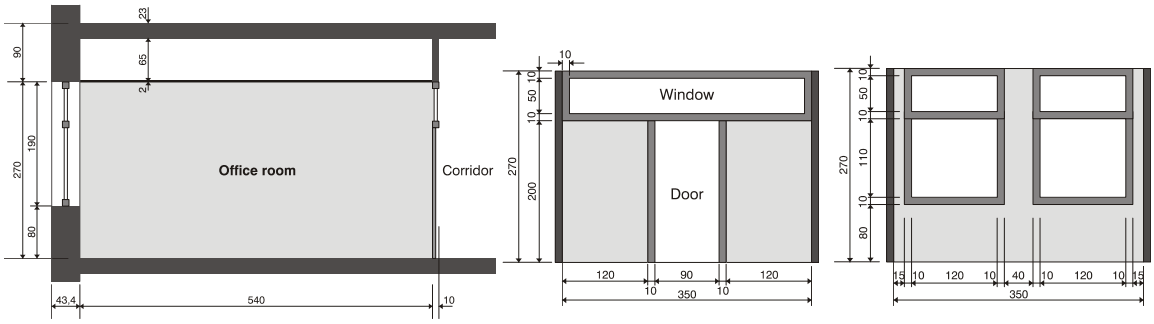

Vertical cross section of office module. Internal wall between office module and corridor. External wall of the office.

Fig. 2. Geometrical data of the office building.

Thermal characteristics:

Building envelope: Roof: U = 0.3 W m^{-2} $°K^{-1,}$ Ground floor: U = 0.379 W m^{-2} $°K^{-1,}$ Opaque part of façade: U = 0.373 W m^{-2} $°K^{-1}$
Low-e double glazing: U=1.8 W m^{-2} $°K^{-1}$, direct solar transmission: 0.62, total solar transmission: 0.708
Double skin: Clear single glass, U-value = 5.33 W m^{-2} $°K^{-1}$, shading factor = 0.76.
Width of the air cavity: 1.2m.
H (double-skin façade) = H (building) + 1m.
Internal gains in the offices: 29.37 W $m^{-2.}$

Climatic data assumptions.

We chose to analyze Belgian standard days (week day). Each modelled day is preceded by the simulation of ten previous days to take account of the effect of inertia.

RESULT OF RESEARCH – WHAT SHOULD BE DONE IN PRACTICE.

Sunny winter day (outside temperature evolves between 0°C and 5.8°C)

Building without double-skin takes directly profit from the solar gains and air exchanges between the sunny and no sunny zones can be privileged.
Heating demand is 539 kWh per day.

In building with double-skin, heating of South offices is useless except 1 or 2 hours the morning. Temperature in the closed DP is

- 34.5°C if shading devices are up
- 41°C if shading devices are down.

If overheating is observed in South offices, shading devices are sufficient to restore comfort.
A very small opening (slit of 2.5 cm) up and down in the double-skin generates great air flows and makes it possible to recover ±11 000 m³/h at 25-26°C. This air can be used as ventilation air of the no sunny zones.
The extraction of the air of the offices via the double-skin makes it possible to recover to air with ± 32°C, but this one must forward by an exchanger whose efficiency is about 0.5. This solution is slightly less profitable than the preceding one.
Heating demand is 438 kWh per day.

Cloudy winter day (outside temperature evolves between 0.8°C and 6.3°C)

In the two building, air exchanges between South and North zones imply a light increase in heating consumptions.
In building without double-skin, heating demand is 647 kWh per day.

In building with double-facade, double-skin must remain closed and temperature in the closed DP is 2°C moreover than the outside temperature. This air layer decreases the losses by transmission of the interior façade and protects this one from the losses by infra-red radiation.
Heating demand is 566 kWh per day.

Sunny spring day (outside temperature evolves between 8°C and 14.6°C)

Building without double-skin takes directly profit from solar gains and air exchanges between sunny and no sunny zones can be privileged.
If overheating is observed shading devices are sufficient to restore comfort. If necessary, little day ventilation removes the cooling need.
Heating demand is 95 kWh per day.

In building with double-skin, heating of South offices is useless due to the hot air layer provided by the double-skin. Indeed, temperature in the closed DP is

- 28°C if shading devices are up
- 32°C if shading devices are down.

Air exchanges between zones S and N allow to remove heating of North offices except 1 or 2 hours the morning. Shading devices are necessary when there are overheating.
Double-skin air can be used to ventilate the halls (only spaces having to be heated between 10 a. m. and 4 p. m.).
Day ventilation increase eliminates cooling needs,

- in southern offices: 3ach from 9 a. m. to 6 p. m.
- in northern offices: 2 ach from 12 a. m. to 2 p. m.

Heating demand is 45 kWh per day.

Sunny summer day (outside temperature evolves between 11.4°C and 23.3°C)

The table 1 compares the cooling load of the office building with and without double-skin façade. We suppose that the openings are adjusted to obtain a day ventilation of 4 ach and a night ventilation of 8 ach at all the floors.

TABLE 1
Comparison of the cooling load of the office building with and without double-skin façade.

	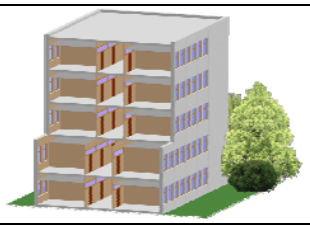	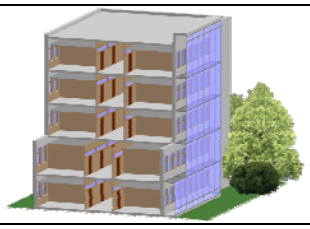
No cooling strategies	1033kWh/day	1147kWh/day
Shading devices	685kWh/day	Closed double-skin: 911 kWh/day Opened double-skin: 850 kWh/day
Day ventilation	Single-sided ventilation: 474 kWh/day. Cross ventilation: 608 kWh/day	Double-skin top windows opened: 805 kWh/day. Double-skin top and down windows opened: 771 kWh/day.
Night ventilation	Single-sided ventilation: 403 kWh/day. Cross ventilation: 425 kWh/day	Double-skin top windows opened: 721 kWh/day. Double-skin top and down windows opened: 665 kWh/day.
Day and night ventilation	Single-sided ventilation: 252 kWh/day. Cross ventilation: 358 kWh/day.	Double-skin top and down windows opened: 513 kWh/day.

Alas, the way in which the building with double-skin is crossed by the ventilation air is a function of the wind orientation and speed.
If double skin is on the windward side, the air flow in the building is due to the wind effect and the movement is reversed except at the lower stages where the stack effect dominates when only the top window of the double-skin is opened. In that case, the upper stages are partially contaminated by the air providing from the lower stages and the cooling loads are important. The cooling consumption for this sunny summer day is 986 kWh/day.
To improve the situation, top opening must be leeward oriented. Knowing the orientation of the wind, just open the window being in depression to improve cross ventilation in the good direction.
Fig. 3 gives the evolution (morning, midday, afternoon) of the zone air change rate during the day in each office for the various floors. When the air change rate is negative, the air flow is done in opposite direction.

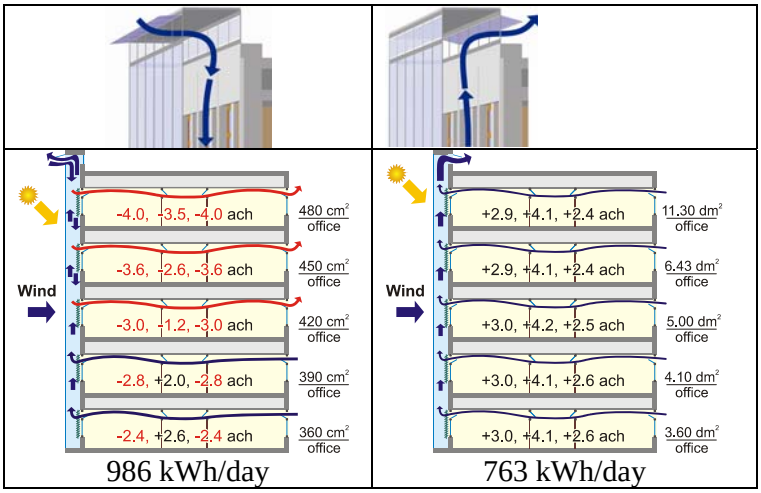

Fig. 3. Office air change rate and air movement when the sunny double skin is on windward side.

During the night, the cross ventilation is totally effective even if the direction of air flow in the building is reversed. Indeed, it is not important since the double-skin temperature is nearly the same than the outside temperature and since the reuse of the air arising from other offices is not a problem since they are not occupied and so not polluted during night.

Cloudy summer day (outside temperature evolves between 14.3°C and 18.1°C)

In the two cases, shading devices are not used because that would diminish daylighting.
With the application of the cooling strategies (day ventilation and night ventilation) cooling demand can be cancelled in building without double-skin.

In building with double-skin, cross day ventilation is effective if DP top opening is leeward oriented. Cross night ventilation is effective even if the direction of air flow is reversed. Indeed, it is not important since the double-skin temperature is the same than the outside temperature. Cooling demand is 181 kWh per day.

Sunny autumn day (outside temperature evolves between 15°C and 26.7°C)

In the two cases, external shading devices must be used, day ventilation is to prevent since outside temperature is upper than 24°C between 11.30 a.m. and 5 p.m. and night ventilation (8 ach) is effective.
In building without double-skin, cooling demand is 395 kWh per day.
In building with double-skin, the double-façade must be largely open (temperature in DP passes from 67°C to 31°C if there is an opening of 50 cm). So the cooling demand is 624 kWh per day.

CONCLUSIONS.

In winter, the air layer decreases the losses by transmission of the interior façade and protects this one from the losses by infra-red radiation
Moreover, if the double-skin is sunny, the air temperatures increase very quickly. This air can be used as ventilation air of the no sunny zones.

During the summer, when the sun is shining, it is difficult to apply the strategy of day natural ventilation. Indeed, cross day ventilation by extraction through the double-skin is delicate and is a function of the wind orientation and of the building wind protection.

REFERENCES.

Allard F. (1998). *Natural ventilation in buildings, a design handbook.* Altener project, James and James, London.
Dickson D. (1998). *Ventilation technology in large non-domestic buildings.* Air Infiltration and ventilation Centre, University of WarWick Science Park, Great Britain.
Gratia E., De Herde A. (2003). Design of low energy office buildings. *Energy and Buildings* **35:5**, 473-491.
Hendriksen, O.J., Sorensen, H., Svenson, A., & Aaqvist, P. (2000). Double skin façades – Fashion or a step towards sustainable buildings. *Proceedings of ISES*. Eurosun 2000.
Jones A. M. (2000). *EDSL Ltd, TAS*, Software package for the thermal analysis of buildings. 13/14 Cofferidge Close, Stony Stratford, Milton Keynes, Mk11 1BY, United Kingdom.
Liddament M. (1996). *A guide to energy efficient ventilation.* Air Infiltration and ventilation Centre, University of WarWick Science Park, Great Britain.
Poirazis H. (2004). *Double skin façades for office buildings* – Literature Review. Report EBD-R-04/3. Division of Energy and Building Design, Lund University.
Rennie D., Parand F. (1998). *Environmental design guide for naturally ventilated and daylit offices.* Building Research Establishment Ltd, Construction Research Communications, Ltd, PO Box 202, Watford, Herts, WD2 7QG.
Wong N., Mahdavi A., Boonyakiat J., Lam K. (2003). Detailed multi-one air flow analysis in the early building design phase. *Building and environment* **38:1**, 1-10.

Airflow simulations in double façades with a perforated inner sheet.

Regina Bokel, Truus de Bruin-Hordijk
Building Physics Group, Faculty of Architecture, Delft University of Technology
PO Box 5043, 2600 GA Delft, The Netherlands
Phone: ++31152784091; Fax: ++31152784178;
E-mail: R.M.J.Bokel@bk.tudelft.nl, G.J.deBruin-Hordijk@bk.tudelft.nl

Abstract
In today's architecture, innovative concepts, such as double skin facades, for the building skin are developed to improve the energy performance of a building and at the same time improve the indoor climate of the building. Various types of double façades can be distinguished. The glass sheets of a double façade, with sun-shading lamellas in between, can be completely air-tight or one of the sheets can allow air exchange with either the interior of the building or with the outside of the building. Double facade buildings are expensive on account of the extra glass sheet. But, most of the time, these buildings are prestigious buildings where economic arguments are not always decisive. For lower budget buildings, alternatives for the extra glass sheet are looked for. An inner sheet which consists of a textile material or consists of a perforated sunshade are possibilities. These options have the advantage that the inner sheet is also a sunshade, the disadvantage is that the view which the building's user has of the outside may be nearly blocked. In this paper cfd-airflow simulations are reported in double facades with an inner perforated sheet in order to research how the main airflow is interrupted by the holes. Naturally, a higher percentage of holes in a non-transparent sheet provides the building's user with a room with a view and also decreases the need for artificial lighting by providing daylight into the room.

1. INTRODUCTION

A double skin facade is said to improve the energy performance and the thermal comfort of a usually transparent building. In this paper double skin facades with an air exchange with the interior of the building (also called air flow windows) is investigated. In cold winters, this glass outer facade skin suffers from a cold downward airflow, thus causing cold feet for those persons sitting right next to the window. With a double skin facade the second skin decreases the cold airflow by forcing the warm air through the small inlet under the inner glass pane. This warmer air is then ventilated out at the top of the cavity. If the velocity of the warm air is high enough (thus the inlet small enough), this warm upward airflow counters the cold downward airflow and the air temperature right next to the double skin facade is significantly higher, thus creating a more comfortable climate for the inhabitants. In hot summers a sunscreen can be lowered in the cavity between the two skins. This sunscreen heats up and can reach very high temperatures. By ventilating this cavity, as in the winter situation described above, it is expected that the excess heat is ventilated out thus creating a cooler indoor climate and thus more thermal comfort.

Double facade buildings, however, are expensive on account of the extra glass sheet. But, most of the time, these buildings are prestigious buildings where economic arguments are not always decisive. For lower budget buildings, alternatives for the extra glass sheet are looked for. An inner sheet which consists of a textile material or consists of a perforated sunshade are possibilities. These options have the advantage that the inner sheet is also a sunshade. A woven cloth can also be perceived as an esthetical addition to the interior space. In addition, the acoustical qualities of a textile material are different from a standard glass pane. The disadvantage of using a non transparent screen, however, is that the view which the building's user has of the outside may be nearly blocked, which can cause disastrous effects [Hendriks, 2004] on the perceived thermal comfort. The benefits of a double skin façade have been shown for an inner facade skin that is impermeable to air, such as a glass inner facade skin. In this paper a screen inner facade skin is investigated. And screens, especially those made from woven or knitted textile

materials, are permeable to air. And permeable screens combined with a forced airflow can lead to totally different airflows in a room.

2. METHOD

2.1 Model geometry

In order to investigate the beneficial effects of an air flow window where the inner glass pane is replaced by a permeable sunscreen, computation fluid dynamics simulations have been performed. Due to increased computer power it is now possible to model the entire room and not only the airflow window. This is also necessary when a permeable screen is used. The room dimensions are 5.4 x 1.8 m2 and a height of 3.0 m, see figure 1. The distance between the outer glass pane and the screen is 0.1 m. The entire outer glass pane is made of glass with an U-value of 3.7 W/m2K. All other walls, the floor and ceiling consist of 0.2 m concrete. In the wall opposite the window an air inlet is constructed at a height of 0.5 above the floor and its size is 0.5 x 1.8 m2. On the outside of the air inlet the air has a temperature of 20 °C. At the top of the cavity between the outer glass pane and the screen an exhaust is modelled with a total forced air flow of 97.2 m3/h (54 m3/h per meter). Outside temperatures were 0 °C for the winter situation (an optimistic representation of the Dutch weather). According to the Novem regulations [Novem brochure], the opening under the screen is 5 mm for a cavity width of 0.1 m. The screen thickness is 5 mm. The inlet for the double skin facade should be over the entire width of the facade to obtain the least turbulent airflow in the cavity. The inlet should be positioned at the bottom for an upward air stream and the inlet should have a limited width (5 to 10 mm) depending on the air exchange rate of 20-60 m3/h per meter cavity width [Novem brochure].

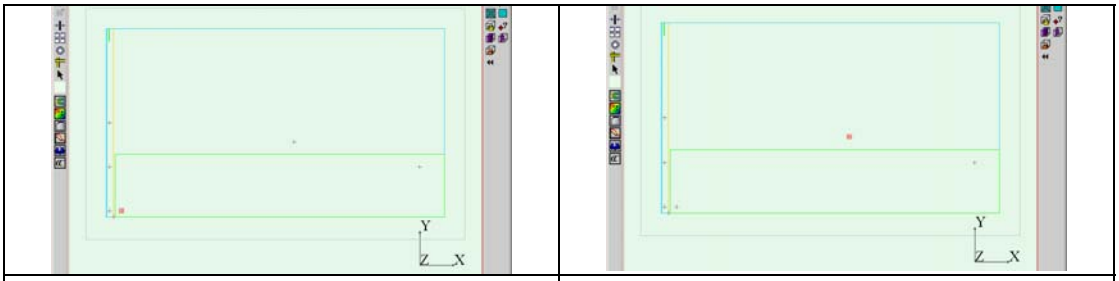

point 5 | point 6

Figure 1: Geometry of the model, the double façade is situated on the left.

2.2 Modelling characteristics

All CFD simulations have been performed with the commercially available package Flovent [Flovent manual]. As we are only interested in the air flow over the airflow window, thus only in the air flow perpendicular to the air flow window, all simulations were performed in only two dimensions. This also allows us to cut down significantly in computer time. All simulations have been performed with the turbulent k-ε model and rectangular grid. The minimum grid size is 2 mm, the maximum grid is 0.05 m in the horizontal direction and 0.01 m in the vertical direction. This leads to a total of around 67000 grid cells. The walls, ceiling and floor were modelled as adiabatic in the winter situation. The air inlet into the room is modelled as a planar resistance, due to convergence problems when both the air inlet and outlet are modelled as a fixed flow. This, however, has the disadvantage that it is possible for the air to flow out through the planar resistance, which is not expected to be a realistic situation. The sunscreen is modelled as an impermeable solid material for the reference simulations. The permeable sunscreen is modelled as a planar resistance with a given permeability. Although this

means that there is a homogenous permeability over the screen which will not always be the case in practical situations, results were interesting enough to mention in this paper. On the other hand, simulating clearly defined holes in the screen is much more difficult and will take much more computing time than available.

Eight variants, which are shown in figure 3 and table 1, were simulated. For reference reasons a room without a screen was modelled as well as a room with an impermeable screen. Further a screen with a permeability of 5 % and a screen that is impermeable at the top and the bottom and has a permeability of 15 % in the middle. All these screen variants were modelled in a winter situation, where the winter situation is also modelled with a heating device at the bottom of the cavity of 500 W.

3. RESULTS

From figure 2 it can be seen that there are significant differences between the different variants. The warm air from the air inlet in the wall will immediately rise up to the ceiling when there is no screen present. This is not surprising, as the downward airflow near the window is quite large due to the low U-value of the window and the low outside temperature of 0 °C. In the presence of an impermeable screen the warm air still rises up near the wall, but the small opening under the impermeable screen effectively counters the cold downward air stream near the window. This positive effect of the impermeable screen can also be seen when the temperatures are compared for the variants with and without an impermeable screen. The temperature near the screen in the room (point 5 in table 1) shows a temperature of 19.4 °C for the impermeable screen which is much higher than the temperature of 15.6 °C for the room without a screen. A permeable screen with only a permeability of 5 %, however, performs much worse than the impermeable screen. Both the airflow pattern and the temperature values resemble the situation without a screen. A permeable screen with only a permeability of 5% is thus not suitable to counter the effect of the cold downward airflow. The next variant is the variant where the screen is impermeable at the top and at the bottom. The bottom part is closed in order to contain the cold downward airflow behind the screen. The top is closed in order to prevent the warm air to disappear immediately though the top of the screen. The middle part is made more permeable to air, which for most screens also means that it is easier to look through, thus improving the inhabitants view. From figure 2 it can be seen that the downward airflow is indeed countered more effectively, and from table 1 it can be seen that the temperatures are higher than for the totally permeable screen, but the improvement is much less than the situation with the impermeable screen.

Screen	Winter, no heating			Winter, 500 W heating		
	T_ 5	T_6	T_exhaust	T_ 5	T_6	T_exhaust
No screen	15.6	17.3	17.6	23.7	21.3	20.9
Impermeable	19.4	19.6	13.2	21.0	21.1	21.2
5% permeable	14.6	17.8	17.1	21.5	21.6	20.2
0% - 15% - 0% permeability	15.2	18.2	16.0	21.7	21.7	19.9

Table 1: Temperature results for various screen configurations.

The more traditional way to counter the cold downward airflow near the facade. is to put a heater under the window. It is now investigated whether a combination of the traditional heater supplied at the bottom of the cavity with a power of 500 W over the entire width of 1.8 m and a screen will increase the thermal comfort. Again air with a temperature of 20 °C was available at the inlet in the wall opposite the window. The

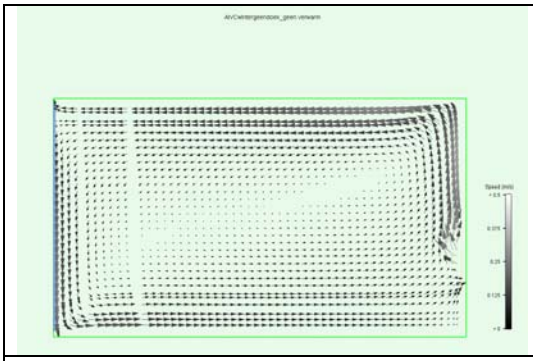	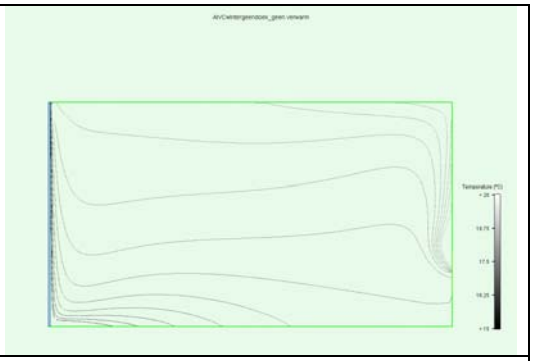
No screen	No screen
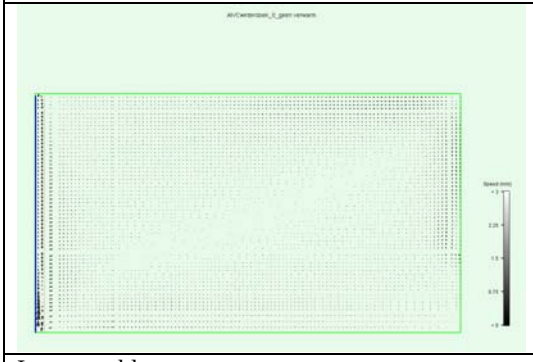	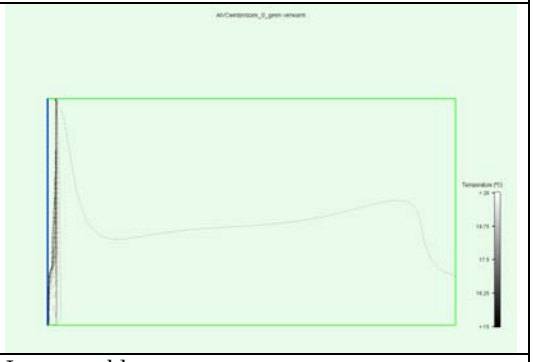
Impermeable	Impermeable
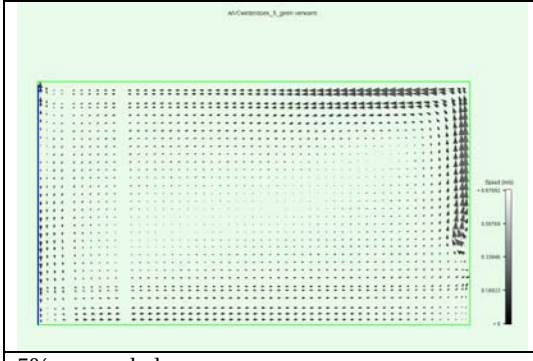	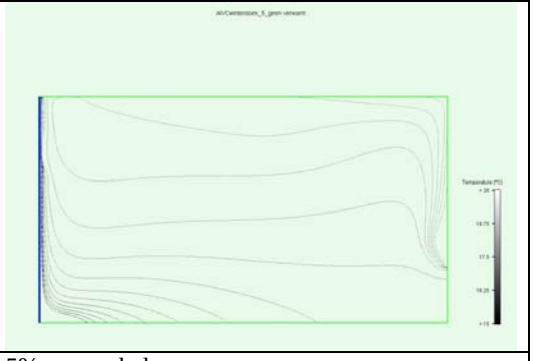
5% permeabel	5% permeabel
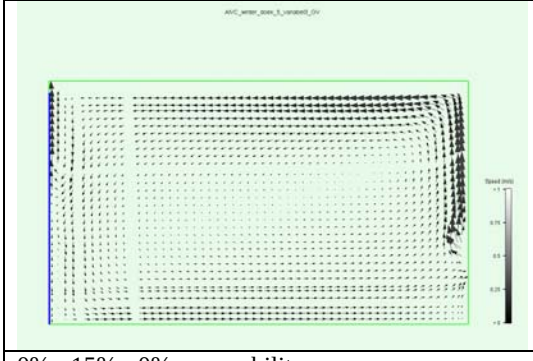	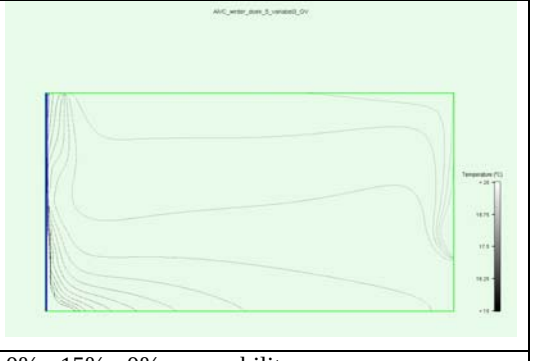
0% - 15% - 0% permeability	0% - 15% - 0% permeability

Figure 2: CFD simulations in the winter situation without heater for different screen variants. Left are the simulated air speeds, right the simulated isotherms.

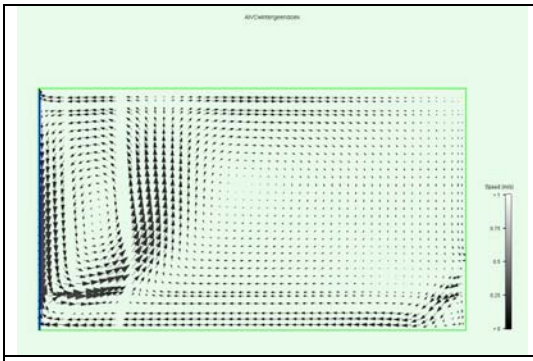	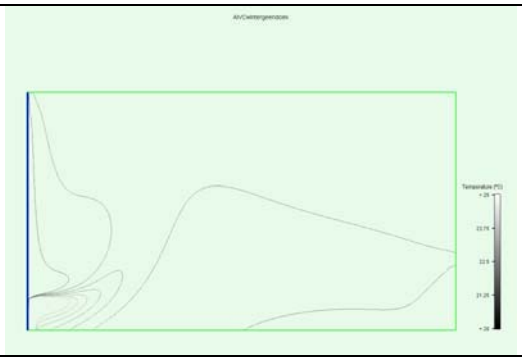
No screen	No screen
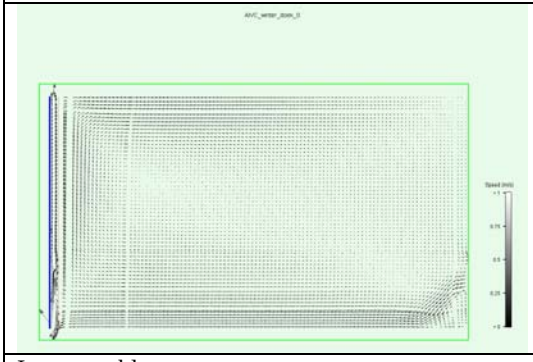	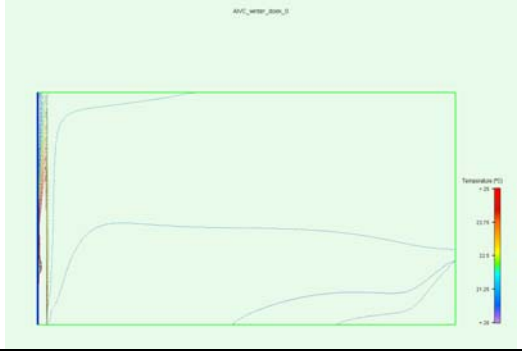
Impermeable	Impermeable
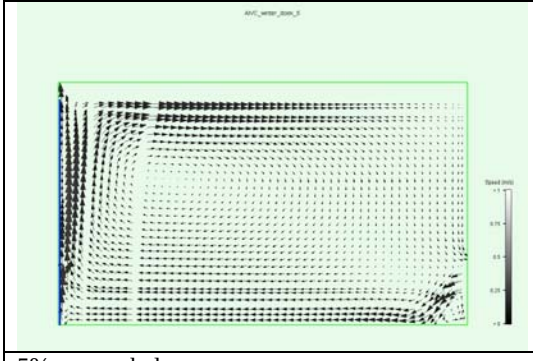	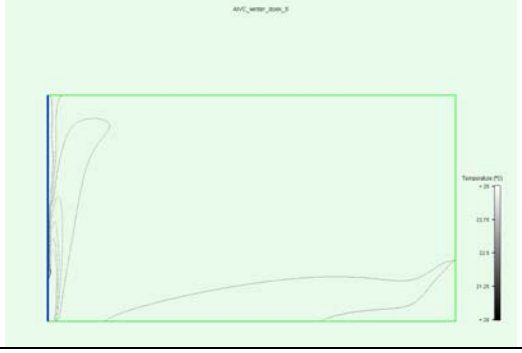
5% permeabel	5% permeabel
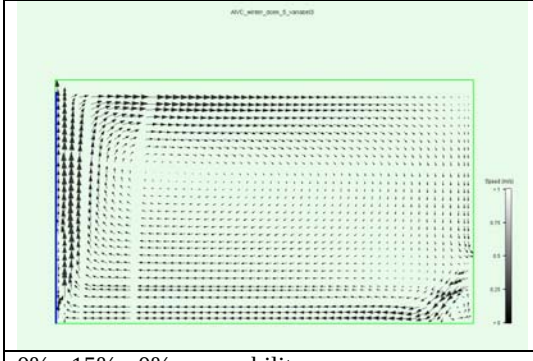	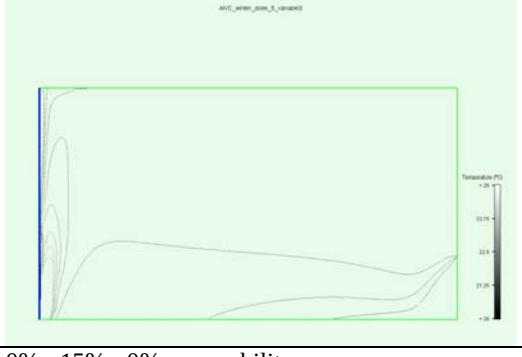
0% - 15% - 0% permeability	0% - 15% - 0% permeability

Figure 3: CFD simulations in the winter situation with 500 W heater for different screen variants. Left are the simulated air speeds, right the simulated isotherms.

results of these calculations are shown in figure 3 and table 1. Due to the presence of the heater all temperatures are higher than in the preceding variants without a heater. This is a positive thing as it should now be possible (not calculated) to decrease the inlet temperature, thereby saving energy which can be used for the heater. Comparing all 4 variants, there are no large differences in the temperatures. The presence of the screen does have an effect on the airflow, however. The screen combined with the low energy heater keeps the cold downward airflow contained in the cavity. In this situation the screen does improve the thermal comfort by creating lower air velocities near the screen. The inhomogeneous screen variant more effectively counters the cold downward airflow, as can be seen in figure 3.

4. DISCUSSION AND CONCLUSION

It was assumed that a screen, even one partly permeable to air, improves the thermal comfort in a room in winter. Problems were expected in the summer situation when the users of the building open the screen for view, thus allowing large amounts of solar heat inside, as reported for the Mercator building in Nijmegen (Netherlands) [Hendriks, 2004]. The initial aim of this research was to investigate various combinations of light and air permeability of the screen in order to improve both view and thermal comfort. However, problems in the winter situation already arose. The CFD-simulations show that the differences between no screen and a permeable screen are small when no extra heating is applied to counter the cold downward flow. When an additional heater is applied at the bottom of the cavity thermal comfort increases with the presence of a permeable skin. Likewise, Tanimoto and Kimura showed that thermal comfort with a screen second skin could be increases by increasing the amount of air flow. In both cases the inlet air temperature can be lowered and the energy saved in this way can be used to heat the heater at the bottom of the cavity or heat the larger volume of air flow. Thermal comfort is thus a very fine balance between the total amount of energy applied to the various air conditioning devices and the distribution of the total amount of energy over the various air conditioning devices.

CFD is very sensitive to the way in which the screen is simulated, as is already described by Safer et al. [2004] and simulations should preferably be checked with experimental data. However, simulations by Tanimoto and Kimura [Tanimoto and Kimura, 1997] using a more simple combined heat and air flow network model, showed that it was impossible to completely avoid the cold draft transmitted with a permeable screen during normal operating conditions, which supports the CFD predictions. Further simulational research should consider the influence of internal heat such as humans and computer, and the influence of infiltration through the edges of the screen.

A screen with a variable permeability creates better comfort in winter. When it is assumed that there is a strong correlation between the air and the view permeability of the screen, a better view is obtained with a more permeable area of the screen in the middle of the screen in the vertical direction. As a future project it is hoped to present the results of the summer situation with a permeable screen as well.

References

Flovent manual , www.flovent.com
Klimaatgevels, stand van de Techniek, brochure published by NOVEM
Hendriks N., Bouwwereld 15, 2004, in Dutch
Safer N, Woloszyn M., Roux J.J, 2004, Solar Energy
Tanimoto J., K. Kimura, Energy and Buildings 26, 1997

ATRIA FOR VENTILATION EFFICIENCY IMPROVEMENT IN URBAN OFFICE BUILDINGS

Chris J. Koinakis

Laboratory of Building and Construction Physics, Dept. of Civil Engineering, Aristotle University, 54006, Thessaloniki, Greece, e-mail: chrisko@civil.auth.gr

ABSTRACT

In this paper the effects of atrium and other similar architectural design features (e.g. shafts) on ventilation efficiency are examined in a multi-storey office building. Attention has been given to simulate the use of the main entrances, the vestibules and the various shafts. An atrium and an non atrium solution were compared for the examined building. Stack effect was the dominating force and wind effect was present yet not significant, but enough to produce negative pressures at the area of the atrium, mainly due to the form of the atrium's roof. Among others, it was concluded that the implementation of the atrium increased ventilation efficiency especially at the upper floors, generating incoming flows from the atrium and increasing the infiltration and ventilation rates, even for high density urban areas. The outcomes are useful for IAQ control during winter and for passive cooling during the summer. Special attention is needed to evaluate the user's behavior, since the effects proved to be intense and often overturn initial ventilation and energy design.

KEYWORDS: atrium, ventilation efficiency, stack effect, natural ventilation, simulation.

INTRODUCTION

The initial purpose of the atrium in ancient Greek and Roman architecture was to allow the daylight to penetrate and the smoke from fire to come out. This form was extended to a larger courtyard area in traditional middle-east architecture. The contemporary form of the atrium was firstly appeared during the 19th century where the cast-iron industry produced extensive iron frames which allow the use of extensive glazed areas. The use of the atrium in modern architecture was spread after 1960's and became popular in large commercial and office buildings, where it was used as a core circulation space (Bednar 1986, Saxon 1994). The last few decades there has been a vast increase in the use of air conditioning especially in urban office buildings, following the tendency to provide improved indoor environmental quality in both new and refurbished buildings in urban Mediterranean climates. Special attention has also been given to hybrid ventilation during recent research projects and several case studies were presented (Aggerholm 2002, Densante et al. 2002, Heiselberg 2002, Koinakis 2004).

In urban environments the possibilities of adjusting the building's envelope and form are usually very limited. In these cases the forming of atria inside a building could be a very effective tool to improve ventilation efficiency and to provide increased solar gains and day lighting capabilities. Atria could also help implementing passive control techniques, decreasing or eliminating the use of HVAC systems.

ATRIA AND OTHER ARCHITECTURAL FEATURES IN VENTILATION DESIGN

Several building architectural features can be utilized for natural ventilation design and most of them are already included in the architectural design. Shafts, elevator shafts, stairwells and chimneys should also be considered together with atria, because of the similarity of the

natural driving forces and the usually increased interactions among different type of building features. For example, shafts and stairwells should be examined as individual ventilation zones in order to avoid unwanted and uncontrolled interzonal flows between an atrium and a stairwell. The distribution of these building elements within the hole building is also important to control intezonal flows (Koinakis 2005). A description of the examined building is presented in Figures 1 and 2.

Shafts

In the examined building shafts are placed near the WC area to serve local ventilation demand without interfering with the rest of the building. The interaction between the shaft and the atrium is strongly depended on the combination of the openings (windows and doors) which are facing the shaft. The air supply at the shaft can be described be the exponential law:

$$Q = C\left(\Delta P\right)^{\frac{1}{2}} \tag{1}$$

The effect of the shaft in the examined cases is strongly depending on the combination of the opened or closed windows and doors between the shafts and the floor zones. The flow coefficients C in the above equation are 100 to 150 greater if the large openings are opened. In this case an interaction between the shaft and the atrium is significant and dispersion of indoor contaminants usually appears, because of the increased horizontal interzonal flows.

Elevator shafts

The modeling of elevator shafts has similarities with stairwells and atria. Experimental data for the flow characteristics in elevator shafts were not traced in the literature. Airtightness measurements implementing pressurization tests are only referred in literature within the frames of test protocols proposed during research projects, not evolving the effect of the lift-cage movement and the use of the elevator (CMHC 2005)

Atria

The atrium is modeled by dividing it vertically to separate zones with very low flow resistances (flow coefficient or shaft resistance less than 0.005). In this way the temperature variations along the atrium's height could be adequately modeled (Dols et al. 2002, Walton et al 2003).

The atrium's roof shape

The ventilation efficiency of the atrium is strongly related to the interactions between the atrium's roof shape, the configuration of the top of the atrium , the wind direction and the effect of the surrounding buildings. Wind tunnel studies were carried out to investigate the airflow performance of various atrium roof shapes for various urban densities (Sharples et al. 2001). It was concluded among others that the shape of the atrium roof and the orientation of the wind affects the ventilation differentials much more than the urban area density. For example a tilted roof with openings on it at the leeward side of a vertical obstacle appeared to produce the strongest pressure differentials for both 0^0 and 45^0 wind direction. These were also the conditions in the examined building. A more efficient roof design is needed to exploit Venturi effects or vortex generation effects but in this case detailed wind data of the close area are needed.

Use of doors.

In multi-storey office buildings a significant amount of airflow is incoming and outgoing from and to outdoor through the entrance doors at the ground level as well as at the floor entrances near the elevator and staircase shafts. Few studies about the air leakage and the large openings airflow through manually swinging doors and automatic sliding doors are

referred in the literature. This phenomenon also appeared at the building examined in this paper, where manual swinging doors were used in both ground floor main entrance and floor stairwell shaft entrances (Figure 1). The main entrance has two double doors with an intermediate vestibule and the floor stairwell shaft entrances have one double door. Due to the heavy use of the building (60 to 85 persons per 5 minutes, according to sample measurements during the peak hours), the entrance inflows and outflows are very important for the ventilation and the overall energy design. Sample velocity measurements at the building main entrance showed mean maximum values of 2.5 m/s ingoing flow during winter and 2.1 m/s during summer.

The use of the various doors was taken into account through the effective opening area. The effect of the use of the double door as a function of the people passing through the door, was simulated implementing the approximation equations of the average opening area proposed by K. Kohri for office building generally (K. Kohri 2001).

$$r = 1.0 - 0.26\exp(-0.036X) - 0.74\exp(-0.0091X) \quad \text{(only outside double door)} \tag{2}$$

$$r = 1.0 + 0.27\exp(-0.019X) - 1.27\exp(-0.0096X) \quad \text{(double doors with vestibule)} \tag{3}$$

where r= the average opening area ratio of doors and X= the number of people passing through the doors

In the case of the central entrance door with a vestibule, the opening area ratio could be calculated implementing the following equations proposed by Kohri (K. Kohri 2001).

$$r = \frac{Ae}{Ae\max}, \text{ where: } Ae = \frac{Cd}{\sqrt{\frac{1}{Ao^2} + \frac{1}{Ai^2}}} \text{ and } Ae\max = \frac{Cd}{\sqrt{\frac{1}{Ao\max^2} + \frac{1}{Ai\max^2}}} \tag{4}$$

where Cd is the discharge coefficient for the large opening (=0.65),
Ao, Ai are the actual opening area of the outside and inside door respectively [m^2]
$Ao\max$, $Ai\max$ are the maximum opening area of the outside and inside door respectively [m^2]

Simulation details

The air movement through an 8-storey building was simulated. For this purpose the multizone airflow model CONTAM was implemented (Dols et al. 2002, Walton et al 2003). The use of the main openings, the interaction of the building architectural features (e.g. shafts, atrium etc) and the air temperatures in various spaces as the result of the operation HVAC systems were obtained from measurements in the existing building. Hybrid ventilation with few low supply fans was the only ventilation system installed in the building. The effective opening area of the doors connecting the zones of the building (entrance, lobby, shafts and atrium) were obtained from in-situ sample measurements (passing persons per door) and from the implementation of the equations 2 to 4.

The elevator and the staircase are sharing the same lobby, while the atrium is independent from the rest of the shafts and extends from the 4th till the 7th floor (Figures 1 and 2). Two modes of door use were examined, one with moderate use and one with extensive use of the doors during peak hours. The wind effects were present yet not dominating, for the most common prevailing winds in the area (wind direction NNW and speed v=1.7m/s during December) for the existing dense wind environment in the location of the examined building. The airflow balance equations were solved for all the building zones.

As derived from Figures 3 and 4, on the lower floors the air enters from outdoors and from the lower parts of the shafts (elevators, staircases etc) and exits from the higher parts of shafts. On the higher floors the air enters from the shafts and the atrium and exits to the outdoor.

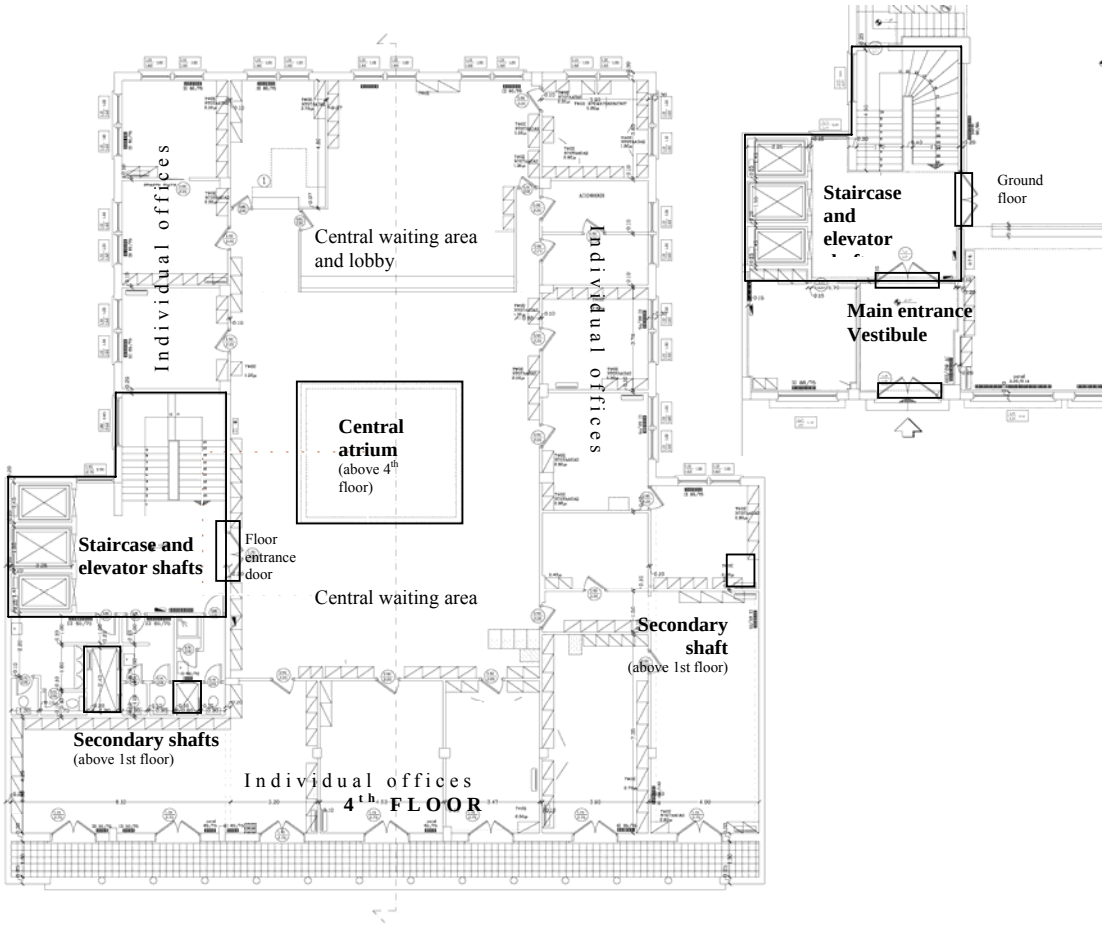

Figure 1. Left: Plan view of a representative floor of the examined building; upper right: main entrance and elevator shaft configuration in the ground floor. (Atrium, shafts and main entrances are highlighted)

RESULTS AND DISCUSSION

The parameters and the remarks mentioned in the above paragraphs were implemented during the simulations. The existing building was used for bulk and qualitative validation of part of the simulation results; special attention has been given to the validation of the direction of the interzonal flows and the zone air temperatures.

The simulations were presented for the two major traffic conditions: moderate and peak-hour use of the main entrances. Two building configurations were examined: one with an atrium above the 4th floor (existing case) and one with no atrium. The results are presented in Figures 3 and 4 for moderate and peak-hours use of main entrances, respectively.

As shown in the above figures the distribution of flows are triangle-like with outdoor air entering mainly at the lower floors and exiting at the higher floors. The outdoor flow rates are at the lower floor (incoming) and at the higher flow (upcoming).

The air change rate due to the incoming air flows from outdoors is 0.7 ach at the ground level. It is slightly increased compared to corresponding infiltration values of the building stock in

Greece according to relevant studies, (Papamanolis et al. 1996), because of the leaky entrance doors.

The atrium contributes significantly to the ventilation efficiency of the upper floors; most of the incoming air supply at the upper floors (approx mean value 55%) is entering from the atrium and not from the elevator and the other shafts. If no atrium exists, the incoming flows are only 0.5 ach/h of probably not fresh air from the lower floors through the shafts. This creates additional problems if the upper half floors are more crowded as in the existing building and therefore more fresh air supply is needed. If the peak-hours scenario is implemented, the incoming shaft flows appeared approximately 80% increased due to the extensive use of the elevators and of the main doors at each floor in both atrium and non atrium cases. Additionally, the triangle like flow and pressure distribution is disturbed due to the non uniform distribution of the traffic during peak hours in every floor. This is more likely to happen in the middle floors, because the interzonal flows there are weaker. For example the flows at the 4th floor are almost tripled during peak hours for both atrium and non-atrium cases. These phenomenon could be increased if there are vestibules at the main entrance of each floor (also see Sharples et al. 2001) .

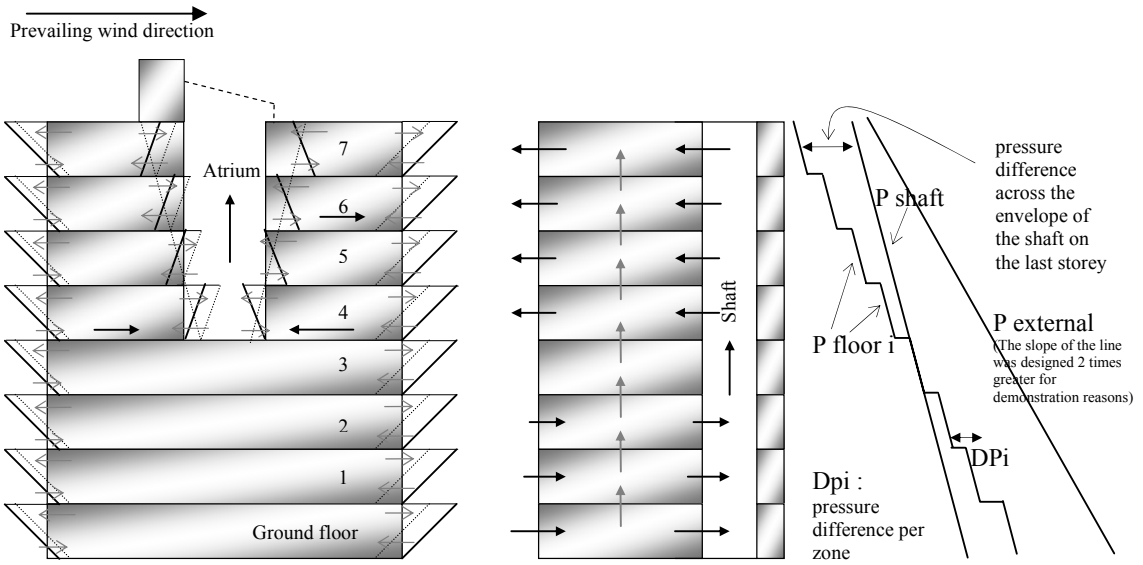

Figure 2. Pressure distribution and interzonal flows in the examined building; left: cross-section at the area of the atrium; middle: cross section at the area of the main shafts; right: internal and external pressure differences (slope lines)

It is therefore clear that it is not always true that "the more you open doors, the more you refresh". On the other hand, it could be said that the incoming flows from the lower floors to the higher floors through the shafts are less contaminated, due to the higher ventilation rates as a result of the extensive use of external doors. This hypothesis is not usually true because the indoor contaminant emissions are also increased due to the crowd. Documented results can be derived only after detailed simulation of the contaminant emissions and validated by proper measurements.

CONCLUSIONS AND FURTHER WORK

The main scope of this paper was to investigate the effects of atrium and other similar architectural design features (e.g. shafts) on ventilation characteristics and the interzonal flows in the zones of a multi-storey office building, for specific conditions and opening area

of frequently used entrance doors in an office building. Simulation results agreed well with the bulk in-situ measurements which carried out mainly for qualitative assessment (e.g. validation of the direction and the magnitude of the interzonal flows). Stack effect was the dominating force and wind effect was present yet not significant, but enough to produce negative pressures at the aria of the atrium, mainly due to the form of the atrium roof. The simulation of the use of the main entrances based on data from literature and sample in-situ measurements proved essential for reliable simulation and affected the ventilation efficiency dramatically. The outcomes are useful for IAQ control during winter and for passive cooling during the summer.

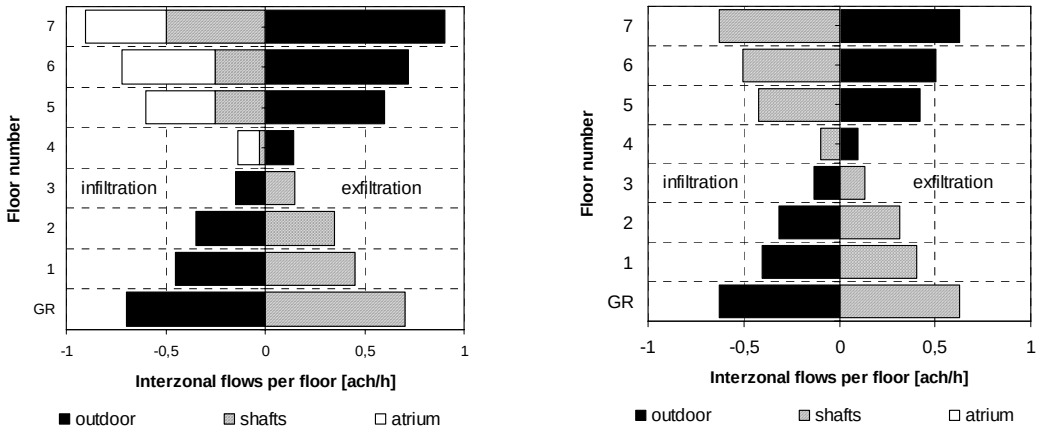

Figure 3. Flow balance per floor for moderate use of main entrances. Left: building with atrium above the 4th floor (existing case). Right: building without the atrium.

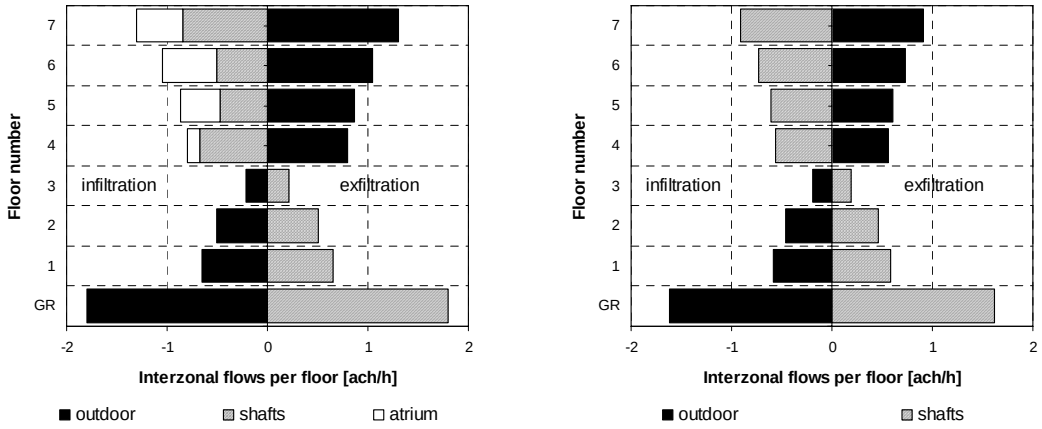

Figure 4. Flow balance per floor for peak-hours use of main entrances. Left: building with atrium above the 4th floor (existing case). Right: building without the atrium.

It was concluded, among others, that the implementation of the atrium increased ventilation efficiency especially at the upper floors creating incoming flows from the atrium and increasing the infiltration and ventilation rates, even for high density urban areas. The process of the simulation results in the form of flow balance per floor, appeared to be practical and comprehensive for the estimation of the airflow effects and for the comparison with the literature.

This work could be further deployed implementing ventilation strategies related to the use of atrium and shafts in the overall energy design. Further experiments and simulations are to be prepared by the author on energy efficient use of atrium in office buildings during winter and summer period. Further work is needed for the evaluation and the simulation of the user behavior, since the effects proved to be intense and sometimes overturn critical design parameters.

REFERENCES

Aggerholm Søren, (2002). Technical report: Hybrid Ventilation and Control Strategies in the Annex 35 Case Studies. Danish Building and Urban Research and IEA Energy Conservation in Buildings and Community Systems.

Bednar M.J., (1986). The new atrium. McGraw-Hill Book Company, New York.

CMHC (Canada Mortgage and Housing Corporation), Technical Series 98-123, (www edition 2005). Establishing the Protocol for Measuring Air Leakage and Air, Flow Patterns in High-Rise Apartment Buildings. Canada.

Densante A., Vic T.A. (editors) (2002). Hybrid ventilation, State of the art review. IEA, Energy Conservation in Buildings and Community Systems, Annex 35 Hybrid Ventilation in New and Retrofitted Office Buildings.

Dols S.W., Walton G.N., (2002). CONTAMW 2.0 User manual. National Institute of Standards and Technology, U.S.A.

Heiselberg Per (editor) (2002). Principles of hybrid ventilation. IEA, Energy Conservation in Buildings and Community Systems, Annex 35 Hybrid Ventilation in New and Retrofitted Office Buildings.

Kohri Kimiko, (2001). A simulation analysis of the opening area of entrance doors and winter airflow into the entrance door of a high-rise office building. 7th IBPSA conference, Rio de Janeiro, Brazil, August 13-15, pp 1017-1022.

Koinakis C.J., (2004). Ventilation retrofitting of public office buildings in Greece. 25th Conference of the Air Infiltration and Ventilation Centre, "Ventilation and Retrofitting", pp 43-50, Prague, Czech Republic.

Koinakis C.J. (2005). The effect of the use of openings on interzonal air flows in buildings: An experimental and simulation approach. Energy and Buildings, Elsevier, volume 37, number 8, pp. 813–823.

Liddament Martin W., (1986). Air Infiltration Calculation Techniques – An application Guide. Air Infiltration and Ventilation Centre, Bracknell, Berkshire, UK.

Papamanolis N., Koinakis C., (1996). Air change rates in buildings in Greece. International Conference on Protection and Restoration of the Environment III, Chania, pp 517-524, Greece.

Saxon R., (1994). The atrium comes of age. Longman, London.

Sharples S., Bensalem R., (2001) Airflow in courtyard and atrium buildings in urban environment: a wind tunnel test. Solar Energy, Vol. 70, No. 3., pp 237-244.

Walton G.N., Dols S.W., (2003). CONTAMW 2.1 Supplemental User Guide and Program Documentation. National Institute of Standards and Technology, U.S.A.

APPLICATION OF PHOENICS TO ATHLETIC HALLS WITH HVAC VENTILATION

O. I. Stathopoulou[1] and V. D. Assimakopoulos[2]

[1]Department of Applied Physics, Faculty of Physics, University of Athens, Build. Phys. 5, University Campus, 157 84 Athens, Greece.

[2]Institute for Environmental Research and Sustainable Development, National Observatory of Athens, I. Metaxa & V. Pavlou str., 152 36 Athens, Greece.

ABSTRACT

The commercial general - purpose Computational Fluid Dynamics (CFD) code PHOENICS is used to study the indoor environmental conditions of a large, mechanically ventilated, athletic hall. The indoor space of the building was simulated in the PHOENICS environment and computations were validated against experimental data obtained during a ten-day campaign in the hall. Data included measurements of airflow characteristics at different indoor locations under different ventilation conditions. Having obtained good agreement from comparing computed and experimental results, different ventilation scenarios of air-conditioning, heating and cooling, were applied in the model to investigate the air velocity and temperature patterns prevailing in the hall in each case. Computed results showed dynamic airflow and temperature patterns significantly altering with the different considered scenarios. Temperature stratification was evident, while distinct recirculating vortices characterized the airflow fields originating from the ceiling air inlet fans of the ventilation system.

KEYWORDS

CFD model, large enclosure, HVAC, indoor conditions, IAQ.

INTRODUCTION

In the last decades indoor air quality has become a public health concern. Research community have concentrated on the measurement of pollutants concentrations in closed spaces such as offices and homes (Lee et al (2002)) with a view to compare different indoor environments and identify pollution sources. Other studies have dealt with the relation of indoor pollutants concentrations to ventilation characteristics (Guo et al (2004)). At the same time CFD codes have become a useful tool in the research field of air quality. They have been applied to environmental studies of wind flow and pollutant dispersion around buildings, to investigations of indoor airflow fields for building design and optimum ventilation purposes (Xing et al (2001)) as well as to simulations of pollutants dispersion in working areas for health and safety reasons (Duci et al (2004)). However, few studies combine theoretical and experimental approaches and little has been done on studying environmental conditions inside large enclosures such as stadiums and athletic halls where many people congest and athletes train and compete while their performance can be affected by the quality of breathing air. Good ventilation and air quality conditions in such places are very important. Since metabolism is intense, supply of fresh air is necessary for achieving comfort conditions. Therefore, this study investigates numerically and experimentally the airflow, temperature and pollutants concentrations fields prevailing in a large mechanically ventilated athletic hall under different ventilation conditions.

METHODOLOGY

Experimental Procedure

A ten-day period experimental campaign in the frame of a national research project took place in an indoor basketball hall built in 2000 and situated in the eastern suburbs of the urban complex of Thessaloniki-Greece. Parking areas and auxiliary athletic facilities surround the hall, while the close vicinity includes heavy-traffic roads at about 500m and the sea at about 1km to the southwest. The building is 30m high, the surface of the arena is 1125m^2 and the capacity of the hall is 8,000 spectators. The windows are normally closed and the Heating – Ventilating – Air Conditioning (HVAC) system operates when necessary. Measurements were taken at different locations in the hall with the HVAC system in operation. Instrumentation included DANTEC FlowMasters (type 54N60) for spot mean air velocity, temperature and turbulence intensity measurements at sets of 1-min. Surface temperatures of indoor materials were measured with infrared thermometer (COLE & PARMER, type 08406) and CO_2 concentration measurements were taken with portable instrumentation (IAQRAE PGM – 5210, indoor air quality monitor).

Theoretical Model – Initial and Boundary Conditions

The PHOENICS CFD code (Spalding (1981)) solves the time averaged conservation equations of mass, momentum, energy and chemical species in steady three-dimensional flows.

$$\frac{\partial}{\partial t}(\rho\Phi) + div\{(\rho\upsilon\Phi - \Gamma_\Phi\, grad\ _\Phi)\} = S_\Phi \qquad (1)$$

where ρ, υ, Γ_Φ and S_Φ are density, velocity vector, "effective exchange coefficient of Φ" and source rate per unit volume, respectively. The discretization of the domain is followed by the reduction of the previous equations to their finite domain form using the "hybrid formulation of the coefficients" and the solution technique employs the SIMPLEST algorithm (an improved version of the well-known SIMPLE algorithm). The standard k-ε turbulence model is applied, while buoyancy effects are considered. To improve convergence, under-relaxation was used.

A three-dimensional rectangular enclosure was considered in Cartesian coordinate system as seen in Figure 1. For symmetry reasons, only one fourth of the indoor space was modelled. The dimensions of the objects modelled are real and geometry is as detailed as possible according to the building's plans and the mechanical ventilation system's blueprint, always taking into account computational efficiency. The domain size is 45m x 45m x 22m and it includes 81 rows of spectators' seats, 23 circular air-inlet fans at the ceiling and 8 air-outlets close to floor level.

The cases studied are as follows and the specific settings for each case are given in Table 1. (1) Basic Case: This case corresponds to a selected day from the experimental campaign. The hall is empty and the HVAC system operates in the air-conditioning mode, without heating or cooling. (2) Heating Case: This case is same as Basic Case, while the HVAC system operates in the heating mode. (3) Cooling Case: This is a hypothetical case of a typical summer day in Thessaloniki-Greece. The hall is considered empty and the HVAC system operates in the cooling mode.

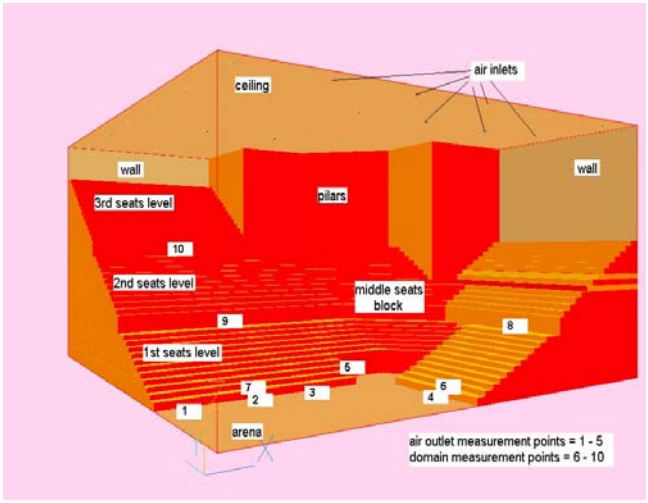

Figure 1: Geometrical domain – Basic

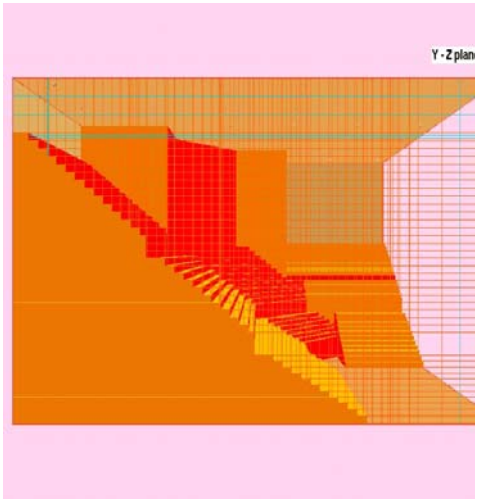

Figure 2: Grid view on Y–Z plane - Basic

The boundary and initial conditions are: (a) Fresh air comes in the hall via the ceiling circular fans (Figure 1), the diameters of which are either 0.4m or 0.63m and mean (axial along -z) velocities and turbulence intensities range from 1.18 to 3.38 m/s and 13 to 31 %, respectively, according to the experimental measurements. (b) The X – Z and Y – Z planes of the domain have symmetry boundary conditions (Figure 1). It is also important to note that many efforts were made to achieve the best balance among convergence, grid independency and saving of run-time due to the very complex domain geometry (Figure 2).

TABLE 1
Information and initialization data. The asterisk (*) corresponds to experimentally measured data.

DATA	BASIC	HEATING	COOLING
Grid cells	71x107x46	71x107x46	71x107x46
Min cell size (m)	0.63x0.42x0.48	0.63x0.42x0.48	0.63x0.42x0.48
Inlet air temp. (^{0}C)	*20.7 – 21.3	*28.8	20
Initial air temp. (^{0}C)	*20.2	*18.15	28
Ceiling surface temp. (^{0}C)	*22	*22	31
Floor surface temp. (^{0}C)	*19	*19	27
East wall surface temp. (^{0}C)	*20	*20	28
North wall surface temp. (^{0}C)	*20	*20	28
Pillars temp. (^{0}C)	*17 - 20	*17 - 20	29
1^{rt} seats level temp (^{0}C)	*18	*18	28
2nd seats level temp (^{0}C)	*18.5	*18.5	29
3rd seats level temp (^{0}C)	*19	*19	30

TABLE 2
Measured and computed velocities and temperatures at measurement points of the domain in Basic Case.

Measurement points of domain	V_{exp} (m/s)	V_{th} (m/s)	T_{exp} (^{0}C)	T_{th} (^{0}C)
1 (air-outlet)	0.43	0.34	21.8	19.3
2 (air-outlet)	0.41	0.20	21.3	19.3
3 (air-outlet)	0.31	0.21	21.5	19.3
4 (air-outlet)	0.19	0.32	21.6	19.3
5 (air-outlet)	0.42	0.25	21.6	19.4
6 (arena level)	0.09	0.06	20.2	20.7
7 (arena level)	0.12	0.10	19.9	20.8
8 (above 1^{rt} seats level)	0.20	0.20	20.2	20
9 (above 1^{rt} seats level)	0.23	0.02	20.4	19.3
10 (above 2nd seats level)	0.29	0.33	20.6	20.9

RESULTS AND DISCUSSION

(1) Basic Case: Computed results of Basic Case present good agreement with experimental results. Table 2 gives the measured and computed velocities (V_{exp} and V_{th}) and temperatures (T_{exp} and T_{th}) at several points of the domain including air-outlets and points at the arena and the seats levels. The disagreement observed for velocities at points 9 and 4 is attributed to the geometric complexity of those areas, which could not be modelled in detail. It is also observed that comparison between computed and measured temperatures at domain points 6 – 10 is better than at the points close to the air abductors of the HVAC system (air-outlets: 1 – 5). Since theoretical results are physically plausible, giving the highest temperatures at high levels and the lowest ones at low levels, the previous difference is attributed to ineffectiveness of the HVAC system in conjunction with certain modelling simplifications that had to be made for computational economy reasons. The airflow field formed in the hall is quite interesting. Figure 3 displays a vector plot of velocity on a Y-Z plane extending from a row of air-inlet fans at the ceiling. Air jets squirt from the ceiling air-inlets with maximum velocity 3.2m/s decreasing to 0.2 m/s at approximately 6.5m above the arena floor. Moving up from 1st seats level to 3rd seats level, jets become more intense with higher velocities reaching 0.9 – 1.3 m/s close to the spectators at the 3rd seats level and 1.5 m/s at the upper seats. Furthermore, large vortices are formed between air jets with air velocity being less than 0.2 m/s, which become more distinct above the seats.

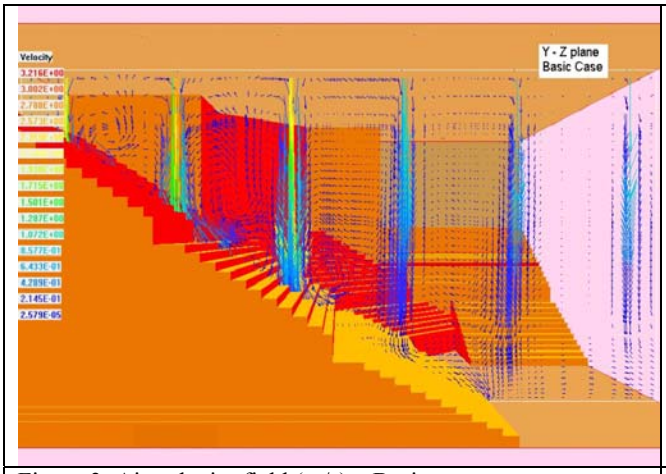

Figure 3: Air velocity field (m/s) – Basic

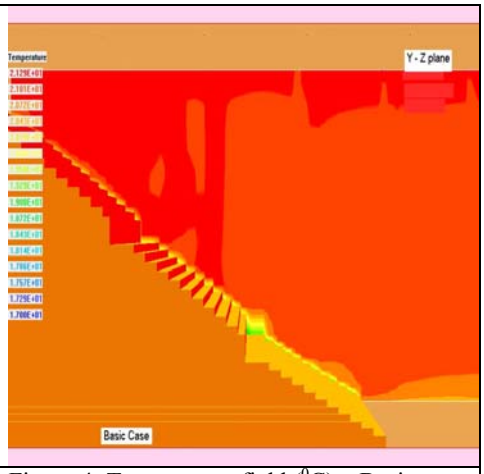

Figure 4: Temperature field (^{0}C) – Basic

Regarding the temperature field, a smooth stratification is formed in the hall ranging from 17 to 21^{0}C (Figure 4). The highest temperatures appear close to the ceiling and the upper seats, while the lowest ones are observed very close to the floor and the air-outlets. It is finally interesting to note that mean air velocity and temperature at the height of 2m above the arena where the athletes train and compete are 0.07 m/s (which is considered very low, according to ASHRAE standard) and 20.8^{0}C, respectively.

(2) Heating Case: This case corresponds to a certain experimental day for which measurements of air velocity and temperature are only available for point 2 – air outlet (Figure 1). Experimental results give 0.48 m/s and 20.2^{0}C for velocity and temperature, while computed results give 0.2 m/s and 21.37^{0}C, respectively. Regarding the air velocity (Figure 5) and temperature (Figure 6) fields prevailing in the hall, they are considerably altered with respect to those in the Basic Case. Temperature stratification is enhanced with values ranging from 17 to 29^{0}C (Figure 6). Warm air jets penetrate to a depth of about 7.5m above the arena and the 1st seats level, while they reach spectators at the upper seats. The highest temperatures

appear close to the ceiling around the jets and at the upper seats, exceeding 26^0C. Such temperatures are observed above the arena and the 1st seats level only at a height of over 10m. Furthermore, temperature decreases to 25^0C at about 0.8m from the floor and become even lower only very close to the surfaces and the air-outlets. It is finally interesting to note that mean air velocity and temperature at the height of 2m above the arena where the athletes train and compete are 0.05 m/s and 25.2^0C, respectively. Owing to the enhanced temperature stratification, air jets originating from the ceiling air inlet fans have smaller penetrating depths, compared to the Basic Case, reaching approximately 13m above the arena and the 1st seats level (Figure 5). Prevailing velocities appear very low (less than 0.05 m/s), whereas close to spectators at the 3rd seats level they increase to 0.8 - 1.5 m/s. Furthermore, vortices between air jets are of smaller scale and less intense with respect to the Basic Case, while they are maintained only at the higher levels close to the ceiling fans. Above the arena and the lower seats, a one-way direction flow is formed moving horizontally towards the centre of the hall. It is also interesting to note that mean air velocity and temperature at the height of 2m above the arena where the athletes train and compete are 0.05 m/s and 25.2^0C, respectively.

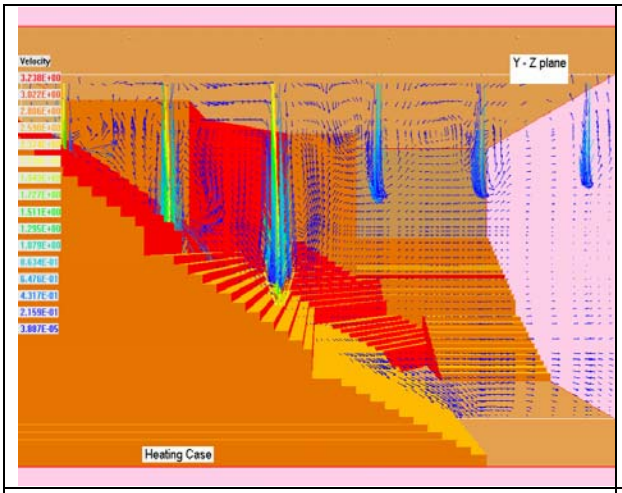

Figure 5: Air velocity field (m/s) – Heating Case

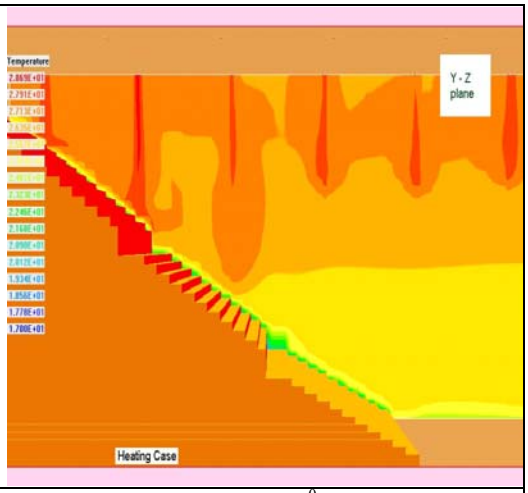

Figure 6: Temperature field (^{0}C) – Heating Case

(3) Cooling Case: A typical summer day is considered in this case with outdoor temperature exceeding 30^0C, according to meteorological data for the experimental site. Boundary and initial conditions are given in Table 1. The air velocity and temperature fields prevailing in the hall under cooling conditions are illustrated in Figures 7 and 8, respectively. Velocity fields are not significantly changed compared with the Basic Case. Air jets have smaller penetrating depths and velocities decrease to 0.2 m/s at approximately 9m from the floor (Figure 7). Going up the seats jets become more intense with velocities slightly increasing to 0.4 m/s close to spectators at the 2nd seats level and further increasing to 0.9 - 1.6 m/s at the upper seats. Large vortices are formed between the jets with low velocities prevailing therein (0.2 – 0.3 m/s). However, air flow above the arena and the 1st seats level until a height of 5m seems one-way directional moving from the arena to the seats. Regarding temperature, considerable stratification is formed in the hall (Figure 8) with the lowest values (20 – 23^0C) being observed very close to the air jets originating from the ceiling inlets, at the area between the 2nd and 3rd seats level until a height of 2m from the spectators' seats as well as at the right hand 1st block of seats. Temperature exceeds 24^0C at a height of approximately 18m above the arena reaching 25^0C very close to the ceiling, while at the rest of the indoor space temperature slightly fluctuates over 24^0C. It is finally interesting to note that mean air velocity and temperature at the height of 2m above the arena where the athletes train and compete are 0.06 m/s and 23.4^0C, respectively.

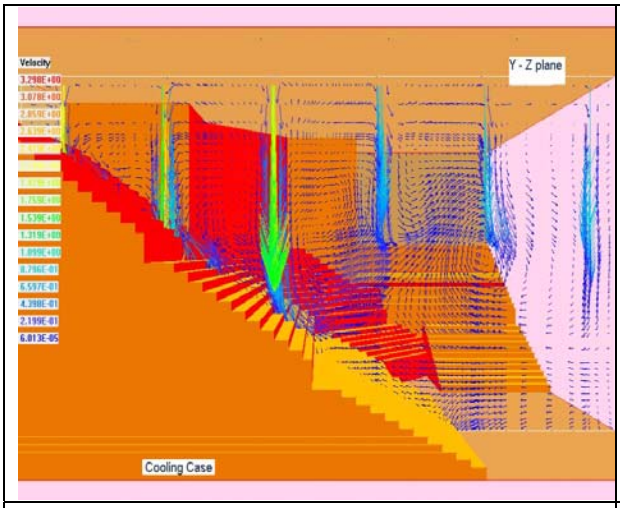

Figure 7: Air velocity field (m/s) – Cooling Case

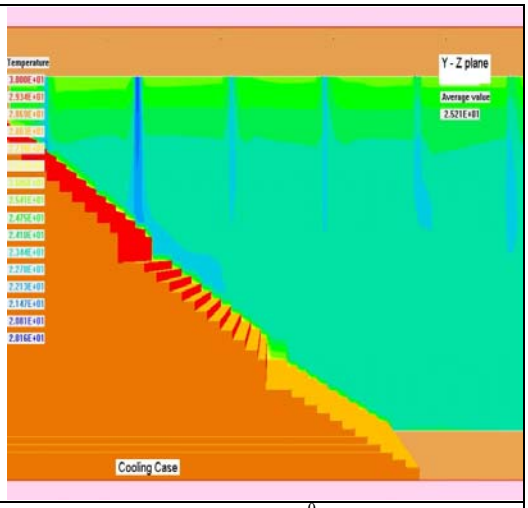

Figure 8: Temperature field (^{0}C) – Cooling Case

CONCLUSIONS

Comparison between experimental and computed results was satisfactory with only discrepancy observed being attributed to simplifications of the model setup for computational economy reasons. Airflow fields were characterised by large distinct vortices extending from top to bottom between air jets originating from the ceiling air inlet fans. Velocities were higher at the upper spectators' seats and temperature depicted a smooth stratification, which was enhanced under heating ventilation conditions. When heating was applied air jets had considerably smaller penetrating depths, vortices were less intense, velocities slightly decreased, while airflow field above the arena turned to one-way horizontal flow. This was also observed under cooling ventilation conditions, whilst overall less significant changes were imposed to the airflow and temperature patterns. Air jets and velocities became slightly smaller compared with the Basic Case (air-conditioning HVAC operation) and temperature stratification was more intense. Further work includes scenarios of different uses of hall and consideration of pollutants. For example, an "athletic event" day has been studied with the hall occupied by spectators and indoor pollutant sources considered as well as infiltration of outdoor originating pollutants. Furthermore, scenarios of different uses of hall under different ventilation conditions and presence of pollution sources including more physical processes are under study.

ACKNOWLEDGEMENTS: This work was supported by IRAKLEITOS Fellowships for Research of the Hellenic Ministry of Education.

REFERENCES

Duci, A., Papakonstantinou, K., Chaloulakou, A. and Markatos, N. (2004). Numerical Approach of Carbon Monoxide Concentration Dispersion in an Enclosed Garage. *Build. Environ*. **39**, 1043-1048.

Guo, H., Lee, S. C. and Chan, L. Y. (2004). Indoor Air Quality Investigation at Air-conditioned and Non-air-conditioned Markets in Hong Kong. *Sci. Total Environ*. **323**, 87-98.

Lee, S. C., Guo, H., Li, W. M. and Chan, L. Y. (2002). Inter-comparison of Air Pollutant Concentrations in Different Indoor Environments in Hong Kong. *Atmos. Environ*. **36**, 1929-1940.

Spalding, D. B. (1981). A General Purpose Computer Program for Multi-dimensional One- and Two-phase Flow. *Mathematics and computers in simulation*. **23**, 267-276.

Xing, H., Hatton, A., Awbi, H. B. (2001). A Study of the Air Quality in the Breathing Zone in a Room with Displacement Ventilation. *Build. Environ*. **36**, 809-820.

INDOOR AIR CLIMATE CONTROL

A. Van Brecht[1], S. Quanten[1], T. Zerihundesta[1], D. Berckmans[1]
[1] Division of Monitoring-Modelling-Management of Bioresponses (M3BIORES), Catholic University of Leuven, Kasteelpark Arenberg 30, B-3001 Leuven, Belgium

ABSTRACT

An on-line mathematical approach was used to model the spatio-temporal temperature distribution in an imperfectly mixed forced ventilated room. A second order model proved to be a sufficiently good description of the temperature dynamics ($R^2 = 0.929$) of the system. Furthermore, it was possible to fully understand the physical meaning of the second order model structure.
Using this model, a Model Based Predictive (MBPC) climate controller was developed for a Single Input Single Output (SISO) system. The controller was able to follow the mean temperature of 4 points, and to robustly react to a random local disturbance.
The results presented in this paper show that Model Based Predictive Control using Data-Based Mechanistic modeling can be of significant importance in the development of a new generation of climate controllers.

KEYWORDS

imperfectly mixed fluids, uniformity, data-based mechanistic modeling, identification, model based predictive control

INTRODUCTION

In everyday life, one is constantly confronted with imperfectly mixed fluids. Every fluid in nature, whether it is a gas or a liquid, is imperfectly mixed and is characterised by spatio-temporal gradients of heat and mass variables. In ventilated airspaces (domestic buildings, office rooms, supermarkets, transport systems, medical facilities, …) and in agricultural and industrial process rooms (greenhouses, animal houses, chemical vessels, bio-reactors, …) it is desirable to control the spatio-temporal heat and mass distribution in the imperfectly mixed fluid in order to achieve optimum process quality (production results, comfort, …) with a minimum use of energy.

In many of these applications one strives to achieve a spatially homogeneous distribution of heat and mass. For example, in egg incubators spatial gradients about the optimum breeding temperature of 37.5 - 37.8 °C must be avoided to guarantee a spatially uniform embryo development and quality (Zhang, Q. *et al.*, 1992; French, N.A., 1994).

There are also many applications in which one strives to achieve a spatially heterogeneous heat and mass distribution. For example, in ventilated rooms which are not entirely occupied, it is important to achieve good air quality and thermal comfort in the occupied zone, without providing too large amounts of fresh air and heat in those parts of the room where it is not required (Sandberg, M., 1981).

This paper has the intention to present the application of Data-Based Mechanistic (DBM) modelling for controlling the temperature dynamics in a forced ventilated room. Most existing models for control purposes can be translated into two main groups: mechanistic or white box models and Data-Based or black box models. Mechanistic models describe a system's behaviour based on a priori known physical, mechanical, chemical and/or biological mechanisms underlying the functioning of the system (France J. *et al.*, 1984; Baldwin R.L., 1995). When applied to the problem of controlling the spatio-temporal heat and mass distribution in an indoor environment such as ventilated airspaces, agricultural and industrial process rooms, these mechanistic models (e.g. Computational Fluid Dynamics (CFD) models) are restrictive owing to their exceptional complexity. One must be aware of the fact that a mechanistic model, such as CFD models, constitutes the culmination of a large number of assumptions and approximations (Bruce J.M. *et al.*, 1979; Oltjen J.W. *et al.*, 1987; Kettlewell, P.J. *et al.*, 1992) resulting in a model that is a valuable tool for design purposes, but lacks the necessary accuracy to be appropriate for control purposes.

Opposite to 'mechanistic or white box modellers' who feel that computer-based models should reflect the perceived complexity of the process, there are scientists with a more 'black box' turn of mind who favor 'data-based' procedures. In the data-based modelling approach, the model structure is inferred and the model parameters are estimated by reference to experimental data using more objective, statistically based methods (e.g. (Aerts J.-M. *et al.*, 2000)). This technique can deliver accurate models but the complete lack of physical insight is a major drawback in control purposes, making it an application specific model.

However, there is an intermediate type of model, that exploits the availability of time-series data in statistical terms but which overtly attempts to produce models which have a physical (mechanistic) meaning. As a hybrid between the extremes of mechanistic and data-based modelling, these so called data-based mechanistic (or grey box) models provide a physically meaningful description of the dominant internal dynamics of heat and mass transfer in the imperfectly mixed fluid (Berckmans, D. *et al.*, 1992a; Berckmans, D. *et al.*, 1992a; Barnett V *et al.*, 1993; Janssens, K. *et al.*, 2004; Janssens, K. *et al.*, 2004). The strength of these models is that they combine the advantages of both mechanistic or white box (generality, knowledge based) and data-based or black box (compact, accurate) models and is, therefore, an ideal basis for model-based control system design (Camacho, E. *et al.*, 1999; Maciejowski, J.M., 2002). In the present paper, the DBM approach to modelling is applied to the problem of modelling imperfect mixing in the forced ventilation of buildings.

MATERIALS AND METHODS

Test installation

The laboratory test room, represented in figure 1, is a mechanically ventilated room with a length of 3 m, a height of 2 m and a width of 1.5 m. It has a slot inlet (1 in figure 1) in the left sidewall just beneath the ceiling and an asymmetrically positioned, circular air outlet (2 in figure 1) in the right sidewall just above the floor. The volume of air in the test room (vol_{room}) is 9 m³. An enveloping chamber of length 4 m, width 2.5 m and height 3 m (6 in figure 1) is built around the test room to reduce disturbing effects of varying laboratory conditions (fluctuating temperature, opening doors, …). The volume of the buffering interspace or buffer zone is 21 m^3. The test room and the enveloping chamber are both constructed of transparent plexiglass through which the airflow pattern can be observed during flow visualization experiments.

A mechanical ventilation system enables an accurate control of the ventilation rate in the range 70 - 420 m^3/h and this with an accuracy of 6 m^3/h. A heat exchanger and a moisture conditioning unit are provided in the supply air duct to regulate the temperature and moisture content of the inflowing air. A series of five aluminium heat sinks (4 in figure 1), in which a semi conductor heat source is used and a shallow hot water reservoir (3 in figure 1) is located at the floor of the test room to simulate the heat and moisture production of the occupant(s).

To measure the spatio-temporal temperature distribution in the test chamber, 36 calibrated type T thermocouples are located in a 3-D measuring grid (5 in figure 1) covering a large part of the room. The temperature sensors are located in two vertical xy-planes: a 'front sensor plane' (0.375 m from the front wall) and a 'rear sensor plane' (0.375 m from the back wall). Thermocouples are further located in the slotted air inlet, in the exhaust outlet, in the buffer zone and in the laboratory hall. The accuracy of the thermocouples is 0.1 °C and the time constant is less than 3 seconds. An intelligent measurement and data collection unit with programmable measurement speed is used for the data acquisition with a sampling rate of 10 s for 36 thermocouple channels. A more detailed description of the laboratory test room is given in literature (Berckmans, D. *et al.*, 1992b; Janssens, K. *et al.*, 2000).

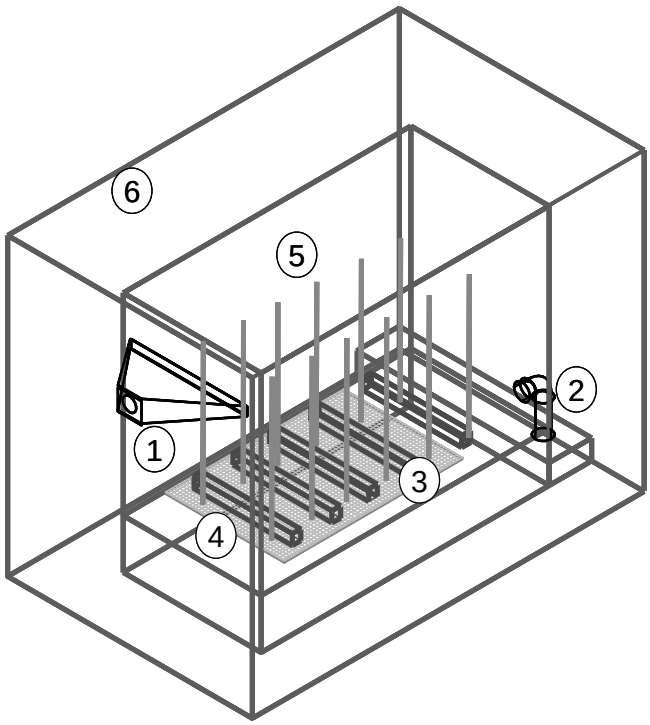

Figure 1: Laboratory test chamber: 1**.** air inlet, 2. air outlet, 3. aluminium conductor heat sink, 4. shallow hot water reservoir, 5. 3-D sensor grid, 6. envelope chamber or buffer zone

Optimization of uniformity

Since in many biological processes one strives to achieve a maximal uniformity of micro-environmental variables to ensure a homogenous product quality, an objective criterium is needed to quantify spatio-temporal uniformity. Moreover, it should quantify the uniformity of e.g. the temperature distribution measured in a three dimensional grid of temperature sensors in the whole installation. Therefore, to measure the variability of the temperature, the standard deviation of the spatial temperature measurements was used.

As pointed out in the introduction, it is very important in many processes to strive to achieve a perfectly mixed airspace with a uniform three-dimensional temperature distribution. Spatial temperature gradients which exceed an acceptable gradient, which is process depending (e.g. in the baking process of Integrated Circuits it is 10°C at 800°C, in the incubation process of chicken eggs it is 0.3°C at 37.8°C), have a negative effect on the quality and efficiency of the process.

The extend to which a process in which heat, moisture and gas production sources are present becomes perfectly mixed, is complex and depends on the air flow pattern (Barber, E.M. *et al.*, 1982; Barber, E.M. *et al.*, 1984). The air flow pattern in a ventilated room is primarily determined by the momentum and trajectory of the air jet and its mixing with the indoor air (Li, Z.H. *et al.*, 1993). The trajectory of an air jet depends on the inlet type and its proximity to the ceiling (1974) and on the ratio of the thermal buoyancy to the inertial forces (Koestel, A., 1955). It is clear that the ventilation rate of the fresh air has a crucial influence on the air flow pattern.

Data-based mechanistic model

In DBM models, the model structure is first identified using objective methods of time series analysis based on a given, general class of time series model (here linear, continuous-time transfer functions (TF) or the equivalent ordinary differential equations). But the resulting model is only considered fully acceptable if, in addition to explaining the data well, it also provides a description that has relevance to the physical reality of the system under study.

Identification of a reduced-order, linear model

The ability to estimate parameters represents only one side of the model identification problem. Equally important is the problem of objective model order identification. This involves the identification of the best choice of orders of the numerator and denominator polynomials together with the time delay. The parameters of a TF model may be estimated using various methods of identification and estimation (Ljung, L. *et al.*, 1983; Young, P.C., 1984; Norton, J.P., 1986; Ljung, L., 1987). However, most of these methods are based on discrete-time TF models and not on their continuous-time model equivalents, which impedes the interpretation of the model in physically meaningful terms. Although Least Squares (LS) is one of the most commonly used model estimation algorithms, the estimated model parameters become asymptotically biased away from their true values in the presence of measurement or disturbance noise (Young, P.C., 1984). The more complex Simplified Refined Instrumental Variable (SRIV) algorithm developed by Young (Young, P.C., 1984), uses the Instrumental Variable (IV) approach coupled with special adaptive prefiltering to avoid this bias and to achieve good estimation performance. The SRIV structure identification criterion has been proven very successful in practical applications (Young, P.C. *et al.*, 1979; Young, P.C. *et al.*, 1980; Wang, C.L. *et al.*, 1988; Quanten, S. *et al.*, 2003). A continuous-time TF model for a single-input single output (SISO) system has the following general form:

$$y(t) = \frac{B(s)}{A(s)} u(t-\tau) + \xi(t) \tag{1}$$

where: s is the time derivative operator, i.e. $s = d/dt$; y(t) is the noisy measured output; $u(t)$ is the model input; τ is the time delay; $\xi(t)$ is additive noise, assumed to be a zero mean, serially uncorrelated sequence of

random variables with variance σ^2 accounting for measurement noise, modelling errors and effects of unmeasured inputs to the process; and finally, *A(s)* and *B(s)* are polynomials in the s operator of the following form:

$$A(s) = s^n + a_1 s^{n-1} + \ldots + a_n \tag{2}$$

$$B(s) = b_0 s^m + b_1 s^{m-1} + \ldots + b_m \tag{3}$$

where $m \leq n$; a_1, a_2,…, a_n and b_0, b_1,…, b_m are the TF denominator and numerator parameters respectively.

RESULTS AND DISCUSSION

Static experiments

In the described laboratory test chamber, experiments was conducted to examine the effect of the ventilation rate on the spatial temperature homogeneity, while keeping the average temperature inside the ventilated chamber constant at 23°C. For different ventilation rates (120, 160, 200, 240 and 300 m³/h) the 3-D temperature distribution was measured in steady state regime. The internal heat and moisture production during the experiments were respectively 300 W and 0.5 l H_2O/h. From the measured 3-D temperature distribution in the experiments the uniformity of the temperature distribution was quantified as the standard deviation of the 36 temperature measurements for different levels of the ventilation rate, which is shown in figure 2.

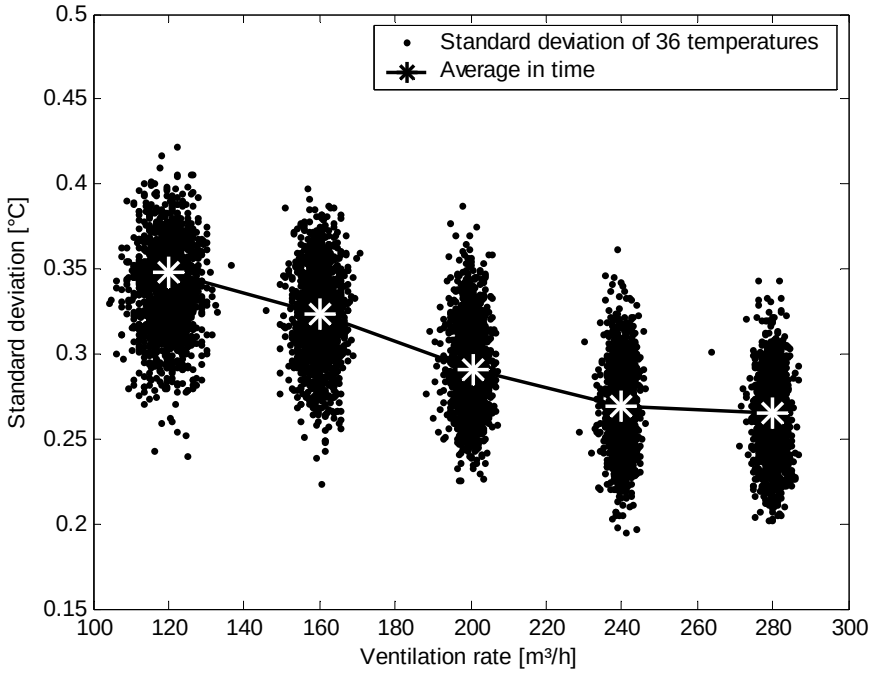

Figure 2: The effect of the ventilation rate on standard deviation of the 36 temperature readings

It is clear from figure 2 that increasing the ventilation rate from 120 to 280 m³/h (or by 133.3%) decreases the standard deviation by 23.9 %. It can be concluded that a ventilation rate of 280 m³/h gives the maximal spatial uniformity. However, increasing the production efficiency is a trade off between energy consumption and product quantity and quality. The decrease in the standard deviation due to an increase of the ventilation level from 240 to 280 m³/h (or by 16.6 %) is only 1.6 %, and would only increase the energy consumption

and not optimise the uniformity of the 3-D temperature distribution. Therefore, the optimal ventilation rate that reduces the variability of the three-dimensional temperature distribution (0.27 °C) in an energy efficient way is 240 m³/h.

Identification of a reduced-order linear model

When a set of usable input-output time-series data is generated, a reduced order, linear model can be estimated to describe the data in a sufficiently accurate way for control purposes. An experiment has been carried out with a step increase in air supply temperature. In this experiment, an initial working point was selected, with the initial supply temperature set at 14.7°C for 25 min in order to establish steady airflow conditions before the required step supply air temperature change was introduced (figure 3). In order to identify and model the temperature dynamics in the test chamber, it would be preferable to perform experiments in which the supply air temperature is changed sharply in a 'sufficiently exciting' manner (Young, P.C., 1984).

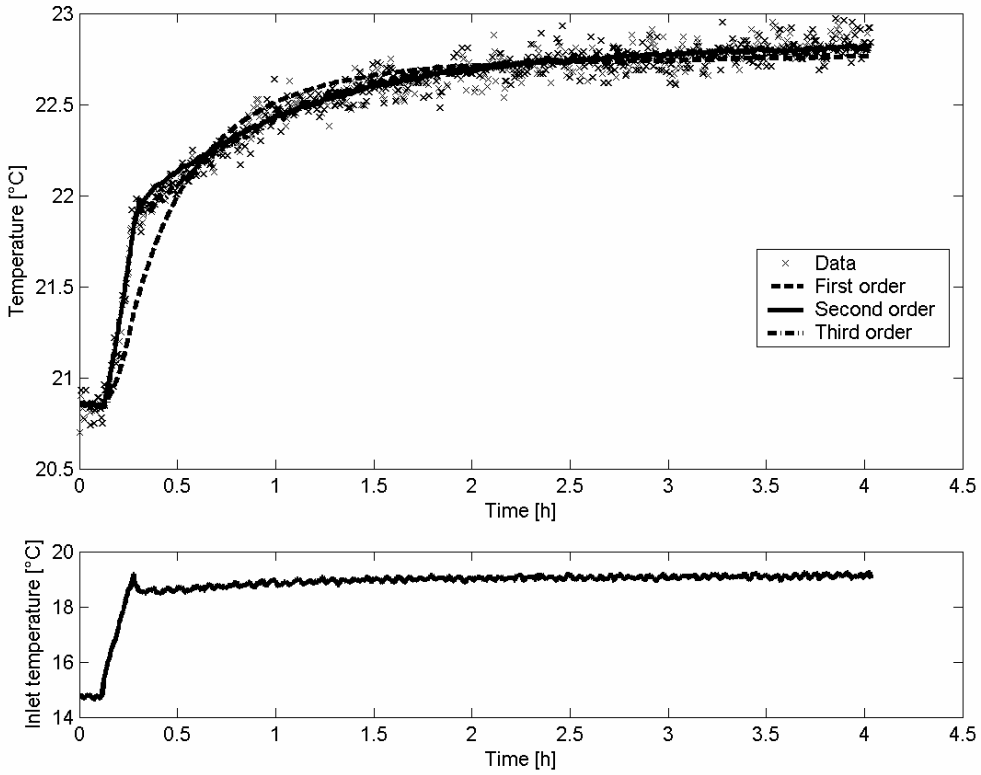

Figure 3: The output of a first order, second order and third order TF model compared with the measured temperature response at sensor position 15

In the present application, a second-order model proves to be a sufficiently accurate description of the temperature dynamics of the system according (figure 3) to the three basic principles of the SRIV algorithm: minimal number of parameters, high reliability of the parameters estimation and high accuracy of the model to proceed with the development of the model-based climate controller, as long as the model provides a physical meaningful description of the temperature dynamics (table 1). When applied to all 36 sensor positions, the second order model describes the data with an average R_t^2 of 0.929 and an average YIC-value of -7.64.

TABLE 1
The model parameter estimates with associated relative standard error, the YIC value and the coefficient of determination R^2_T of a first, second and third order continuous-time TF model for sensor position 15

order of TF	parameter estimates	relative standard error [%]	RT² [-]	YIC value [-]
[1 1 0]	a_1 = 0.010	$\xi(a_1)$= 0.66	0.961	-12,656
	b_0 = 0.004	$\xi(b_0)$= 0.61		
[2 2 10]	a_1 = 0.060	$\xi(a_1)$= 1.58	0.981	-10,048
	a_2 = 0.000	$\xi(a_2)$= 3.13		
	b_0 = 0.016	$\xi(b_0)$= 1.13		
	b_1 = 0.000	$\xi(b_1)$= 3.05		
[3 3 9]	a_1 = 0.749	$\xi(a_1)$= 8.10	0.982	-1,134
	a_2 = 0.460	$\xi(a_2)$= 14.18		
	a_3 = 0.002	$\xi(a_3)$= 13.10		
	b_0 = 0.010	$\xi(b_0)$= 423.47		
	b_1 = 0.106	$\xi(b_1)$= 13.98		
	b_2 = 0.001	$\xi(b_2)$= 13.13		

Data-based mechanistic model

The DBM approach represents the imperfectly mixed fluid in a process room by a number of well mixed zones (WMZ) which are defined around the nodes of a sensor grid. A well mixed zone is a zone of improved mixing with a certain volume wherein acceptably low spatial gradients occur. The value of these acceptable gradients and consequently the number of the WMZ's are determined by the application itself.
These WMZ's exist in every imperfectly mixed fluid. A schematic representation of a WMZ in a process room with fluid flow rate V (m^3/s) and with internal production of heat is given in figure 4.

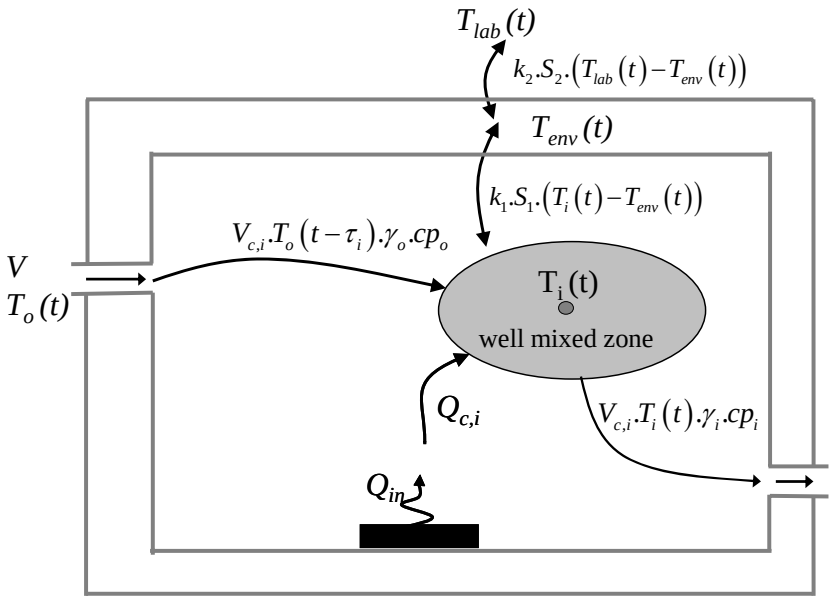

Figure 4: *Schematic representation of the WMZ concept.*

To describe the dynamic behaviour of temperature in the considered *n* WMZ's, standard heat transfer theory can be applied. In case of a constant ventilation rate, a linear, first-order differential equation can be formulated as:

$$\frac{dT_i(t).vol_i.\gamma_i.cp_i}{dt} = V_{c,i}.T_o(t-\tau_i).\gamma_o.cp_o - V_{c,i}.T_i(t).\gamma_i.cp_i + Q_{c,i} + k_1.S_1.\left(T_{env}(t) - T_i(t)\right) \quad (4)$$

$$\frac{dT_{env}(t).vol_{env}.\gamma_{env}.cp_{env}}{dt} = k_1.S_1.\left(T_i(t) - T_{env}(t)\right) + k_2.S_2.\left(T_{lab}(t) - T_{env}(t)\right) \quad (5)$$

where t is the time (s), τ_i is the advective time delay or travel time of the fresh supply air before it enters WMZ i (s); T_i is the temperature in the WMZ i (ºC); T_o is the supply air temperature (ºC); T_{env} is the temperature of the stagnant air in the enveloping zone (ºC); T_{lab} is the temperature in the outside laboratory remaining approximately constant throughout the experiments (ºC); vol_i is the volume of the WMZ i (m^3); vol_{env} is the volume of the enveloping zone (m^3); $V_{c,i}$ is the part of the ventilation rate entering WMZ i (m^3); $Q_{c,i}$ is the part of the total heat production in the room entering the WMZ i (Watt); k_1 and S_1 are the total heat transfer coefficient (Watt/m^2.°C) and the surface area of heat exchange (m^2) between the WMZ i and the enveloping zone; k_2 and S_2 are the total heat transfer coefficient (Watt/m^2.°C) and the surface area of heat exchange (m^2) between the enveloping zone and the laboratory; γ_i and cl_i are the density (kg/m^3) and the heat capacity (J/kg.°C) of the air in WMZ i; γ_0 and cl_0 are the density (kg/m^3) and the heat capacity (J/kg.°C) of the supply air.

The enveloping zone consists of a volume of air between the central chamber walls and the envelope chamber walls (6 in figure 7). There is no mass exchange between the air inside this buffer zone and the air in the central chamber, but heat is exchanged between the air in the buffer zone and the air in the central chamber.
In contrast to the zonal and nodal models in literature (Dalicieux, P. *et al.*, 1992; Li, Y. *et al.*, 1992), the different WMZ's are here considered as decoupled or non-interactive zones. Since the air inlet conditions are responsible for the thermal characteristics of the zone, the model only creates a link between the inlet and individual zones.

Since every living organism in a bio-process needs an adequate amount of oxygen rich fresh air, the focus on the WMZ model concept is to model the movement of fresh air to a particular zone. This is established by using local fresh air flow rate. The local fresh air flow rate is the air flow rate with the same temperature like the incoming air at the inlet that would have created the aggregate effect of the convective flux interaction with the neighbouring zones on the well mixed zone in consideration. This is a very useful assumption, because it creates a direct relationship between individual zones without the need for modelling zonal interactions. When considering non-interactive WMZ's, the spatio-temporal model is also less complex and it is an excellent basis for control purposes. The assumption results in n models (the response of each WMZ to changes in the inlet conditions is described by a single model, resulting in n 1st order models for n WMZ's that can be used for controlling the conditions in the n well-mixed zones each time only using the air inlet conditions.

The advective time delay τ_i in equation (4) is a function of location, i.e., zones which are in the main jet has smaller advective time delay than zones in recirculation zone. In other words, it shows the time elapsed before a zone feels the change in temperature at the inlet.

Under steady state conditions, simplifying these equations and gives:

$$\frac{dt_i(t)}{dt} = \beta_i \cdot t_o(t-\tau) + K_1 \cdot t_{env}(t) - \alpha_1 \cdot t_i(t) \quad (6)$$

$$\frac{dt_{env}(t)}{dt} = K_3 \cdot t_i(t) - (K_3 + K_2) \cdot t_{env}(t) \quad (7)$$

where,

$$\begin{cases} \beta_i = \dfrac{V_{c,i}}{vol_i} \\ K_i = \dfrac{k_1 \cdot S_1}{vol_i \cdot \gamma_i \cdot cp_i} \\ \alpha_i = \dfrac{V_c}{vol_i} + \dfrac{k_1 \cdot S_1}{vol_i \cdot \gamma_i \cdot cp_i} = \beta_i + K_i \\ K_2 = \dfrac{k_2 \cdot S_2}{vol_{env} \cdot \gamma_{env} \cdot cp_{env}} \\ K_3 = \dfrac{k_1 \cdot S_1}{vol_{env} \cdot \gamma_{env} \cdot cp_{env}} \end{cases}$$

Converting (6) and (7) into the frequency domain using the Laplace operator and combining these transfer functions, we obtain the following second order, continuous-time transfer function model for the central chamber – envelope zone system:

$$t_i(t) = \frac{b_0 s + b_1}{s^2 + a_1 s + a_2} t_0(t - \tau) \tag{8}$$

where,

$$\begin{cases} b_0 = \beta_i \\ b_1 = \beta_i \cdot (K_2 + K_3) \\ a_1 = \alpha_i + (K_2 + K_3) \\ a_2 = (K_2 + K_3) \cdot \alpha_i - (\alpha_i - \beta_i) \cdot K_3 \end{cases}$$

It has been shown that the parameter β_i (s^{-1}) in equation (13) has a physical meaning (Janssens, K. *et al.*, 2004): it is the local refreshment frequency or the local outside air change rate in the WMZ.
The well mixed zone concept, that results in the formulation of the DBM model, and the associated heat balance differential equation can be applied to each of the spatially distributed monitoring positions in the test room.

The DBM model and classical heat transfer theory

It is clear from the relationships between the parameters in the TF model (8) and the equivalent parameters in the estimated TF model, that the classical heat transfer coefficients are not uniquely 'identifiable' from the experimental data. On the other hand, the heat transfer dynamics of the chamber are completely specified by the DBM parameters, which can be interpreted as specific combinations of these classical parameters. Consequently, this DBM model represents an alternative approach to modelling the system in physically meaningful, albeit not the normal, classical terms. And the model, in this identifiable form, is entirely adequate for both understanding the heat transfer dynamics of the chamber and designing a ventilation control system. It provides, in other words, an alternative way of presenting heat transfer theory within the context of imperfectly mixed flow processes, such as those encountered in real forced ventilation systems.

Parameter contour plots

Figure 5 shows the spatial contours of the parameter β_i (s^{-1}) in the front and the rear sensor plane of the test installation at a ventilation rate of 240 m³/h. The front sensor plane is the vertical xy-plane of the test chamber which consists of the temperature sensors 4, 5, 6, 10, 11, 12, 16, 17, 18, 22, 23, 24, 28, 29, 30, 34, 35 and 36 and which lies at a z-distance of 0.375 m from the front wall of the chamber (see figure 1). The rear sensor plane consists of the sensors 1, 2, 3, 7, 8, 9, 13, 14, 15, 19, 20, 21, 25, 26, 27, 31, 32 and 33 and lies at a z-distance of 0.375 m from the back wall of the chamber (see figure 1). The lower sensors in both

sensor planes lie at a height of 0.8 m above the floor, the upper sensors lie 0.4 m beneath the ceiling, the left sensors are positioned 0.4 m from the inlet wall and the right sensors are positioned 0.6 m from the outlet wall.

Further, the contour plots relate well to the air flow pattern, which is presented in figure 6. At high ventilation rates, the incoming fresh air rapidly moves across the top of the chamber, hits the right sidewall and then descends towards the exit at the lower right, where some of the airflow recirculates in a clockwise direction. A decrease in the air freshness in the direction of the air flow is quite noticeable from the contours of the local volumetric concentration of fresh air flow rate β_i.

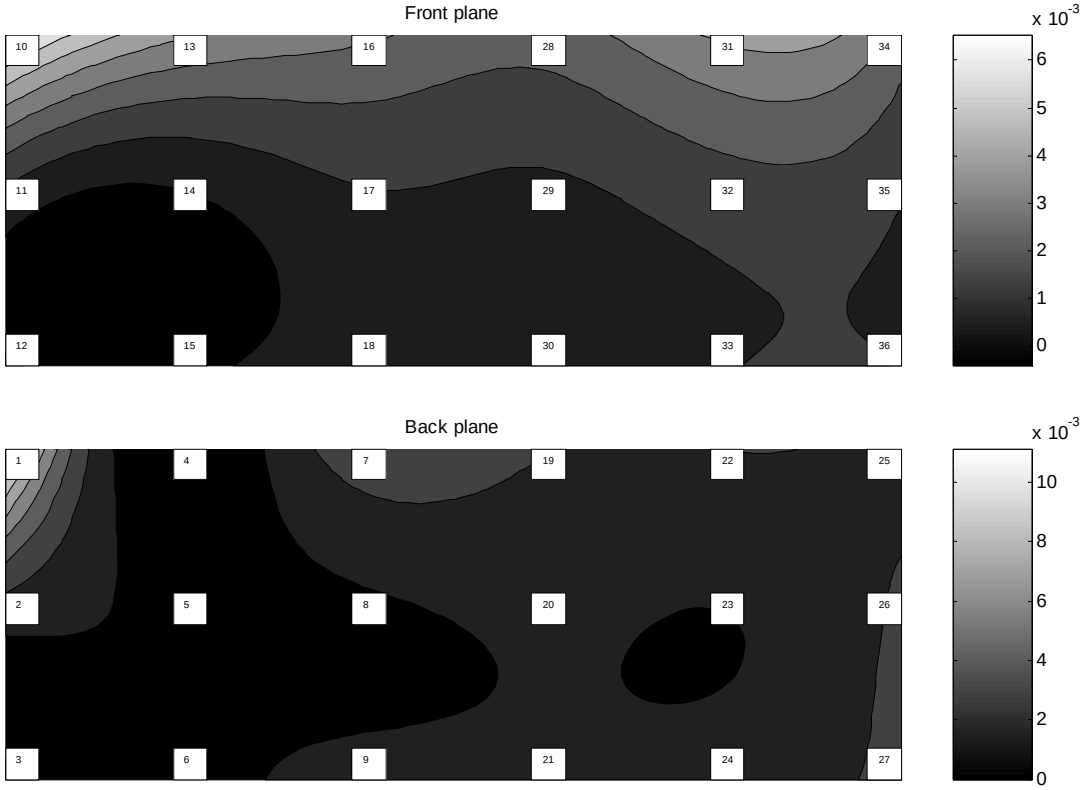

Figure 5: Spatial contour plots of parameter β_1 (s^{-1})

Figure 6: The visualised air flow pattern at 240 m³/h

Development of a model based control system

For achieving the objective of making an introduction in the development of a new generation of climate controllers, the Model Based Predictive Control (MBPC) approach is used, which has been introduced by Richalet et al. (Richalet, J. *et al.*, 1978) and Cutler and Ramaker (Cutler, C.R. *et al.*, 1980) in the late seventies. MBPC involves the computation of a sequence of imminent control moves such that the predicted behaviour of the process over a certain horizon is as close as possible to the reference trajectory (usually defined by the user) and subject to a given constraint. The theoretical background of the control algorithm is described in more detail in literature by Clarke et al. (Clarke, D.W. *et al.*, 1987a; Clarke, D.W. *et al.*, 1987b) and Garcia et al. (Garcia, C.E. *et al.*, 1989).

MBPC has proved to be a very successful controller design strategy, both in theory and practice (Van den Boom, T.J.J., 1996). The provided high performance controllers are readily applicable to high-order and multivariable processes. MBPC are known as quite robust to disturbances and to uncertainties in the model parameters, which might originate from environmental conditions that are not included in the model.

It is important to investigate to what extent the control system is able to facilitate an optimal control of the spatial temperature distribution in the considered ventilation test room, allowing different control objectives to be realized (e.g. spatial homogeneity, spatial heterogeneity, tracking of reference trajectories at positions of interest,…). Also, aspects like the robustness of the control system to disturbances and tracking capability of the reference trajectory need to be checked.

The last stage in this approach involves the evaluation of the MBPC controller. In most processes, it is the aim is to achieve a uniform temperature distribution through the volume of the process. This means that the difference or the variability of the levels of the air temperature in time and space need to be reduced. When having *n* points in space in between the temperature difference and variability need to be reduced, this can be accomplished by *n* independent control inputs that affect the temperature of these *n* points. However, in this test installation, there are not enough inputs to control e.g. 4 points independently, since there is only one air inlet of which air temperature and ventilation level can be changed. Therefore, the ventilation level at which the uniformity is optimal (240 m³/h) is chosen to evaluate a MBPC of the average temperature of 4 points in space: two sensors in the front plane (13 and 15) and two sensors in the rear plane (22 and 24). The TF

describing the average temperature response of these sensor positions to changes in temperature of the supply air temperature is calculated by combining the TF's of the four sensor positions in series and dividing by 4 (equation (9)).
The controller behaviour is evaluated on a simulation basis and by performing a control experiment. In the present simulation and experiment, a sampling rate of 10 seconds is used and the control actions are subjected to hard constraints with maximum and minimum inlet temperature limits of 20 °C and 9 °C respectively. The allowable dynamic raise and drop in inlet temperature is set to 0.011 °C and 0.025 per 10 seconds respectively.

$$t_i(t) = \frac{b_0 s^7 + b_1 s^6 + b_2 s^5 + b_3 s^4 + b_4 s^3 + b_5 s^2 + b_6 s + b_7}{s^8 + a_1 s^7 + a_2 s^6 + a_3 s^5 + a_4 s^4 + a_5 s^3 + a_6 s^2 + a_7 s + a_8} \cdot t_0(t)$$

$$\begin{aligned} b_0 &= 0.09054 & a_1 &= 1.177 \\ b_1 &= 0.03285 & a_2 &= 0.2038 \\ b_2 &= 0.003071 & a_3 &= 0.01278 \\ b_3 &= 9.711 \cdot 10^{-5} & a_4 &= 0.0003111 \\ b_4 &= 8.07 \cdot 10^{-7} & a_5 &= 2.205 \cdot 10^{-6} \\ b_5 &= 2.503 \cdot 10^{-9} & a_6 &= 6.057 \cdot 10^{-9} \\ b_6 &= 2.855 \cdot 10^{-12} & a_7 &= 6.266 \cdot 10^{-12} \\ b_7 &= 8.878\mathrm{e} \cdot 10^{-16} & a_8 &= 1.778 \cdot 10^{-15} \end{aligned} \qquad (9)$$

In the simulation, measurement noise with a standard deviation of 0.2 °C was added to the plant model. To assess the robustness of the controller, a constant input disturbance of 0.2 °C and an output disturbance which switches from -5 °C to 5 °C after 5 hours was simulated and the result is shown in figure 6. The prediction horizon was optimised to 150 samples and the control horizon was 1 sample. The controller demonstrates its robustness for disturbance effects by immediately responding at the inlet temperature profile as the disorder is detected. Consequently the disturbance effect is compensated and the output trajectory follows a path that brings the process output trajectory as close as possible to the desired reference trajectory of the system.

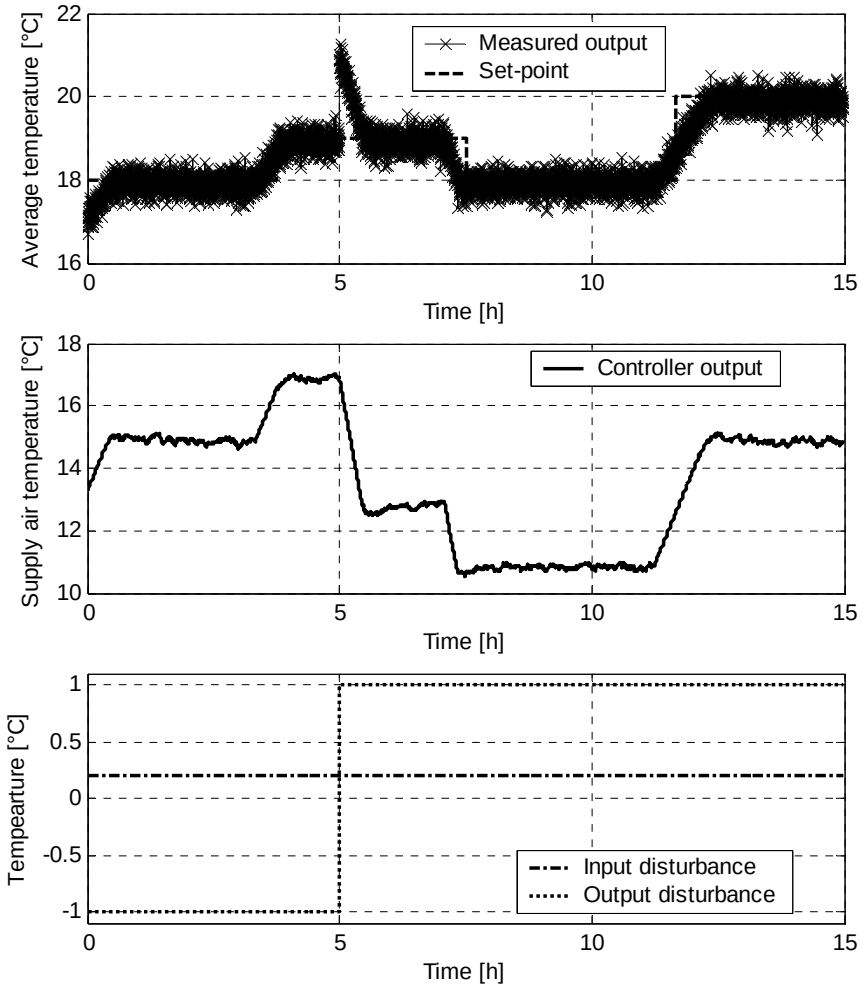

Figure 7: Simulation of the temperature response with measurement noise, input and output disturbances

The result of implementing this MBPC of the average temperature of 4 points in space is shown in figure 7. Also here, the controller demonstrates its robustness to possible modelling errors and measurement noise. The output trajectory follows the desired reference trajectory of the system. The average difference between the desired setpoint and the average measured temperature at the 4 points was 0.057 °C. The average variability of the temperature measurements was 0.27 °C, which is in the optimal level (figure 2).

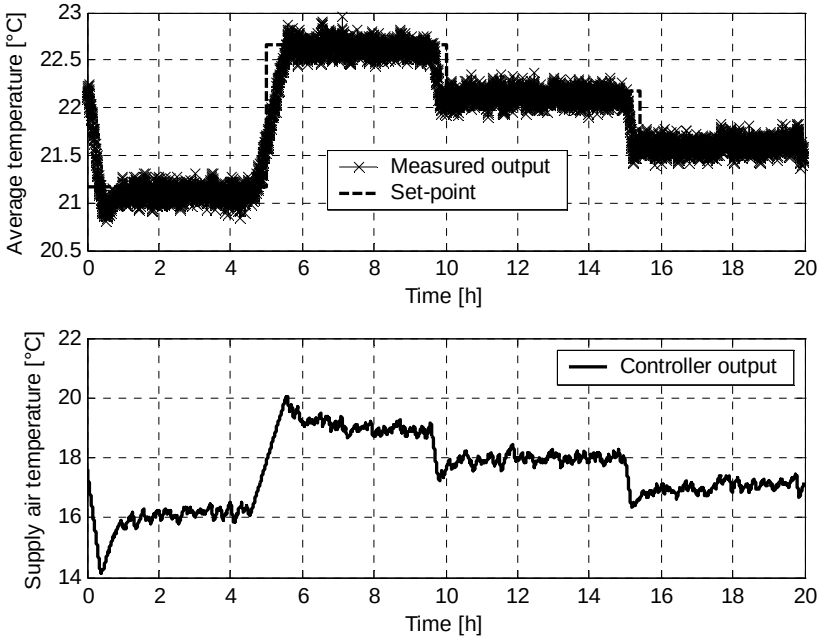

Figure 8: Temperature response as a result of the implemented MBPC

CONCLUSIONS

This paper has reported recent developments in the modelling and control of the forced ventilation in imperfectly mixed processes. It was shown that by using the ventilation rate, the variability of the air temperature distribution could be reduced to 0.27°C.

It has concentrated on the Data-Based Mechanistic (DBM) approach to modelling applied to data obtained from initial planned experiments in forced ventilated room. Here, in contrast to the normal hypothetico-deductive procedures that are most popular in this area of research, a minimally parameterised transfer function model is first identified and estimated from the experimental data without any prior assumptions about the physical nature of the system. Having objectively identified the dominant modes of dynamic behaviour in this manner, however, the model is then interpreted in physically meaningful terms, which have been shown to be in correspondence to the air flow pattern. This model not only explains the data very well (average $R_t^2 = 0.929$), with the minimum number of identifiable parameters, but it is also in a form that can provide the basis for the design of Model Based Predictive Control (MBPC) systems.

The MBPC behaviour to control the average temperature of 4 sensor positions was evaluated on simulation basis, where the robustness for disturbance effects is shown. Moreover, it has been shown by applying the developed MBPC to the forced ventilated room, that a reference trajectory of an average temperature could be achieved, while the variability of the air temperature distribution was still 0.27°C.

The results here presented can form the basis of the development of a MIMO climate controller. Based on the experiments performed and described in this paper, it becomes theoretically possible to control the three dimensional temperature distribution in ventilated processes. An even further extension can be achieved by including more input variables (like air flow direction, air flow pattern, opening of the air inlets,…) so that even more positions inside the car can be controller. This will enable the climate control system to achieve a spatially homogeneous or heterogeneous distribution of heat and mass. Future enhancements to climate controllers in ventilated spaces will include the integration of information from the central process part itself: the living organism.

All these innovations can sparkle off the development of a new generation of intelligent climate control systems, and increasing both optimal process quality (production results, comfort, …) with a minimum use of energy.

REFERENCES

Aerts J.-M., Berckmans D., Saevels P., Decuypere E., and Buyse J., 2000. Modelling the static and dynamic responses of total heat production of broiler chickens to step changes in air temperature and light intensity . *British Poultry Science*, **41**, p. 651-659

Baldwin R.L., 1995. Modeling ruminant digestion and metabolism. Chapman & Hall, London,

Barber, E.M. and Ogilvie, J.R., 1982. Incomplete mixing in ventilated airspaces, part 1: theoretical considerations. *Canadian Journal of Agricultural Engineering*, **24**, p. 25-29

Barber, E.M. and Ogilvie, J.R., 1984. Incomplete mixing in ventilated airspaces, part 2: scale model study. *Canadian Journal of Agricultural Engineering*, **26** (2), p. 189-196

Young P.C. and Lees M., 1993. The active mixing volume: a new concept in modelling environmental systems. In: Statistics for the environment, Barnett V and Turkman K.F. John Wiley & Sons, New York, p. 3-43

Berckmans, D., De Moor, M., and De Moor, B., 1992a,New model concept to control the energy and mass transfer in a three-dimensional imperfectly mixed ventilated space ,Proceedings of Roomvent, Sept. 2-5, Aalborg, Denmark, p.151-168

Berckmans, D., De Moor, M., and De Moor, B., 1992b,Test installation to develop a new model concept to model and control the energy and mass transfer in a three dimensional imperfectly mixed space ,Proceedings of Roomvent, p.399-416

Bruce J.M. and Clark J.J., 1979. Models of heat production and critical temperature for growing pigs. *Animal Production*, **28**, p. 353-369

Camacho, E. and Bordons, C., 1999. Model predictive control. Springer-Verlag, London, pp. 280

Clarke, D.W., Mohtadi, C., and Tuffs, P.S., 1987a. Generalized predictive control – Part I: the basic algorithm. *Automatica*, **23** (2), p. 137-148

Clarke, D.W., Mohtadi, C., and Tuffs, P.S., 1987b. Generalized predictive control – Part II: extensions and interpretations. *Automatica*, **23** (2), p. 149-160

Cutler, C.R. and Ramaker, B.L., 1980,Dynamic matrix control – a computer control algorithm ,Proceedings JACC, San Francisco, USA,

Dalicieux, P., Bouia, H., and Blay, D., 1992,Simplified modelling of air movements in room and its first validation with experiments ,Proceedings of Roomvent '92, Aalborg, Denmark, p.383-397

France J. and Thornley J.H.M., 1984. Mathematical models in agriculture. Butterworths, London,

French, N.A., 1994. Effect of Incubation-Temperature on the Gross Pathology of Turkey Embryos. *Br. Poult. Sci.*, **35** (3), p. 363-371

Garcia, C.E., Prett, D.M., and Morari, M., 1989. Model predictive control: Theory and practice- a survey. *Automatica*, **25** (3), p. 335-348

Janssens, K., Berckmans, D., and Van Brecht, A., 2000,Modelling the spatio-temporal temperature distribution in an imperfectly mixed ventilated room ,Proceedings of Roomvent 2000, 7th Int. Conference on Air Distribution in Rooms, July 9-12, Reading, UK, 223-228

Janssens, K., Van Brecht, A., Zerihun Desta, T., Boonen, C., and Berckmans, D., 2004. Modelling the internal dynamics of energy and mass transfer in an imperfectly mixed ventilated airspace. *Indoor Air*, **14** (2), pp. 13

Katz, L., 1974. Luftstromung im Raum. In: Lehrbuch der Klimatechnik, Bd. 1 Grundlagen, p. 141-200

Kettlewell, P.J. and Moran, P., 1992. A study of heat production and heat loss in crated broiler chicken: a mathematical model for a single bird. *British Poultry Science* , **33**, p. 239-252

Koestel, A., 1955. Path of horizontally projected heated and chilled air jets. *ASHRAE Transactions*, **61**, p. 213-232

Li, Y., Sandberg, M., and Fuchs, L., 1992. Vertical temperature profiles in rooms ventilated by displacement: full-scale measurement and nodal modelling. *Proceedings of Indoor Air '92*, **2**, p. 225-243

Li, Z.H., Zhikov, A.M., Christianson, L.L., and Zhang, J.S., 1993. Characteristics of diffuser air jets and airfl in the occupied regions of mechanically ventilated rooms - a literature review. *ASHRAE Transactions*, **1**, p. 119-1127

Ljung, L., 1987. System identification: theory for the user. Prentice Hall, Englewood Cliffs, New Jersey, pp.

519
Ljung, L. and Soderstrom, T., 1983. Theory and practice of recursive identification. MIT Press, Cambridge, pp. 529
Maciejowski, J.M., 2002. Predictive Control with constraints. Prentice Hall, U.K., pp. 331
Norton, J.P., 1986. An introduction to identification. Academic Press, London, pp. 310
Oltjen J.W. and Owens F.N., 1987. Beef cattle feed intake and growth: empirical bayes derivation of the kalman filter applied to a nonlinear dynamic model . *Journal of Animal Science*, **65**, p. 1362-1370
Quanten, S., McKenna, P., Van Brecht, A., Van Hirtum, A., Janssens, K., Young, P.C., and Berckmans, D., 2003. Model-based PIP control of the spatial temperature distribution in a car. *International Journal of Control*, **16** (1628-1634),
Richalet, J., Rault, A., Testud, J.L., and Papon, J., 1978. Model predictive heuristic control: applications to industrial processes. *Automatica*, **14** (5), p. 413-428
Sandberg, M., 1981. What is ventilation efficiency? *Building and Environment*, **16** (2), p. 123-135
Van den Boom, T.J.J., 1996,Model based predictive control. Status and perspectives ,Proceedings of the CESA'96 IMACS Multiconference, Lille, France, p. 1-12
Wang, C.L. and Young, P.C., 1988. Direct digital control by input-output, state variable feedback. *International Journal of Control*, **47**, p. 97-109
Young, P.C., 1984. Recursive estimation and time-series analysis. Springer-Verlag, Berlin,
Young, P.C., 1984. Recursive estimation and time-series analysis. Springer-Verslag, Berlin,
Young, P.C. and Jakeman, A.J., 1979. Refined instrumental variable methods of recursive time-series analysis: part II, single input output systems. *International Journal of Control*, **29**, p. 1-30
Young, P.C. and Jakeman, A.J., 1980. Refined instrumental variable methods of recursive time-series analysis: part III, extenions. *International Journal of Control*, **31**, p. 741-764
Zhang, Q. and Whittow, G.C., 1992. The effect of incubation temperature on oxygen consumption and organ growth in domestic-fowl embryo's. *J. Therm. Biol.*, **17** (6), p. 339-345

EFFECT OF MOISTURE INERTIA MODELS ON THE PREDICTED INDOOR HUMIDITY IN A ROOM

A. Janssens[1] and M. De Paepe[2]

[1]*Department of Architecture and Urban Planning, Ghent University (UGent), B-9000 Gent, Belgium*
[2]*Department of Flow, Heat and Combustion Mechanics, Ghent University (UGent), B-9000 Gent, Belgium*

ABSTRACT
This paper investigates the sensitivity of indoor humidity models to the numerical description of water vapour buffering in porous materials in the room. Three different numerical models are compared: a lumped capacity model, which lumps the moisture inertia in a single capacity for the room, a two-node model, which differentiates between the room air humidity and the representative humidity of an equivalent humidity buffering material, and finally a room-wall model, which describes the water vapour transfer and storage in the building fabric through a continuum model.

KEYWORDS

Moisture buffer, numerical simulation, HAM

INTRODUCTION

Various applications in building design require a proper assessment of the indoor humidity in buildings during the design stage. The indoor humidity should be controlled within a certain range for instance to improve the acceptability of the indoor environment to occupants, or to prevent deterioration of artefacts and materials in museums or libraries. For this purpose mechanical systems, such as ventilation and humidification systems, may be incorporated in the building design. In order to evaluate the need and performance of such systems, a sufficiently accurate dynamic model is needed to predict the achieved indoor humidity and to size the mechanical systems.
Today different numerical models are available to describe the transient water vapour balance of a room and predict indoor humidity. A typical room moisture balance includes water vapour production by moisture sources (humans, plants,…), convective water vapour transfer with ventilation air, and water vapour exchange with the building fabric and furniture. The water vapour exchange between room air and surrounding materials (walls and furniture) is governed by three physical processes: the transfer of water vapour between the air and the material surface, the moisture transfer within the material and the moisture storage within the material. The existing models mainly differ in the way this last part of the moisture balance is described.
A first group of indoor humidity models are the ones incorporated in the commercial thermal building simulation codes, e.g. TRNSYS or EnergyPlus. The main focus of these models is to predict the temperature fluctuations and energy demands of individual rooms. As a result the water vapour exchange with surrounding materials is described in a simplified way. Two approaches are found. In the simplest approach it is assumed that the room and material humidity's are always the same, and so the moisture capacities of walls and furniture are combined into a single room moisture capacity (the so-called effective capacitance or lumped capacity model). In the second approach a differentiation is made between the room humidity and a representative material humidity. In this case the material, which exchanges moisture

with the room air, is represented by a single equivalent volume representative of the average moisture transfer and storage in the material (the so-called effective moisture penetration depth model). In the TRNSYS code this approach is further elaborated by dividing the equivalent volume into a surface layer and a deep layer.
A second group of indoor humidity models are the ones produced by combining the previous models for thermal building simulation with models for heat-, air and moisture transfer in building components (HAM-models). Several HAM-models have been developed and validated worldwide in the last decade (Hens 1996, Trechsel 2001). Since HAM-models are capable of describing heat and mass transfer within the layers of the building envelope in a very precise way, the exchange of water vapour between the room air and the surrounding walls may be accurately defined. Working combinations of such integrated hygrothermal simulation models are about to be developed and may be available to the practitioner in the near future (Künzel et al. 2005).
Both groups of models described above are so-called multi-zone models. They have one basic simplification in common, namely that the air in a room is well mixed, such that the room conditions (temperature, humidity, air pressure) are equal in the whole zone. A new generation of indoor humidity models is currently under development in order to make a prediction of humidity variations within the room air possible. To achieve this, models to describe the vapour exchange between air and porous materials are combined with CFD-codes (Computational Fluid Dynamics). Examples of this approach are given by Steeman et al. (2006).

The scope of this paper is however limited to the multi-zone models. At the moment there is no guidance on the validity and accuracy of the simplified humidity models incorporated in the existing commercial codes. Therefore this paper presents results of a sensitivity study where the different approaches are compared to describe the moisture exchange between the air and surrounding materials. In a first part the numerical description of the various models is explained. The second part presents the calculation results.

INDOOR HUMIDITY MODELLING

Governing equations

Eqn. 1 gives the non-steady-state moisture balance for the indoor air in a room, in terms of the partial pressure of water vapour.

$$\dot{M}_{prod} + \dot{M}_{sys} + \frac{nV}{R_v T_i}(p_e - p_i) = 3600\left[\frac{V}{R_v T_i}\frac{dp_i}{dt} + \sum_j A_j \beta_i (p_i - p_{s,j})\right] \qquad (1)$$

The left hand side contains all moisture sources: indoor vapour production M_{prod} by the users (kg/h), vapour addition by the HVAC-system M_{sys} (kg/h) and vapour gains by ventilation. The right hand side contains the terms describing the vapour storage in the air, and the convective vapour transfer from the air to the interior surfaces of the enclosure walls. Further symbols are: p_i and p_e for the partial water vapour pressures of the indoor and outside air (Pa), R_v the gas constant for water vapour (462 J/kg/K), T_i the indoor air temperature (K), n the ventilation rate (ac/h), V the room volume (m^3), A_j the area of the interior surface of wall j (m^2), β_i the convective surface film coefficient for vapour transfer (s/m) and $p_{s,j}$ the vapour pressure at the interior surface of wall j (Pa).
This latter variable couples the enclosure moisture balance to the moisture conservation equations of the walls and materials surrounding the enclosure. Eqn. 2 describes the mass balance equation for 1D-transfer and storage of water vapour in a wall with porous building materials:

$$\frac{\partial}{\partial x}\left[\delta(\varphi)\frac{\partial p}{\partial x}\right]=\rho\xi(\varphi)\frac{\partial}{\partial t}\left[\frac{p}{p_{sat}(\theta)}\right] \quad (2)$$

where δ is the vapour permeability (s), φ the relative humidity (-), $\rho\xi$ the moisture capacity in terms of relative humidity, derived from the material sorption isotherm (kg/m^3) and $p_{sat}(\theta)$ the water vapour pressure at saturation at temperature θ. Vapour transfer and storage properties are typically a function of ambient humidity.
Finally the boundary condition at the interior material surface is:

$$\beta_i \cdot (p_i - p_s) = -\delta(\varphi)\left.\frac{\partial p}{\partial x}\right|_s \quad (3)$$

Simplified approaches

In the simplified approaches incorporated in thermal building simulation codes, Eqn. 2 and 3 are solved by assuming that only a thin layer near the interior surface interacts with the indoor air. This thin layer with uniform moisture content absorbs and releases moisture to the room air when exposed to cyclic air humidity variations. This approach implies that water vapour transfer between inside and outside through exterior walls is neglected. The depth of the affected layer is related to the effective moisture penetration depth EMPD associated with the period of typical fluctuations in the vapour pressure at the wall surface (Cunningham 2003):

$$EMPD = \sqrt{\frac{\delta \cdot p_{sat}(\theta) \cdot T}{\rho\xi \cdot \pi}} \quad (4)$$

In Eqn. 4 T is the period of the cyclic variation (s). For porous building materials the effective penetration depth for moisture exchange is typically in the order of millimetres for daily variations and in the order of centimetres for yearly fluctuations. It can be shown that 95% of the moisture exchange between the wall and the air occurs in a region of 3 times EMPD near the wall surface.
In the assumption that the wall-air interaction occurs in a humidity buffering layer with thickness Δ and uniform humidity conditions equal to the surface conditions, than the equations 2 and 3 are reduced to a single equation:

$$\beta_i (p_i - p_s) = \rho\xi(\varphi_s)\Delta\frac{d}{dt}\left[\frac{p_s}{p_{sat}(\theta_s)}\right] \quad (5)$$

The calculation of indoor humidity as a function of time now requires the numerical solution of the set of ordinary differential equations 1 and 5. In the existing building simulation codes three different approaches are found to do so:

1. Eqn. 5 is applied to all wall surfaces. The number of equations to be solved per room is j+1. Non-isothermal conditions are assumed: the surface temperature that appears in Eqn. 5 follows from the solution of the energy conservation equations for the individual walls. The moisture capacity of the intervening layer is a function of the relative humidity of the layer. This more complete approach is used in the computer code EnergyPlus (so-called EMPD-model, EnergyPlus 2005).
2. Eqn. 5 is applied to a single humidity buffering layer with properties representative of the average moisture storage properties of all room surrounding surfaces. Isothermal conditions are assumed when solving the buffering layer mass balance: the temperature of the humidity buffering layer is constant. Also the moisture capacity is constant and independent of the layer humidity. This simplified approach may be used in the computer code Trnsys (so-called buffer storage humidity model, SEL et al. 2004).
3. The previous approach is further simplified by assuming that the thermal and humidity conditions in the humidity buffering layer are the same as in the room air. Hence the vapour pressure of the layer is eliminated from Eqn. 1, and the set of 2 equations reduces

to Eqn. 6. This simplest approach may also be used in the Trnsys code (effective capacitance humidity model). The factor on the right hand side is then treated as a constant capacitance, independent of temperature.

$$\dot{M}_{prod} + \dot{M}_{sys} + \frac{nV}{R_v T_i}(p_e - p_i) = 3600\left[\frac{V}{R_v T_i} + \frac{(A\rho\xi)_{eq}\Delta}{p_{sat}(\theta_i)}\right]\frac{dp_i}{dt} \quad (6)$$

HAM-model

In the following these three simplified approaches based on the humidity buffering layer are compared to a solution where the water vapour transfer within the whole of the surrounding walls is described by means of a HAM-model. In this case the coupled set of Eqn. 1, 2 and 3 is solved simultaneously. In the numerical solution a control volume formulation is used here for discretization in space and a fully implicit scheme for discretization in time (Janssens 1998).

The use of a HAM-model also allows a more detailed investigation of the influence of moisture on the heat transfer in the wall and on the resulting heating and cooling demand of a room. This may be explained by means of Eqn. 7, which shows the governing energy conservation equation for a wall.

$$\frac{\partial}{\partial x}\left[\lambda(w)\frac{\partial\theta}{\partial x}\right] + h_{ev}\frac{\partial}{\partial x}\left[\delta(\varphi)\frac{\partial p}{\partial x}\right] = \frac{\partial}{\partial t}\left[(\rho c + c_w w)\theta\right] \quad (7)$$

In this equation λ is the thermal conductivity (W/mK), w the moisture content (kg/m^3), θ the temperature (°C), h_{ev} the latent heat of evaporation (J/kg), ρc the volumetric heat capacity of the material (J/m^{3}K) and c_w the specific heat capacity of water (J/kgK). The first term in the left hand side represents the volumetric heat efflux by heat conduction in the material. The second term describes the latent heat sink as a result of absorption and desorption processes in the material. The right hand side is the rate of heat storage in the material. As the equation shows the presence of moisture affects the heat transfer in two ways: first through the moisture dependency of the apparent heat transfer and storage properties, second through the latent heat of absorption and desorption.

MODEL COMPARISON

Calculation case

For the model comparison a room geometry was adopted from a hypothetical base case building used in the IEA BESTEST procedure. Peuhkuri and Rode (2005) added information to perform an analysis of the indoor and building envelope moisture conditions on the BESTEST building as an input for the work performed for the Annex 41 of the IEA-ECBCS-program (Hens 2003).

TABLE 1: Material properties and boundary conditions (Peuhkuri and Rode 2005)

Internal surface coefficient for heat transfer	8.3 W/(m²K)
External surface coefficient for heat transfer	29.4 W/(m²K)
Internal surface coefficient for vapour transfer β_i	$2.0\ 10^{-8}$ kg/(m²sPa)
External surface coefficient for vapour transfer β_e	$6.25\ 10^{-8}$ kg/(m²sPa)
Aerated concrete dry density ρ	600 kg/m^3
Aerated concrete dry heat capacity c	840 J/kgK
Aerated concrete thermal conductivity λ	$0.18+ 8\ 10^{-4}$w W/mK
Aerated concrete vapour permeability δ	$2\ 10^{-11}+ 1\ 10^{-12}$ exp(4.2φ) kg/(msPa)
Aerated concrete sorption isotherm w	$300(1-909\ln\varphi)^{-0.5}$ kg/m^3

The internal dimensions of the BESTEST building (one single room) are 6m by 8m by 2.7m. For simplicity it is assumed that the building walls, roof and floor are made of monolithic aerated concrete with thickness 15 cm and face the outdoor air on every side of the building. This means that the exterior and interior boundary conditions for walls, roof and floor are the same. One of the walls contains windows with a total surface area of 12 m². Table 1 lists the remaining information on material properties and boundary conditions.
It can be shown that the EMPD of aerated concrete, according to the definition of Eqn. 4, amounts to 11 mm for a cyclic period of 24 h and ambient conditions of 20°C and 50% RH.

Preliminary isothermal analysis

In literature little guidance exists on the choice of the buffering layer thickness Δ to be used in the simplified humidity models. Therefore a preliminary analysis is performed to study the effect of the chosen buffering layer thickness on the predicted indoor humidity. The analysis is performed for constant boundary conditions: indoor and outdoor temperature 20°C, outdoor relative humidity 50% and air exchange rate 0.5 volumes/h. Only the release of water vapour is variable: it is released in the room from 9.00h until 17.00h at a constant rate of 0.5 kg/h. No heat source is present.
The periodic state solution of the indoor relative humidity is calculated by means of the three models described above: the effective capacitance model (EC), the effective moisture penetration depth model (EMPD) and the HAM-model. In all cases the differential equations are solved numerically using a fully implicit scheme for discretization in time and a time step of 1 hour. In the HAM-model the aerated concrete wall contains 30 control volumes in total. In the center of the wall the discretization is 5 mm, near the surface the discretization refines to 1 mm in steps of 1 mm.
Table 2 lists the results of the calculations in terms of the average and daily variation of the periodic state solution. Figure 1 compares the solution of the three models, represented as the humidity variation around the daily average. The EC- and EMPD-models were solved for different values of the buffering layer thickness to show the influence of the choice of Δ. In these two models material properties were taken constant and evaluated at 50% RH.
The results in Table 2 show that the predicted humidity variation is very sensitive to the choice of the buffering layer thickness, both for the EC- and the EMPD-model. In case the buffering layer thickness is taken equal to the effective moisture penetration depth, the order of magnitude of the daily variation predicted by the simplified models corresponds to the variation predicted by the HAM-model. However, as Figure 1 shows, the simplified models are not able to predict the initial fast response of indoor humidity to changes in moisture production, compared to the HAM-model. Further the simplified models overestimate the daily average indoor humidity. This is due to the fact that these models neglect the transmission of water vapour through the exterior walls. In this exercise, the vapour diffusion transfer through the aerated concrete walls is not insignificant: it amounts to 28% of the convective transfer by ventilation.

TABLE 2: Periodic state solution: daily average and variation of indoor relative humidity (%) (EMPD = 11mm)

Model		Daily average	Daily variation (max-min)
EC	Δ = 0	64.9	42.9
	Δ = 0.5*EMPD		14.3
	Δ = EMPD		8.0
	Δ = 3*EMPD		2.8
EMPD	Δ = 0.5*EMPD	64.9	14.8
	Δ = EMPD		9.0
	Δ = 3*EMPD		4.3
HAM		61.8	9.9

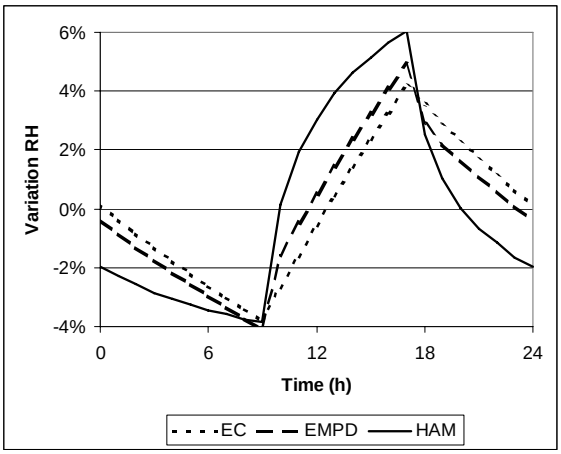

Figure 1: Periodic state solution of three models: relative humidity variation around the daily average

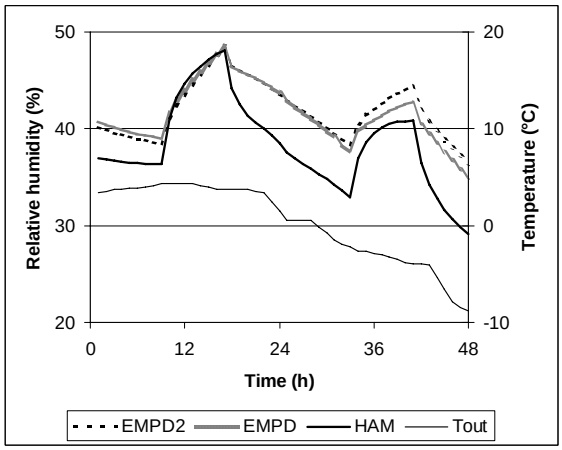

Figure 2: Predicted relative humidity of three models during outside temperature drop (9-10 December)

Model comparison

The evolution of indoor humidity is now predicted in response to variations of exterior climate and building use. A weather file with hourly mean climate data describes the exterior conditions: the IWEC-file for the location of Copenhagen is used. Only temperature and humidity data are considered, solar radiation is not taken into account. Again water vapour is released at a constant rate of 0.5 kg/h from 9.00h until 17.00h every day. Also a heat source is active during these hours with a total power of 800 W (100% convective). An ideal convective heating and cooling system keeps the air temperature in between 20°C and 27°C. The ventilation rate is 0.5 air changes per hour continuously.
As in the preliminary analysis this case is solved with the three models. Based on the previous results the thickness of the humidity-buffering layer in the EC- and EMPD-models is taken equal to the effective moisture penetration depth (11 mm). The two versions of the EMPD-model described above are now part of the comparison. In the first version, referred to as EMPD, changes in the indoor surface temperature have an impact on the water vapour balance of the humidity-buffering layer (non-isothermal assumption). In the second version, referred to as EMPD2, the factors in the vapour balance equation for the humidity-buffering layer have constant values (isothermal assumption).

Table 3: Predicted inside conditions for the different models

OUTSIDE	mean	minimum	10-percentile	90-percentile	maximum
Temperature	8.3	-9.6	0.2	17.0	26.8
Vapour pressure	892	191	470	1389	2162
R. Humidity	77	21	56	94	100
INSIDE	mean	minimum	10-percentile	90-percentile	maximum
HAM					
Temperature	20.1	20	20	20	26.8
Vapour pressure	1177	589	798	1610	2404
R. Humidity	50	25	34	67	78
EMPD					
Temperature	20.1	20	20	20	26.5
Vapour pressure	1244	557	847	1721	2483
R. Humidity	53	24	36	72	84
EMPD2					
Temperature	20.1	20	20	20	26.5
Vapour pressure	1243	577	847	1709	2318
R. Humidity	53	25	36	71	95

Table 3 gives a summary of calculation results. Figures 2-4 show some details of the simulations. Since the solutions of the EC- and the EMPD2-model appeared to match quite well, the results of the EC-model are not listed and not discussed anymore.
As the table shows, the indoor air temperatures predicted by the HAM-model during free floating conditions (no heating nor cooling) slightly deviate from the results of the EMPD-models. This is caused by the fact that the HAM-model incorporates the dependency of thermal material properties on moisture content.
With regard to the predicted humidity, some clear differences appear between the results of the HAM-model and the EMPD-models. In addition to the explanation made in the preliminary analysis, a major cause of observed deviations lies in the interaction between the heat transfer in the walls and the moisture balance in the enclosure. This interaction is accurately described in the HAM-model, but totally absent in the EMPD2-model (the humidity buffering layer is considered isothermal). The effect of this interaction becomes clear during periods with sudden changes in exterior or interior temperature. Figure 2 shows the evolution in relative humidity during a drop in exterior temperature. The HAM-model predicts a faster humidity decrease than the EMPD-models. This is explained by the fact that the temperature in the hygroscopic monolithic walls drops in response to the exterior temperature, after which the absorption of water vapour by the walls increases. For, the immediate effect of a drop of temperature in a hygroscopic material is to leave the moisture content and corresponding relative humidity unchanged, but to decrease the vapour pressure (Cunningham 2003). Since this effect is not modelled in the EMPD2-model, changes in outdoor temperature do not affect the predicted relative humidity (as far as the outside vapour pressure does not change).
A similar response is observed during changes in interior temperature, as shown in Figures 3-4. Here the indoor temperature increases above the heating set point of 20°C during the day, followed by an increase of the interior surface temperature of the walls, and a resulting release of absorbed moisture to the interior. As the EMPD-model incorporates the interaction between interior surface temperature and moisture balance of the humidity buffering layer, its results are well in line with the HAM-simulations. However the results of the isothermal EMPD2-model deviate from the other two.

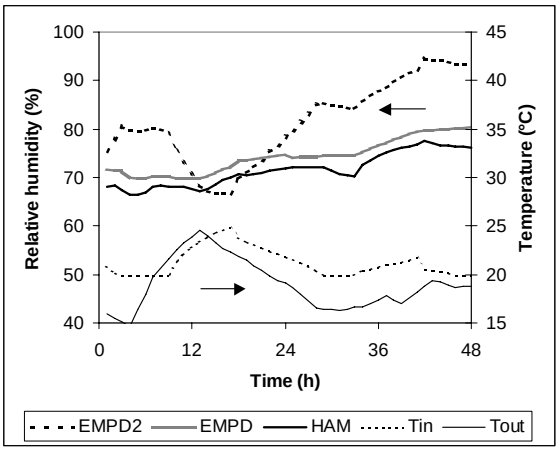

Figure 3: Predicted relative humidity of three models during warm summer days (7-8 August)

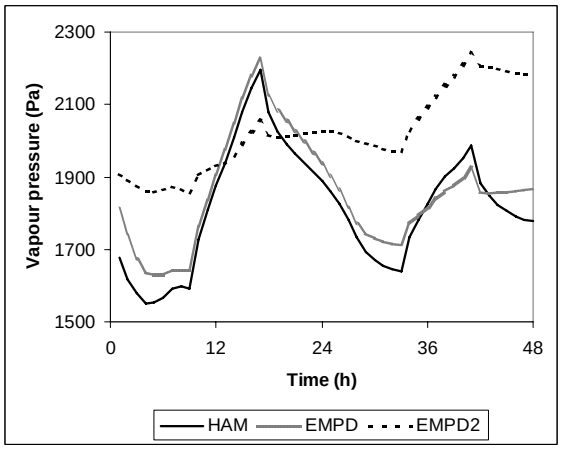

Figure 4: Predicted water vapour pressure of three models during warm summer days (7-8 August)

CONCLUSIONS

This paper investigated the sensitivity of indoor humidity models to the numerical description of water vapour buffering in porous materials in the room. Three different numerical models were compared: an effective capacitance model, an effective moisture penetration depth model, which differentiates between the room air humidity and the representative humidity of an equivalent humidity buffering layer, and finally a room-wall model, which describes the water vapour transfer and storage in the building fabric through a continuum HAM-model. Deviations between calculation results of the various models have been related to different assumptions in modelling. The results of the simplified models appeared sensitive to the choice of thickness of the humidity buffering layer. The interaction between the temperature and the moisture balance of the hygroscopic materials had a major impact on humidity predictions and should be well described.

ACNOWLEDGMENTS

This analysis is part of the research work on Whole Building Heat, Air and Moisture Response (MOIST-ENG) in the frame of Annex 41 of the International Energy Agency ECBCS-programme.

REFERENCES

Cunningham M.J. 2003. The building volume with hygroscopic materials: an analytical study of a classical building physics problem. Building and Environment 38, 329-337.
Energyplus. 2005. Engineering reference. http://www.eere.energy.gov/buildings/energyplus.
Hens H. 1996. Heat, air and moisture transfer in highly insulated envelope parts, task 1: modeling. IEA-EXBCS-Annex 24 Final Report, Acco, Leuven.
Hens H. 2003. Whole building heat air and moisture response. ECBCS News Issue 38, 1-3.
Janssens, A. 1998. Reliable control of interstitial condensation in lightweight roofs: calculation and assessment methods. Doctoral thesis, K.U.Leuven, Laboraatory of building physics.
Künzel H.M., A. Holm, D. Zirkelbach, A. Karagiozis. 2005. Simulation of indoor temperature and humidity conditions including hygrothermal interactions with the building envelope. Solar Energy 78, 554-561.
Peukuhri R. and C. Rode. 2005. Common exercise 1 ‘realistic case’: whole building heat and moisture analysis. IEA-ECBCS-Annex 41 Internal paper.
SEL, TRANSSOLAR, CSTB, TESS (2004). *Trnsys 16: a Transient System Simulation Program*, University of Wisconsin, Madison, USA.
Steeman, H.J., C. T’Joen, A. Willockx, M. De Paepe, A. Janssens. 2006. CFD modelling of HAM transport in buidings: boundary conditions. Submitted to the 3th International Building Physics Conference, Montréal.
Trechsel H.R. (ed.) 2001. Moisture analysis and condensation control in the building envelope. ASTM Manual 40. West Conshohoken PA.

NUMERICAL SIMULATIONS OF ENERGY PERFORMANCE OF A VENTILATION SYSTEM CONTROLLED BY RELATIVE HUMIDITY

M. Woloszyn, J. Shen, A. Mordelet and J. Brau

CETHIL, CNRS UMR 5008 – UCBL – INSA de Lyon, bat. Freyssinet, 69 621 Villeurbanne Cedex, France

ABSTRACT

High levels of indoor relative humidity are one of the main causes of moisture damage in buildings. That cause can be removed by an appropriate ventilation system. Relative humidity controlled ventilation systems were designed to increase energy performance of buildings without exposing them to moisture damage. The study of the performance of such a system in terms of energy savings and maximum relative humidity is proposed here using numerical simulations with an appropriate whole building heat, air and moisture modelling approach that is developed in the frame of IEA Annex 41. In the studied dwelling the benefits of relative humidity controlled ventilation system were found only in terms of indoor climate (relative humidity) and not in terms of energy savings. Moreover the study showed that for the predictions of global energy consumption some simplifications, such as using monozone calculations and neglecting moisture buffering effect of materials can be admitted. However for estimations of the indoor climate in each room (temperature and relative humidity) multizone simulations and modelling of moisture interactions between air and materials are necessary.

KEYWORDS

Energy, Relative humidity, Ventilation, Numerical Simulation, Moisture buffering, Multizone

INTRODUCTION

High levels of indoor relative humidity are one of the main causes of moisture damage in buildings. They stimulate mould growth on surfaces and condensation problems inside the building envelopes. Indoor moisture is mainly due to human presence and activities, and can be removed by an appropriate ventilation system. Ventilation has a considerable impact on the energy performance of the building, especially in modern, very well insulated dwellings, where the heat loss due to the air renewal can account for as much as half of the total heat loss. It seems then, that the reduction of the amount of new cold air introduced into the building contributes to bringing down the energy consumption. However, in order to avoid long term damage due to moisture problems caused by insufficient ventilation this type of solutions must be carefully studied. The performance of a ventilation system in terms of energy savings and of maximum relative humidity can be analysed using numerical simulations with an appropriate modelling approach.

A comparative study of two ventilation systems, one with the airflow controlled by relative humidity (called RHC in the following) and one with a constant airflow rate is proposed in this paper. A second objective of the work was to analyse the impact of different simplifying hypothesis on the numerical simulations results.

HUMIDITY CONTROLLED VENTILATION SYSTEM

Ventilation systems with the airflow controlled by relative humidity were designed in order to increase the energy performance of buildings without exposing them to moisture damage. The special feature of these systems is their air outlet or sometimes their air inlet equipped with a humidity sensitive membrane acting on the cross section of the vent. The airflow increases for high indoor humidity values and decreases when the indoor air gets drier. An additional advantage of these systems, used in dwellings in France, is a good correlation between relative humidity and most of the air pollutants.

Former studies (Woloszyn et al. 2000, Enache et al. 2002), already showed that energy savings can be insignificant. Anyhow, the real energy performance of such a system should not only depend upon moisture production in the dwelling but also upon moisture buffering capacity of all materials in contact with the indoor air.

WHOLE BUILDING MODELLING APPROACH

Numerical simulations of a ventilation system controlled by relative humidity must be carefully conducted using the whole building heat, air and moisture approach. In this case the energy (used to heat the dwelling), the air (ventilation system) and the moisture (controlling parameter of the ventilation system) have very strong interactions that must be taken into account. Such models are being developed now in the frame of the international collaboration in the Annex 41 project from ESBCS program of IEA (Rode et al. 2005).

In the following study, Clim2000 software was used to perform the numerical simulations (Guyon and Rahni, 1997, Plathner and Woloszyn, 2002). The model library of this modular open code includes more than hundred elements representing various building components such as the layer of a wall, a window, an electric heater, different vents, moisture buffering capacity of furniture, etc. Numerical resolution is done by simultaneous solving of a system of algebraic-differential equations generated by the assembly of the global model. The dynamic behaviour is assessed by using an implicit solver with auto-adaptative time step. This method allows for true representation of all the interactions described in the physical model.

CASE STUDY

Building

The BESTEST building from the Common Exercise 0 of the Annex 41 of IEA (Rode et al. 2005), originally proposed by Judkoff and Neymark (1995) in Annex 21, is used as a support for this study. The indoor space of about 50 m² is divided into one big living room with a separated bathroom and kitchen, as showed in Figure 1. The building has heavyweight structure (see Table 1). The heaters are situated in the living room and are controlled by the indoor air temperature (set point temperature: 20°C). Internal loads represent 2 persons, equipments, lighting and moisture production due to human activity (showers, cooking, etc.) with the scenario of Table 2 over a typical day. The building is situated in Trappes in northern France. The simulations were run over one cold month (February) and some results are focusing on the 3 first days of this month.

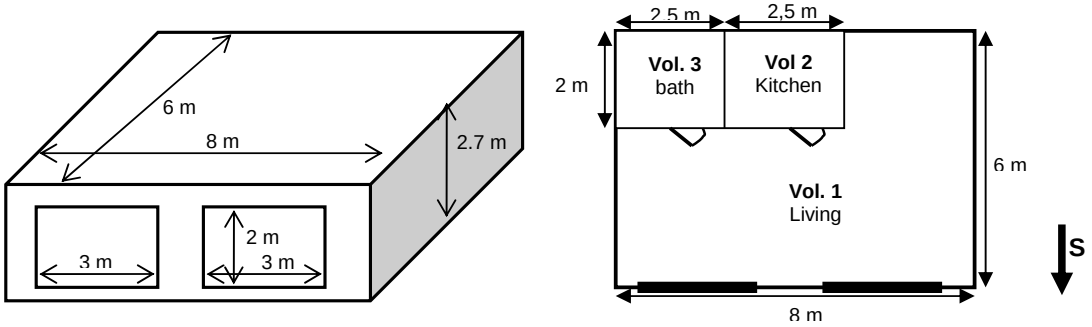

Figure 1: Test building

TABLE 1
Description of the envelope of the test building

Wall	Materials	Area [m²]	U [W/Km²]
Vertical walls	Concrete block (0.51 m) + Foam insulation (0.04 cm) + Wood siding (0.14 m)	63.6	0.512
Floor	Concrete slab (0.08 m) + Insulation (1.007 m)	48	0.039
Roof	Plasterboard (0.16 m) + fibreglass (0.04 m) + roofdeck (0.14 m)	48	0.318
Windows	Double-pane	3	12

TABLE 2
Total daily internal loads

	Load [kWh/day]	Moisture production [kg/day]
Occupants	1,2495	1,575
Bathroom	0,12	3,12
Cooking	1,85	3,7
Equipments + Lighting	1,077	
TOTAL	4,2965	8,395

Ventilation system and indoor moisture content

Two ventilation systems are compared:

- A first with the airflow controlled by relative humidity (RHC), with a minimum flow rate of 80 m^3/h (RH_{indoor} < 30%) and a maximum of 160 m^3/h (RH_{indoor} > 70%) and with linearly interpolated airflow rate in between.
- A second with a constant airflow of 120 m^3/h.

The values of the flow rates were determined by preliminary simulations in order to keep the indoor relative humidity at a suitable level. In both systems the inlet is situated in the living room and the exhausts equally distributed in the bathroom and the kitchen.

Moisture interactions between air and indoor materials are represented using the hygroscopic buffer model proposed by Duforestel et al. (1994), and successfully used by Plathner et al. (2002). The model represents all materials as a lumped capacity with an internal moisture content found by preliminary simulations in order to keep a good balance on a long time period. Here, for the ventilation rate used, the internal moisture content of the hygroscopic buffer was found to be 9.1 g/m^3.

Numerical simulations

The parameter study was conducted to compare the performance of the two ventilation systems but also to define the level of detail necessary to conduct the study. The

simplifications concerned both the geometry and physical representation. The compared cases include:

- RHC and constant ventilation,
- Neglecting or not the moisture buffering capacity of indoor materials,
- Using one-zone (whole dwelling = one zone) or multi-zone (whole dwelling = 3 rooms = 3 zones) approach.

In the case of a multi-zone approach the 3 air zones (bathroom, kitchen and living room) are separated by doors. The doors can be opened (air recirculation is possible) or closed (air is passing only in one direction).

RESULTS AND DISCUSSION

Mono-zone vs. multi-zone approach

The results of relative humidity and of energy use showed that when the doors remain open the difference between the two representations is insignificant. Because of the recirculation flow through the doors, the air in the whole apartment is well mixed. A typical situation is presented in figure 2. The net dry air flow follows the ventilation principle and goes from the living room to the kitchen but the net vapour flow goes the opposite way. This situation happens when the moisture content in the kitchen is higher than in the living room.

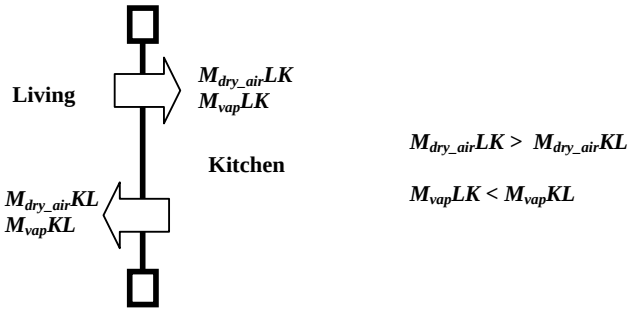

Figure 2: Typical recirculating air flow through the kitchen door during peak vapour production in the kitchen.

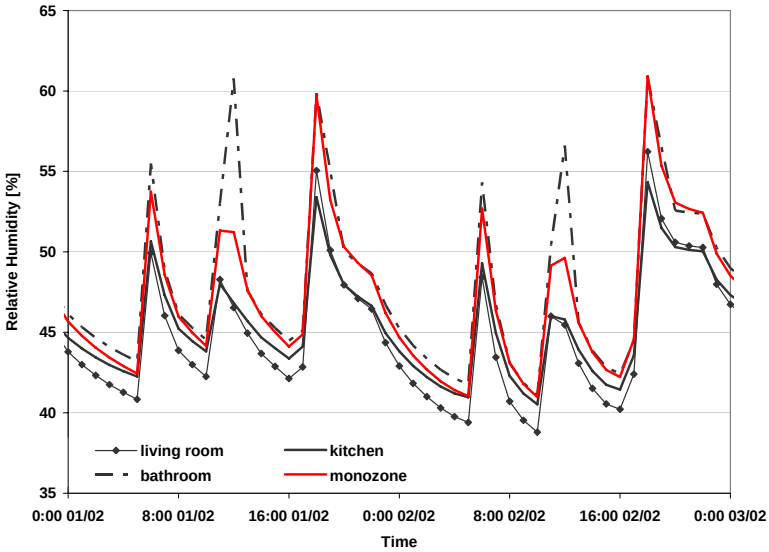

Figure 3: Indoor relative humidity in case of RHC ventilation for both modelling approaches: mono- and multi-zone (doors closed).

On the opposite, when the doors are closed some differences in the indoor climate can be seen. The temperatures in the kitchen and bathroom vary from 18 to 22°C and the peaks of relative humidity are much higher in the kitchen and the bathroom than in the living room (figure 3).

Moisture interactions between air and constructions

The figure 4 shows indoor relative humidity computed, neglecting or not, moisture buffering capacity of materials. As expected, neglecting this phenomenon results in much higher amplitude of relative humidity variations and in peak values overestimated by about 10%.

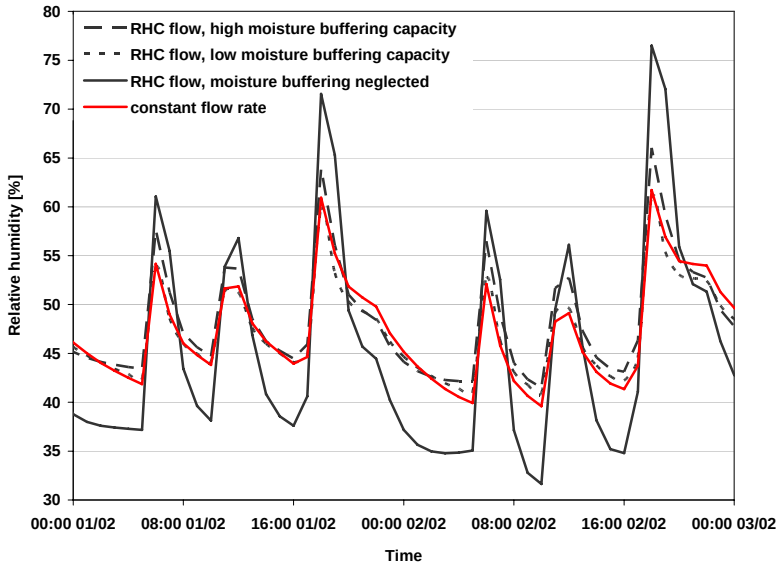

Figure 4: Indoor relative humidity for different moisture buffering representations of indoor materials

RHC vs. constant flow ventilation systems

The energy use for space heating for the most significant cases is given in table 3. As mean ventilation rates in both systems are similar, all results are comparable and RHC ventilation has no real impact on the energy consumption of the studied dwelling. A constant rate ventilation performs even better in terms of energy consumption than RHC ventilation, but the difference is only about 4% (case 2 vs.1 and 5 vs. 4). Moreover the differences between the energy uses estimated by mono- or multi-zone modelling are less than 1% (case 2 vs. 5 and case 1 vs. 4). Also neglecting moisture buffering capacity of materials gives still a correct estimation of the global energy use: no difference was found for constant ventilation (cases 2 and 3) and a small difference of about 2% in case of RHC system (case 4 vs. 6).

TABLE 3
Energy use for heating in February for different cases

Case	Number of zones	Moisture buffering	Ventilation system	Energy use [kWh]	Difference [%]
1	3 (closed doors)	Yes	RHC	767	0
2	3 (closed doors)	Yes	Constant	736	-4.05
3	3 (closed doors)	No	Constant	735	-4.07
4	1	Yes	RHC	773	+0.78
5	1	Yes	Constant	737	-3.92
6	1	No	RHC	757	-1.25

Figure 5 shows the differences in the indoor relative humidity for the two ventilation systems. In the living room the differences are lower than 4% when the moisture buffering effect of indoor materials is represented.

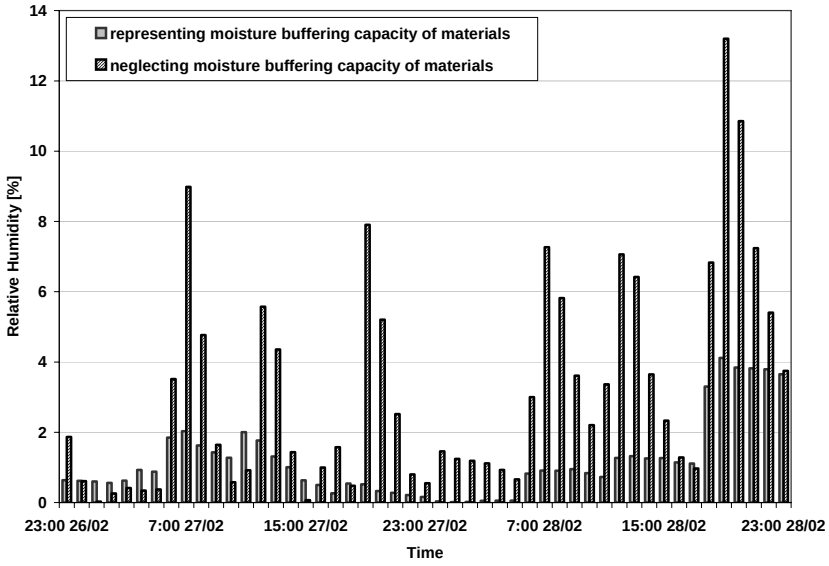

Figure 5: Differences in relative humidity in the living room between the two ventilation systems for two modelling possibilities: neglecting or not moisture buffering capacity of materials.

CONCLUSIONS

In the studied dwelling no energy savings were found due to the use of relative humidity controlled ventilation system. Concerning the indoor climate, when a good mixing of the air can be assumed (open doors) a constant flow ventilation system is enough to ensure correct conditions. However, when the doors are closed RHC system helps to maintain adequate climate in rooms with high moisture production. It seems though that the benefits of RHC system should be estimated in terms of indoor climate (relative humidity or risks of moisture damage…) and not of energy savings.

For predictions of global energy consumption some simplifications, such as using mono-zone calculations and neglecting moisture buffering effect of materials, can be admitted. However these simplifications are not allowed when correct estimations of the indoor climate (temperature and relative humidity) are the objective. When the doors are often kept closed, multizonal simulations are necessary and for correct estimations of indoor relative humidity the moisture interactions between air and materials must be taken into account.

REFERENCES

Duforestel, T. and Dalieux, P. (1994). A model of hygroscopic buffer to simulate the indoor air humidity behaviour in transient conditions. *Proceedings of European Conference on Energy Performance and Indoor climate in Buildings*, Lyon, France, vol3. 791-797

Enache, D., Colda, I. and Vartires A. (2002). The modelling of humidity-control ventilation in habitat buildings. *V-th International HVAC+R Technology Symposium*, Istanbul, Turcia, april 29 – may 1, 2002.

Guyon G. and Rahni N. (1997). Validation of building thermal model in CLIM2000 simulation software by using full-scale experimental data, sensitivity analysis and uncertainty analysis, Proc. *Building Simulation* 97, Prague, Czech Republic

Plathner, P. and Woloszyn, M. (2002). Interzonal air and moisture transport in a test house. Experiment and modelling. *Buildings and Environnement*, **37:2**, 189-199.

Judkoff, R., and J. Neymark. 1995. *Building energy simulation test (BESTEST) and diagnostic method*. NREL/TP-472-6231. Golden, Colo.: National Renewable Energy Laboratory.

Rode, C., Peuhkuri, R., Woloszyn, M., and L. Hedegaard (2005). IEA Annex 41 Subtask 1 – Modelling principles and common exercises. To be presented at *AIVC Conference*, Brussels, September 21-23, 2005

Woloszyn, M., Rusaouën, G., Hubert, J.-L. and Aude, P. (2000). Modélisation hygro-thermo-aéraulique des bâtiments pour l'étude de la ventilation hygroréglable. *Congrès français de thermique, SFT 2000*. Lyon (France) : Elsevier, 753-758.

INDOOR CLIMATE DESIGN FOR A MONUMENTAL BUILDING WITH PERIODIC HIGH INDOOR MOISTURE LOADS

A.W.M. (Jos) van Schijndel

Technische Universiteit Eindhoven
Department of Building and Architecture, Building Physics and Systems (BPS)
VRT 6.29, P.O.Box 513
5600 MB Eindhoven, the Netherlands
email: A.W.M.v.Schijndel@bwk.tue.nl

ABSTRACT
The paper presents a study of the indoor climate of a monumental building with periodic high indoor moisture loads. Several scenarios of the past performance and new control classes are simulated and evaluated. The results include the influence of hygric inertia on the indoor climate and (de)humidification quantities of the HVAC system. It is concluded that: (1) The past indoor climate can be classified as ASHRAE control C with expected significant occurrences of dry (RH below 25%) and humid (RH above 80%) conditions; (2) ASHRAE control C is not suitable for the new hall. The climate control classification for the new hall ranges from B to AA.; (3) The demands on the HVAC system to facilitate pop concerts in the new hall are 40 kW heating power, between 100 and 200 kW cooling power, between 40 and 80 kW humidification power and 125 kW dehumidification power; (4) In case of control class AA, placing additional hygroscopic material has no significant effect. In case of control class B, the placing of additional moisture buffering material (5 air-volume-equivalents) does not decrease the (de)humidification power and it decreases the (de)humidification energy by 5%.

KEYWORDS
Indoor climate, moisture load, model, simulation, monumental building

1. INTRODUCTION
A monumental theatre, formerly used as a cinema, is renovated. The interior of the theatre, containing monumental paintings, wood and plaster, is well preserved. It is concluded that the past heating of the building had no significant impact on the monumental interior. A new destination of the renovated theater is to facilitate (pop) concerts. This will cause a much higher indoor moisture load as before. An important demand is that the indoor climate may not deteriorate compared to the past situation. Currently the building is under construction, so measurement of the original situation is not possible. Therefore simulation is the only tool that can be used to check the indoor climate performances of the past situation and new designs. The objectives of this paper are twofold: (I) Demonstration of the use of a new simulation and visualization tool by: Characterization of the past performance of the indoor climate; classification for the new climate control and calculating the required HVAC capacities. (II) A preliminary study of the effect of moisture buffering on the (de)humidification energy of the HVAC system. The outline of the paper is as follows: Section 2 presents background information on the building and its monumental interior, performance criteria for the indoor climate and the used simulation tool HAMLab. Section 3 provides simulation results of the past indoor climate of the Luxor hall and new designs with and without placing additional hygroscopic material, using the new visualization chart. In Section 4, a discussion on the simulation results is presented. Section 5 shows the conclusions.

2. BACKGROUND

The current building and its monumental interior

The Luxor theatre, designed by Willem Diehl, was built in 1915 at Arnhem (Netherlands). The main hall (volume about 1800 m^3) has no windows. The outdoor walls are made of brick (0.8m) with air gap. The roof is made of tiles. It's monumental interior consists of a wooden stage frame, gypsum/wooden ceiling artifacts and paintings on wood and paper. Figure 1 provides an impression of the building and the hall.

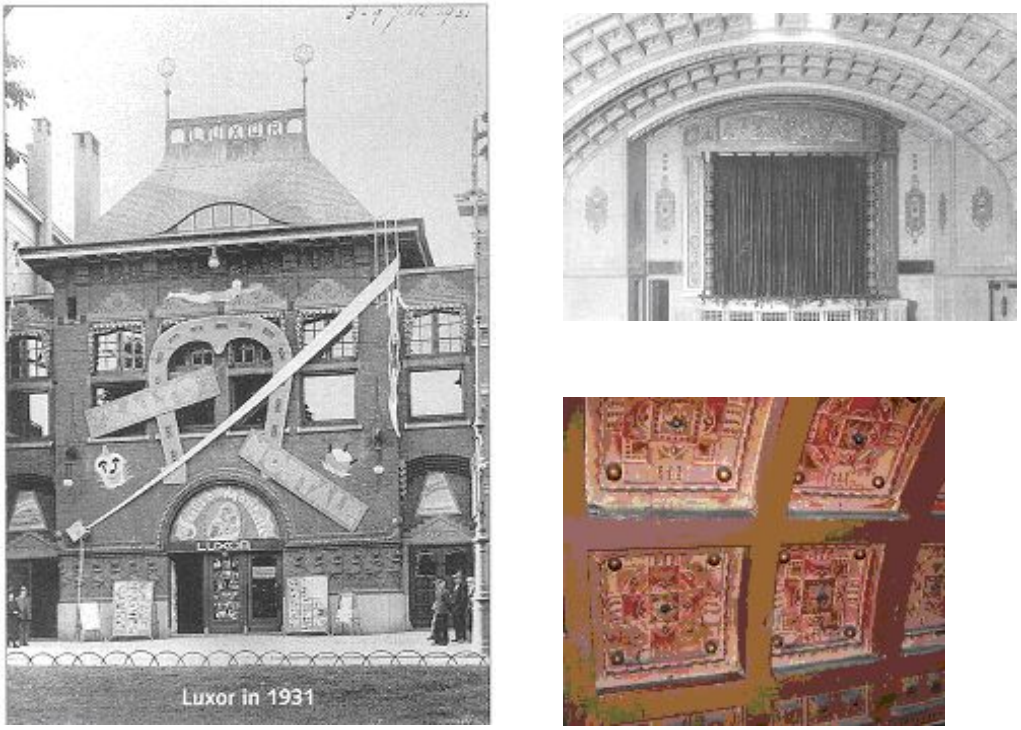

Figure 1: Left: The Luxor Theatre in 1931; Right top: The monumental wooden stage frame; Right bottom: Gypsum/wooden ceiling artifacts.

The performance criteria and classification of the indoor climate

The performance criteria for the indoor climate are based on control classes (ASHRAE 1999). Details can be found in Section 3.

The modeling tool HAMLab

HAMLab (Heat, Air & Moisture Laboratory) is used as simulation tool (van Schijndel & Hensen, 2005). It is implemented in the scientific computation software MatLab. HAMLab provides a collection of models, functions and data to assist scientific computations in the research area 'whole building HAM response and control'. It is also one of the tools involved at the current IEA Annex 41. In this paper, HAMLab is mainly used to simulate indoor climates. Background information on the physics and implementation is provided by (van Schijndel & de Wit, 2005). Validation results are published in: (Schellen 2002), (van Schijndel & de Wit, 2003), (van Schijndel & Schellen 2005).

3. SIMULATION RESULTS

Climate Evaluation Chart (CEC)

All simulated scenarios are presented by Climate Evaluation Charts (CEC). Because there is a lot of information in the chart, an explanation of the CEC is presented now. Figure 2 presents an typical example of a CEC. The interpretation of the chart is explained below (the data itself are not important at this moment)

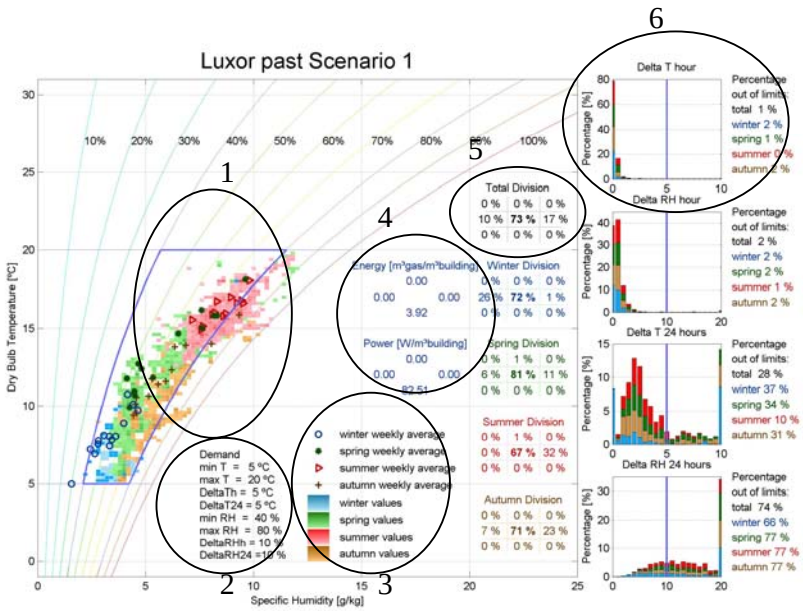

FIG. 2: Example CEC. Note: Some parts of the CEC rely on color

The background of the chart is a standard psychometric chart for air, with on the horizontal axis: the specific humidity, on the vertical axis: the temperature and curves for the relative humidity. Area 2 shows the demanded performance (demands) on: (1) climate boundaries: maximum and minimum temperature and relative humidity (min T, max T, min RH and max RH) and (2) climate change rate boundaries: maximum allowed hourly and daily changes (DeltaTh, DeltaT24, DeltaRHh, DeltaRH24). Area 1 shows the climate boundaries and the simulated climate of one (Dutch standard test reference) year. The simulated climate is presented by seasonal (Spring from March 21 till June 21, etc.) colors representing the percentage of time of occurrence and seasonal weekly averages. The colors visualize the climate distribution. For example, a very stable climate produces a narrow spot, in contradiction to a free floating climate which produces a large cloud. Area 3 provides the corresponding legend. Area 5 shows the total percentage of time of occurrence of areas in the in the psychometric chart (9 areas). In this example 73% of the time the climate is within the climate boundaries; The area to the left (too dry) occurs 10% of the time, the area to the right (too humid) occurs 17% of the time. The climates in the other 6 regions do not occur. Below area 5 the same can be found for each season. Area 4 shows the energy amount (unit: m^3 gas / m^3 building volume) and required power (unit: W / m^3 building volume) used for heating (lower), cooling (upper), humidification (left) and dehumidification (right), assuming 100% efficiencies. In this example the energy amount is 3.92 m^3 (gas / m^3 building volume) and required power is 82.51 (W / m^3 building volume) used for heating. Cooling, humidification and dehumidification are zero in this example. Area 6 presents the occurrence in percentage of time outside the climate change rate boundaries. In the example the demand of maximum allowed hourly change of temperature of 5 (^{o}C/hour) is shown as a blue line. The distribution per season is provided together with the percentage of time of out of limits. In this example, area 6 shows that only 1% of the time, the hourly temperature change rate is out of limits.

This is also specified for each season. Below area 6 the same can be found for the other climate change rate boundaries. All simulation results will be presented below.

Simulated scenarios
All simulations are performed using a test reference year for the Netherlands. The past performance is simulated using two scenarios, representing past periodic and intensive use of the hall. The goal of these scenarios is to simulate worst-case conditions. The results are used for comparison with new control class designs. The future use of the hall includes (pop) concerts. This will cause a much higher moisture load in the hall. This effect is included in all future scenarios. The simulated control class scenarios (ASHRAE, 1999) start with the lowest class, representing the same type of HVAC system as in the past and end with the highest class, representing precision control. Furthermore, extra scenarios are included with the use of additional hygroscopic material. The goal of these scenarios is to study the effect of moisture buffering on the indoor climate, energy amount and required power. After presenting all scenarios the results will be discussed in Section 4.

The hall used as cinema The hall was heated and ventilated by an air system. During a performance (duration 4 hours, 200 sitting people producing 17 kW heat and 2.5 g/sec moisture) the system provided an estimated ventilation rate of 10 ACH. During the day (duration 10 hours, 2 people) this was estimated as 2 ACH and 1 ACH for the rest (including infiltration). In order to estimate the past indoor climate, two extreme scenarios are simulated. The assumption is made that the past indoor climate was somewhere between the next two past scenarios: (1*) periodic use of the hall*: 2 times a week a performance, the hall is only heated during these performances. Furthermore a minimum air temperature of 5 ^{o}C is maintained. (2) *intensive use of the hall*: 6 times a week a performance, the hall is also heated during the day. A minimum air temperature of 10 ^{o}C is maintained. The results are presented in figure 3 and 4.
A control class C design All new designs have to facilitate: (a) 2 concerts a week (duration 4 hours, 700 moving people producing 63 kW heat, 27 g/sec moisture) with a designed ventilation rate of 10 ACH; (b) 3 meetings a week (duration 4 hours, 100 people producing 8 kW heat, 1 g/sec moisture) with a designed ventilation rate of 10 ACH; (c) During the day (duration 10 hours, 10 people, 2 ACH) and 1 ACH for the rest (including infiltration).
First, a control class C design will be evaluated. Class C, defined as 'prevent all high risk extremes', usually consists of basic heating and ventilation. Two scenarios are presented: (1) *HVAC system: heating, ventilating, without additional hygroscopic material*, (2) *HVAC system: heating, ventilating, with additional hygroscopic material*. The results are presented in figure 5 and 6 (Note: There are no 'percentages out of limits' presented in these CECs, because (ASHRAE) control class C does not specify a limitation of the allowable change rates).
A control class B design Also, a control class B design will be evaluated. Class B, defined as 'precision control, some gradients plus winter temperature setback', is usually a HVAC system, including cooling and (de)humidification . Two scenarios are provided: (1) *HVAC system: climate control, without additional hygroscopic material*. (2) *HVAC system: climate control, with additional hygroscopic material*. The demanded performance and results are presented in figure 7 and 8.
A control class AA design Finally a control class AA design will be evaluated. Class AA, defined as 'precision control, no seasonal changes', is usually a high-tech HVAC system, including cooling and (de)humidification. One scenario is presented: *HVAC system: climate control*. The demanded performance and results are presented in figure 9.

Periodic use of the hall

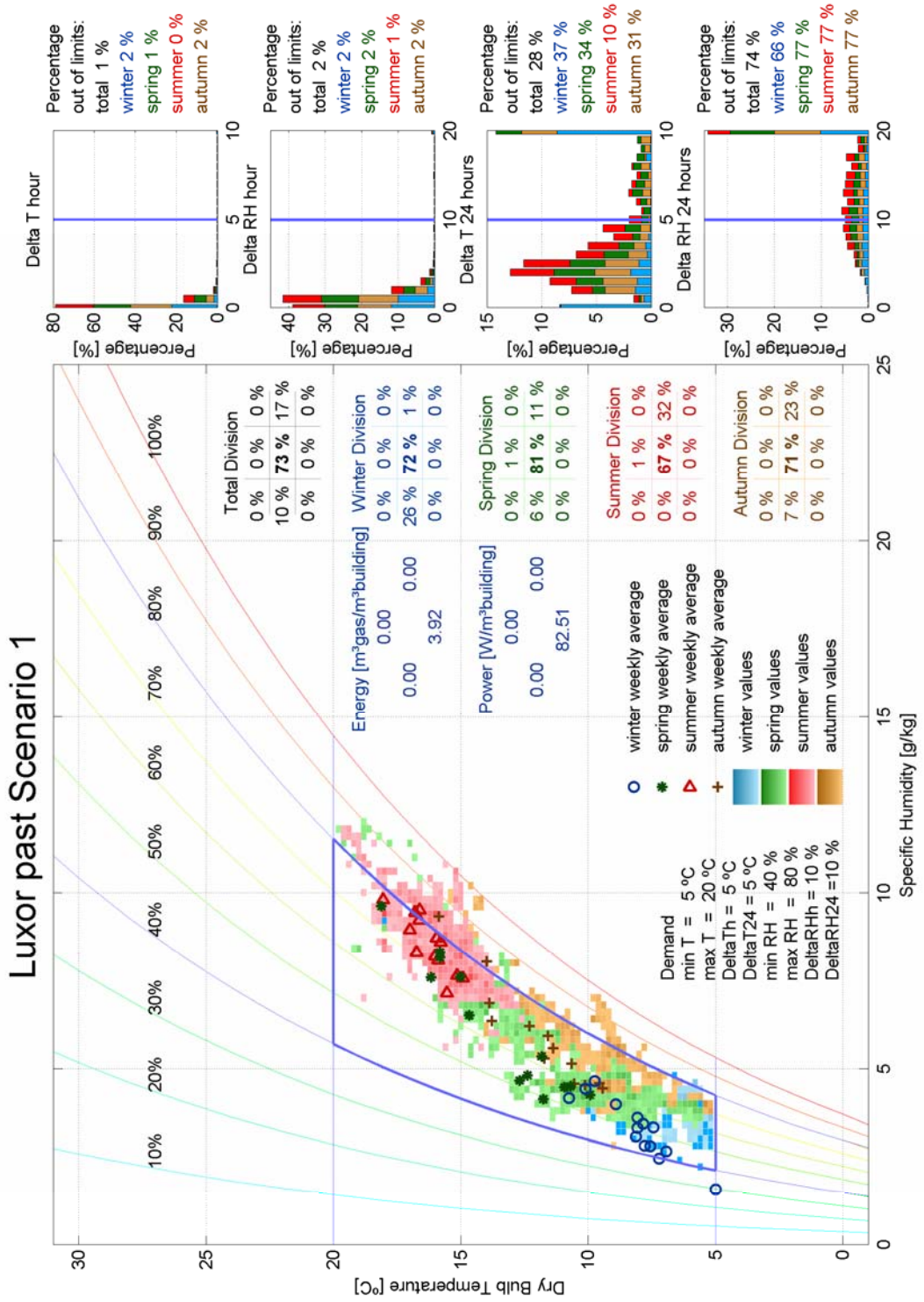

FIG. 3: The CEC of Scenario ‘periodic use of the hall’

Intensive use of the hall

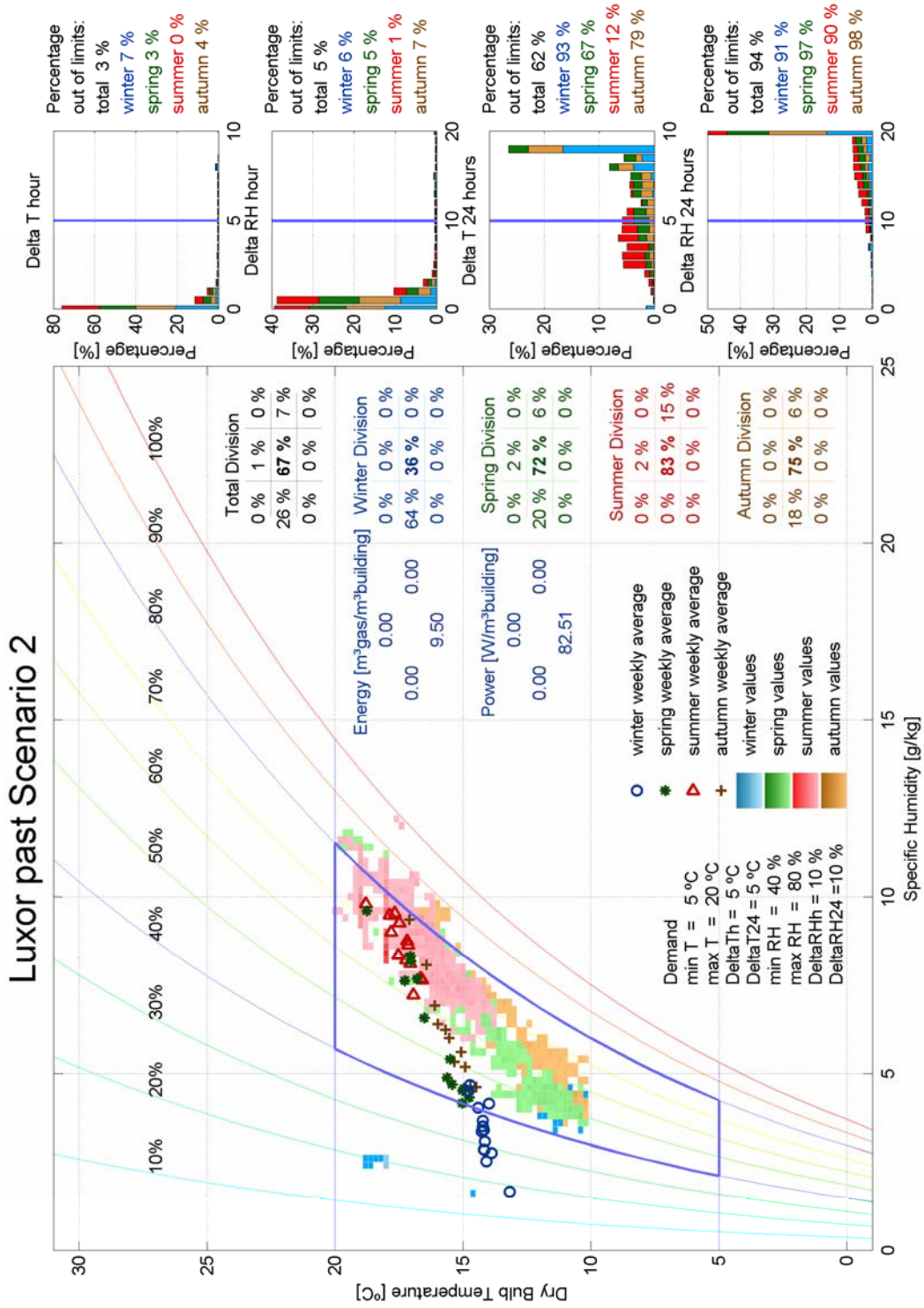

FIG. 4: The CEC of Scenario ‘intensive use of the hall’

HVAC system: heating, ventilating, without additional hygroscopic material

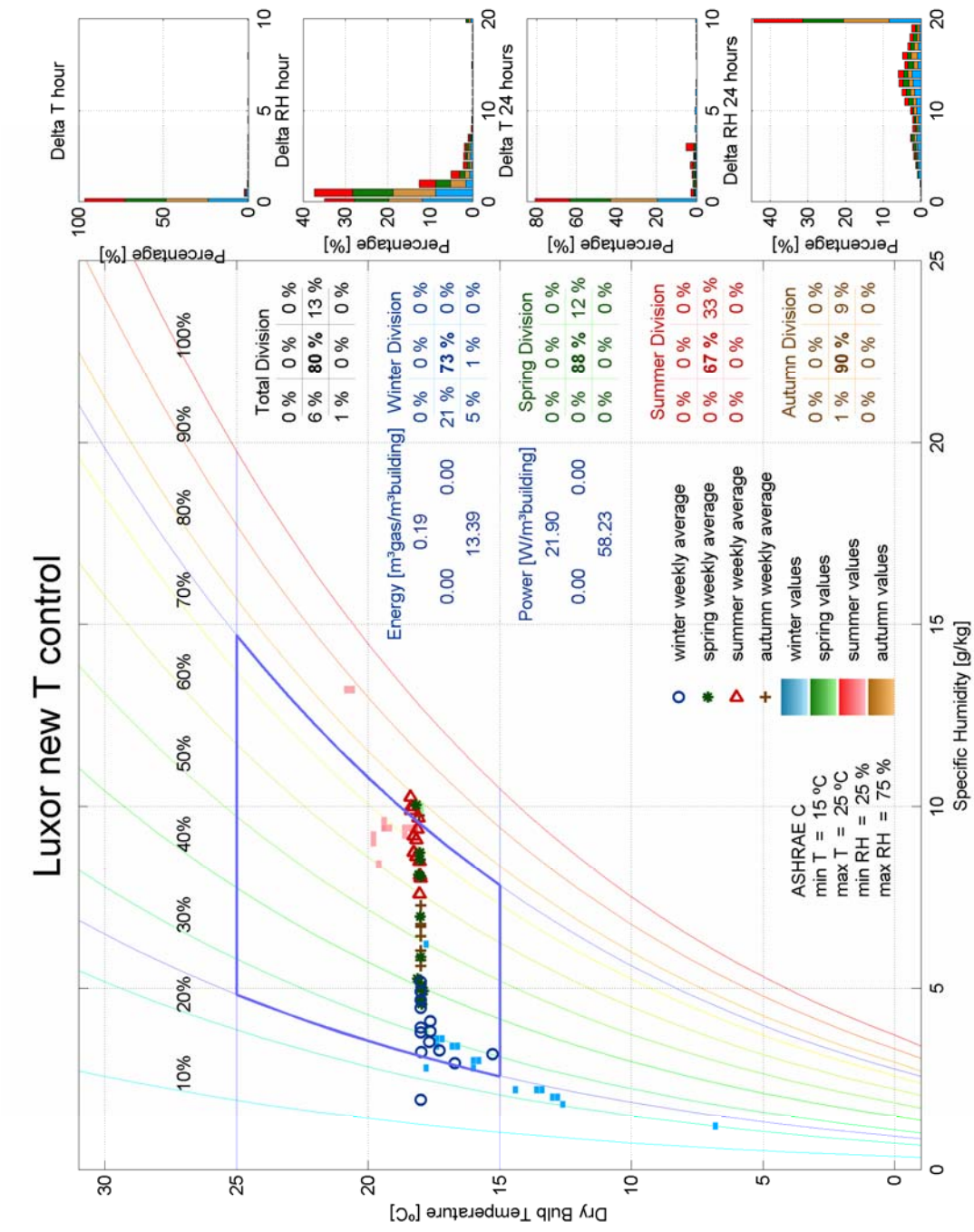

FIG. 5 The CEC of Scenario ‘control class C design without additional hygroscopic material’

HVAC system: heating, ventilating, with additional hygroscopic material

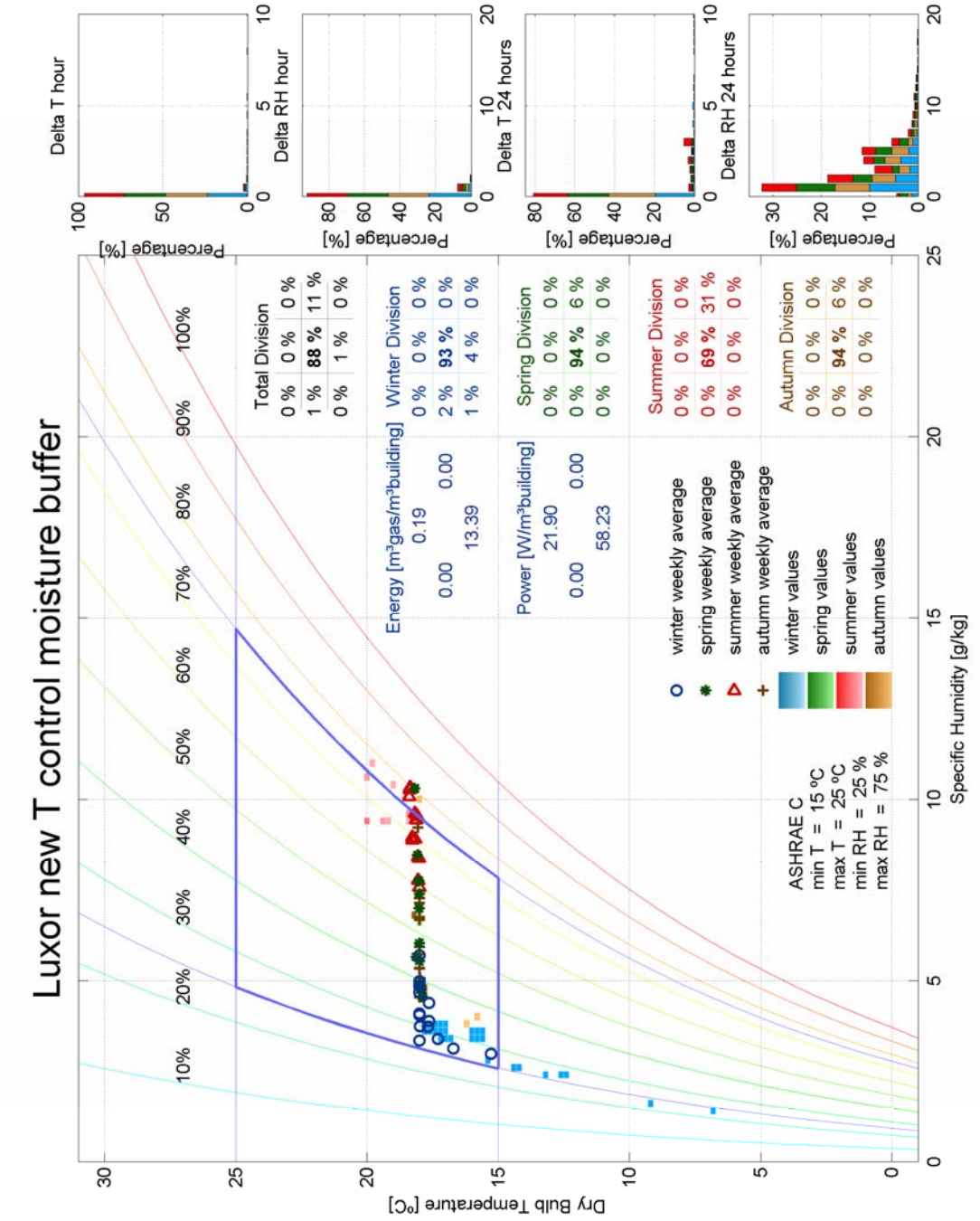

FIG. 6: The CEC of Scenario ‘control class C design with additional hygroscopic material’

HVAC system: climate control B, without additional hygroscopic material

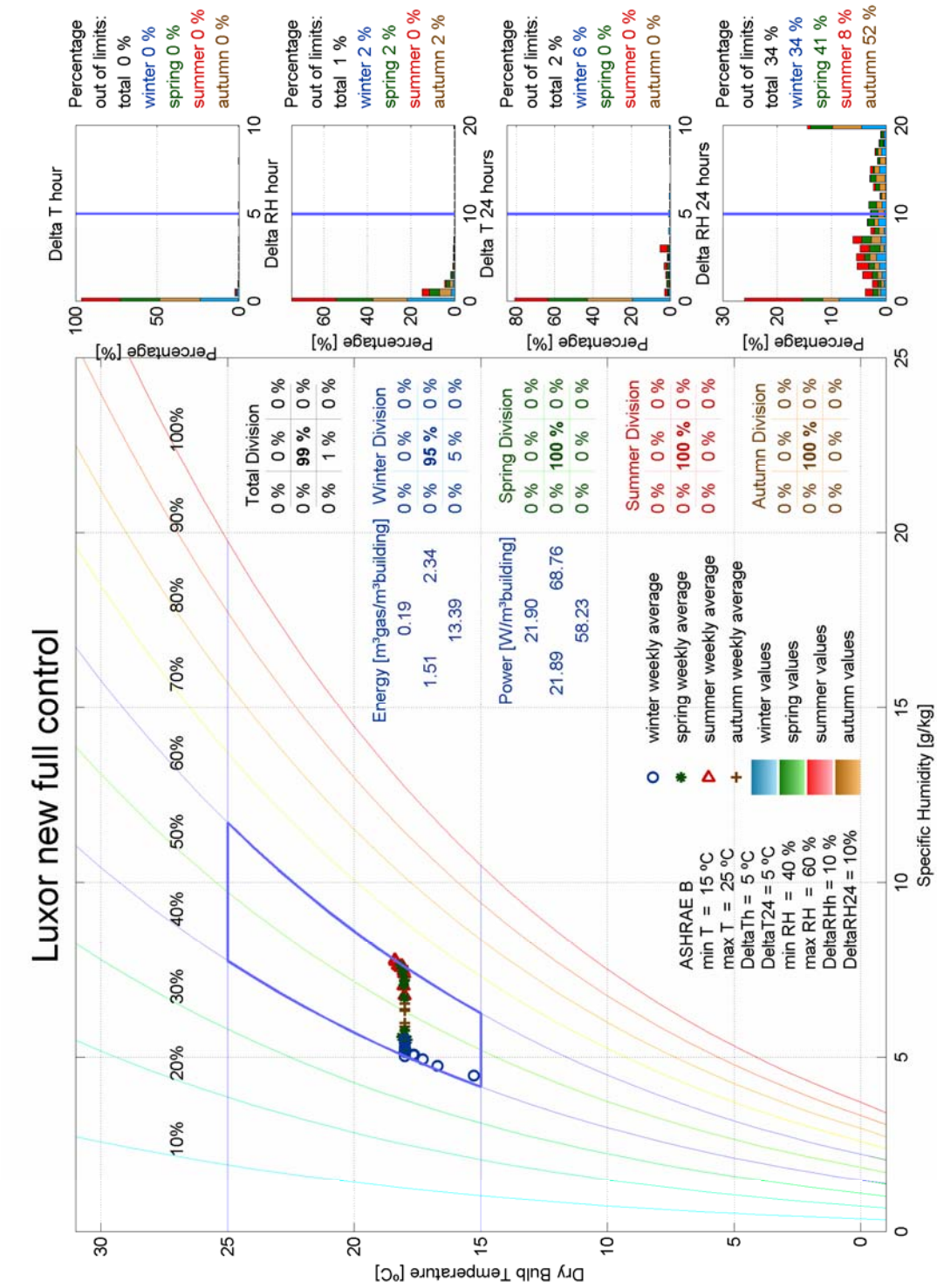

FIG. 7 The CEC of Scenario ‘control class B design without additional hygroscopic material’

HVAC system: climate control B, with additional hygroscopic material

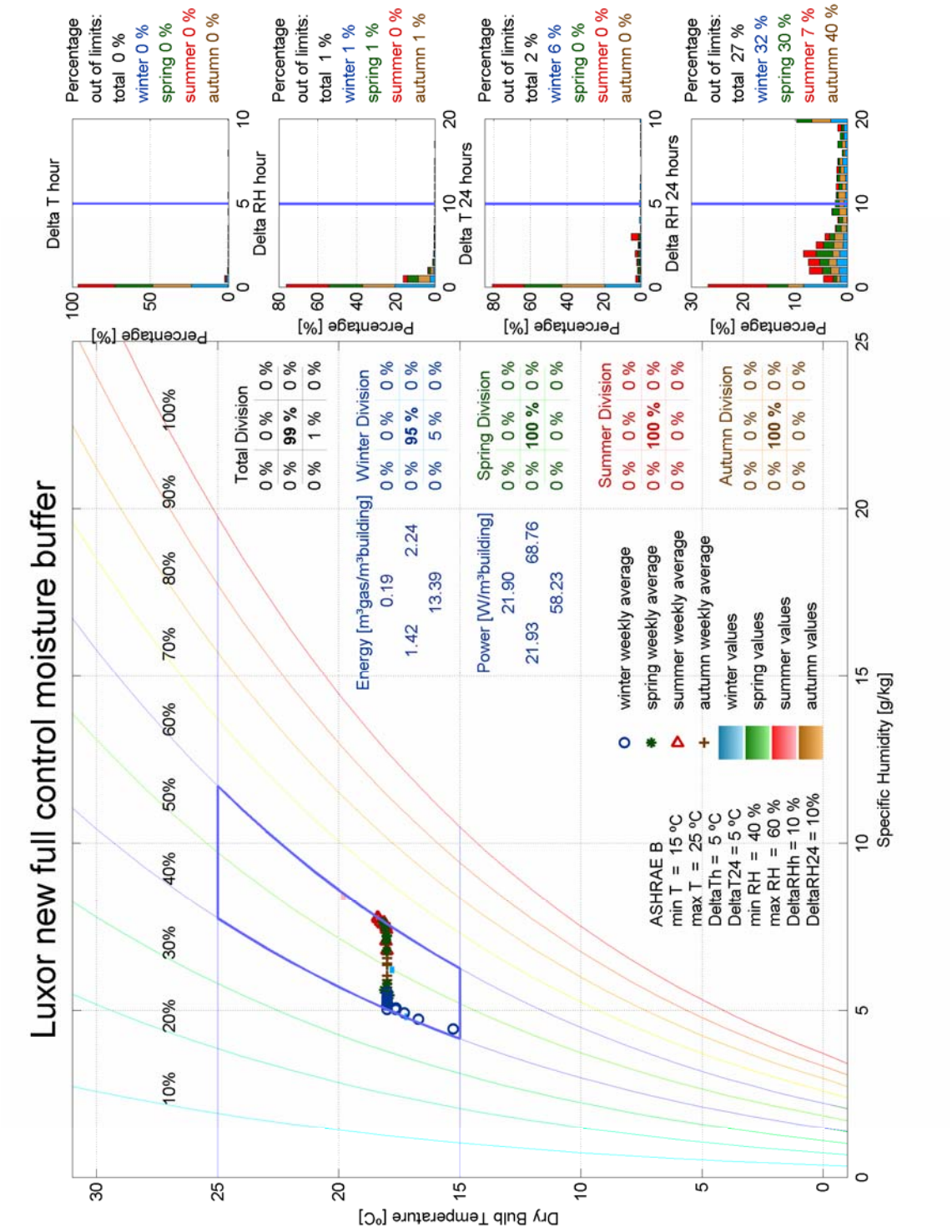

FIG. 8: The CEC of Scenario ‘control class B design with additional hygroscopic material’

HVAC system: climate control AA

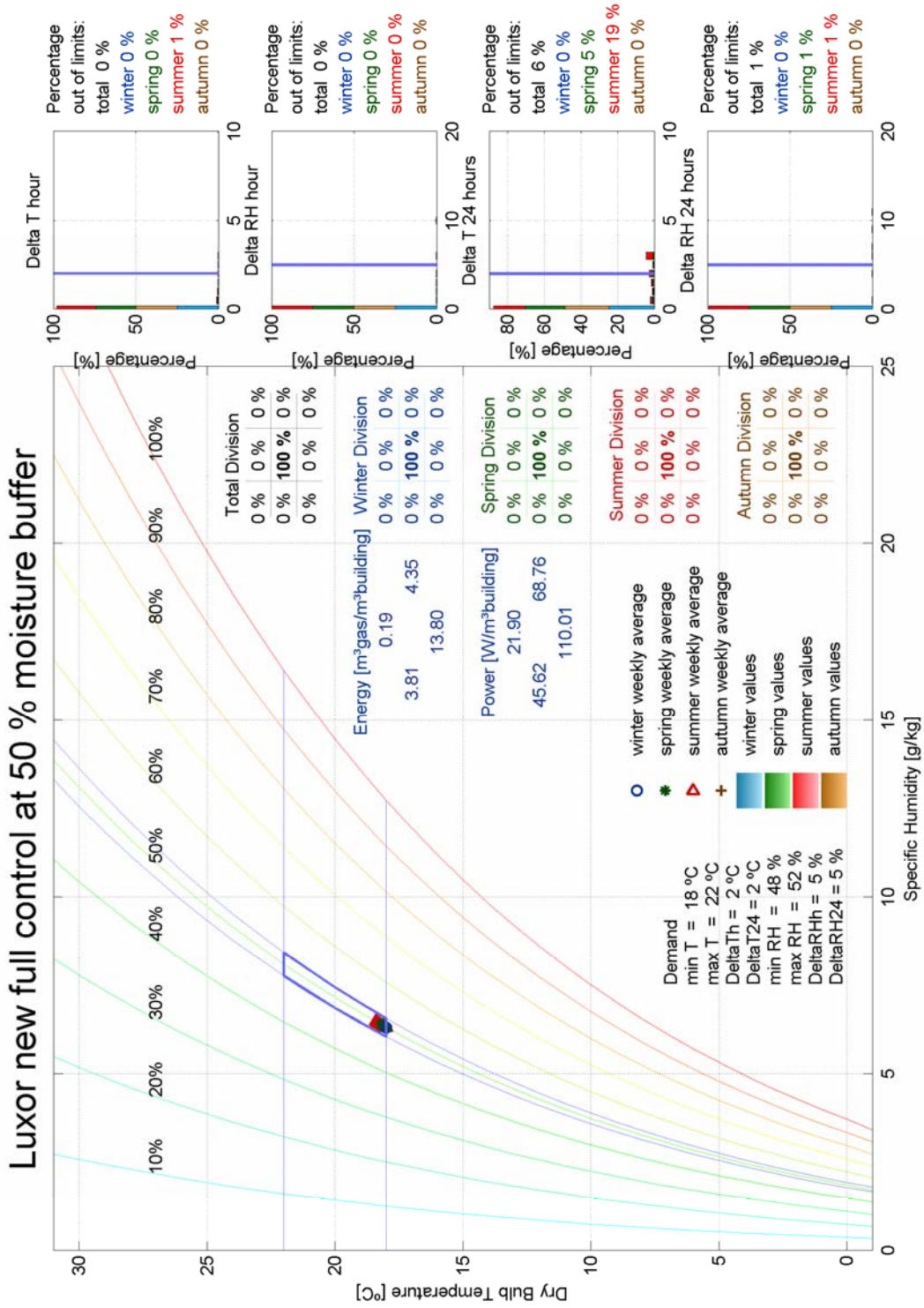

FIG. 9: The CEC of Scenario ‘control class AA design.

4. DISCUSSION OF THE RESULTS

4.1 Evaluation of the scenarios

Past performance

Both past performance scenario results show high RH change rates (up to 94% of time out of limits). Although this did not lead to visible damage to the monumental interior so far, it should be reduced to prevent future damage. Furthermore the scenario in figure 3 results in high humidity's (up to 17% of time is too humid) and the other scenario in figure 4, results in low humidity's (up to 26% of time is too dry). Both problems should be prevented in the future.

Control class C design

This design contains only heating and ventilation. Figure 5 shows that this is not an acceptable design because: (a) during the winter the RH is 21% of the time below 25% and (b) 40% of the time the daily RH fluctuation is above 20%. Figure 6 shows that both problems are solved if a very large amount of additional moisture buffering material (100 air-volume-equivalents) is placed. The amount of additional moisture buffering material is expressed in air-volume-equivalents (of the 1800 m^3 hall). This means 1 air-volume-equivalent (at 20 ^oC/50%) equals 14 kg of moisture. If wood fiberboard is selected as buffering material, 1 m^3 wood can buffer 12 kg moisture (daily change rate of Rh 20%, density wood = 300 kg/m^3, (de)sorption = 0.04 $kg_{moisture}/kg_{wood}$). 100 wood slices of 1 cm x 1m x 1m separated by 1 cm air gap fills 2 m^3 of space. Thus 100 air-volume-equivalent takes 230 m^3 of space. However, due to the monumental roof and walls, it will be very difficult to place such amount of buffering material. This means that moisture control will be inevitable.

Control class B design

This design contains full climate control with RH between 40% and 60%. Figure 7 shows that the only problem left is that still 34% of the time the daily RH fluctuation is above 20%. Figure 8 shows that if a reasonable amount of additional moisture buffering material (5 air-volume-equivalents, taking 12 m^3 of space) is placed, then: (a) it has only small effects on the humidification energy (decrease of 6%) and dehumidification energy (decrease of 4%); (b) it has no significant effect on the (de)humidification power and (c) the daily RH fluctuations remain too high. Note that these climate conditions are expected to be better than the past performance. One could argue that the monumental interior has not deteriorated in the past, so it probably will not deteriorated in better climate conditions. In this case control class B would be appropriate. But one can also argue that it is pure luck that the monumental interior has not deteriorated so far. In this case control class B would not be appropriate and a more stringent control class is required.

Control class AA design

This design contains full climate control with RH between 48% and 52%. This means there is almost no of moisture buffering due to the steady RH. Figure 9 shows that the climate meets the demanded performance very well. The disadvantages compared to the previous class B design are: (a) a much higher humidification energy (increase of 270%) and dehumidification energy (increase of 200%) and (b) a significant effect on the humidification power (increase of 200%) and cooling power (increase of 190%).

4.2 Evaluation of the moisture buffering effects on the HVAC performance

From figure 7 and 8 it follows that the humidification energy drops from 1.51 to 1.42 [m^3 gas / m^3 building volume] and the dehumidification energy drops from 2.34 to 2.24 [m^3 gas / m^3 building volume] by placing 5 air-volume-equivalents moisture buffering material. The next figure presents the (de)humidification energy as a function of the placed additional buffering material in more detail.

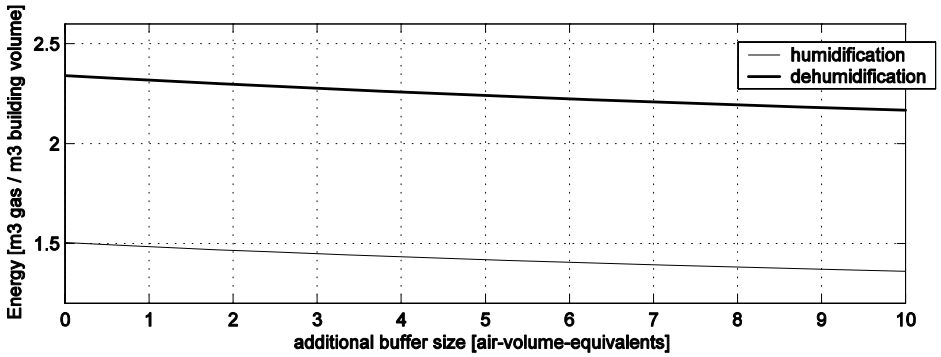

Figure 10. The (de)humidification energy as a function of the placed air-volume-equivalents.

Figure 10 shows an almost linear decrease of 0.01 [m^3 gas / m^3 building volume] per air-equivalent additional buffering material.

5. CONCLUSIONS

Revisiting the objectives of Section 1, it is concluded that:

Concerning the use of the new simulation and visualization tool: (1) The past indoor climate can be classified as ASHRAE control C with expected significant occurrences of dry (RH below 25%) and humid (RH above 80%) conditions. (2) ASHRAE control C is not suitable for the new hall. The climate control classification for the new hall ranges from B to AA. Further research in the form of detailed HAM transport calculations in the (monumental) constructions are needed select the appropriate class. (3) The demands on the HVAC system to facilitate pop concerts in the new hall are 40 kW heating power, between 100 and 200 kW cooling power, between 40 and 80 kW humidification power and 125 kW dehumidification power. All these quantities are based on 100% process efficiencies.

Concerning the effect of moisture buffering on the (de)humidification energy of the HVAC system: (4) In case of control class AA, placing additional hygroscopic material has no significant effect. In case of control class B, the placing of additional moisture buffering material (5 air-volume-equivalents) does not decrease the (de)humidification power and it decreases the (de)humidification energy by 5%.

ACKNOWLEDGEMENT

Rogier Lony provided input data for the models. This is greatly acknowledged by the author.

REFERENCES

ASHRAE, (1999). Heating, ventilating and Air-Condioning Applications, Chapter 20, museums, libraries and archives. ISBN 1-883413-72-9,

Schellen, H.L. (2002). Heating Monumental Churches, Indoor Climate and Preservation of Cultural heritage; Dissertation, Eindhoven University of Technology.

Schijndel, A.W.M. van & Wit, M.H. de , (2003). Advanced simulation of building systems and control with SimuLink, 8TH IBPSA Conference Eindhoven. August 11-14.

Schijndel, A.W.M. van & Schellen H.L. (2005). Application of an integrated indoor climate & HVAC model for the indoor climate performance of a museum. *7TH Symposium on Building Physics in the Nordic Countries, Jun13-15 2005.*

Schijndel, A.W.M. van & Hensen J.L.M. (2005). Integrated heat, air and moisture modeling toolkit in Matlab. *Building Simulation Conference August 15-18 2005.*

Schijndel, A.W.M. van & Wit, M.H. (2005). HAMlab, http://sts.bwk.tue.nl/hamlab/

DEVELOPMENT AND VALIDATION OF A MODEL TO CALCULATE WIND SPEEDS IN URBAN CANYONS

Chrissa Georgakis[*] , Mathaios Santamouris[*]

[*]*Group of Building Environmental Physics, University of Athens, Building Physics 5, University Campus, 157 84 Athens, Greece*

Abstract

Studies on air circulation became of great importance in recent years, since are crucial for the energy consumption of buildings, for the pollutant dispersion within cities and for the good comfort conditions for the pedestrians and the habitants. The semi-empirical model developed in this study aims to accurate wind speed computation inside street canyons.

In the framework of the Urbvent European Research project, an extended experimental campaign took place in five different urban street canyons in the centre of Athens during the summer of 2001. Wind speed and direction measurements took place, every 30 seconds at several heights within the canyon, as well as and above on the rooftop of the buildings. Wind speed measured near the building facades using the same time interval. The experimental campaign lasted three days per canyon.

The experimental data were grouped into different categories based on the measurements of the wind speed above the rooftop of the buildings and the incidence angle on the canyon axis. For all of the derived categories existing algorithms were gathered and grouped into a semi-empirical model.

By the use of the above mentioned model wind speed calculated inside the canyons at exactly the same spots where wind speed was measured during the measuring campaign. After comparing between measured and computed wind speed values, derived from the semi-empirical model, we resulted into agreement.

KEYWORDS

Wind speed and direction calculated values; wind speed and direction measured inside and outside canyon; urban canyon; semi-empirical algorithm.

INTRODUCTION

Wind characteristics around buildings and inside the urban canyons of a city, in different heights from the ground, it is of great importance for the safety and the comfort of its inhabitants. Increased wind speeds and turbulence can create a hostile environment for the inhabitants of the city and its structures. A model able to esteem

*Corresponding author Tel: +30-210-7276849; fax: +30-210-7295282; email address: cgeorgakis@phys.uoa.gr

wind speed inside a city would be important for the calculation of maximum wind loads expected close to the buildings and for the dispersion of atmospheric pollutants in a specific region. The already knowledge for wind is based either in numerical studies (Hunter et al., 1990/1991) or either in wind tunnel studies (Wedding et al., 1977; Hoydysh and Dabbert, 1988; Kastner-Klein, 1999). Studies based on measured wind speed values are limited (De Paul and Sheih, 1986; Nakamura and Oke, 1988; Santamouris et al., 1999).

In the framework of URBVENT, a European Research project, wind flow characteristics were measured through an extended experimental campaign. The measuring procedure included wind speed and direction measurement of wind outside and inside the canyons. The measurements took place inside the canyons at four different height levels from the ground and also close the canyons facades. The model calculates wind speed inside an urban canyon, based on the already known algorithms, for the cases of ambient flow higher than the threshold value of 4 m/sec. For very low ambient wind flow the model uses the experimental data in order to calculate wind speed in the center of the canyon and close to its facades.

Analysis for all wind's incidence angles and speeds higher or lower than 4 m/sec, proved that the proposed model operates within sufficiently accuracy. However limitations were posed due to model's assumptions and simplifications.

1. FIELD EXPERIMENTS

Table 1 presents the geometrical characteristics of the five canyons. Also it presents in which specific spots per canyon were wind flow inside and outside the canyons was measured. Analytical the set up was the following:

1. In the centre of each canyon the meteorological station of the University of Athens was placed, for three days and for twelve hours per day. The mobile meteorological station was installed on a vehicle equipped with a telescopic PT8 Combined Collar Mast Assembly with extended height of 15.3 meters. On the telescopic mast the following anemometers were attached at four different heights (3.5 – 7.5 – 11.5 – 15.5 meters) in order to record and storage every 30 seconds wind speed and direction in the middle of the canyon.

- Wind speed in the middle of the canyon was measured withA100K Pulse output anemometers
- Wind direction in the middle of the canyon was measured with W200 Porton Windwane ($\pm 300^0$ range) anemometers.

2. Simultaneously wind speed was measured near the facades of the canyon on three orthogonal axes, as well as wind speed and direction outside the canyon, with the following anemometers:

- A three-axis anemometer was used to measure the three components of wind speed inside the canyon adjacent to the facades. The anemometer was mounted on the exterior façade of a building facing into the canyon at a distance of 3 m from the wall.
- A cup anemometer was placed at a distance of 6 m above the top of the canyon to measure the wind speed and direction out of the canyon.

2. DESCRIPTION OF THE DEVELOPED SEMI-EMPIRICAL MODEL

When the predominant direction of the airflow was approximately normal (say $\pm$ 20 degrees) to the long axis of the street canyon, three types of airflow regimes were observed as a function of the building (L/H) and canyon (H/W) geometry, (Oke,

1988). When the buildings are well apart, (H/W>0.05), their flow fields do not interact. At closer spacing the wakes are disturbed. When the height and spacing of the array combine to disturb the bolster and cavity eddies, characterized by secondary flows in the canyon space where the downward flow of the cavity eddy is reinforced by deflection down the windward face of the next building downstream. At even greater H/W and density, a stable circulatory vortex is established in the canyon because of the transfer of momentum across a shear layer of roof height and a flow regime occurs where the bulk of the flow does not enter the canyon.
If the wind speed out of the canyon is below some threshold value the coupling between the upper and secondary flow is lost, (Nakamura and Oke, 1988), and the relation between wind speeds above the roof and within the roof is characterized by a considerable scatter. End effects or finite –length canyon effects, play an important role in the airflow distribution inside canyons. For canyons with $L/W \approx 20$ (Yamartino and Wiegand, 1986) was reported that, finite-length canyon effects begin to dominate over the vortex. Similar phenomena reported by Santamouris et al, (1999). Thus, prediction of the airflow in high aspect ratio canyons may concentrate on cases where end effect does not dominate the flow.
The orientation of the canyon, the geometrical characteristics (width, height and length of the canyon without intersections) and a file with ambient flow data (wind speed and direction outside canyon) are the inputs used by the model. By defining the coordinates (x, y) of a point the model predicts a wind speed value at the specific spot.

The flow chart of the proposed model is presented in Figure 1.

I. The model calculates based on the input data, if the aspect ratio of the canyon (H/W) is greater than 0.7 so it is a canyon situation or otherwise the space between the buildings is not a street canyon.

II. The next calculation is if the ratio of the building length between main intersections and the width between buildings (L/W) is greater than 20. If the ratio L/W is less than 20 then, the end effects dominate inside the canyon and extended experimental analysis indicated that a wind speed value of 0.5 m/s could be considered as mean (Results of the European Projects URBVENT Part 1, 2004). If it is greater than 20, it means that there is a wind circulation in the canyon and the calculations of the model continue.

III. Consequently, if the wind speed outside the canyon is less than 4 m/s and its direction is perpendicular or oblique to the canyon, the values from Table 2 (Empirical Values) can be used.

IV. If the wind's incidence angle was parallel to the main axis of the canyon (with wind speed greater or less than 4 m/sec) the following algorithms were used:

In the obstructed sublayer $0 \le z \le h_b$ the following exponential law describes the variation of wind with height below rooftops:

$$u_p = U_0 \cdot \exp(\frac{y}{z_2}) \quad (1)$$

and

$$z_2 = 0.1 \cdot h_b^2 / z_0 \quad (2)$$

Where U_0 was a constant reference speed, z_2 was the roughness length for the obstructed sub-layer, h_b the mean buildings height, y was the height from ground in

which wind speed could be calculated and z_0 the aerodynamic roughness length of the area.

The aerodynamic roughness length z_0 is defined as the height where the wind speed becomes zero. Although the roughness length is not equal to the height of the individual roughness elements on the ground, there is one to one correspondence between those roughness elements and the aerodynamic roughness length. Once the aerodynamic roughness length is determined for a particular surface, it does not change with wind speed, stability and stress.

Typical values of the aerodynamic roughness length are presented by Stull (1997) based on plenty of studies. As expected higher roughness elements are associated with larger aerodynamic roughness lengths. For the centres of large towns and cities the proposed vale is z_0=1, while for the Rocky Mountains the proposed value is z_0=100. For the centres of cities with very tall buildings the proposed value is z_0=2-3. For the centre of the city of Athens where the mean buildings height is close to 30 meters, we considered for z_0 the value 3.

<u>If the wind's incidence angle was perpendicular/oblique to the main axis (and its speed greater than 4 m/sec) of the canyon the following algorithms were used:</u>

The following part of the model is based on the study of Hotchkiss and Harlow, (1973). Use of the proposed algorithms permits the calculation of the cross and vertical wind speed component (u, v). The algorithms consider incompressible flow, absence of sources or sinks of vorticity within the canyon, and appropriate boundary conditions for the simple two-dimensional rectangular notch of depth H and width W. The proposed algorithms are the following:

$$u = \frac{\mathrm{A}}{k} \cdot \left[e^{ky}(1+ky) - \beta \cdot e^{-ky}(1-ky) \right] \cdot \sin(kx) \quad (3)$$

And

$$v = -\mathrm{A} \cdot y \cdot \left(e^{ky} - \beta \cdot e^{-ky} \right) \cos(kx) \quad (4)$$

Where

$$k = \pi / W \quad (5)$$

$$\beta = \exp(-2kH) \quad (6)$$

$$\mathrm{A} = k u_0 / (1-\beta) \quad (7)$$

$$y = z - H \quad (8)$$

And u_0 is the wind speed above the canyon and at the point x=W/2, z=H.

The above-mentioned algorithms were tested and approved by Yamartino and Wiegard (1986). The same authors have proposed the following expression to calculate the along canyon component, $w(z)$:

$$w(z) = w_r \cdot \log[(z+z_0)/z_0] / \log[(z_r+z_0)/z_0] \quad (9)$$

Where w_r was the wind speed values measured outside the canyon at z_r meters above the ground and z_0 was the surface roughness.

The horizontal wind speed inside the canyon was:

$$v_h = (u^2 + v^2)^{0.5} \quad (10)$$

So, the total wind speed inside canyon at any point (x, y) was:

$$v_t = (v_h{}^2 + w^2)^{0.5} \quad (11)$$

The results of the experimental procedure are given in the form of box-plots. A box-plot was used as a graphic representation of the data distribution, which shows the locations of percentiles. The line in the middle of the box is the median, or the 50^{th} percentile of the sample. The lower and upper lines of the box are the 25^{th} and the 75^{th} percentiles, representing the lower and upper quartile, respectively. The length of the box represents the interquartile range. The lower and upper "whiskers" show the range of data, if there are no outliers. Data are considered outliers if they are located 1.5 times the interquartile range away from the top or bottom of the box. In each box plot two red lines are plotted in order to present the calculated values derived from the model. For the goodness of fit between the experimental measurements of wind speed inside a canyon and the ones raised from the application of the theoretical model, the t-test of the differences of mean values was applied, taking into account the variation of the samples (Georgakis, 2004). The comparison for the two set of values led to the conclusion that the model's prediction could be characterized as satisfactory.

3. DISCUSSION OVER THE EXPERIMENTAL AND THE COMPUTED WIND SPEED VALUES

3.1 Wind speed outside the canyon less than 4 m/sec

The box plot analysis, present in Diagrams 1-5, 11-15 and 20-24 regards the cases when the ambient flow was less than 4 m/sec and parallel, perpendicular and oblique to the main axis of the canyons. For the case of parallel flow together with the box plot for the wind speed outside the canyon, six box plots present the experimental and the computed values at the four level heights from the ground and also close the canyon facades. For the cases of perpendicular flow the first box plot depicts the ambient wind speed and the four following box plots depict the experimental vertical values close to the canyon facades (uplifts depicted with negative values and down lifts depicted with positive values) for the two perpendicular flows ($\pm 90^0$ and $\pm 270^0$ to the main axis of the canyon). Also, the last four box plots in these diagrams regard only the experimental values in the centre of the canyon, at the four level heights from the ground, in order to integrate the total flow inside the canyon. For the cases of oblique flow the diagrams are similar to the ones which regard to the perpendicular flow, except of the fact that now there are four different flows close to the canyons facades, so the total amount of box plots are thirteen.
For Voukourestiou canyon lack of experimental wind speed values, due to technical problems during the experimental procedure, obstruct a representative box plot analysis close both the canyon facades. Also, for this canyon there was no box plot analysis for the case of perpendicular flow with ambient wind flow less than 4 m/sec, since there were no experimental values for the specific case.

For the case of parallel flow outside the canyon, the computed average values for the four height levels of 3.5-7.5-11.5-15.5 meters and for the different heights near to each canyons facades, are close to the average measured values for the respectively heights. Some overestimation or underestimation for the computed values of the specific flow are due to thermal effects and intermitted vortices that dominate close to canyon corners. For the case of perpendicular and oblique flow to the main axis of the canyon, experimental and computed values depicted the flow close to canyon facades. The agreement between experimental and computed mean values was satisfactory.

For Ermou canyon technical difficulties during the experimental procedure derived to not very representative plots about the specific canyon.

3.2 Wind speed outside the canyon greater than 4 m/sec

The box plot analysis, present in Diagrams 6-10, 16-19 and 25-29, regard the cases when the ambient flow was greater than 4 m/sec and parallel, perpendicular and oblique to the main axis of the canyons. Each of the above mentioned diagrams include seven box plots. The first one depicts the ambient wind flow and the four following the experimental and computed values inside the canyon at the four different height levels. The last two-box plots regard wind flow close the canyon's facades.

The computed average values for the four height levels and close to the canyons facades are very close to the average measured values for the respectively spots, for the cases of deep canyons (Dervenion and Voukourestiou). This analysis indicated a very good agreement between experimental and model values. For Ermou canyon lack of experimental wind speed values, due to technical problems during the experimental procedure, obstruct a representative box plot analysis. For Miltiadou and Kaniggos canyons their aspect ratio L/W were less than 10 (Table 1). One of the first criteria in the semi-empirical model, was that only if the aspect ratio L/W was greater than 20, the calculations of the model could take place, otherwise end effects dominate and the mean wind speed inside canyon at any height level is close to 0.5 m/sec. In order to prove to verity of the above-mentioned criterion of the model, calculation took place for both Miltiadou and Kaniggos canyon. The computed values overestimated wind speed values inside both canyons. So, the substance of the model was proved.

4. CONCLUSIONS

- Average wind speed values measured inside canyons and the computed ones indicated stratification proportionally to wind speed values measured outside canyon.
- After extended analysis for the case of ambient flow parallel to the main axis of the canyon below the threshold value of 4 m/sec, it was proved that the computed values derived from the model are in good agreement with the experimental ones (Georgakis, 2005). So, there is no need for empirical values for this case, contrarily with the case of perpendicular or oblique flow to the main axis of the canyon.
- When the aspect ratio L/W was greater than 10, the calculations of the model could take place, otherwise end effects dominate and the mean wind speed inside canyon at any height level is close to 0.5 m/sec.
- Model tends to overestimate inside canyon velocities compared to experimental ones for the cases of parallel flow and ambient flow greater than 4 m/sec. For ambient wind less than 4 m/sec and wind incidence angle parallel to the main axis of the canyon the model tends to underestimate wind speed velocities inside canyons.
- In deep the canyons such as Dervenion and Voukourestiou, there was a very good agreement between experimental and computed values for perpendicular/oblique type of flow, and for ambient wind speed greater than 4 m/sec. This model is a good practical tool for deep canyon cases.

Acknowledgements

The present study was partly financed by the European Commission, Directorate General for Science, Research and Technology under the contract "Urbvent": Natural ventilation in urban areas - Potential assessment and optimal facade design, ENK6-CT-2000-00316, The contribution of the Commission is gratefully acknowledged.

References

1. De Paul, F.T. and Sheih, C.M.: “Measurements of Wind Velocities in a Street Canyon”, Atmospheric Environment, Vol.20, p.p. 455-459, 1986.
2. Georgakis, C., Niachou, K., Livada, I., Santamouris, M.: "On the prediction of natural ventilation rates in urban environment”, 5th ISES Europe Solar Conference, EuroSun 2004, Volume 3, Topic 11 Energy Meteorology, p.p.797-804, 2004.
3. Georgakis, C., Santamouris. M.: “Canyon effects: Calculation of wind speed in an urban street canyon with the aid of a semi-empirical model based on experimental data”, International Conference “Passive and Low Energy Cooling for the Built Environment”, p.p. 117-124, 2005.
4. Hoydysh W. and Dabbert W. F.: “Kinematics and Dispersion characteristics of flows in asymmetric street canyons”, Atmospheric Environment, Vol.22, p.p. 2677-2689, 1988.
5. Hotchkiss R.S. and Harlow F.H.: “Air pollution transport in street canyons”. Report by Los Alamos Scientific Laboratory for US Environmental Protection Agency, EPA-R4-73-029, NTIS PB-233 252, 1973.
6. Hunter, L.J., Watson, I.D., Johnson, G.T.: “Modeling Air Flow Regimes in Urban Canyons, Energy and Buildings”, Vol. 15-16, p.p. 315-324, 1990/91.
7. Kastner-Klein, P., Plate, E.J.: “Wind tunnel study of concentrations fields in street canyons”, Atmospheric Environment, Vol.33, p.p. 3973-3979, 1999.
8. “Natural Ventilation in Urban Areas – Results of the European Projects URBVENT Part 1: Urban Environment”, submitted in Building and Environment, 2004.
9. Nakamura, Y., Oke, T.R.: “Wind temperature and stability conditions in an E-W oriented urban canyon”, Atmospheric Environment, 1988.
10. Nicholson, S.: “A pollution model for street-level air”, Atmospheric Environment Vol.9. p.p. 19-311 1975.
11. Oke T.R: “Street Design and Urban Canopy Layer Climate”, Energy and Buildings, 11, p.p 103-113, 1988.
12. Santamouris, M., Papanikolaou, N., Koronakis, I., Livada, I., and Assimakopoulos, D.N.: '“Thermal and Air Flow Characteristics in a Deep Pedestrian Canyon and Hot Weather Conditions”, Atmospheric Environment, In Press, 1999.
13. Stull, R.B.: “An Introduction to Boundary Layer Meteorology”, Kluwer Academic Publishers, 1997.
14. Yamartino, R.J., Wiegand, G.: '“Development and evaluation of simple models for the flow, turbulence and pollution concentration fields within an urban street canyon”, Atmospheric Environment 20, 2137-2156, 1986.
15. Wedding J.B., Lombardi D.J. and Cermak J.E.: “A wind tunnel study of gaseous pollutants in city street canyons'” Journal of the Air Pollution Control Association, Vol.27, p.p. 557-566, 1977.

Street Canyon		**Ermou**	**Miltiadou**	**Voukourestiou**	**Kaniggos**	**Dervenion**
Orientation from the North	Degrees	92	45	45	12	327
Canyon width	Meters	10	6	10	8	7
Canyon length	Meters	200	50	100	70	200
Buildings height	Meters	20	12	30	28	23
Canyon aspect ratio	*H/W*	2	2	3	3.5	3.3
Wind speed and direction inside the canyon	Meters from ground	3.5-7.5-11.5-15.5	3.5-7.5-11.5-15.5	3.5-7.5-11.5-15.5	3.5-7.5-11.5-15.5	3.5-7.5-11.5-15.5
Height of the	Meters	7.5-	8.0-8.0	5.0-8.0	5.0-10.0	20.0-10

two Three-axis anemometer	from ground	10.5				
Wind speed and direction anemometer, outside the canyon	Meters from ground	26	18	36	34	29

Table 1 Description of the experimental sites, definition of the measurement points, the experimental period of every canyon

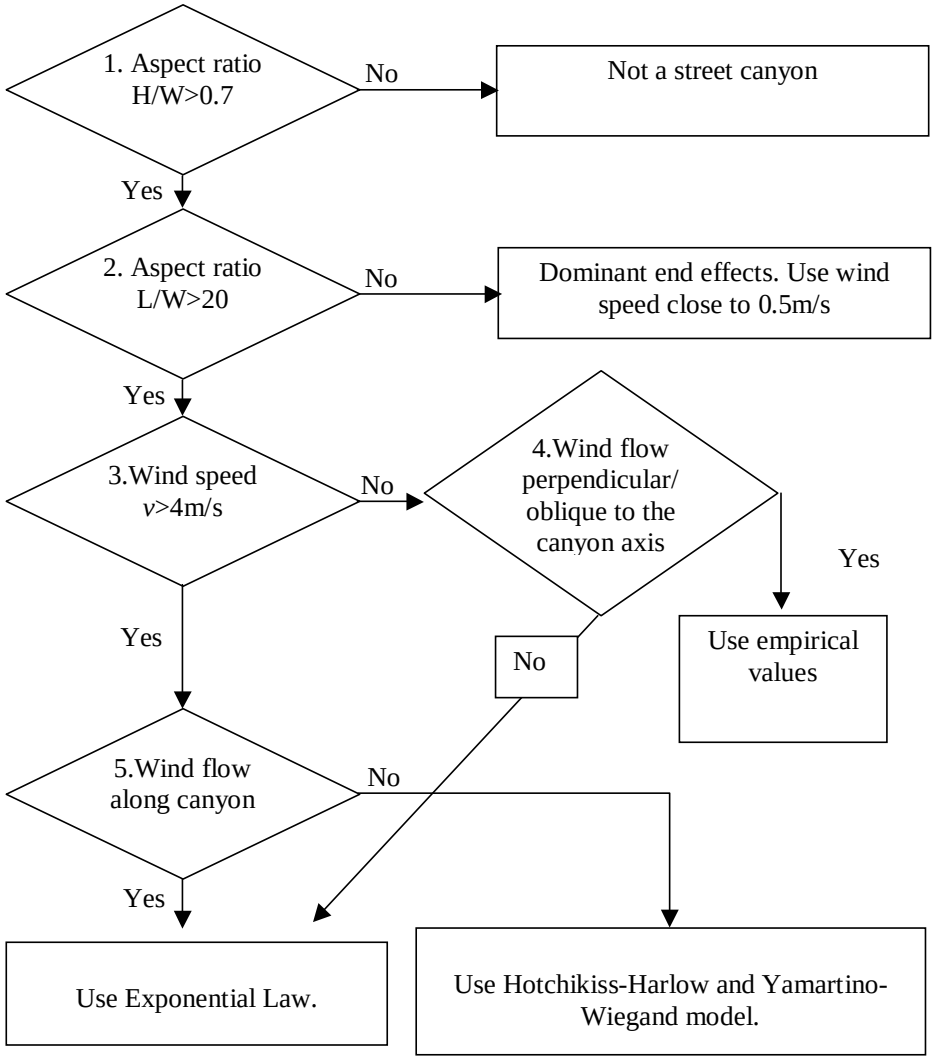

Figure 1 Flow-chart of the algorithms and the empirical values used by the model for computing wind speed inside street canyons

Wind speed outside the canyon (U)	Wind speed inside the canyon		
	Near the windward facade of the canyon		Near the leeward facade
	Lowest part	Highest part	
U=0	0 m/s	0 m/s	0 m/s
0<U<1	0 m/s	75% of the corresponding maximum wind speed value recorded at the top of the canyon, for this cluster	50% of the calculated wind speed value close the windward façade
1<=U<2	0 m/s	75% of the corresponding maximum wind speed value recorded at the top of the canyon, for this cluster	50% of the calculated wind speed value close the windward façade
2<=U<3	0 m/s	75% of the corresponding maximum wind speed value recorded at the top of the canyon, for this cluster	50% of the calculated wind speed value close the windward façade
3<=U<4	0 m/s	75% of the corresponding maximum wind speed value recorded at the top of the canyon, for this cluster	50% of the calculated wind speed value close the windward façade

Table 2 Empirical Values for perpendicular/oblique canyon wind speed inside the canyon

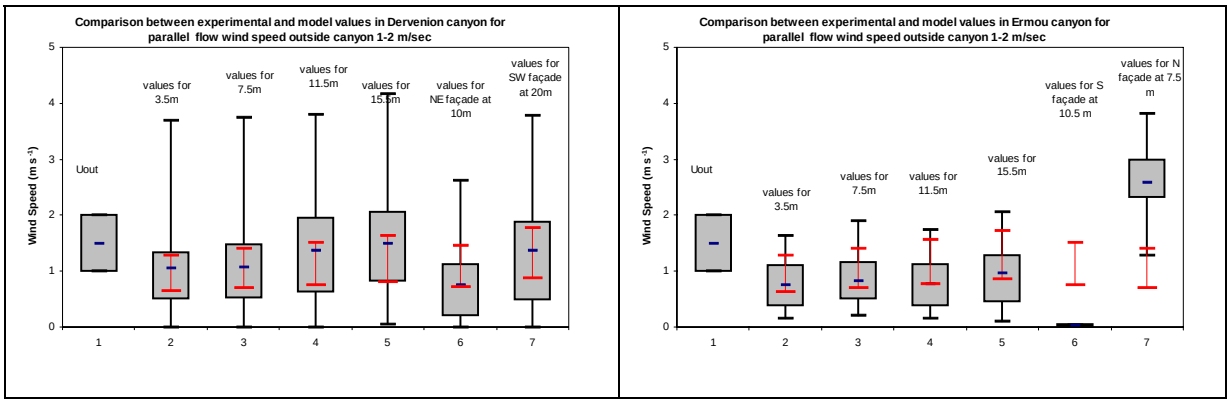

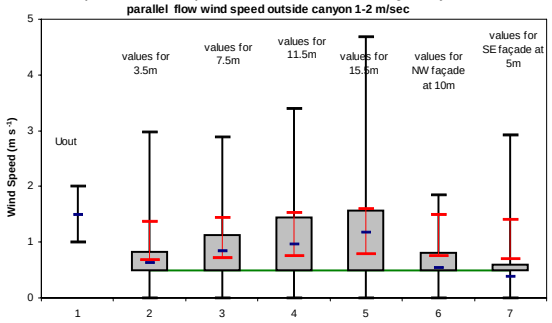

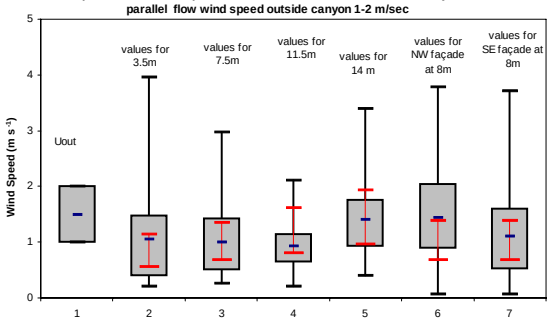

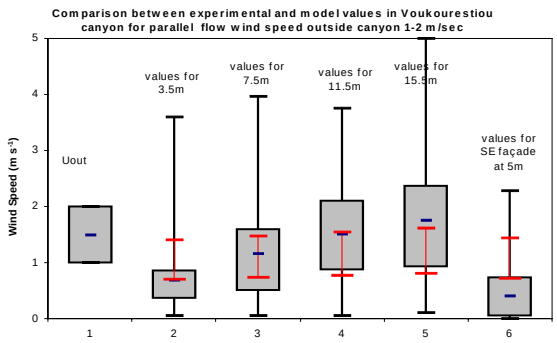

Diagrams 1-5: Experimental and computed vales of wind speed in the centre of the canyons and near the canyons facades, for incidence angle parallel to the main axis of the canyon, and wind speed outside canyon less than 4 m/sec

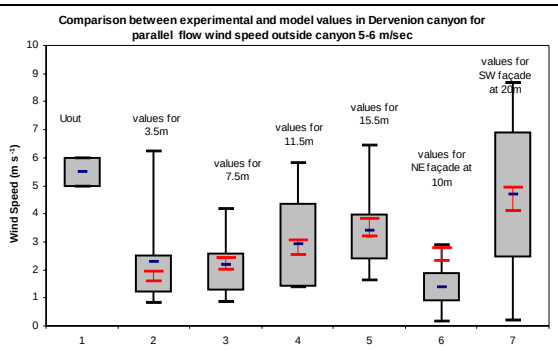

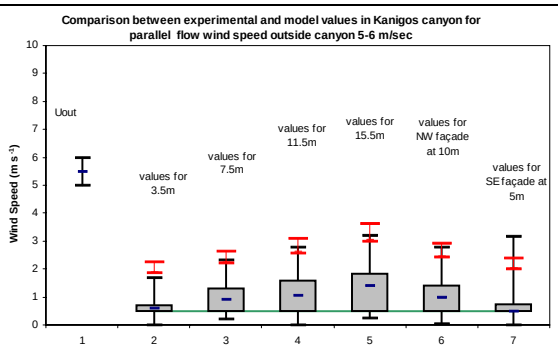

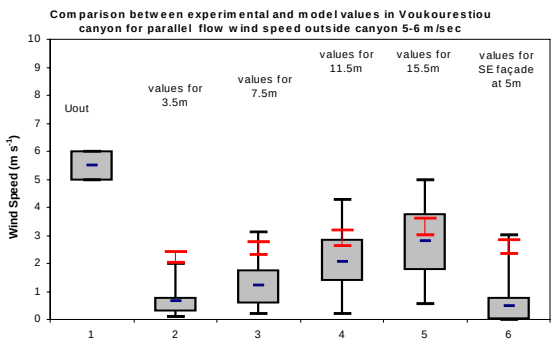

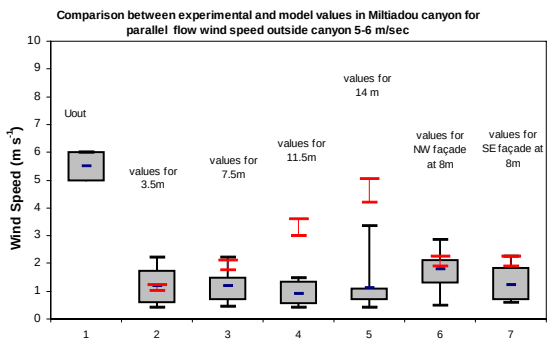

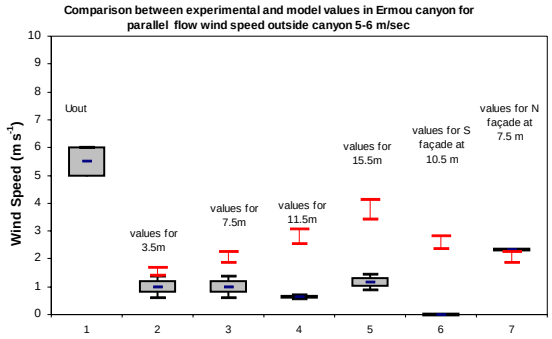

Diagrams 6-10: Experimental and computed vales of wind speed in the centre of the canyons and near the canyons facades, for incidence angle parallel to the main axis of the canyon, and wind speed outside canyon greater than 4 m/sec

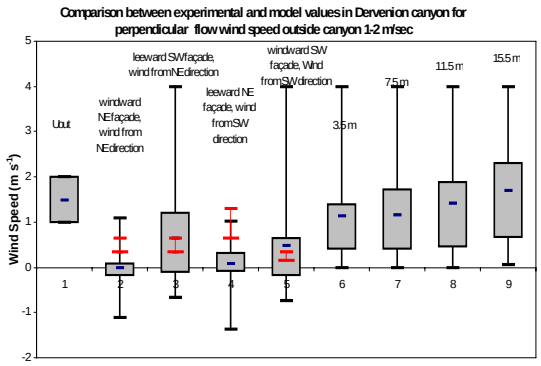

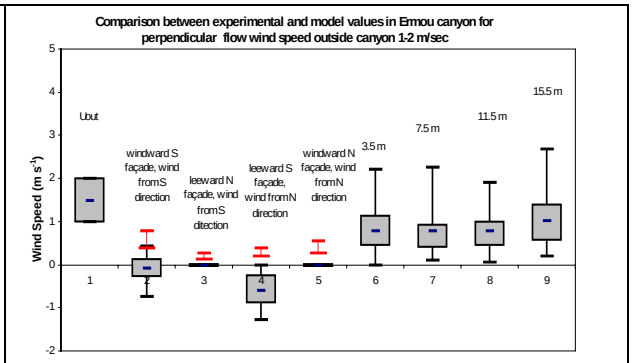

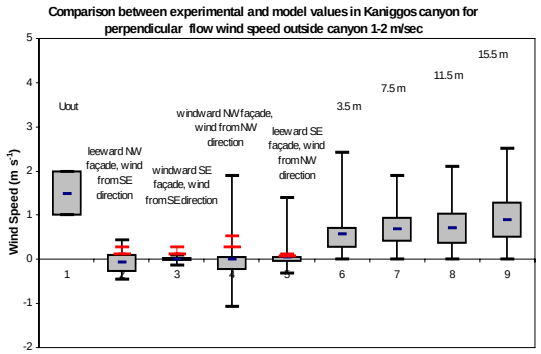

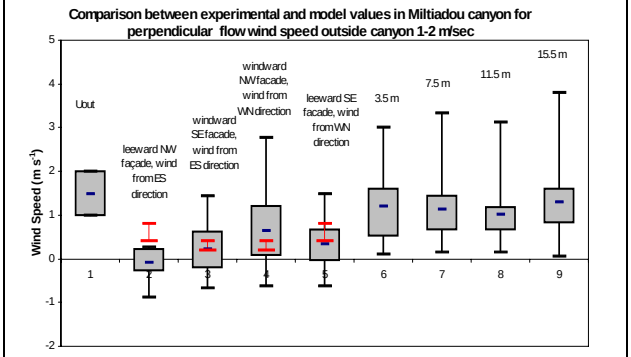

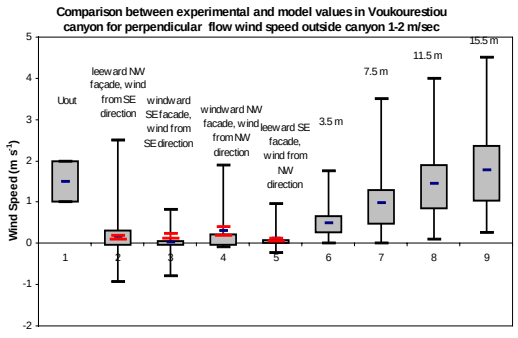

Diagrams 11-15: Experimental and computed wind speed values near the canyons facades for perpendicular incidence angle to the main axis of the canyon, and wind speed outside canyon less than 4 m/sec

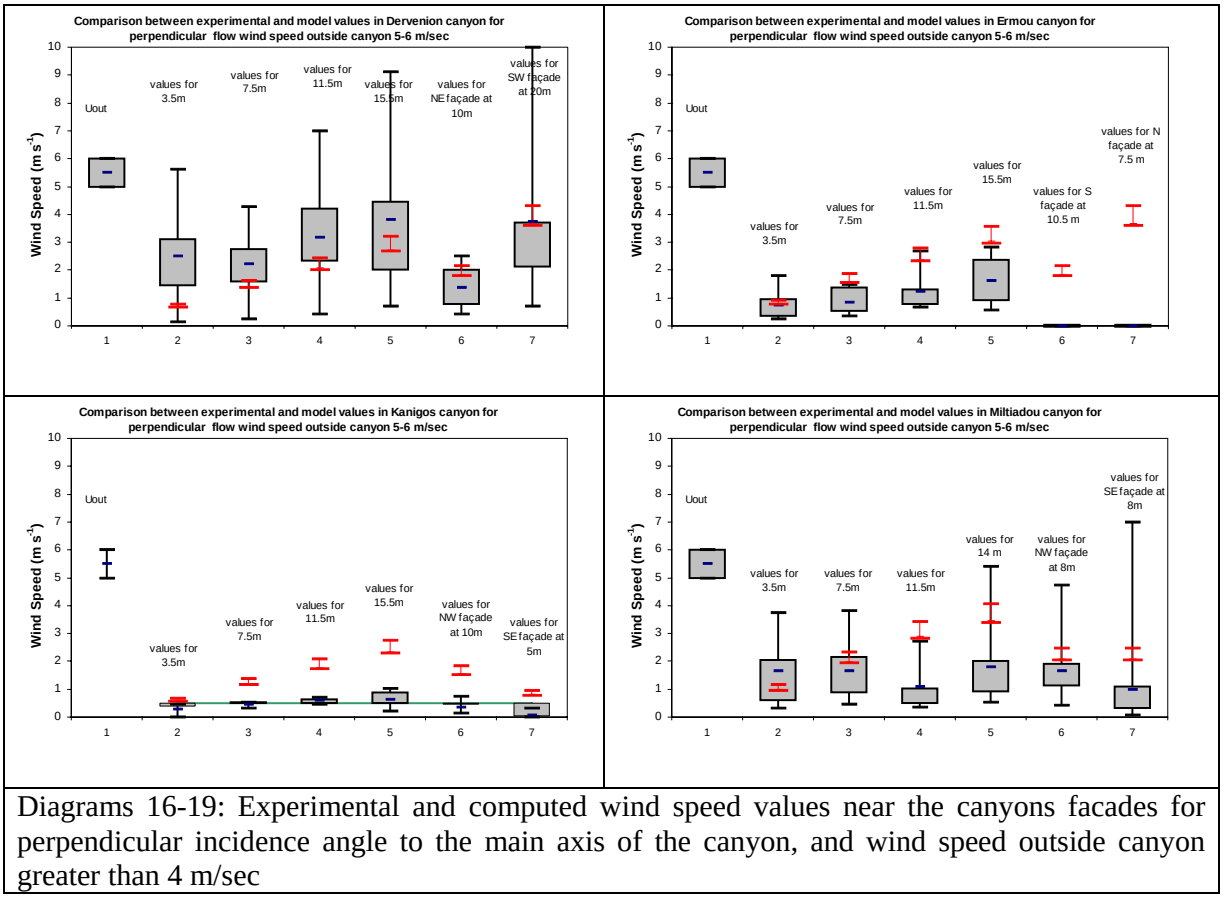

Diagrams 16-19: Experimental and computed wind speed values near the canyons facades for perpendicular incidence angle to the main axis of the canyon, and wind speed outside canyon greater than 4 m/sec

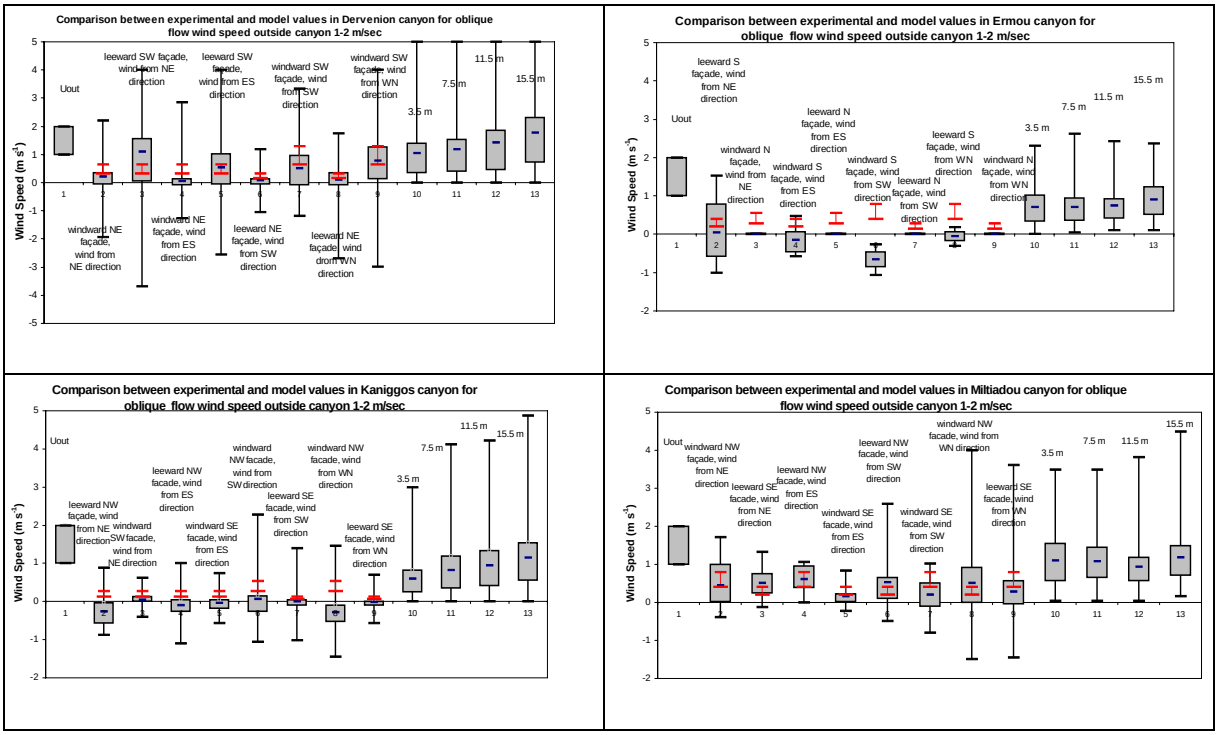

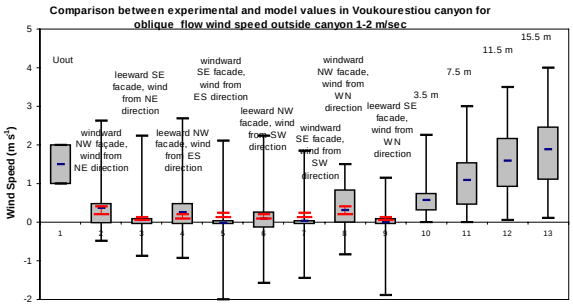

Diagrams 20-24: Experimental and computed wind speed values in the centre of the canyons and near the canyons facades for oblique incidence angle to the main axis of the canyon, and wind speed outside canyon less than 4 m/sec

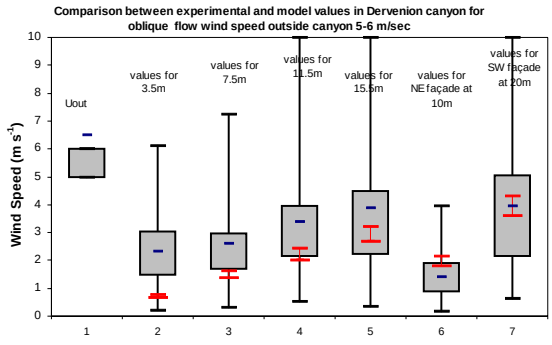

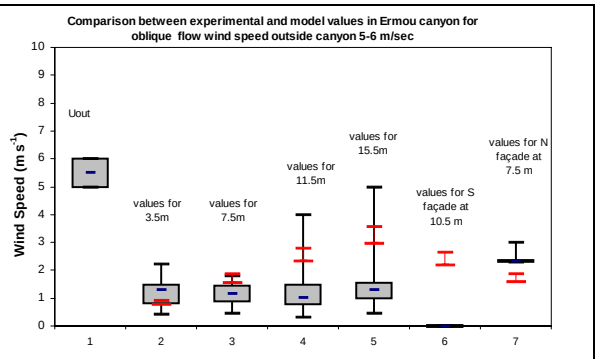

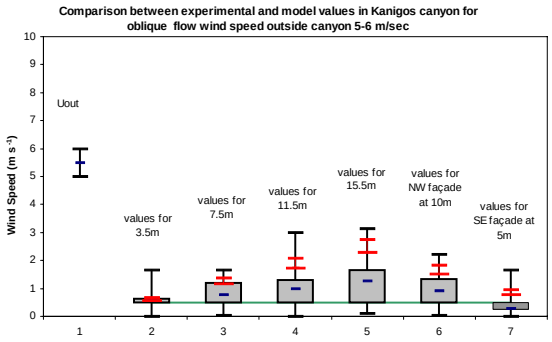

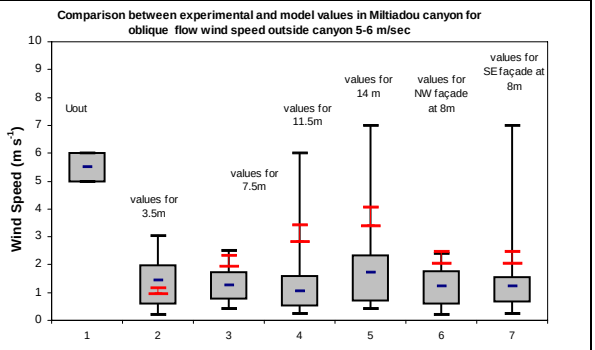

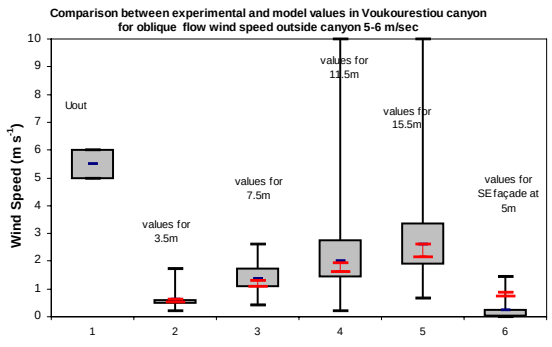

Diagrams 25-29: Experimental and computed wind speed values in the centre of the canyons and near the canyons facades for oblique incidence angle to the main axis of the canyon, and wind speed outside canyon greater than 4 m/sec

Probabilistic model PROMO for evaluation of air change rate distribution

Krystyna Pietrzyk [1] and Carl-Eric Hagentoft [2]

[1] *Swedish Testing and Research Institute, Department of Energy Technology, Building Physics, Borås, SE-50115, Sweden*
[2] *Chalmers University of Technology, Department of Building Technology, Building Physics, Gothenburg, SE-41296, Sweden*

ABSTRACT: The probabilistic model (PROMO) applied to the problem of air infiltration in low-rise buildings is presented. The PROMO model allows the estimation of the effect of variations of climatic conditions on air exchange in a building. In PROMO, experimental data are used in order to evaluate the parameters and types of the distributions of temperature, wind speed, and wind direction. Those distributions are employed to evaluate the distributions of air change rate caused by air infiltration and can be used to estimate probability of inadequate ventilation. FORM (First-Order Reliability Method) technique is used for probabilistic approximations. For validation of the PROMO model, the probability density functions of the air change rate for the test house situated near Gothenburg are estimated from the results of full-scale measurements of pressure differences across the envelope and compared to those calculated by PROMO from the climatic parameters measured at the site. The agreement of the results obtained in these two ways is very good.

KEYWORDS: air infiltration, air change rate, probabilistic model, reliability, FORM

INTRODUCTION

The main subject of the paper is a study of climate-induced air infiltration in low-rise buildings. The probabilistic model PROMO, allowing the estimation of probability density functions of air change rate has been developed and validated with the help of experimental data. It can be used to evaluate the contribution of air infiltration to ventilation and energy balance and the influence of that contribution on the reliability of air exchange or reliability of energy performance of a building. In the context of air exchange, air infiltration constitutes a complement to the design of ventilation. This complement is often disregarded, or considered in a very simplified manner. The tendency of relying to larger degree on natural ventilation calls for better modelling techniques for air infiltration. An attempt to create such a modelling technique is presented. A modelling approach proposed seems very well suited to handling the natural driving forces governing the rate of air infiltration. It also gives a possibility to quantify the probability of insufficient or excessive air exchange (Pietrzyk, 2000).
Physical relationships for air infiltration and ventilation in buildings, which form the background to the probabilistic modelling can be found in the AIVC publications (for ex. in Liddament, 1986), or in (Etheridge & Sandberg, 1996). FORM technique is used for the probabilistic approximations of air change rate (Pietrzyk & Hagentoft, b, Pietrzyk 2000) and reliability analysis (Pietrzyk, 2000, c). The description of FORM can be found in (Haldar, 2000, Ditlevsen, 1996) and also in (Pietrzyk & Hagentoft, a).

PROBABILISTIC MODEL PROMO

The probabilistic model PROMO has been created under the following assumptions: a low-rise building with single ventilation and temperature zone, the steady-state conditions of air

flow, the leakage area uniformly distributed over a building component except for the big openings. The detailed description of the model can be found in (Pietrzyk & Hagentoft, b).

Input data to the infiltration model

The input data to the infiltration model consist of random variables (italic bold text) and deterministic parameters. The probability density functions of random variables are estimated from the series of hourly experimental data. The family of distributions, typical for certain climatic parameters can be chosen.

1. Environmental data (description of the site and climatic data):
wind speed and ***wind direction*** from the nearest meteorological station (the set of measurements or parameters of the statistical distributions) for each wind direction sector d: surface roughness, the evaluation of the sheltering effect of the nearest surrounding, ***external temperature*** (the set of measurements or parameters of the statistical distribution), correlation coefficient between wind speed and external temperature

2. Parameters of a building:
geometry of the building (the area of building components A_j, the volume of the house V, etc.), the leakage characteristics of the house estimated for each building component and/or for the whole building, the location of neutral pressure layer, the orientation of the building against different wind directions, the pressure coefficients Cp_{ext} and Cp_{int} for different facades and wind direction sectors accounting for the sheltering effect of the surroundings

3. Serviceability data:
assumed ***internal temperature*** during heating season, intentional openings

Infiltration model

The infiltration model given by Equation 1 is based on the superposition of wind and stack effect (Etherige,1996). Temperature difference across envelope, and wind speed v evaluated for each direction sector d are treated as random variables.

$$ACH_d = \sqrt{s_1 \Delta T^2 + s_2 |\Delta T| + s_3 |\Delta T|^{1.5} + w_{d,1} v_d{}^4 + w_{d,2} v_d{}^2 + w_{d,3} v_d{}^3} \qquad (1)$$

where s_1, s_2, s_3 are deterministic coefficients dependent on the parameters of the flow balance for the stack effect, $w_{d,1}$, $w_{d,2}$, $w_{d,3}$ are deterministic coefficients dependent on the flow balance for various wind directions d.

$$s_1 = \left(\frac{3600}{V}\right)^2 \left(0.044 \frac{2}{\rho}\right)^2 \left(\sum_{j=1}^{n} A_j a_j |z_j|\right)^2$$

$$s_2 = \left(\frac{3600}{V}\right)^2 0.044 \frac{2}{\rho} \left(\sum_{j=1}^{n} A_j b_j \sqrt{|z_j|}\right)^2$$

$$s_3 = 2\left(\frac{3600}{V}\right)^2 \left(0.044 \frac{2}{\rho}\right)^{1.5} \left(\sum_{j=1}^{n} A_j a_j |z_j|\right) \left(\sum_{j=1}^{n} A_j b_j \sqrt{|z_j|}\right)$$

$$w_{d,1} = \left(\frac{3600}{V}\right)^2 \left(\sum_{j=1}^{n} A_j a_j \left|C_{p,d,j}\right|\right)^2$$

$$w_{d,2} = \left(\frac{3600}{V}\right)^2 \left(\sum_{j=1}^{n} A_j b_j \sqrt{\left|C_{p,d,j}\right|}\right)^2$$

$$w_{d,3} = 2\left(\frac{3600}{V}\right)^2 \left(\sum_{j=1}^{n} A_j a_j \left|C_{p,d,j}\right|\right)\left(\sum_{j=1}^{n} A_j b_j \sqrt{\left|C_{p,d,j}\right|}\right)$$

The coefficients a_j and b_j describe leakage characteristics of the building component j. They can be evaluated from the results of blower door tests carried out on the standard components or they can be assumed according to design values of the leakage area. Parameter z_j gives the location of the component related to the neutral pressure layer.
The probabilistic distributions of the air change rate are approximated using FORM. The air change rate follows different probability distributions depending on the contribution and the quantity of the stack and wind forces as well as leakage distribution over the envelope.

CASE STUDY

Description of the test house

The object of the study is a two-story timber-framed one family detached house with a concrete basement situated near Gothenburg. There is an open passage between the basement and the living area. The house is surrounded by a forest with trees of different heights excluding the southern side of a building exposed to an open area. The house was constructed in 1979 with the intention of using it for experimental studies in building physics with focus on ventilation and energy saving. The garage with doors facing south is located in the extended south part of the cellar as shown in Figure 1.

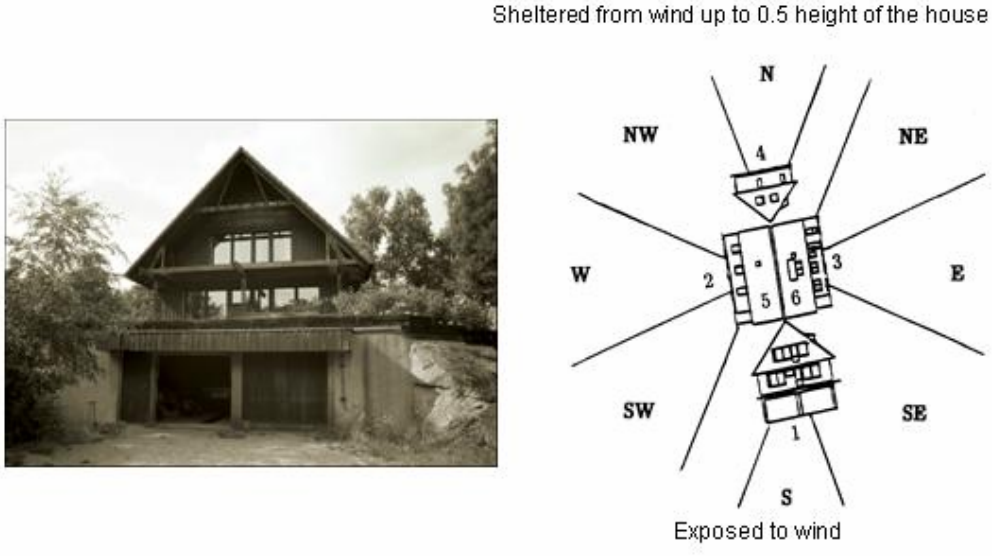

Figure 1. Object of the study

Measurement program

The following parameters have been measured, as is shown in Figure 2: leakage characteristics of the house using blower door tests, mean value of pressure difference across the 6 building components with Validyne pressure transducers, wind speed and wind direction with the anemometer located on a small hill about 25 m from the house, internal and external temperatures. The measurement program was carried out for 8 months. As a result, hourly mean data have been obtained.

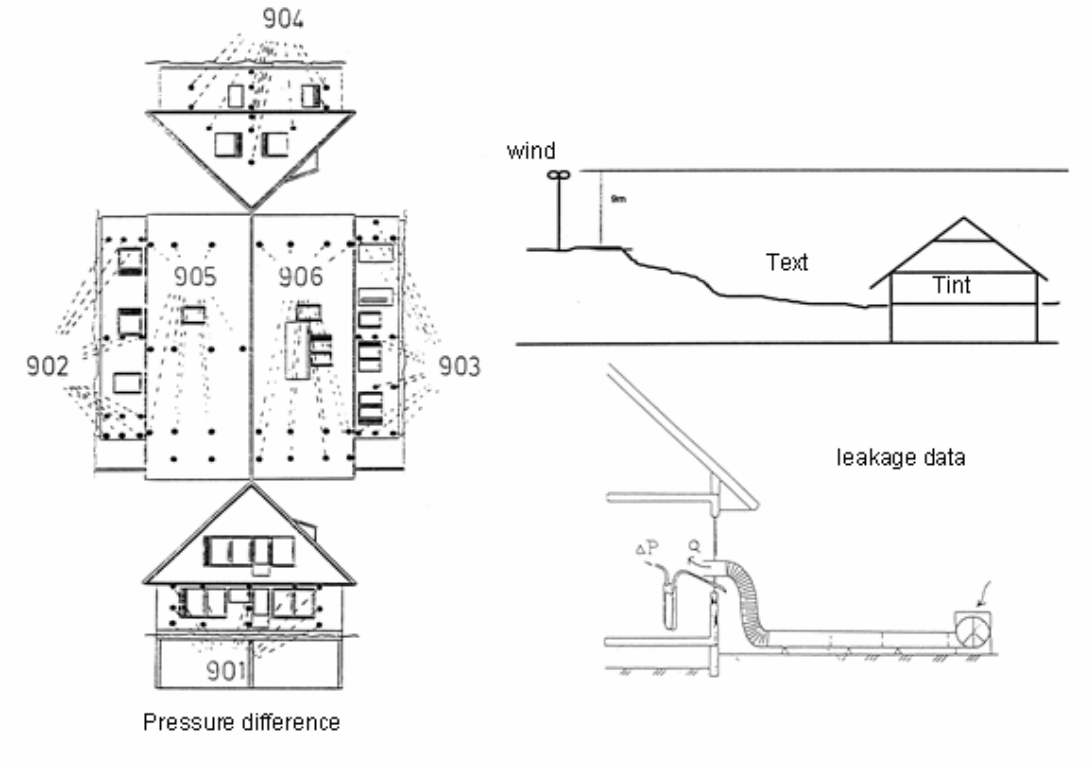

Figure 2. Measurement program for validation of probabilistic model of air infiltration

The results of the pressure drop measurements have been used to calculate the air exchange through the envelope. An opening under the garage door has been treated separately in the calculation model (see Pietrzyk & Hagentoft, b, Pietrzyk, 2000).

Case study with the help of PROMO model

The modelling flow for the PROMO model together with the results obtained is shown in Figure 3. For each wind direction sector the modelling procedure has been performed. Eventually, two cases have been distinguished. The first one considering those wind direction sectors to which the opening under the garage door has been exposed and the second one concerning all remaining wind direction sectors. The probability density functions of the air change rate for these cases approximated using the first order reliability method FORM (Pietrzyk & Hagentoft, a) are presented in Figure 3. For the case one (the opening exposed to wind) a log-normal probability density function has given the best fit according to Kolmogorov-Smirnov test with significance level of 0.05. For the other case, a normal probability density function has been fitted.

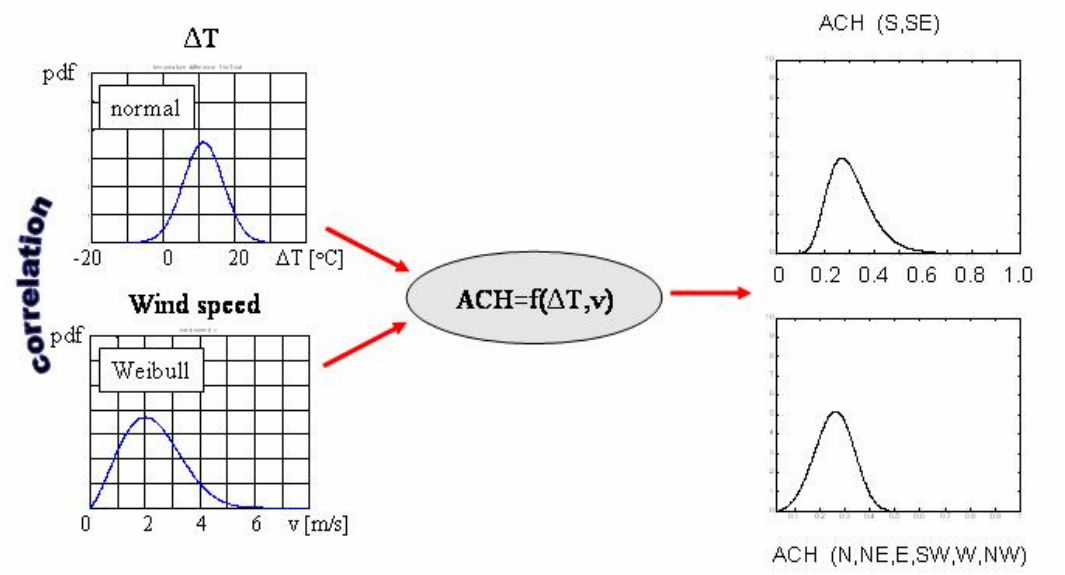

Figure 3. Modelling flow and the results obtained from probabilistic approximations using FORM

Validation of the PROMO model

The probabilistic model of air infiltration has been validated on the basis of full-scale pressure difference measurements carried out on the test house. The validation model is described in (Pietrzyk & Hagentoft, b). The results of air change rate calculations have been shown in Figure 4 in the form of histograms and probability density functions fitted to those results. They present the same cases as approximated with the help of the PROMO model. The mean value, the standard deviation, the skewness and the peakedness of validation results agree with the moments calculated for the probabilistic approximations. Eventually, the recommended types of distributions are similar (see Figures 3 and 4).

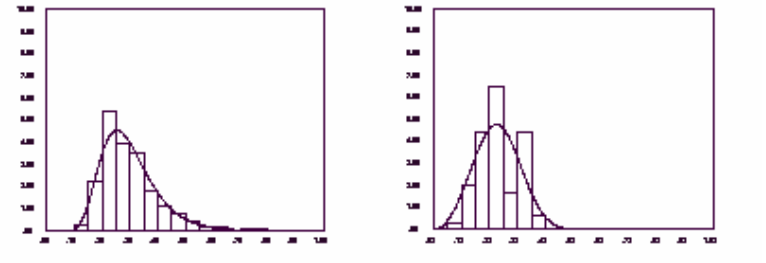

Figure 4. The results of validation of the PROMO model in the form of histograms and probability density functions of ACH estimated for the case 1- left (wind directions: S, SE) and the case 2 - right (other wind directions).

APPLICATION OF PROMO RESULTS

The probability density functions of air change rate can be used to evaluate the reliability of natural ventilation for a building but also to evaluate the reliability of the energy performance of the building envelope. In the context of energy balance, air infiltration constitutes one of many possible processes of heat exchange between the interior and the exterior of a building. Air infiltration can also be considered from the point of view of its influence on the properties

(thermal and structural) of building components. Some parameters of the buildings, usually treated as deterministic, are in reality dependent on climate-induced airflow through the structure and those should be treated as random variables. For some building technologies, especially those involving lightweight timber frame with mineral wool filling, and loose mineral wool layers for roof insulation one can speak about the dependence of the thermal properties of building components on air infiltration. It is very clear for the, so called, "dynamic wall" (Anderlind & Johansson, 1983), specially designed to save energy. The interaction between thermal transmittance and airflow through the components should be considered while calculating heat loss through a building envelope. The thermal transmittance becomes the most interesting parameter that can vary with the climatic parameters and should be treated as a random variable. Probabilistic description of air filtration through the wall is an important input to probabilistic model of thermal transmittance (Pietrzyk & Hagentoft, 2004). Eventually, reliability of energy performance for building envelope components exposed to various environmental and climatic conditions can be analysed. Different design options concerning also the effect of air infiltration on variations of thermal transmittance of the envelope can be calculated in the form of probability density functions of heat loss characterising energy performance of the envelope. Additionally, different ventilation strategies can be considered in terms of reliability (Pietrzyk, c).

CONCLUSIONS

The probabilistic model PROMO for the approximation of probability density function of air change rate for a naturally ventilated house on the basis of the probabilistic description of climatic data is developed and validated with the help of the results of full-scale pressure difference measurements.
The probability density functions of air change rate can be used to evaluate the reliability of natural ventilation for a building but also to evaluate the reliability of the energy performance of building envelope.

ACKNOWLEDGMENT

Financial support of the Swedish Council for Building Research is gratefully acknowledged.

REFERENCES

Anderlind G, Johansson B. (1983). *Dynamic insulation. A theoretical analysis of thermal insulation through which a gas or fluid flows*, The Swedish Council for Building Research, Stockholm,

Ditlevsen O., Madsen H.O. (1996). *Structural reliability methods*, England, John Wiley & Sons

Etheridge D., Sandberg M. (1996). *Building Ventilation: Theory and Measurements*, John Wiley & Sons

Haldar A., Mahadevan S. (2000). *Probability, Reliability and Statistical Methods in Engineering Design*, John Wiley & Sons.

Liddament, M.W. (1986). *Air Infiltration Calculation Techniques - An Applications Guide,* AIVC, Great Britain

Pietrzyk K. (2000). *Probabilistic modelling of air infiltration and heat loss in low-rise buildings*. Ph.D. thesis, ISSN 0346-718X, School of Architecture, Chalmers University of Technology, Gothenburg, Sweden.

Pietrzyk K., Hagentoft C-E. (a). Reliability analysis in building physics design. Accepted for publication in *Building and Environment*

Pietrzyk K., Hagentoft C.-E. (b). Probabilistic analysis of air infiltration. Accepted for publication in *Building and Environment*

Pietrzyk K., Hagentoft C.-E. (2004). Probabilistic modelling of dynamic U-value. Performance of Exterior Envelopes of Whole Buildings IX, Florida, USA

Pietrzyk K. (c). Probability-based design in ventilation. Submitted for publication to *The International Journal of Ventilation.*

MODELING AND CONTROL OF LIVESTOCK VENTILATION SYSTEMS AND INDOOR ENVIRONMENTS

Zhuang Wu[1], Per Heiselberg[2], Jakob Stoustrup[3]

[1] *Department of Control Engineering, Aalborg University, Fredrik Bajersvej 7C, DK-9220, Aalborg East, Denmark*
[2] *Department of Building Technology and Structural Engineering, Aalborg University, Sohngaardsholmsvej 57, DK-9000, Aalborg, Denmark*
[3] *Department of Control Engineering, Aalborg University, Fredrik Bajers Vej 7C, DK-9220, Aalborg East, Denmark*

ABSTRACT

The hybrid ventilation systems have been widely used for livestock barns to provide optimum indoor climate by controlling the ventilation rate and air flow distribution within the ventilated building structure. The purpose of this paper is to develop models for livestock ventilation systems and indoor environments with a major emphasis on the prediction of indoor horizontal variation of temperature and concentration adapted to the design of appropriate controlling strategy and control systems. The Linear Quadratic (LQ) optimal control method taking into account of the effect of necessary constraints and random disturbances is designed through system linearization. The well designed control systems are able to determine the demand ventilation rate and airflow pattern, improve and optimize the indoor Thermal Comfort (TC), Indoor Air Quality (IAQ) and energy use.

KEYWORDS

Livestock Ventilation, Thermal Comfort, Indoor Air Quality, LQ Optimal Control.

NOMENCLATURE

c_p	Heat capacity	q	Volume flow rate
ρ	Air density	*subscripts*	
P	Pressure	i	Zone i
H	Average height of inlet vent and leakage	o	Outside
A	Area of openings and leakage	in	Flow in
U	Heat transfer coefficient of building envelope	out	Flow out
V_{ref}	Wind speed	NPL	Neutral Pressure Level
$\dot{m}$	Mass flow rate	$wall$	Building envelope

INTRODUCTION

Hybrid ventilation systems have been widely used for livestock buildings. Livestock ventilation is concerned with comfort interpreted through animal welfare, behavior and health, and most importantly, it is concerned with factors such as conversion ratio, growth rate and mortality (J.A.Clark, 1984). Most existing analyses for the livestock ventilation system assume that the indoor air temperature and concentration is uniform. However, the actual indoor environment at any controlling sensor (especially when the sensors are located horizontally) will depend on the air flow distribution that is usually depicted as a map of the

dominant air paths. Therefore, the control system for large scale livestock barns neglecting the horizontal variations could obviously result in significant deviations from the optimal environment for the sensitive pigs or chickens in the livestock barn.

In this paper, the livestock indoor environment and its control system will be regarded as a feedback loop in which the controller provide the optimal actions to the actuators taking into account of the necessary disturbances and random noises based upon the developed indoor climate model and ventilation equipment models. The purpose of this paper is to design an appropriate controlling strategy to improve the indoor animal Thermal Comfort (TC) and Indoor Air Quality (IAQ) through an optimal energy approach.

MATHEMATICAL MODELLING

The fan assisted natural ventilation principle will be investigated in this work. As seen in Figure 1(a), 1(b) and 1(c), the system consists of evenly distributed fans and fresh air openings on the walls. From the view of direction A and B, Figure 1(A) and 1(B) provide a description of the dominant air flow map of the building includes the airflow interaction between each conceptual zone by applying the multi-conceptual zone method. In each zone, it is possible to monitor the zonal climate and concentration and effect of the control signals through the actuators movements: inlet vents and exhaust fans.

The necessary simplifying assumptions for developing models are as follows:

- The interactive airflow between internal zones, which is influenced by the inlet air jet trajectory, thermal buoyancy forces and convective heat are assumed to be constant.
- Heat gain from animals and solar radiation are assumed to be constant.
- The rate of the heat loss by evaporation is neglected.
- The thermal properties of the airflow are assumed to have bulk average values.
- Airflow involves no mass accumulation inside the building.
- The heat transfer coefficient of building envelope is assumed to be constant.
- The pressure is assumed to be constant on each building surface (same value of pressure coefficient C_p is used for all openings on the same side of the building).
- A hydrostatic pressure distribution is assumed in the space.
- Opening characteristics are assumed independent on flow rate, pressure difference and outside temperature (constant discharge coefficient C_d are used for all openings).

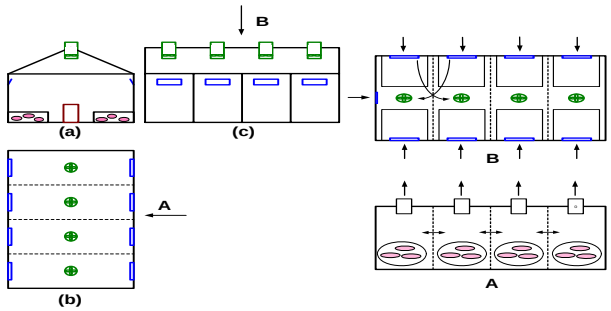

Figure 1: Synoptic of Large Scale Livestock Barn and the Dominant Airflow Map of the Barn

Models of Indoor Climate

A conceptual multi-zone method will be employed to analyze and develop the indoor climate model. The livestock building will be divided into several macroscopic homogeneous conceptual zones horizontally so that the nonlinear differential-algebraic Eqn. 1 and Eqn. 2

relating the zonal temperature T_i and zonal concentration $C_{r,i}$ can be derived by applying the theory of conservation of energy and mass. By substituting *i* with the zone number into Eqn. 1 and Eqn. 2, we could derive four coupled differential equations for indoor thermal comfort in terms of zonal temperature and indoor air quality in terms of zonal air concentration respectively.

For Eqn. 1, the rate of energy $\dot{Q}$ transferred by mass flow can be calculated by Eqn. 3. $\dot{Q}_{i+1,i}, \dot{Q}_{i,i+1}$ indicate the heat exchange due to the air flow across the conceptual boundary of zone *i* and zone *i*+1, while for the middle zones which have heat exchange with neighbor zones on each side, two more parts $\dot{Q}_{i-1,i}, \dot{Q}_{i,i-1}$ will be added to Eqn. 1. The value of interactive mass flow between internal zones is the sum of influence from air jets, heat plume, thermal buoyancy and air exchange rate. $\dot{Q}_{inlet,i}, \dot{Q}_{outlet,i}, \dot{Q}_{leakage,i}$ represent the heat transfer by mass flow through inlet, outlet and leakage of the zone respectively. The convective heat loss through the building envelope is denoted by $\dot{Q}_{conve}$ and described as $U \cdot A_{wall} \cdot (T_i - T_o)$. The heat source of the zone $\dot{Q}_{source,i}$ includes the heat gain from animal heat production, solar radiation and heating system. For Eqn. 2, the rate of concentration is indicated as $C_r \cdot n$, where C_r represents the concentration level and the air exchange rate *n* is calculated by Eqn. 4. For the middle zones which have mass flow interaction with neighbor zones on both sides, two more parts $C_{r,i} \cdot n_{i,i-1}, C_{r,i-1} \cdot n_{i-1,i}$ should be added to Eqn. 2. The rate of contaminant generation is denoted by G_i and the zonal volume is denoted by V_i.

$$M_i c_{p,i} \frac{dT_i}{dt} = \dot{Q}_{i+1,i} + \dot{Q}_{i,i+1} + \dot{Q}_{in,i} + \dot{Q}_{out,i} + \dot{Q}_{leakage,i} + \dot{Q}_{conve,i} + \dot{Q}_{source,i} \tag{1}$$

$$\frac{dC_{r,i}}{dt} = C_{r,i} \cdot n_{out} + C_{r,o} \cdot n_{in} + C_{r,i+1} \cdot n_{i+1,i} + C_{r,i} \cdot n_{i,i+1} + \frac{G_i}{V_i} \tag{2}$$

$$\dot{Q} = \dot{m} \cdot c_p \cdot T_i \tag{3}$$

$$n = \frac{\dot{m} \cdot 3600}{\rho \cdot V} \tag{4}$$

Models of Inlet Vent and Motor Fan System

$$\sum q_{in} \cdot \rho_o \cdot \frac{\Delta P}{|\Delta P|} + \sum q_{out} \cdot \rho_i = 0 \tag{5}$$

$$q = C_d A \cdot \sqrt{\frac{2|\Delta P|}{\rho}} \operatorname{sgn}(\Delta P) \tag{6}$$

$$\Delta P = \frac{1}{2} C_P \rho_o V_{ref}^2 - P_i + \rho_o g \frac{T_i - T_o}{T_i} (H_{NPL} - H) \tag{7}$$

Eqn. 5 gives the relationship between the volume flow rate and pressure difference across the openings based on mass balance equation with single zone method. The ventilation flow rate can be determined from Eqn. 6 and the pressure difference is the combing driving forces of

thermal buoyancy and wind as Eqn. 7. Therefore, Eqn. 5 will then result in a linear equation from which we can solve for the internal pressure P_i. With fan law, the straightforward relationship between total pressure difference, volume airflow rate and motor speed is clarified in a nonlinear static equation (P.Heiselberg, 2004).

Performance Simulation

The open loop dynamic performances of zonal variation for indoor temperature and CO_2 concentration within a day based on the developed TC model and IAQ models are demonstrated in Figure 2(a) and (b). The system started from operating points which maintain the system behavior (indoor climate and indoor air quality) at the required condition with exceptionally low horizontal variation. The system is stimulated by a serious of step changes of the indoor zonal heat source and zonal contaminant load during the entire time horizon. The simulation is implemented with stochastic external temperature, ambient concentration and wind speed disturbances generated from random sources through low-pass filters.

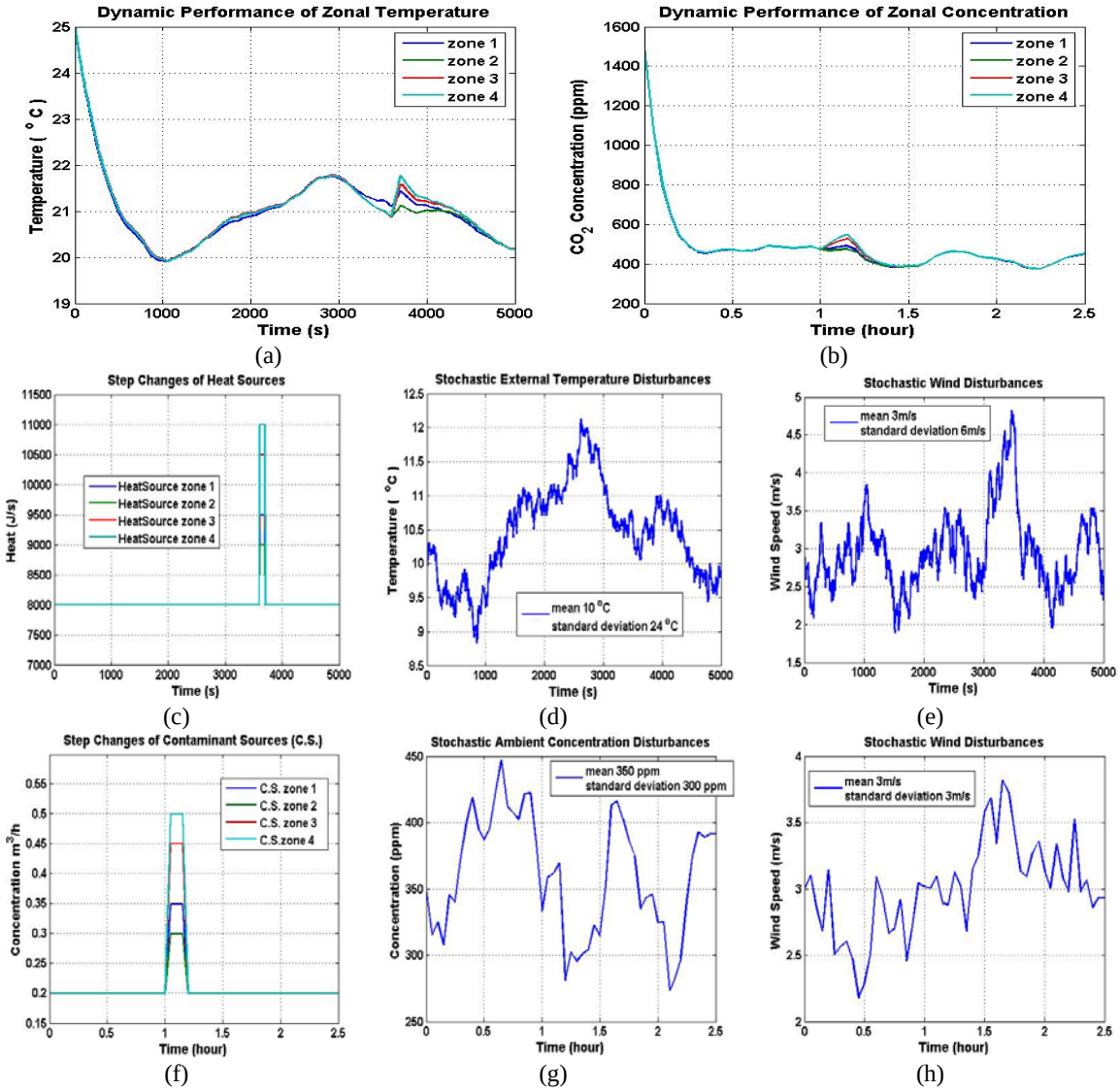

Figure 2: Open loop Dynamic Performance for (a) Zonal Temperature and (b) Zonal CO_2 Concentration; Step Changes of (c) Heat Source (f) Contaminant Source; Stochastic Wind Speed (e) and external temperature (d) for TC model; Stochastic Wind Speed (h) and Ambient CO_2 Concentration (g) for IAQ model.

It proves to be evident from the simulation results, that the conceptual multi-zone models for TC and IAQ contain significant information on horizontal variation which is not able to be captured by the single zone model with mean temperature and concentration, under the circumstances that the zonal disturbances changes.

DESIGN OF CONTROL SYSTEM

The entire livestock ventilation system and indoor environment is a Multiple Input and Multiple Output (MIMO) dynamic nonlinear process and strongly coupled intrinsic system. It is exposed to external disturbances and noise and has actuators with saturation. Consequently, it is necessary to explore the application of advanced control algorithms, such as the optimal control, predictive control etc. to satisfy the equilibrium between the indoor air quality, thermal comfort and energy consumption. Linear Quadratic (LQ) optimal control is a good method for ventilation control system analysis before applying other more complex control schemes. The LQ control deals with a linear state space model which is derived from the system linearization around the equilibrium points, where the Thermal Neutral Zone and animal demand concentration are selected to be the reference values.

The performance function for LQ control is:

$$\min \sum_{k=0}^{N-1} \left[x^T(k) Q_1 x(k) + u^T(k) Q_2 u(k) \right] + x^T(N) Q_N x(N) \tag{8}$$

where k denotes the sample time, x is measurable states or controlled variables (zonal temperature and zonal concentration) matrix, and u is control signal or manipulated variables (inlet vents and fan speed) matrix, N denotes the time horizon, the weighting matrices Q_1 and Q_N are positive definite and Q_2 is positive semi-definite, and they are defined as diagonal matrices. The diagonal elements are the inverse value of the square of the maximum allowed deviations in the states and the control signals (G.F.Franklin *et al.*, 1998). By using Dynamic Programming, we could obtain a linear time varying controller, where the dynamic gain is determined by the *Riccati* Equations. The optimal control signals are generated from this linear feedback MIMO controller taking into account of the disturbances variables (external temperature, heat source, ambient concentration and contaminant load). Then, this generated control signals are input to the process to predict the zonal temperature and concentration. The sensor and motor dynamics is relatively fast compared with the entire system response and could be neglected.

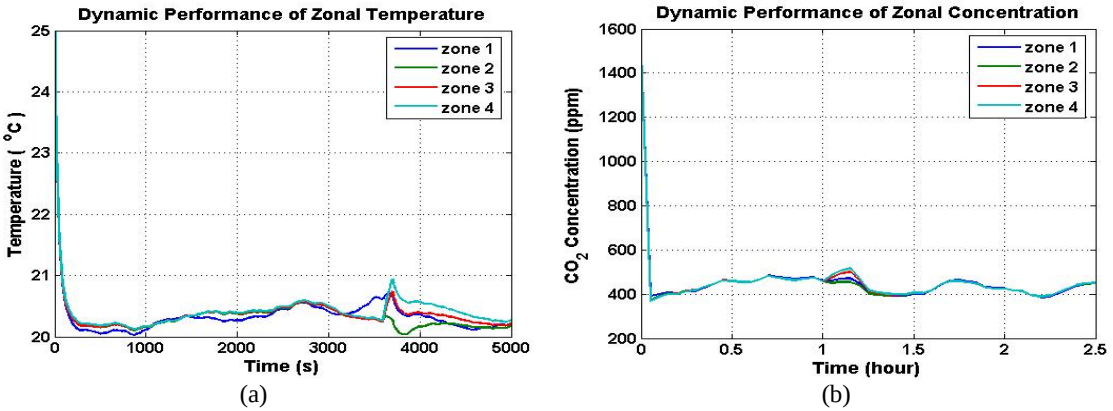

(a) (b)

Fig. 3 Close Loop Dynamic Performance with Feedback Gain for (a) Zonal Temperature, (b) Zonal CO_2 Concentration.

Figure 3 illustrates the close loop dynamic performances of the indoor temperature and air concentration with a linear feedback gain for animal thermal comfort and indoor air quality by applying the same variation of the disturbances for open loop simulation as shown in Figure 2. A certain amount of trial and error is required with an interactive computer simulation before a satisfactory design is obtained, for example, one of possibilities is to adjust the weighting matrix. Through comparing the close loop and open loop of the simulation results, we could recognize that the system with controller has much shorter response time to reach the steady state and has the capability to reject the indoor and outdoor disturbances oscillation and noise relatively by adjusting the air flow rate through eight inlet vents and four exhausted fans.

DISCUSSION

Aiming at improvement of performances and optimization of energy, the main achievement of this work is the successful application of the LQ optimal controller for livestock ventilation systems analyzed by a conceptual multi-zone method. The results prove to be fruitful that the designed control scheme is feasible and flexible to satisfy the purpose.

Some parameters of the mathematical models will be identified through experiment in a real scale livestock barn equipped with hybrid ventilation systems. The interfacial mixing parameters which describe the airflow interaction of internal zones will be calibrated with experimental measurement by using gas tracer. Advanced control methods, dynamic disturbances models, estimator for weather condition, augmented control signals for more actuators such as the operation of the heating system for cold weather, air-conditioning systems for warm weather, shade screen for solar radiation will be applied in future and the result will be compared with those obtained with currently used classical PID controller.

AKNOWLEDGEMENT

The authors would like to acknowledge financial support from the Danish Ministry of Science and Technology (DMST) and Center for Model Based Control (CMBC) with Grant number: 2002-603/4001-93.

BIBLIORAPHY

G.F.Franklin, J.D.Powell and M.L.Workman (1998). *Digital Control of Dynamic Systems*. 3rd edition. Reading Mass.: Addison-Wesley.

J.A.Clark (1981). *Environmental Aspects of Housing for Animal Production*. Butterworth Heinemann. England.

J.P.Bourdouxhe, M.Grodent and J.Lebrun (1998). *Reference Guide for Dynamic Models of HVAC Equipment*. American Society of Heating, Refrigerating and Air-Conditioning Engineers. Atlanta.

K.Zhou, J.C.Doyle and K.Glover (1996). *Robust and Optimal Control*. Prentice-Hall. New Jersey.

P.Heiselberg (2002). *Principles of Hybrid Ventilation*. IEA Energy Conservation in Buildings and Community Systems Program, Annex 35: Hybrid Ventilation in New and Retrofitted Office Building.

P.Heiselberg (2004). *Natural and Hybrid Ventilation*. Aalborg University. Denmark.

COMPARATIVE ANALYSIS OF THE ENERGY IMPACT OF AIR INFILTRATION FOR DIFFERENT VENTILATION SYSTEMS

A. Voeltzel and F.R. Carrié

Centre d'Etudes Techniques de l'Equipement de Lyon
46 rue Saint Théobald
F – 38081 L'Isle d'Abeau Cedex, France

ABSTRACT

This work presents simulations results exploring the influence of the building air-tightness on the energy consumption of buildings for different hypothesis on the type of ventilation system. It shows that the energy impact is different depending on the ventilation system, and that buildings ventilated with a supply-extract ventilation system, even those without heat exchanger, are much more sensitive to air infiltrations than buildings ventilated with an extract ventilation system.

KEYWORDS

air infiltrations, leakage, energy consumption, supply-extract ventilation system, heat recovery

INTRODUCTION AND OBJECTIVES

Airborne energy losses represent from 30 % to 50 % of heating needs of dwellings equipped with an extract ventilation system. This proportion can be even higher for buildings built with high standards of thermal insulation like the Passiv Houses in Germany for instance.

Airborne energy losses depend on the air flow rates procured by the mechanical ventilation system and the air infiltrations. Poor building air-tightness can be responsible for cross air flows increasing significantly the total air change rate and consequently the energy consumption of a building.

The building air-tightness has a different impact on the energy consumption depending on the ventilation system. In buildings with an extract ventilation system, the ventilation system maintains the building at a depression of a few Pascals (Figure 1(a)). In buildings equipped with a supply-extract ventilation system, the pressure difference across the buildings envelope is much lower (Figure 1(b)). This makes the buildings equipped with a supply-extract ventilation system more sensitive to cross ventilation due to wind and poor air-tight building envelope.

A way to reduce the energy consumption of buildings consists in installing energy efficient ventilation systems like supply-extract ventilation system with heat recovery. Nevertheless, the global efficiency of the system can be affected if the air leaving the building doesn't flow through

the heat exchanger. This happens when part of the air flow leaves the building through exfiltrations (Figure 1 (b)).

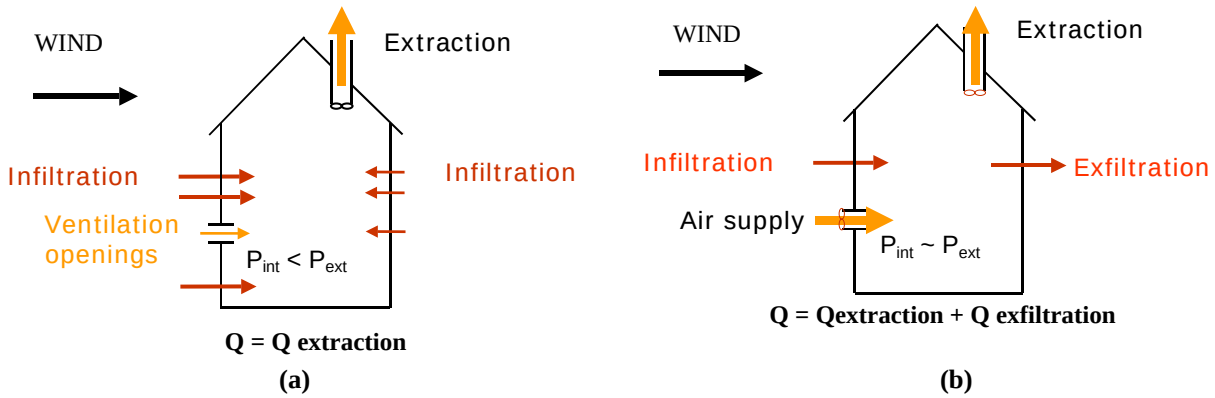

Figure 1 : Influence of the ventilation system on the total air change rate of a building. Case of a good air-tightness : (a) building ventilated with an extract ventilation system, (b) : building ventilated with a supply-extract ventilation system.

Thus, as shown in Figure 1, the presence of air infiltrations does not systematically increase the total ventilation rate of a building. It depends on the capability of the ventilation system to maintain a sufficient pressure difference across the building envelope to fight the wind forces on the building facades.

The work presented in this paper aims at comparing and quantifying the energy impact of the building air-tightness on the energy consumption of a building for different ventilation systems.

The approach was based on the use of the simulation tool developed for the French thermal regulation RT2000 (Réglementation Thermique 2000) **[1]**. This simulation code computes the total energy consumption of a building, taking into account the energy needed to heat the building, to produce hot water, and for non residential buildings also for lighting. Results are given in primary energy, defined as the total energy needed including the generation-, transmission- and emission energy losses.

PHYSICAL MODELLING OF AIR FLOW RATES

Air infiltration modelling in the French thermal regulation RT2000

The model used in RT2000 is based on EN 13465 **[2]** for the computation of the ventilation and infiltration flow rates in the building, and on the ISO 13790 **[3]** for the computation of the heating needs. The model described in EN 13465 is based on a mono zone pressure code that compute the pressure inside the building according to the exterior pressures on the building facades, the characteristics of the ventilation system, and the airflow laws of openings in the building envelope. Each element of the building envelope (ventilation openings and air infiltration cracks) is described by an airflow law of the form (Eq. 1). The pressure inside the building is obtained by solving the mass conservation equation, and the airflows through the different openings are then given by applying Eq. 1.

$$Q = K(\Delta P)^n \qquad \textbf{Eq. 1}$$

Q	airflow through the opening	[m3.h^{-1}]
K	opening coefficient	[m3.h^{-1}.Pa^{-n}]
ΔP	pressure difference across the opening	[Pa]
n	flow exponent	[-]

The coefficient K is related with the effective leakage area, and the value of n gives some information on the shape of the openings: values next to 0.5 correspond to large openings, whereas values next to 1 means that the openings are very small and diffuse.

The parameter used in the French regulation RT2000 to characterize the air-tightness of the building envelope (I_4) is the leakage airflow under a pressure difference of 4 Pa across the building envelope, divided by the area of the "cold surface" which is defined as the building envelope area separating the heated volume from the outside or from a non heated room, excluding the bottom floor from this definition (Eq. 2).

$$I_4 = \frac{Q_{4Pa}}{A_c} \qquad \textbf{Eq. 2}$$

A_c	Area of the "cold surface"[1] of the building envelope	[m^2]
Q_{4Pa}	Leakage airflow through the building envelope at a pressure difference of 4 Pa	[m^3.h^{-1}]
I_4	Leakage airflow per m^2 of "cold surface" at a pressure difference of 4 Pa	[m^3.h^{-1}.m^{-2}]

Reference values for building air-tightness in the French thermal regulation RT2000

The RT2000 introduces reference and default values. The reference value is the value that lead to the reference consumption if all others characteristics of the building are also at the reference value. The default value is the value that a designer can use if he doesn't have an idea of or doesn't know the real value at the stage he makes the computation. This value increases the energy consumption and has to be compensated by a performance higher than the reference on an other part of the building.
The reference- and default values in the regulation depend on the building use. They are summarized in Table 1. For a typical French single family dwelling[2], the reference value of the leakage airflow under a pressure difference of 4 Pa (0.8 m^3.h^{-1} .m^{-2}) is equivalent to the airflow through a hole of about 200 cm^2 at the same pressure difference.

Table 1 : Reference and default values for the building air-tightness defined in the French regulation RT2000

	Leakage airflow Q at ΔP = 4 Pa [m^3.h^{-1} .m^{-2}]	
	Reference value	Default value
Single family dwellings	0.8	1.3
Multiple family dwellings	1.2	1.7
Tertiary sector buildings	1.2	1.7
Others buildings	2.5	3.0

[1] defined as the building envelope area separating the heated volume from the outside or from a non heated room, excluding the bottom floor from this definition.
[2] One level house, 110 m^2 of floor area, a heated volume of 280 m^3, and 230 m^2 of "cold surface".

Fields measurement results of the air-tightness of French buildings

Figure 2 shows the air-tightness performances measured on French buildings, resulting from a test sample of 71 dwellings and 17 non residential buildings. One can see that dwellings are much more airtight than others buildings. Only one third of the non residential buildings that have been tested in this sample have an I_4 value better than the reference value defined by the French thermal regulation (1.2 or 2.5 $m^3.h^{-1}.m^{-2}$ depending on the type of ventilation, see Table 1). On the other hand, about 40 % of the single family dwellings and 90 % of the multiple family dwellings have an I_4 value better than the RT2000 reference value (Figure 2(a)).

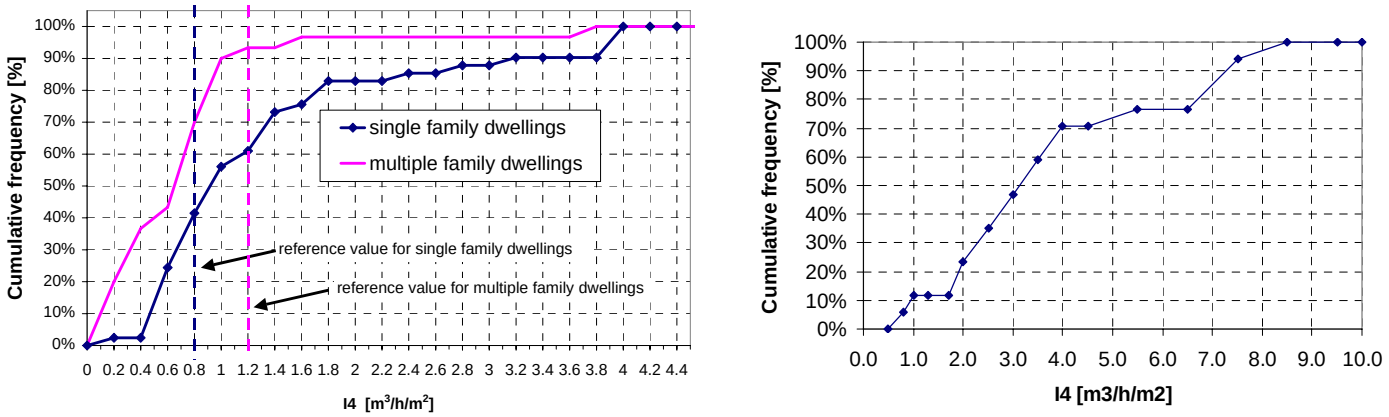

(a) **(b)**

Figure 2 : Cumulative frequency of indicator I4 measured on French buildings. (a): dwellings (sample : 41 single family dwellings, 30 multi family dwellings), (b): non residential buildings (office buildings, industrial buildings, village halls, gymnasiums) (measurement sample : 17 buildings). Source : [4]

SIMULATION RESULTS AND DISCUSSION

Simulations have been made with the simulation code THCmotor (release 2.1.1) specially developed for the French thermal regulation RT2000. The total energy consumption has been computed for a single family dwelling and an office building for different assumptions concerning the ventilation system installed (extract ventilation system, supply-extract ventilation systems with or without heat recovery).

Influence of building air-tightness on total energy consumption

Figure 3 (a) and (b) presents the influence of the building air-tightness on the global energy consumption for respectively a single family dwelling ventilated with a mechanical extract ventilation system, and an office building ventilated with a supply-extract ventilation system without heat recovery. These figures show that the energy consumption grows for increasing values of the air leakages airflow, which is logical as the total ventilation rate is increased by the air infiltrations. Nevertheless, Figure 3 (a) also shows that for values of I_4 lower than 0.8 $m^3.h^{-1}.m^{-2}$, the amelioration of the building air-tightness does not decrease any more the energy consumption of the building ventilated with an extract ventilation system. This can be explained by the fact that for air-tight buildings ventilated with an extract ventilation system, the depression induced by the ventilation system is sufficient to drive the air flow through the mechanical extraction and fight exfiltrations.

On the other hand, for the simulated office building ventilated with a supply-extract ventilation system, the improvement of the building air-tightness is always beneficial for the energy consumption, even for low value of I_4 (Figure 3(b)). This illustrates the fact that buildings ventilated with a supply-extract ventilation system are much more sensitive to air infiltrations than those ventilated with an extraction ventilation system, because of the lower value of the pressure difference caused by the ventilation system across the building envelope (Figure 1(b)).

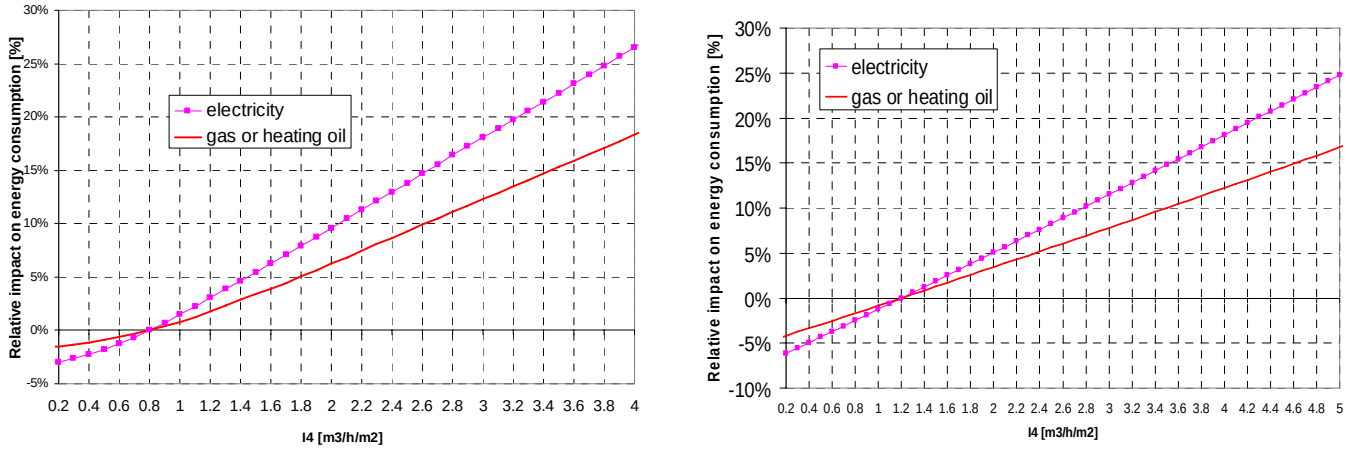

Figure 3 : Influence of the building envelope air-tightness on the total energy consumption. (a): single family dwelling ventilated with an extract ventilation system, simulation file : CSTB file MI4 THC-APP-04 ref.thc, (b): office building ventilated with a supply-extract ventilation system without heat exchanger, simulation file : CSTB file bureaux2 THC-APP-14 ref.thc.

Figure 4 compares the energy consumptions for the same office building supposing in one case that the building is ventilated with an extract ventilation system, and in the other case with a supply-extract ventilation system without heat recovery. For I_4 greater than 1.1 $m^3.h^{-1}.m^{-2}$, the energy consumption is higher when the building is ventilated with a supply-extract ventilation system without heat exchanger. This is due on one side to the increased electricity consumption because of the presence of two fans, and on the other side to the air infiltrations.

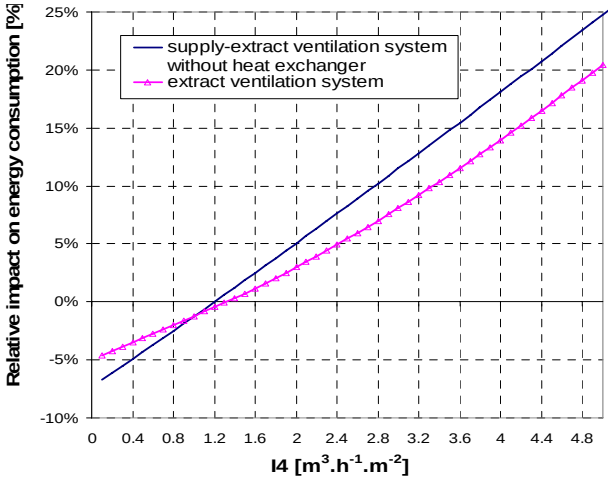

Figure 4 : Influence of the building air-tightness for an office building ventilated respectively with an extract – and a supply extract system. Sim. file : CSTB file bureaux2 THC-APP-14 ref.thc.

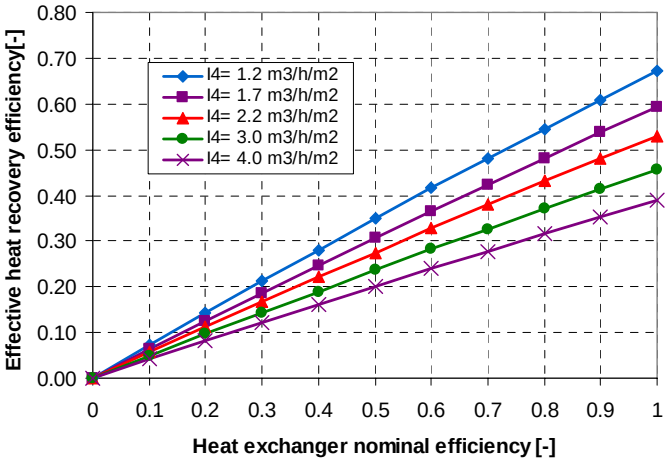

Figure 5 : Influence of the building air-tightness on the effective heat recovery for an office building ventilated with a supply-extract ventilation system. Sim. file : CSTB file bureaux2 THC-APP-14 ref.thc.

Influence of building air-tightness on the heat recovery efficiency

Figure 5 presents the evolution of the effective heat recovery efficiency, defined as the part of the enthalpy flux leaving the heated volume that is recovered to pre heat the entering air, as a function of the nominal heat exchanger efficiency, for different hypothesis of the building air-tightness. This simulation has been made for an office building ventilated with a supply-extract ventilation system. For poor air-tight building envelopes, the effective heat recovery efficiency can drop to very low values. For instance, for a building envelope with an I_4 value of 4.0 $m^3.h^{-1}.m^{-2}$, the effective heat recovery efficiency is three times lower than the nominal efficiency of the heat exchanger.
Taking into account that one third of the French non residential buildings that have been tested have an I4 value greater than 4.0 $m^3.h^{-1}.m^{-2}$ (see Figure 2(b)), this shows potential energy savings that lay in bettering the building air-tightness.

CONCLUSION

Air-tightness is becoming a growing concern for energy efficient buildings. Simulations of the impact of air infiltrations on energy consumptions depending on the type of ventilation system installed have been made with the simulation tool specially developed for the French thermal regulation RT2000.
The simulations showed that the energy consumptions of buildings equipped with a supply-extract ventilation system can be significantly increased by leaky building envelopes, and that these buildings are much more sensitive to air infiltrations than buildings equipped with an extract ventilation system. Moreover, when the supply-extract ventilation includes a heat exchanger, the effective heat recovery of the system can be deeply limited by air infiltrations, even for very efficient heat exchangers.
Theses results indicate that particular attention should be paid to the verification of the building air-tightness performance of buildings equipped with supply-extract ventilation systems, especially with low-energy buildings.

REFERENCES

[1] Réglementation thermique française RT2000. Décret n° 2000-1153 du 29 novembre 2000 relatif aux caractéristiques thermiques des constructions modifiant le code de la construction et de l'habitation. Direction Générale de l'urbanisme, de l'Habitat et de la Construction.

[2] EN 13465 : Ventilation for buildings - calculation methods for the determination of air flow rates in dwellings.

[3] ISO 13790 : thermal performance of buildings - calculation of energy use for space heating.

[4] Guillot K. and Litvak A. (2000). Field measurement campaign of 70 French dwellings, ADEME, France.

ANALYSIS OF VENTILATION SYSTEMS IN HIGH PERFORMANCE HOMES IN COLD CLIMATES

Christine E. Walker[1] and Douglas Kosar[1]

[1]*Building Sciences Group, Energy Resources Center, University of Illinois at Chicago, Chicago, IL 60607-7054, USA*

ABSTRACT

The performance of three different ventilation systems in cold climate homes is discussed. Comparisons are presented of monitored datasets by contrasting operations of the three ventilation systems, the energy impacts on the overall HVAC systems, and resulting indoor environmental conditions. Whole building simulation results, based on ventilation system models using EnergyGauge® and validated in part by the monitored datasets, provide normalized comparisons of HVAC system energy use. Finally, the economics of the three ventilation system approaches are discussed based on representative installed equipment costs and energy prices, so practitioners from policymakers, code developers, builders, on down to homeowners better understand the first and operating cost tradeoffs.

KEYWORDS

Ventilation systems, monitoring, modeling, residential

INTRODUCTION

Sustained higher heating fuel costs, more energy efficient building codes, and emerging residential ventilation standards are fostering needed research on mechanical means for providing fresh air in cold climate homes to maintain acceptable indoor air quality (IAQ). These more energy efficient homes are adopting construction methods that include applying greater insulation levels throughout the building envelope, along with tighter overall building methods. The combination of these high performance envelopes and tight construction lead to very low air changes per hour (ACH) in residential structures. In order to meet indoor air quality standards, such as those specified by the American Society of Heating, Refrigerating, and Air-Conditioning Engineers (ASHRAE) Standard 62.2-2003 *Ventilation and Acceptable Indoor Air Quality in Low-Rise Residential Buildings*, these homes require the installation of mechanical ventilation systems.

One of three types of ventilation systems was installed in each of three neighboring single-family, detached houses in South Chicago, Illinois, USA. The homes were similarly constructed, using high performance structural insulation panels, and all located within the same housing development. The homes were outfitted with continuous monitoring equipment to record the run-times, inlet and/or outlet air conditions, and energy consumption of mechanical equipment, along with the temperature, relative humidity, and carbon dioxide levels in key areas of the homes. Each house had a blower door test to measure the overall ACH due to natural infiltration. This test not only provided the baseline infiltration for each house, but also ensured that the homes were tightly constructed as designed. Additionally, the individual ventilation systems were tested with flow hoods to measure the actual ventilation airflows.

This paper presents findings for the three ventilation systems that were installed, monitored and modeled for each high performance home. The ventilation systems are described, followed by a discussion of the methodology used in evaluating the monitored data and modeling runs for the ventilation systems. Finally the overall monitoring results for each ventilation system are presented and then compared to the other systems in a normalized manner using the modeled data.

MECHANICAL VENTILATION SYSTEMS

The three ventilation systems were selected based on their respective indoor air quality, initial cost, and operating cost attributes. The three systems evaluated are: 1) Exhaust-Only system, 2) Air-Cycler system, and 3) Energy Recovery Ventilation system. The systems were installed on nearly identical 1728 ft^2 3-bedroom, 2-story homes with basements. Based on ASHRAE Standard 62.2-2003 (ASHRAE 2003), each home required 60 cfm of mechanical ventilation air. Details of each ventilation system are presented below.

Exhaust-Only System

This system uses two bathroom exhaust fans to induce, by design, uncontrolled infiltration through the building envelope which also creates a load on the heating and cooling system of the home. There is no ductwork associated with this ventilation system, which may not distribute air as effectively as the other systems. The fans cycle on and off throughout the day and night, with the fan on for 35 minutes every hour to meet the fresh air requirements via the induced infiltration. The first floor bathroom exhaust fan had a measured flow rate of 59 cubic feet per minute (CFM), while the second floor bathroom exhaust fan had a measured flow rate of 56 CFM. A total energy usage of 45-50 Watts for both fans was measured.

Air-Cycler System

This ventilation system uses a supply-only strategy, introducing outside air when needed to meet fresh air requirements. The air-cycling system is a ducted system that draws outdoor air to the return duct, mixes it with the return air, and then distributes the mixed air throughout the home. A controller operates a damper in the outside air duct that will close if the outdoor air volume requirement has been met. When there are no heating or cooling requirements, the controller will turn on the furnace or AC system supply fan periodically to guarantee that fresh air requirements are met. The air-cycling system used in the test home had a programmable timer used to actuate the outside air damper and initiate supply fan operation, as needed. The timer was set to turn on for 15 minutes and then remain off for 5 minutes, resulting in a 75% run-time. The air-cycling system had a measured flow rate of 80 CFM with negligible measured energy use for the damper motor.

Energy Recovery Ventilation (ERV) System

The ERV system utilizes an enthalpy exchanger (with two small fans) to exchange both heat and moisture between an incoming fresh air stream and outgoing exhaust air stream. This system, like the air-cycling system, requires ductwork and relies on the heating/cooling system to distribute the fresh air throughout the home. When there are no heating or cooling requirements, the heating/cooling system fan turns on periodically in order to meet fresh air requirements. The preconditioning of incoming fresh air with the ERV saves operating energy

for heating and humidifying in the winter, and cooling and dehumidifying in the summer. The ERV controller cycled on 75 percent of the time, or 45 minutes per hour. The ERV supply air was measured at 80 CFM, while the exhaust was measured at 54 CFM. This difference was caused by the pressure drop across the filters. The ERV consumed an additional 102 Watts over the 700-800 Watts consumed by the heating/cooling system fan.

METHODOLOGY

Both building monitoring and whole-building simulation was used in evaluating the operation of the ventilation systems. Building monitoring provided data that could then be used in validating the building simulation model. These methods are seen as complimentary; validating energy consumption and performance data with each other. In this section an overview of both the monitoring procedure and building simulation method are presented.

Long-Term Remote Monitoring

The three homes were outfitted with monitoring equipment to ascertain the overall performance of each ventilation system, based on the energy used in operation and the resulting indoor environment. The focus of the research was on cold climates, particularly the heating energy consumption of these ventilation systems. The monitoring was carried out beginning in October 2004 and finishing in May 2005. A fifteen-minute recording interval was utilized for the long-term monitored data.

Measured data covered indoor air conditions, ventilation system operations, and energy usages. Indoor air quality was evaluated by monitoring temperature, humidity, and carbon dioxide levels at several locations throughout the home. Depending on the ventilation system, several measurements were recorded including the intake or mix air temperature and relative humidity, exhaust air temperature and relative humidity, and intake and exhaust airflow rates. As part of the assessment of the homes, a blower door test was performed to determine the natural leakage of each house. The houses were measured to range from 0.04-0.06 ACH, compared to the U.S. Department of Energy (DOE) Building America Benchmark of 0.65 ACH. The overall energy consumption of the homes was measured along with several one-time energy usage measurements already noted. In addition, the furnace/AC fan on-time was monitored. It was not feasible however, to separate out fan calls for heating or cooling from requirements for outside air only within those 15 minute interval datasets.

Whole Building Modeling

To obtain a normalized annual performance, the EnergyGauge® computer simulation (FSEC 2005) was used to model the homes and their different ventilation systems. This software has an easy-to-use graphic user interface over the DOE 2.1E simulation engine and is specifically designed for modeling of residential buildings. The construction specifications and floor plans of the homes were used for the input data to the EnergyGauge® model. Structural insulation panels were specified for the envelope construction, with an R-42.5 rating for the roof and R-24.7 for the walls, and a low infiltration rate based on the measured data. The U.S. DOE Building America Benchmark schedules (Hendron 2005) were used as the input for the lighting, appliance, plug, and water heating loads, which are considered to be the baseline when comparing residential buildings. The building model consisted of a first floor and second floor with an unconditioned basement. The thermostat temperature set point used for

all three homes was 76°F for the cooling season and 71°F for the heating season. The actual heating and cooling system capacities and efficiencies of the equipment installed in the homes were used in the building simulations. For heating, the homes had identical 92.5% AFUE high efficiency gas-fired furnaces of 62,780 Btu/hr capacity. Only one of the three homes (the ERV home) was equipped with a 3.5 ton (42,000 Btu/hr), 10 SEER air conditioner, but all homes were modeled with this air conditioner. The supply ventilation for each system was set to 60 CFM for the simulations.

Although this software did contain existing menu selectable options for various mechanical ventilation supply and exhaust systems, it was determined that certain system features such as induced infiltration, furnace/AC fan run-time interlocks, and over-venting damper controls were not yet adequately modeled. So a base case simulation was performed on an unventilated home and then an 8760 hour post-processing spreadsheet analysis of the three ventilation system operations was generated to provide their respective energy usage results.

RESULTS

In evaluating the ventilation systems, annual energy usage and cost was of interest, in addition to meeting indoor air quality standards. First the operation of each ventilation system had to be determined to understand what percentage of time during any hour the ventilation system operated, especially those times independent of the thermostat. Then the internal environments for the homes were compared, followed by the normalized simulation results.

Monitored Home Data

The monitored data for the ventilation systems was separated into monthly datasets, and the run-time fraction of the furnace fan separated into 0.1, or 10% increments. The furnace operating between 70 and 80 percent of a given fifteen minute interval would appear above the '0.8>F>=0.7' label in the figures. This provided a preliminary estimate of the operation of each ventilation system, thereby allowing the comparison of their control strategies. The pattern and number of run-time hours for each system is indicative of the fan energy requirements of each system, as well.

The Air-Cycler System is on for fifteen minutes and then off for 5 minutes for fresh air requirements, resulting in most of the datasets falling above a 60% run-time. The ERV system operates 45 minutes on and 15 minutes off per hour. Much of the data for the ERV is at 100% run-time. The Exhaust-Only system on the other hand operates for 35 minutes each hour, but its operation is not interlocked with the furnace fan, so there are periods of time when it is not in operation, represented by high number of furnace run-time hours of zero (Furnace=0).

The December data is presented in Figure 1, with the ERV system operating at full operation (F=1) over the fifteen minute interval for the most number of hours. In April, when there is a reduced heating requirement, the ERV and Air-Cycler systems operate a reduced number of hours at full operation, but still much more often than the Exhaust-Only system, as seen in Figure 2. The average carbon dioxide level was determined using the measured carbon dioxide levels from the three areas within each home -- the first floor, master bedroom, and second bedroom. The average outside carbon dioxide level, 409 ppm, was subtracted from this average interior level, providing some measure of the indoor air quality. Table 1 presents the number of hours that this difference in carbon dioxide levels exceeded 700 ppm for the 4728 hours of the monitoring period mid October 2004 through May 2005.

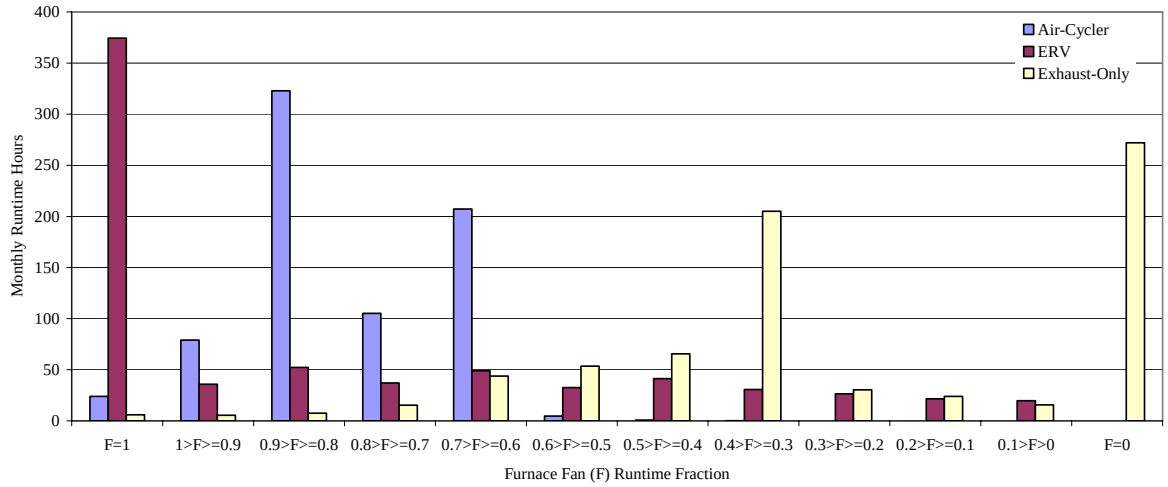

Figure 1: December Monthly Run-Time Hours for the Three Ventilation Systems

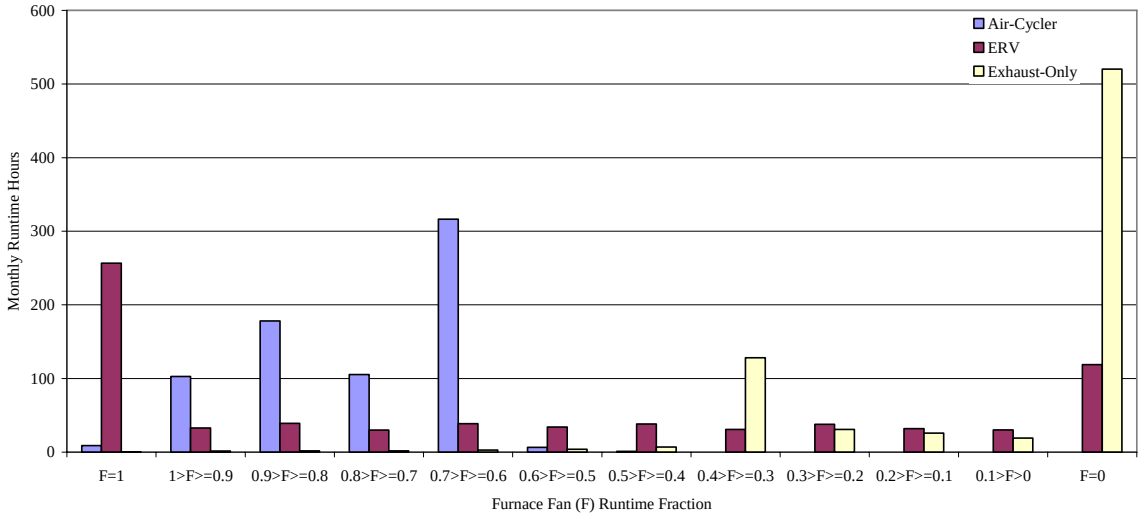

Figure 2: April Monthly Run-Time Hours for the Three Ventilation Systems

EnergyGauge® Simulations

The EnergyGauge® simulations and post-processing spreadsheet analysis allowed a normalized operation of the ventilation systems. The homes were modeled with the same building orientation, temperature set points, internal loads, etc. This provided a direct comparison of the home energy consumption based purely on differences in their ventilation systems. The simulation results for the energy required to condition the home for the three ventilation cases are presented in Table 1. Also included is a base case that represents the high performance home without any ventilation system, providing an additional energy baseline but unacceptable indoor air quality. The heating or cooling energy is the thermal and electrical energy required to condition the supply air. The heating or cooling fan energy is the electrical energy required to distribute the supply air. The ERV system clearly saves heating and cooling energy, but the fan energy associated with exhausting or ventilating air was the significant factor. This was especially true for the interlocking operation with the furnace/AC fan of the Air-Cycler and ERV systems that resulted in substantial supply fan energy requirements solely for ventilation. These operating results are similar to those determined in a companion study by Steven Winter Associates (Aldrich 2005).

TABLE 1

EnergyGauge® Simulation Annual Energy Usage

Energy End Use	*Base Case*	*Exhaust-Only*	*Air Cycler*	*ERV*
Heating (62.78 kBtu/hr) --therms	497	634	634	536
Supply Fan Heating -- kWh	406	524	524	441
Cooling (42 kBtu/hr) -- kWh	1247	1323	1323	1269
Supply Fan Cooling -- kWh	229	244	244	234
Exhaust Fan -- kWh	---	210	---	---
Supply Fan Ventilating -- kWh	---	---	3440	3532
ERV Fan -- kWh	---	---	---	670
Total -- kWh	1881	2302	5531	6147
Total -- therms	497	634	634	536
Annual Energy Cost -- $/yr at $0.60/therm and $0.10/kWh	$486	$611	$934	$936
System Installed Cost Premium ($)		$230	$300	$1200
Air Quality(monitored data Oct'04–May '05)				
Number of Hours CO2 Levels above 700ppm	unacceptable	138	124	314

SUMMARY

Through monitoring and simulation of alternative ventilation systems, a better understanding was attained regarding their operating characteristics and energy implications. The systems were designed to meet minimum indoor air quality requirements, as set by ASHRAE Standard 62.2, and then the energy consumption associated with the operation of these ventilation systems was assessed. The interlock of the Air-Cycler and ERV systems with the supply fan, to meet minimum run-times for indoor air ventilation requirements in addition to heating/cooling requirements, caused substantial energy consumption increases, made worse when furnace/AC systems were oversized and already had short run-times. The energy usage for the Exhaust-Only system was substantially lower than the other two systems, as it only required a 50 Watt power draw, as opposed to the 750 Watt interlocked furnace fan power draw. The Exhaust-Only system is also projected to have the lowest installed cost premium of the three systems as well, if a single exhaust fan and controller can be used as priced in Table 1.

ACKNOWLEDGEMENTS

The authors would like to thank the National Center for Energy Management and Building Technologies and the Department of Energy for their financial support of this research and Steven Winters Associates for sharing their monitored home data and providing technical assistance with the data analysis.

References

Aldrich, R. (2005) Research and Ideas: Furnace Fan Penalty. Energy Design Update. Aspen Publishers. **25:6**. June 2005.

ASHRAE Standard 62.2 (2003) *Ventilation and Acceptable Indoor Air Quality in Low-Rise Residential Buildings*. American Society of Heating, Refrigerating, and Air-Conditioning Engineers, Atlanta, GA, USA.

Florida Solar Energy Center (2005), EnergyGauge® USA Residential, A Residential Energy Design Software, Cocoa, FL, USA, www.energygauge.com/USARes/default.htm .

Hendron, R. (2005). Building America Research Benchmark Definition, Updated December 29, 2004, National Renewable Energy Laboratory, Golden, CO, USA.

USE OF THE STAIRWELL AS A COMPONENT OF NATURAL VENTILATION SYSTEMS IN RESIDENTIAL BUILDINGS. COMPARISON OF TECHNOLOGIES FOR THE EXTERNAL ENVELOPE.

F. Iannone and F. Fiorito

Department of Architecture and Urban Planning, Politecnico di Bari, Bari, Italy

ABSTRACT

The design and realisation of natural ventilation systems is an important research topic into the ability of buildings to respond to climatic conditions, using parts of the buildings themselves as indoor microclimate control systems. This research aims to evaluate how the stairwell can be an essential element of natural ventilation in low-rise buildings. In this study, the main innovation is the different architectural and functional conception of traditional building components such as the stairwell.

The stairwell is used as a chimney in order to increase the air exchange rate in cold and hot seasons. While previous works of the author were focused on the ventilation in winter, when the heating of dwellings enhances the stack effect in the stairwell, in this paper the summer behaviour of similar systems has been be investigated. The hypothesised driving forces causing air movement are the stack effect and the "solar chimney effect".

In this paper the application of the described systems is analysed on common building types, such as blocks of "in-line" housing. These consist of three to five storeys with a single stairwell and two apartments on each floor.

The natural ventilation system studied is characterized by easy implementation in energy retrofitting of buildings as well as inexpensive installation and management. In order to increase the "solar chimney" behaviour, two different technical envelope solutions have been evaluated, namely painting external surfaces black and external insulation. The effects produced by the implementation of different façade systems (equipped with PV systems, transparent insulating materials, air collectors and advanced envelope systems) will be compared in future works.

Finite elements and Computational Fluid Dynamics codes were used in order to design and verify the intervention efficiency and the behaviour of the system as a whole . The first results of CFD simulations here presented highlight that the fluid patterns can play a fundamental role. The complex geometry and the dynamic thermal boundary conditions of a typical stairwell substantially modify the hypothesised "solar chimney behaviour" of the system at night.

KEYWORDS

Natural Ventilation, Stairwell, Residential Buildings, CFD

INTRODUCTION

This research aims to evaluate how stairwell can be an essential element of natural ventilation in low-rise buildings and follows on from previous research by the authors (Catalano et al., 2004).

This study focuses on building types that are very common, such as blocks of in-line housing. While previous works have evaluated the behavior of the stairwell as an extractor chimney during winter, in this paper the mechanism of the optimized winter system is evaluated during summer conditions.

1. THE NATURAL VENTILATION SYSTEM: THE MODEL AND ITS BOUNDARY CONDITIONS.

The analyzed system is a typical stairwell of an in-line multi-family building of five storeys, with two dwellings per floor. The following figures show the typical plan and sections of the adopted model. The same system has been analysed in typical winter boundary conditions. Furthermore, the behaviour of a stairwell with a sloped roof (see figure 1) has been verified.

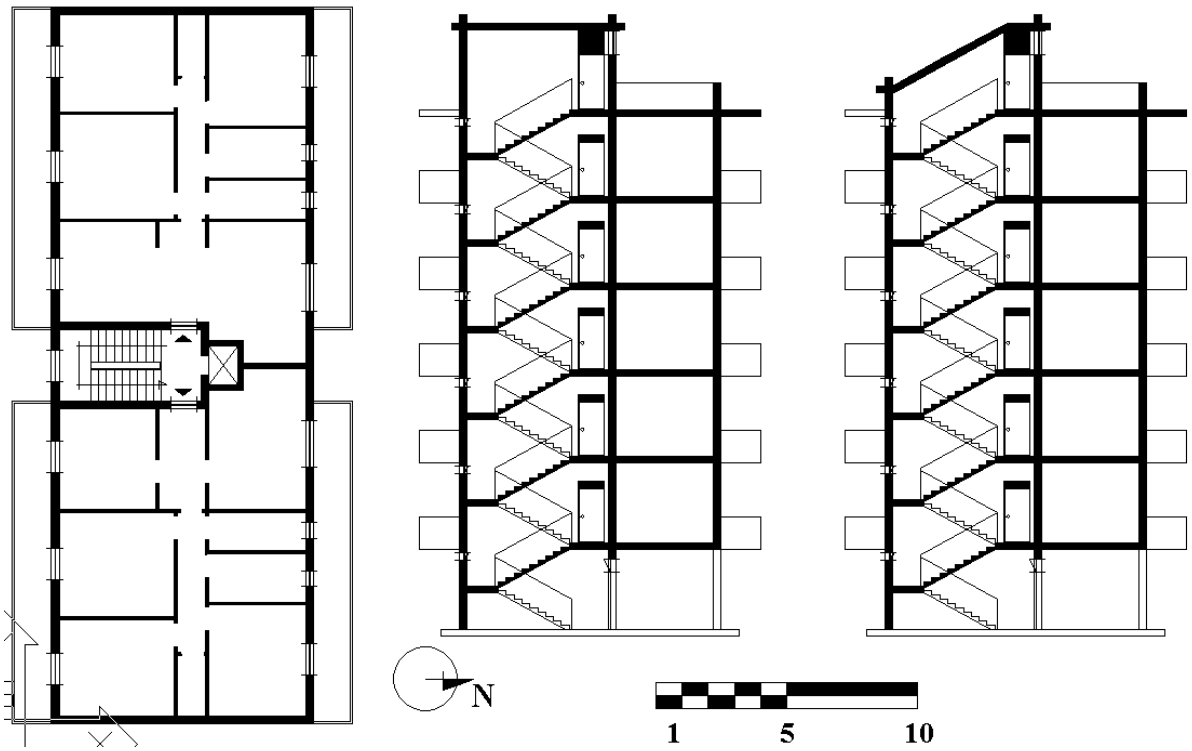

Figure 1: the adopted model: typical plan and section

The main components of the ventilation system for each apartment are:

- wind-sheltered inlets located near windows or heating devices (for example, a grille mounted into an external wall or windowsill, equipped with adjustable deflectors);
- air-transfer device (for example, grilles mounted into the internal doors);
- operable louvers mounted at the top of the entrance unit;
- semi-automatic control system (each occupant can manually adjust the air-inlets of some or all the rooms to suit personal requirements).

The natural ventilation system has been designed in order to extract the exhausted air from each apartment and each unit is sealed off from the others. These are important characteristics of the ventilation system in order to avoid a short-circuit and guarantee adequate indoor air quality (IAQ) in each unit.

Citing the conclusions of the previous works (Catalano et al., 2004), during winter, the studied stairwell is able to improve indoor ventilation, thanks to the pressure gradient between the stairwell and apartments, given by an internal temperature gradient.

The general aim of the developing research is to evaluate the summer behavior of this system with the following hypothesis:

- it is necessary to consider the behavior of the global system in transient state, providing variable external and internal heat fluxes, and simulating the real thermal inertia of the envelope;

- in order to verify the behavior of the model during summer, the effects of total solar radiation incident on the stairwell surfaces (the south wall, the walls at the top and the roof) have been taken into account (no shading of the envelope);
- no flat is equipped with an HVAC system: the only way to cool the apartments is natural ventilation. In this way, by eliminating the effect of internal heat loads, the internal air temperature is the same as the external one.

The hypothesised driving forces causing air movement are:

- the stack effect;
- the "solar chimney effect": the south wall warms air in the stairwell, causing it to rise toward the roof; this warmed air is extracted at the top of the stairwell and, consequently, fresh air is supplied to each dwelling.

The wind effects were ignored (the above mentioned mechanisms may be more affordable and continuous than wind-induced ventilation, especially in urban areas).

With the aim of maximizing the solar contribution, a statistical mean day in the month of July was chosen as the simulation date (in which, both the outdoor temperature and total vertical irradiance reach maximum values).
The city chosen as the location for simulations is Bari (41° 7' N – 16° 46' E), in the south of Italy. For this location, implementing solar radiation models (Muneer, 2004), mean values of hourly global solar radiation were estimated. Furthermore the external hourly mean temperatures were obtained from CNR (1982).

As previously mentioned, the effect of the thermal inertia of the traditional stairwell envelope was taken into account, trying also to suggest retrofitting intervention able to improve the "solar chimney effect", by means of a suitable shifting of the thermal wave and to enable the energetic upgrading of the envelope in general.

For this reason, during a first simulation step the heat transmission of traditional and retrofitted walls were evaluated (also reported in table 1) while in the second step a CFD simulation of the global stairwell model was carried out.

TABLE 1: thermo-physical characteristics of external traditional walls (1-4) and retrofitting intervention (5-7)

Id number	Type name	layers	width [cm]	λ [W/m °C]	c [MJ/m^3°C]
1-2	Single layer perforated brick wall (20-30 cm)	External plaster	2	0.9	1.62
		Perforated brick	20-30	0.35	0.47
		Internal plaster	1	0.8	1.62
3	Concrete wall (30 cm)	Concrete	30	2.7	1.83
4	Single layer tufa wall	External plaster	2	0.9	1.62
		Tufa	30	0.65	1.65
		Internal plaster	1	0.8	1.62
5	Externally insulated perforated brick wall	External plaster	2	0.9	1.62
		Insulation (polystyrene)	4	0.024	0.059
		Perforated brick	30	0.35	0.47
		Internal Plaster	1	0.8	1.62
6	Externally insulated concrete wall	External plaster	2	0.9	1.62
		Insulation (polystirene)	4	0.024	0.059
		concrete	30	2.7	1.83
7	Externally insulated tufa wall	External plaster	2	0.9	1.62
		Insulation (polystyrene)	4	0.024	0.059
		Tufa	30	0.65	1.65
		Internal plaster	1	0.8	1.62

2. ANALYSIS OF HEAT TRANSFER THROUGH EXTERNAL WALLS

In order to compare different envelope solutions we simulated the thermal behavior of traditional (local) walls and retrofitted ones using the following methodology.
For the temperature affecting the exterior surfaces, a theoretical temperature was used, considering the effect of the outdoor air temperature and the absorbed solar energy and indicating periodical change. In this way the so-called "sol-air temperature" was calculated using the following formulation (Threlkeld, 1998):

$$T_{sa} = T_{out} + \frac{\alpha}{h_{out}} R_{tv} - \frac{\varepsilon \, \Delta R}{h_{out}}, \qquad \text{Eqn. 1}$$

where T_{sa} is the sol-air temperature, T_{out} is the outdoor air temperature, α is the absorptivity of the external surface, h_{out} is the outdoor convective heat transfer coefficient, R_{tv} is the total radiation for vertical surfaces. The last term in Eqn.1, the correction factor, is assumed to be equal to 0 for vertical surfaces, following the ASHRAE recommendations.

Regarding the absorptivity of external surfaces, the solutions of white-painted (α=0.25) and black-painted external surfaces (α=0.90) were evaluated and, consequently, hourly values of sol-air temperature were calculated.

The internal heat flows (Q_{in} and Q_{out}) and surface temperatures were calculated with the aid of Heat 2.0 software, developed by the Department of Building Physics of the University of Lund (Sweden). The walls simulated, often used for the stairwell envelope in the south of Italy, are those in table 1. The results of these simulations are in the following table 2 and figure 2.

The simulations conducted show how concrete walls, both traditional and externally insulated, are able to maximize internal heat exchanges thanks to their considerable heat storage masses, also providing a good delay of the thermal wave.
The highest shift is, however, given by tufa walls, that also provide good heat exchange.
It is also necessary to consider that the differences between the behavior of analyzed systems will decrease in the global CFD model, which also takes into account internal surfaces and masses.

TABLE 2: results of the simulations: internal heat flows (Q_{out}= heat transmitted to the stairwell, Q_{in}=heat transmitted to the wall) and hours of flux inversions.

Id number	Type name	flux inversion	Q_{out} [Wh/m^2]	Q_{in} [Wh/m^2]	flux inversion	Q_{out} [Wh/m^2]	Q_{in} [Wh/m^2]
		painted white (α=0.25)			painted black (α=0.90)		
1	Single layer perforated brick wall (20 cm)	5:30 A.M. 1:30 P.M.	116	65	5:30 A.M. 11:30 A.M.	250	47
2	Single layer perforated brick wall (30 cm)	5:30 A.M. 3:30 P.M.	110	73	6:30 A.M. 1:30 P.M.	201	53
3	Concrete wall (30 cm)	6:30 A.M. 3:30 P.M.	243	105	7:30 A.M. 11:30 A.M.	591	37
4	Single layer tufa wall	7:30 P.M. 5:30 P.M.	159	97	7:30 P.M. 3:30 P.M.	295	46
5	Externally insulated perforated brick wall	6:30 A.M. 5:30 P.M.	86	72	6:30 A.M. 4:30 P.M.	115	57
6	Externally insulated Concrete wall	7:30 A.M. 7:30 P.M.	158	149	7:30 A.M. 6:30 P.M.	190	120
7	Externally insulated tufa wall	6:30 P.M. 7:30 P.M.	103	122	6:30 P.M. 6:30 P.M.	130	98

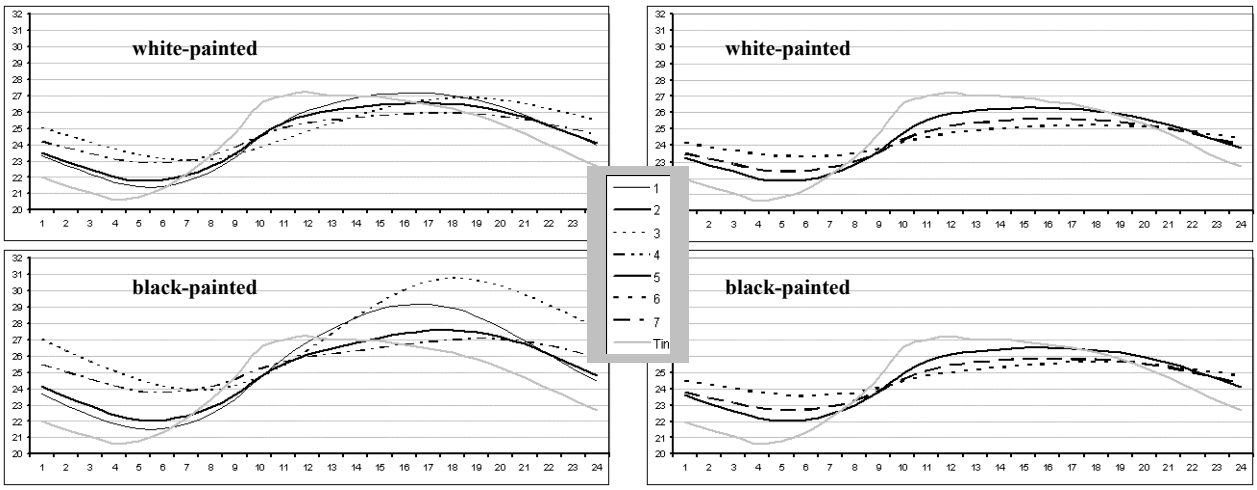

Figure 2: internal surface temperature for traditional (1-4) and retrofitted (5-7) walls

3. THE NUMERICAL CFD SIMULATIONS: RESULTS AND DISCUSSION

The model used in CFD simulations was simplified in order to optimise the computational time:

- the pressure losses in the apartment path were collapsed into a single resistance (therefore, only the stairwell was modelled);
- the stairwell geometry was simplified and reduced to the essential components (flights of stairs, landings, steps);
- the openings were modelled as simple resistance or as simple sloping planes.

The locations, the sizes and the pressure losses of openings were optimised in order to extract the air and to balance the airflow rate from each dwelling. The balanced system described in Catalano et al. (2004) (optimised for winter regime) has been used for the summer period.
The CFD numerical simulations were run in order to evaluate:

- the behaviour of the stairwell as an extraction device in summer (chimney and solar chimney);
- the effects of different envelope solutions (traditional and refurbished ones);
- the effects of different roof solutions at the top of the stairwell (flat and sloped roof);
- the behaviour of the system for different ventilation strategies (24 hours or night ventilation).

The CFD simulations highlight that the system is characterised by two different mechanisms (stack effect behaviour in day-time and solar chimney behaviour at night) :

- in the day-time, the air exhausted from dwellings rises in the stairwell, flowing along two main patterns: the first flow path is helicoidal in shape (just below the flights of stairs and landings), the second is a vertical path along the core of the stairwell; the results shown in figure 3a highlight that the air is extracted from all the dwellings
- at night, at lower levels (first to fourth floor), the air near the external wall is heated up and then rises along the walls, the landings and the flight of stairs. This warmed air mixes with the colder air extracted from dwellings, flows downward along the flight of stairs and returns back to the external wall (figures 3b and 4).

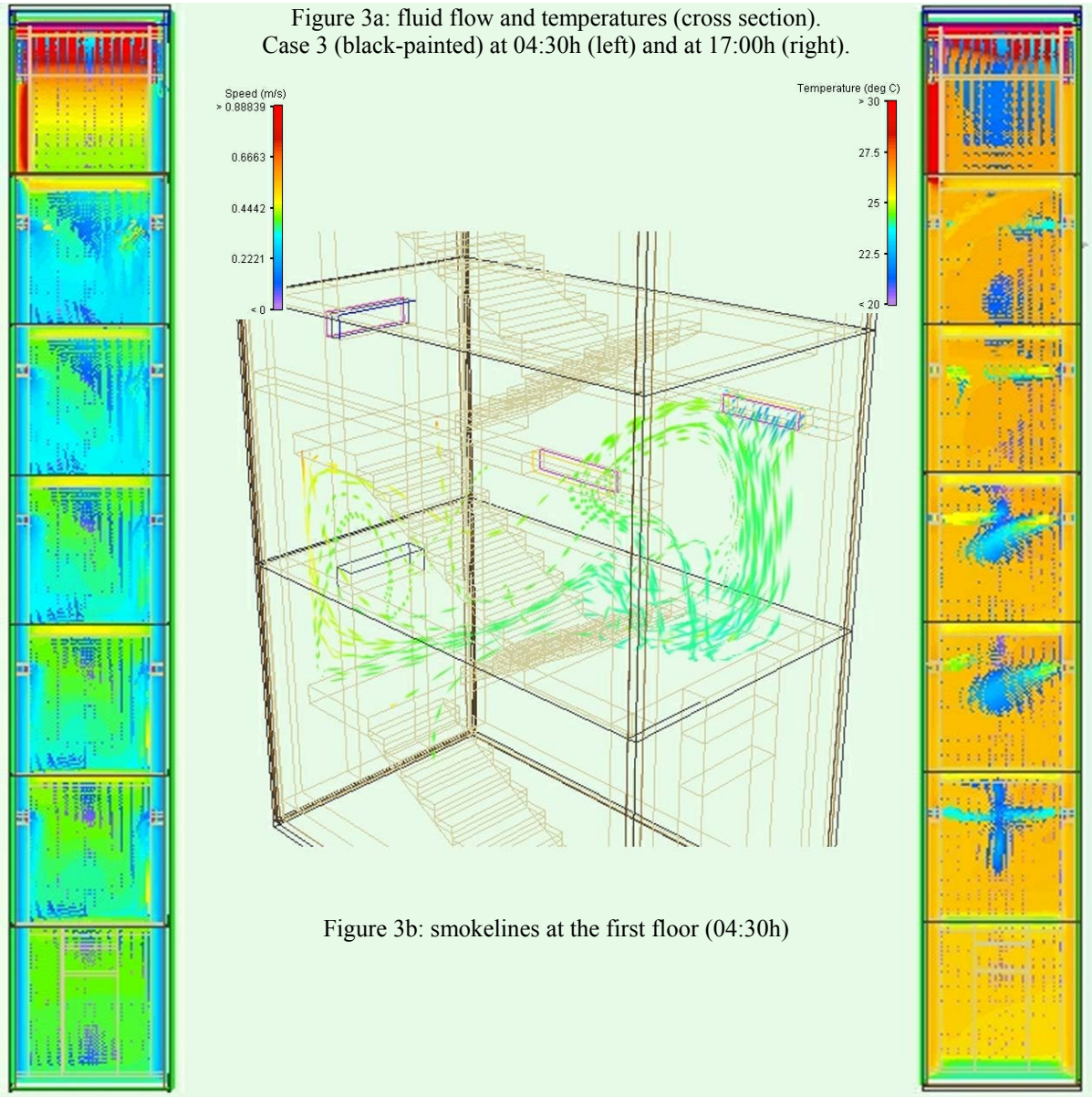

Figure 3a: fluid flow and temperatures (cross section).
Case 3 (black-painted) at 04:30h (left) and at 17:00h (right).

Figure 3b: smokelines at the first floor (04:30h)

In detail, the CFD simulations highlight that (figures 4 and 5):

- thermal inversion (the air enters the dwellings at night) is observed when the heat stored in the external walls is low or the delay of heat released to the stairwell is low (case 1, perforated brick wall, 20 cm);
- the airflow rates are high in day-time and low at night;
- the airflow rates increase with the heat accumulated in the external walls;
- the shift in maximum and minimum airflow rates is related to the delay of the thermal wave but not as expected;
- the effects of a sloped roof on the main behaviour of the system are poor (except for the fifth and the fourth floor);
- the ventilation strategies (24 hour or night ventilation) do not affect the main behaviour of the system;
- the refurbished external walls (painted black or covered by an external thermal insulation layer) allow higher airflow rates both in day-time and at night, but the airflow rates seem to be inadequate for night ventilation strategies.

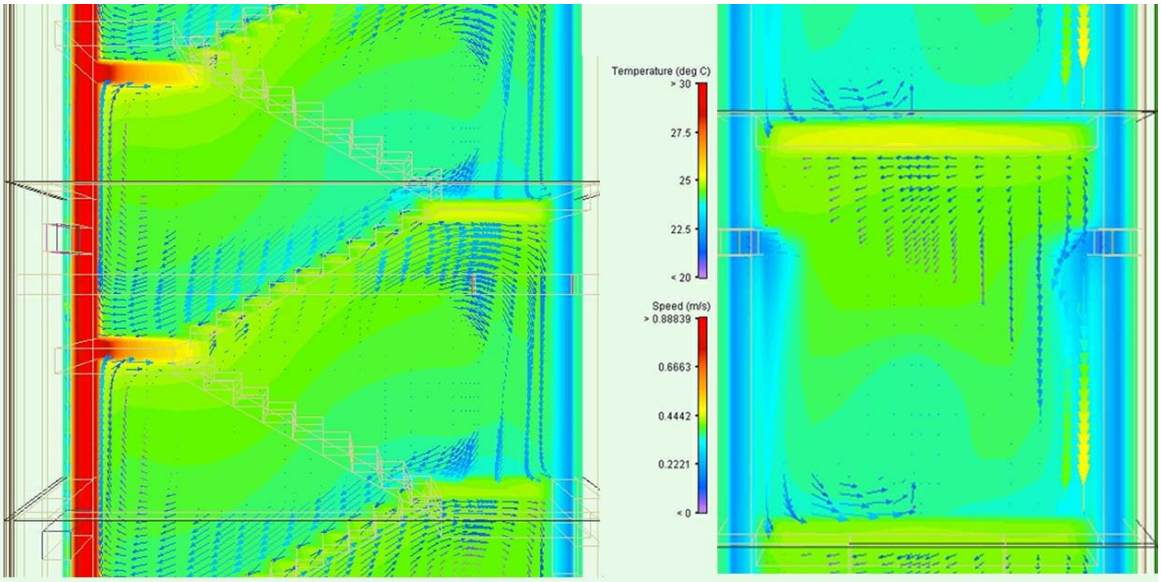

Figure 4:details of fluid flow and temperatures at the first floor (longitudinal and cross section). Case 3 (black-painted) at 04:30h (above) and at 17:00h (below).

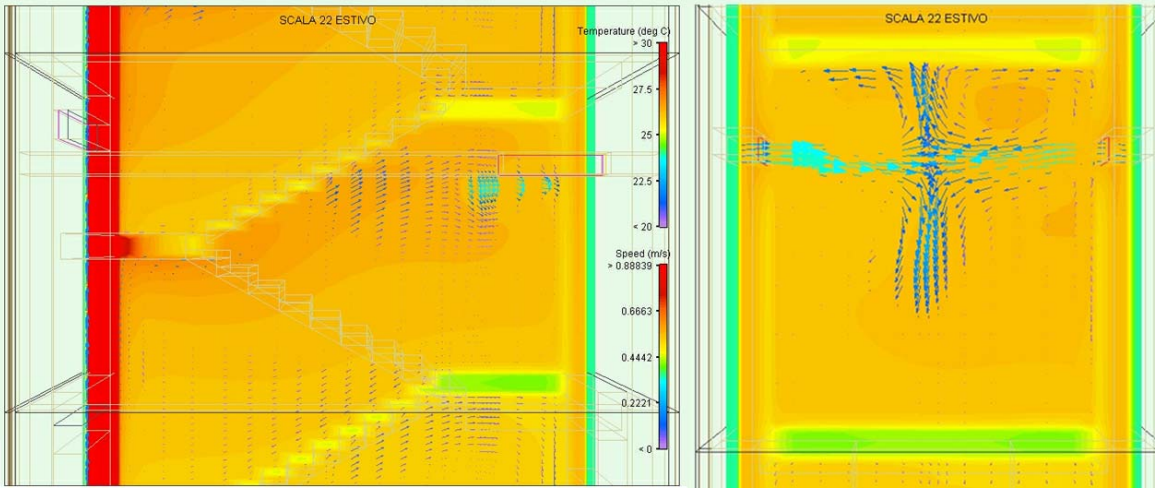

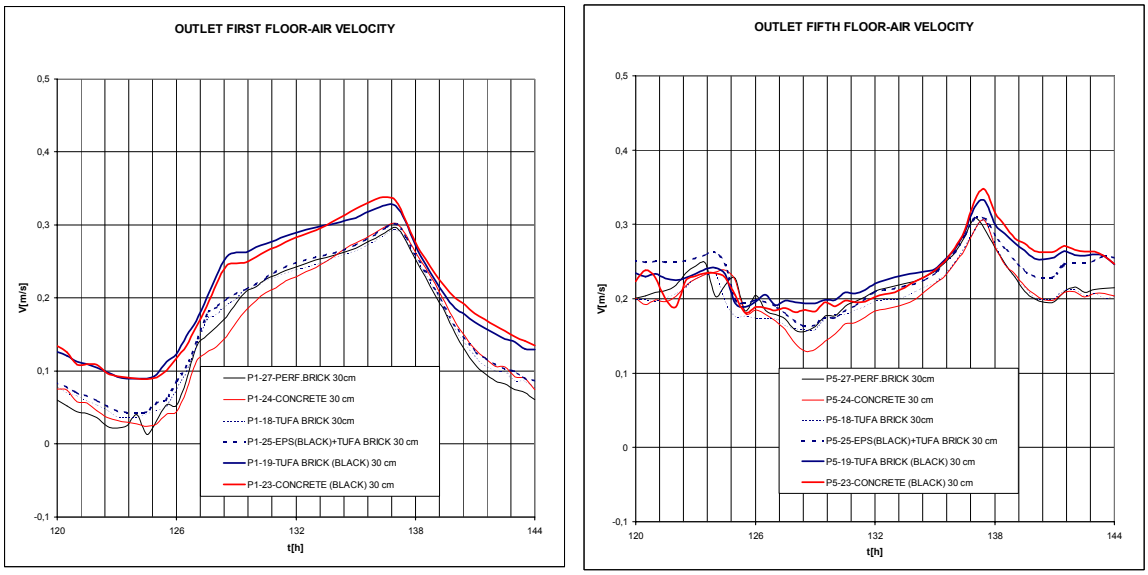

Figure 5: air velocity near the air-transfer device at the top of the entrance unit (grilles at the first and fifth floors).

In conclusion, the CFD simulations show that fluid patterns can have a fundamental role: the complex geometry and the dynamic thermal boundary conditions of a typical stairwell substantially modify the hypothesised behaviour of the system at night. It is worth noting that the temperature of air extracted from dwellings is generally higher than that hypothesised and this temperature is related to the internal thermal loads and the ventilation rates.
Further simulations will be run to test different systems that can enhance the "solar chimney behaviour" at night. The first idea is to break the thermal loop shown in figure 3b by means of openings located on the half landing or by adding conveyers at the bottom of the half landings that drive the warmed air toward the central void of the stairwell. In addition, methods of refining air temperatures of dwellings will be evaluated.

REFERENCES

Blomberg, T. (1996). Doctoral Thesis. *Heat conduction in two and three dimensions. Computer modeling of Building Physics applications.* Department of Building Physics, Lund University, Sweden.

Catalano, M. , Dell'Osso, G. R. , Iannone, F. (2004). Natural ventilation for controlling the indoor microclimate. *Proceeding of International Conference Eurosun 2004*. Freiburg im Breisgau, Germany.

CNR (1982). *Dati climatici per la progettazione edile ed impiantistica*. Consiglio Nazionale delle Ricerche – Progetto Finalizzato Energetica, Rome, Italy.

Muneer, T. (2004). *Solar radiation and daylight models.* Elsevier Butterwoth-Heinmann, Linacre House, Jordan Hill, Oxford.

Threlkeld, J. L. (1998). *Thermal Environmental Engineering*. Prentice Hall, Englewood Cliffs, NJ.

CONTRIBUTORS

F. Iannone planned and supervised the study, executed the CFD simulations and analysed the data (paragraphes 1 and 3). F. Fiorito codesigned the study and executed the analysis of heat transfer through external walls (paragraphes 1 and 2).

The Air Infiltration and Ventilation Centre was inaugurated through the International Energy Agency and is funded by the following seven countries:

Belgium, Czech Republic, France, Greece, The Netherlands, Norway and United States of America.

The Centre provides technical support in air infiltration and ventilation research and application. The aim is to provide an understanding of the complex behaviour of the air flow in buildings and to advance the effective application of associated energy saving measures in both the design of new buildings and the improvement of the existing building stock.

Air Infiltration and Ventilation Centre
Operating Agent and Management
INIVE EEIG
Boulevard Poincaré 79
B -1060 Brussels - Belgium

www.aivc.org

Tel: +32 2 655 77 11
Fax: +32 2 653 07 29
inive@bbri.be
www.inive.org